NSSDC WDC-A-R&S
National Space Science Data Center/
World Data Center A For Rockets and Satellites
80-05

Coordinated Ionospheric and Magnetospheric Observations from the ISIS 2 Satellite by the ISIS 2 Experimenters

Volume 3

High-Latitude Charged Particle, Magnetic Field and Ionospheric Plasma Observations During Northern Summer

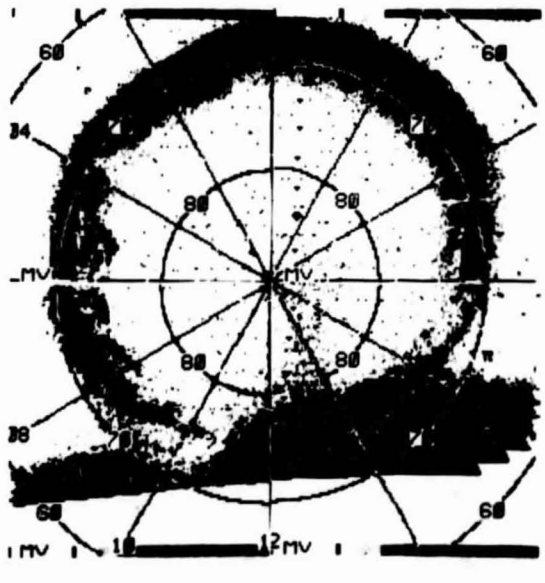

November 1980

COORDINATED IONOSPHERIC AND MAGNETOSPHERIC OBSERVATIONS FROM THE ISIS 2 SATELLITE BY THE ISIS 2 EXPERIMENTERS

VOLUME 3

HIGH-LATITUDE CHARGED PARTICLE, MAGNETIC FIELD, AND IONOSPHERIC PLASMA OBSERVATIONS DURING NORTHERN SUMMER

Coordinator: D. M. Klumpar
University of Texas at Dallas

November 1980

The Experimenters are grateful to the National Space Science Data Center, Greenbelt, Maryland for making this publication possible.

This Data Book is dedicated

to the memory of John H. Chapman,

through whose efforts the Alouette-ISIS

satellite program became a reality.

TABLE OF CONTENTS

I. INTRODUCTION

ISIS 2 is the fourth and final satellite launched in the Alouette/ISIS series. In this International Satellites for Ionospheric Studies program, Canada provided the spacecraft, data acquisition, and satellite control. The USA provided the launch capability, tracking, and data acquisition. Satellite instruments and data processing support were provided by both countries. During the course of the program these countries contributed telemetry support and collaborative data analysis: Australia, Finland, France, India, Japan, New Zealand, Norway, and the United Kingdom.

Alouette 1 won recognition mainly through the success of the topside sounder, but subsequent evolution led to a highly coordinated ISIS 2 satellite, having the capability for both direct measurements and remote sensing. Launched on April 1, 1971, into a near-circular near-polar orbit at 1400 km, it was essentially an observatory-type satellite with the potential of making fundamental measurements of both the ionosphere and magnetosphere, thereby yielding important information on the coupling processes between these regions.

At the time the program was planned, no provision was made for the generation or presentation of uniform and coordinated data sets, as this concept did not emerge until much later. This work has been done, for a selected number of passes, by the ISIS Experimenters Committee, and this publication is the result of their coordinated efforts.

The purpose of this work is to provide at the end of the data acquisition phase of the ISIS program, a representative set of data from ISIS 2 covering a range of operating modes and geophysical conditions. The data presented here show the typical values and range of ionospheric and magnetospheric characteristics, as viewed from 1400 km with the ISIS 2 instruments. For any scientist using ISIS data, this book should give a useful background and helpful perspective as to what is available. For others, this publication should be helpful in providing typical and extreme values of ionospheric and magnetospheric parameters, or may even provide research material. Anyone making serious quantitative use of these data may wish to contact the experimenters themselves. Original data from the instruments have been deposited in the National Space Science Data Center (NSSDC), NASA/GSFC, Greenbelt, Maryland 20771.

The overall publication comprises seven data sets in four volumes. The definition of each data set depends partly on geophysical parameters and partly on satellite operating mode. Preceding the data set is a description of the organizational parameters and a review of the objectives and general characteristics of the data set. The data are shown as a selection from 12 different data formats. Each data set has a different selection of formats, but uniformity of a given format selection is preserved throughout each data set. A description of how to interpret each format is given in the introductory sections. Most of the data that are plotted linearly in time are on one of two possible scales, corresponding to either 12 min/page or 20 min/page. Thus easy comparison of data is made possible. To summarize, each data set consists of a selected number of passes, each comprising a format combination that is most appropriate for the particular data set. Following

this introduction is a list of ISIS 2 experimenters, with addresses and telephone numbers, then a brief description of the ISIS 2 satellite, followed by more detailed instrument descriptions, format descriptions, data set descriptions, and the data themselves. At the end of Volume 1 is a bibliography of ISIS 2 published papers. This bibliography was produced from a computerized technical reference file at the National Space Science Data Center. Comprehensive bibliographies for the other satellites of the Alouette-ISIS program also are available from NSSDC.

II. LIST OF ISIS 2 EXPERIMENTERS (as of 1980)

Communications Research Centre - Department of Communications P.O. Box 11490, Station "H", Ottawa, Ontario, Canada K2H 8S2

H. G. James - Topside sounder, VLF, Cosmic Noise (613-596-9279)
D. Muldrew - Topside sounder (613-596-9101)
J. H. Whitteker - " " "
J.D.R. Boulding - Satellite controller (613-596-9539)

Goddard Space Flight Center, Greenbelt, MD, USA 20771

L. H. Brace - Cylindrical electrostatic probe, Code 961 (301-344-8575)
E. J. Maier - Retarding potential analyzer, Code 963 (301-344-8912)
C. Freeman - Data analyst (301-344-6374)

National Research Council - Herzberg Institute of Astrophysics, Ottawa, Ontario, Canada K1A OR6 (613-992-2734)

I. B. McDiarmid
J. R. Burrows
D. D. Wallis
M. D. Wilson
} Energetic Particle Detector and Fluxgate Magnetometer

University of Calgary, Physics Department, Calgary, Alberta, Canada T2N 1N4 (403-284-6340)

C. D. Anger
L. L. Cogger
J. S. Murphree
} Auroral Scanning Photometer

University of Texas at Dallas, Center for Space Sciences, MS F02.2, P.O. Box 688, Richardson, TX, USA 75080

W. J. Heikkila
J. D. Winningham
D. M. Klumpar
} Soft Particle Spectrometer (214-690-2835)

J. H. Hoffman - Ion Mass Spectrometer (214-690-2840)
W. H. Dodson - " " " "

York University, Centre for Research in Experimental Space Science, 4700 Keele Street, Downsview (Toronto), Ontario, Canada M3J 1P3 (416-667-3221)

G. G. Shepherd - Red Line Photometer
F. W. Thirkettle - Data Analyst

III. SATELLITE DESCRIPTION

ISIS 2 (Figure 1) was launched from the Western Test Range, California on April 1, 1971 (Franklin and Maclean, 1969; Daniels, 1971). The orbital parameters are: apogee 1423 km, perigee 1356 km, inclination 88.16°, and period 113.55 min. ISIS 2 carries 12 instruments (Figure 2), 10 of which are described in detail below. The other two are the Beacon experiment for measuring ionospheric irregularities and the Cosmic Noise experiment for measuring the cosmic or natural background noise level.

The satellite is an approximate oblate spheroid with a height of 119 cm, a diameter of 127 cm, and a weight of 260 kg. Its attitude is controlled by torquing coils and is measured by a 6-probe fluxgate magnetometer and a solar aspect sensor. The spin rate varies between about 2.5 and 3.5 rpm and can be changed by about 0.10 - 0.15 rpm/orbit. The spin axis is normally kept in the orbital plane (orbit-aligned) or at right angles to the orbital plane (cartwheel). For the orbit-aligned configuration the attitude can be changed by 2.0° - 2.5°/orbit and in the cartwheel configuration, by about 0.5°/orbit. The spacecraft contains about 11,000 solar cells and 3 Ni-Cd batteries. It was capable of operating for about 9 hours/day at launch and presently (1980) is capable of operating for about 2.5 hours/day. It has 3 telemetry transmitters at 136.08, 136.59, and 401.75 MHz and a tracking beacon at 136.41 MHz. Data are telemetered to several ground stations situated around the world. The spacecraft has a tape recorder and clock, but these failed in 1971 and 1974, respectively.

IV. INSTRUMENT DESCRIPTION AND DATA PROCESSING

AURORAL SCANNING PHOTOMETER (ASP)

The ISIS 2 dual wavelength auroral scanning photometer (Anger et al, 1973) is designed to map the distribution of auroral and airglow emissions at 5577Å and 3914Å over the portion of the dark Earth visible to the spacecraft.

Franklin, C. A., and M. A. Maclean, The design of swept-frequency topside sounders, Proc. IEEE, 57, 897-929, June 1969.

Daniels, F., The ISIS-II spacecraft, Communications Research Centre Report No. 1218, Department of Communications, Ottawa, March 1971.

Anger, C. D., T. Fancott, J. McNally, and H. S. Kerr, ISIS 2 scanning auroral photometer, App. Optics, 12, 1753-1766, Aug. 1973.

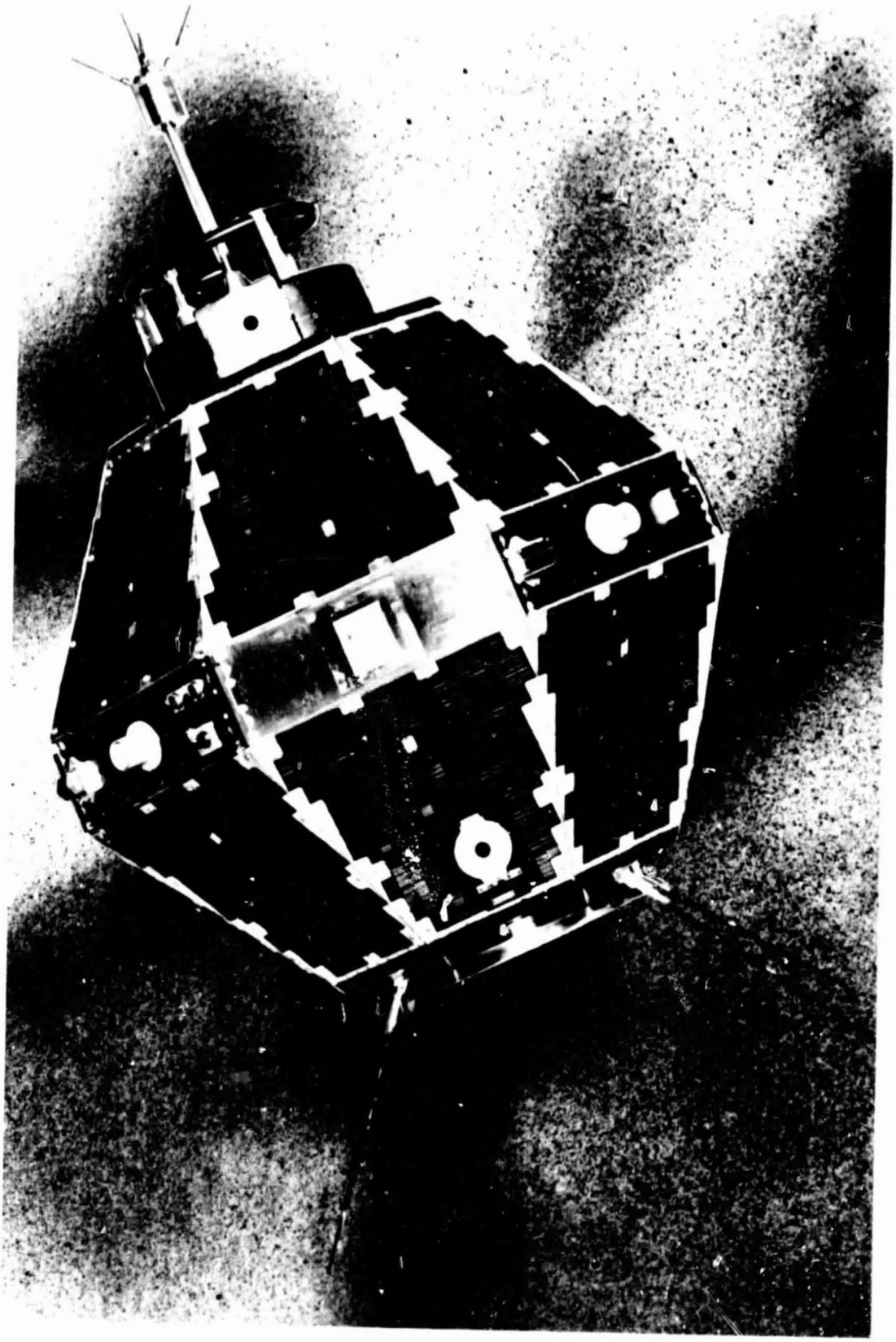

Figure 1. ISIS 2 Spacecraft.

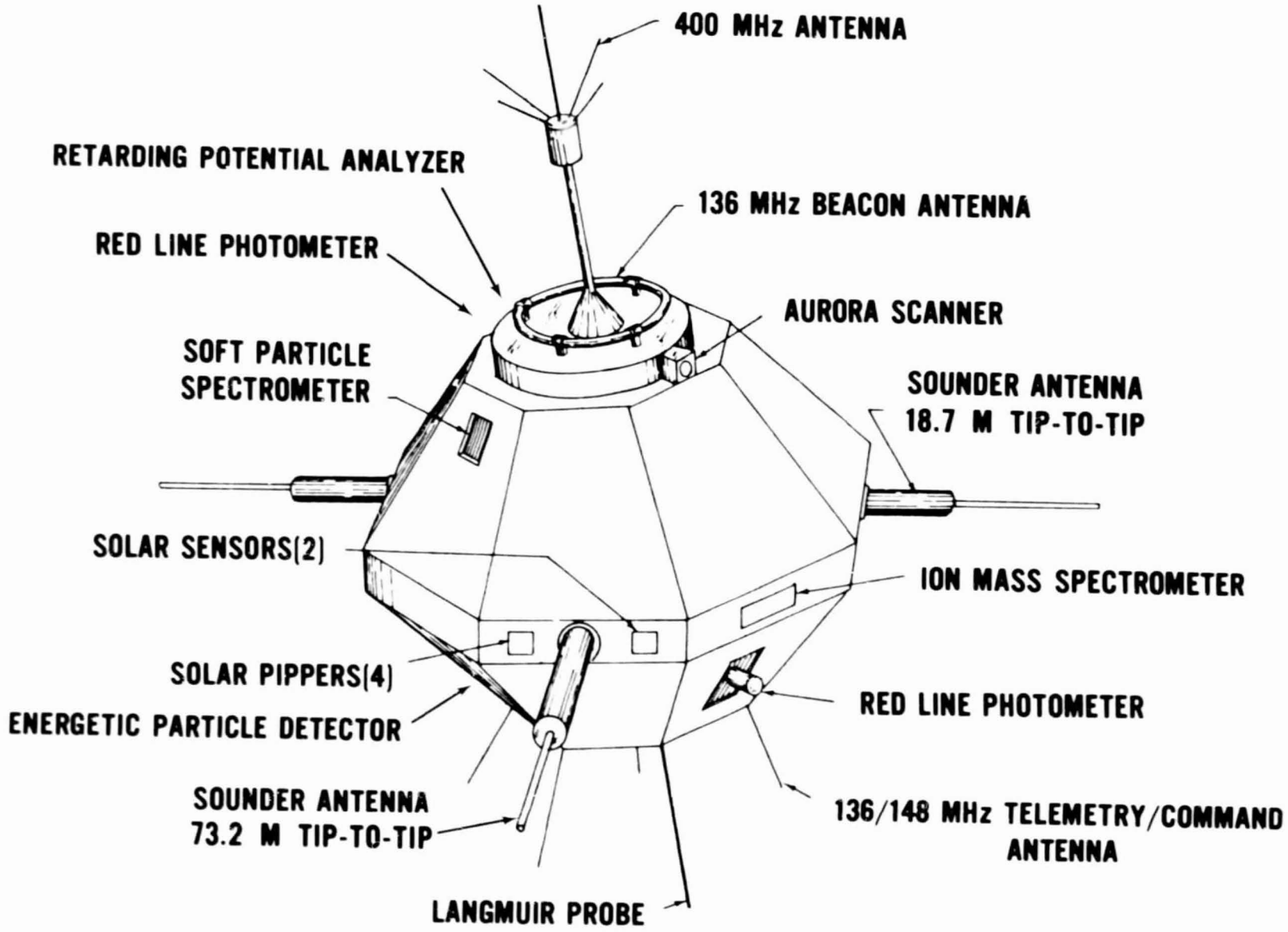

Figure 2. ISIS 2 Instrumentation.

Meaningful optical observations are possible at angles between the viewing direction of the instrument and the Sun direction of >60° and <120° due to a two-stage baffle system which shields the optics. The optical system consists of two separate barrels which are 180° apart so that only one barrel can look at the Earth at a time. The light from each of the barrels passes through its own interference filter (5581 ± 9Å or 3914 ± 13Å), lens, and mirror, and then is focused at a common point on a single-image dissector photomultiplier tube. This tube is similar to an ordinary photomultiplier tube except that an electrostatic imaging system and aperture are interposed between the cathode and first dynode. At any instant, only those photoelectrons from a small region of the cathode can pass through the aperture and be multiplied. This region is scanned across the photocathode by a magnetic scanning coil, thus generating a 13-element linear scan which is oriented at 90° to the direction of motion produced by rotational motion of the spacecraft (see Figure 3). The instantaneous field of view of each of these elements is 0.4° x 0.4°, resulting in an average output of one photoelectron pulse for ~250 rayleighs (R) from each point viewed, and hence a signal to noise ratio of one. The spatial resolution at 100 km directly under the spacecraft is ~8 km for each element.

Each photoelectron passing through the imaging electron optics and aperture of the image dissector tube is multiplied by about 10^7 by the dynode chain. The resulting output pulse is amplified by a pulse preamplifier, which produces standard pulses suitable for driving high-speed digital logic. Pulses from the preamplifier are accumulated in a digital logarithmic accumulator, the seven-bit output of which is transferred to a buffer and shifted out in standard PCM format at 630 words per second. As one frame of data consists of the 13 elements in a scan plus a frame synchronization word, there are 45 frames of data output per second.

The photometer scans the Earth by a combination of the rotational and translational motions of the spacecraft together with the internal electronic scanning performed by the image dissector (see Figure 3). The spacecraft spin axis and orbital plane remain essentially fixed in space as the spacecraft orbits the Earth, and, therefore, each rotation of the spacecraft results in the scanning of a strip, which, for the orbit-aligned mode of the spacecraft, is at right angles to the orbital plane. The width of the strip (5°) is chosen so that it will just join onto the strip scanned during the previous rotation. The image dissector repetitively scans at high speed across the narrow dimension of each strip, dividing it into 13 separately resolved regions (0.4° x 0.4°). Similar strips are scanned at each of the two wavelengths, although they differ in time by half the rotation period.

RED LINE PHOTOMETER (RLP)

The RLP (Shepherd et al, 1973) was designed to measure the emission of 6300Å aurora and airglow from the F-region of the Earth's ionosphere. It has two optical inputs, 180° apart and at 90° to the satellite spin axis. One input is characterized by a 10Å bandwidth filter and the other by an 88Å bandpass. They have roughly equal responses to white light, but the responses to

Shepherd, G. G., T. Fancott, J. McNally, and H. S. Kerr, The ISIS-II atomic oxygen red line photometer, Appl. Opt. 12, 1767 (1973).

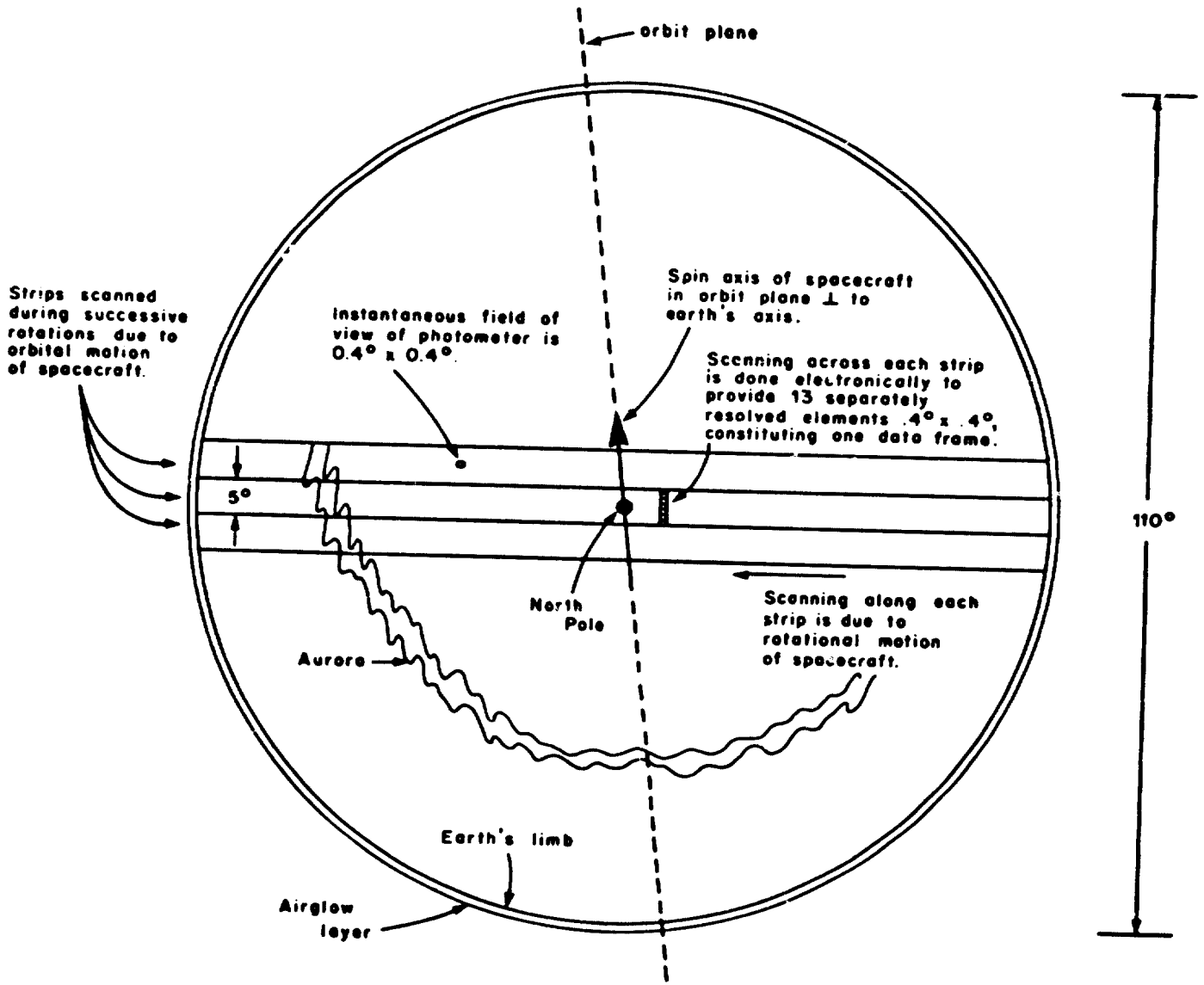

Figure 3. The Earth as it would appear from the spacecraft 1400 km above the pole, with scanning pattern of photometer superimposed.

6300Å emission are in the ratio of 9:1. The field of view of both is 2.5° in diameter. These optical inputs enter the same telescope system, and the intensities are summed onto one photomultiplier detector. As one input views the Earth the other views the dark sky, allowing the signals to be separated. Corrections for the starlight background intensity are made in data analysis. Intensities are measured at a rate of 30 samples/sec.

With the satellite spin axis in the plane of the orbit, the Earth scans caused by satellite rotation (19-second period, normally) form a raster-like scan pattern, generating two pictures per orbit; one as seen through the 10Å filter, the other by the 88Å filter. These pictures are combined to eliminate the white light background, leaving the 6300Å intensities. These intensity values are contoured in "spin coordinates," and then transformed to magnetic invariant coordinates using the method of Boyd (1977) . The details are described under Format 8.

When the spin axis is perpendicular to the orbit plane (cartwheel configuration), the RLP scans repeatedly along the satellite track. The output in this case is presented as intensity along the spacecraft track as a function of spacecraft time. The details are described under Format 1.

SWEPT-FREQUENCY SOUNDER

The sounder is essentially a radar, operating between 0.1 and 20 MHz, which transmits pulses approximately 100 μs in duration, and then listens for reflected signals. The pulses are repeated at the rate of 45 per second, as the frequency is gradually swept through its range. The received signal is displayed in the form of an ionogram, in which the density of the display at any point depends on the signal level.

An ionogram is shown in Figure 4. In a well-behaved (horizontally stratified) ionosphere, there will be at most two echoes for a given frequency. For each echo, the time delay is determined by the electron density (N) as a function of altitude (h). The delay-time scale is marked in units of distance (apparent range), corresponding to a signal propagating at the speed of light. In a plasma, the signal travels more slowly than this, and the delay time depends on an integral of group refractive index along the path. The ionogram provides apparent range as a function of frequency, and with this information, the integral can be inverted to give the vertical electron density profile N(h). A procedure for this inversion is described by Jackson (1969).

The trace in the lower portion of the ionogram represents the automatic gain control (AGC) voltage. Zero voltage is given by the horizontal line that is designated 2800 km apparent range, and the maximum AGC voltage of 5 volts is shown by the 2400 km apparent range marker. The AGC voltage can be used as a measure of the background noise level at the satellite.

Boyd, J. S., Invariant geomagnetic coordinates for epoch 1977.25, Planet. Space Sci. 25, 411 (1977).

Jackson, J. E., The reduction of topside ionograms to electron-density profiles. Proc. IEEE, 57, 960-976, June 1969.

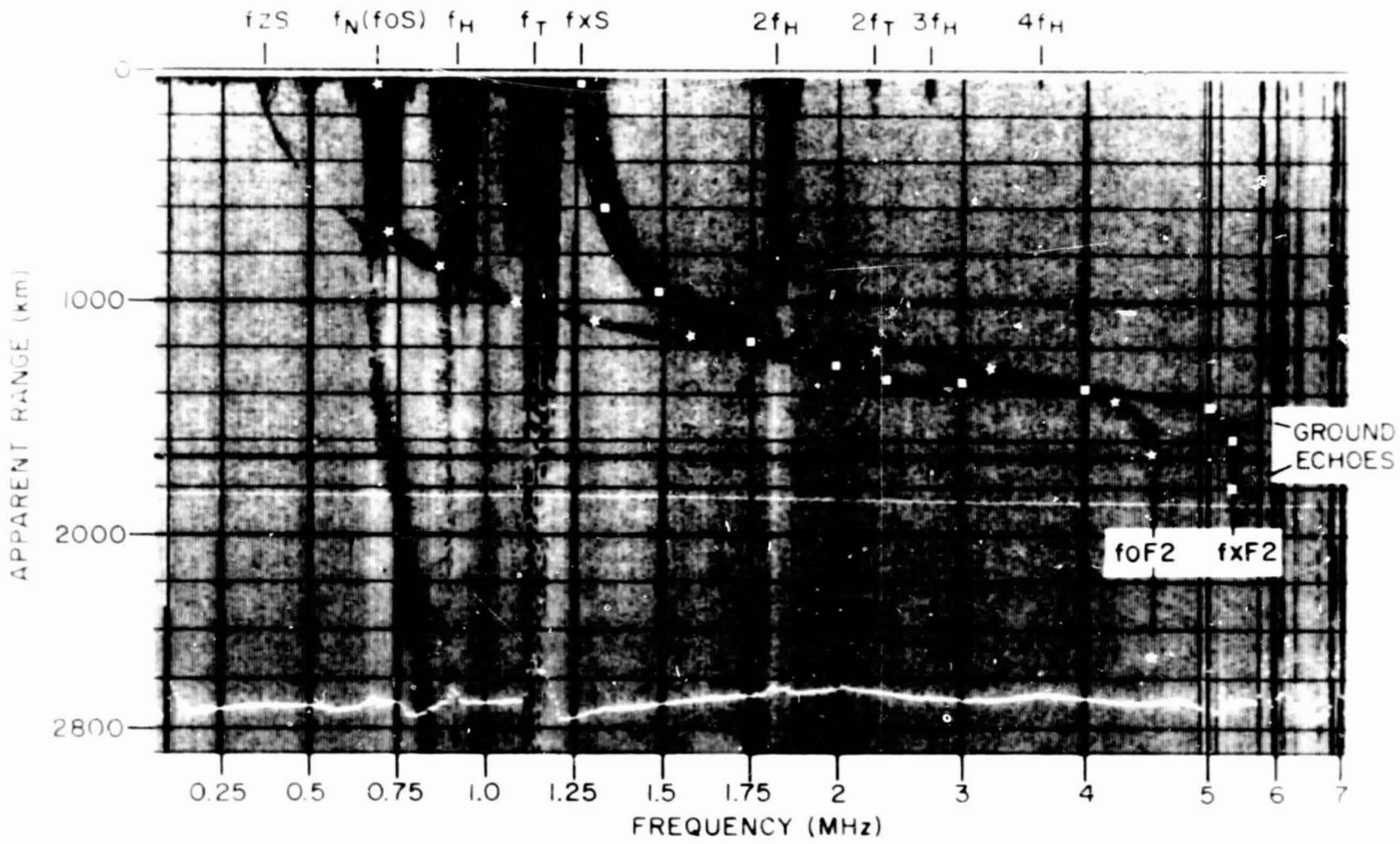

Figure 4. ISIS 2 Ionogram.

The sounder is described in more detail by Franklin and Maclean (1969). In the same issue of Proc. IEEE, there are several other articles on topside sounding. A short review on topside sounding is given by Jackson et al (1980).

CYLINDRICAL ELECTROSTATIC PROBE (CEP)

The CEP is a Langmuir probe instrument which measures the electron density (N_e) and temperature (T_e) of the ionospheric plasma. The instrument consists of a pair of thin wire collectors projecting from the spacecraft spin axis at both ends. The two collectors are operated independently in a time-shared fashion by a common electronic unit which applies an appropriate voltage waveform and measures the resulting volt-ampere characteristics of the collectors. Details of similar instruments used on the Alouette 2 and Explorer 31 satellites are discussed elsewhere (Findlay and Brace, 1969).

A typical CEP plot of N_e and T_e is shown in Figure 5. The plot format reflects the details of the instrument design. Points are shown at 6-second intervals, reflecting the repetition rate of the sweep voltage waveform. Each collector is assigned to the electronics during alternate 30-second intervals, thus alternate groups of five measurements are derived from different probes. Owing to damage of one of the probes at launch, which introduced a spin modulated error in its N_e measurement, only one probe is employed for N_e measurements. Both probes are capable of good T_e measurements, although wake effects on one or the other may cause slight disagreement in their T_e measurements at certain points in the orbit. This will be evident as an offset in alternate groups of five T_e points in the plots. The T_e values are given either by solid points or by question marks (?) in the case of poor curves caused by ionospheric irregularities, as discussed later.

The N_e measurements are made in the range of about 10^2 to $10^5/cm^3$. The lower limit arises from electrostatic shielding by the spacecraft sheath which grows out over the collectors at very low densities.

The T_e measurements can be made when N_e exceeds about $200/cm^3$ when the collectors are not in sunlight. When in sunlight, photoelectrons leaving the collectors prevent a proper ion current reference to be established until N_e exceeds about $10^3/cm^3$. T_e may be resolved between 500°K and 15,000°K when the above N_e conditions are attained.

Franklin, C. A. and M. A. Maclean, The design of swept-frequency topside sounders, Proc. IEEE, 57, 897-929, June 1969.

Jackson, J. E., E. R. Schmerling, and J. H. Whitteker, Mini-review on topside sounding, IEEE Transactions on Antennas and Propagation, Vol. AP-28, No. 2, 284-288, March 1980.

Findlay, J. A. and L. H. Brace, Cylindrical electrostatic probes employed on Alouette 2 and Explorer 31 satellites, Proc. IEEE, 57, 1054-1056, June 1969.

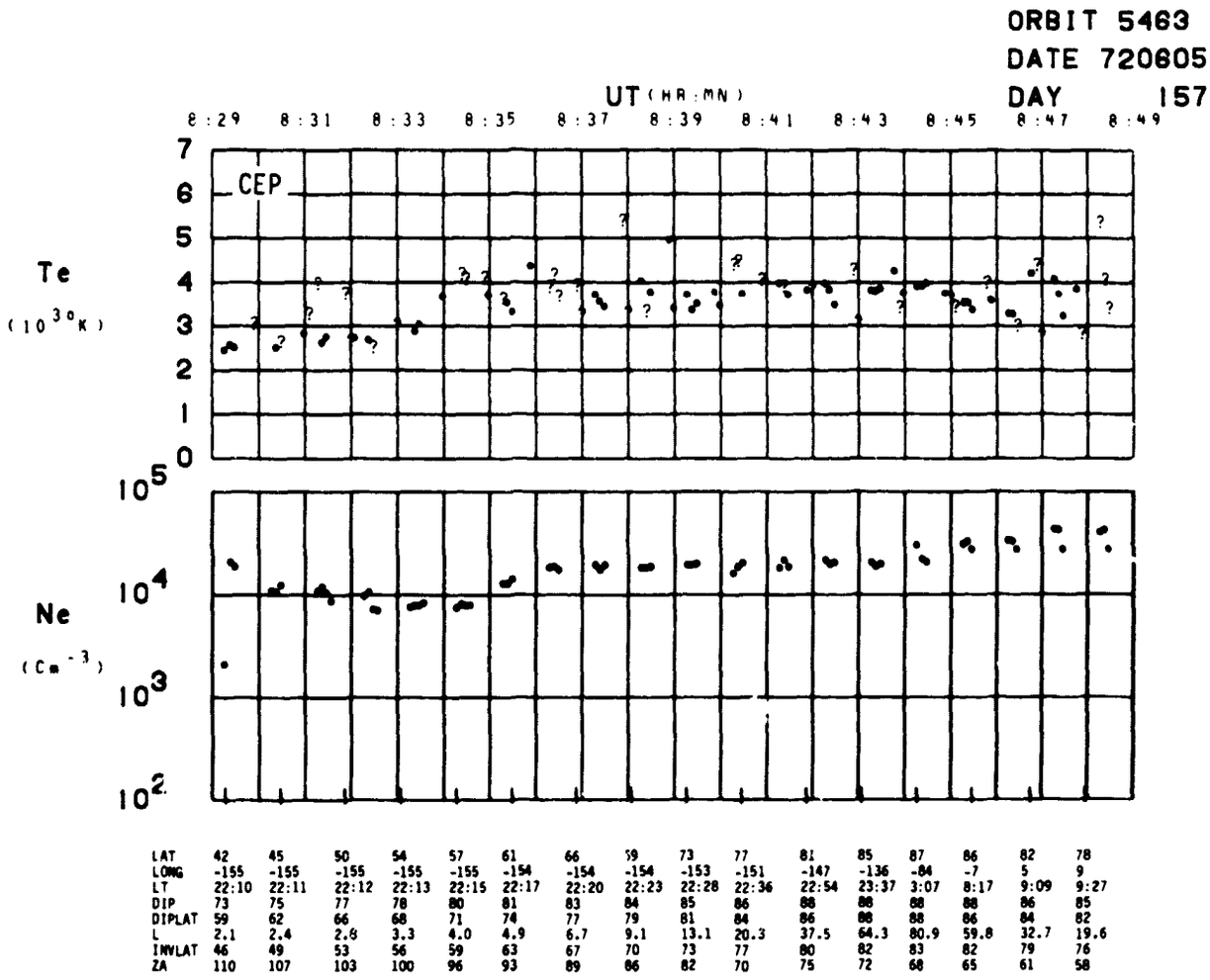

Figure 5. Example of CEP data.

The main sources of error in N_e are wake effects and inadequacies of the theory for the conversion of electron current to density. Comparisons with the sounder and the other direct measurements on ISIS 2 show that the errors seldom exceed a factor of two, even when wake effects are ignored. Thus we have not eliminated N_e data on the basis of spacecraft orientation.

The main source of error in T_e arises from the irregular structure of the high-latitude ionosphere which introduces distortions in the volt-ampere characteristics. When a solid point is employed to plot T_e, the error is probably less than 10 percent. Larger errors may be expected when question marks are used. No T_e value is plotted if the plasma is so structured as to distort the curve beyond recognition to the curve fitting program. In general, question mark symbols should be used only when solid T_e points are not available, and then only as an estimate of T_e.

ENERGETIC PARTICLE DETECTOR (EPD)

The EPD instrument was designed to provide directional flux measurements of electrons (from 0.15 keV to 2 MeV) and positive ions (from 2 keV to 20 MeV with some gaps). A diversity of sensors are used. A stepped electrostatic analyzer provides an 8-point electron spectrum ($0.15 < E < 10$ keV) and an 8-point positive ion spectrum ($2.0 < E < 26$ keV), each once per second. However, only three of these electron differential channels are displayed in the normal EPD format. Geiger counters and solid state detectors provide integral flux measurement at 12 different threshold energies starting at $E > 22$ keV for electrons and $E > 150$ keV for protons. Only three of these integral channels are included in Format 3, averaged to one second time resolution. The instrumental time resolution is $\sim$1/4 second. The energy bandpass ($\Delta E/E$) of the electrostatic analyzer is 30 percent for electrons and 15 percent for positive ions.

All of the sensors but one have the axis of their fields of view fixed in the same direction in the plane perpendicular to the spacecraft's spin axis. One geiger counter axis is along the spin axis. The fields of view of the integral detectors are conical. The electrostatic analyzer differential spectrometer has a rectangular field of view defined by a collimator with half angles 1.5° x 1.7°.

The electron differential channels are unaffected by positive ion fluxes but do give spurious counts due to solar ultraviolet light when viewing the Sun. The integral channels respond to both electrons and protons in general at different threshold energies. In Format 3, channel I(210) has had the positive ion flux removed. The $I_{\parallel}(40)$ channel includes both electron ($E > 40$ keV) and positive ions ($E > 150$ keV) fluxes. The latter flux is negligible except during solar proton events. Both I(40) and $I_{\parallel}(40)$ also sometimes have spurious Sun counts.

The gain of the differential spectrometers' channeltron detector decreased quickly between April and October 1974 and should be regarded as quantitatively inaccurate after April 1974. The geiger counter, $I_{\parallel}(40)$, failed in June 1973.

The instrumentation and detector characteristics are more fully described by Venkatarangan et al, 1975. Some relevant EPD detector characteristics are tabulated below.

Detector	Type	Energy Threshold keV	Geometric Factor cm^2 ster	Collimator Half-Angle
I(210)	solid state	e^- 210	8.15×10^{-3}	7.0°
I(40)	solid state	e^- 40 p^+ 150	7.84×10^{-3}	6.8°
$I_{\parallel}$(40)	geiger	e^- 40 p^+ 600	1.03×10^{-3}	5.6°
I(22)	geiger	e^- 22 p^+ 240	8.83×10^{-4}	5.5°
Ip(750)	solid state	$750<p^+<4000$	4.9×10^{-2}	11.3°

ION MASS SPECTROMETER (IMS)

The ion mass spectrometer (Hoffman et al, 1974) is a magnetic sector type mass spectrometer with two electron multiplier detectors located on two different radii within the sector. The incoming ions are accelerated by a potential that makes a complete sweep in 1 second such that the mass range 1 to 9 AMU is sampled on one channel and, simultaneously, the mass range 8 to 64 AMU is sampled on the other channel. Thus the mass spectrum from 1 to 64 AMU is sampled each second. The output current from the electron multipliers is then converted to an ion concentration using conversion constants determined by in-flight calibration using the electron density obtained from the topside sounder also located on the ISIS satellite.

The ion concentration is given in number of ions per cubic centimeter of the five dominant ions found at 1400 km, each plotted as a function of time in 20-minute segments. Each data point has been obtained by curve fitting the spacecraft spin-modulated cartwheel data and determining the maxima and time of maxima of the fitted curve. Thus the absence of data for a given ion may indicate that a good curve fit was not possible; this generally occurs at concentrations less than 10 ions/cm^3.

Venkatarangan, P., J. R. Burrows, and I. B. McDiarmid, On the angular distributions of electrons in 'inverted V' substructures, J. Geophys. Res. 80, 66-72, Jan. 1975.

Hoffman, J. H., W. H. Dodson, C. R. Lippincott, and H. D. Hammack, Initial ion composition results from the ISIS 2 satellite, J. Geophys. Res. 79, 4246, 1974.

RETARDING POTENTIAL ANALYZER (RPA)

The retarding potential analyzer (Kayser et al, 1978) is a planar multigrid instrument designed to measure ionospheric density and temperature parameters over the range 10 to 10^6 ions/cm^3 and 500-10,000°K, respectively. This is accomplished by performing an electrostatic retardation of the ions flowing into the instrument at the spacecraft velocity when the instrument is oriented in the nearly forward direction. The instrument is mounted in the equatorial plane of the spacecraft, with the sensor normal directed radially outward. Thus the viewing angle scans a variety of directions as the spacecraft rotates at the nominal 3-rpm spin rate. In the cartwheel mode, in which the spacecraft spin axis is perpendicular to the orbit plane, the sensor scans the full angle range 0° to 360° between the sensor normal and the velocity vector every (nominally) 20 seconds. In the orbit aligned mode, in which the spacecraft spin axis is in the orbit plane, the sensor cannot scan the forward direction at all latitudes. In particular, at high latitudes, the sensor normal is almost perpendicular to the velocity vector, thus precluding data collection when the optical instruments are obtaining "spin scan" images. Thus only the cartwheel data sets contain results from the RPA.

Plasma analysis is performed by applying programmed voltages to the various grids within the ion trap and measuring the current transmitted to the collector as a function of the applied potentials (Moss and Hyman, 1968). The resulting current voltage (I-V) response is fitted to a predicted response to provide the estimates of the ambient parameters. Results presented in this data book are based on the assumptions that the ions present in significant concentrations (>1 percent of the total) may be H^+, He^+, and O^+, all assumed to be at a common temperature T. Useful data are obtained only when the sensor normal is within 35° of the spacecraft velocity vector. The combination of the 3-second instrument program cycle and the 20-second spacecraft spin period yields a limit of 1 or 2 plasma analyses per 20-second interval. This nominal rate of 3 per minute may not be attained for several reasons. (1) Operation of the sounder transmitter sometimes perturbs the local plasma, yielding non-geophysical results. (2) Photoemission effects within the instrument sometimes preclude analysis of the I-V curve when the Sun is within the field of view of the instrument. This is most significant in regions of low plasma density. (3) Highly structured plasma often cannot be analyzed if the local plasma variations are fast on the 1-second time scale on the instrument. This is usually the reason for the apparent data gaps in the auroral zone. (4) Extreme spacecraft potentials are sometimes encountered, exceeding the range of the applied sweep voltages. For all of these cases, appropriate tests are used to delete, or correct, data points before analysis and to select results based on the quality of their fit to the theoretical I-V curve.

Kayser, S. E., E. J. Maier, and L. H. Brace, Quiet time plasma irregularities at 1400 km in the cleft region, J. Geophys. Res. 83, 2533, 1978.

Moss, S. J., and E. Hyman, Minimum variance technique for the analysis of ionospheric data acquired in satellite retarding potential analyzer experiments, J. Geophys. Res. 73, 4315, 1968.

SOFT PARTICLE SPECTROMETER (SPS)

The ISIS 2 Soft Particle Spectrometers measure the fluxes and energy spectra of electrons and positive ions over the energy range from 5 eV to approximately 15 keV.

There are two independent electrostatic analyzers (SPS's) on the ISIS 2 satellite, each of which is capable of measuring electrons and/or positive ions in either an energy step dwell mode or a spectral sweep mode. Each of the spectrometers, referred to as "top beam" and "bottom beam," are mounted looking in identical directions perpendicular to the satellite spin axis. The top detector is normally operated in an electron sweep mode and as such has a geometric factor of 4.95×10^{-4} cm^2 ster and an energy bandpass ($\Delta E/E$) of 24.7 percent with center energies from 13.15 keV to 5.5 eV in 38 levels. The bottom detector is normally operated in a positive ion sweep mode and in this mode has a geometric factor of 1.27×10^{-3} cm^2 ster and an energy bandpass ($\Delta E/E$) of 35.5 percent with center energies from 14.675 keV to 5.0 eV in 39 levels. Both spectrometers have rectangular fields of view with a full width of 5 degrees by 25 degrees for the top beam (electron mode) and 10 degrees by 25 degrees for the top beam (ion mode) and the bottom beam in both electron and ion modes. In both cases the long dimension of the field of view is parallel to the spin axis and the short dimension is in the equatorial plane. A similar instrument flown on ISIS 1 is described by Heikkila et al (1970).

VERY LOW FREQUENCY RECEIVER (VLF)

The center of the VLF instrument is a broadband receiver covering the frequency range from 50 Hz to 30 kHz (Franklin et al, 1960). A receiving antenna connects to the receiver through a protective low pass filter. Normally, the antenna is the 73.2-m dipole shared with the topside sounder. Also, the receiver input can be connected instead to the spacecraft torquing coils used for attitude adjustment; however, the torquing coils have not produced meaningful data. VLF emissions are observed over a wide amplitude range and consequently the receiver has been designed with a dynamic range of 68 dB, most of which is achieved by use of automatic gain control (AGC).

Output from the receiver directly modulates an FM telemetry transmitter and has a dynamic range of 3 dB above the AGC threshold. The AGC is sampled 60 times per second and telemetered to ground via the PCM data channel. The receiver threshold is 20 μV across an input impedance of 16 kΩ.

On ISIS 2 the VLF experiment also includes an exciter connected to the short (18.7 m) sounder dipole. It sweeps logarithmically from 15 to 0.05 kHz

Heikkila, W. J., J. B. Smith, J. Tarstrup, and J. D. Winningham, The soft particle spectrometer in the ISIS 1 satellite, Rev. Sci. Instr. 41, 1393, 1970.

Franklin, C. A., T. Nishizaki, and W. E. Mather, A wideband VLF Receiver for the Alouette II and ISIS-A satellites, DRTE Technical Memorandum 522, Department of National Defence, Ottawa, Canada, May 1960.

once every 5 or 10 seconds. In addition, the short-dipole impedance can be measured by recording the amplitude and phase of the current drawn by the dipole in response to the VLF exciter. These data are telemetered via the PCM system.

TRIAXIAL FLUXGATE MAGNETOMETER

The orthogonal set of magnetometers (McDiarmid et al, 1978) is mounted in the body of the spacecraft with one component oriented along the spin axis (designated the z-magnetometer) and the other two in the plane perpendicular to the spin axis (designated x-y plane). The x-and z-magnetometers each have two ranges, ± 60,000 nT (± 600 milligauss) and ± 20,000 nT. The former range has digitization steps of 480 nT while the latter has 160 nT. The y-magnetometer has only the ± 60,000 nT range. All components are sampled at the rate of 1 sample/sec. There is no in-flight calibration capability. There is an induced field due to the surrounding spacecraft mass and wiring harness which is of the order of 1 percent of the external field. This field and some other periodic sources of interference from spacecraft equipment are removed in the data processing.

In this data book, only data from the axial (z) component are presented since its processing is more straightforward than for the spinning components. Only data sets in which the spin axis is nearly perpendicular to the orbit plane (i.e., cartwheel) have magnetometer measurements included, since it is desirable to use the higher sensitivity (± 20,000 nT) range. In cartwheel, the axial component is aligned approximately in the East-West direction when crossing the auroral ovals.

V. DATA FORMAT DESCRIPTIONS

The data most appropriate, and available, for a particular study are presented in formats selected from the following list. A format may contain data from a single instrument or from several instruments. A description of the information provided by each instrument is provided in this section. The following table specifies what instrument and quantities are plotted in each format. Unless otherwise specified all quantities plotted are profiles along the spacecraft track.

McDiarmid, I. B., J. R. Burrows, and M. D. Wilson, Comparison of magnetic field perturbation at high latitudes with charged particle and IMF measurements, J. Geophys. Res. 83, 681, 1978.

Format Number	Instrument	Quantity Plotted
1	Auroral Scanning Photometer	5577Å, 3914Å intensity
	Red Line Photometer	6300Å intensity
	Soft Particle Spectrometer	Electron energy flux
2	Topside Sounder	Electron density contours at different altitudes
	Magnetometer	Magnetic field deviation
3	Energetic Particle Detector	Electron and proton flux/energy
4	Cylindrical Electrostatic Probe	Electron density and temperature
	Ion Mass Spectrometer	Concentration of H^+, He^+, O^{++}, N^+, O^+
5	Retarding Potential Analyzer	Concentration of H^+, O^+, He^+ and ion temperature
6	Soft Particle Spectrometer	Electron and positive ion spectrograms
7	Auroral Scanning Photometer	Grey-scale two dimension co-ordinate transform of 5577Å, 3914Å intensities and the 5577Å/3914Å ratio
8	Red Line Photometer	Contour plot of 6300Å intensity
9	Auroral Scanning Photometer	5577Å E and F region latitude profiles
	Red Line Photometer	6300Å latitude profile
10	Cylindrical Electrostatic Probe	Electron density and temperature
	Topside Sounder	Electron density contours at different altitudes
11	VLF	VLF spectra
12	Auroral Scanning Photometer	Height profiles of 5577Å slant intensity

FORMAT 1 (ASP, RLP and SPS)

The sample of Format 1 shown in Figure 6 has been retouched for clarity, but it corresponds to the direct computer plot reproduced in the ISIS 2 data book. This format contains a combination of Soft Particle Spectrometer (SPS) electron data and optical data from the Auroral Scanning Photometer (ASP) and Red Line Photometer (RLP). A minimum-time-delay algorithm is used, in which the time delay between the satellite crossing of a particular field line and the optical viewing of the emission from the foot of the field line is minimized. This delay can be kept to within one-half of a spin period, by selecting optical data from the most appropriate spin for a given latitude range, and splicing it together to form a continuous sequence. For this data set the satellite has its spin axis perpendicular to the orbit plane and the optical scans are repeatedly along the spacecraft track. Thus, there is adequate redundancy for the above procedure.

The electron data and optical data are then plotted as a function of Universal Time, corresponding to the time of the spacecraft motion (the time of the SPS measurement), which will be somewhat different from the optical viewing time as described above. The start time is shown at the lower left and minute values are given on the horizontal axis. The atomic oxygen 6300Å emission intensity from the RLP and the atomic oxygen 5577Å and N_2^+ 3914Å emission intensities from the ASP are plotted in kR on a logarithmic scale at the bottom. These intensities have not been corrected for airglow background or albedo. The SPS electron energy fluxes have been integrated over four energy bands as shown on Figure 6: 5 -60 eV, 60 -300 eV, .3 -1. keV, 1 -15 keV and plotted on vertically separated scales, with the ordinate labeled in units of the logarithm of the energy flux in erg cm^{-2} sr^{-1} sec^{-1}.

The modulation that appears on these fluxes results from the rotation of the spacecraft. The detectors look outward in the equatorial planes, sweeping through a pitch angle coverage shown by the sawtooth at the top of the plot. A downward sawtooth corresponds to downward-going particles.

At the top of Figure 6 the following geophysical quantities are indicated along the horizontal axis: INVL - invariant latitude, INVT - invariant time, SDEP - local solar depression angle at the location of the viewed emission, CDEP - solar depression angle at the magnetic conjugate point to the viewed emission.

The 5577Å and 3914Å data plotted are derived from the slow-speed PCM data link, the same as used for the 6300Å data, but not the same as the high speed data link employed for the high-resolution ASP photos. To achieve this reduced data rate the intensity across a 13-element scan is averaged into essentially a single value by filtering. Because of this, the PCM data should be used with caution when accurate intensities are desired. Optical observations from satellites (and rockets) include in addition to the real emission intensity, a variable contribution from ground scattering. In principle this contamination can be quantitatively removed using the method of Hays and Anger (1978) assuming

Hays, P. B. and C. D. Anger, Influence of ground scattering on satellite auroral observations, Appl. Opt. 17, 1898-1904, June, 1978.

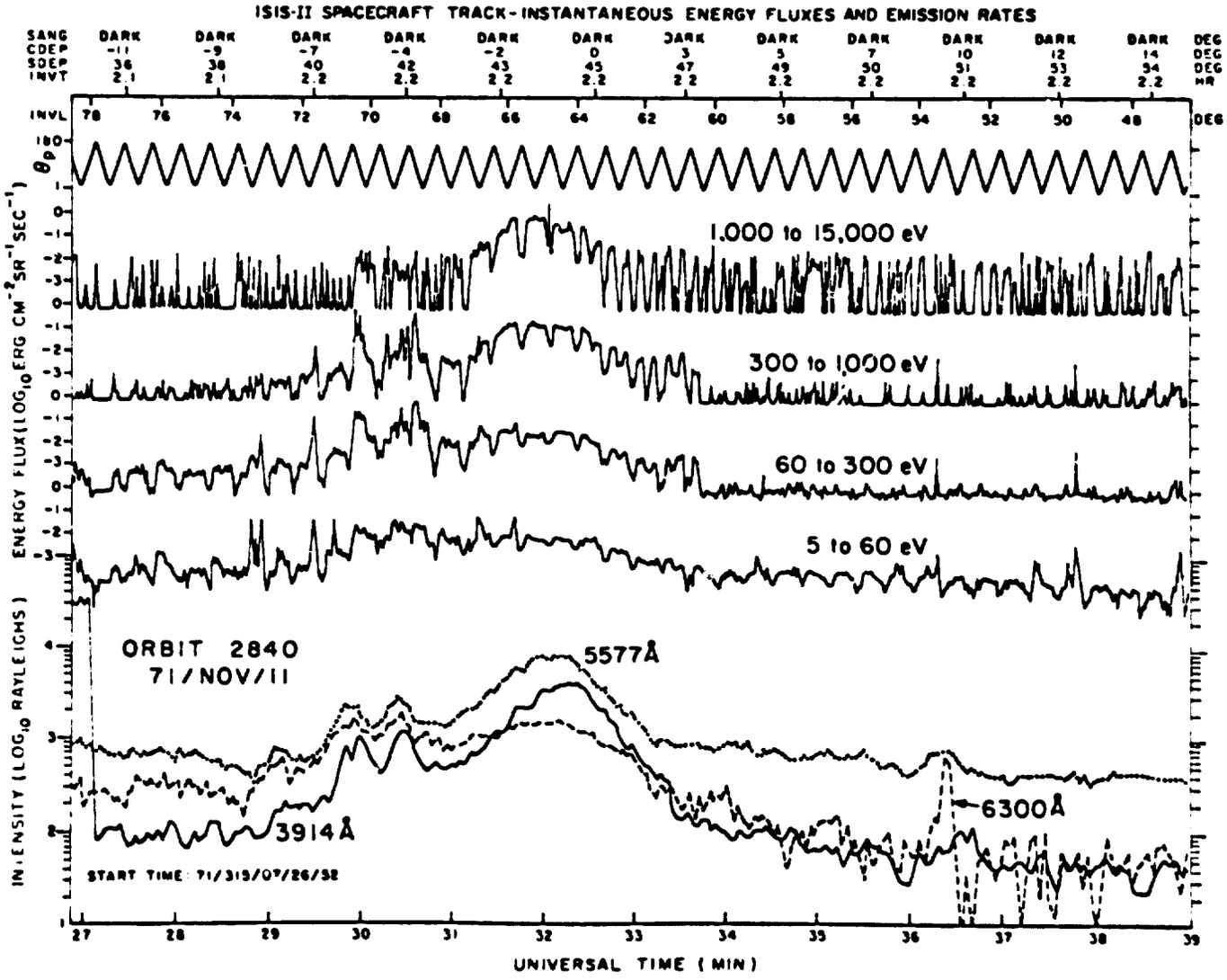

Figure 6. Example of Format 1 (Optical data and SPS).

the altitude of the emission and the spectral albedo of the surface are known. Practical experience has shown that the factor by which to divide an observed intensity (5577Å or 3914Å) varies from 2 for a large-scale, reasonably uniform region to 1 (i.e., no correction) for thin discrete arcs (Murphree et al, 1978). This correction factor is not as serious for the 6300Å emission because of its higher altitude and consequently lower susceptibility to contamination.

FORMAT 2, TOP (MAGNETOMETER)

The axial magnetometer plot is Format 2, combined on the same page with the sounder isodensity height profile plot. They have a common abscissa labeled in minutes of Universal Time. The orbit number and Universal Time at the beginning of the plot appear at the bottom. The ordinate is in units of nanoteslas (nT). The quantity plotted is the residual deviation of the filtered axial component from the GSFC 06/74* model field computed in the direction of the inferred spacecraft spin axis orientation. The residual baseline is offset from zero by an amount of the order of 400 to 1000 nT, in different orbits, depending on field contributions from electrical subsystems in the spacecraft. The offset from these sources remains unchanged for the duration of any plot. The data are low pass filtered with a 9-point filter and plotted at 1 point/sec. The principal source of noise is the digitization step size. After filtering, the typical RMS noise from this source is ~40 nT. Where deviations exceed the statistical fluctuations, negative-trending deviations correspond to Birkeland currents flowing into the ionosphere and positive-trending deviations correspond to Birkeland currents flowing out of the ionosphere.

FORMAT 2, BOTTOM (SOUNDER)

For each chosen value of electron density, the altitude at which that density was observed to occur is plotted as a function of UT. The values chosen for these plots are powers p of 10 such that 4p is integral, e.g., p= 3.0, 3.25, 3.5, 3.75, 4.0, etc. Units are cm^{-3}. Data points are indicated by * symbols on the contours for integral powers of 10, and by + symbols on the others. All the symbols in a vertical line represent the density information obtained from one ionogram.

The broken line at the top of the plot represents the position of the spacecraft (for ISIS 2 this line is straight and horizontal). The broken line at the bottom represents the lowest altitude from which density information was obtained. In favorable cases, this will be close to the peak of the F layer, but it can be any distance above the peak.

The altitudes are obtained under the assumption that the radio propagation from the topside sounder was vertical. At high latitudes, the propagation is more likely to be along the magnetic field. When this occurs, the altitudes shown are too low. At very high latitudes, the difference is small, but close to 60° magnetic latitude, it can amount to 50 km.

Murphree, J. S., I. W. H. Robertson, C. D. Anger, and L. L. Cogger, Rocket observations of auroral albedo over snow, Appl. Opt. 17, 1849-1850, June 1978.

*Cain, J. C., private communication, 1974.

The usual sampling rate for the topside sounder is about 4 per minute. On many passes, two consecutive samples are taken, then two missed. This mode was chosen on most cartwheel passes to provide the ion probes with interference-free intervals. Where data points are missing at irregular intervals, it is because some ionogram traces were too weak or too irregular to be scaled properly.

FORMAT 3 (EPD)

With two exceptions, the traces represent electron fluxes as a function of time. Those labeled D are differential channels while those labeled I are integral channels. The number in parentheses indicates the detected energy (keV) for the differential channels or the threshold energy for the integral detectors. Units are designated by R for 'counts per second' and I for 'electrons cm^{-2} sec^{-1} $ster^{-1}$ keV^{-1}'.

All of the above vertical scales are logarithmic.

The bottom trace, $\bar{E}$, indicates the average energy (keV) computed from the complete electrostatic analyzer energy range (0.15 to 9.6 keV); it does not include the integral detectors. The vertical scale is linear.

The top trace, I(22)/I(40), shows the ratio of geiger counter flux (electrons E > 22 keV and protons E > 240 keV) to the solid state detector flux (electrons E > 40 keV and protons E > 150 keV). Since the electron fluxes are normally greater than the positive ion fluxes, the ratio normally exceeds unity. However, when the proton flux between 150 and 240 keV predominates, the ratio is less than unity.

Shown across the bottom of each plot are the Universal Time (minutes), Invariant Latitude (degrees), magnetic local time (hours), B - the intensity of the magnetic field measured at the spacecraft (gauss), and Theta z - the angle between the spacecraft spin axis and the local magnetic field vector (degrees). Theta z (θ_z) is defined to be zero in both hemispheres for downward-coming field-aligned particles.

Detector $I_{\parallel}(40)$ thus looks at θ_z to the local magnetic field while all other detectors execute pitch angle scans from $90°-\theta_z$ to $90°+\theta_z$. Consequently, fluxes are often modulated at twice the spin frequency for anisotropic fluxes or at the spin frequency in regions of isotropic precipitation. The nominal spacecraft spin frequency is 3 rpm.

The integral channels record a small component of background counts due to penetrating electron flux (e.g., outer zone electrons near invariant latitude of 60°) or due to penetrating proton flux in the inner zone and during solar flare events, over the polar cap. At other places, the penetrating background counts are negligible relative to the directional flux entering the collimator.

FORMAT 4, TOP (CEP)

CEP measurements of electron density, N_e, and temperature, T_e, are plotted independently. T_e is plotted either as a point or a question mark (?) depending upon the quality of fit of the exponential portion of the volt-ampere characteristic, as described in the CEP instrument description. T_e measurements

of highest reliability are plotted as points, and those of lower reliability are plotted with question marks. If the plasma is highly structured or too low in density, no T_e measurement will be made.

The values of N_e are plotted as solid points. The points come in groups of five during alternate 30-second intervals as discussed in the instrument description.

Universal Time is given at 2-minute intervals and is represented by vertical lines at 1-minute intervals.

FORMAT 4, BOTTOM (IMS)

The date and time of the start of the frame are given in the upper left hand corner. The date is given in day, month, year, and Julian day in brackets. The time is given in hours, minutes, seconds, and second of day. The orbit number is given in the upper right hand corner and is the orbit number of the start of the data frame. The orbit is incremented on the north-bound crossing of the geographic equator. The orbital data at the bottom of the plot has been interpolated to an even 2-minute point on the plot. The description and units of the orbital data are given below:

	Description	Units
UT	Universal Time	HH:MM
LAST	Local apparent solar time	HH:MM
MLT	Magnetic local time	HH:MM
DLAT	Dip latitude	Degrees
INVL	Invariant latitude	Degrees
GLAT	Geodetic latitude	Degrees
GLNG	Geodetic longitude	Degrees
SZEN	Solar Zenith Ang.	Degrees
ALT	Height above the geoid	Kilometers

The ion species are identified as follows:

Symbol	Species	Mass	Units
H	H^+	1	cm^{-3}
+	He^+	4	cm^{-3}
Δ	O^{++}	8	cm^{-3}
N	N^+	14	cm^{-3}
O	O^+	16	cm^{-3}

FORMAT 5 (RPA)

Geophysical parameters deduced from the RPA as described in the instrument section are plotted on two graphs using the standard 20-min. abscissa. The lower frame shows the H^+ (symbol H) and O^+ (symbol O) densities plotted against a logarithmic ordinate scale. The density grid shown is usually over the range 10 to 10^5 cm^{-3}, but occasionally is truncated if there are no data to allow more space for an extended scale on the second plot. The upper frame shows the ion temperature on a linear scale (symbol T) and the He^+ density (symbol 4) on a logarithmic scale. The temperature scale is usually 0° to 5000°K, but occasionally may be truncated at the lower limit (if no data are present) to permit extension of the upper limit. The scale factor in the plot (degrees/cm) is constant, regardless of scale truncation.

Universal Time is used for the standard 20-min. long linear abscissa, with a vertical line every 2 minutes. Additional abscissa values are shown to identify the local time, magnetic local time, dip latitude, invariant latitude, geodetic latitude, geodetic longitude, solar zenith angle, and altitude of the spacecraft as defined under Format 4, IMS.

FORMAT 6 (SPS)

Data from these instruments are displayed as energy versus time grey-shaded spectrograms where the plotted grey-scale intensity is proportional to the log of the instrument count rate at each energy level. Due to the operational characteristics of the instrument, the count rate at a particular energy, and thus the grey-scale intensity, is an indicator of the directional energy flux per unit energy at the measured energy. In the mode of operation for data presented here, one complete electron spectrum and one complete positive ion spectrum are obtained each second.

The upper and center panels of the plot contain the electron and positive ion spectrograms, respectively. The vertical scales are logarithmic in energy from 1 eV to over 10^4 eV. The lower panel contains pitch angle information and average energies. The pitch angle denotes the instrument look direction such that 0° refers to downward-moving particles, 90° to locally mirroring particles, and 180° refers to particles coming from below the spacecraft. Note that the

range of pitch angles sampled by the detectors, which look radial to the spacecraft spin axis, depends upon the angle between the spacecraft spin axis and the local magnetic field. This angle is denoted by θ_z and appears along the upper edge of the electron spectrogram. For θ_z=90° the spin axis is perpendicular to the magnetic field, and all pitch angles from 0° to 180° are sampled each half spin period. The average energies in the lower panel are computed once each second for electrons and for positive ions and represent the average energy per particle over the range 5 eV to approximately 15 keV. The horizontal axis is time ordered with the beginning Universal Time printed at the lower left hand corner. Each succeeding minute of Universal Time is indicated along each horizontal axis. Geographic latitude, geographic longitude, and local time are given at the bottom of the plots for the first and last data points. The quantities called "ECAL" are calibration indicators for internal use. The spacecraft location in Magnetic Local Time and Invariant Latitude at 1-minute intervals appears along the top horizontal axis. Orbit number and satellite altitude also are shown above the plots.

FORMAT 7 (ASP)

Because of the large dynamic range of the Auroral Scanning Photometer (ASP), it is necessary to use a grey-scale representation and a sequence of varying upper and lower intensity limits to display the data. An example of the plotted data is shown in Figure 7. The data are plotted on an electrostatic dot matrix plotter and arranged in three independent rows with the leftmost picture in each row containing the coordinate system. There is, in addition, header information at the top of the page giving basic information about the pass and how the data were transformed. In all cases, the coordinates are corrected geomagnetic latitude (CGL) (Hakura, 1965) and time (see Murphree and Anger, 1980, for a description of the transform procedure). This magnetic coordinate system is denoted by the "M" in the lower left-hand corner of each coordinate picture. The accompanying "V" indicates that the intensity data have been corrected for look direction, i.e., van Rhijn effect. However, the data are not corrected for ground scattering and thus real intensity levels will be less depending on the spectral albedo of the surface under the auroral emissions. Latitudes are labeled in general every 10° and the Magnetic Local Time (MLT) every 6 hours. The geomagnetic pole is represented by a " + ".

The spacecraft track projected down to 100 km along magnetic field lines is given by the sequence of triangles, the approximate orbital motion being defined as the direction of the apex of the triangle. The triangles represent the position of the spacecraft exactly on the minute, the particular minute being derivable from the sequence of triangle shapes as follows. The basic shape

Hakura, Y., Tables and maps of geomagnetic coordinates corrected by the higher order spherical harmonic terms, Rep. Ionosph. Space Res., Japan, 19, 121, 1965.

Murphree, J. S., and C. D. Anger, An observation of the instantaneous optical auroral distribution, Can. J. Phys., 58, No. 2, 214-223, Feb. 1980.

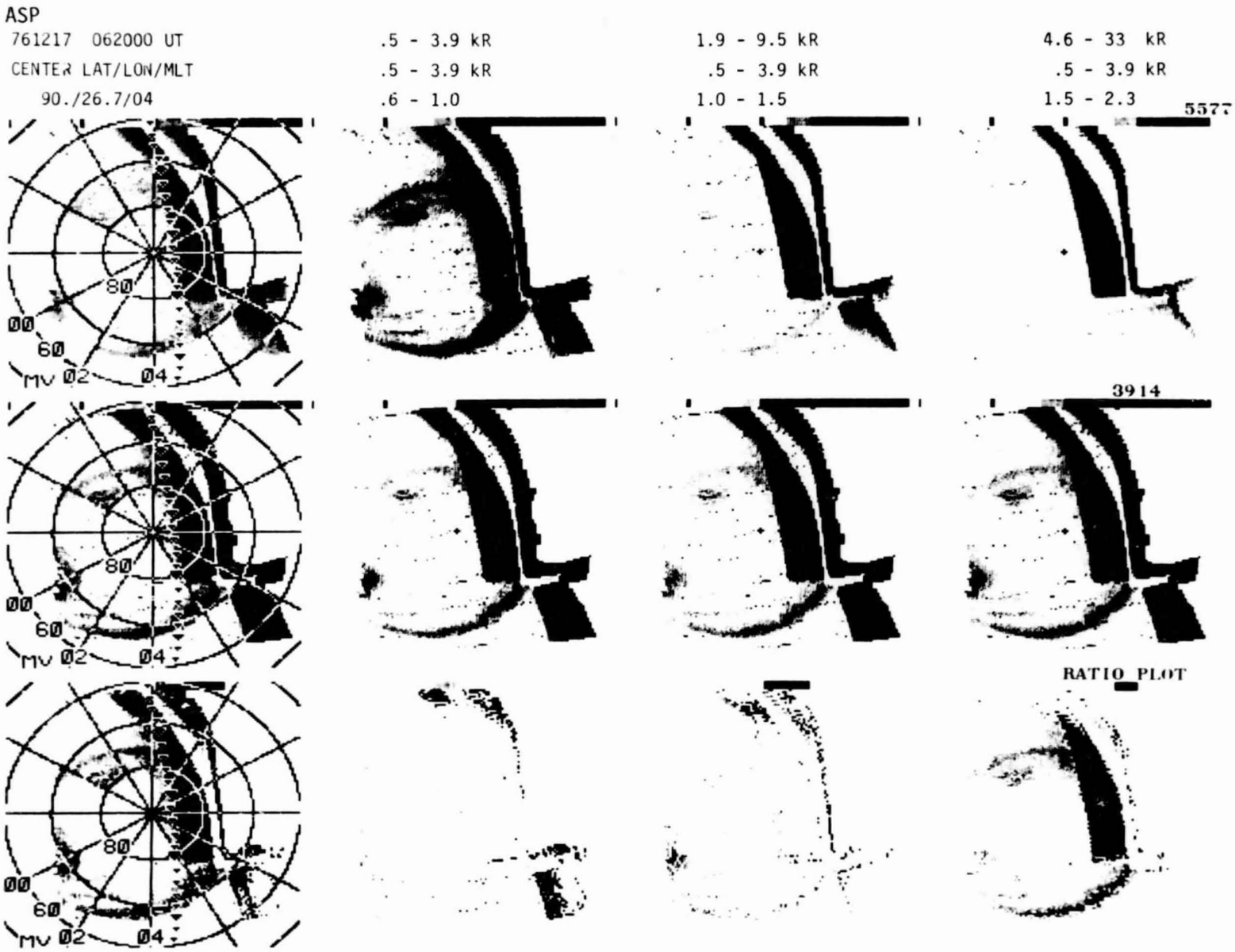

Figure 7. Example of Format 7 (ASP).

consists of filled (or a blank, depending on the surrounding background) blocks denoted below by "x":

```
  x
 xxx - represents any minute not specified in the following


  x
 xxx - one of the following:  5, 15, 25, 35, 45, 55 UT minute
xxxxx


  x
 xxx  - UT minute 10 or 50
xxxxx
  x



  x
 xxx
xxxxx  - UT minute 20 or 40
 xxx


  x
 xxx  - UT minute 0 or 30
xxxxx
xxxxx
```

The actual time values can be obtained by noting the start time in the header and identifying the first time symbol in the coordinate picture.

The start and/or end of a pass may or may not be apparent in the given transform, depending on the range (in degrees) to which it was desired to transform the data, but the spacecraft track indication will continue to the end of the coordinate system. If start or end does occur within the range of the transform, the data will be truncated in a straight line. In contrast to this, the limit of optical observations at 90° to the spacecraft track (its limbs) will form a pair of irregular lines parallel to and equidistant from the spacecraft track.

The data appearing in each picture in each row are a grey-scale representation of the intensity for the appropriate wavelength. Each picture element is represented by a 3 x 3 square matrix of dots and anywhere from 0 (at or below the bottom of the desired intensity range) to 9 (at or above the top of the range) of the dots are blackened so as to provide a grey scale. For example, if the picture is labeled .6 - .95 (the numbers representing kR for intensities and ratio values for ratio plots), then any points with intensities less than or equal to .6 kR will be white while any elements greater than or equal to .95 kR will be black. The three rows of pictures represent 5577Å intensity, 3914Å intensity and the ratio I(5577Å)/I(3914Å), respectively. In general, the 5577Å data are displayed in the three rightmost pictures of the

first row with three different intensity ranges (in kR), e.g., .5 - 3.9, 1.9 - 9.5, 4.6 - 33, while 3914Å uses a single range for all three pictures, this range being the same as that for the lowest 5577Å range. The picture onto which the coordinate system is overlayed has a range equal to the entire range of intensities covered by all of the pictures in the row. For example, in the above 5577Å ranges, the coordinate picture would contain .5 - 33 as the kR range.

In the pass shown in Figure 7, the 5577Å and 3914Å data illustrate the northern hemisphere polar cap on 761217 at 0620 UT. The satellite track is basically from 16 MLT to 5 MLT as the data show well-defined auroral emissions in the evening (16 - 21 MLT) and morning (00 - 07 MLT) sectors. The midnight sector of the auroral emissions was beyond the limb on this pass as indicated by the irregular boundary of the data in that MLT sector. The dayside is contaminated by scattered sunlight as is illustrated by the high intensity, regular feature in both wavelengths. This is a common feature because of the difficulty in combining the correct satellite altitude with both time of year and UT to optimize dayside viewing conditions. Such features are usually easily distinguished from auroral emissions because they are aligned with the spacecraft track rather than with the magnetic coordinate system.

Because of contrast problems, it is necessary to approach the ratio in a different manner. Each of the three pictures in the ratio plot row represents different ratio ranges which are always chosen to be: 0.6 - 1.0, 1.0 - 1.5, 1.5 - 2.3. The ratio for each element (i.e., position in the coordinate system) in each picture is calculated. If it falls within the specified range as given above, then the 3914Å intensity at the point is plotted based upon the 3914Å intensity thresholds in the same column of the previous row (this is why all 3914Å thresholds are identical). The result is three pictures which show where 3914Å emissions are observed (and their intensity) for the three ratio ranges. The composite (i.e., the leftmost picture with the superimposed coordinate grid) then should be similar to the composite 3914Å given in the previous row. Any missing points in the composite picture will correspond to ratio values outside the range 0.6 - 2.3.

FORMAT 8 (RLP)

In this format the isointensity contours of atomic oxygen 6300Å emission are shown, obtained with the Red Line Photometer (RLP) and plotted in a polar invariant projection. The perimeter corresponds to 50° invariant, and dashed circles indicate 60°, 70°, and 80° invariant. Invariant noon is at the top and morning (06 h) on the right. The intensities corresponding to the contours selected are listed on the upper right, and the contours themselves are labeled in units of tens of rayleighs (25 = 250R). The orbit number, date, day number, and Universal Time for the first and last spins of the pass are given on the upper left. The hatched line shows the track of the spacecraft traced down to the 250 km level, the height assumed for the altitude of emission; each hatch mark indicates one rotation (spin) of the spacecraft, and every tenth spin is labeled. The spin axis is nearly parallel to the orbit plane. The Universal Times that correspond to each spin number are given on the far right-hand side.

The intensities given are not corrected for albedo and so over regions of widespread emission they may be too large by a factor of two. If the label at the top reads "6300 angstrom intensity" then a correction for white light background has been applied. If it reads "10 angstrom bandpass intensity" then

there has been difficulty with white light subtraction in part of the picture and the 10Å channel data are shown uncorrected. The intensities shown for these cases will be less accurate than for the others.

The example shown in Figure 8 illustrates some aspects of the data and some of the peculiarities. The features discussed below correspond to contours that have been labeled, A → G.

A. These contours arise from sunlight scattered from the Earth. They can be recognized by their proximity to noon and by their steep gradient.

B. These linear contours are caused by scattering in the RLP baffle system, and the steep gradient is caused by one critical baffle element. When the solar illumination leaves this element the baffle scattering falls rapidly and the auroral contours become visible.

C. These linear contours, having a steep gradient, are generated by the passage of the spacecraft from sunlight into darkness, with the cessation of baffle scattering. These contours are perpendicular to the spacecraft track, and the rectangular pattern of B/C normally can be recognized readily.

D. Dayside auroral contours. The morning extension of the dayside auroral contours are evident here, extending from the region of baffle scattering. When baffle scattering is not present this pattern is normally roughly symmetric about noon.

E. Night auroral contours. These contours define the region of brighter nightside aurora.

F. Equatorward auroral boundary. These contours define the equatorward boundary of 6300Å aurora. The termination after midnight is caused by the scans reaching the "edge" of the Earth; i.e., the limb.

G. Poleward auroral boundary. These contours define the poleward auroral boundary and normally form a near-circular region in the polar cap.

FORMAT 9 (ASP AND RLP)

This format provides latitude profiles of airglow emission rate at 5577Å and 6300Å obtained from the ASP and RLP. In the cartwheel mode of operation, the fields of view of the photometer sweep along the path of the orbit to provide data over a large range of latitudes but a very small range of longitudes. Pole-to-pole coverage can be achieved in a time interval of about 30 minutes.

The latitude profiles are based on airglow limb data which result in a measurement at the leading and trailing limb for each limb. This ensures that the data are free from cloud and ground albedo effects and contamination by other sources of light. It also permits the separation of the 5577Å airglow into the E- and F-region components (see Format 12), both of which are plotted. The maximum of the E region airglow is defined to occur at 95 km for the 5577Å data and the F region is then referenced to that level. The emission rates given correspond to what would be observed in the zenith from below at the location of the airglow limbs. The plots therefore represent the vertical

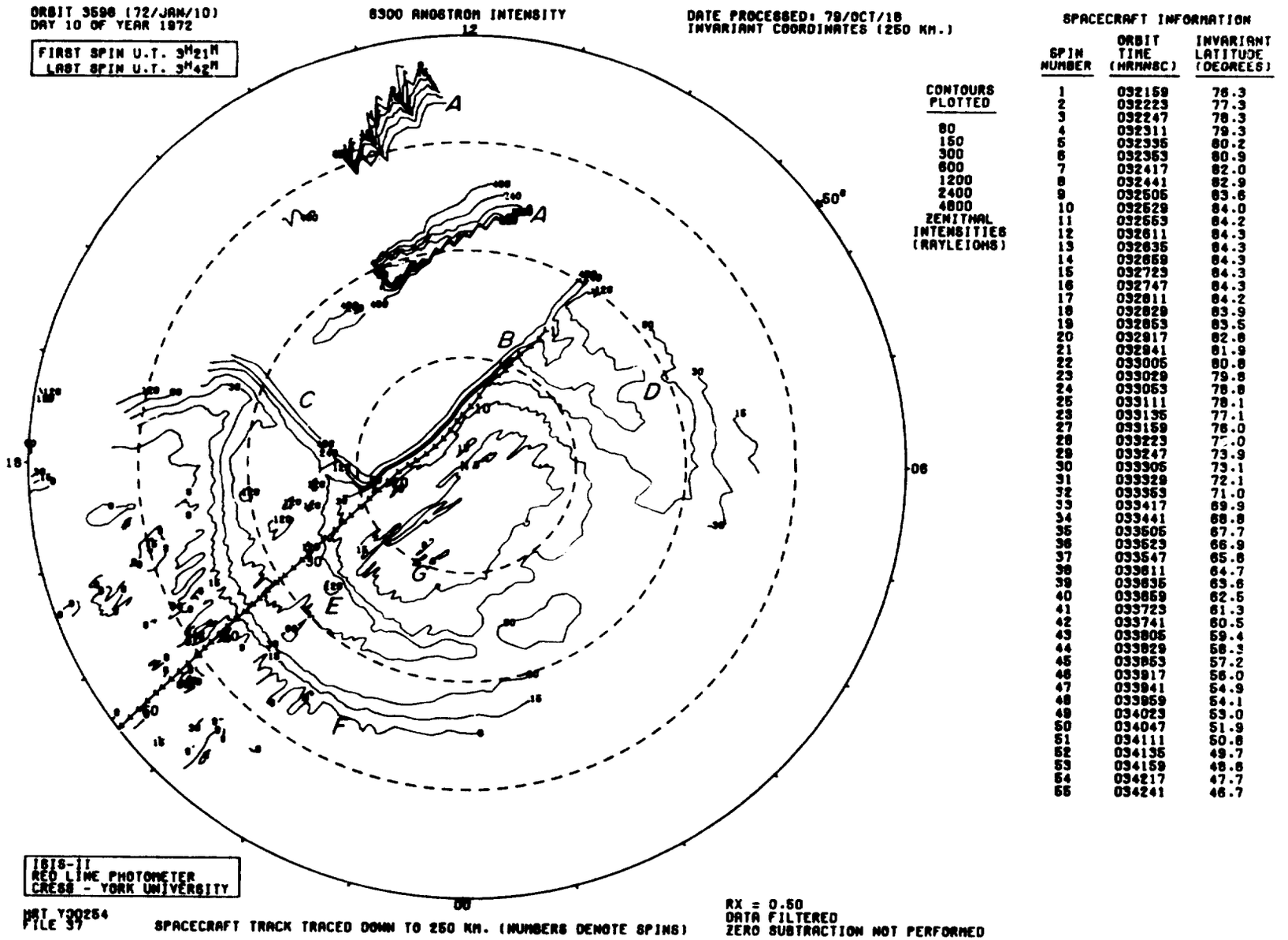

Figure 8. Example of Format 8 (RLP) with the events A through G.

emission rate in rayleighs as a function of geographic latitude. The points are not independent due to the fact that the optical viewing path in the atmosphere is longer than the spatial sample interval which is determined by the orbital speed of the satellite. As a consequence the plots correspond to a running mean of the emission rate.

In practice, the latitude range is restricted to low and mid-latitudes due to the presence of aurora at higher latitudes. The difference between leading and trailing limb values when they overlap in the plot is due either to the small difference in longitude or to temporal variation in the airglow.

FORMAT 10, TOP (CEP)

See Format 4 (Top) description. The latitude, longitude, local time, dip angle, dip latitude, L value, invariant latitude, and solar zenith angle are given below the graphs.

FORMAT 10, BOTTOM (SOUNDER)

See Format 2 (Bottom) description.

FORMAT 11 (VLF)

VLF data published herewith are presented in the conventional amplitude-frequency-time display wherein signal corresponds to the dark parts of the display. These data are from routine 35-mm records having the frequency axis across the film and the time along the film. This data book has room only for interesting excerpts of the receiver film record. In data set C of Volume 4 the VLF film has been printed at 2X magnification to illustrate the details of a variety of typical phenomena observed by ISIS 2. In the other data sets, film is printed at 1X magnification. The VLF receiver was off during the majority of the passes. Excerpts of the VLF record for receiver-on passes have been chosen to show the highlights of those passes. In many cases, the VLF exciter was on and its periodic frequency downsweeps can be seen.

The example of the data format given in Figure 9 shows the frequency axis running linearly from 0 to 21 kHz, and the Universal Time axis running linearly from 06:41:10 to 06:41:39 (hours:minutes:seconds). Both the frequency and time limits are to be associated with the extremes of the film. In the example given, the broad diffuse patches are a natural emission, VLF hiss. The record also contains four instances of the received exciter signal. Two of these are on the fast duty cycle, at 06:41:15 and 06:41:21, and two on the slow cycle, at 06:41:23 and 06:41:34.

FORMAT 12 (ASP)

This format provides examples of the 5577Å airglow limb profiles obtained during a pass. The selection was made to demonstrate the variation of the two components of the airglow. The vertical axis gives the tangential height. In all cases the reference height of 95 km has been arbitrarily assigned to the maximum of the E- region airglow response. The slant intensity in kilorayleighs (kR) is plotted along the horizontal axis. The profiles, obviously broadened by the finite field of view of the instrument, do not give information about the detailed vertical distribution; they merely demonstrate the resolution of the main components.

71/299/0639

Excerpts of VLF Spectral film for the period 0641 - 0642

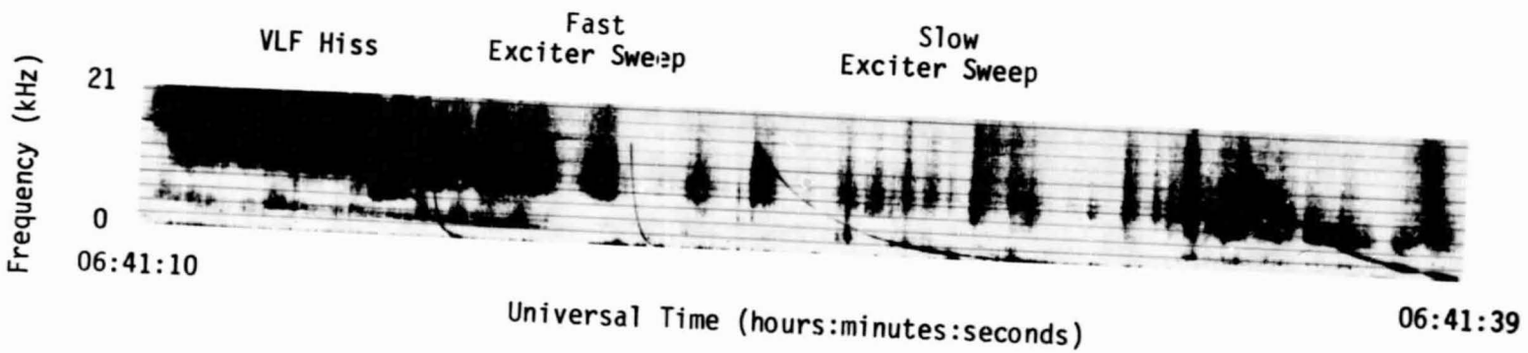

Figure 9. Example of Format 11 (VLF).

VI. GEOPHYSICAL DATA SET: HIGH-LATITUDE CHARGED PARTICLE, MAGNETIC FIELD, AND IONOSPHERIC PLASMA OBSERVATIONS DURING NORTHERN SUMMER

DATA SET DESCRIPTION

This data set consists of charged particle, magnetic field, and ionospheric plasma (remote and in situ) observations from ISIS 2 obtained at high magnetic latitudes over the Northern Hemisphere during the period May through August of 1972. The data were obtained during an interval of satellite operation that optimized plasma, field, and particle measurements but precluded significant optical auroral observations.

The selection of passes for this data set was contingent upon the satellite having its spin axis oriented perpendicular to the orbit plane. In this configuration the particle instruments measure nearly the entire pitch angle distribution every half-spin of the satellite and the thermal plasma detectors alternately look in the ram and wake directions. Data formats presented in this volume contain either 12- or 20-minute intervals of data along the satellite track with the 12-minute segment of each pass chosen to be centered on the regions of auroral particle precipitation. For most passes, the data extend in latitude from the approximate location of the plasmapause well into the polar cap. An attempt was made to include a representative sample of passes through all local times and during periods of both relative quiet and relatively moderate magnetic activity as measured by the 3-hour K_p index.

The 40 auroral zone crossings that make up this data set are thus to be regarded as individual examples of high-latitude observations during a wide range of magnetic activity and Magnetic Local Time (MLT). No single pass should be construed to represent the "average" or "usual" situation in any particular circumstance.

The objective of this data set is to present examples of observations at 1400 km of plasma, particle, and magnetic field perturbations around the auroral oval over a range of magnetic activities. These data form a relatively comprehensive measure of the magnetospheric particle input to the ionosphere over an energy range from 5 eV upwards. In situ observations of plasma density, electron temperature, ion temperature, and ion concentrations depict the state of the ionosphere along the ISIS 2 orbit. Topside sounder height profiles provide a determination of ionospheric density at altitudes below the satellite down to the altitude of F2max. Magnetic perturbations show the signatures of local field-aligned currents measured at the satellite. Plasma waves at the satellite over the frequency range 0 - 20 kHz are measured by the VLF receiver. Thus these data represent a highly coordinated set of observations of the particle, plasma and electromagnetic state of the topside auroral ionosphere/magnetosphere interface.

The data in this volume appear in two groups: the first for magnetically quiet periods ($K_p \leq 1+$) and the second for moderately active ($3- \leq K_p \leq 5+$) periods. The data are ordered within each group sequentially by increasing MLT of the satellite passage over the 70° invariant latitude circle.

Figures 10 and 11 are summary plots showing the spacecraft track in MLT and invariant latitude coordinates for the 12-minute segment of each pass for the quiet and moderately active periods, respectively. The approximate location of the auroral oval is shown for reference in each figure. Tables 1 and 2 are ordered by MLT and list the passes by date, day of year, Universal Time, MLT at 70° invariant latitude, and 3-hour K_p value.

For each data interval a complete data suite consists of the following data formats in order of their appearance.

1. Format 6: Soft Particle Spectrogram (12 min)
2. Format 2: Sounder plus Magnetometer (12 min)
3. Format 3: Energetic Particle Detector (12 min)
4. Format 4: Cylindrical Electrostatic Probe plus Ion Mass Spectrometer (20 min)
5. Format 5: Retarding Potential Analyzer (20 min)
6. Format 11: VLF Receiver

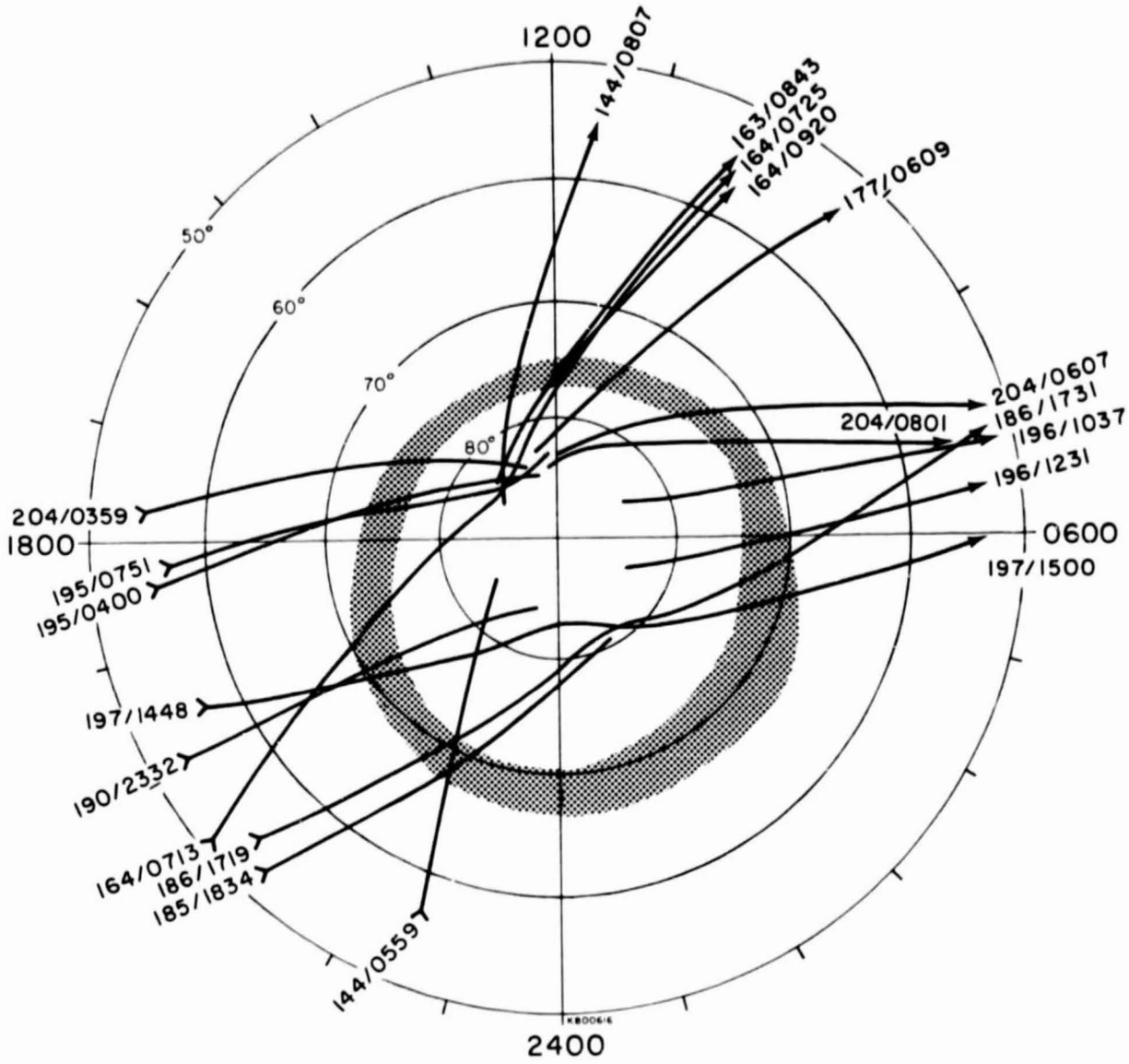

Figure 10. Magnetic Local Time - Invariant Latitude Orbit Tracks for Section 1 (Low K_p)

Table 1 Data Set Pass List for Section 1 (Low K_p)

Date**	Day** Number	Universal Time†	MLT at 70° invar.	3-hr K_p	Page	Data Set
July 15	197	1500	05.0	1-	39	1
July 4	186	1731	05.6	1-	44	2
July 14	196	1231	06.0	0+	51	3
July 14	196	1037	06.95	0+	56	4
July 22	204	0801	07.5	0+	61	5
July 22	204	0607	08.2	0+	66	6
June 25	177	0609	10.0	1+	71	7
June 12	164	0725	11.0	0+	76	8
May 23	144	0807	12.3	0+	83	9
June 11	163	0843	13.1*	1	88	10
June 12	164	0920	13.3*	0	93	11
July 22	204	0359	16.9	0+	100	12
July 13	195	0400	17.7	1+	105	13
July 13	195	0751	17.7	0+	110	14
June 12	164	0713	19.7	0+	115	15
July 8	190	2332	20.25	1-	122	16
July 15	197	1448	20.4	0+	127	17
July 4	186	1719	22.0	1+	132	18
May 23	144	0559	22.2	0+	139	19
July 3	185	1834	22.5	1+	144	20

**All data are from 1972.
†Universal Time is the start time for the 12-minute pass segments.
*MLT at 80° invariant latitude.

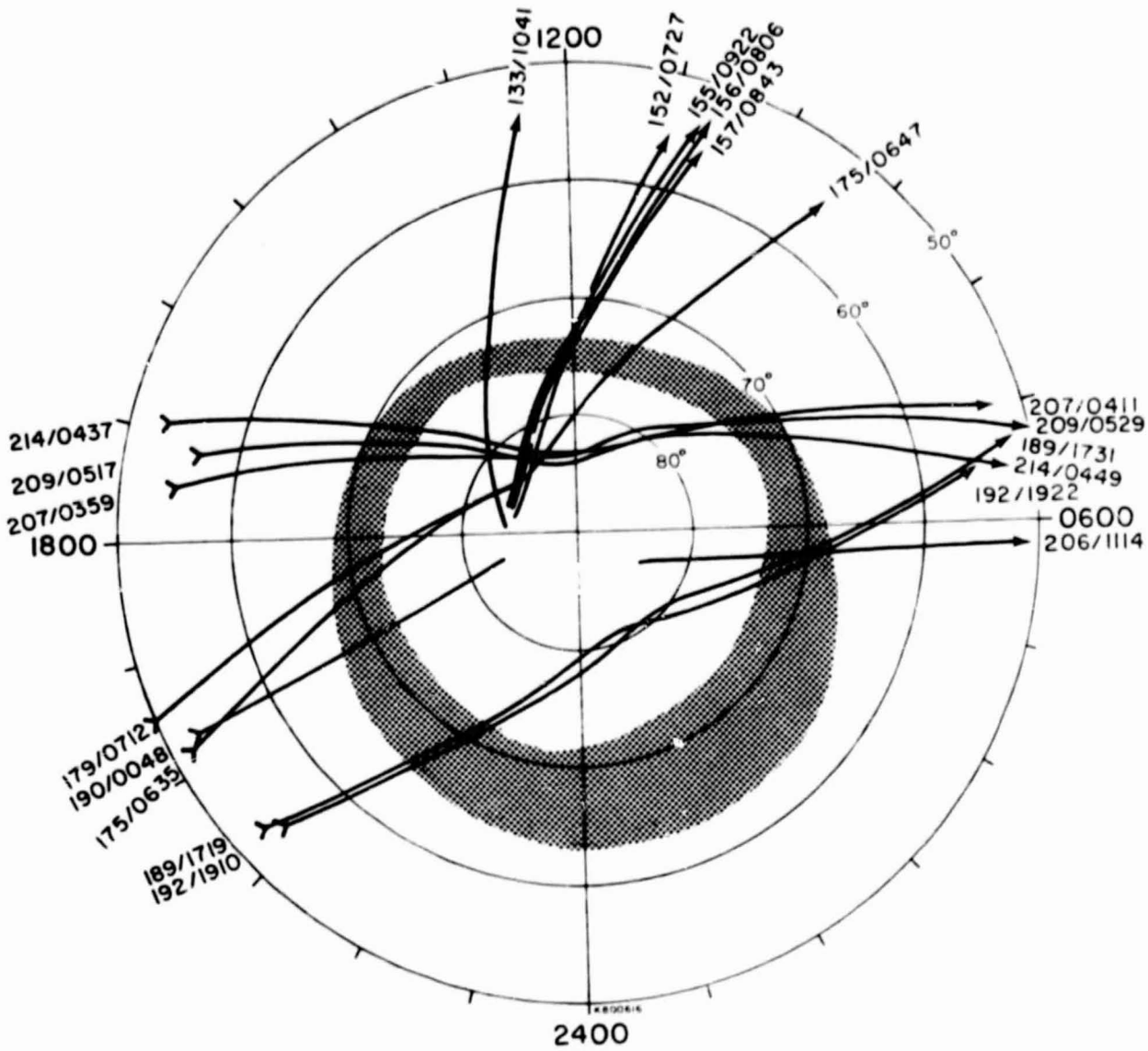

Figure 11. Magnetic Local Time - Invariant Latitude Orbit Tracks for Section 2 (High K_p)

Table 2 Data Set Pass List for Section 2 (High K_p)

Date**	Day** Number	Universal Time†	MLT at 70° invar.	3-hr K_p	Page	Data Set
July 7	189	1731	05.4	3	149	21
July 10	192	1922	05.5	3-	154	22
July 24	206	1114	05.5	3	159	23
Aug. 1	214	0449	07.5	4	164	24
July 27	209	0529	07.8	4-	171	25
July 25	207	0411	08.0	5-	176	26
June 23	175	0647	10.2	3+	182	27
June 4	156	0806	11.6	3-	187	28
May 31	152	0727	13.1*	3	192	29
June 5	157	0843	13.2*	3	196	30
June 3	155	0922	13.6*	3-	201	31
May 12	133	1041	15.2*	3-	206	32
Aug. 1	214	0437	16.1	4	213	33
July 27	209	0517	16.5	4-	220	34
July 25	207	0359	16.7	5-	225	35
June 27	179	0712	18.5	3	231	36
June 23	175	0635	19.0	3+	236	37
July 8	190	0048	19.6	3	241	38
July 7	189	1719	21.9	3	246	39
July 10	192	1910	22.0	3-	251	40

**All data are from 1972.
†Universal Time is the start time of the 12-minute pass segments.
*MLT at 80° invariant latitude.

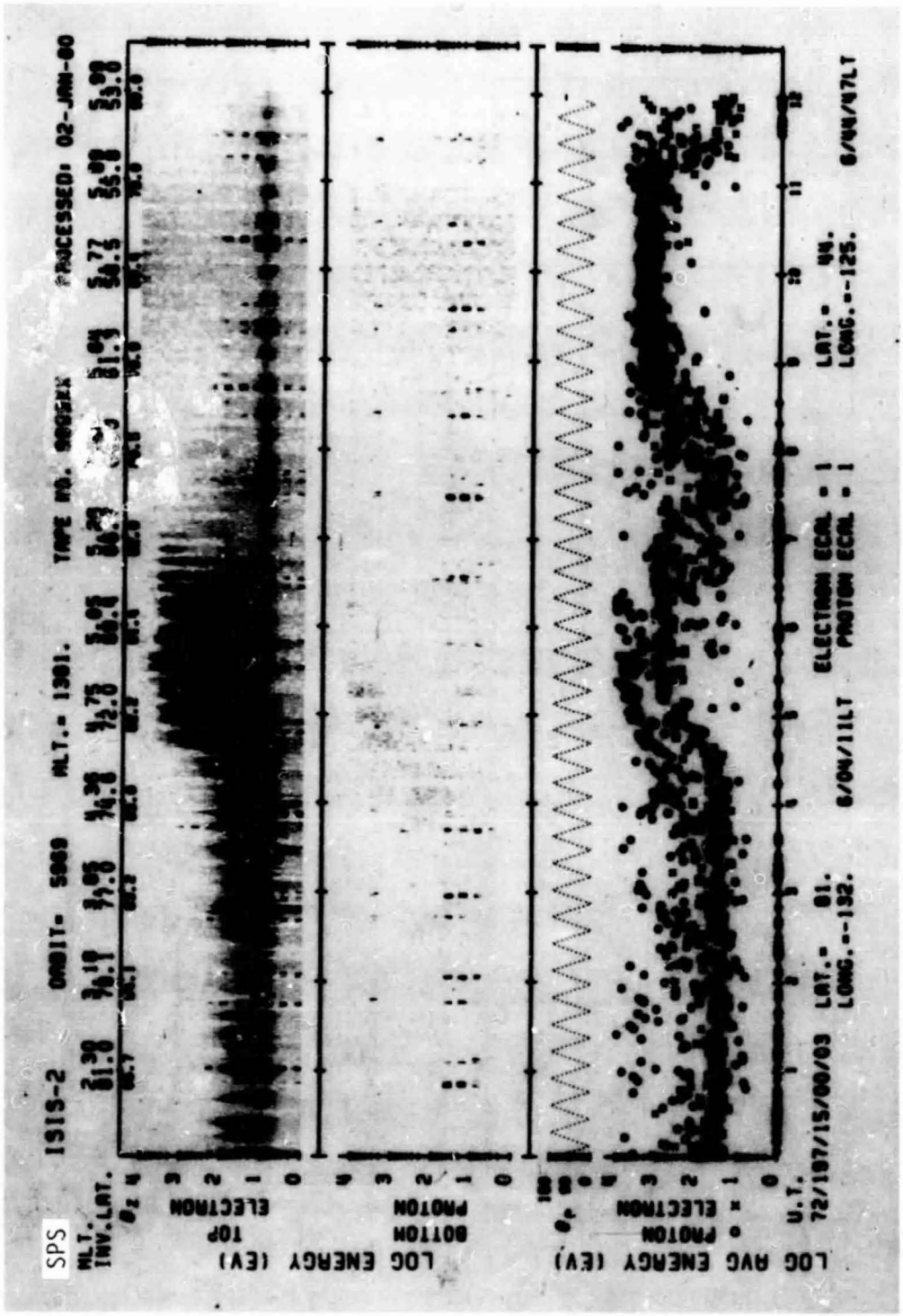

SET 1, FORMAT 6

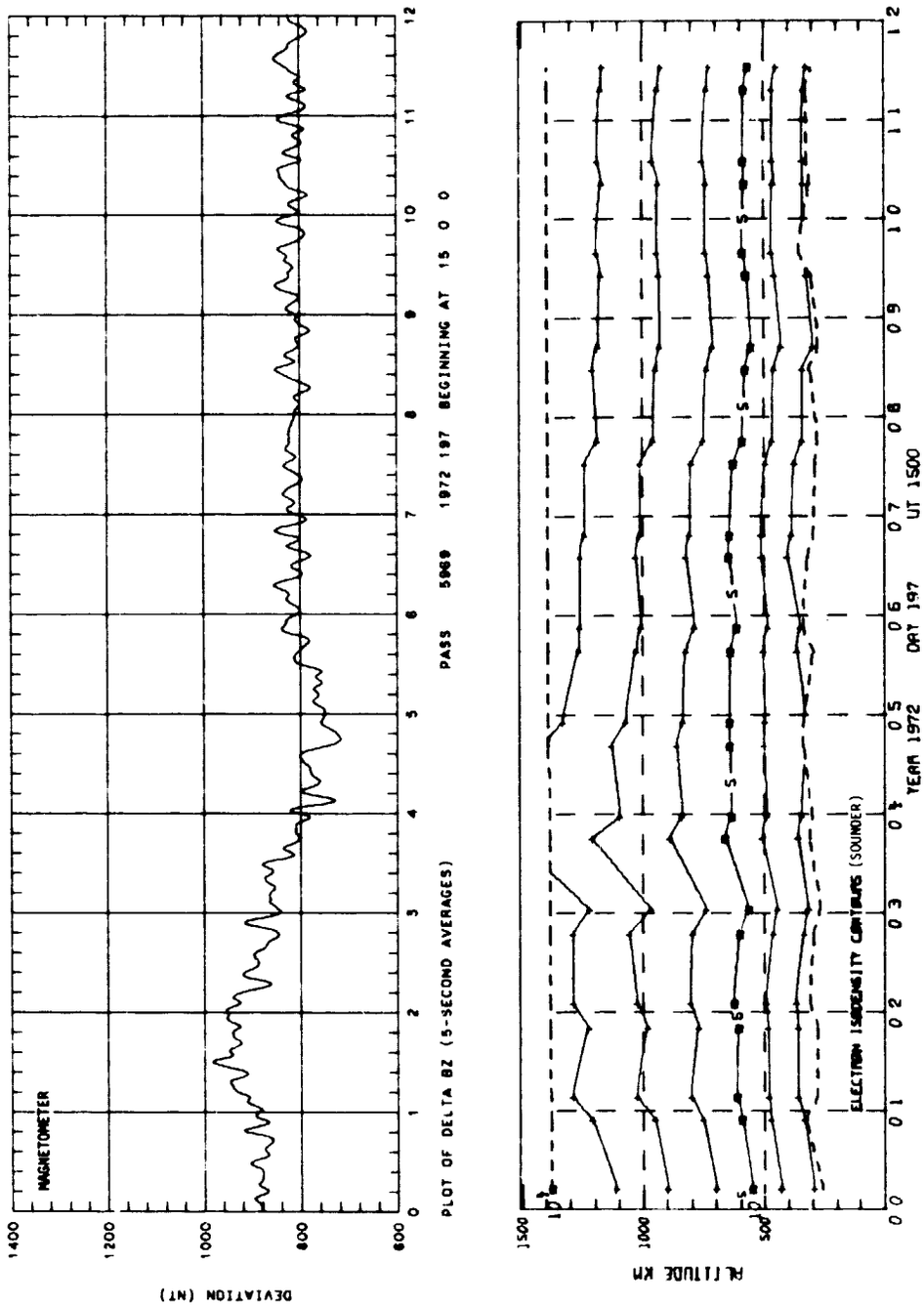

SET 1, FORMAT 2

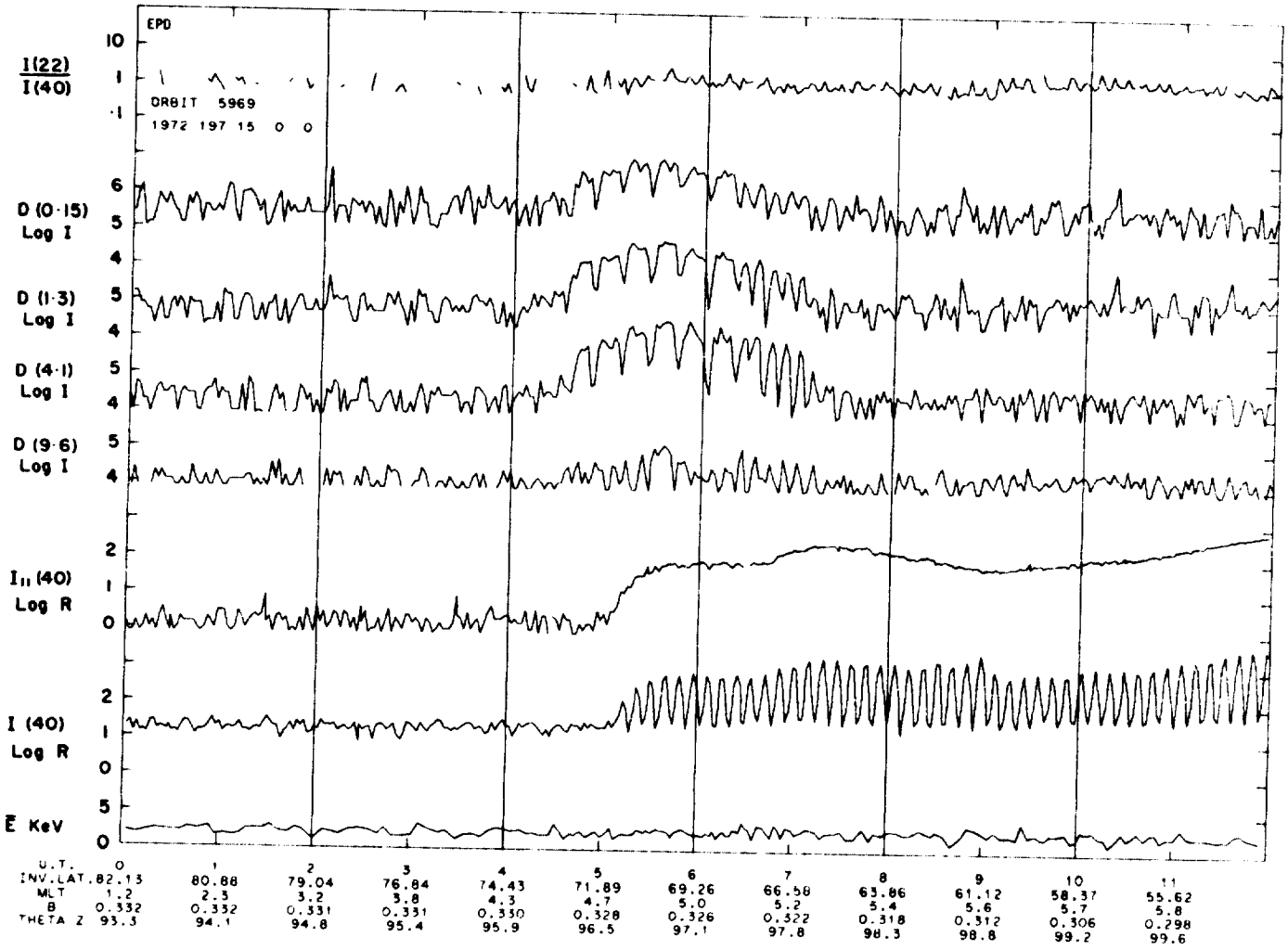

SET 1, FORMAT 3

ORBIT 5969
DATE 720715
DAY 197

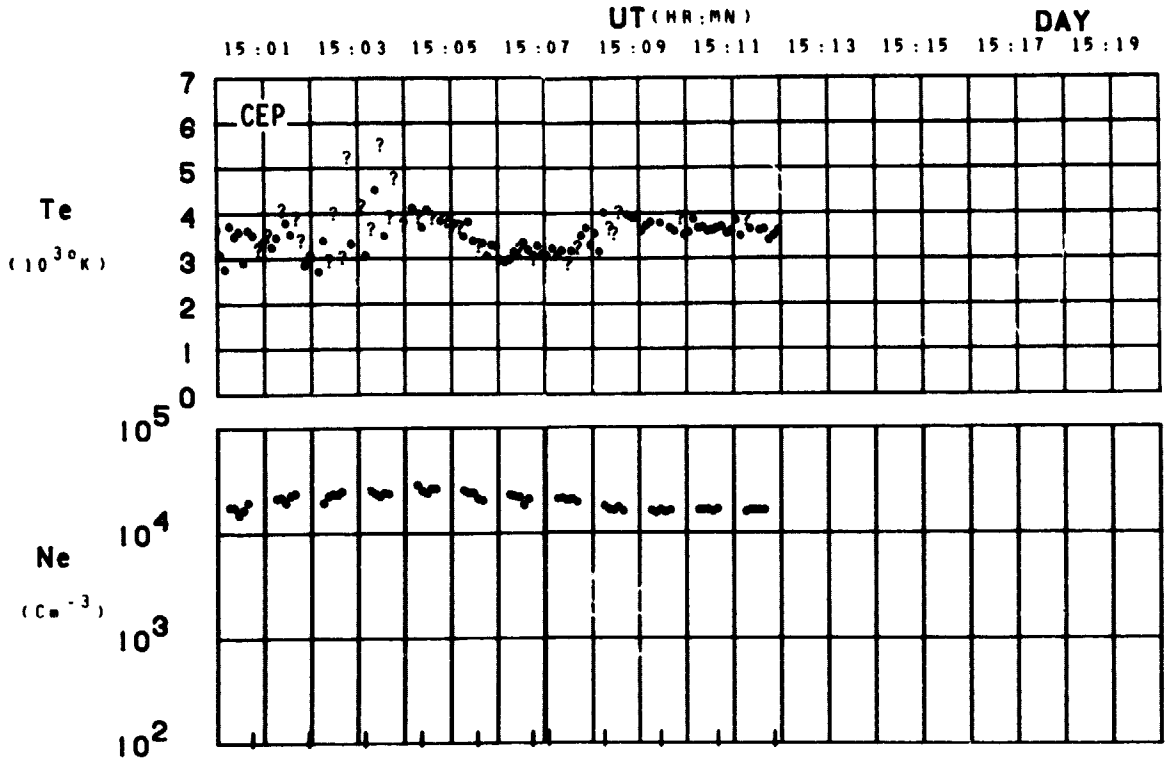

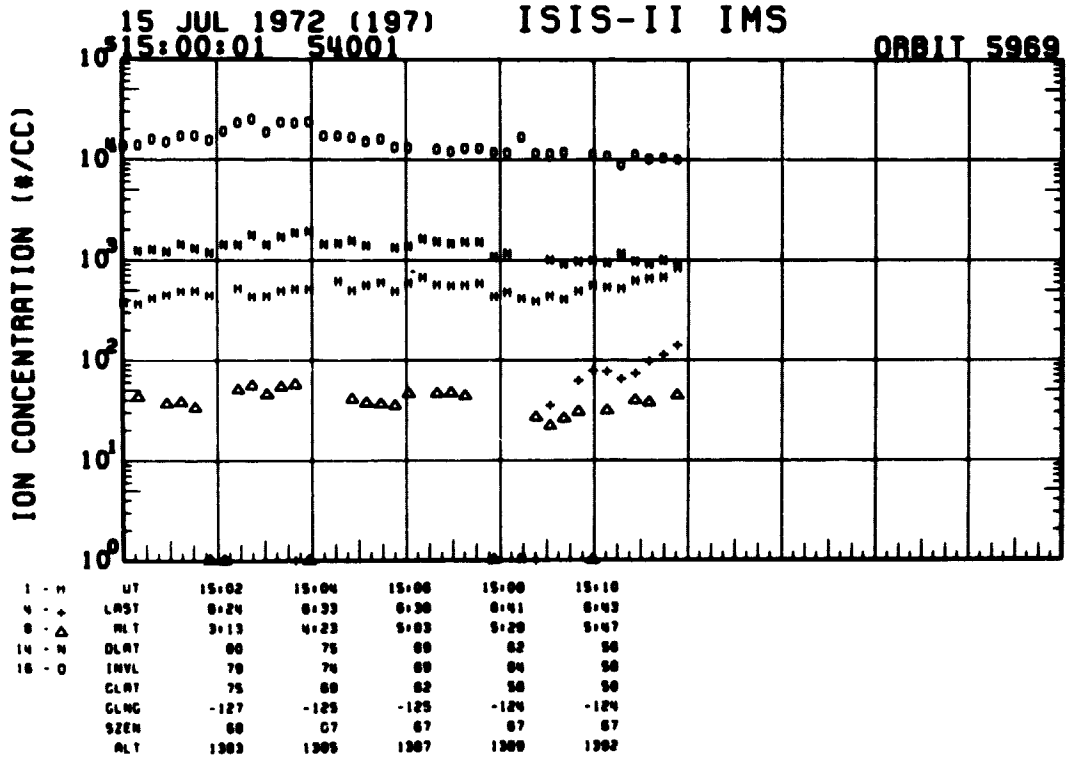

SET 1, FORMAT 4

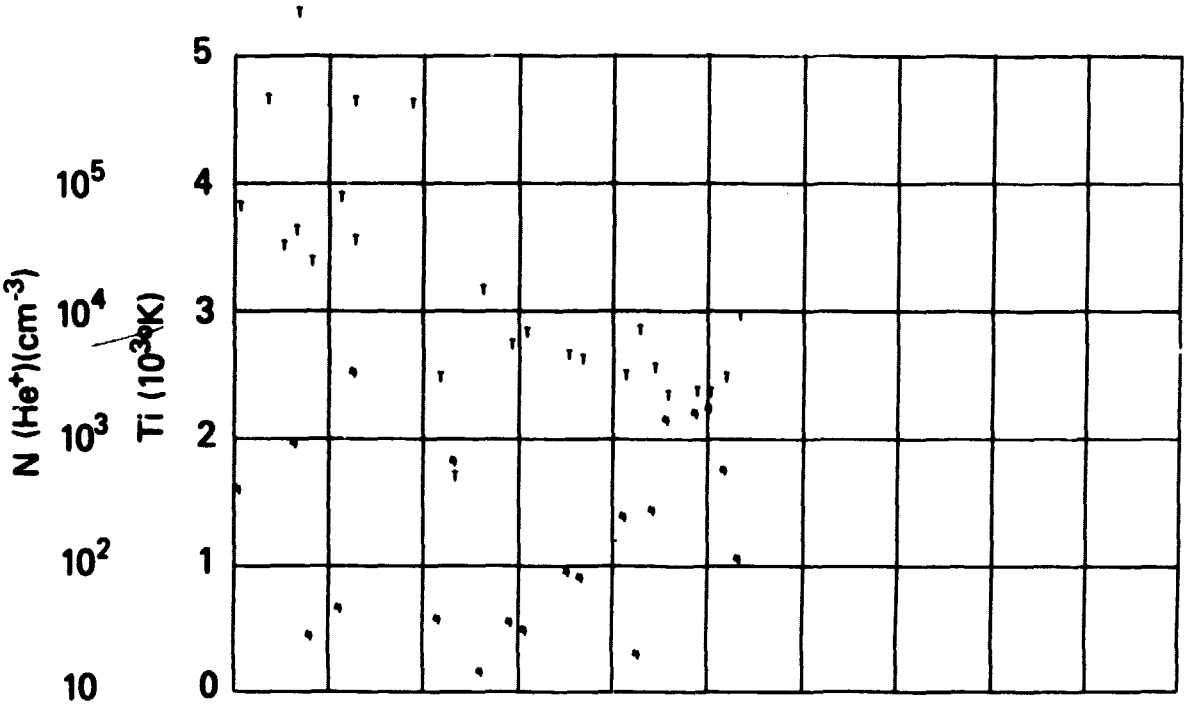

UT	15:02	15:04	15:06	15:08	15:10
LAST	6:24	6:33	6:38	6:41	6:43
MLT	3:13	4:23	5:03	5:29	5:47
DLAT	80	75	69	62	56
INVL	78	74	69	64	58
GLAT	75	69	62	56	50
GLNG	-127	-125	-125	-124	-124
SZEN	68	67	67	67	67
ALT	1383	1385	1387	1389	1392

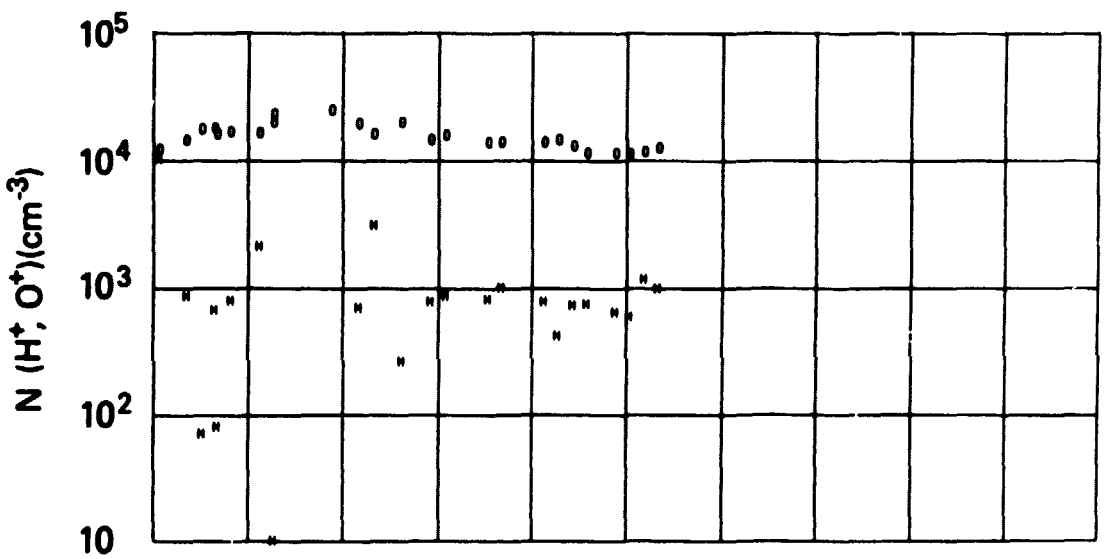

SET 1, FORMAT 5

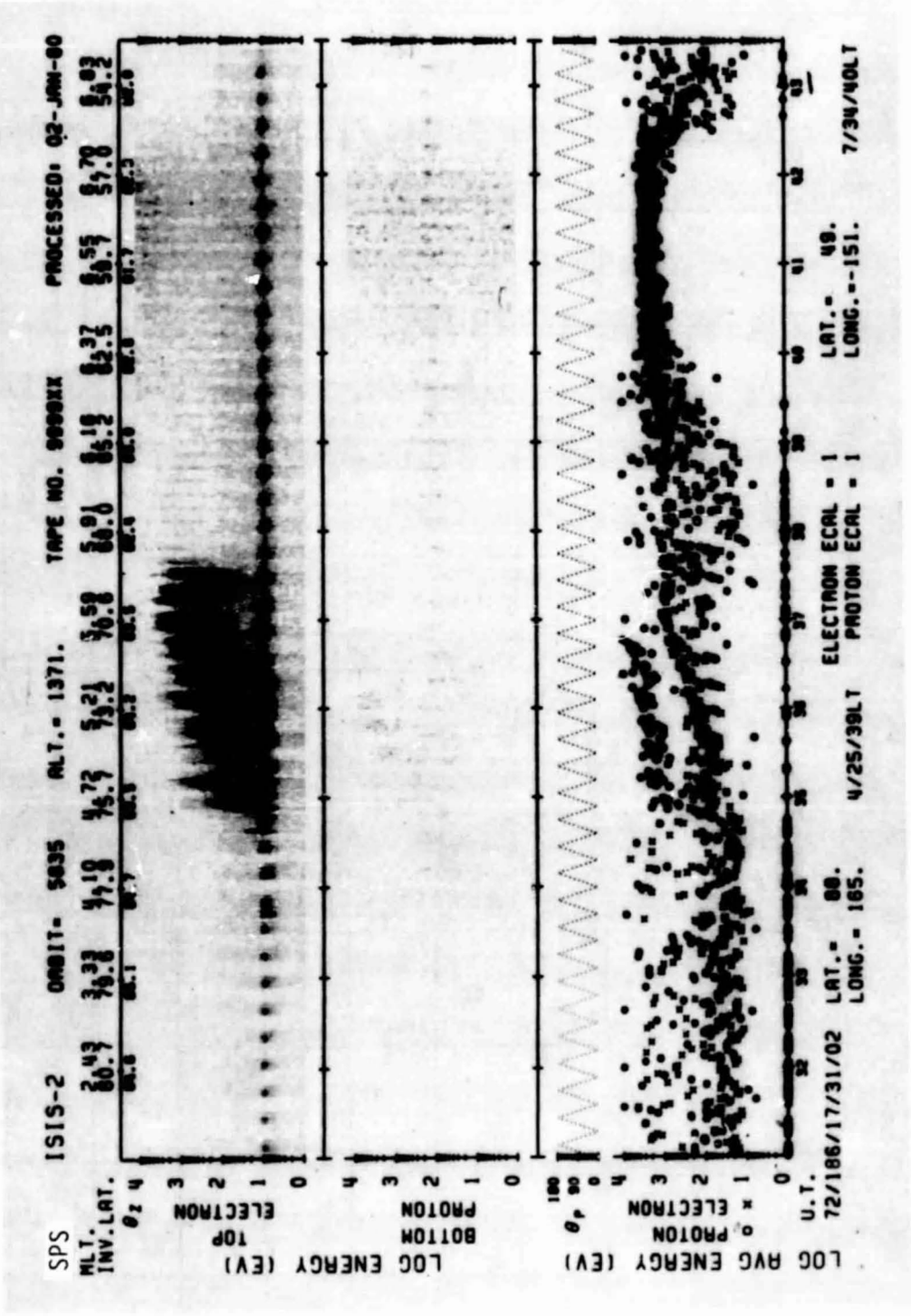

SET 2, FORMAT 6

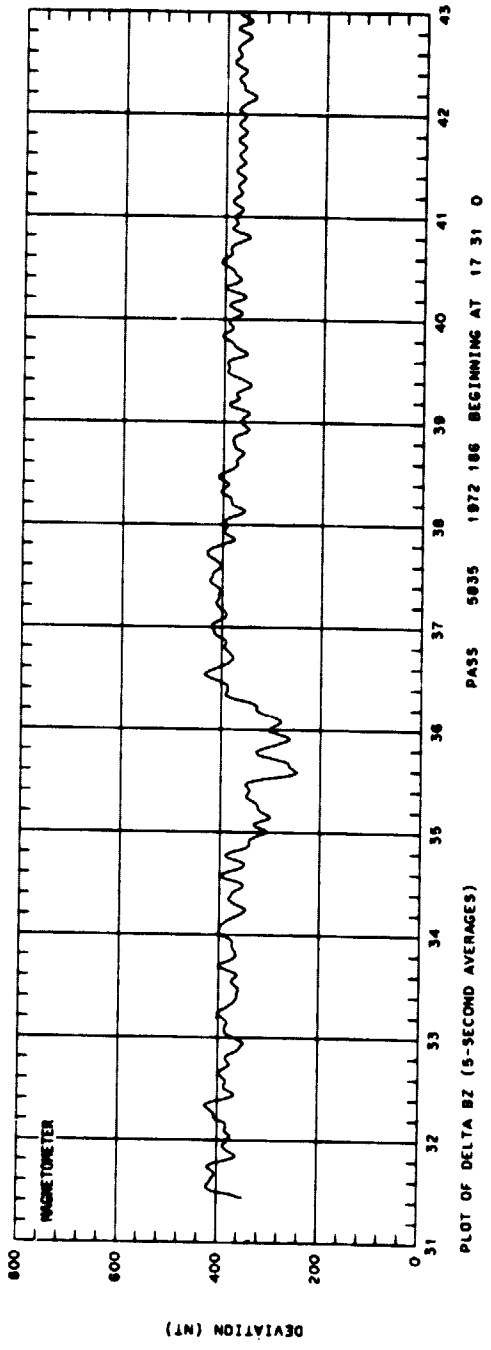

SET 2, FORMAT 2

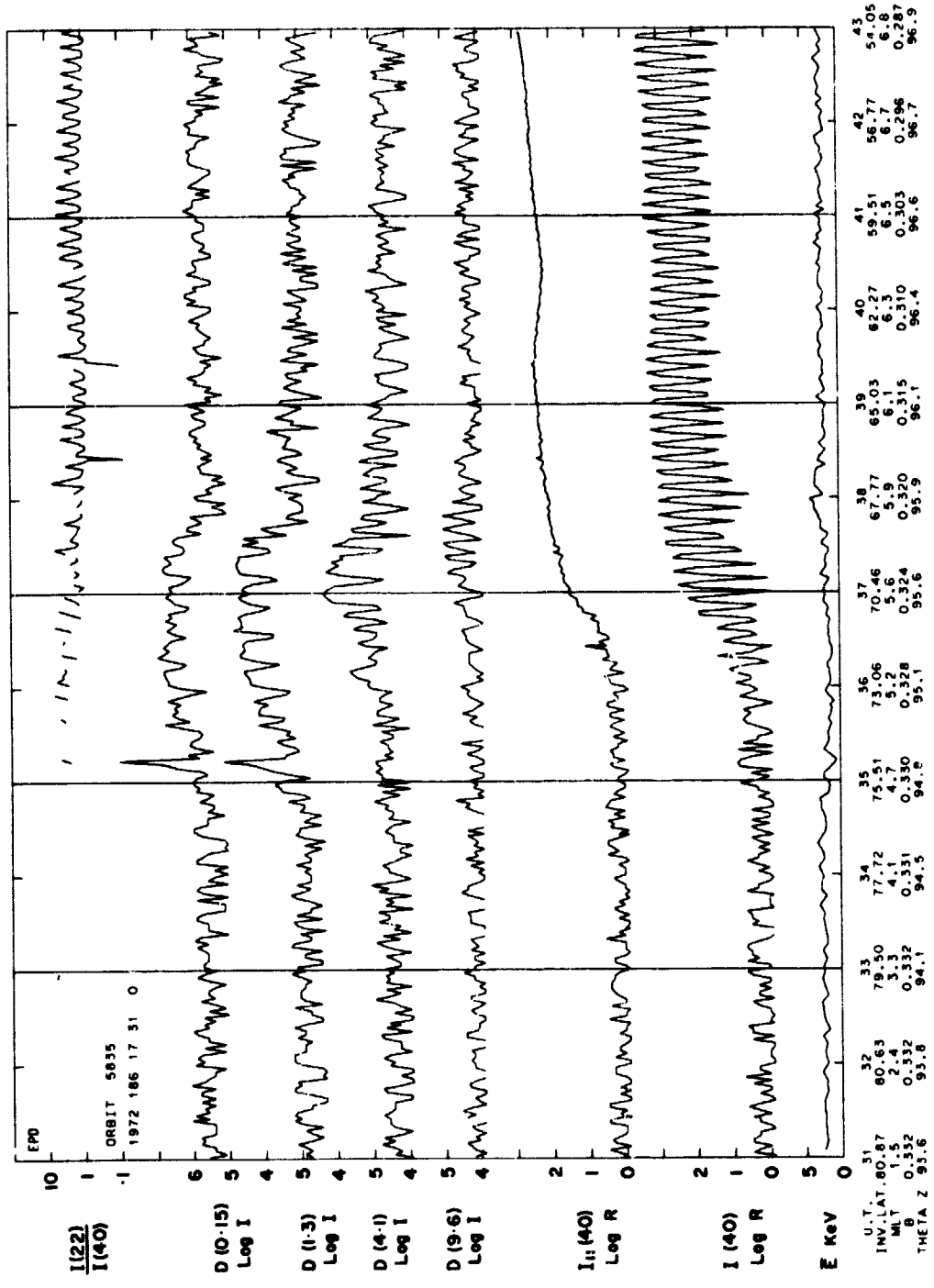

SET 2, FORMAT 3

ORBIT 5835
DATE 720704
DAY 186

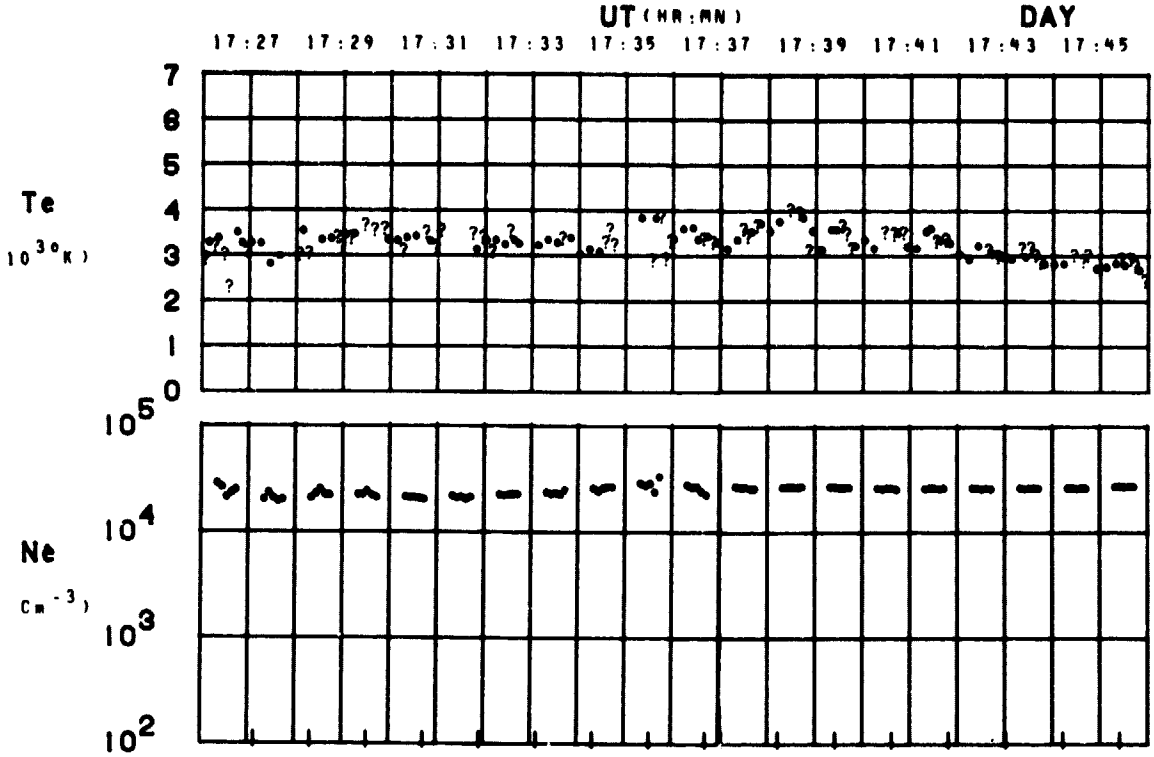

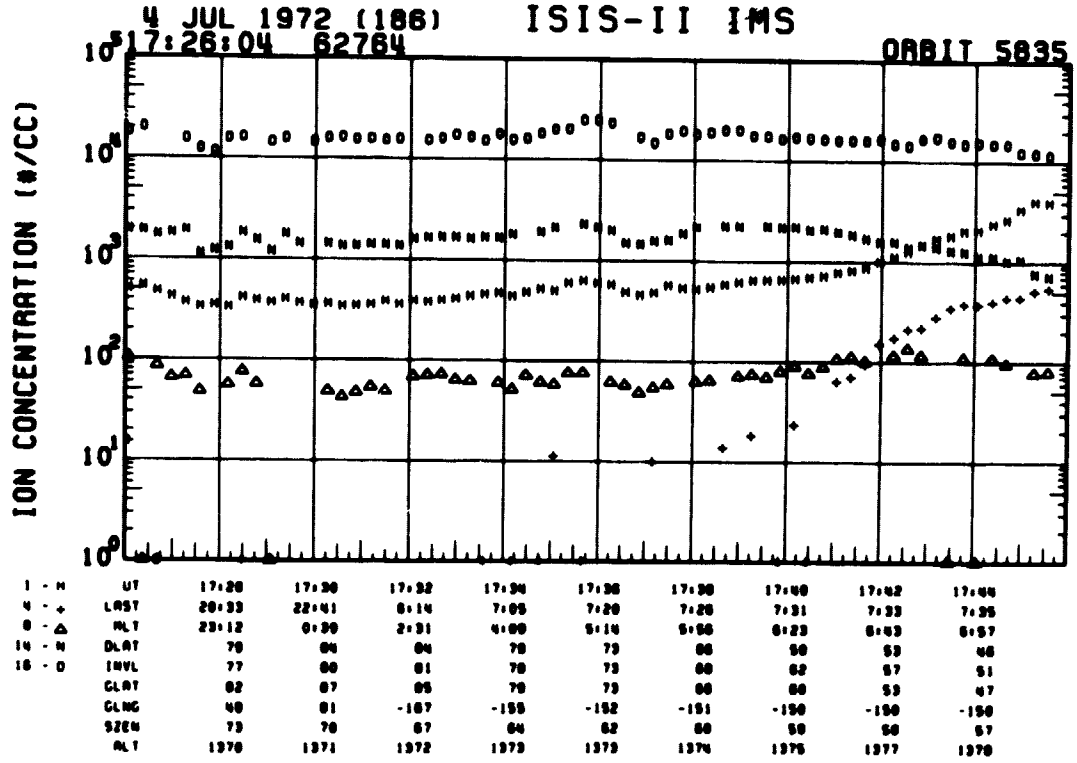

1 - H	UT	17:26	17:30	17:32	17:34	17:36	17:38	17:40	17:42	17:44
4 - +	LAST	20:33	22:41	0:14	1:05	1:20	1:26	1:31	1:33	1:35
8 - △	MLT	23:12	0:20	2:31	4:00	5:14	5:56	6:23	6:43	6:57
14 - N	DLAT	70	64	64	70	73	66	58	53	48
16 - O	INVL	77	80	81	78	73	66	62	57	51
	GLAT	62	67	65	70	73	66	60	53	47
	GLNG	48	81	-167	-155	-152	-151	-150	-150	-150
	SZEN	73	70	67	64	62	60	58	56	57
	ALT	1370	1371	1372	1373	1373	1374	1375	1377	1378

SET 2, FORMAT 4

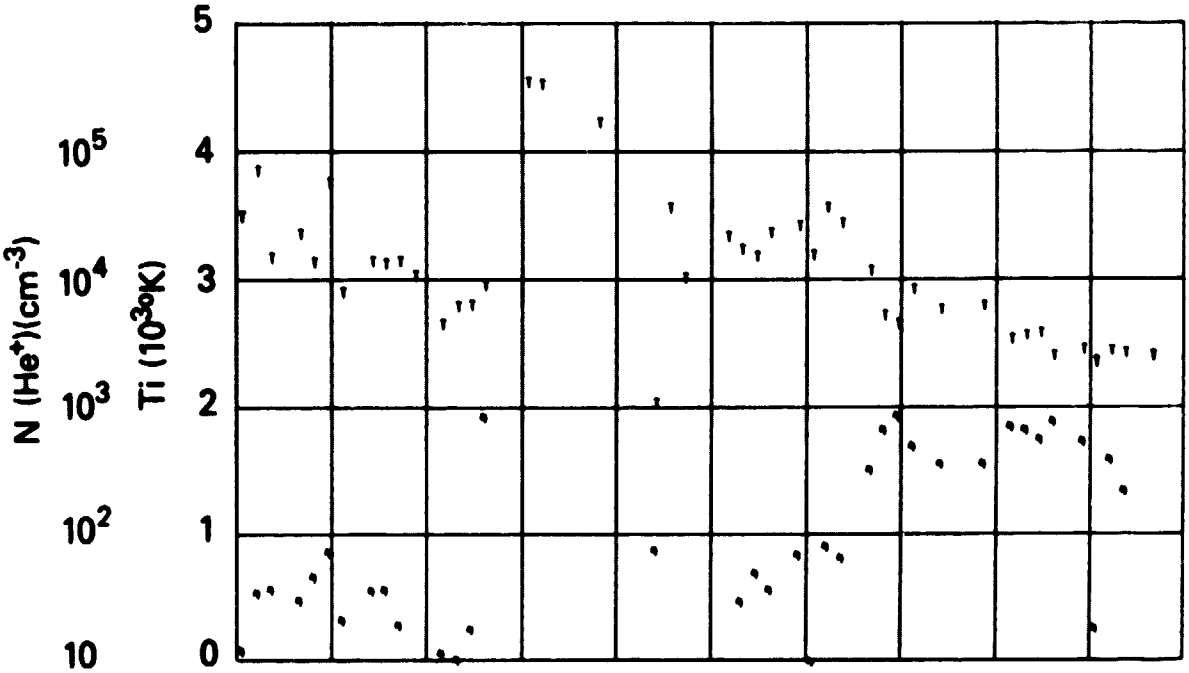

UT	17:28	17:30	17:32	17:34	17:36	17:38	17:40	17:42	17:44
LAST	20:33	22:41	0:14	7:05	7:20	7:28	7:31	7:33	7:35
MLT	23:12	0:38	2:31	4:09	5:14	5:56	6:23	6:43	6:57
DLAT	79	84	84	78	73	68	59	53	48
INVL	77	80	81	78	73	68	62	57	51
GLAT	82	87	85	78	73	68	60	53	47
GLNG	48	81	-167	-155	-152	-151	-150	-150	-150
SZEN	73	70	67	64	62	60	59	58	57
ALT	1370	1371	1372	1373	1373	1374	1375	1377	1378

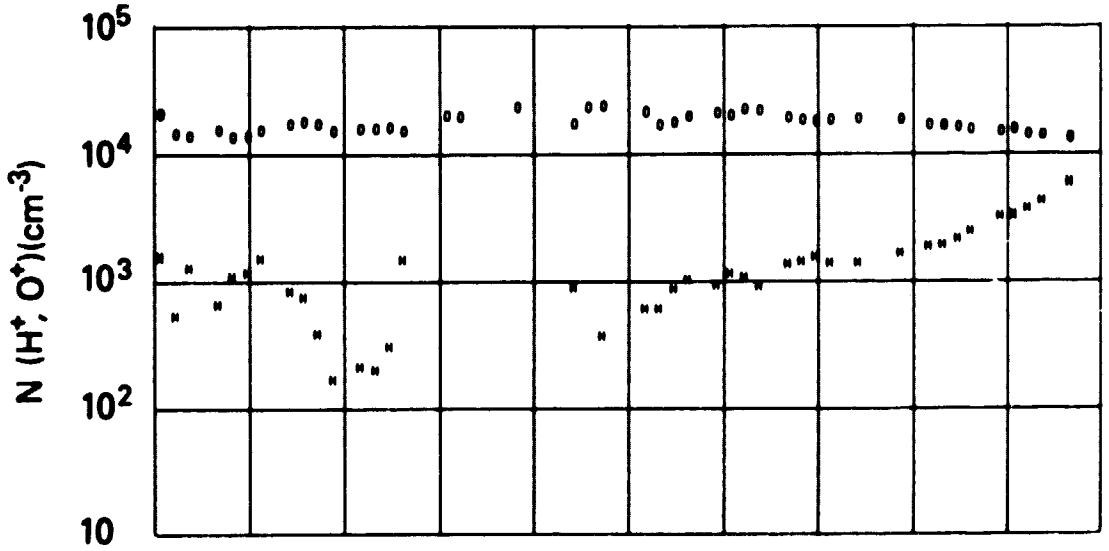

SET 2, FORMAT 5

72/186/1731

Excerpts of VLF Spectral film for the period 1733 - 1743

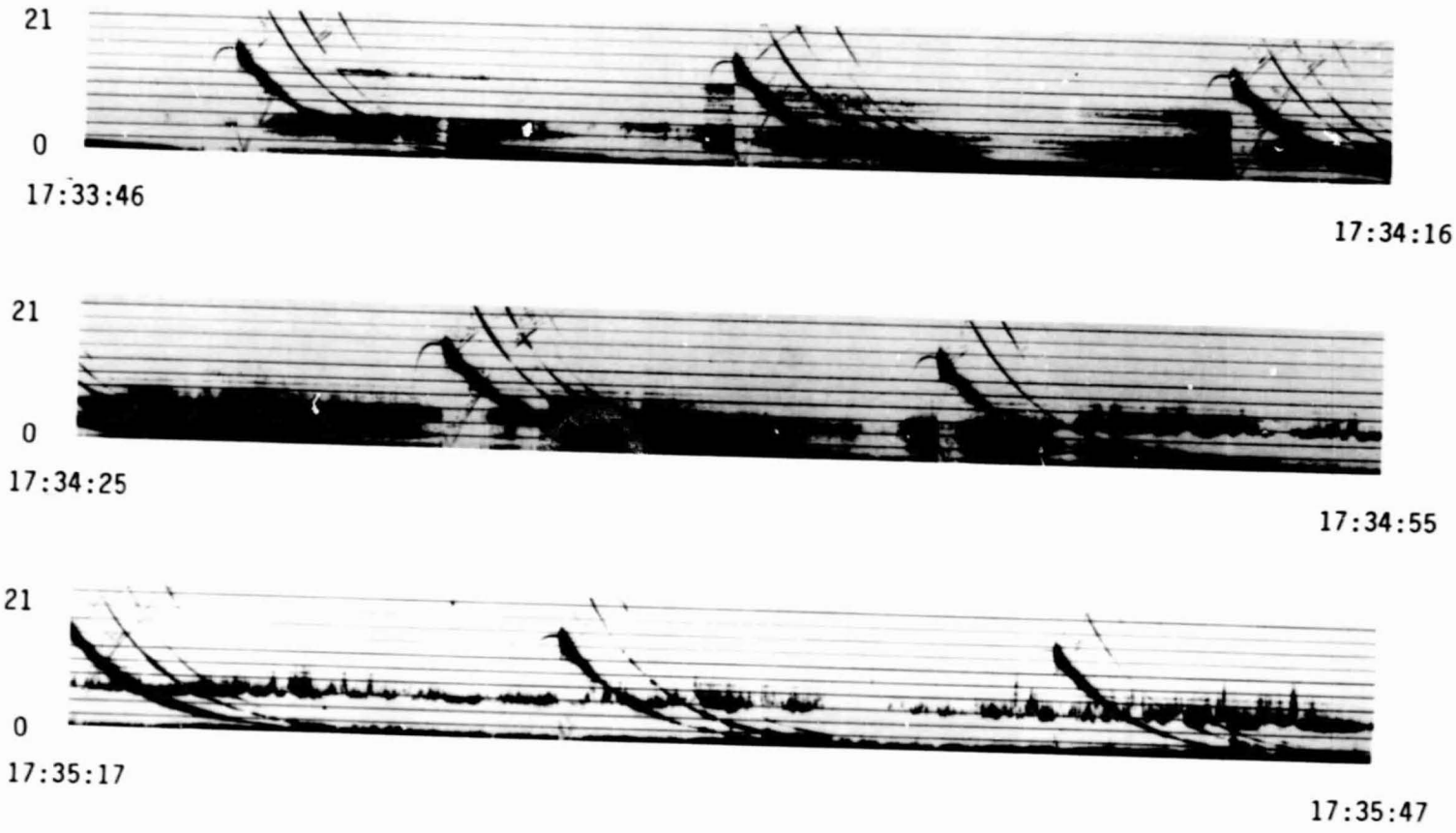

SET 2, FORMAT 11

72/186/1731

Excerpts of VLF Spectral film for the period 1733 - 1743

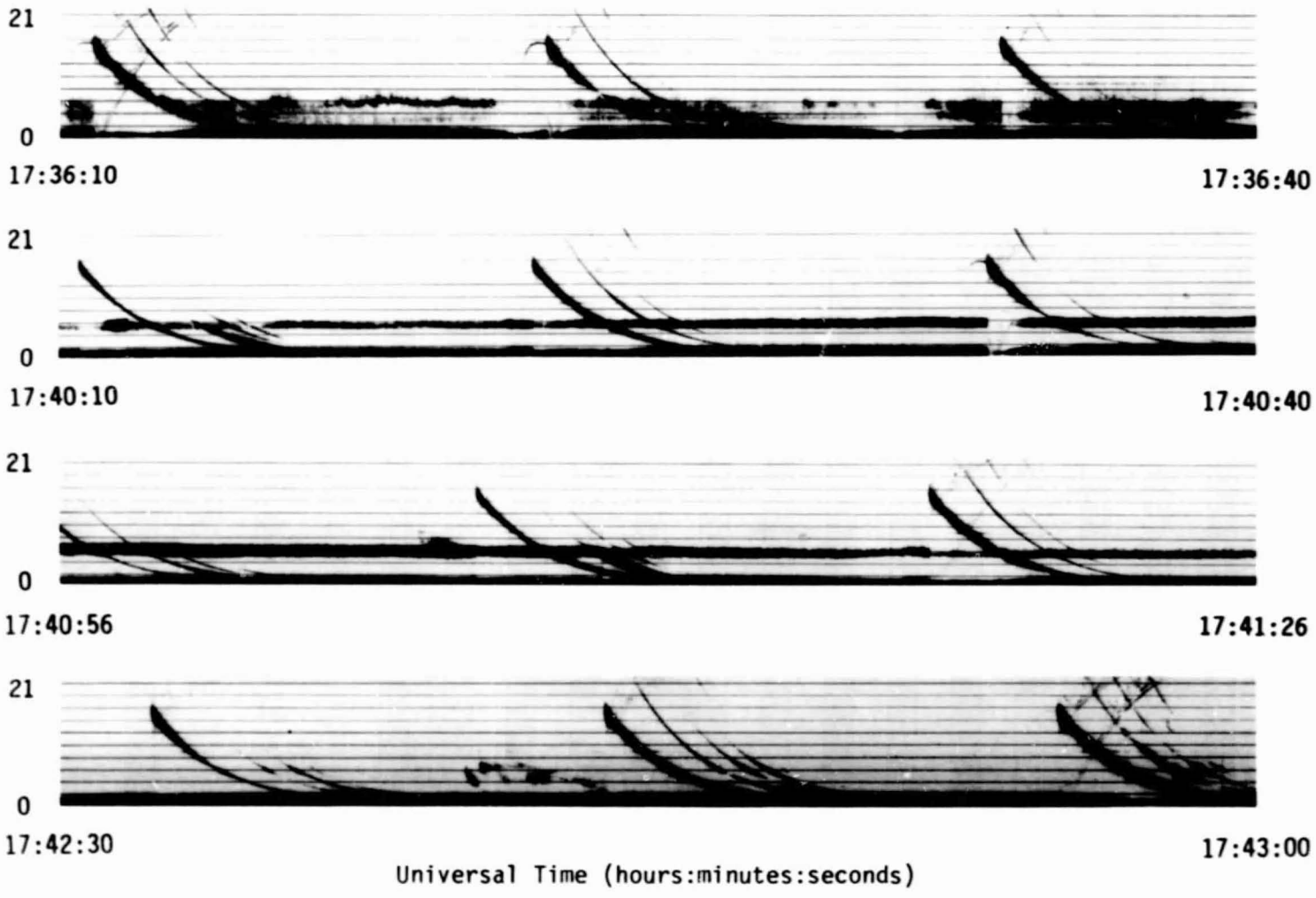

SET 2, FORMAT 11

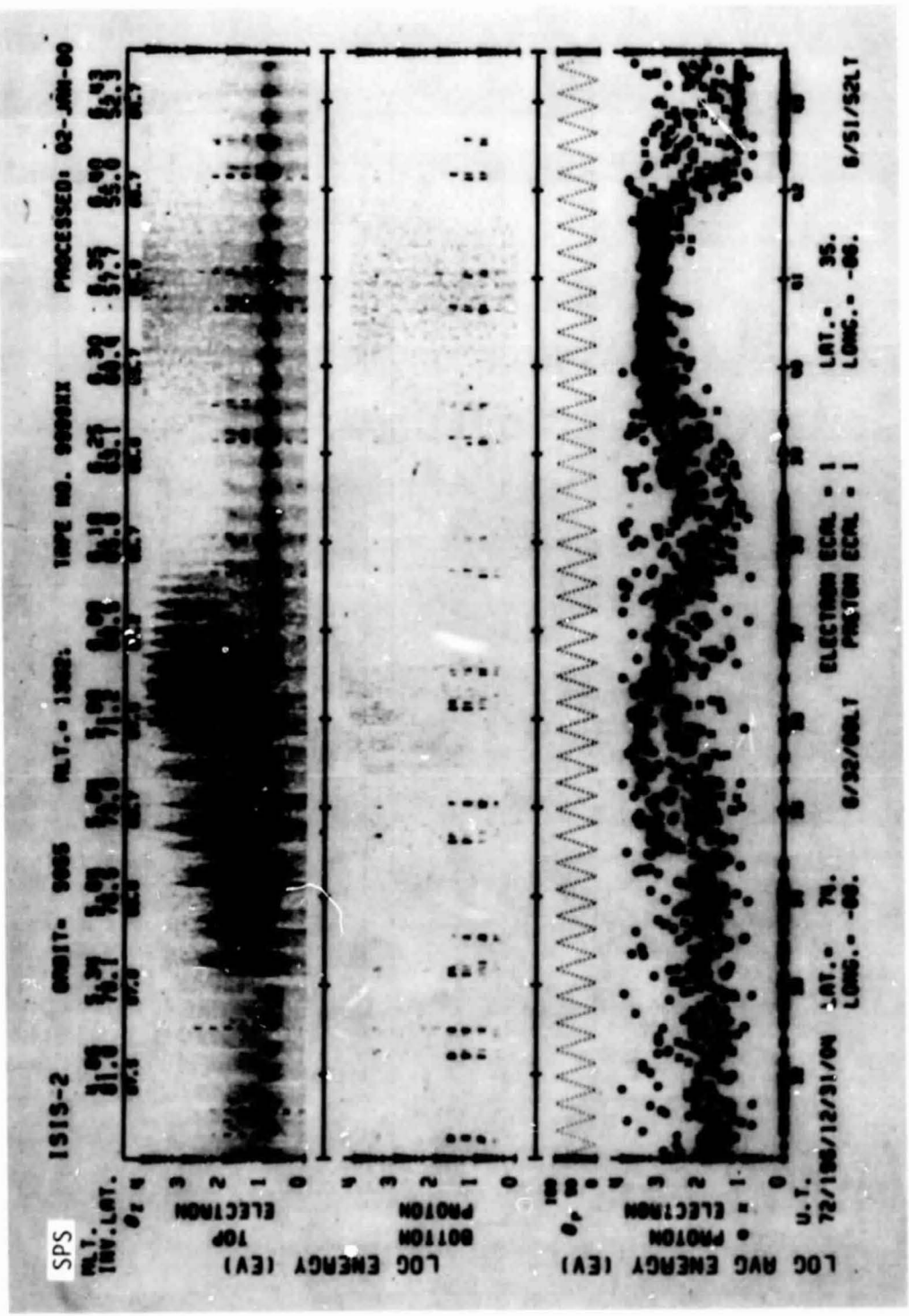

SET 3, FORMAT 6

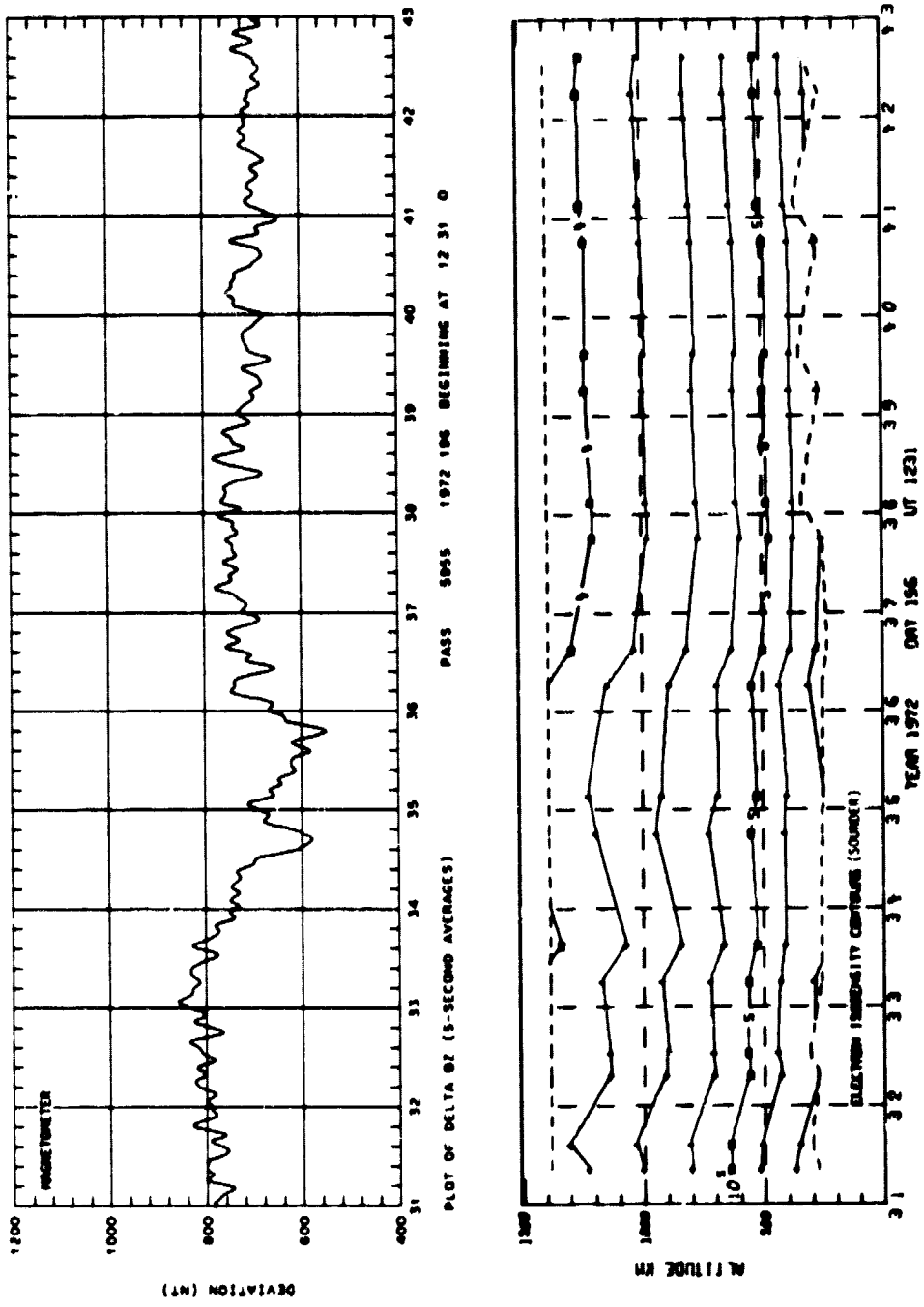

SET 3, FORMAT 2

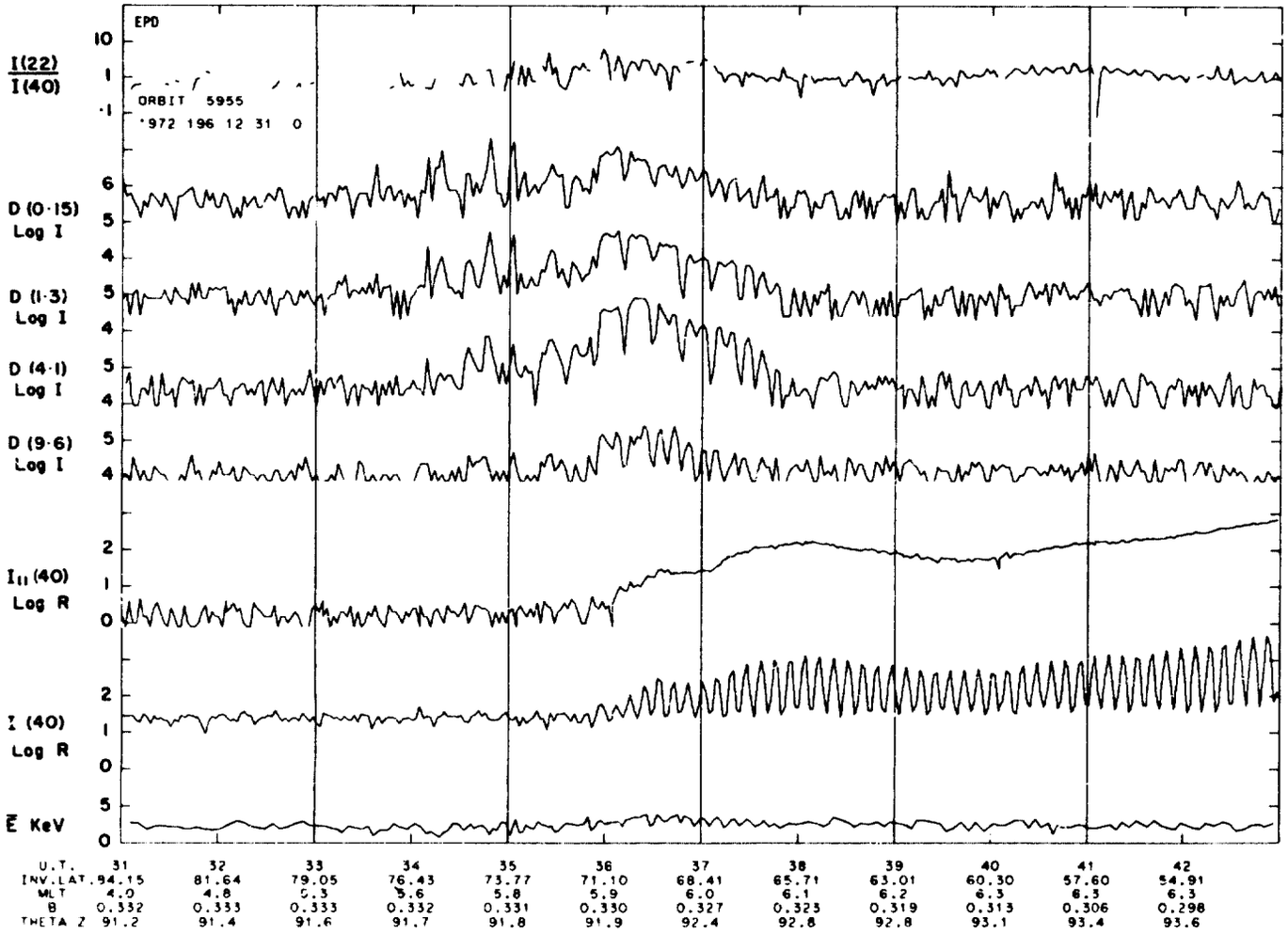

SET 3, FORMAT 3

ORBIT 5955
DATE 720714
DAY 196

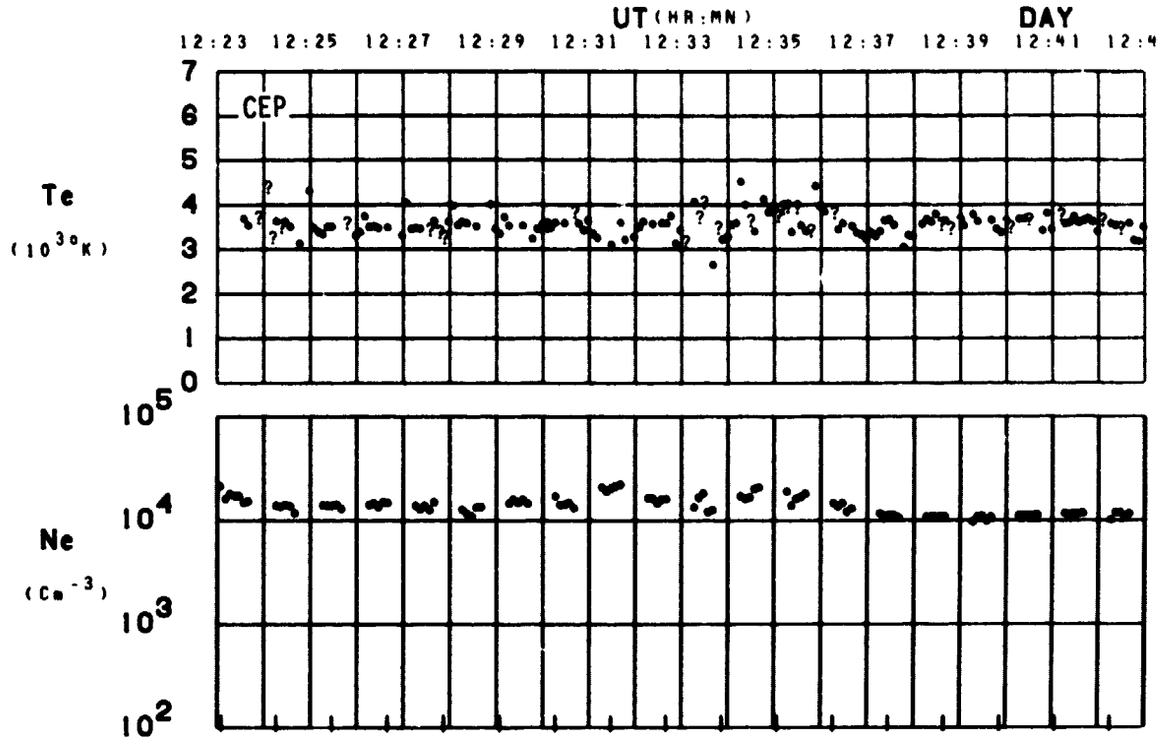

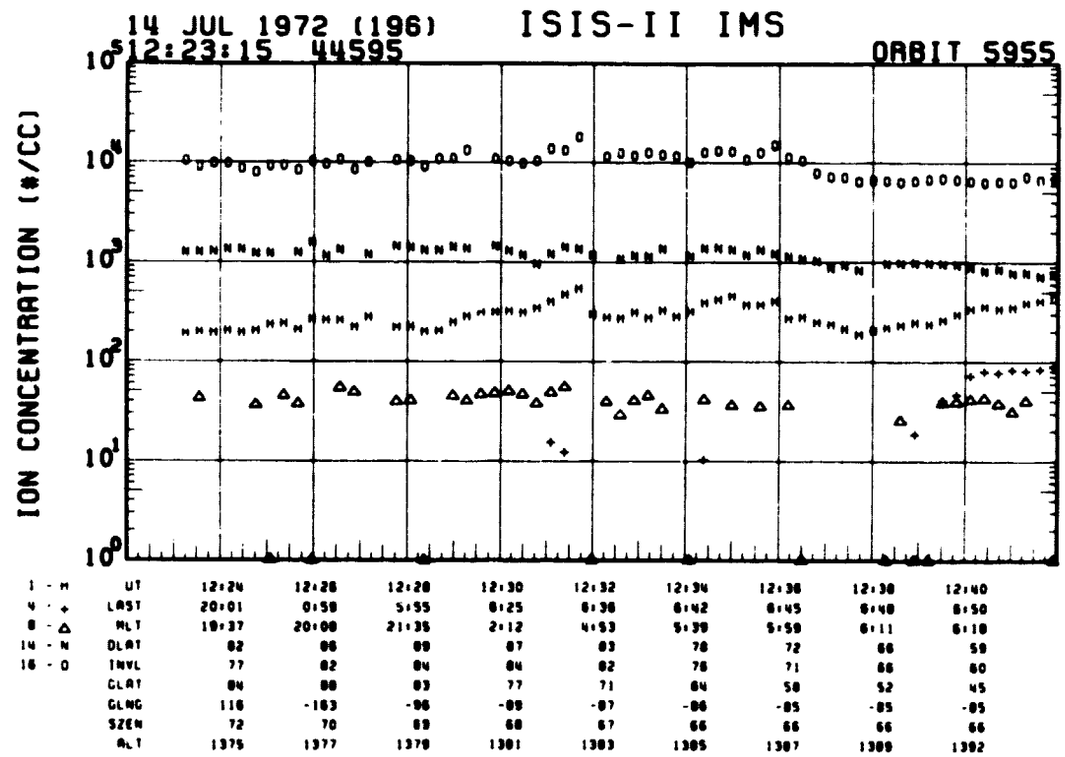

1 - H	UT	12:24	12:26	12:28	12:30	12:32	12:34	12:36	12:38	12:40
4 - +	LAST	20:01	0:58	5:55	8:25	8:38	8:42	8:45	8:48	8:50
8 - △	ALT	19:37	20:08	21:35	2:12	4:53	5:39	5:59	6:11	6:18
14 - N	DLAT	82	86	89	87	83	78	72	66	59
16 - O	INVL	77	82	84	84	82	78	71	66	60
	GLAT	84	88	83	77	71	64	58	52	45
	GLNG	116	-163	-96	-89	-87	-86	-85	-85	-85
	SZEN	72	70	69	68	67	66	66	66	66
	ALT	1375	1377	1378	1381	1383	1385	1387	1389	1392

SET 3, FORMAT 4

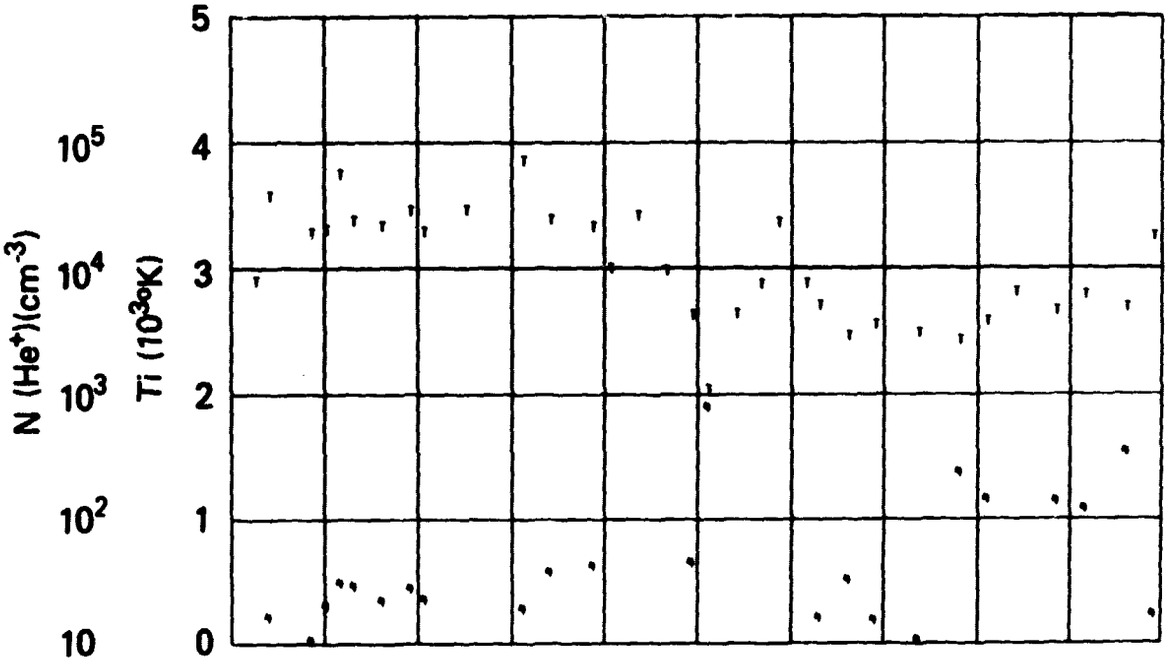

UT	12:24	12:26	12:28	12:30	12:32	12:34	12:36	12:38	12:40
LAST	20:01	0:59	5:55	6:25	6:36	6:42	6:45	6:48	6:50
MLT	19:37	20:08	21:35	2:12	4:53	5:30	5:59	6:11	6:18
DLAT	82	86	89	87	83	78	72	66	59
INVL	77	82	84	84	82	78	71	66	60
GLAT	84	88	83	77	71	64	58	52	45
GLNG	116	-163	-96	-89	-87	-86	-85	-85	-85
SZEN	72	70	69	68	67	66	66	66	66
ALT	1375	1377	1378	1381	1383	1385	1387	1389	1392

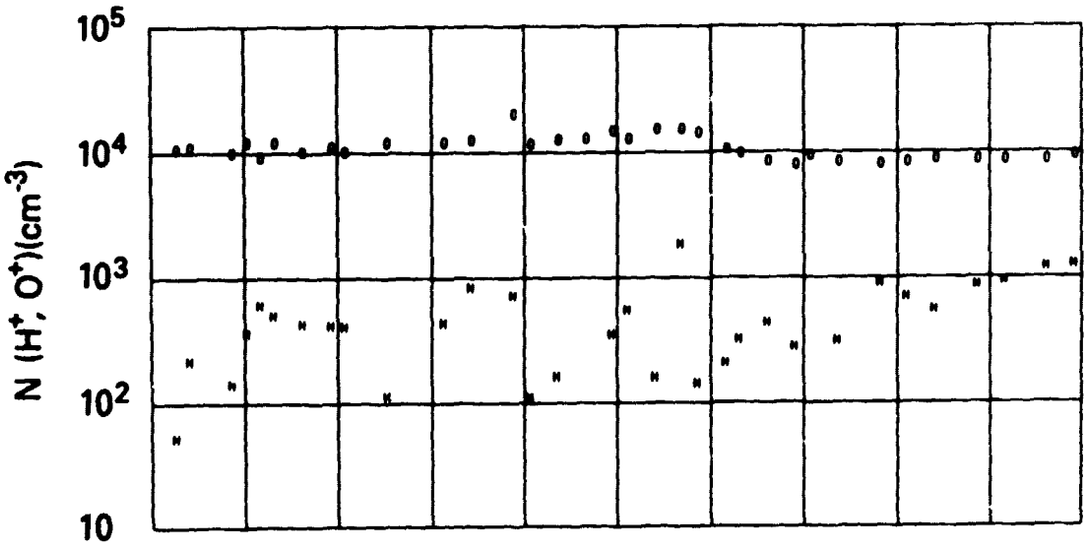

SET 3, FORMAT 5

SET 4, FORMAT 6

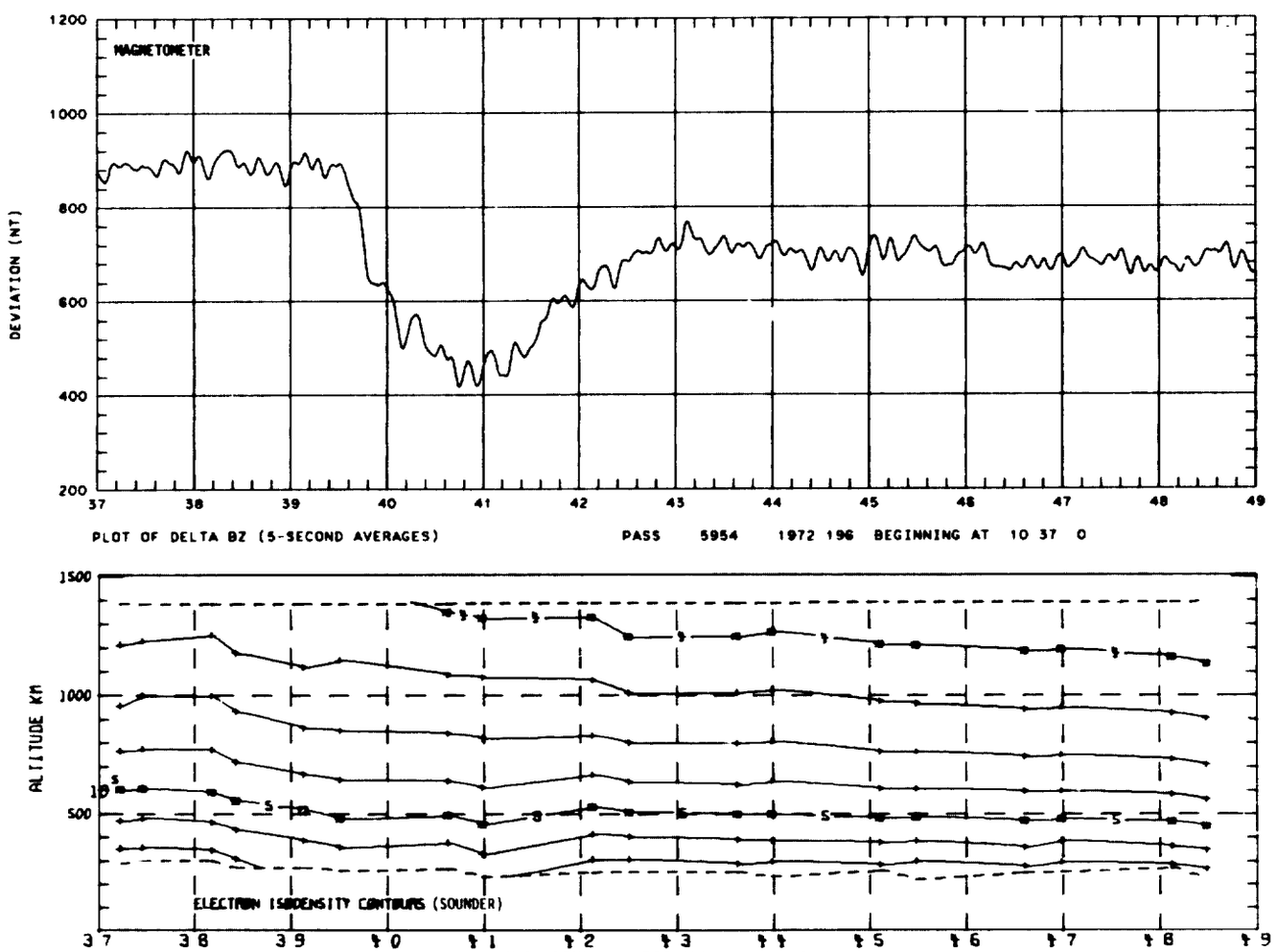

SET 4, FORMAT 2

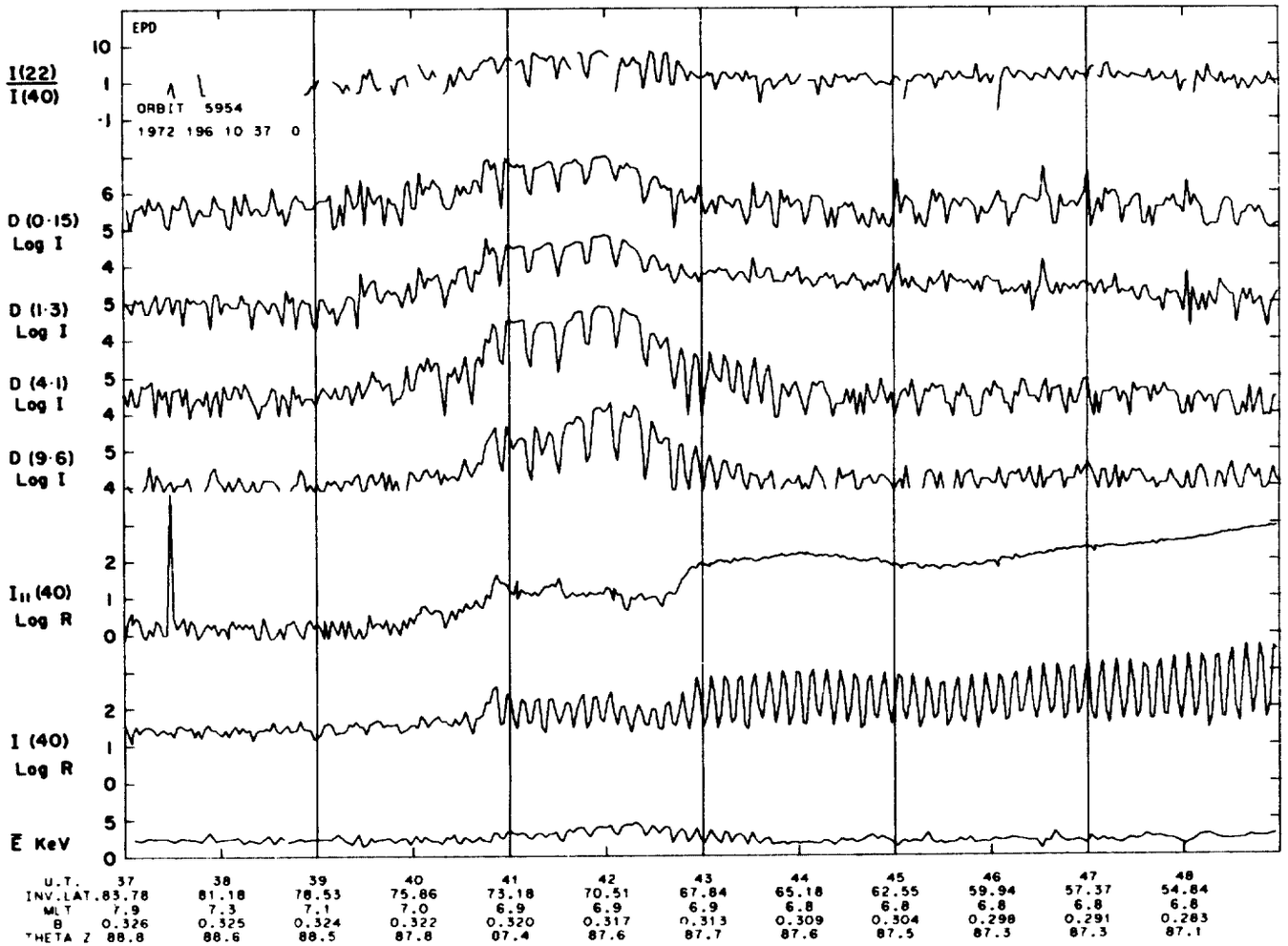

SET 4, FORMAT 3

ORBIT 5954
DATE 720714
DAY 196

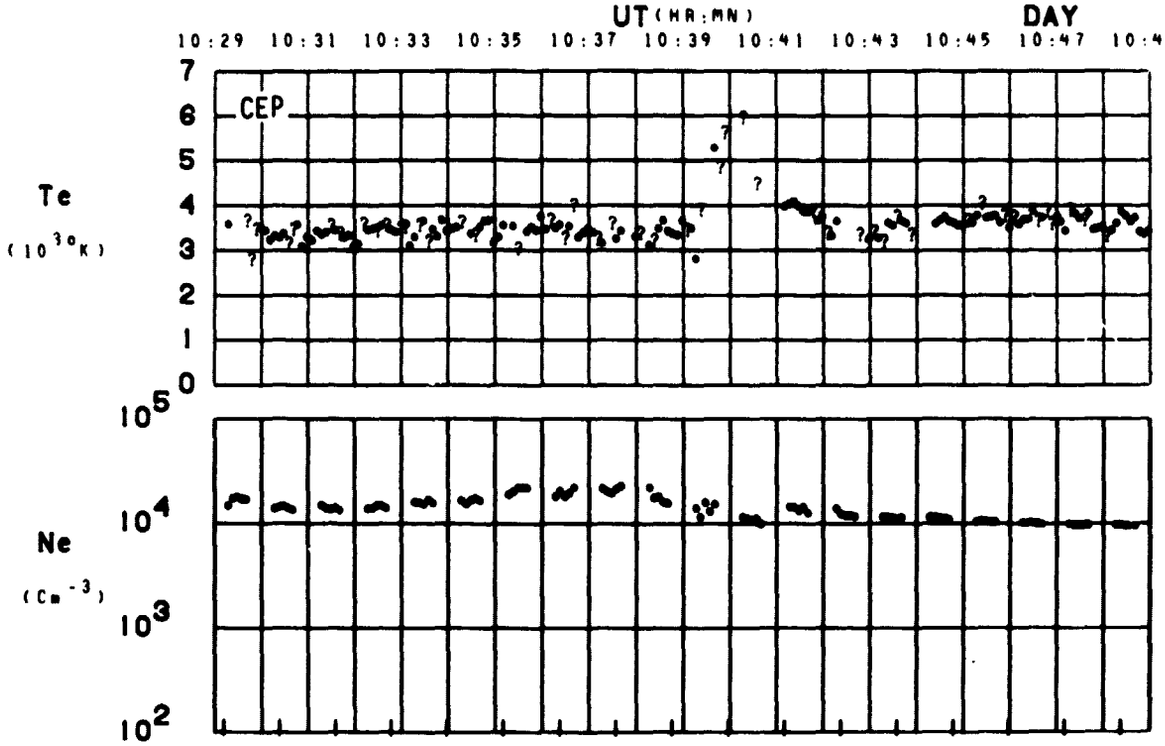

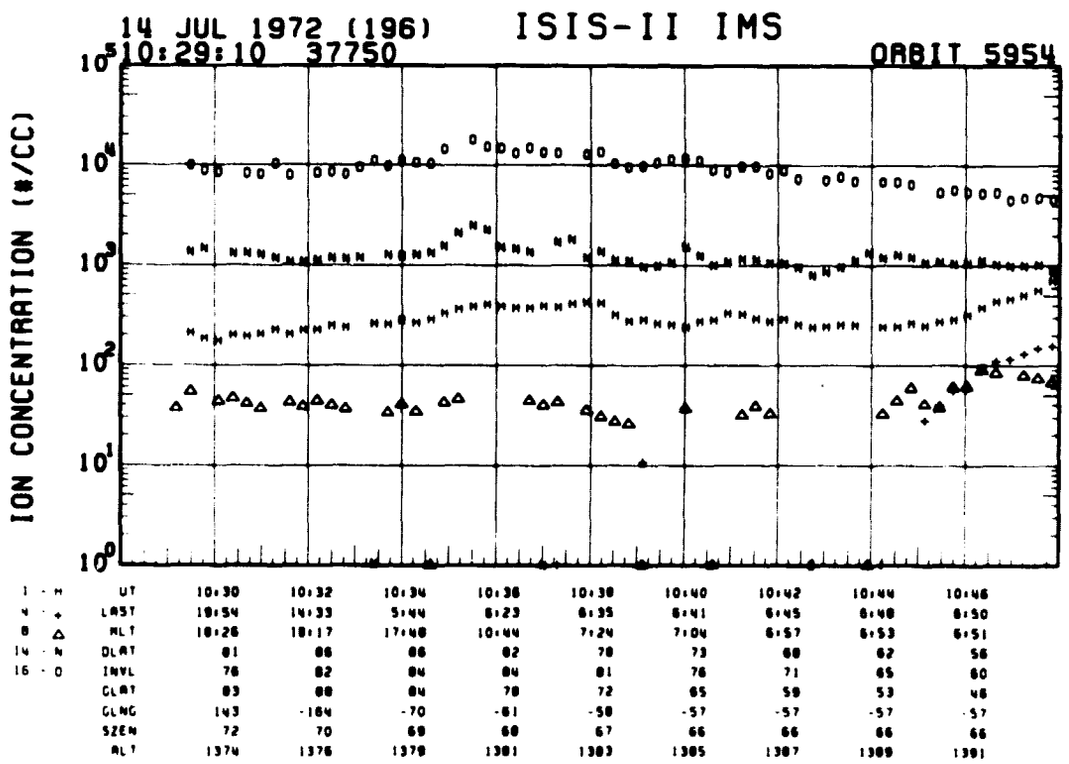

1 - H	UT	10:30	10:32	10:34	10:36	10:38	10:40	10:42	10:44	10:46
H - +	LAST	19:54	14:33	5:44	6:23	6:35	6:41	6:45	6:48	6:50
8 - △	MLT	18:26	18:17	17:48	10:44	7:24	7:04	6:57	6:53	6:51
14 - N	DLAT	81	86	88	82	78	73	68	62	56
16 - O	INVL	76	82	84	84	81	76	71	65	60
	GLAT	83	88	84	78	72	65	59	53	48
	GLNG	143	-164	-70	-81	-58	-57	-57	-57	-57
	SZEN	72	70	69	68	67	66	66	66	66
	ALT	1374	1376	1378	1381	1383	1385	1387	1389	1391

SET 4, FORMAT 4

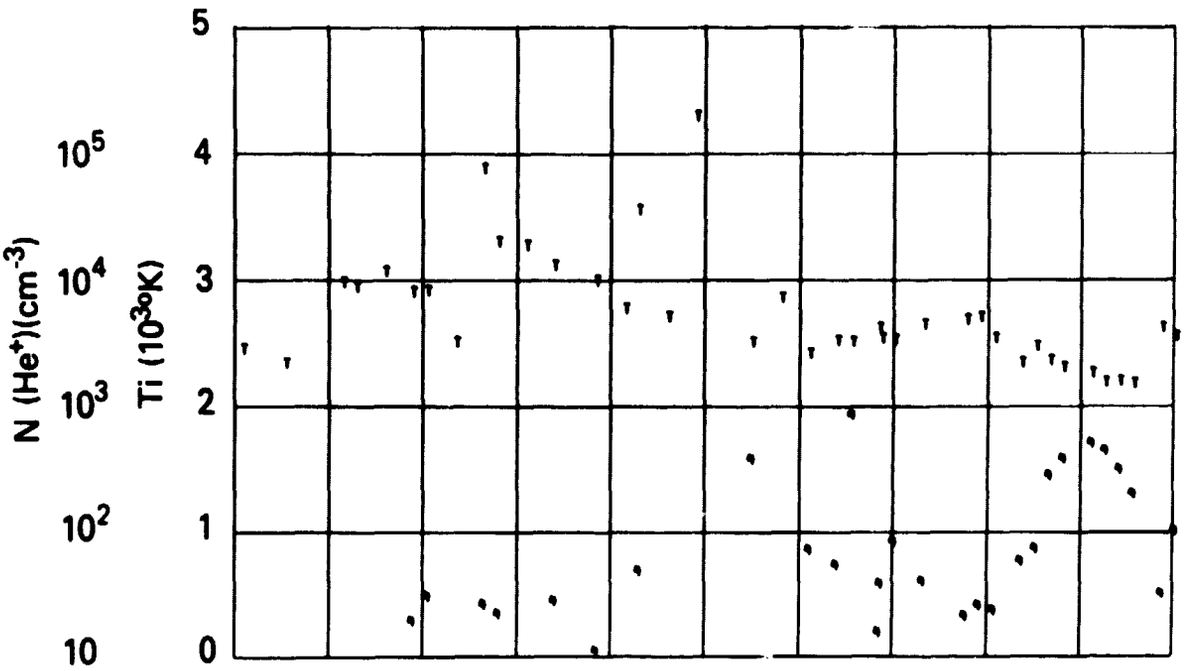

UT	10:30	10:32	10:34	10:36	10:38	10:40	10:42	10:44	10:46
LAST	19:54	14:33	5:44	0:23	0:35	0:41	0:45	0:48	0:50
MLT	18:26	18:17	17:48	10:44	7:24	7:04	6:57	6:53	6:51
DLAT	81	86	86	82	78	73	68	62	56
INVL	76	82	84	84	81	76	71	65	60
GLAT	83	88	84	78	72	65	58	53	48
GLNG	143	-164	-70	-61	-58	-57	-57	-57	-57
SZEN	72	70	69	68	67	66	66	66	66
ALT	1374	1376	1379	1381	1383	1385	1387	1389	1391

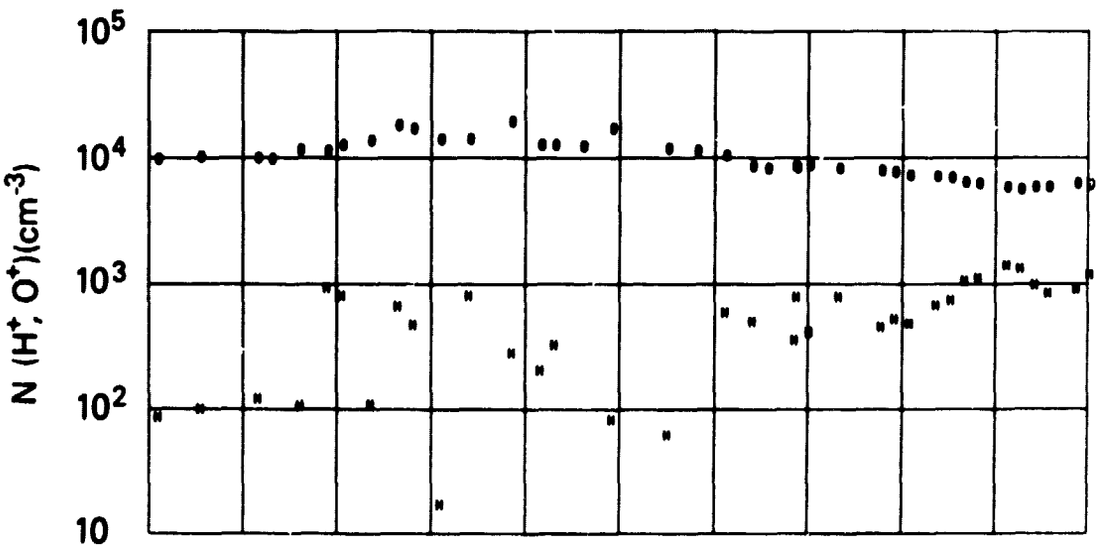

SET 4, FORMAT 5

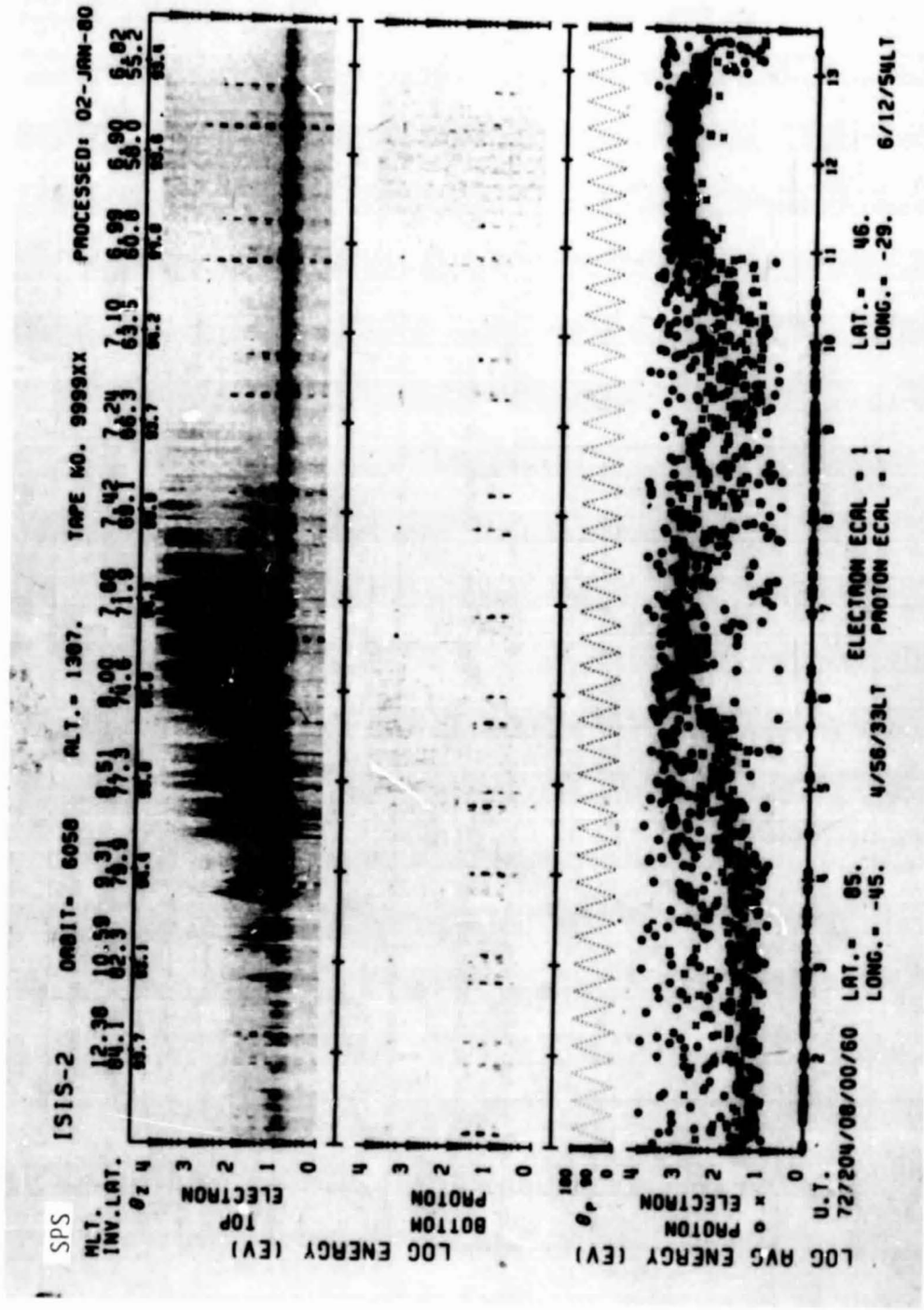

SPS

SET 5, FORMAT 6

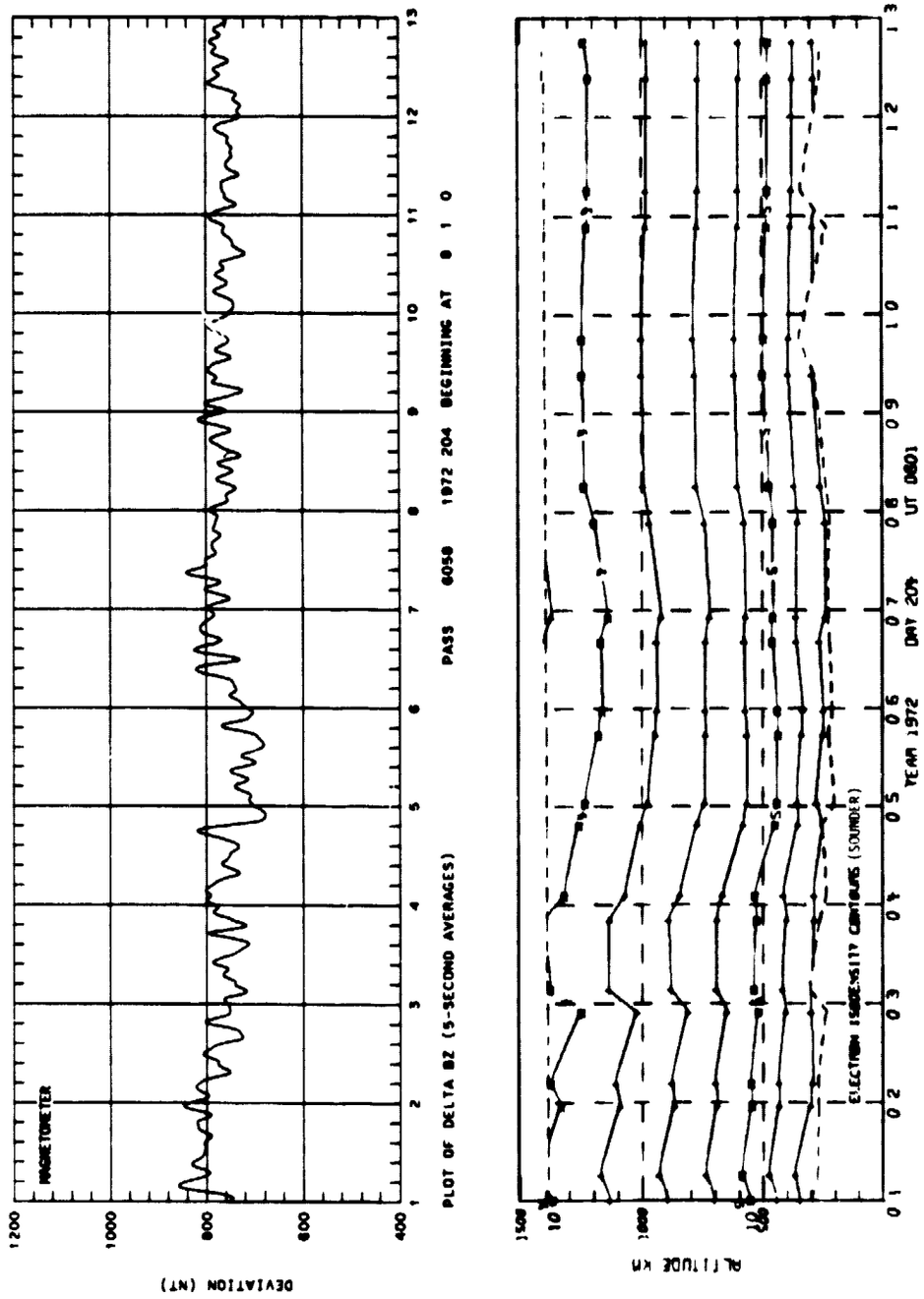

SET 5, FORMAT 2

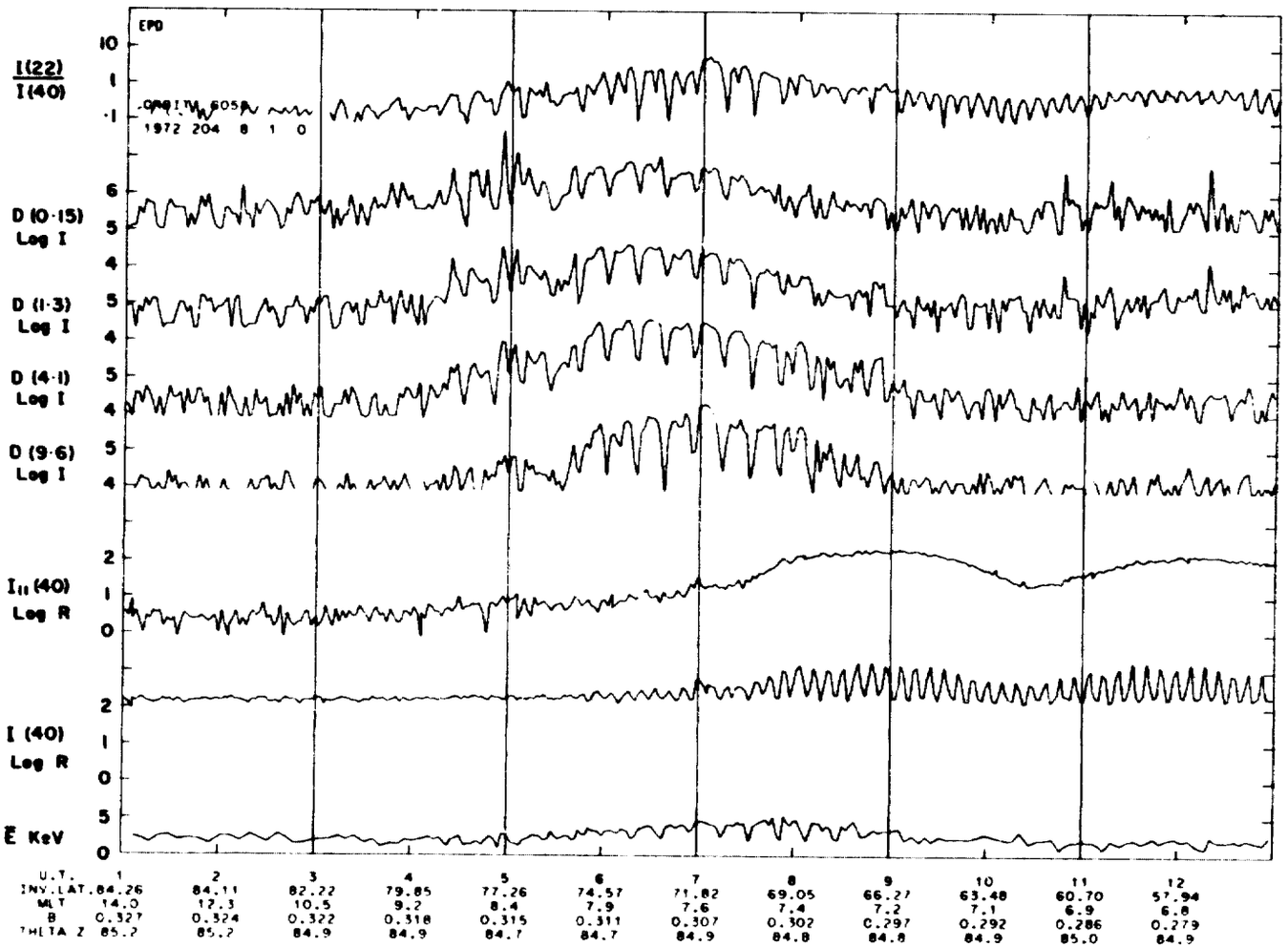

SET 5, FORMAT 3

ORBIT 6058
DATE 720722
DAY 204

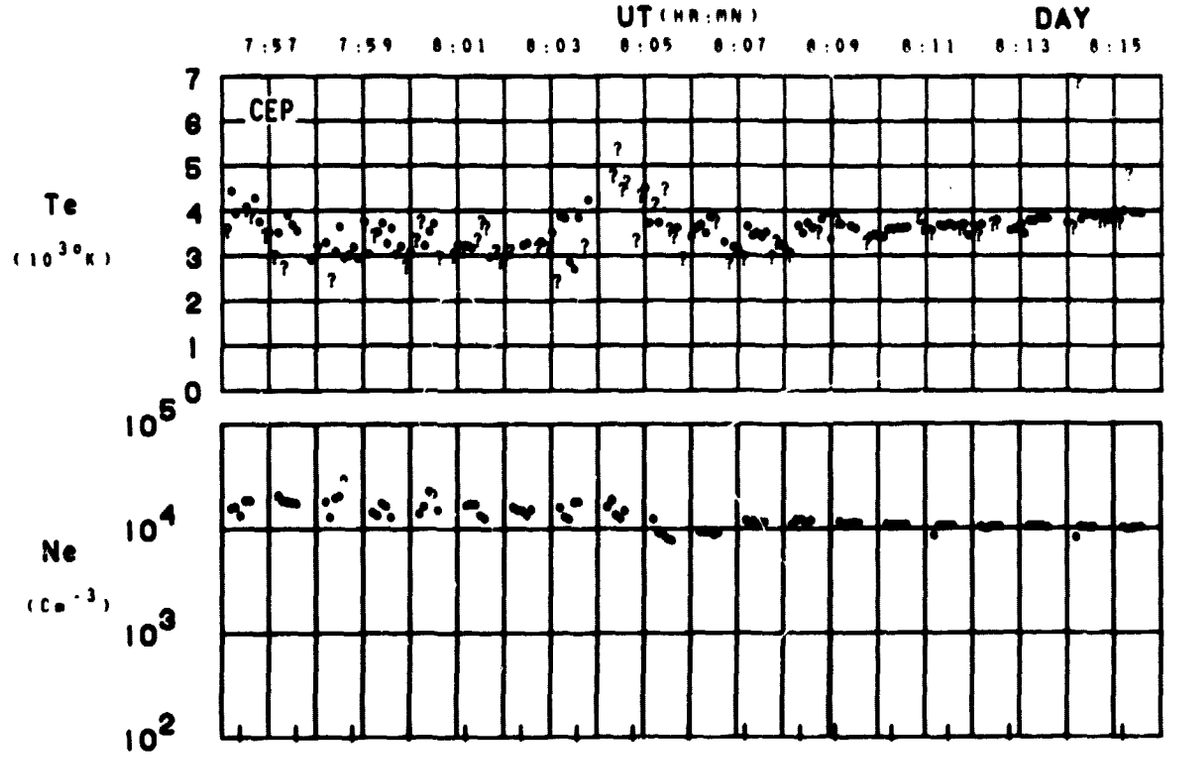

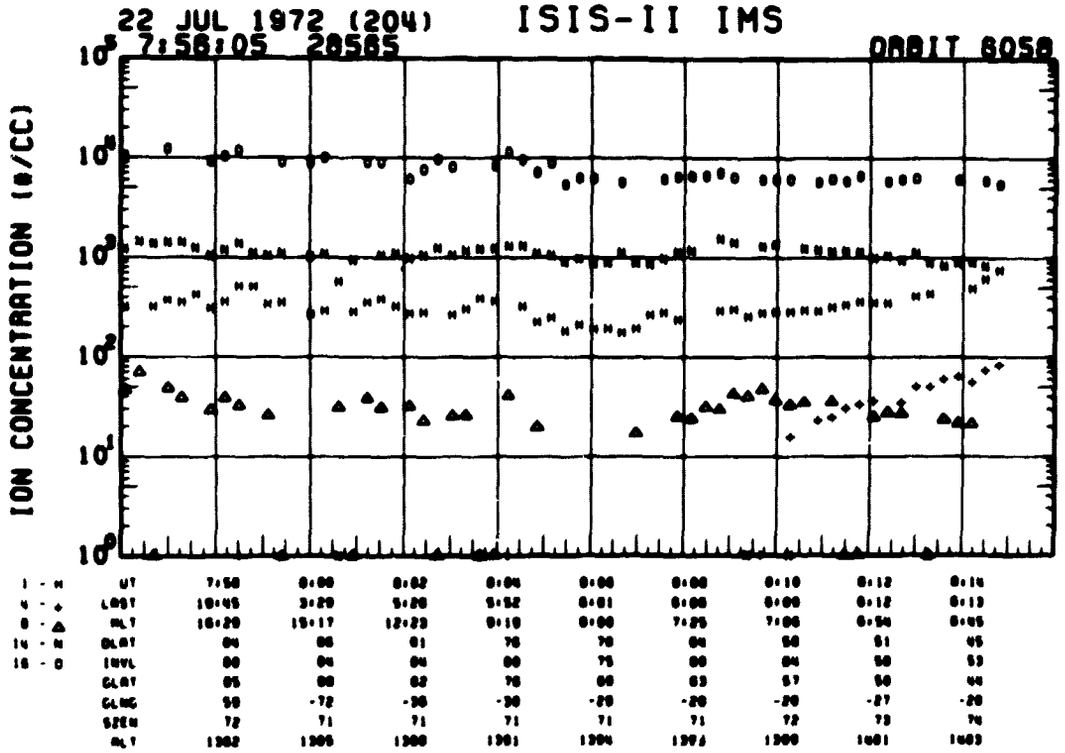

SET 5, FORMAT 4

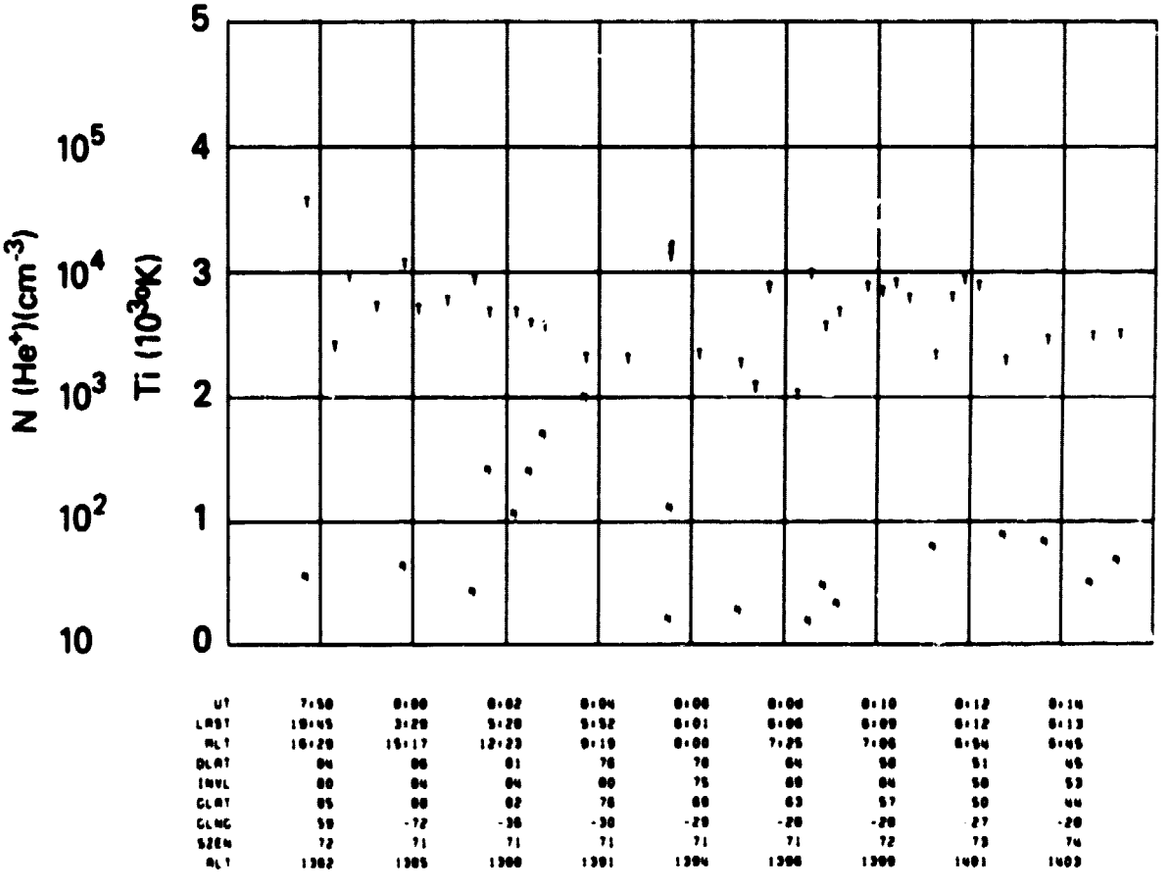

UT	7:58	8:00	8:02	8:04	8:06	8:08	8:10	8:12	8:14
LAST	19:45	3:28	5:28	5:52	6:01	6:06	6:09	6:12	6:13
MLT	16:29	15:17	12:23	9:19	8:08	7:25	7:06	6:54	6:45
DLAT	84	86	81	76	70	64	58	51	45
INVL	88	84	84	80	75	69	64	58	53
GLAT	85	88	82	76	68	63	57	50	44
GLNG	59	-72	-36	-30	-28	-28	-28	-27	-28
SZEN	72	71	71	71	71	71	72	73	74
ALT	1382	1385	1388	1391	1394	1398	1399	1401	1403

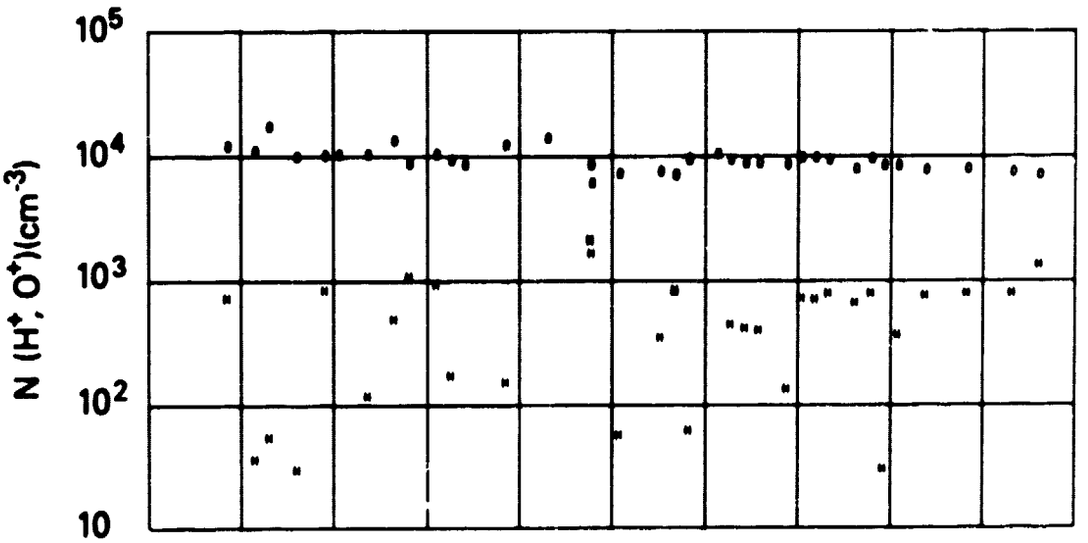

SET 5, FORMAT 5

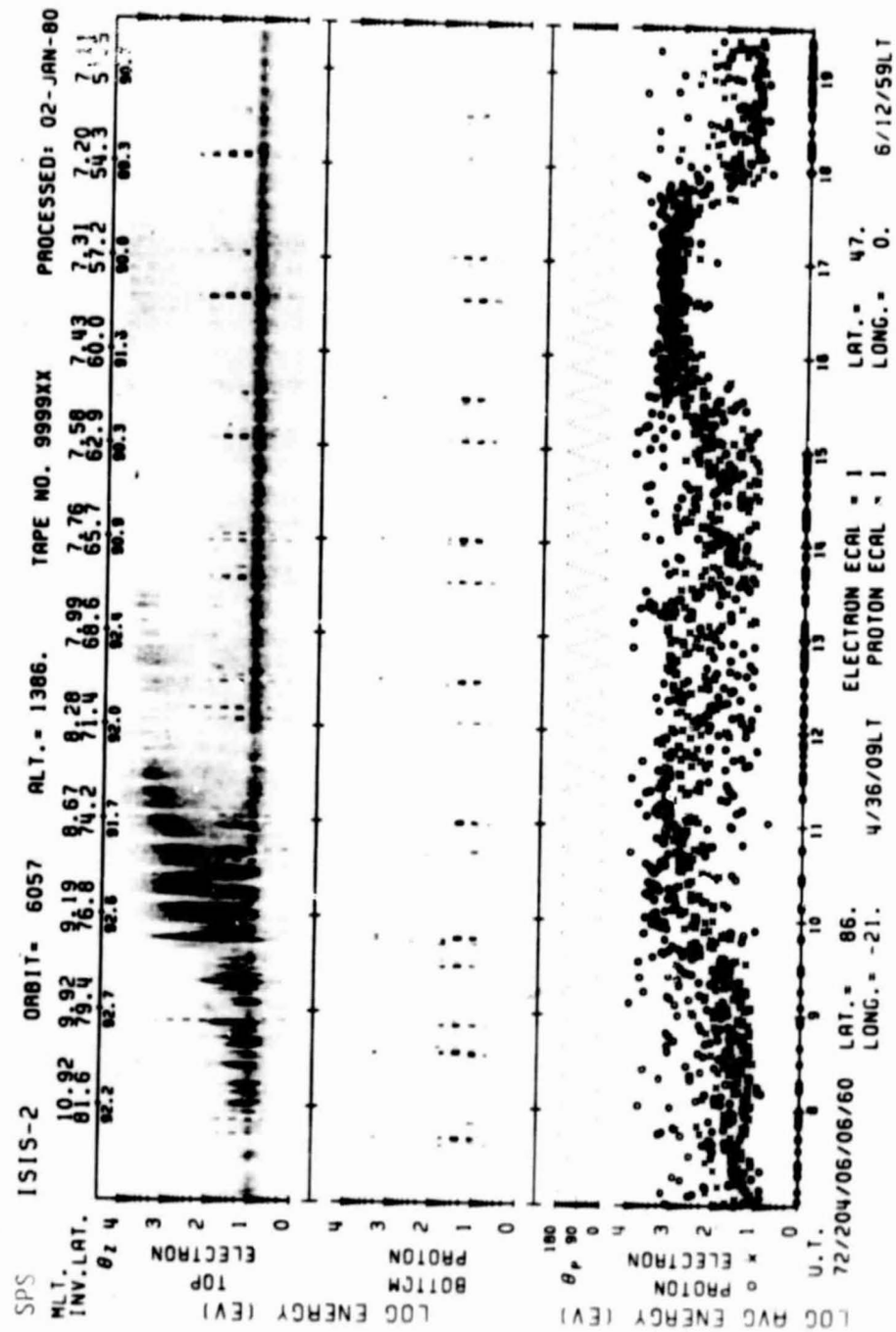

SET 6, FORMAT 6

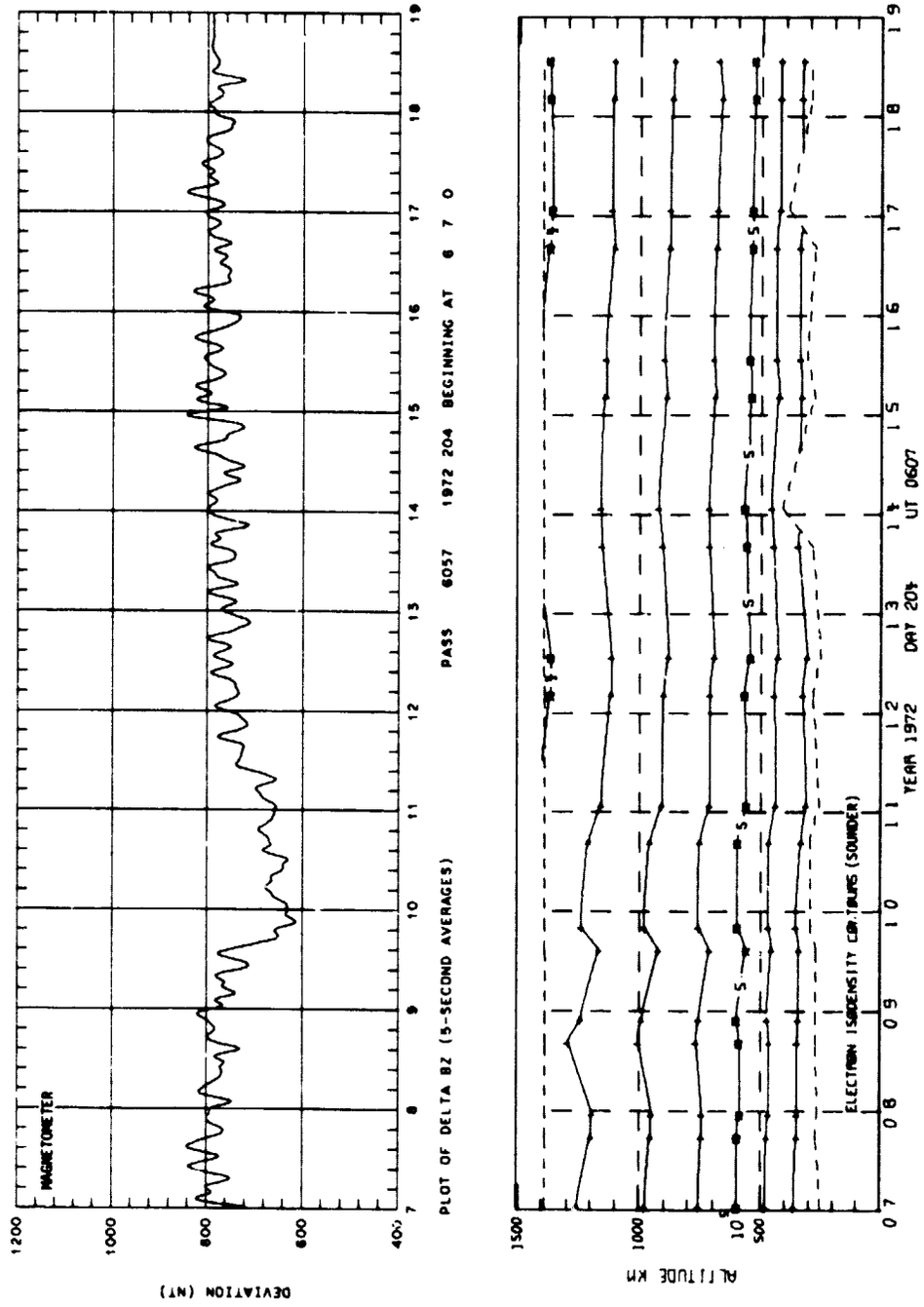

SET 6, FORMAT 2

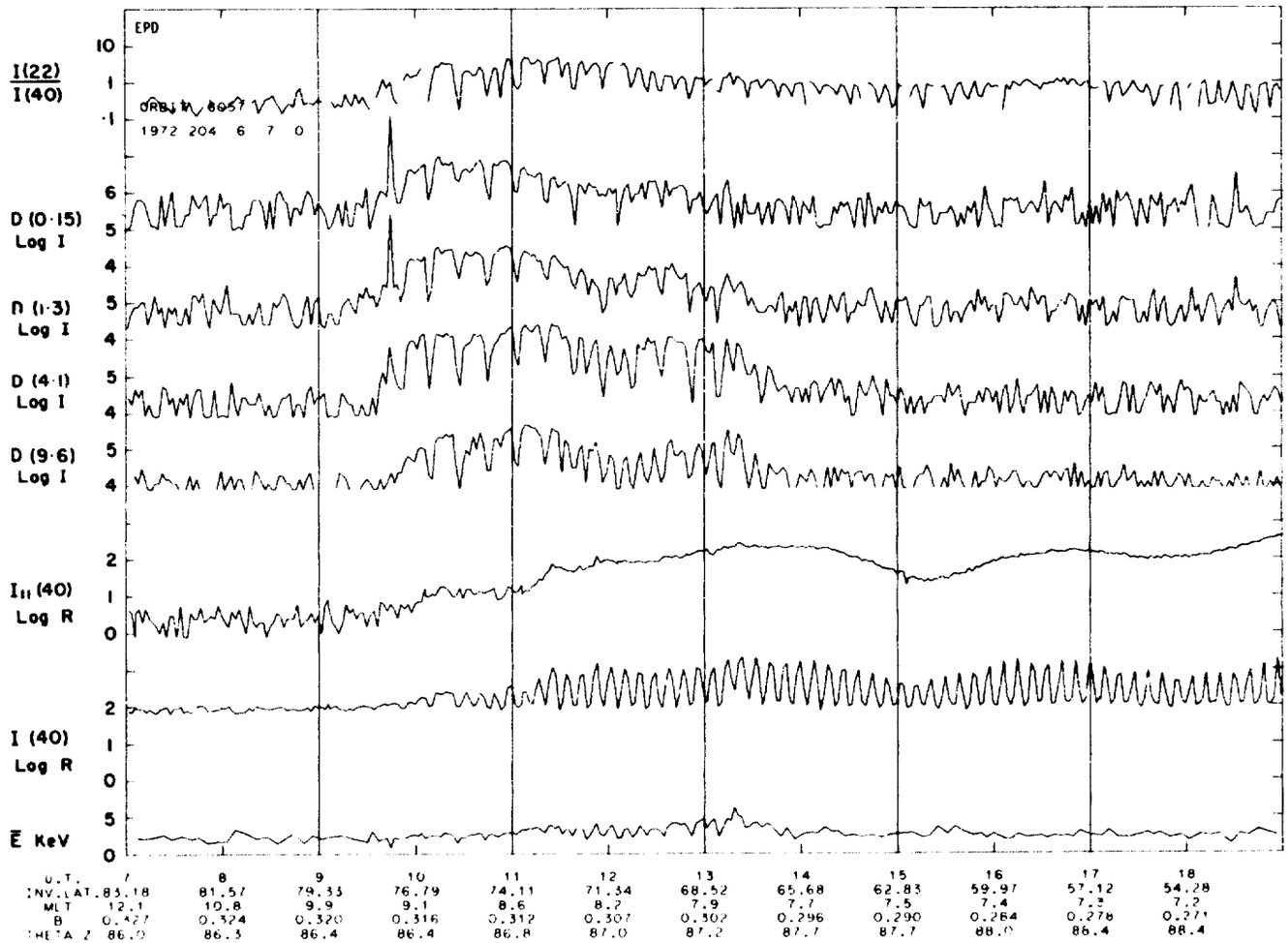

SET 6, FORMAT 3

ORBIT 6057
DATE 720722
DAY 204

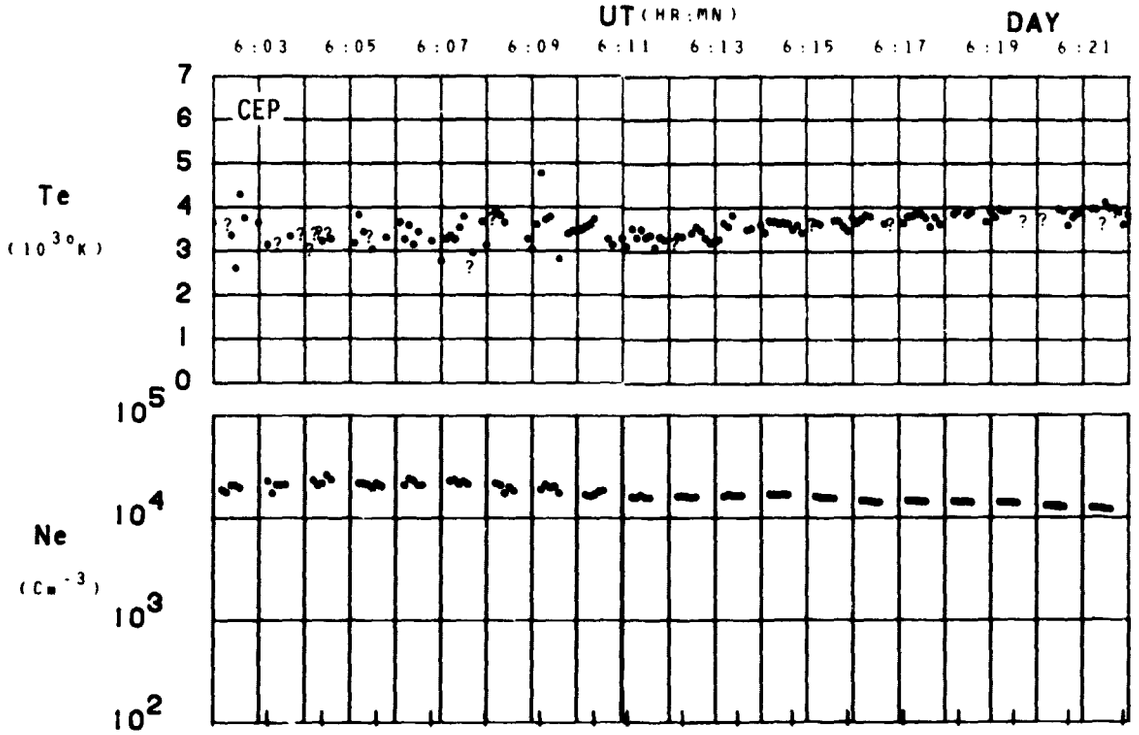

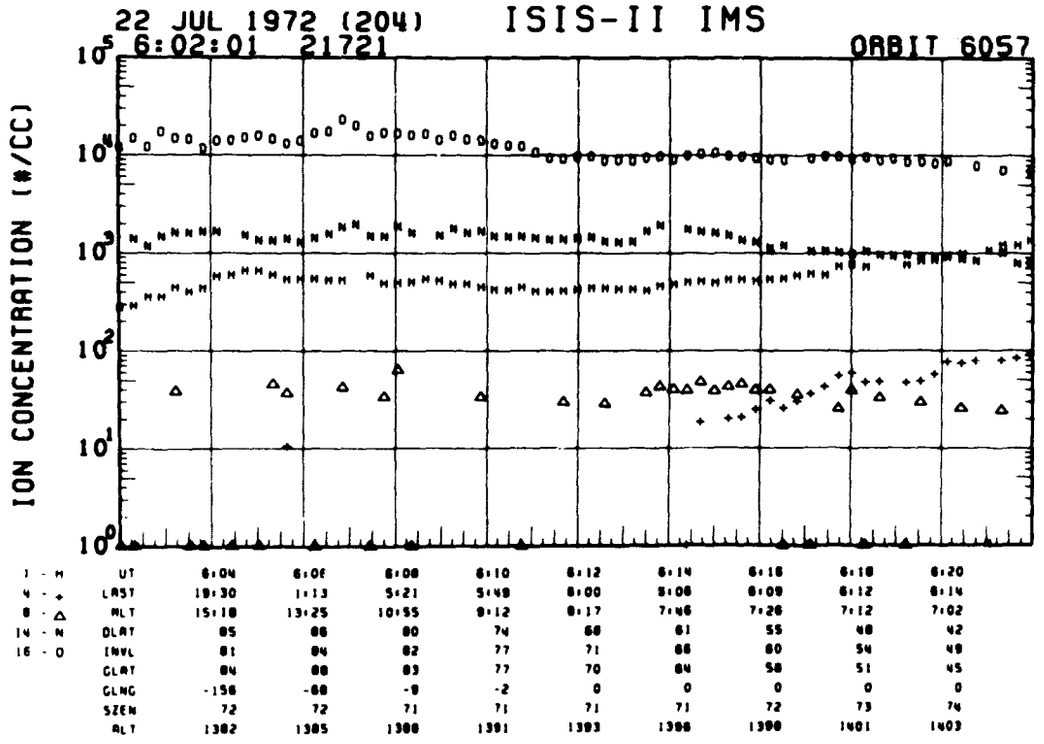

1 - H	UT	6:04	6:06	6:08	6:10	6:12	6:14	6:16	6:18	6:20
4 - +	LAST	19:30	1:13	5:21	5:48	8:00	5:08	6:09	6:12	6:14
8 - △	MLT	15:18	13:25	10:55	9:12	8:17	7:46	7:26	7:12	7:02
14 - N	DLAT	85	86	80	74	68	61	55	48	42
16 - O	INVL	81	84	82	77	71	66	60	54	48
	GLAT	84	88	83	77	70	64	58	51	45
	GLNG	-156	-68	-9	-2	0	0	0	0	0
	SZEN	72	72	71	71	71	71	72	73	74
	ALT	1382	1385	1388	1391	1393	1398	1398	1401	1403

SET 6, FORMAT 4

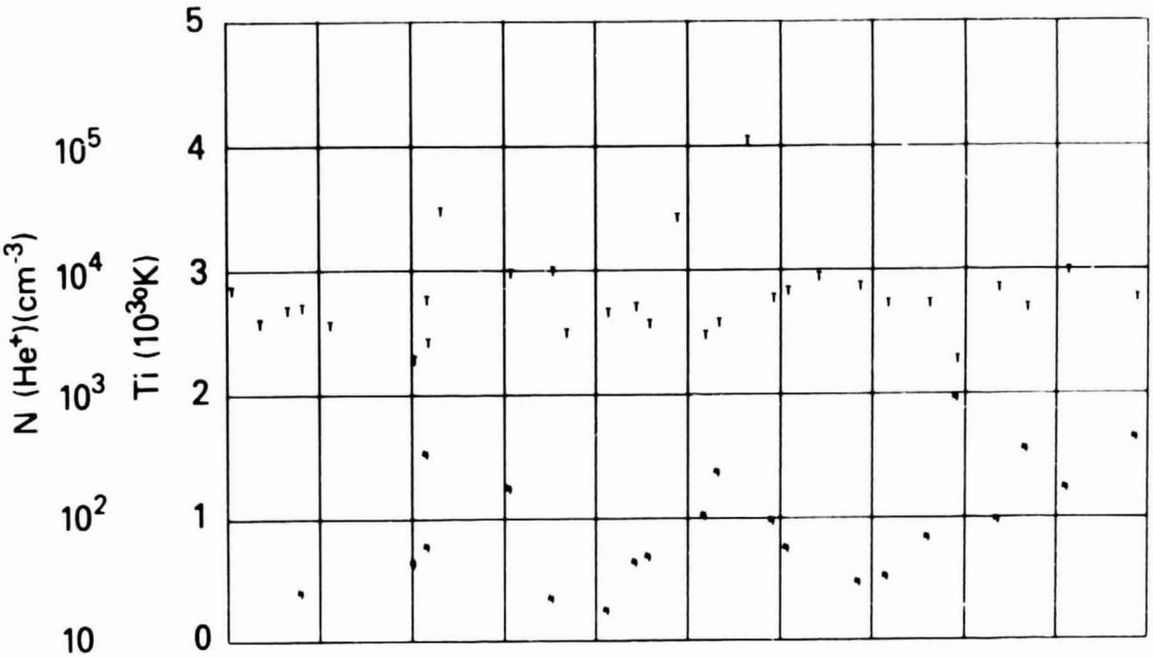

UT	6:04	6:06	6:08	6:10	6:12	6:14	6:16	6:18	6:20
LAST	19:30	1:13	5:21	5:49	6:00	6:08	6:09	6:12	6:14
MLT	15:18	13:25	10:55	9:12	8:17	7:46	7:26	7:12	7:02
DLAT	85	86	80	74	68	61	55	48	42
INVL	81	84	82	77	71	66	60	54	49
GLAT	84	88	83	77	70	64	58	51	45
GLNG	-156	-68	-9	-2	0	0	0	0	0
SZEN	72	72	71	71	71	71	72	73	74
ALT	1382	1385	1388	1391	1393	1396	1398	1401	1403

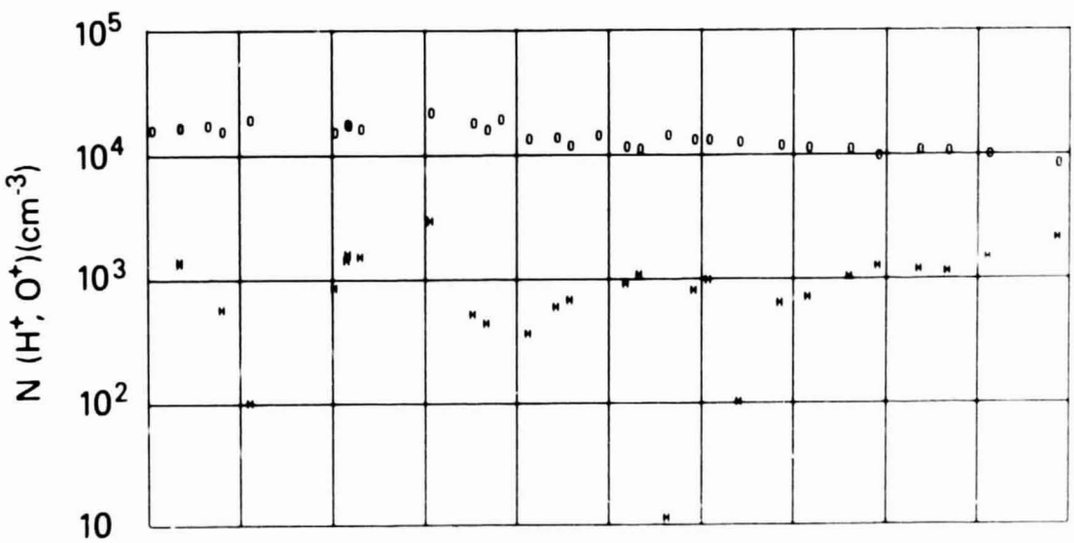

SET 6, FORMAT 5

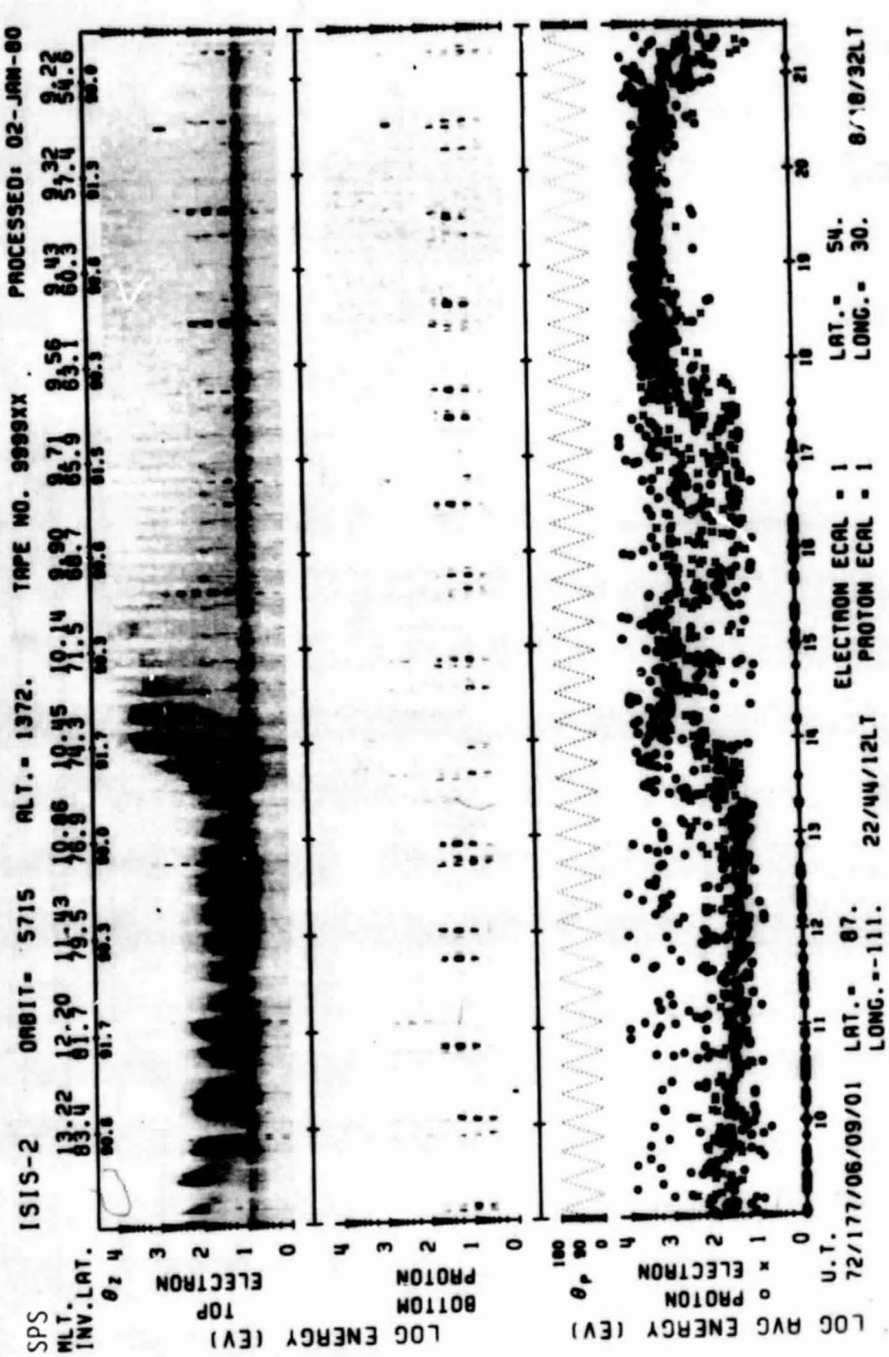

SET 7, FORMAT 6

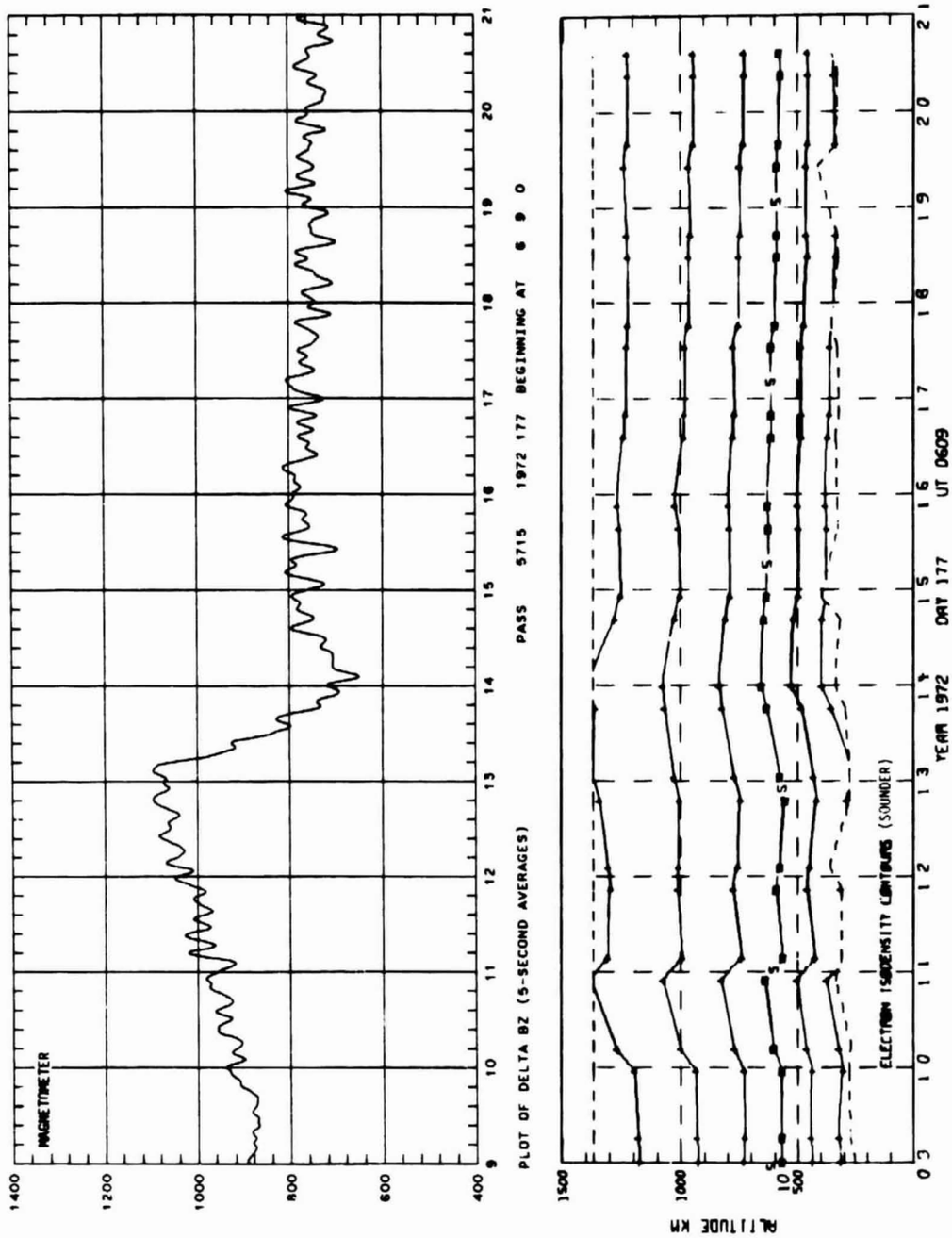

SET 7, FORMAT 2

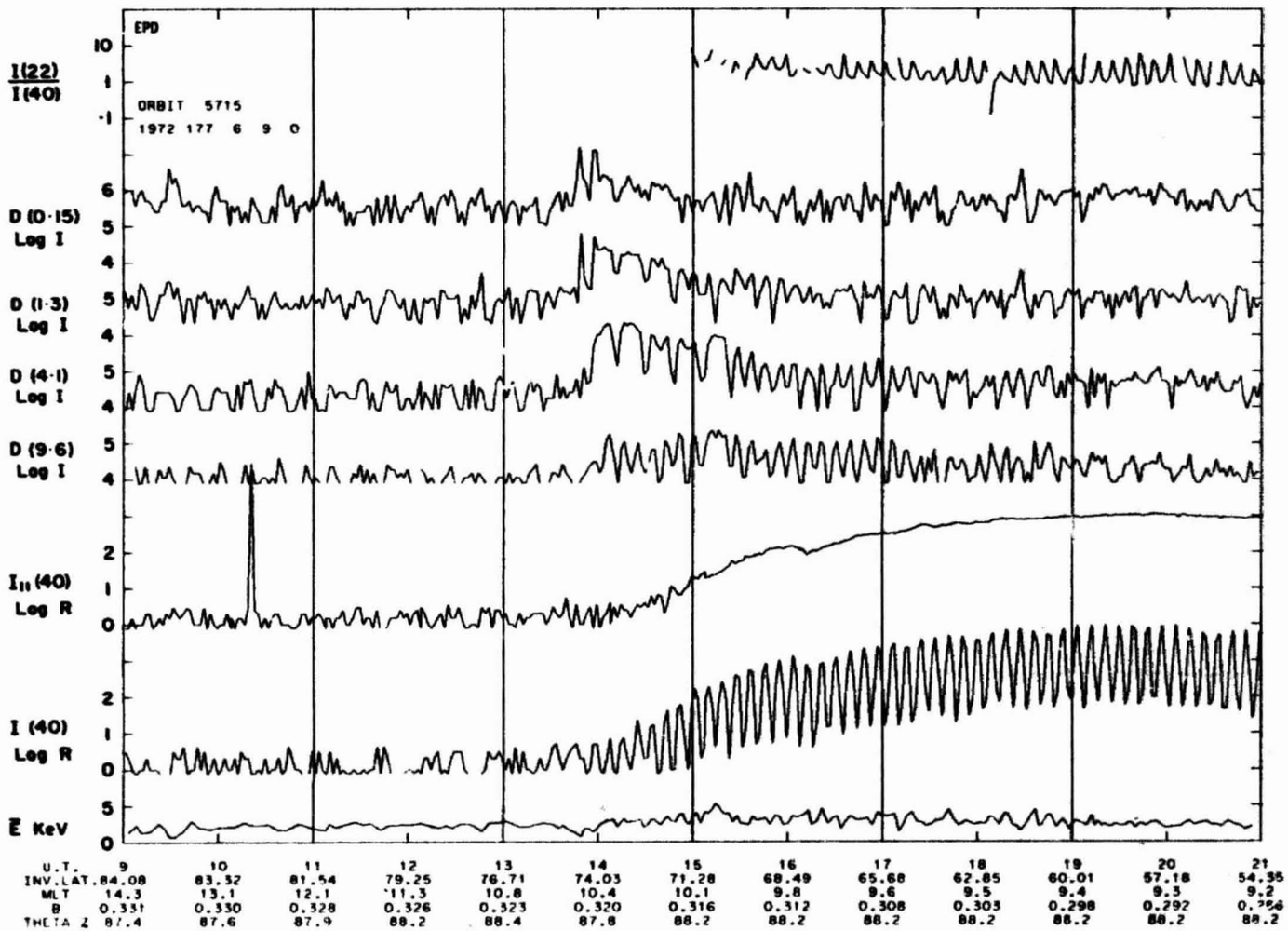

SET 7, FORMAT 3

ORBIT 5715
DATE 720625
DAY 177

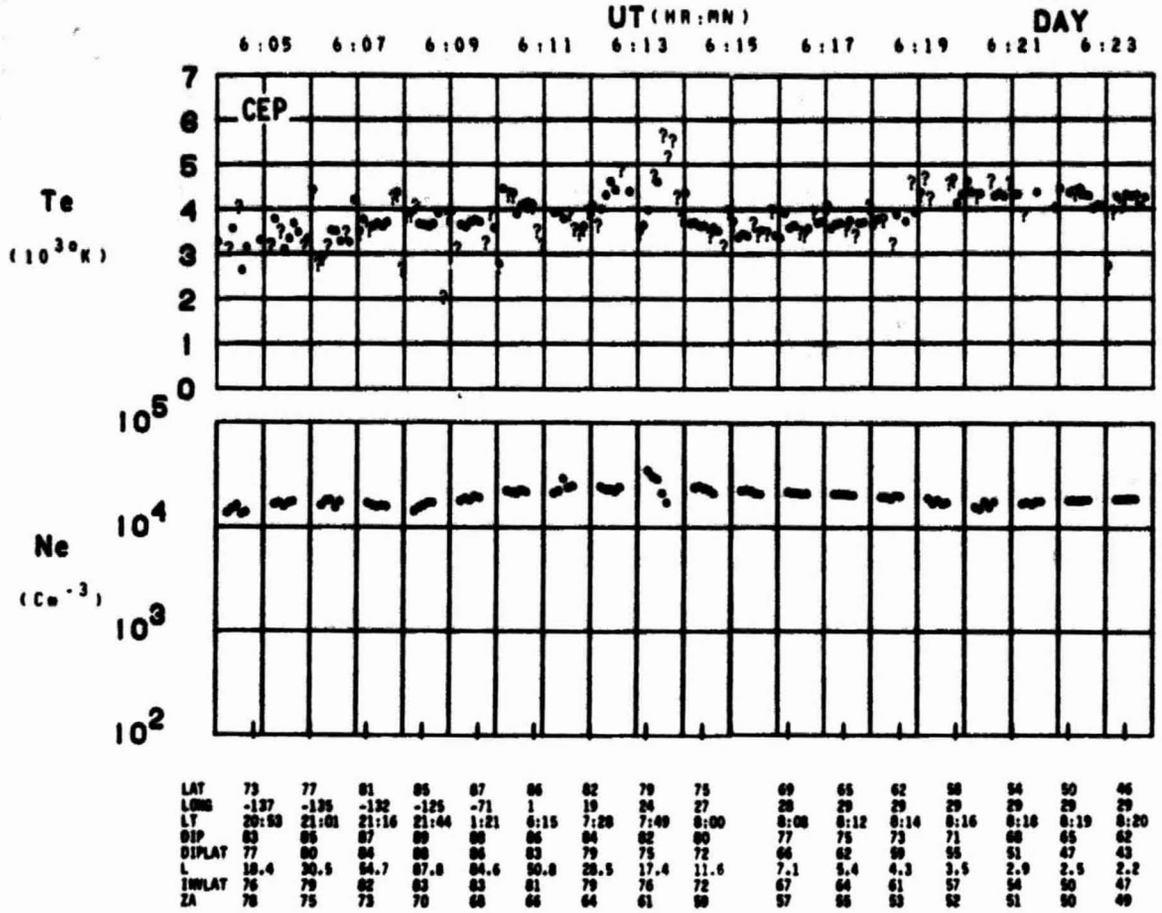

LAT	73	77	81	85	87	86	82	79	75	69	65	62	58	54	50	46
LONG	-137	-135	-132	-125	-71	1	19	24	27	28	29	29	29	29	29	29
LT	20:53	21:01	21:16	21:44	1:21	6:15	7:28	7:49	8:00	8:08	8:12	8:14	8:16	8:18	8:19	8:20
DIP	83	86	87	89	88	86	84	82	80	77	75	73	71	68	65	62
DIPLAT	77	80	84	88	86	83	79	75	72	66	62	59	55	51	47	43
L	10.4	30.5	64.7	87.8	84.6	50.8	28.5	17.4	11.6	7.1	5.4	4.3	3.5	2.9	2.5	2.2
INVLAT	76	79	82	83	83	81	79	76	72	67	64	61	57	54	50	47
ZA	78	75	73	70	68	66	64	61	59	57	55	53	52	51	50	49

SET 7, FORMAT 4

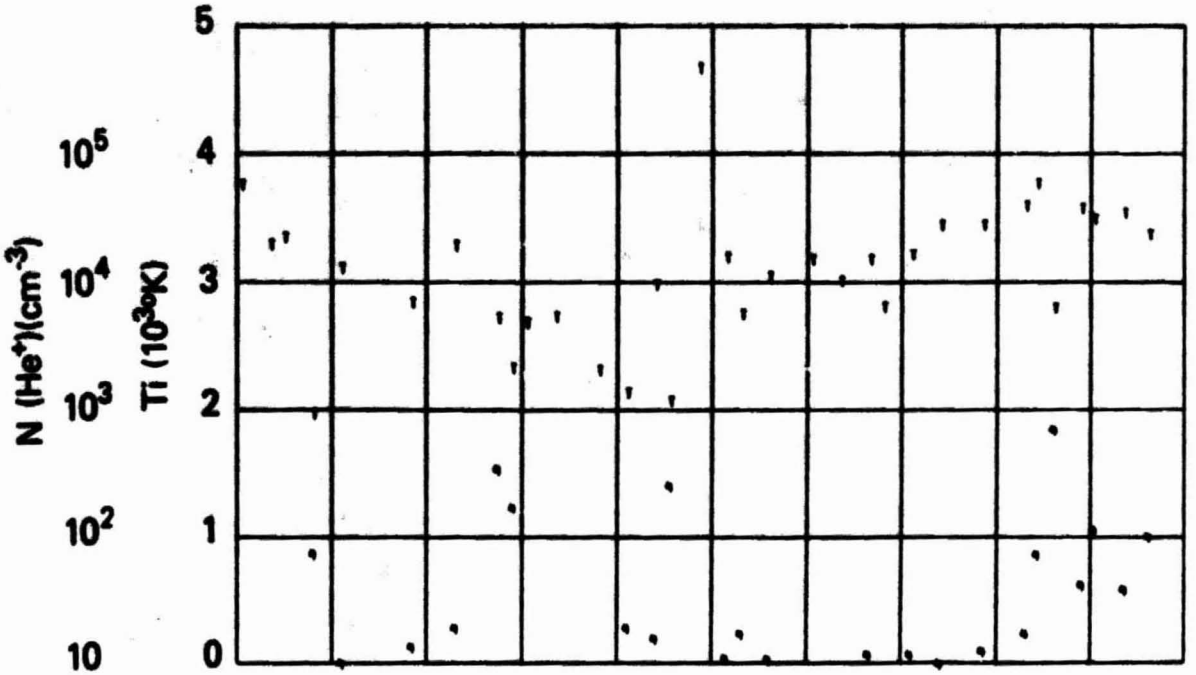

UT	06:06	06:08	06:10	06:12	06:14	06:16	06:18	06:20	06:22
LAST	21:01	21:36	03:17	07:28	07:57	08:08	08:13	08:17	08:19
MLT	17:43	15:24	12:10	10:30	09:45	09:21	09:06	08:56	08:49
DLAT									
INVL	79	83	83	79	77	69	63	57	52
GLAT	78	84	88	83	77	70	64	58	52
GLNG	-136	-127	-43	20	25	29	30	30	30
SZEN	75	71	67	64	60	57	54	52	50
ALT	1373	1372	1371	1370	1369	1369	1368	1368	1368

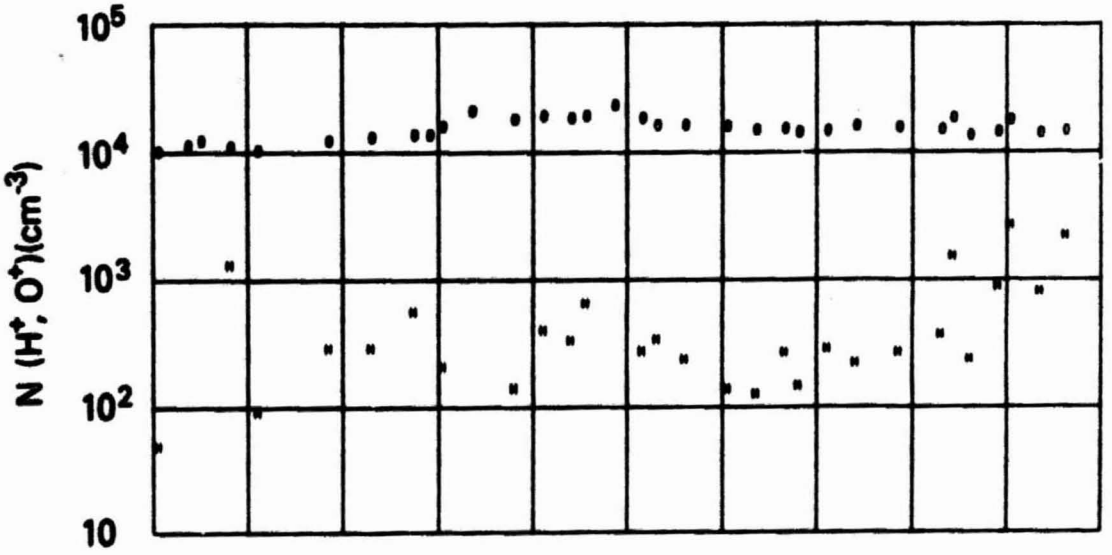

SET 7, FORMAT 5

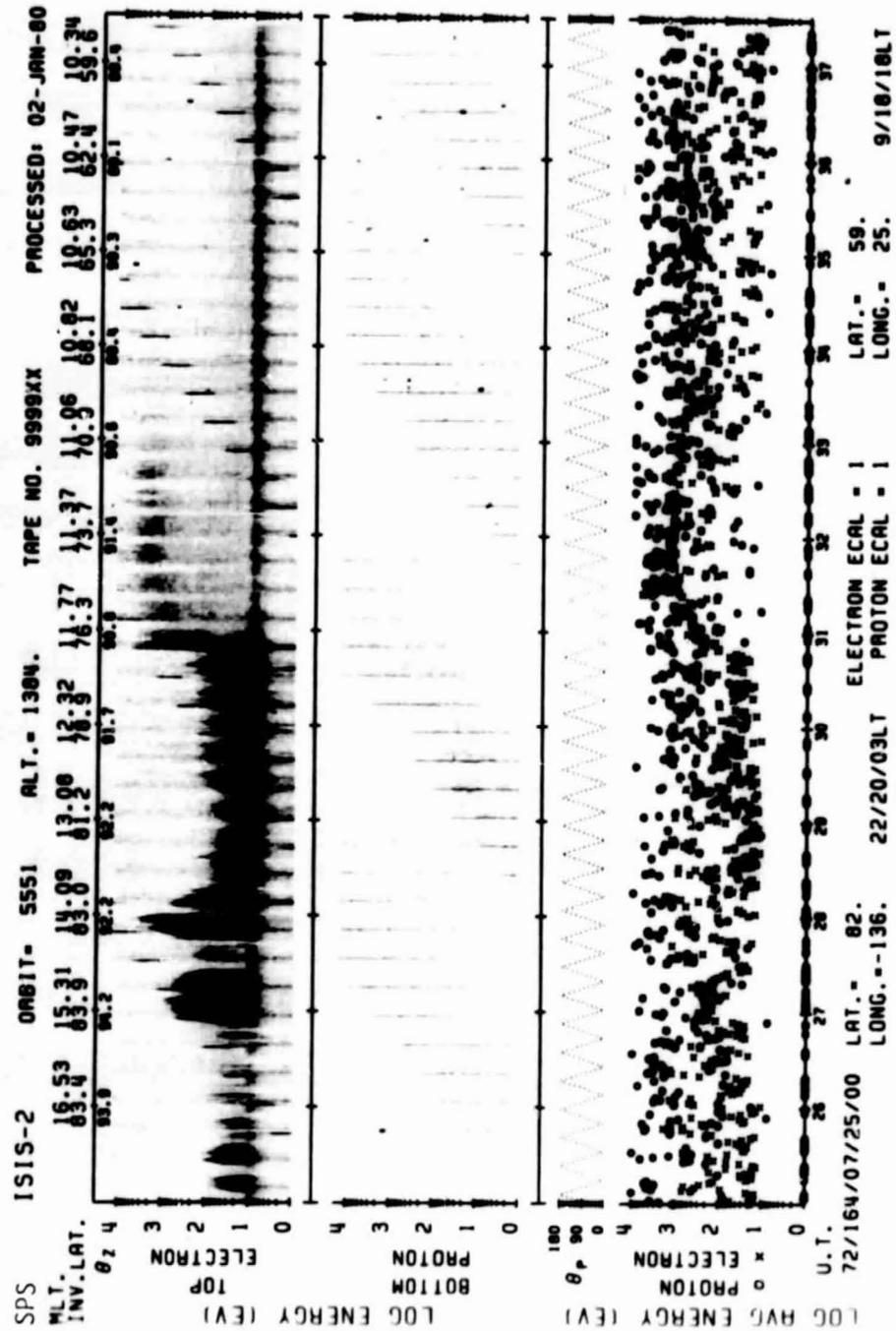

SET 8, FORMAT 6

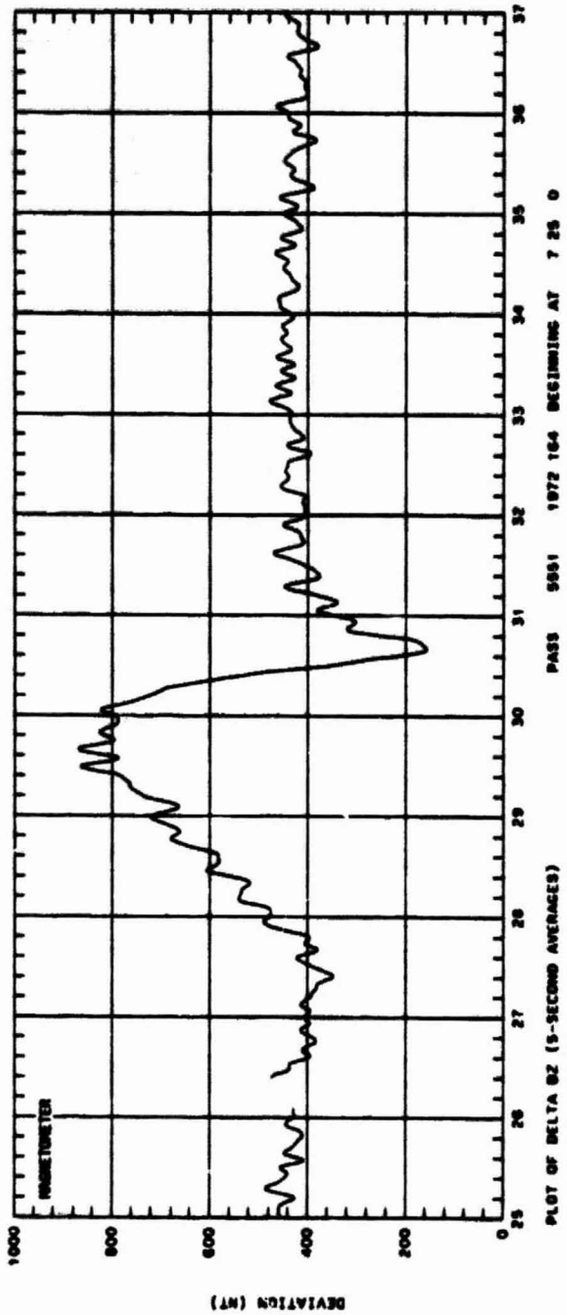

SET 8, FORMAT 2

SET 8, FORMAT 3

ORBIT 5551
DATE 720612
DAY 164

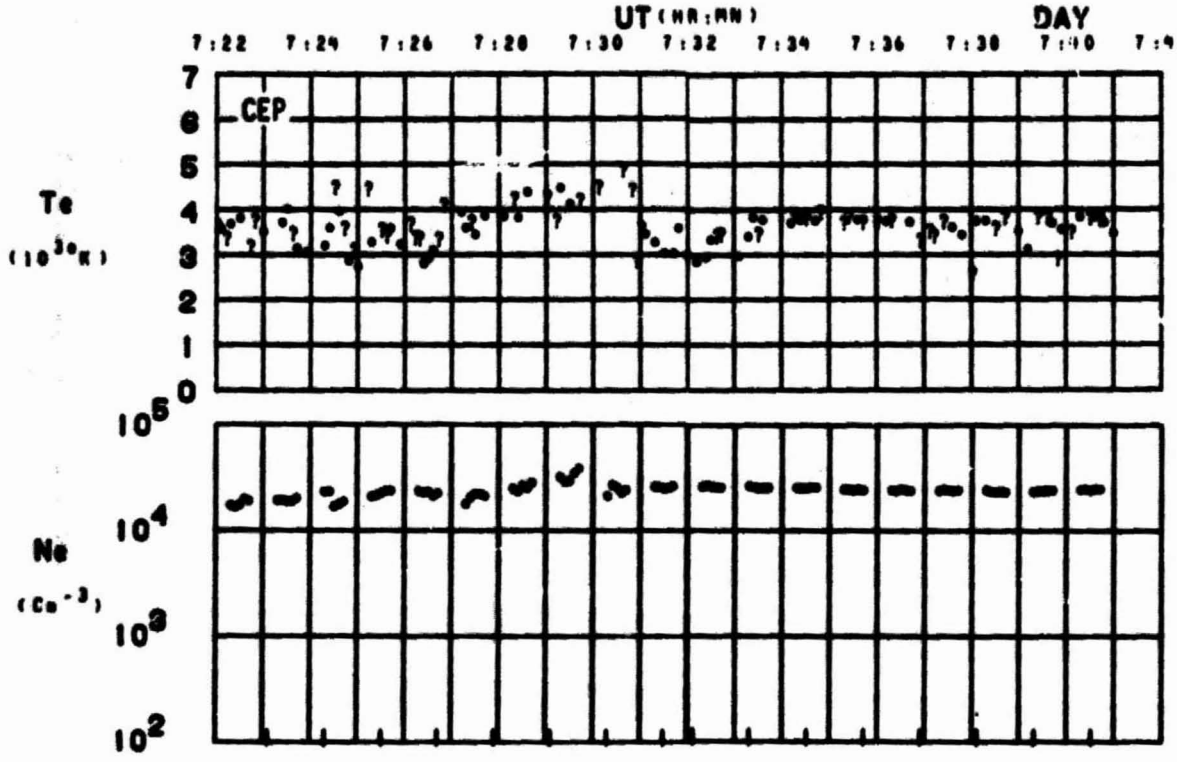

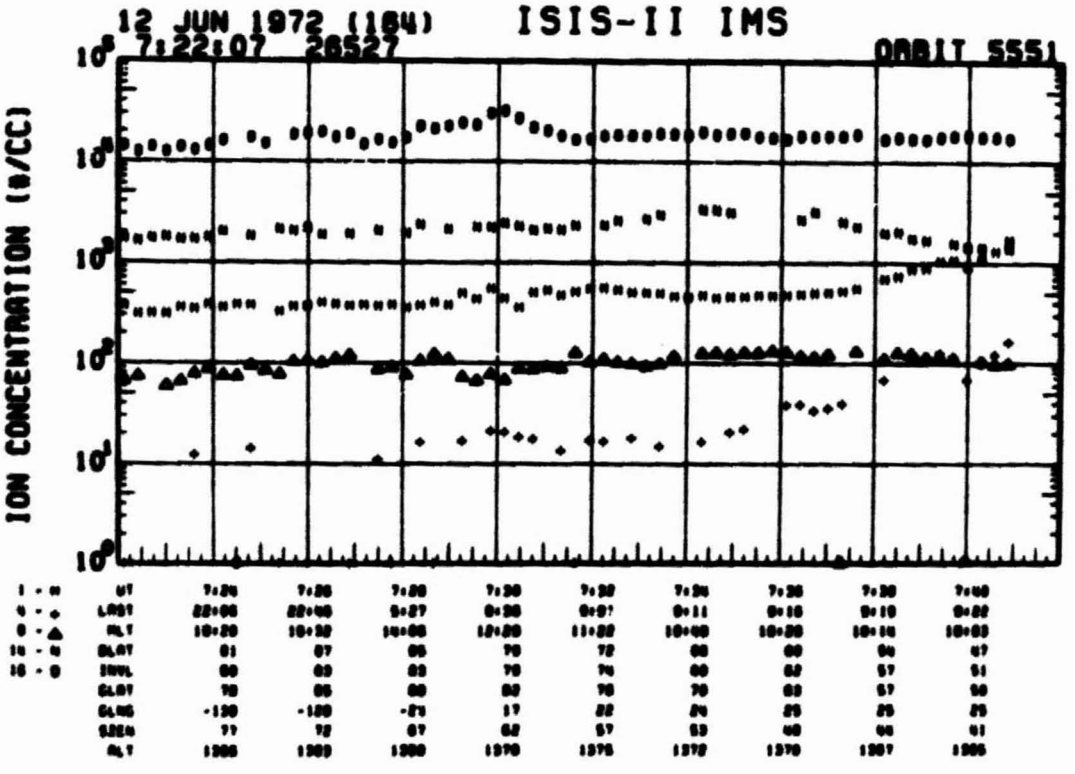

SET 8, FORMAT 4

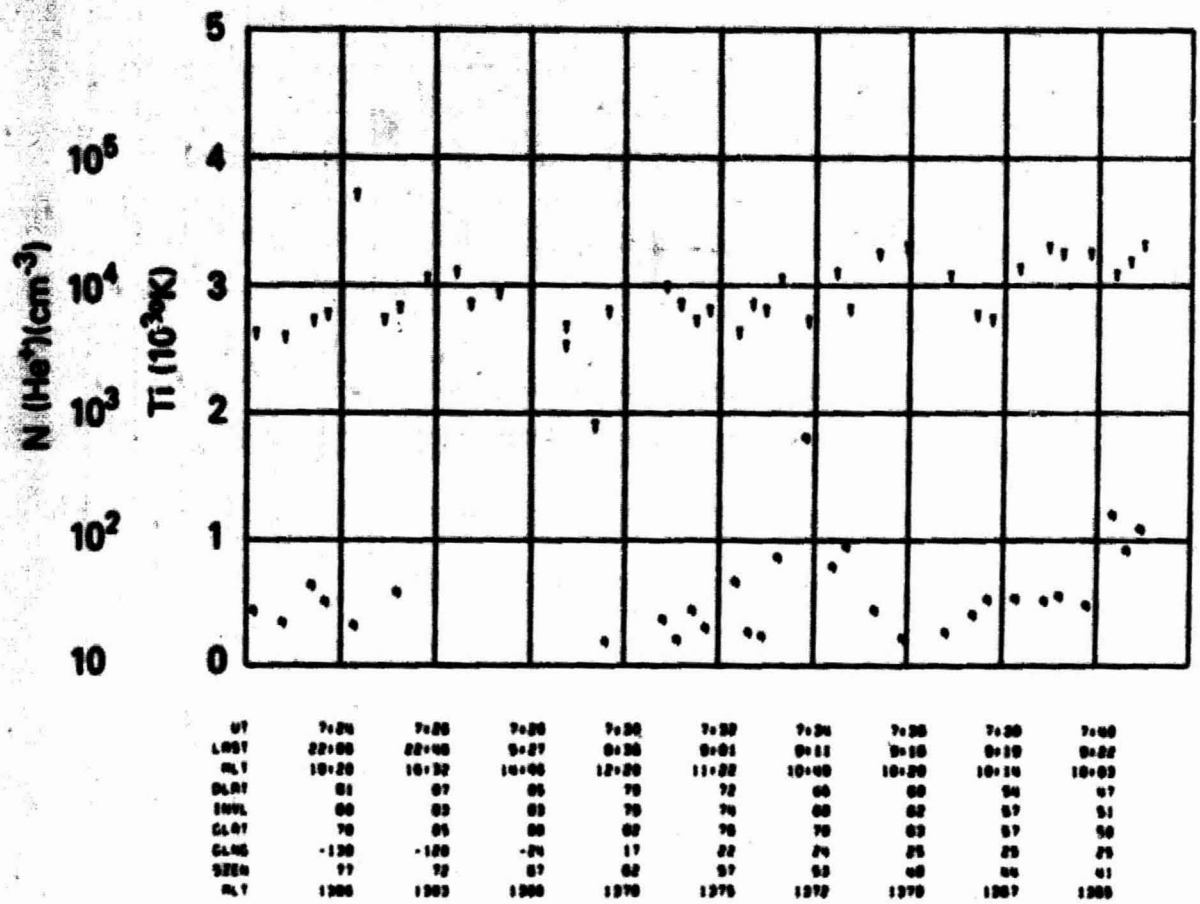

UT	7:24	7:26	7:28	7:30	7:32	7:34	7:36	7:38	7:40
LAT	22:08	22:48	9:27	9:36	9:01	9:11	9:19	9:19	9:22
MLT	10:20	10:32	10:08	12:20	11:02	10:48	10:20	10:14	10:03
GLAT	81	87	85	79	72	66	60	54	47
GLON	60	83	83	79	76	68	62	57	51
GLAT	70	85	88	82	76	70	63	57	50
GLON	-130	-120	-24	17	22	24	25	25	25
SZEN	77	72	67	62	57	53	48	44	41
ALT	1386	1383	1380	1378	1375	1372	1370	1367	1365

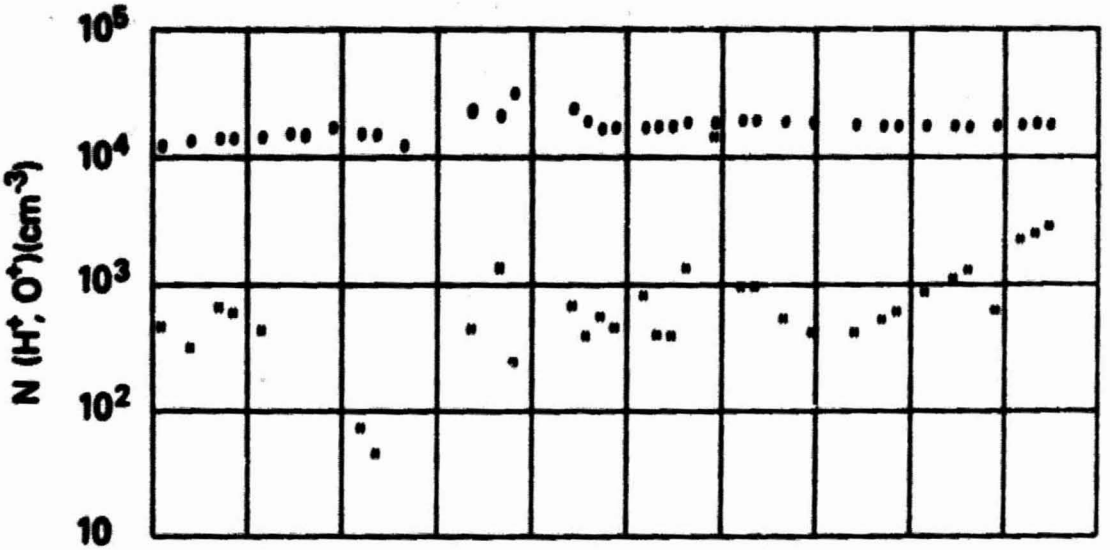

SET 8, FORMAT 5

72/164/0725

Excerpts of VLF Spectral film for the period 0725 - 0727

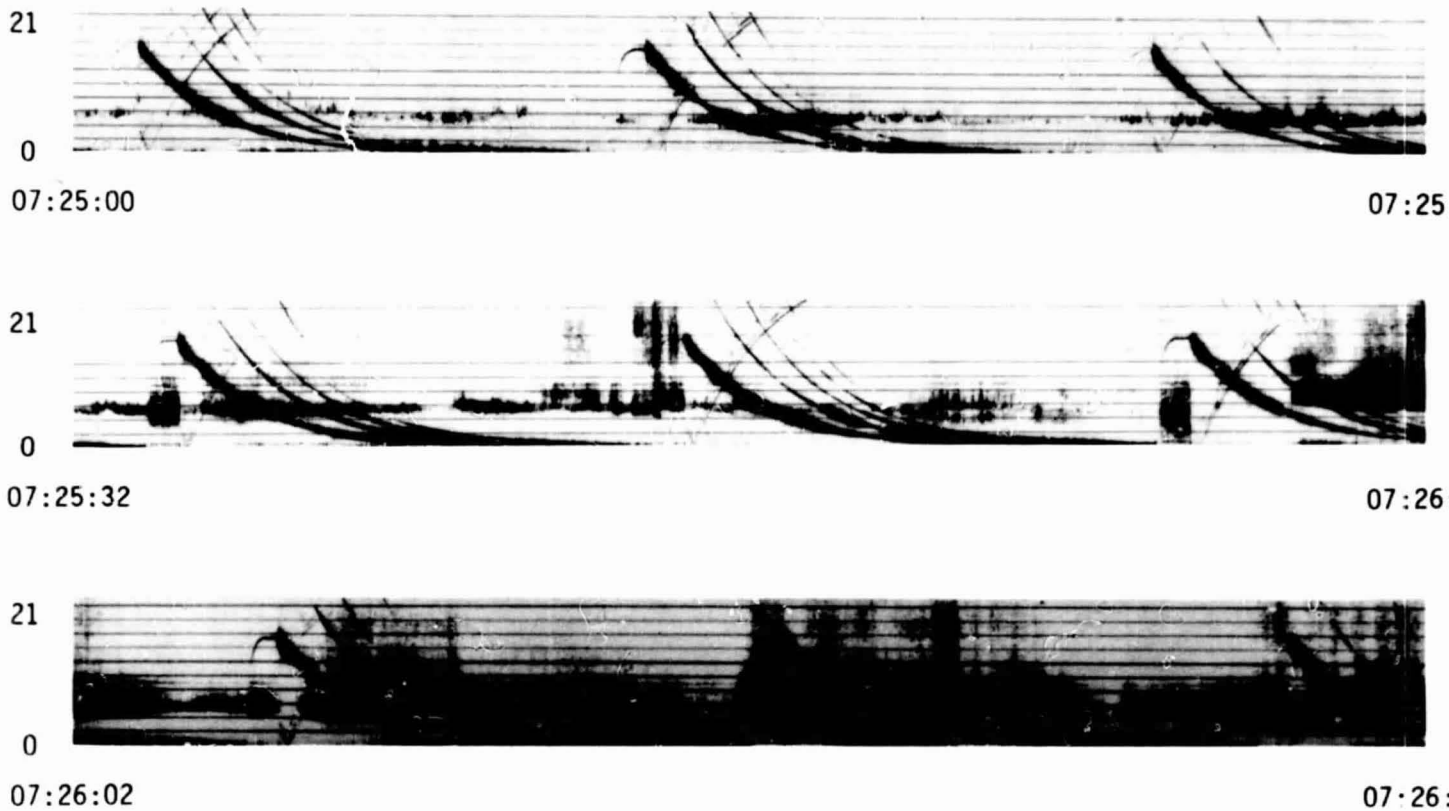

SET 8, FORMAT 11

81

72/164/0725

Excerpts of VLF Spectral film for the period 0725 - 0727

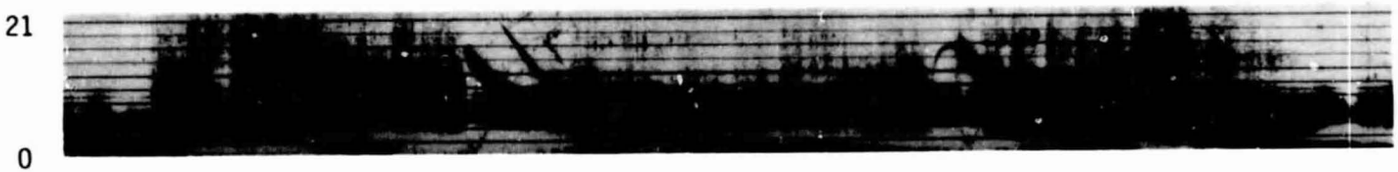

Frequency (kHz)

Universal Time (hours:minutes:seconds)

SET 8, FORMAT 11

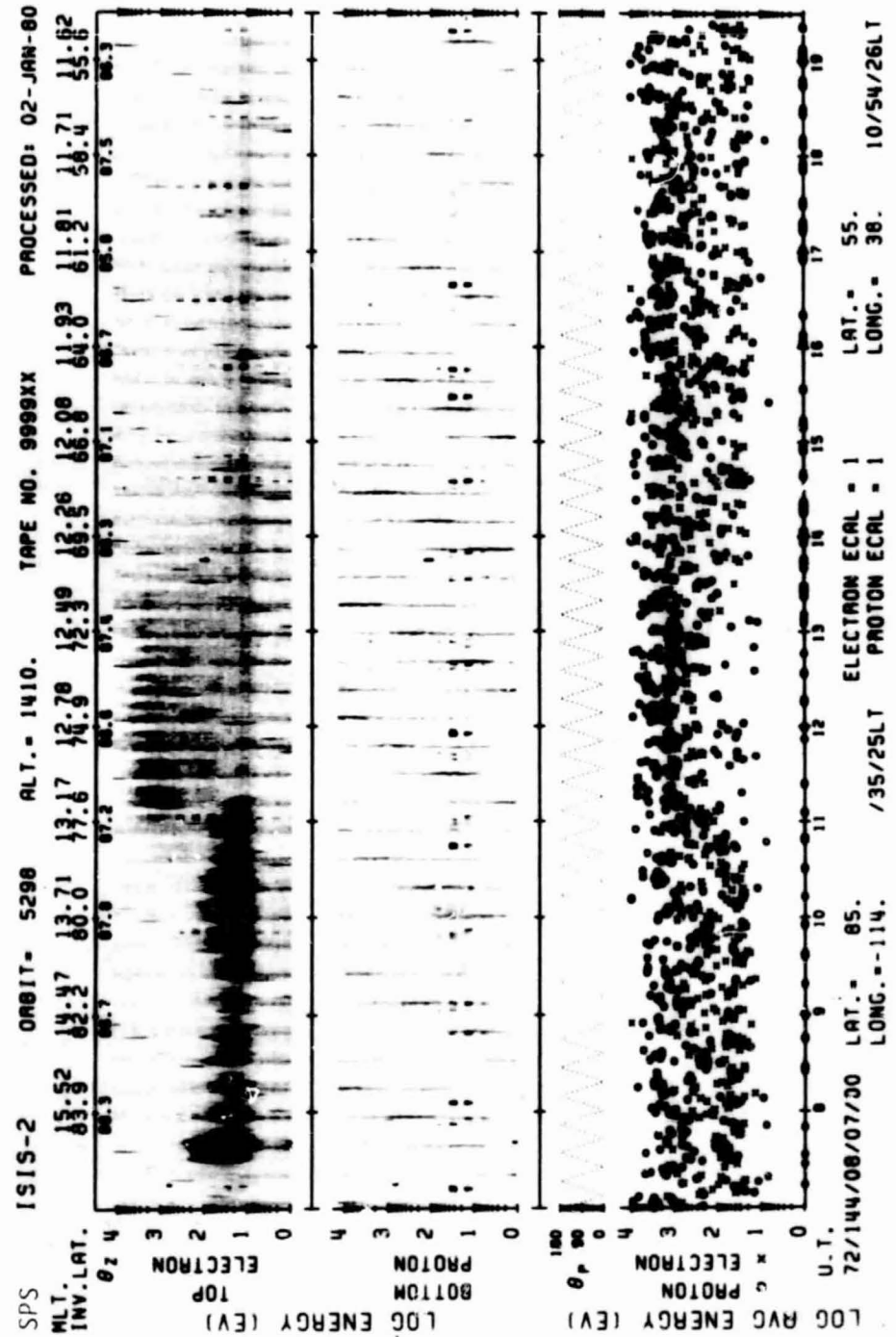

SET 9, FORMAT 6

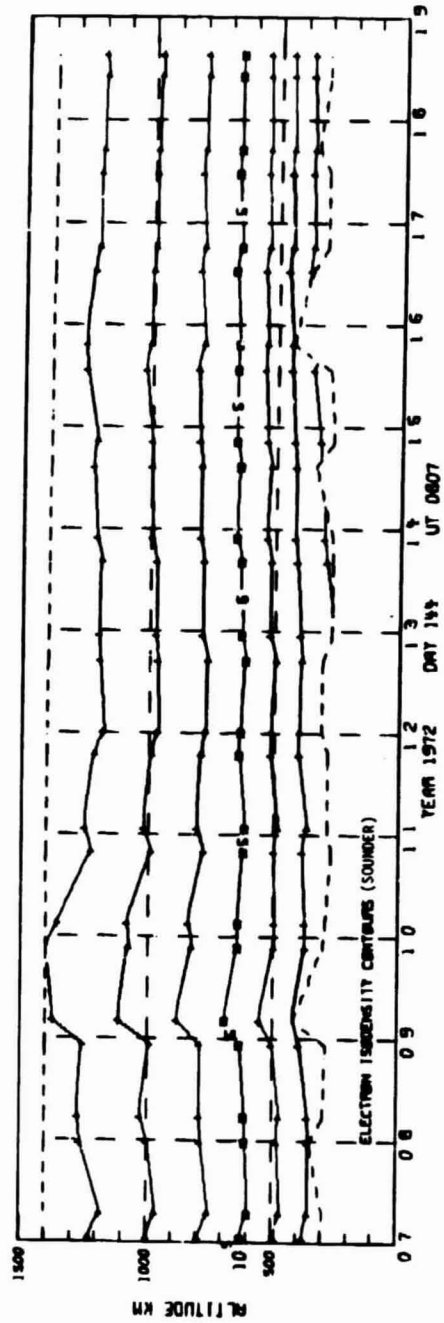

SET 9, FORMAT 2

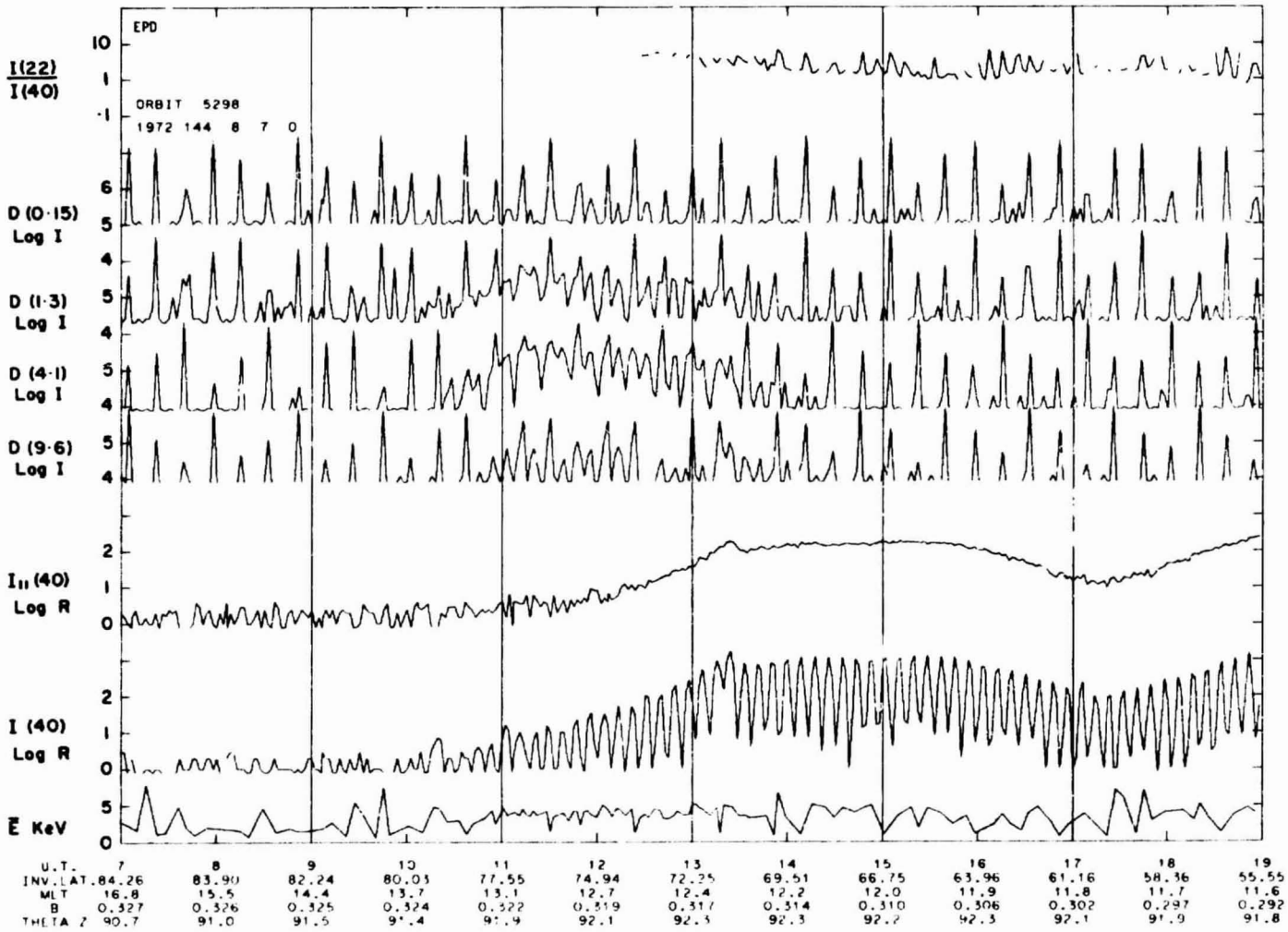

SET 9, FURMAT 3

ORBIT 5298
DATE 720523
DAY 144

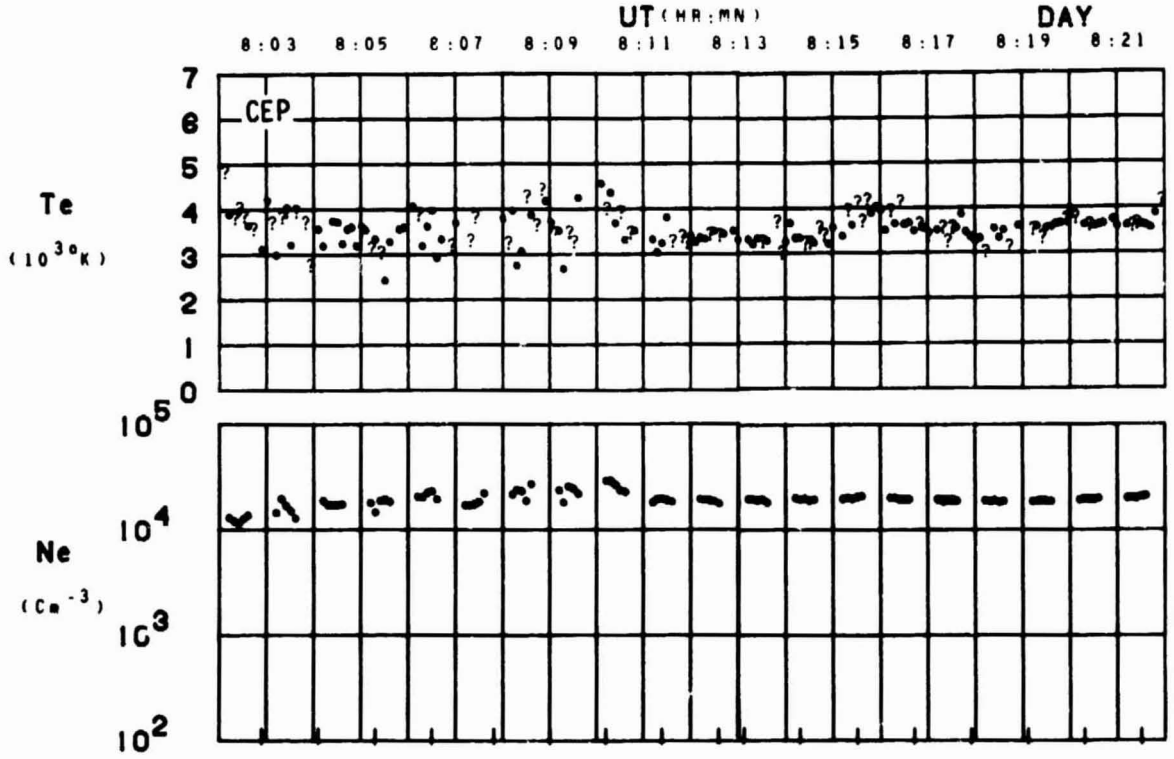

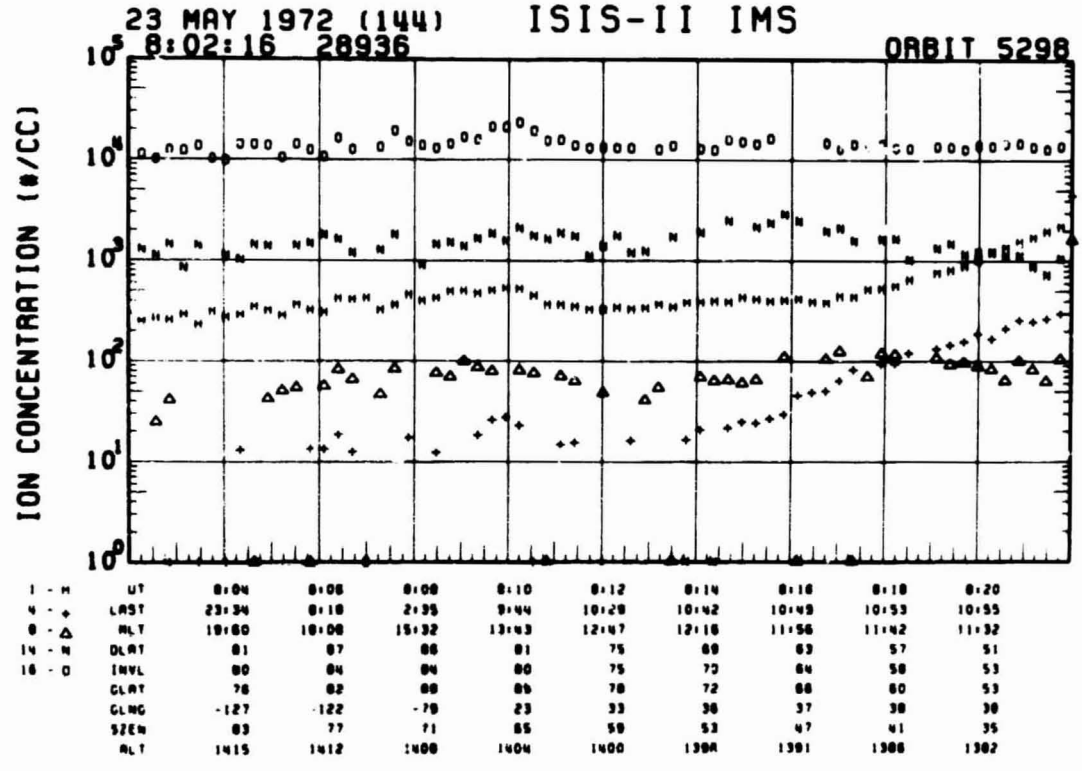

UT	8:04	8:06	8:08	8:10	8:12	8:14	8:16	8:18	8:20
LAST	23:34	0:18	2:35	9:44	10:28	10:42	10:49	10:53	10:55
MLT	19:60	19:06	15:32	13:43	12:47	12:16	11:56	11:42	11:32
DLAT	81	87	86	81	75	69	63	57	51
INVL	80	84	84	80	75	70	64	58	53
GLAT	76	82	88	86	78	72	66	60	53
GLNG	-127	-122	-78	23	33	36	37	38	38
SZEN	83	77	71	65	59	53	47	41	35
ALT	1415	1412	1408	1404	1400	1398	1391	1388	1382

1 - H
4 - +
8 - △
14 - N
16 - O

SET 9, FORMAT 4

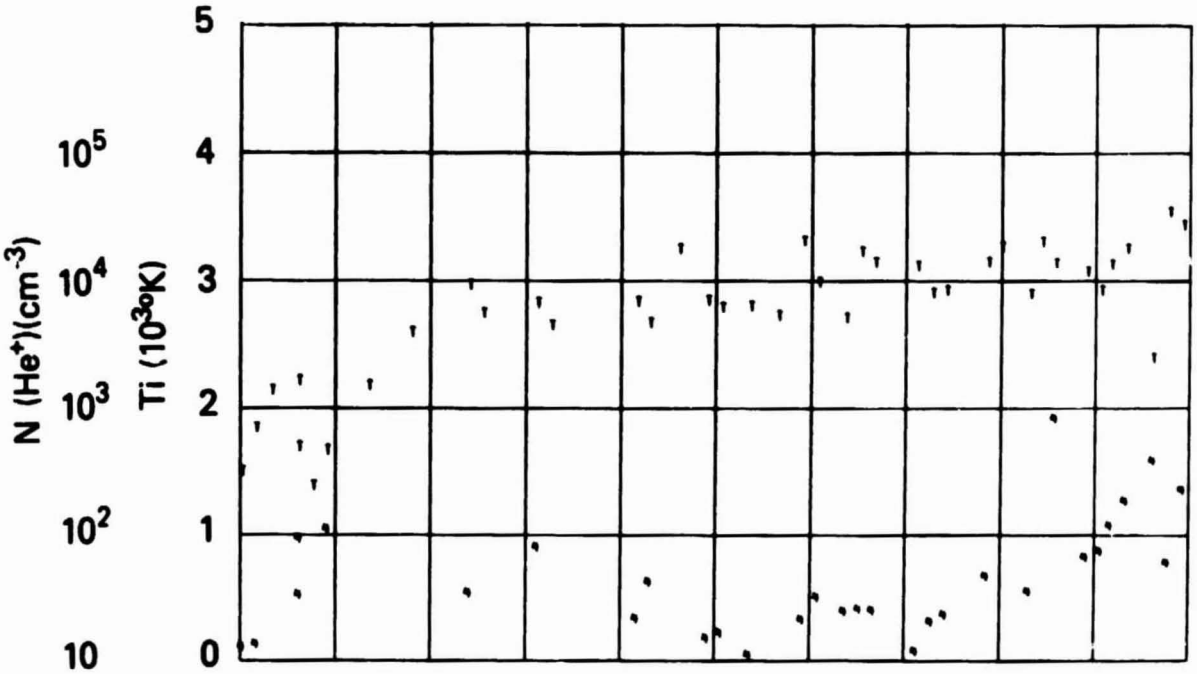

UT	8:04	8:06	8:08	8:10	8:12	8:14	8:16	8:18	8:20
LAST	23:34	8:18	2:35	9:44	10:28	10:42	10:49	10:53	10:55
MLT	19:60	18:08	15:32	13:43	12:47	12:18	11:56	11:42	11:32
DLAT	81	87	86	81	75	69	63	57	51
INVL	80	84	84	80	75	70	64	58	53
GLAT	76	82	88	85	78	72	66	60	53
GLNG	-127	-122	-79	23	33	36	37	38	38
SZEN	83	77	71	65	59	53	47	41	35
ALT	1415	1412	1408	1404	1400	1398	1391	1388	1382

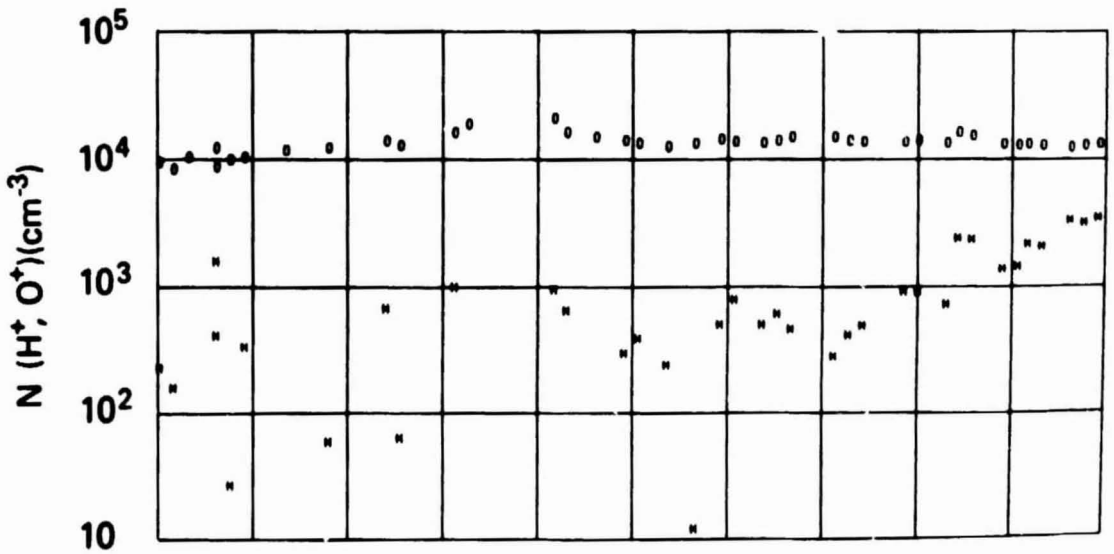

SET 9, FORMAT 5

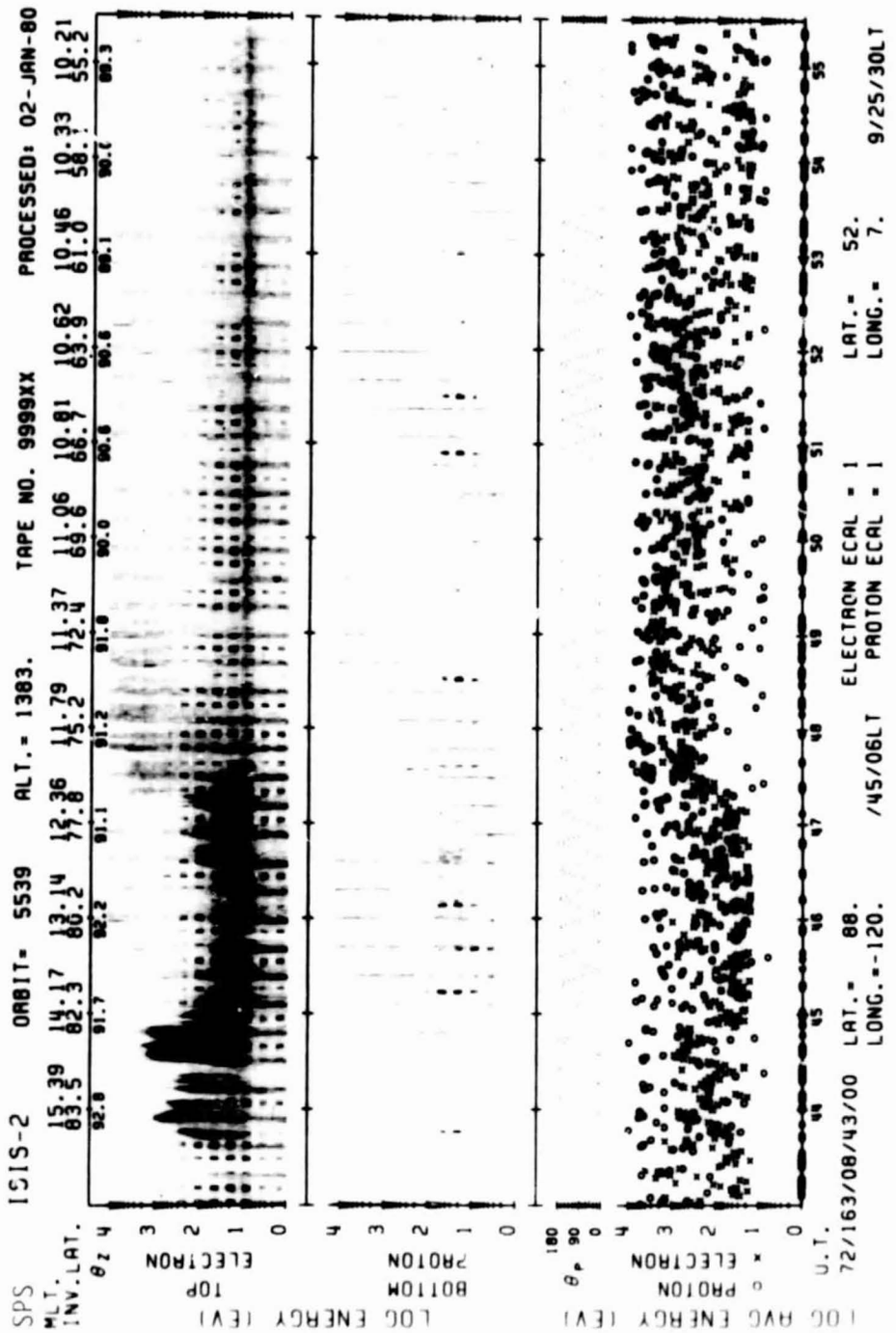

SET 10, FORMAT 6

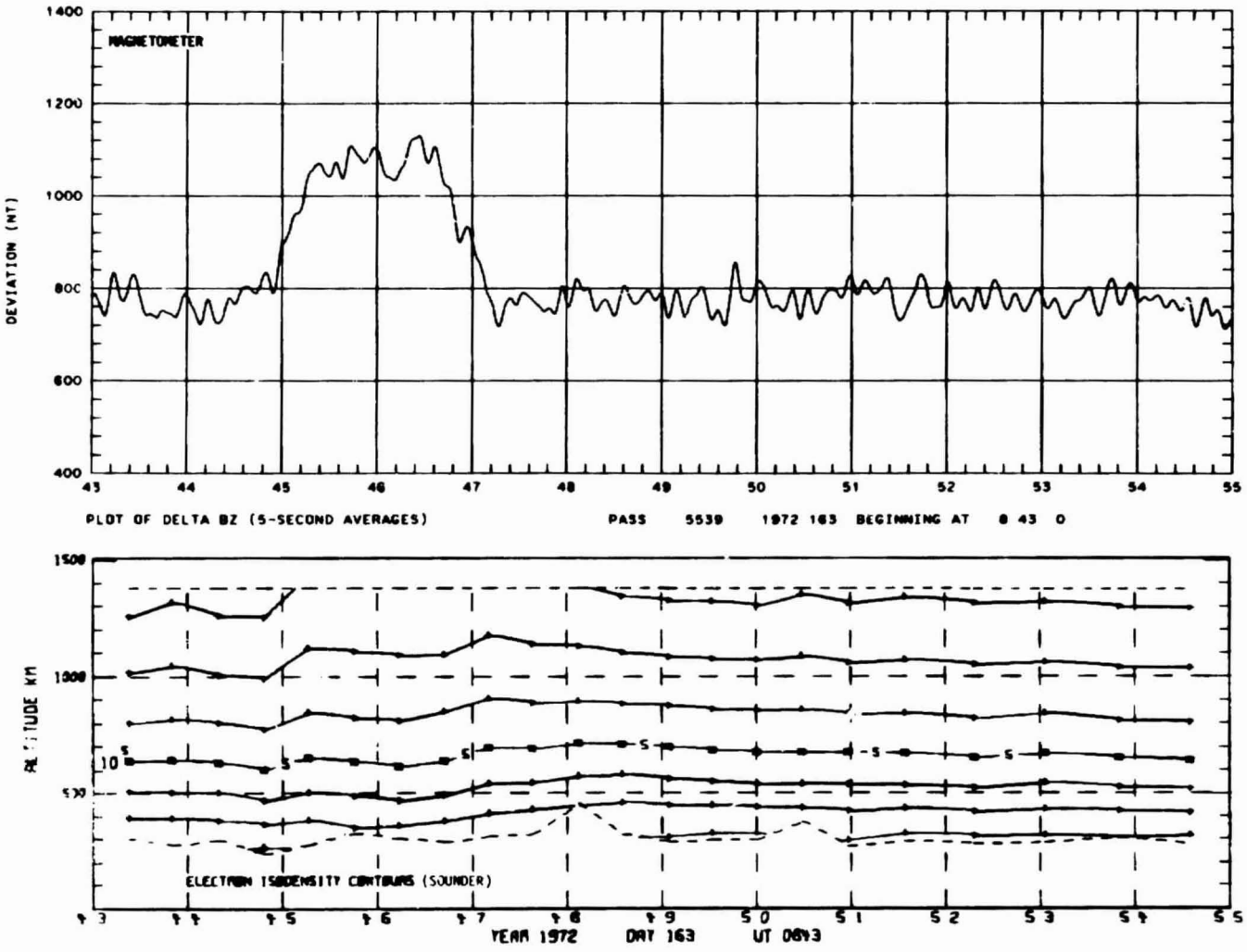

SET 10, FORMAT 2

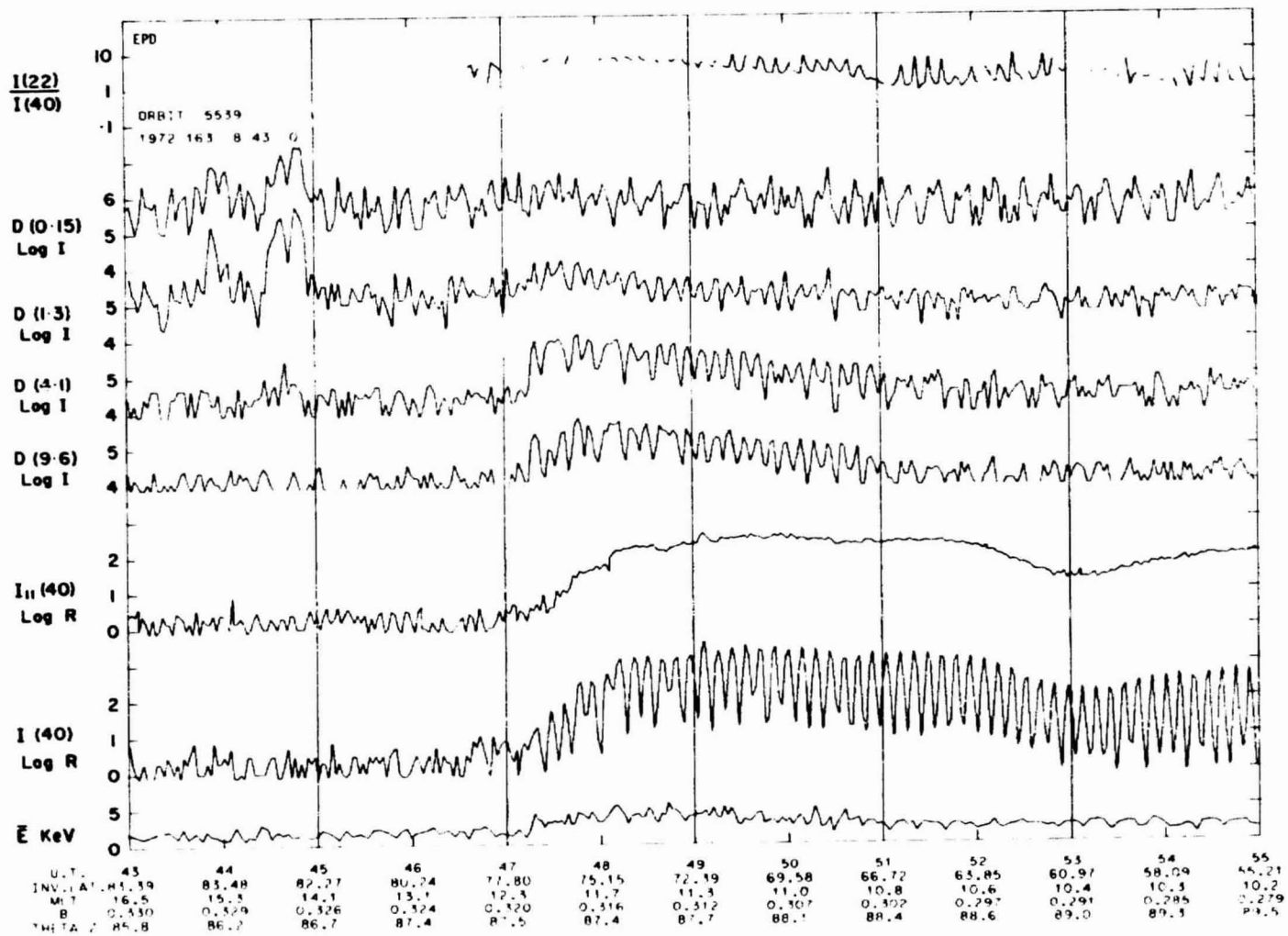

SET 10, FORMAT 3

ORBIT 5539
DATE 720611
DAY 163

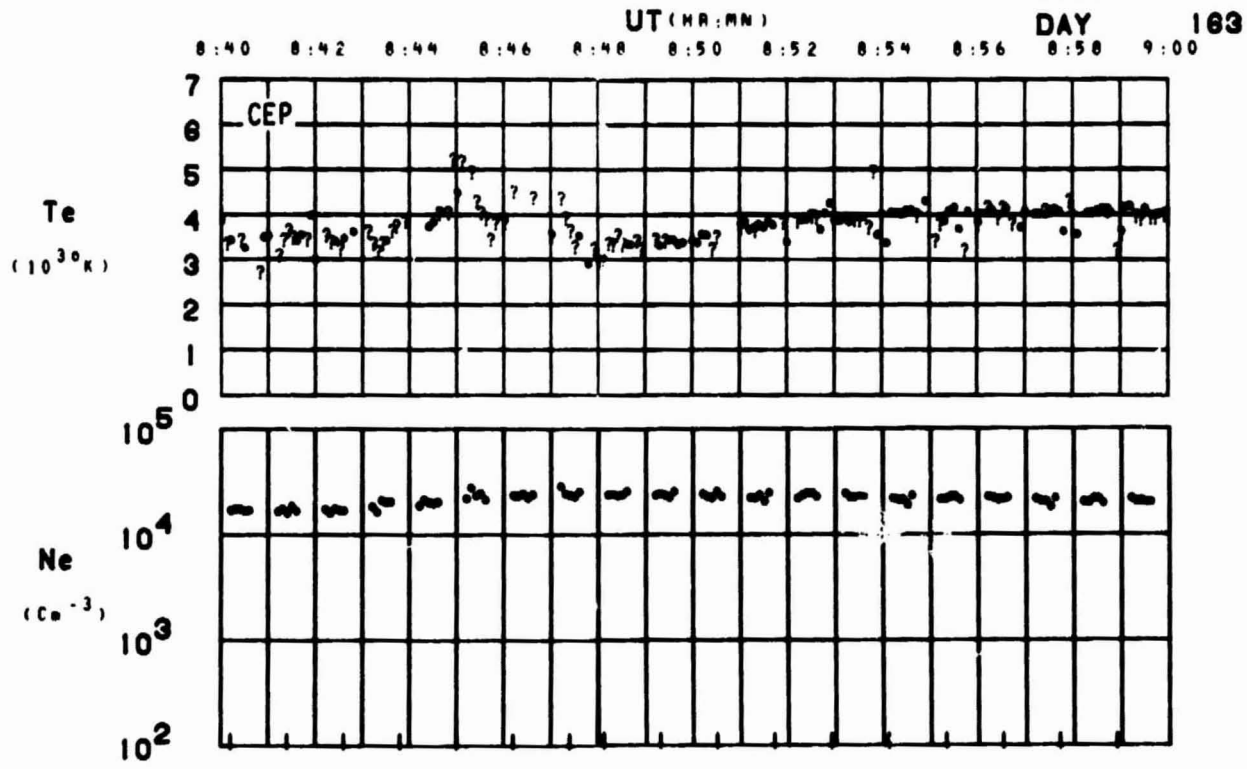

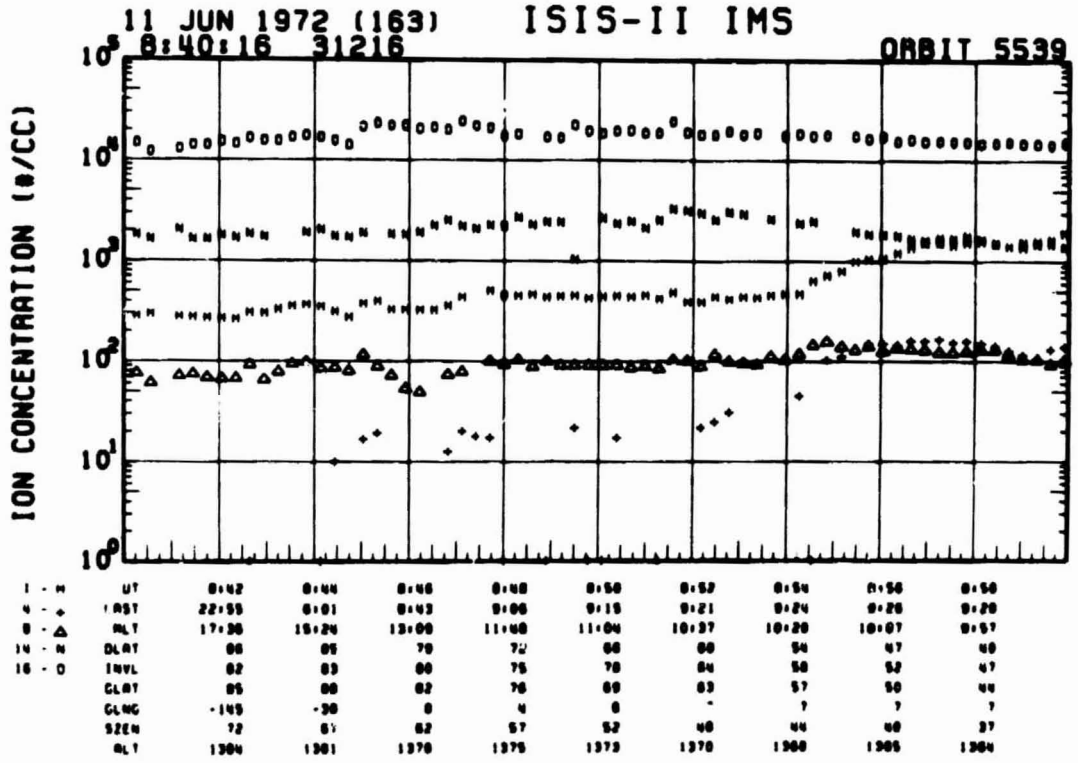

SET 10, FORMAT 4

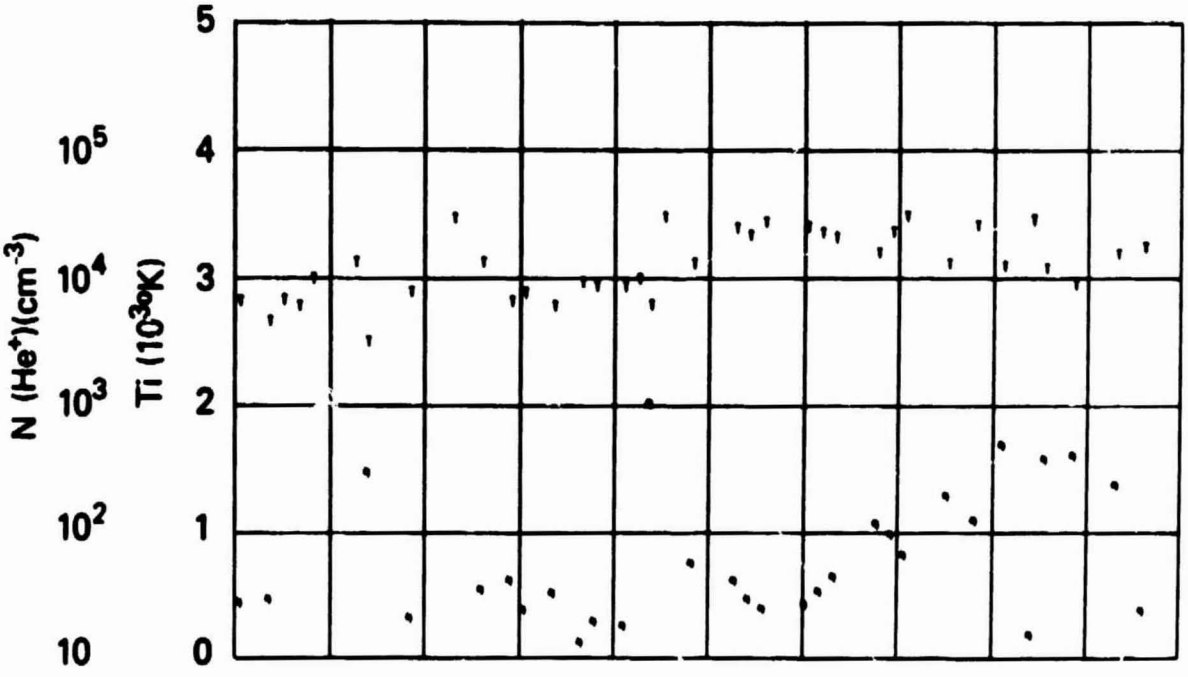

UT	8:42	8:44	8:46	8:48	8:50	8:52	8:54	8:56	8:58
LAST	22:55	0:01	0:43	9:08	9:15	9:21	9:24	9:28	9:28
MLT	17:36	15:24	13:09	11:48	11:04	10:37	10:20	10:07	9:57
DLAT	86	85	78	72	66	60	54	47	40
INVL	82	83	80	75	70	64	58	52	47
GLAT	85	80	82	78	69	63	57	50	44
GLNG	-145	-30	0	4	8	7	7	7	7
SZEN	72	67	62	57	52	48	44	40	37
ALT	1384	1381	1378	1375	1373	1370	1368	1365	1364

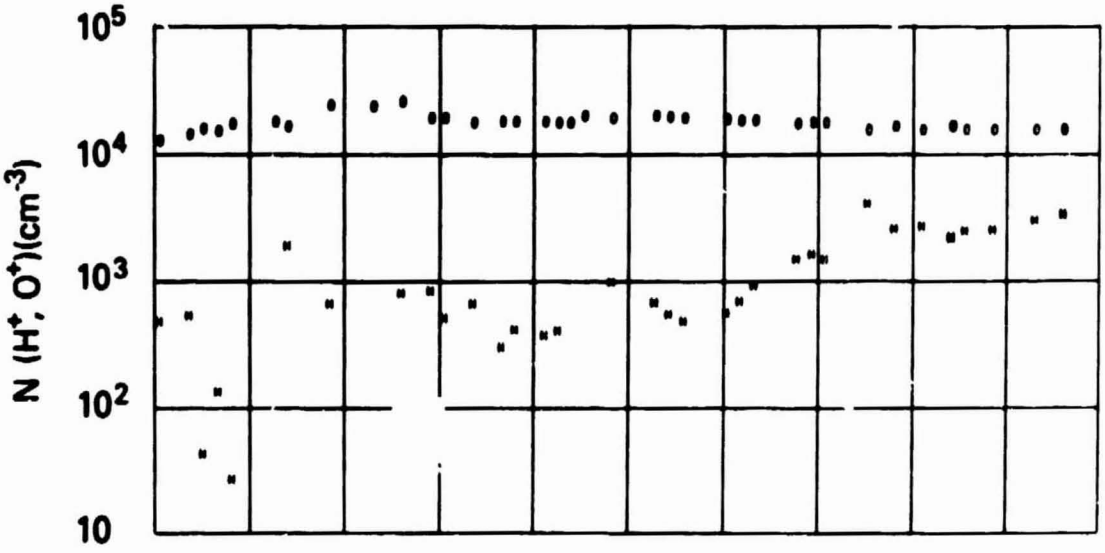

SET 10, FORMAT 5

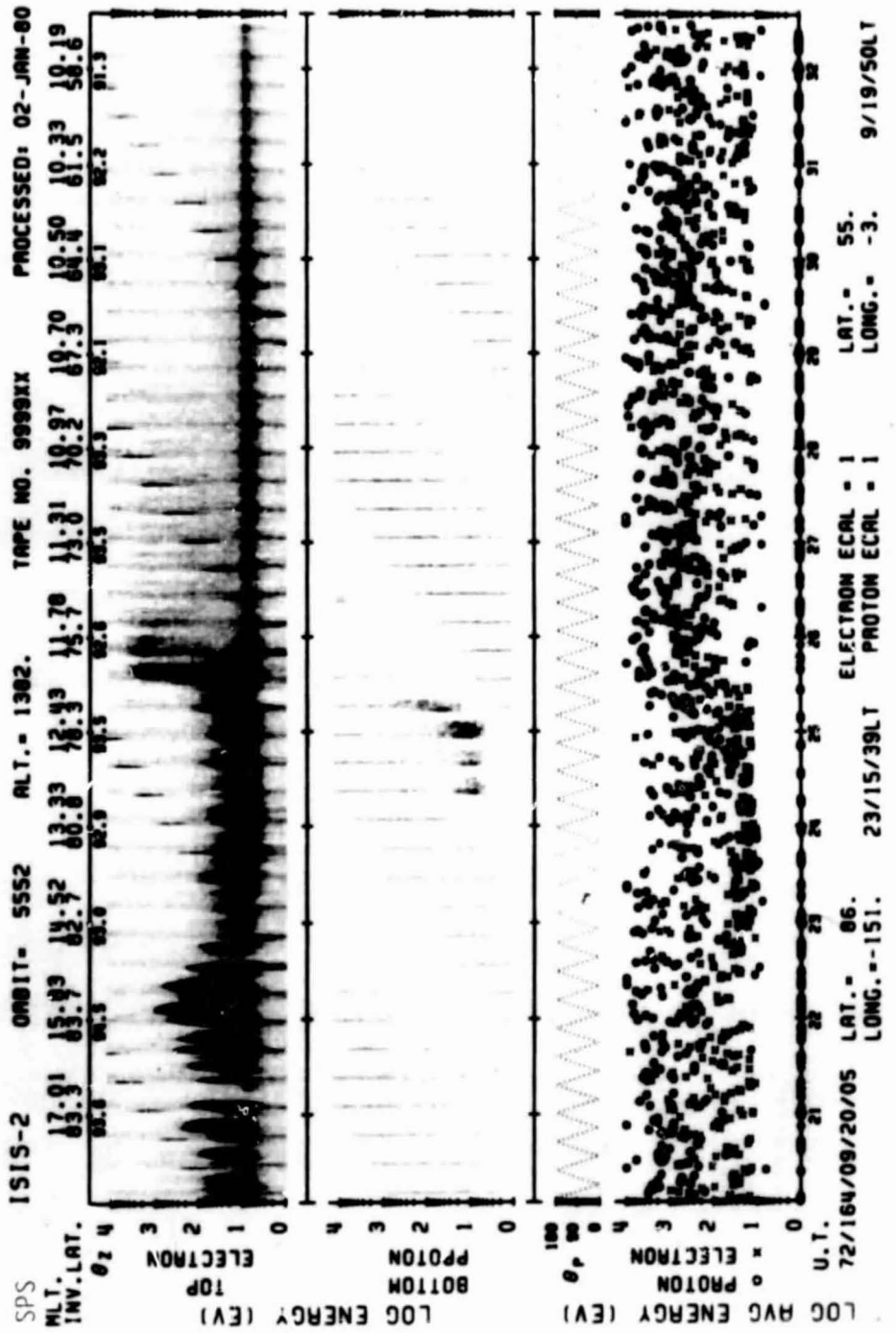

SET 11, FORMAT 6

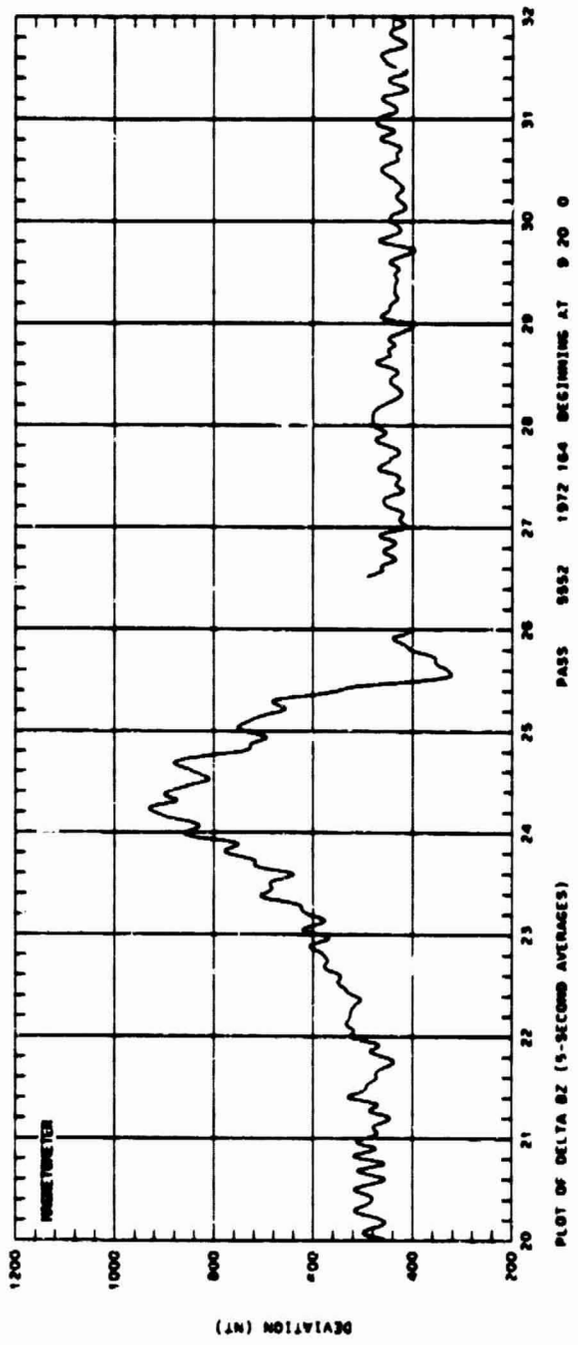

SET 11, FORMAT 2

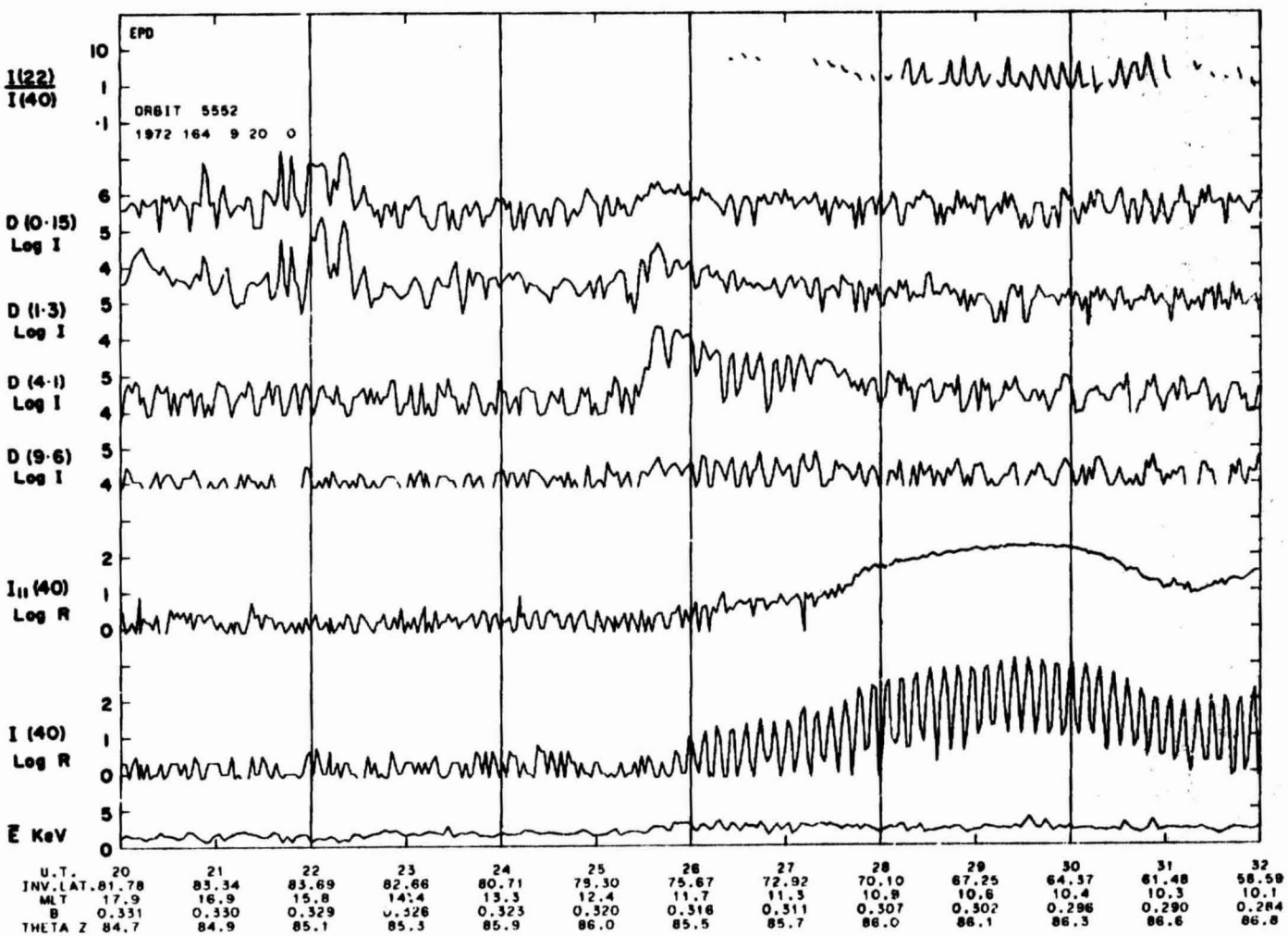

C-2

SET 11, FORMAT 3

ORBIT 5552
DATE 720612
DAY 164

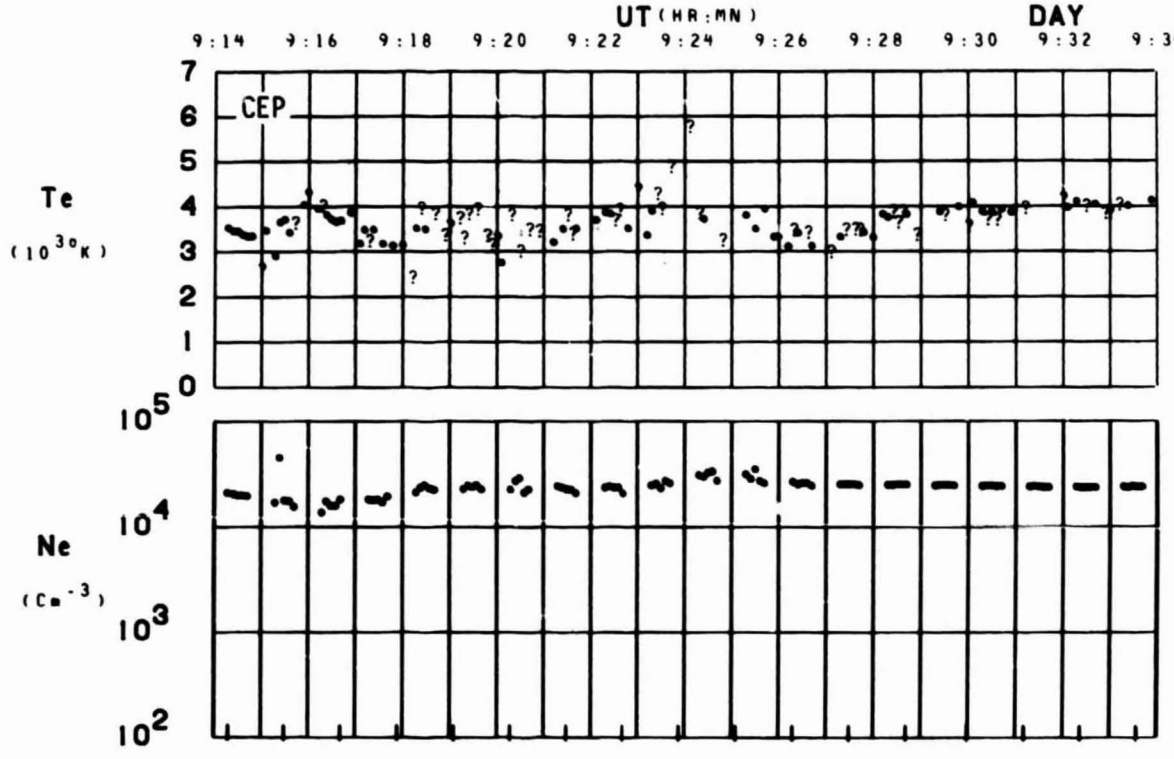

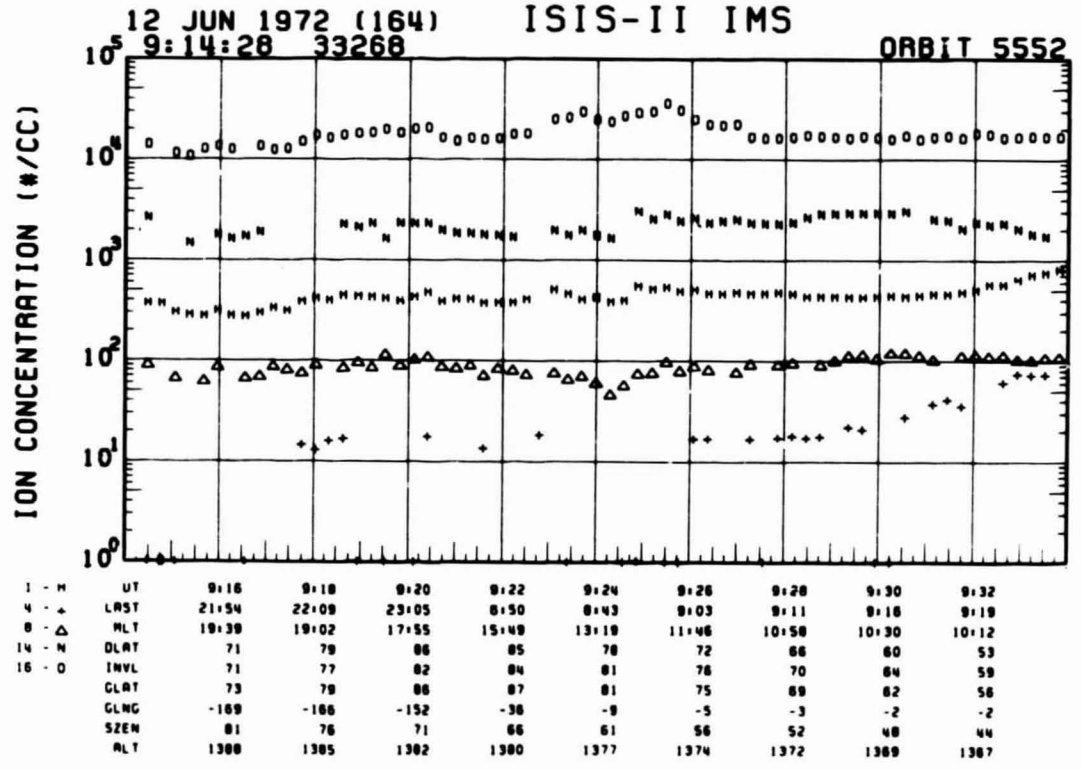

	9:16	9:18	9:20	9:22	9:24	9:26	9:28	9:30	9:32
UT	9:16	9:18	9:20	9:22	9:24	9:26	9:28	9:30	9:32
LAST	21:54	22:09	23:05	0:50	0:43	0:03	0:11	0:16	0:19
ALT	19:39	19:02	17:55	15:49	13:19	11:46	10:58	10:30	10:12
DLAT	71	79	86	85	78	72	66	60	53
INVL	71	77	82	84	81	76	70	64	59
GLAT	73	79	86	87	81	75	69	62	56
GLNG	-169	-166	-152	-36	-9	-5	-3	-2	-2
SZEN	81	76	71	66	61	56	52	48	44
ALT	1388	1385	1382	1380	1377	1374	1372	1369	1367

SET 11, FORMAT 4

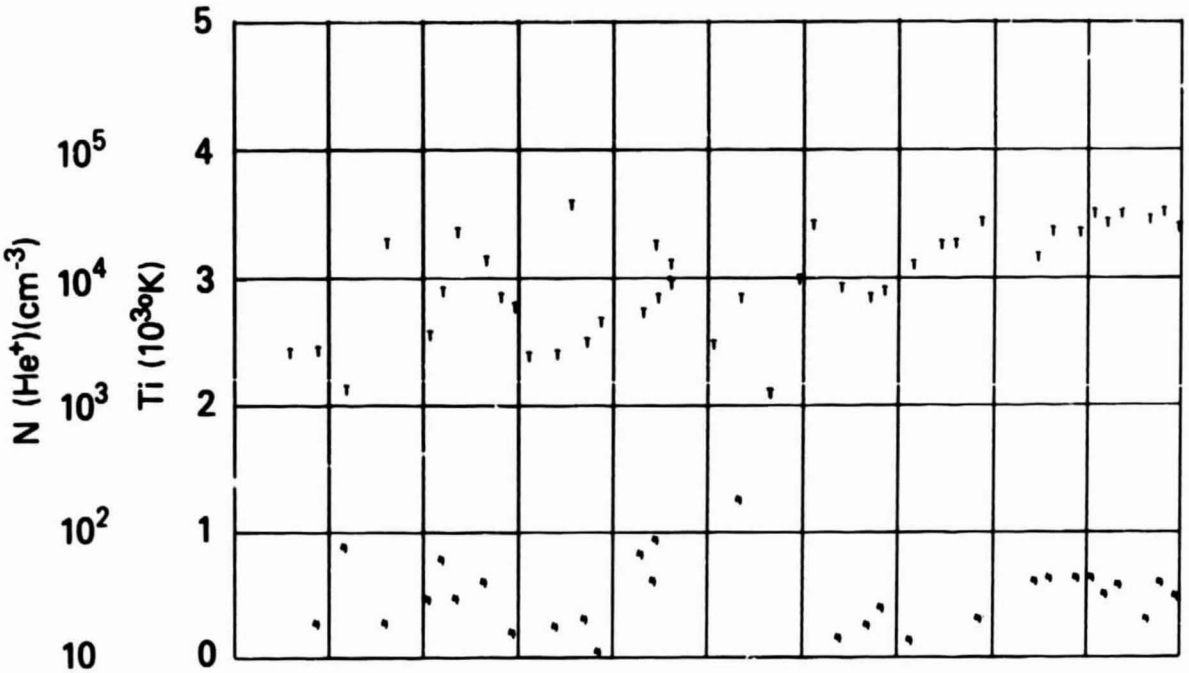

UT	9:16	9:18	9:20	9:22	9:24	9:26	9:28	9:30	9:32
LAST	21:54	22:09	23:05	8:50	8:43	9:03	9:11	9:16	9:19
MLT	19:39	19:02	17:55	15:49	13:19	11:46	10:58	10:30	10:12
DLAT	71	78	86	85	78	72	66	60	53
INVL	71	77	82	84	81	76	70	64	59
GLAT	73	78	86	87	81	75	69	62	56
GLNG	-169	-166	-152	-36	-9	-5	-3	-2	-2
SZEN	81	76	71	66	61	56	52	48	44
ALT	1388	1385	1382	1380	1377	1374	1372	1369	1367

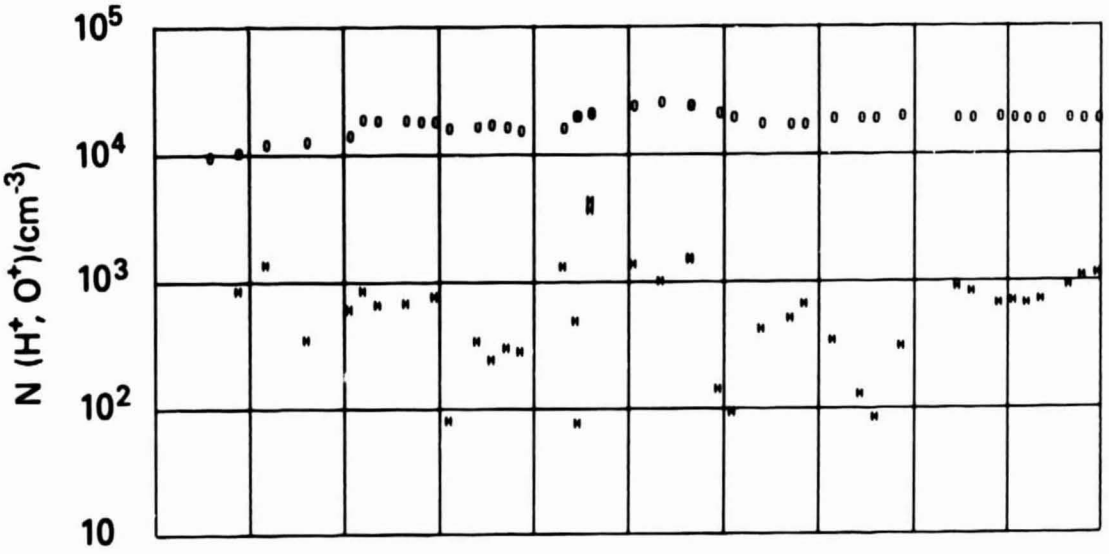

SET 11, FORMAT 5

72/164/0920

Excerpts of VLF Spectral film for the period 0921 - 0927

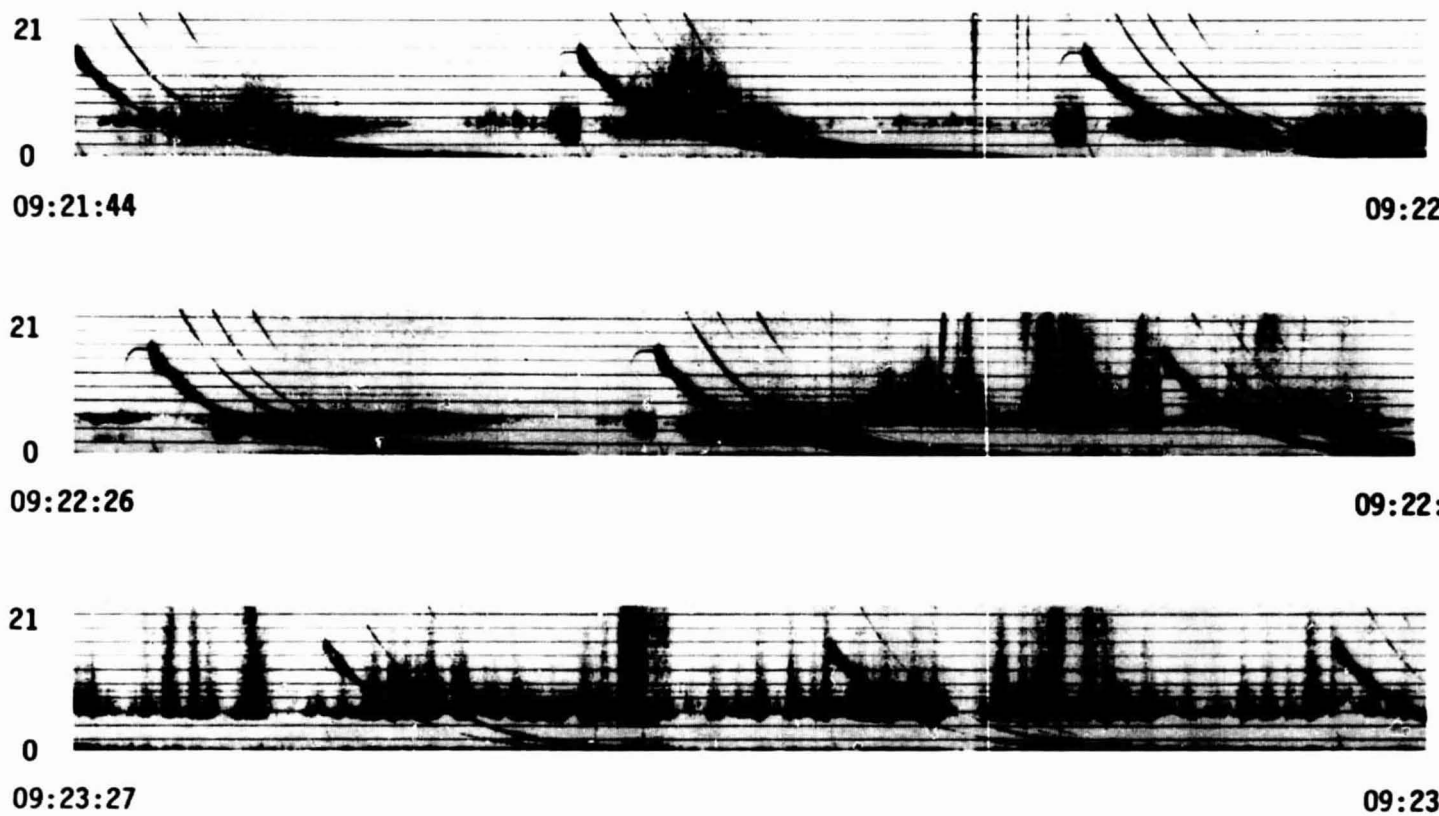

SET 11, FORMAT 11

72/164/0920

Excerpts of VLF Spectral film for the period 0921 - 0927

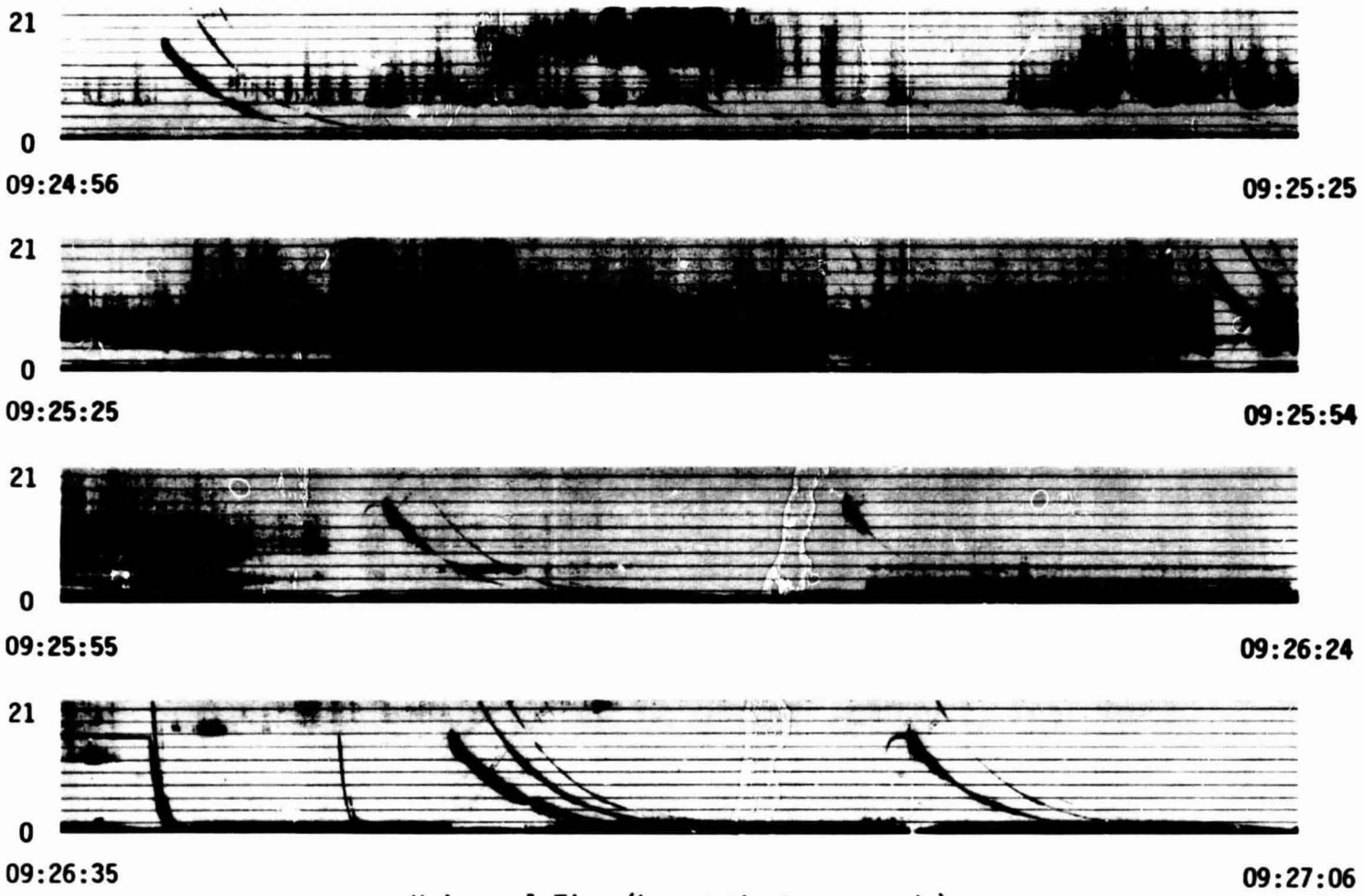

SET 11, FORMAT 11

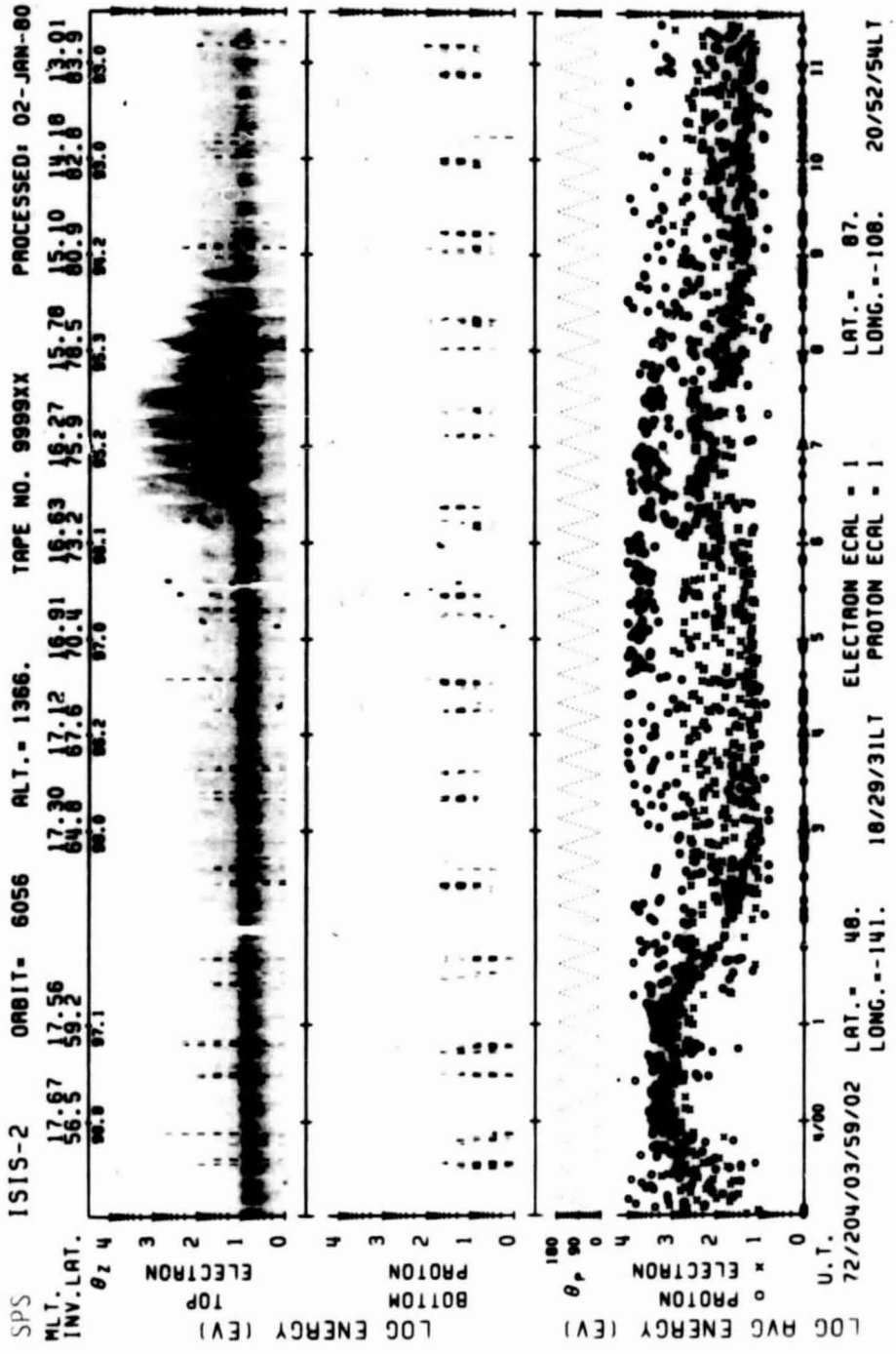

SET 12, FORMAT 6

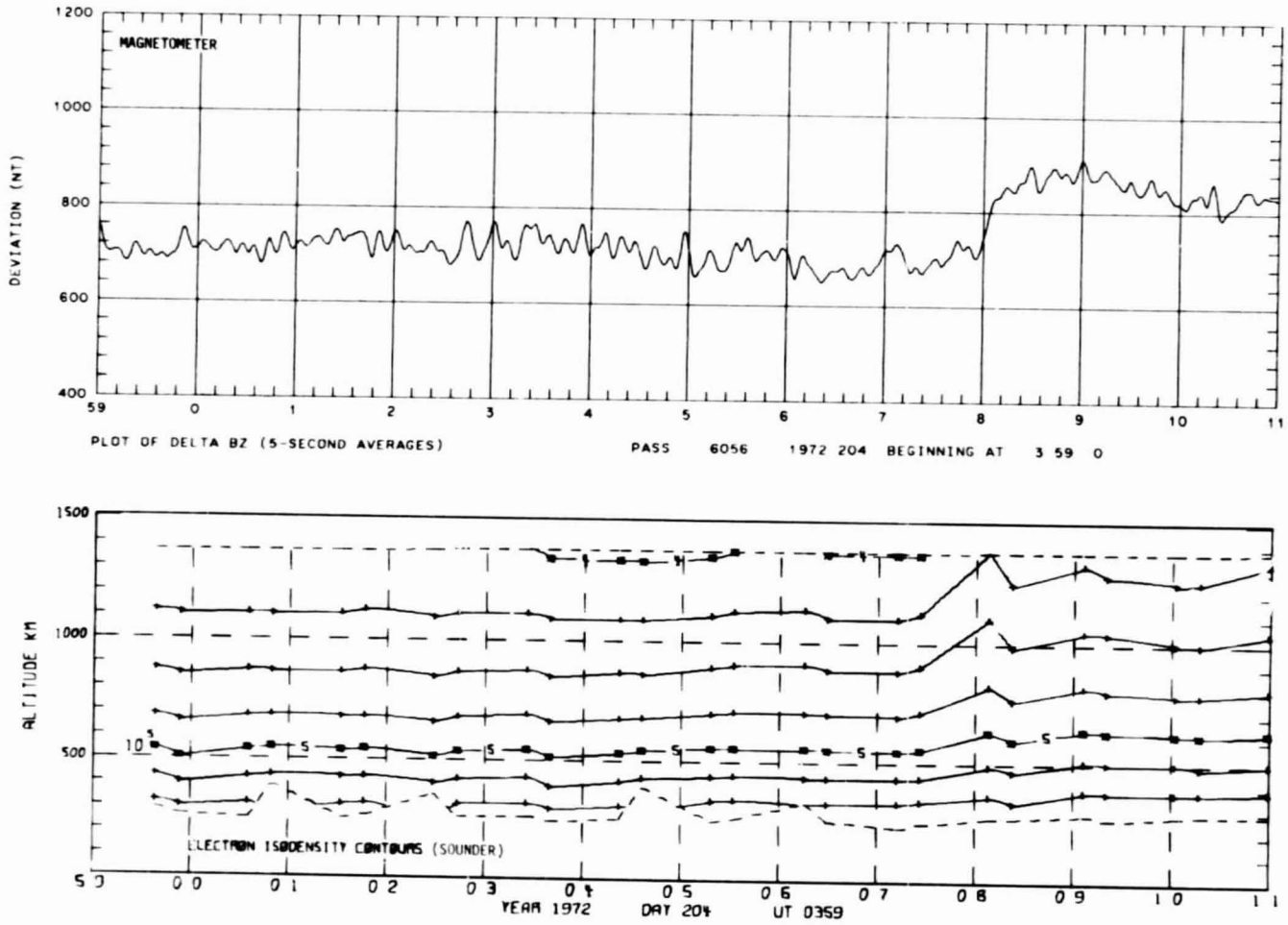

SET 12, FORMAT 2

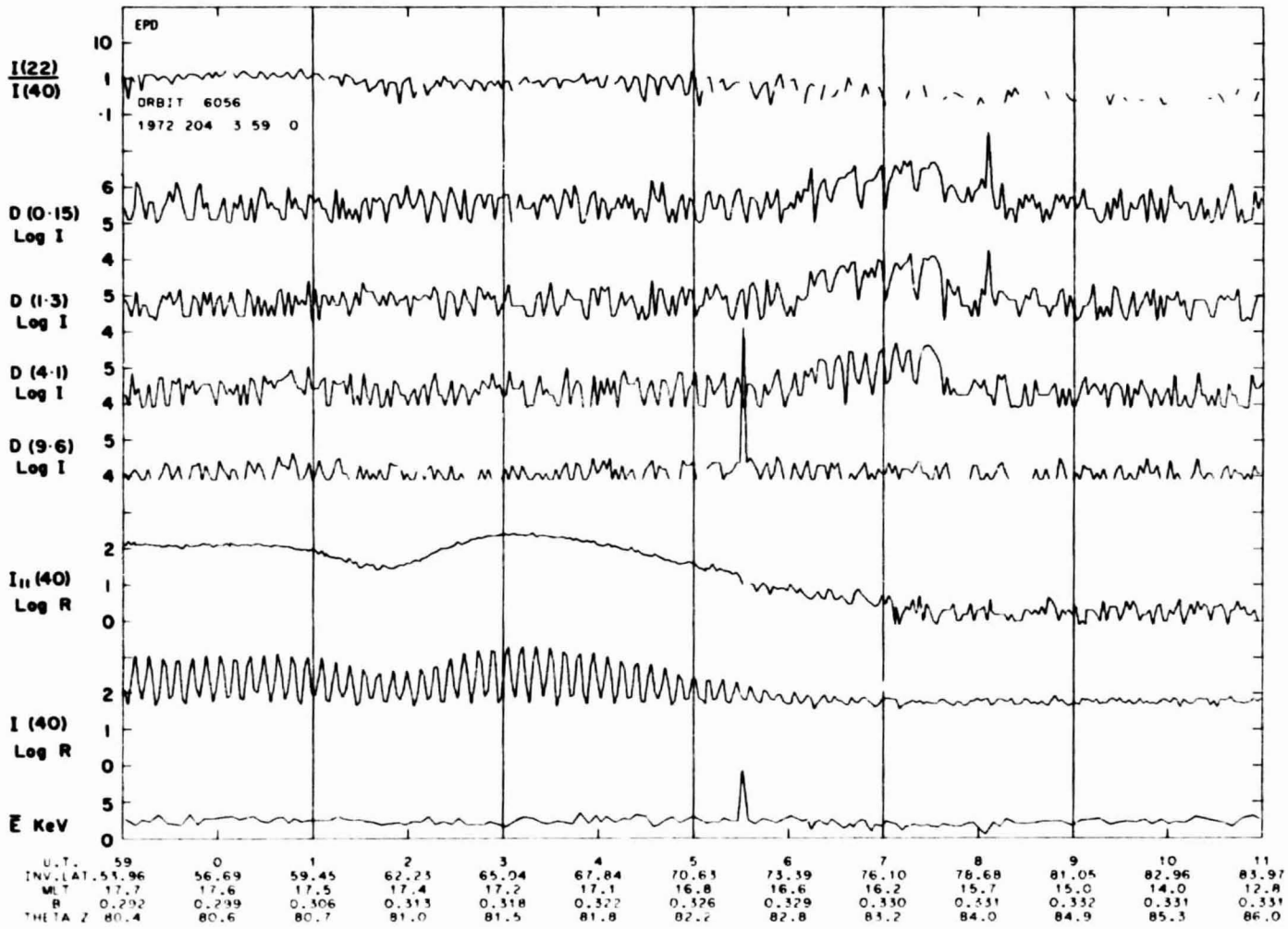

SET 12, FORMAT 3

ORBIT 6056
DATE 720722
DAY 204

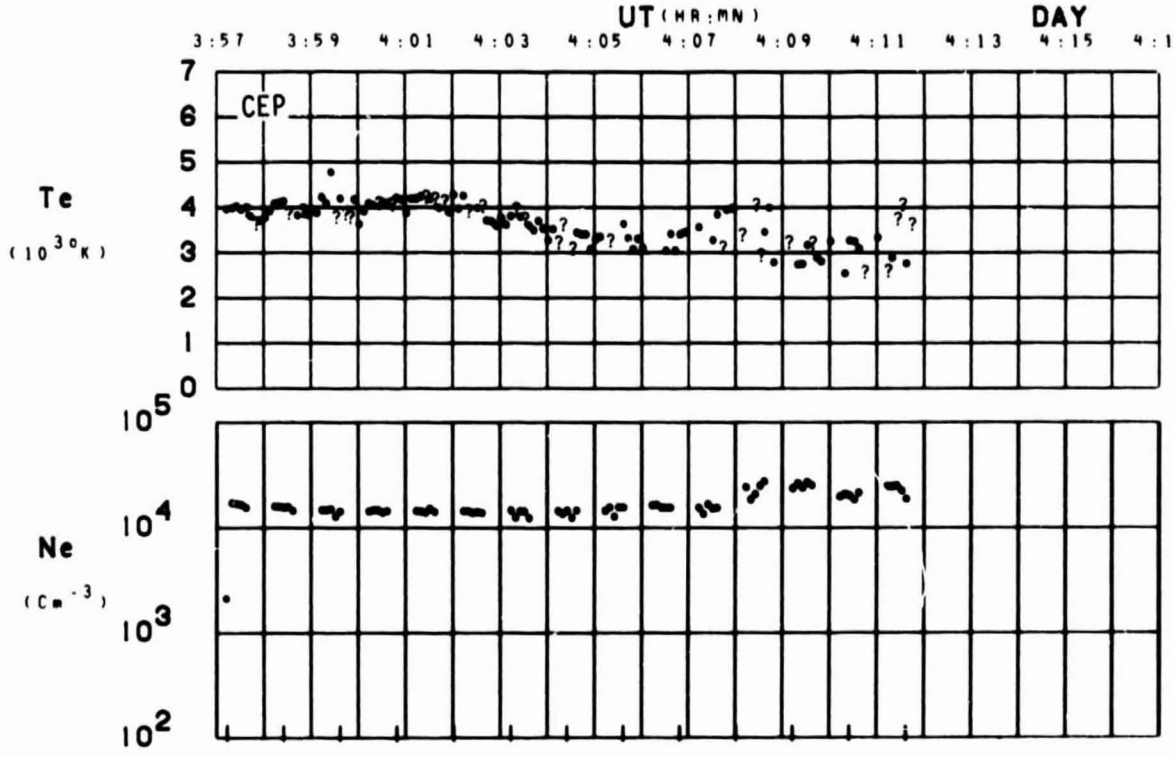

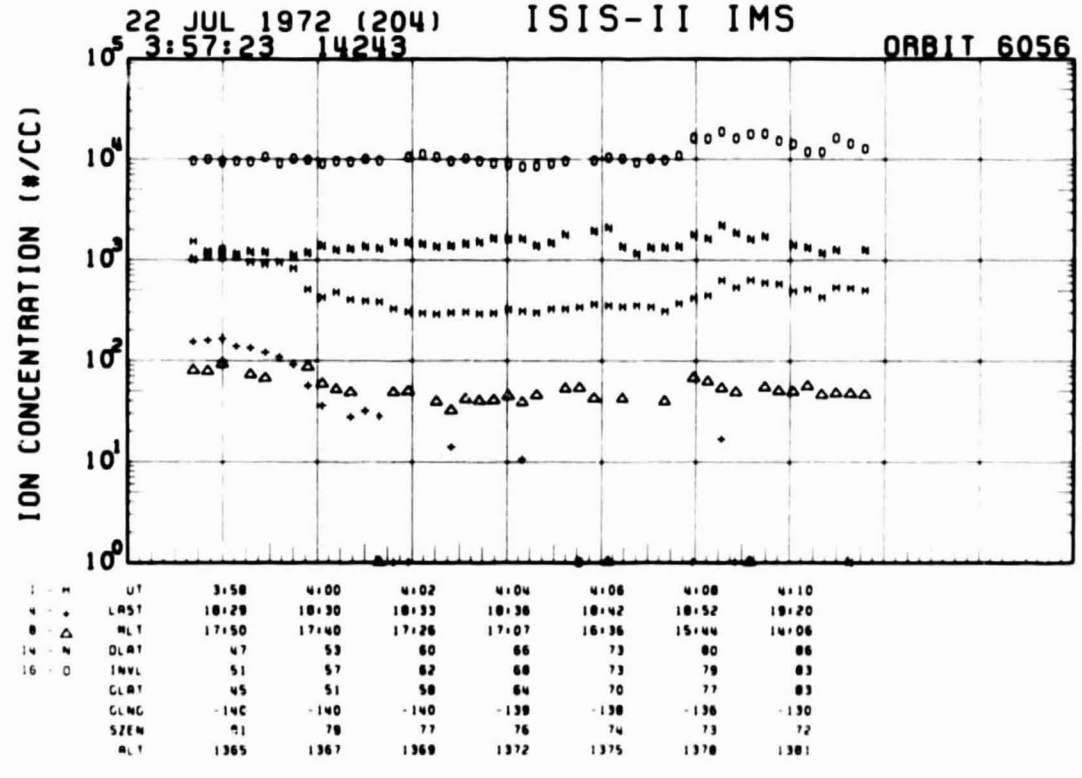

UT	3:58	4:00	4:02	4:04	4:06	4:08	4:10
LAST	18:29	18:30	18:33	18:36	18:42	18:52	19:20
MLT	17:50	17:40	17:26	17:07	16:36	15:44	14:06
DLAT	47	53	60	66	73	80	86
INVL	51	57	62	68	73	78	83
GLAT	45	51	58	64	70	77	83
GLNG	-140	-140	-140	-139	-138	-136	-130
SZEN	81	78	77	76	74	73	72
ALT	1365	1367	1369	1372	1375	1378	1381

SET 12, FORMAT 4

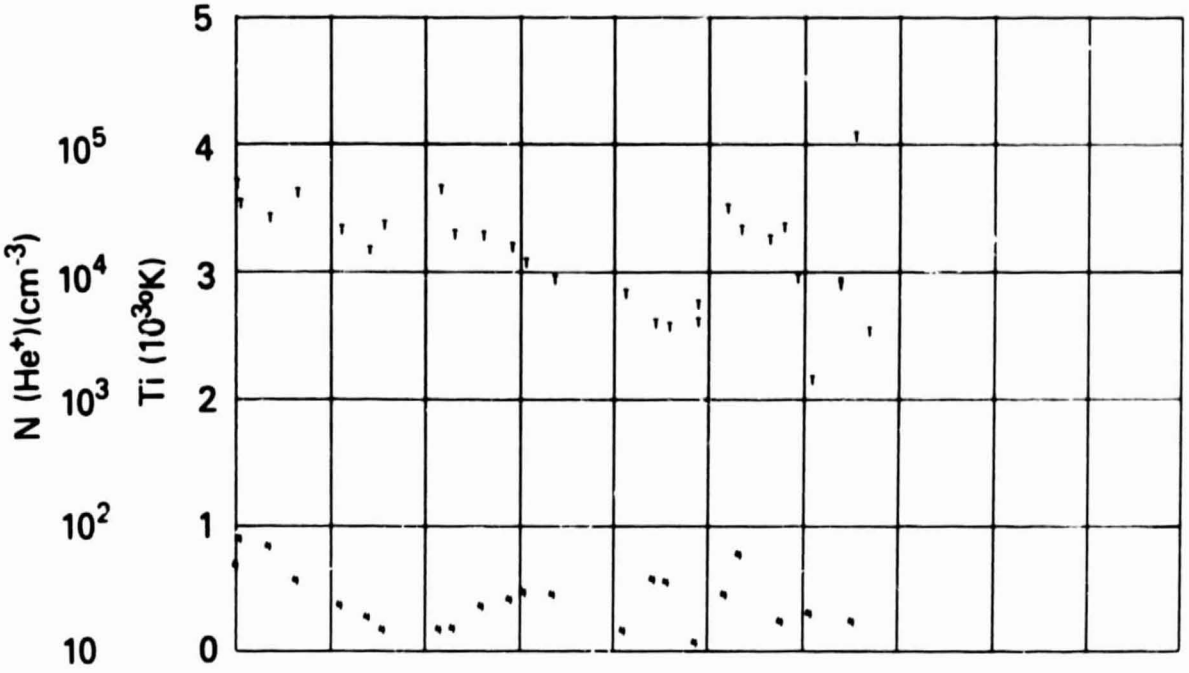

UT	3:58	4:00	4:02	4:04	4:06	4:08	4:10
LAST	18:28	18:30	18:33	18:36	18:42	18:52	19:20
MLT	17:50	17:40	17:26	17:07	16:36	15:44	14:06
DLAT	47	53	60	66	73	80	86
INVL	51	57	62	68	73	79	83
GLAT	45	51	58	64	70	77	83
GLNG	-140	-140	-140	-139	-138	-136	-130
SZEN	81	79	77	76	74	73	72
ALT	1365	1367	1369	1372	1375	1378	1381

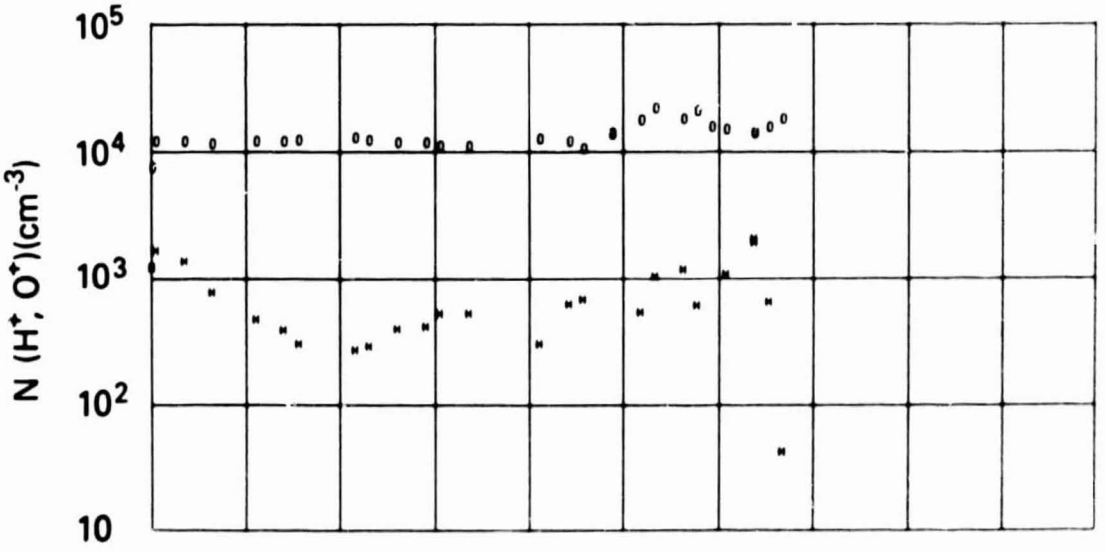

SET 12, FORMAT 5

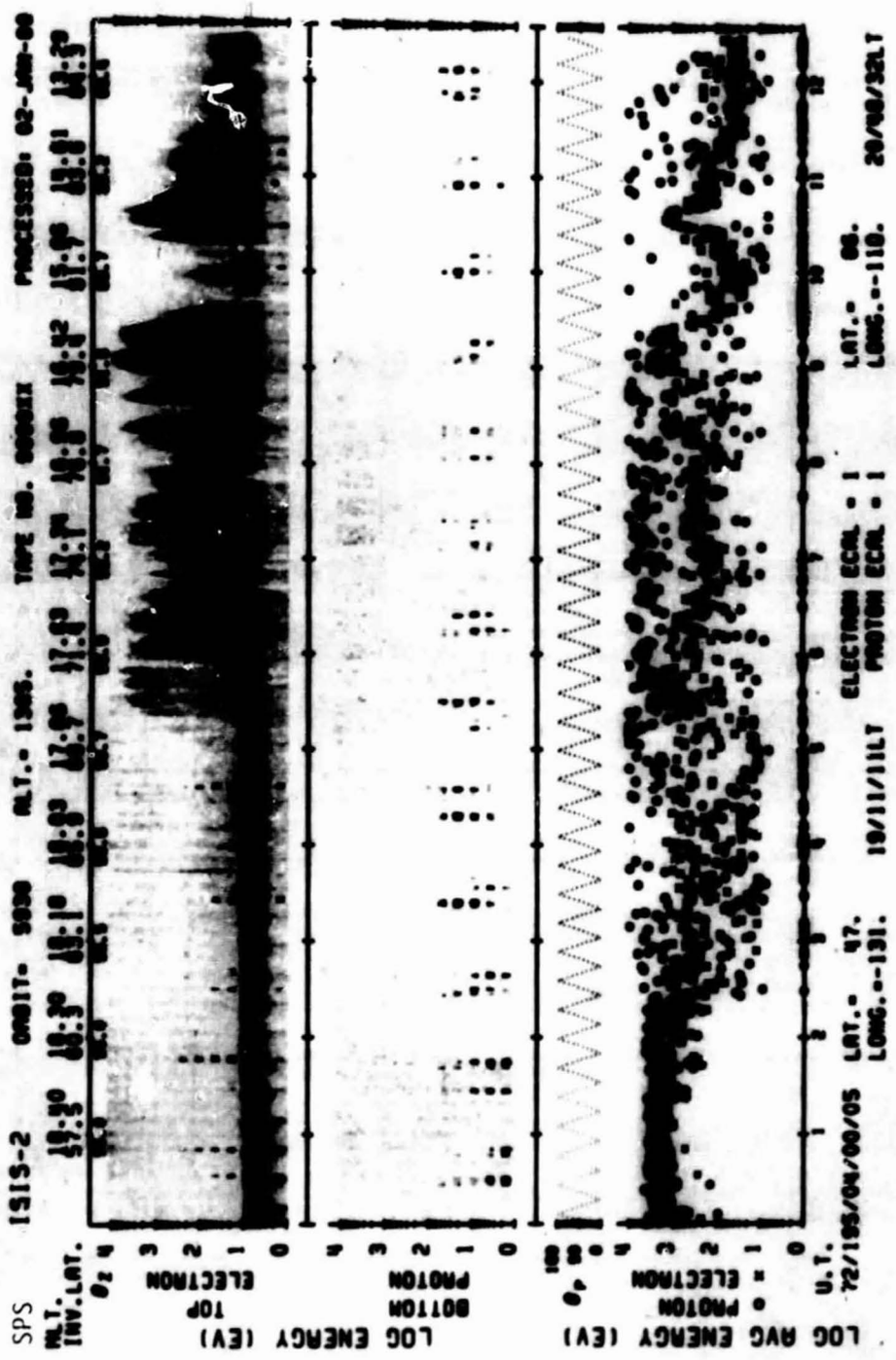

SET 13, FORMAT 6

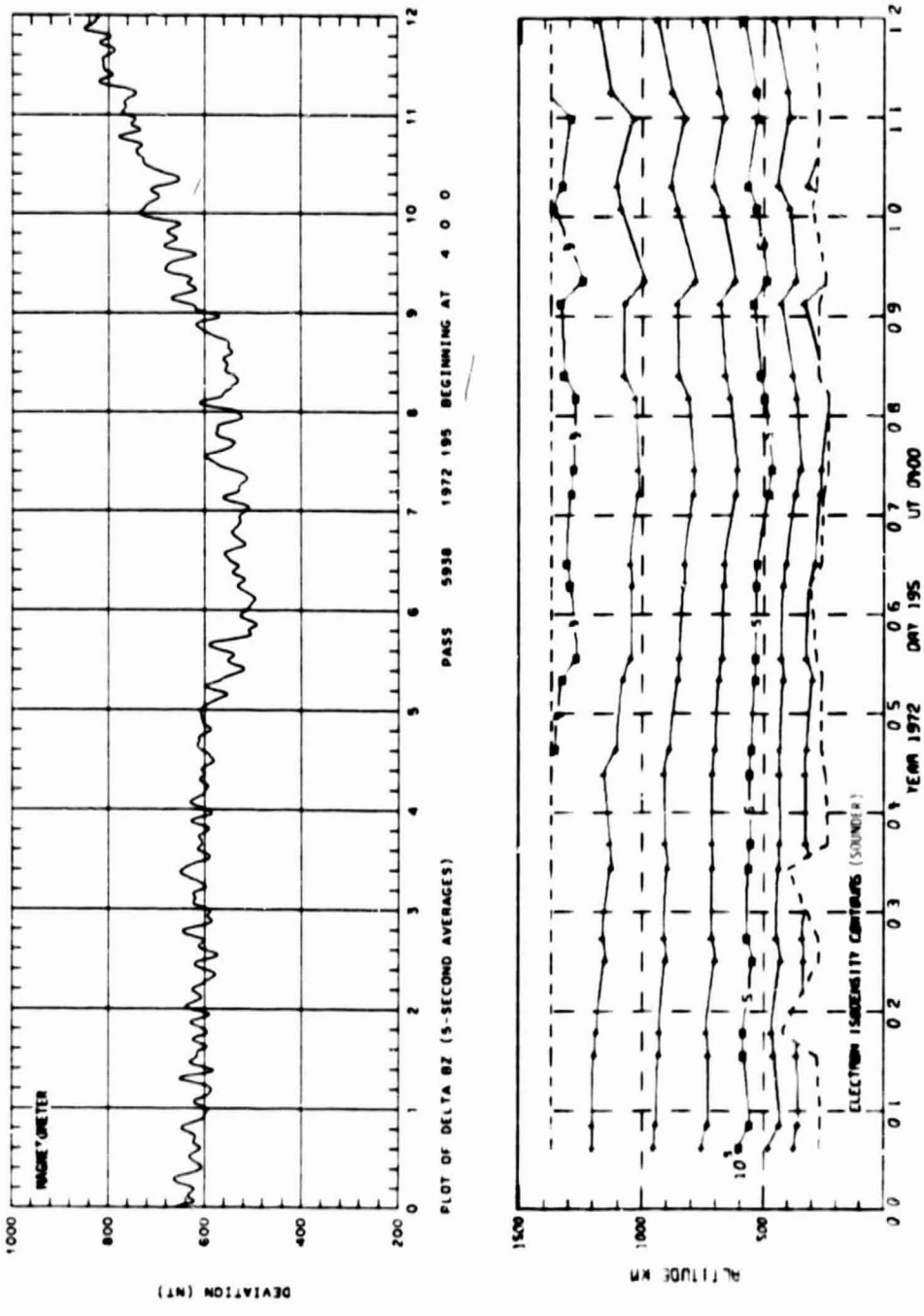

SET 13, FORMAT 2

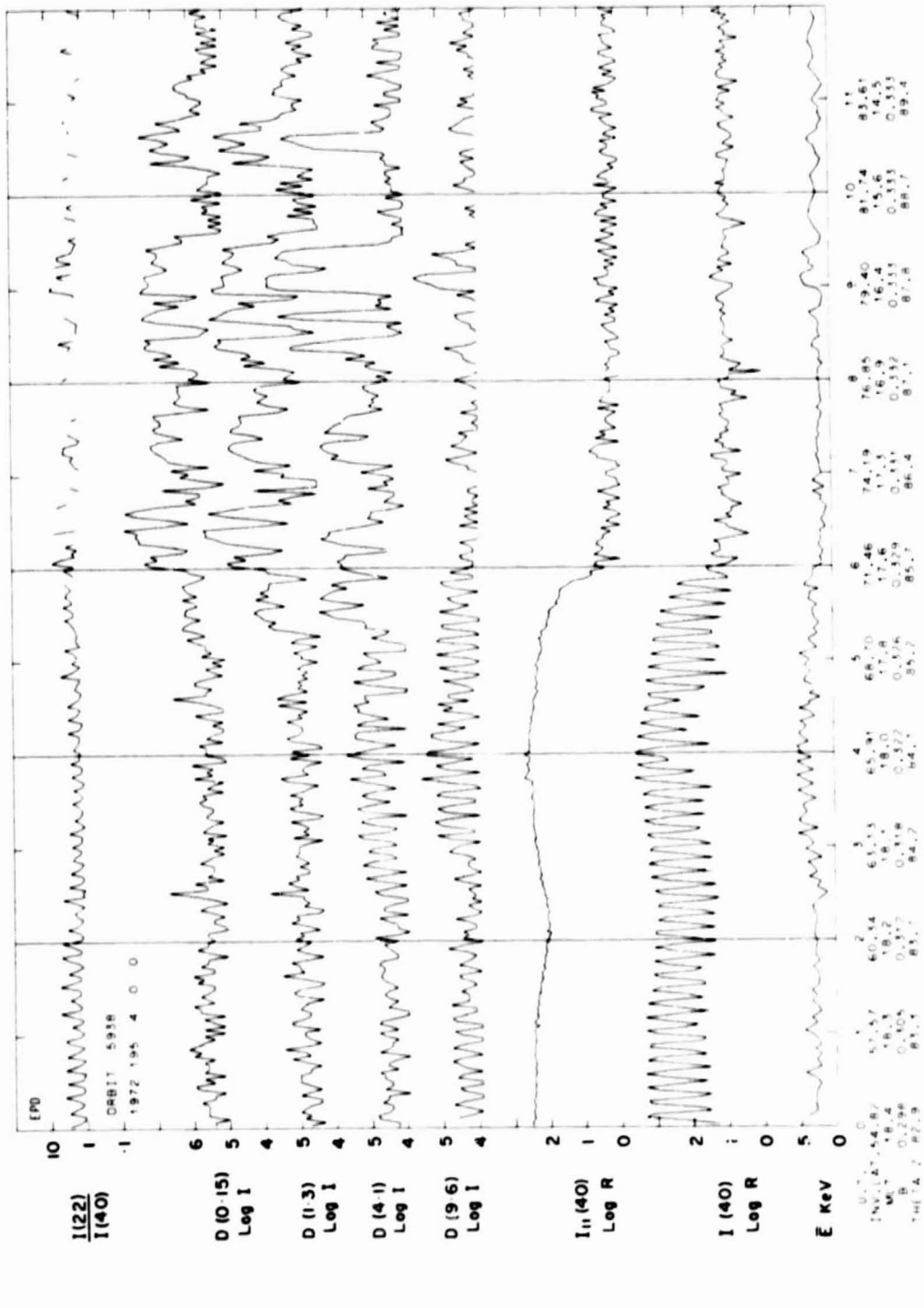

SET 13, FORMAT 3

ORBIT 5938
DATE 720713
DAY 195

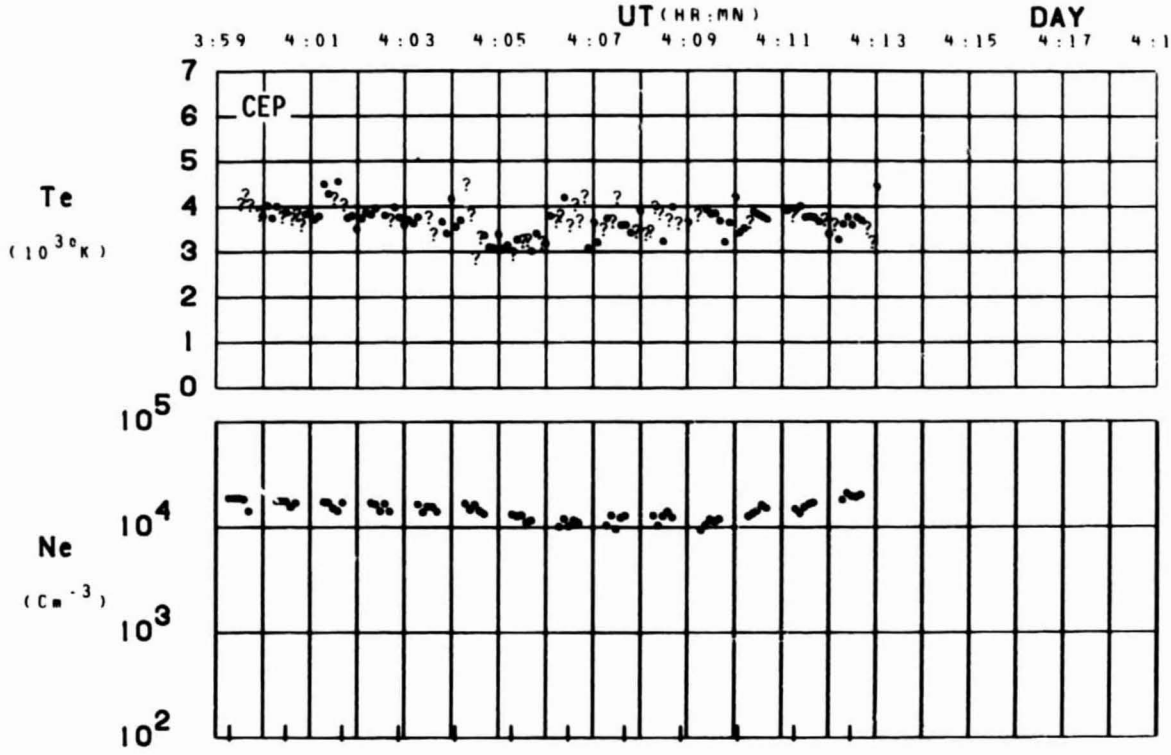

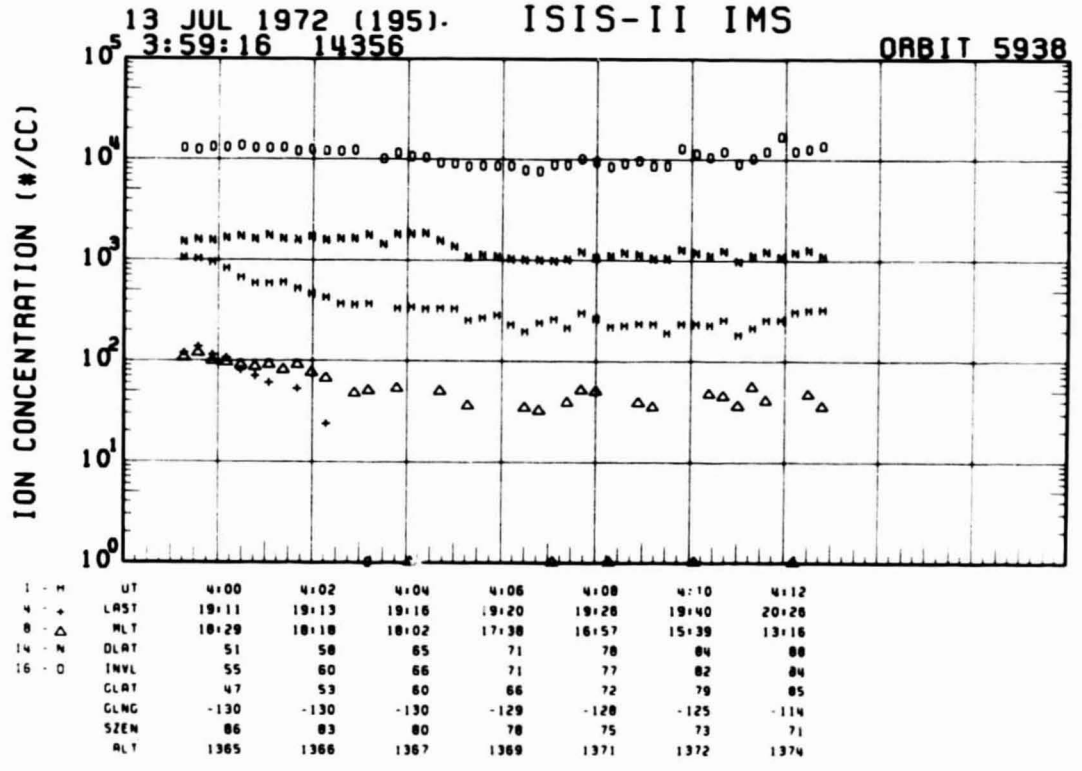

1 - H	UT	4:00	4:02	4:04	4:06	4:08	4:10	4:12
4 - +	LAST	19:11	19:13	19:16	19:20	19:26	19:40	20:26
8 - △	MLT	18:29	18:18	18:02	17:38	16:57	15:39	13:16
14 - N	DLAT	51	58	65	71	78	84	88
16 - O	INVL	55	60	66	71	77	82	84
	GLAT	47	53	60	66	72	79	85
	GLNG	-130	-130	-130	-129	-128	-125	-114
	SZEN	86	83	80	78	75	73	71
	ALT	1365	1366	1367	1369	1371	1372	1374

SET 13, FORMAT 4

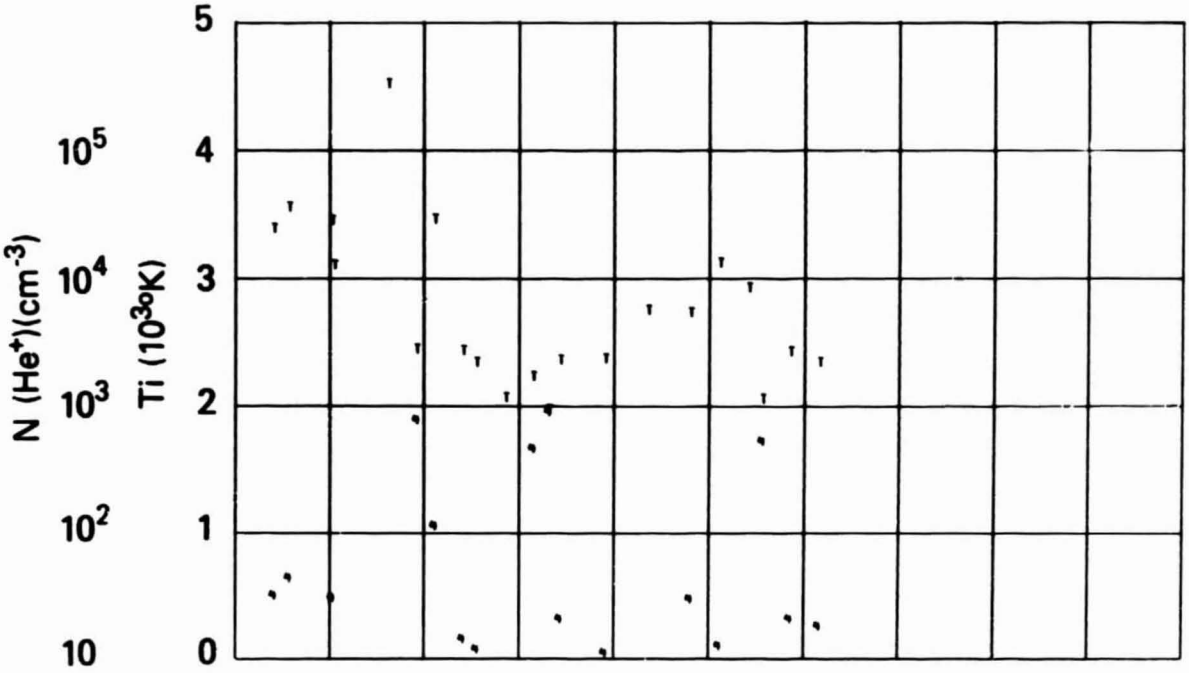

UT	4:00	4:02	4:04	4:06	4:08	4:10	4:12
LAST	19:11	19:13	19:16	19:20	19:26	19:40	20:26
MLT	18:29	18:18	18:02	17:38	17:57	15:39	13:16
DLAT	51	58	65	71	78	84	88
INVL	55	60	66	71	77	82	84
GLAT	47	53	60	66	72	79	85
GLNG	-130	-130	-130	-129	-128	-125	-114
SZEN	86	83	80	78	75	73	71
ALT	1365	1366	1367	1369	1371	1372	1374

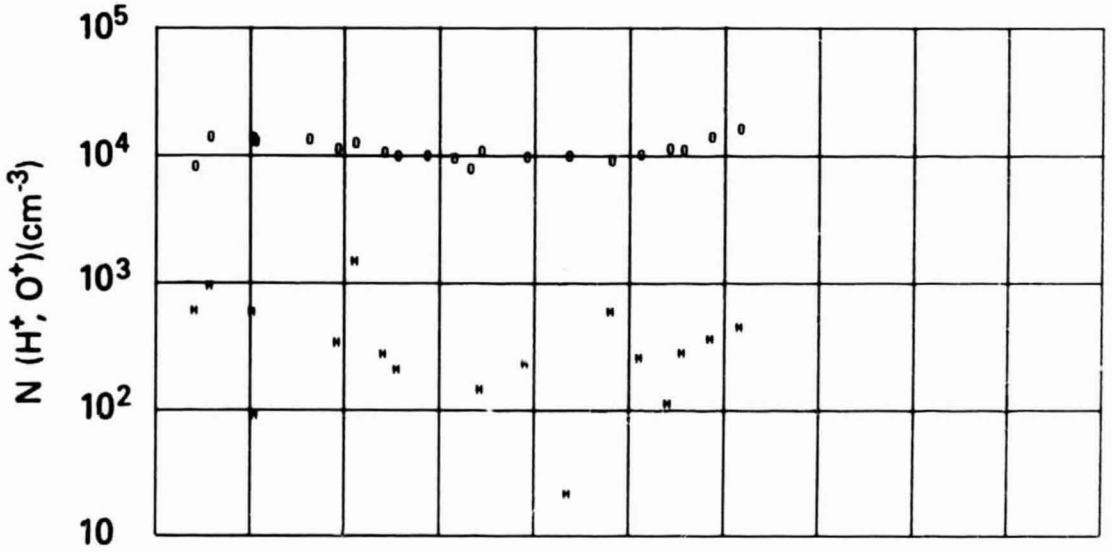

SET 13, FORMAT 5

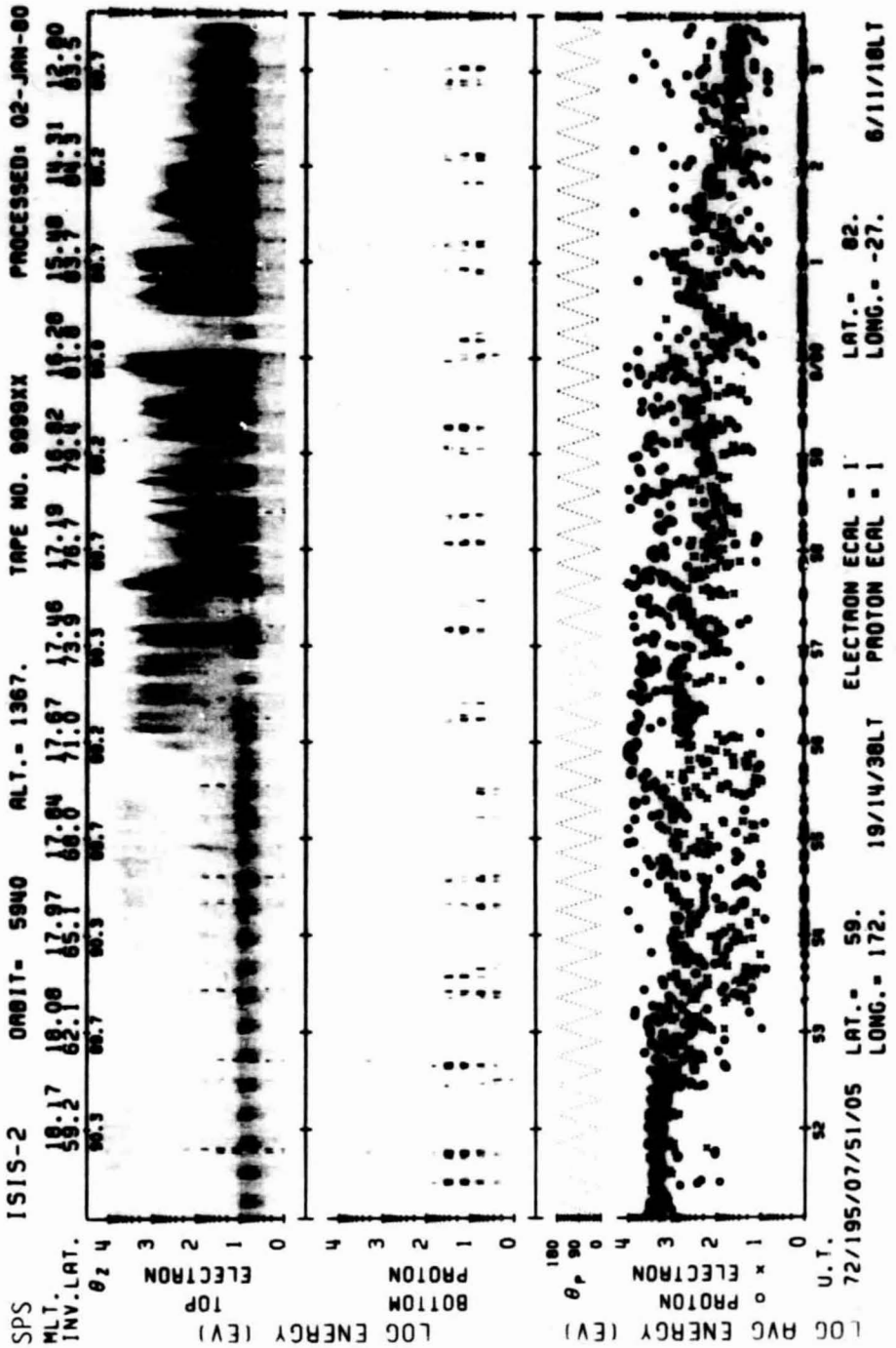

SET 14, FORMAT 6

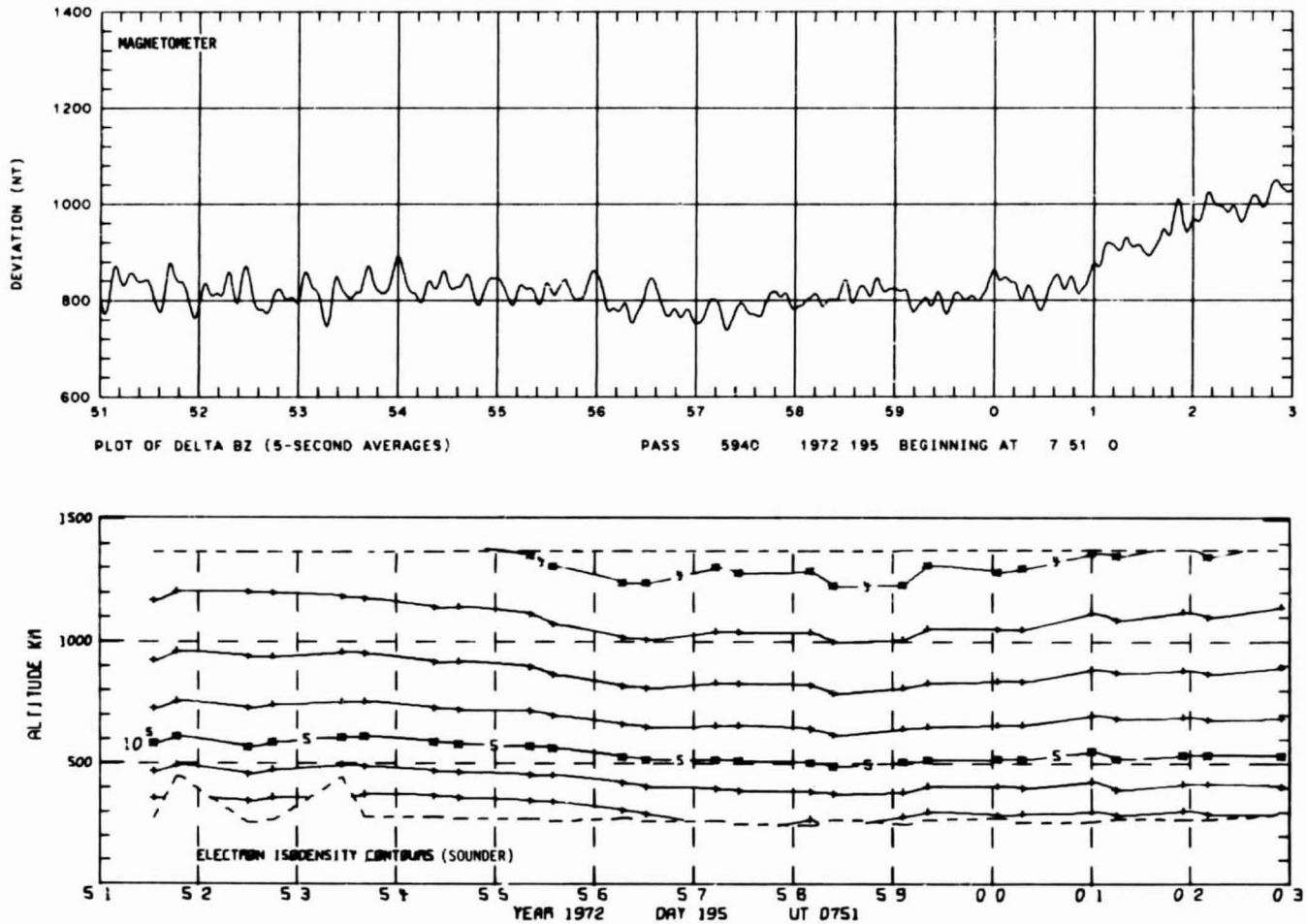

SET 14, FORMAT 2

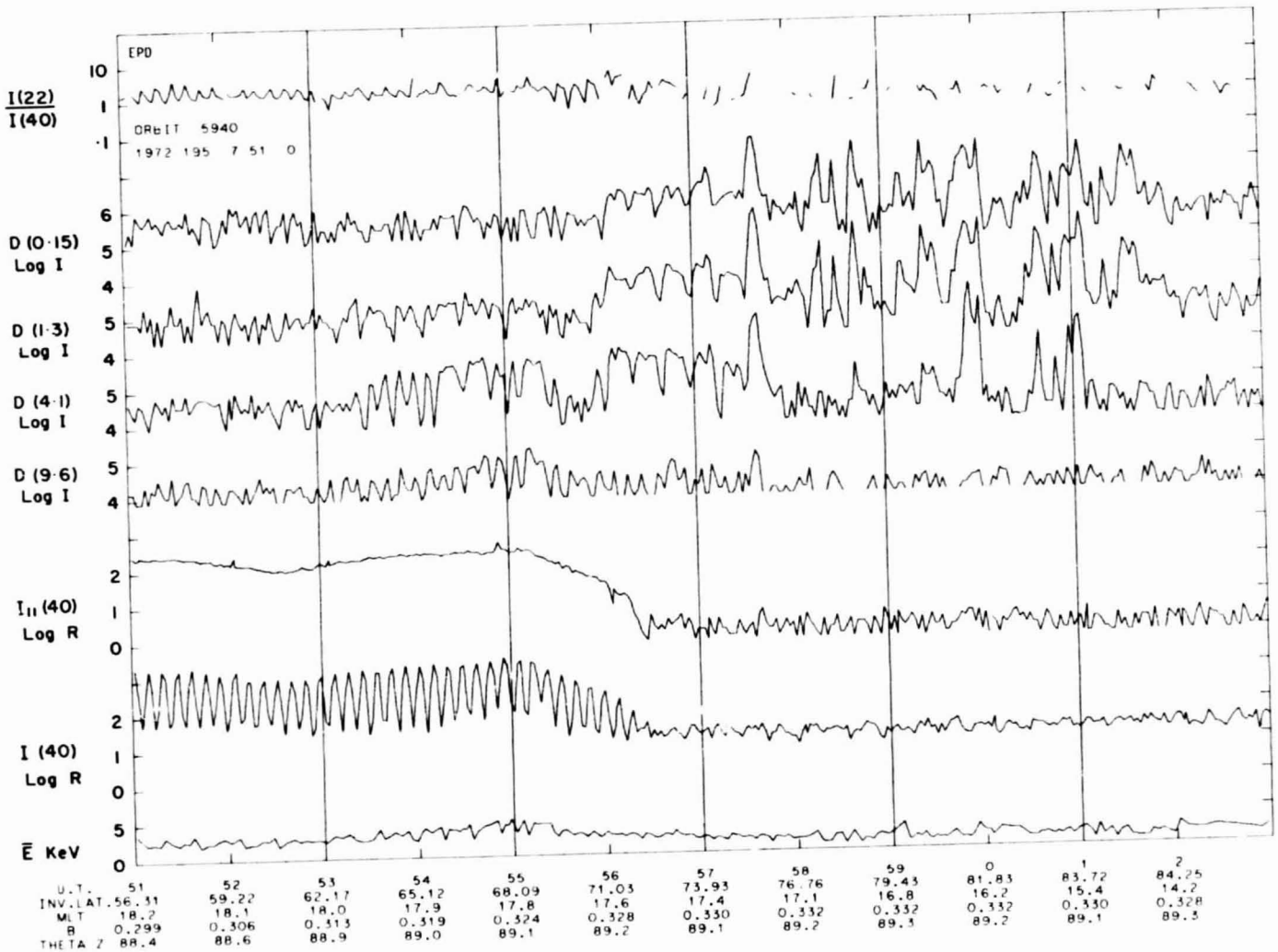

SET 14, FORMAT 3

ORBIT 5940
DATE 720713
DAY 195

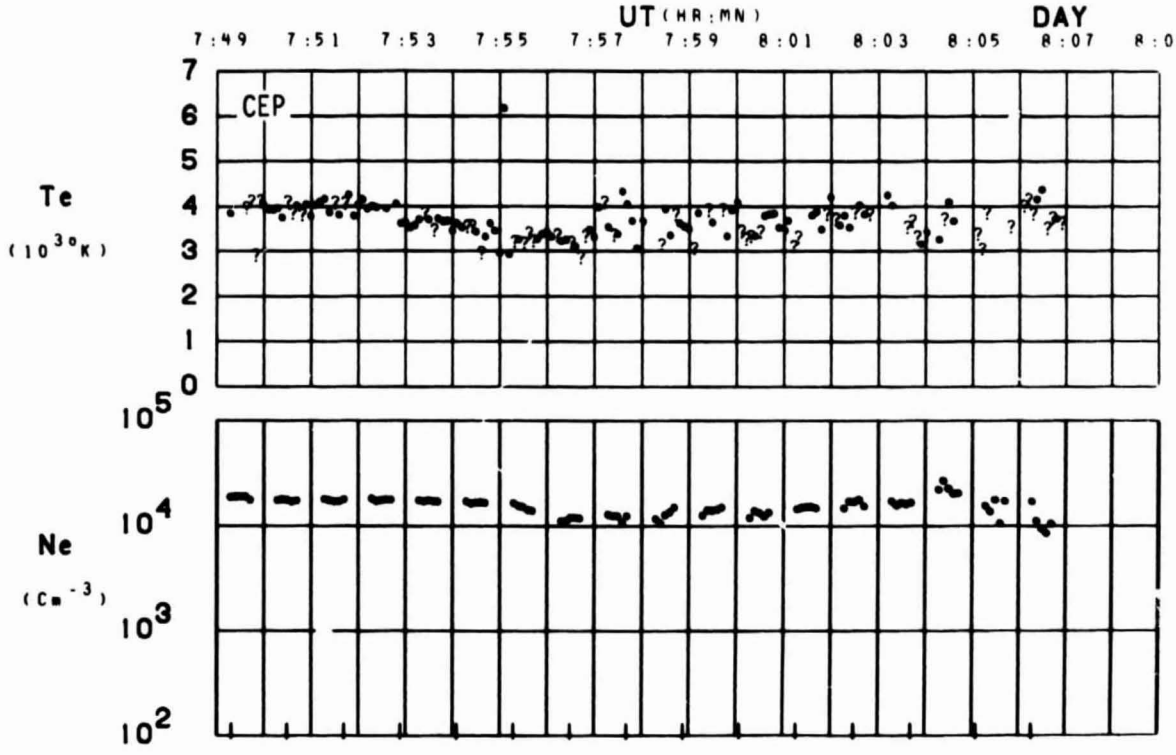

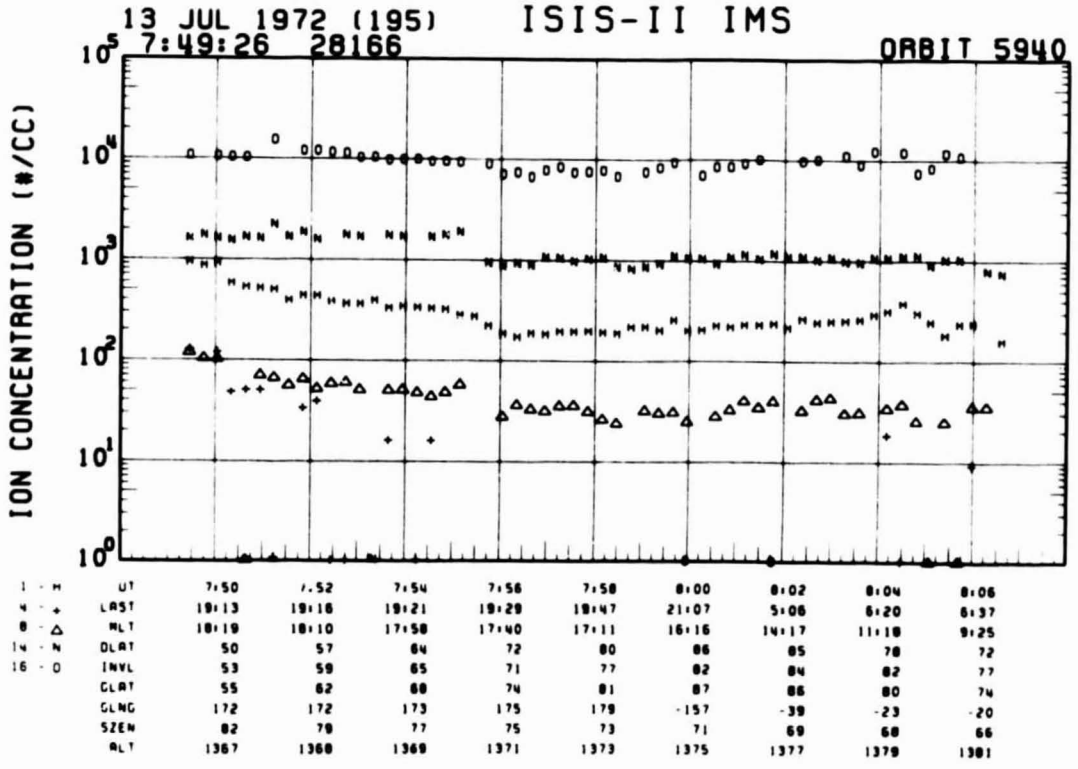

1 - H	UT	7:50	7:52	7:54	7:56	7:58	8:00	8:02	8:04	8:06
4 - +	LAST	19:13	19:16	19:21	19:29	19:47	21:07	5:06	6:20	6:37
8 - Δ	MLT	18:19	18:10	17:58	17:40	17:11	16:16	14:17	11:18	9:25
14 - N	DLAT	50	57	64	72	80	86	85	78	72
16 - O	INVL	53	59	65	71	77	82	84	82	77
	GLAT	55	62	68	74	81	87	86	80	74
	GLNG	172	172	173	175	179	-157	-39	-23	-20
	SZEN	82	78	77	75	73	71	69	68	66
	ALT	1367	1368	1369	1371	1373	1375	1377	1379	1381

SET 14, FORMAT 4

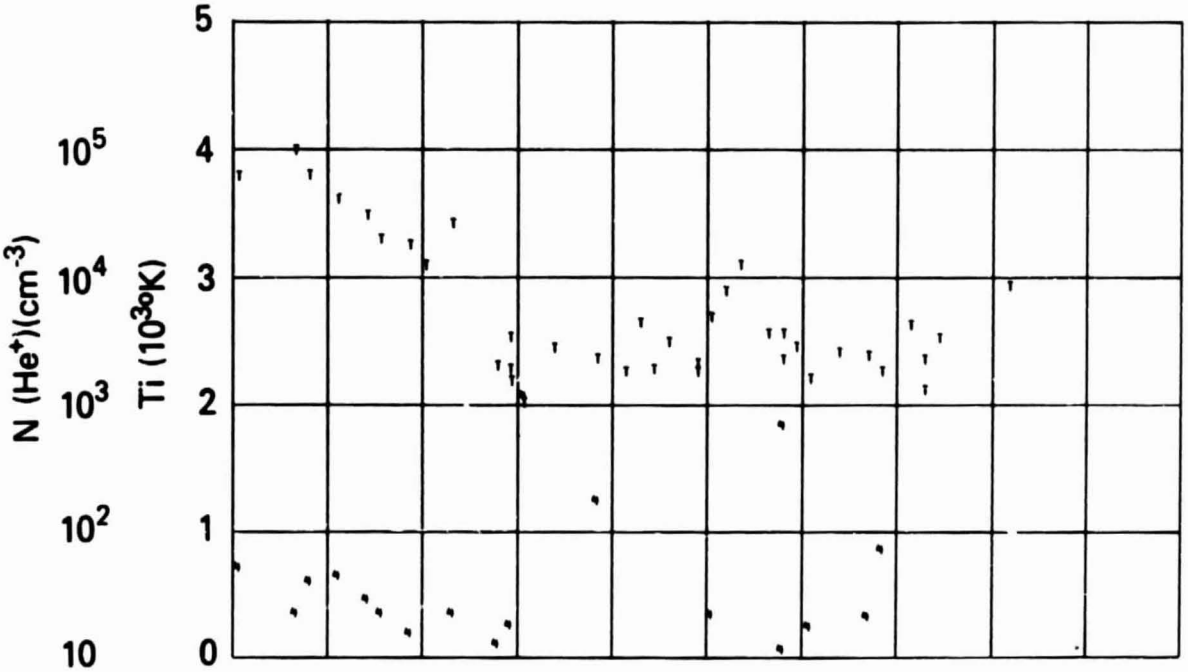

UT	7:50	7:52	7:54	7:56	7:58	8:00	8:02	8:04	8:06
LAST	19:13	19:16	19:21	19:29	19:47	21:07	5:06	6:20	6:37
MLT	18:19	18:10	17:58	17:40	17:11	16:16	14:17	11:18	9:25
DLAT	50	57	64	72	80	86	85	78	72
INVL	53	59	65	71	77	82	84	82	77
GLAT	55	62	68	74	81	87	86	80	74
GLNG	172	172	173	175	179	-157	-39	-23	-20
SZEN	82	79	77	75	73	71	69	68	66
ALT	1367	1368	1369	1371	1373	1375	1377	1379	1381

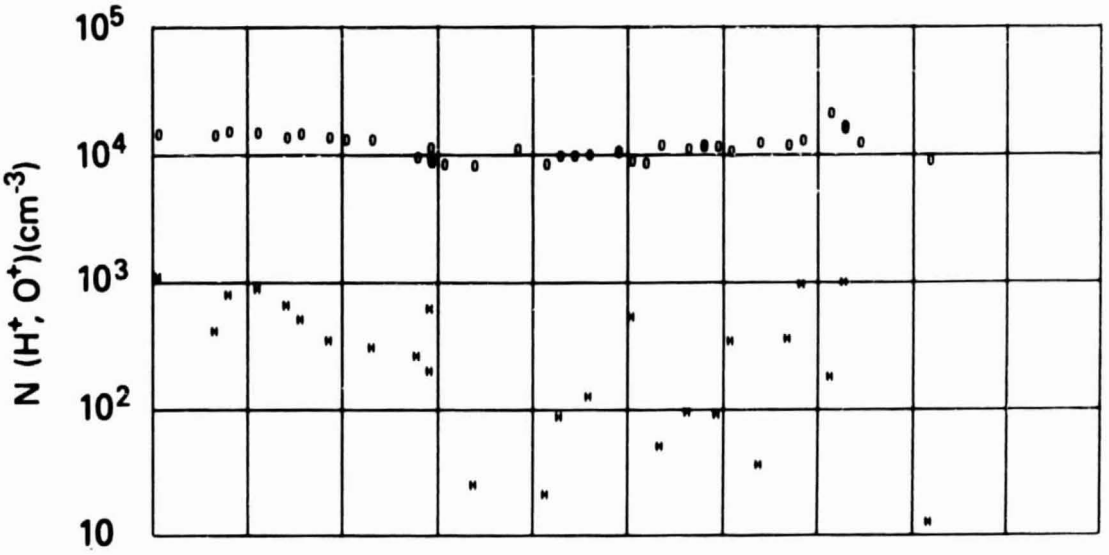

SET 14, FORMAT 5

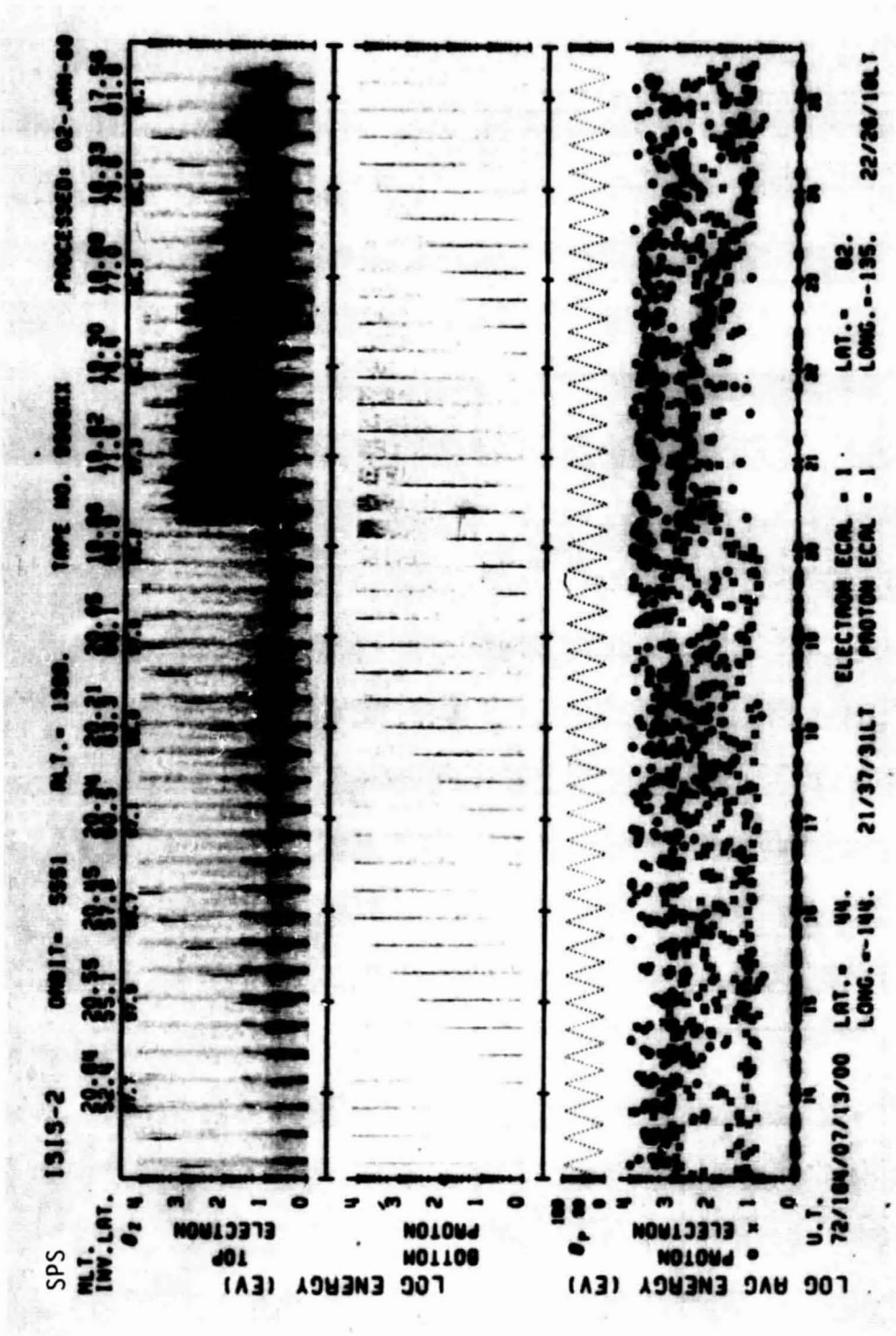

SET 15, FORMAT 6

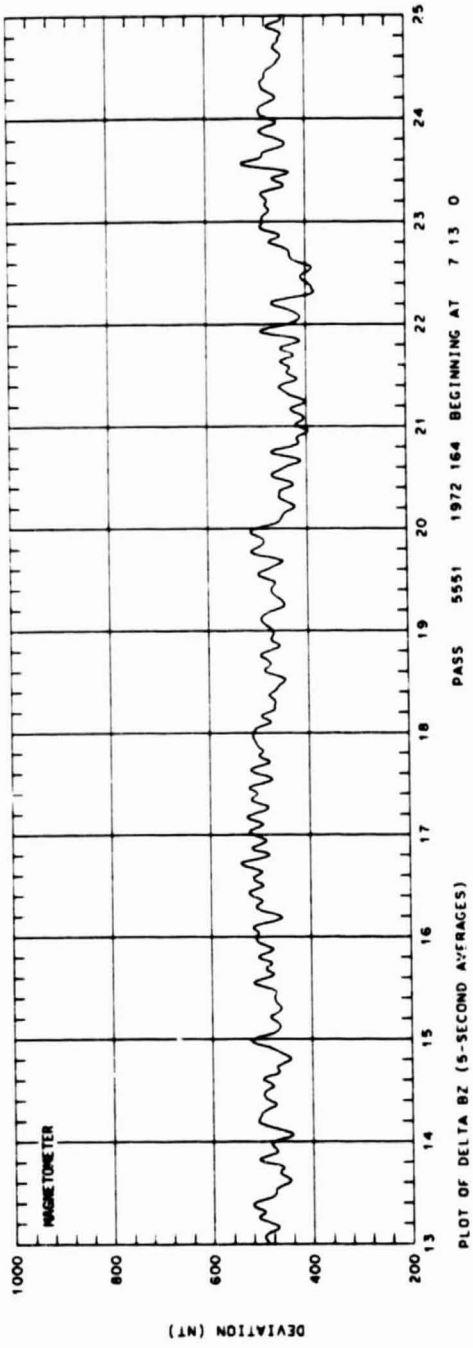

SET 15, FORMAT 2

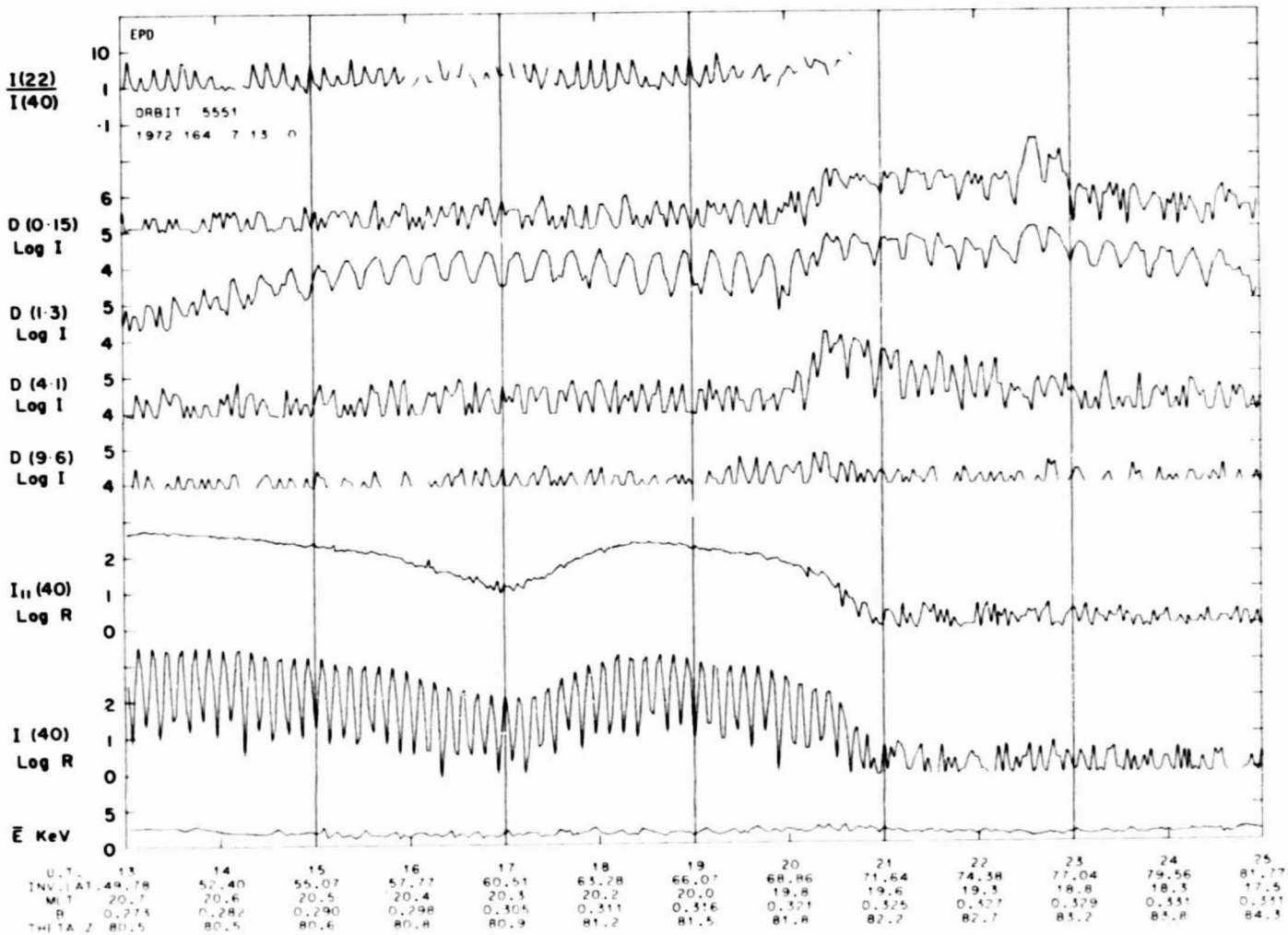

SET 15, FORMAT 3

ORBIT 5551
DATE 720612
DAY 164

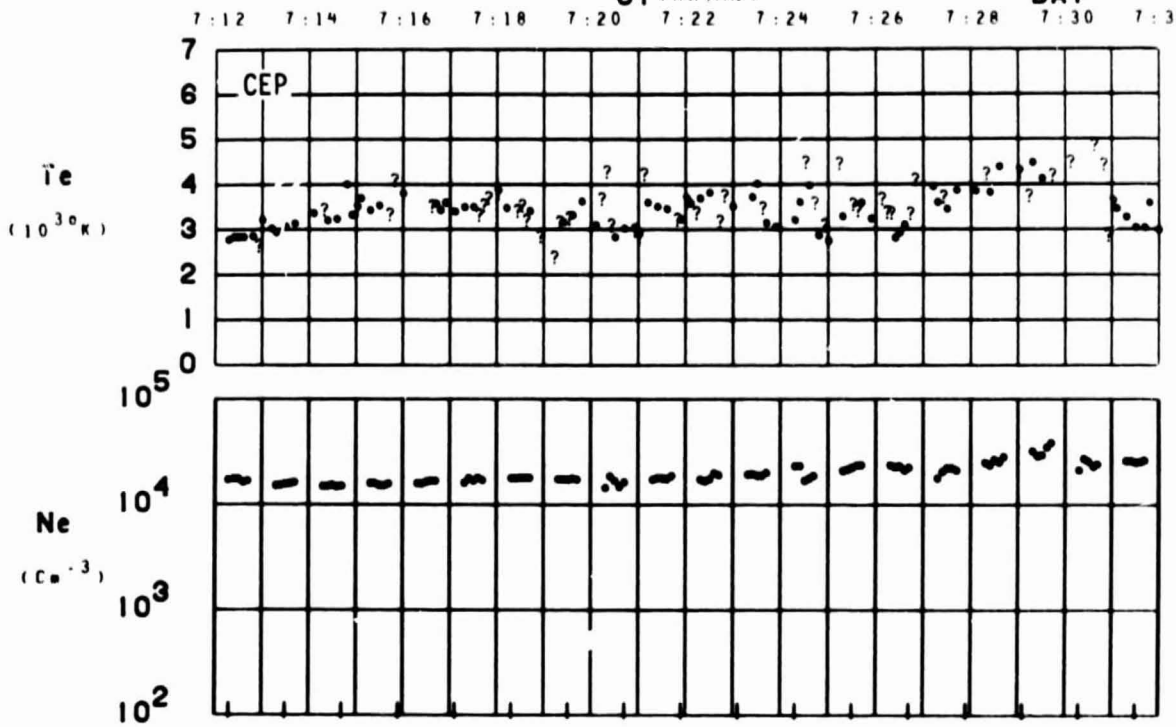

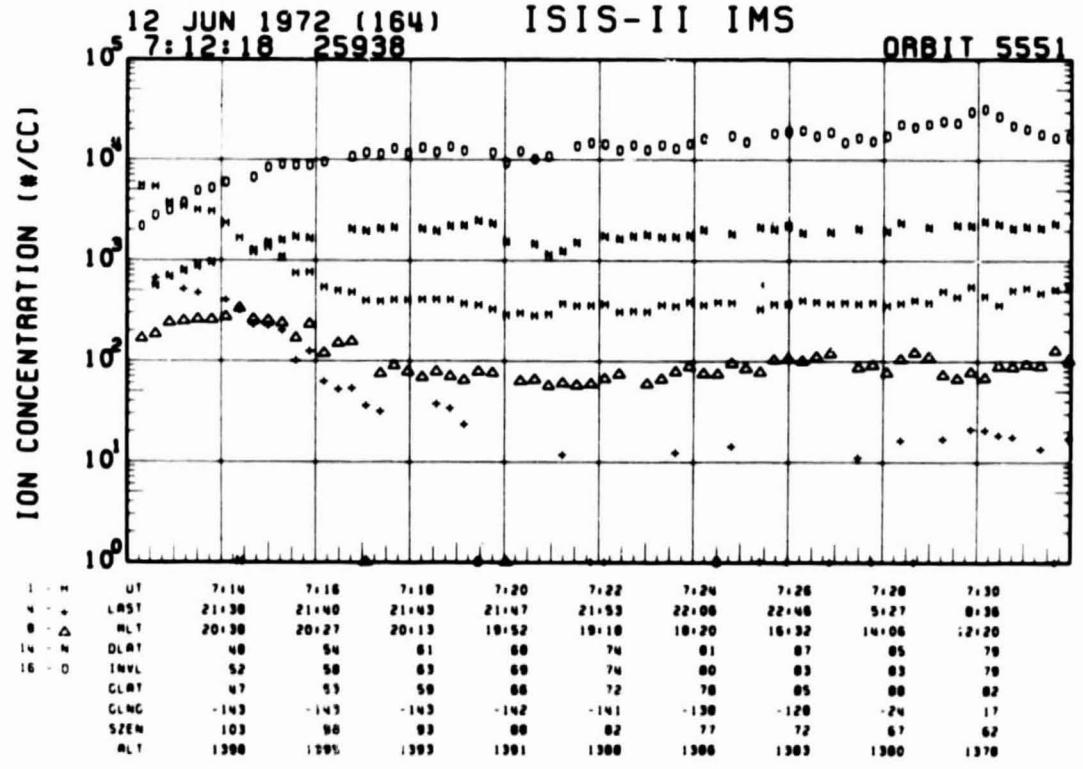

UT	7:14	7:16	7:18	7:20	7:22	7:24	7:26	7:28	7:30
LAST	21:38	21:40	21:43	21:47	21:53	22:06	22:46	5:27	8:36
ALT	20:38	20:27	20:13	19:52	19:18	18:20	16:32	14:06	12:20
DLAT	48	54	61	68	74	81	87	85	79
INVL	52	58	63	69	74	80	83	83	79
GLAT	47	53	59	66	72	78	85	88	82
GLNG	-143	-143	-143	-142	-141	-138	-128	-24	17
SZEN	103	98	93	88	82	77	72	67	62
ALT	1398	1395	1393	1391	1388	1386	1383	1380	1378

H - H
+ - +
Δ - Δ
N - N
O - O

SET 15, FORMAT 4

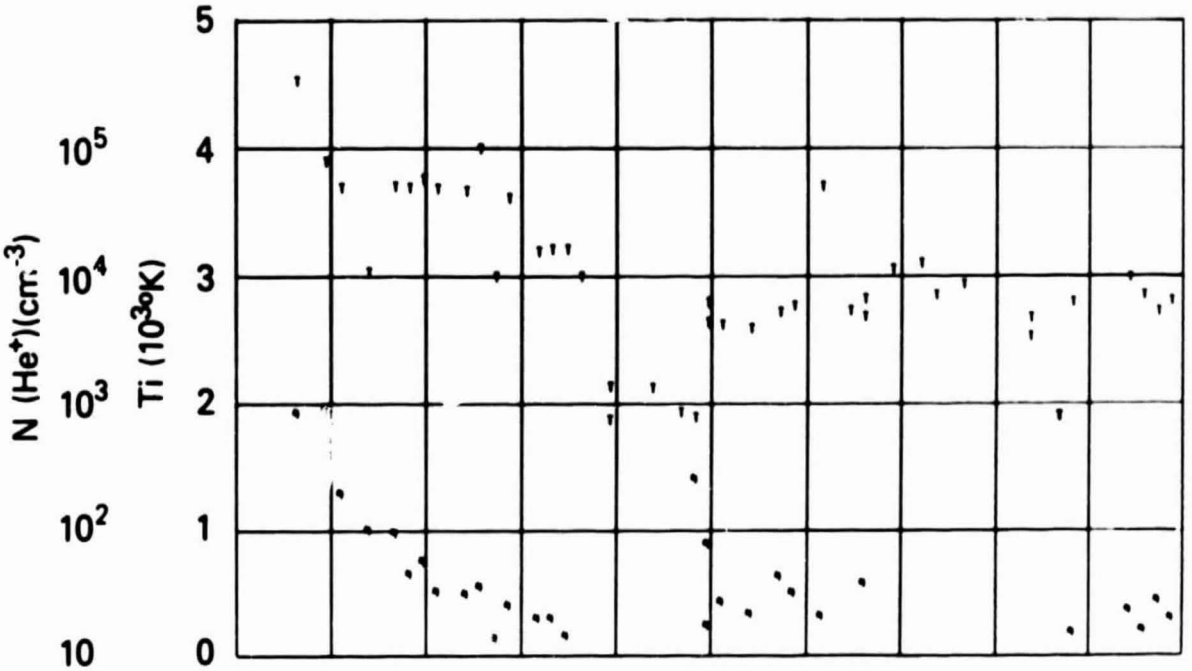

UT	7:14	7:16	7:18	7:20	7:22	7:24	7:26	7:28	7:30
LAST	21:38	21:40	21:43	21:47	21:53	22:06	22:46	5:27	8:36
MLT	20:38	20:27	20:13	19:52	19:18	18:20	16:32	14:06	12:20
DLAT	48	54	61	68	74	81	87	85	79
INVL	52	58	63	69	74	80	83	83	79
CLAT	47	53	59	66	72	78	85	88	82
CLNG	-143	-143	-143	-142	-141	-138	-128	-24	17
SZEN	103	98	93	88	82	77	72	67	62
ALT	1390	1395	1383	1391	1388	1386	1383	1380	1378

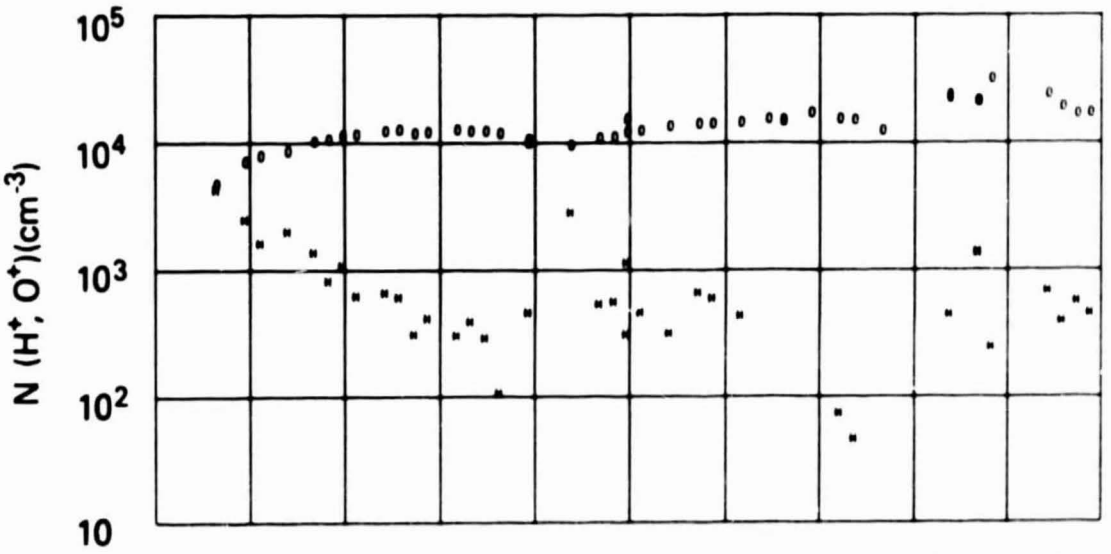

SET 15, FORMAT 5

72/164/0713

Excerpts of VLF Spectral film for the period 0713 - 0725

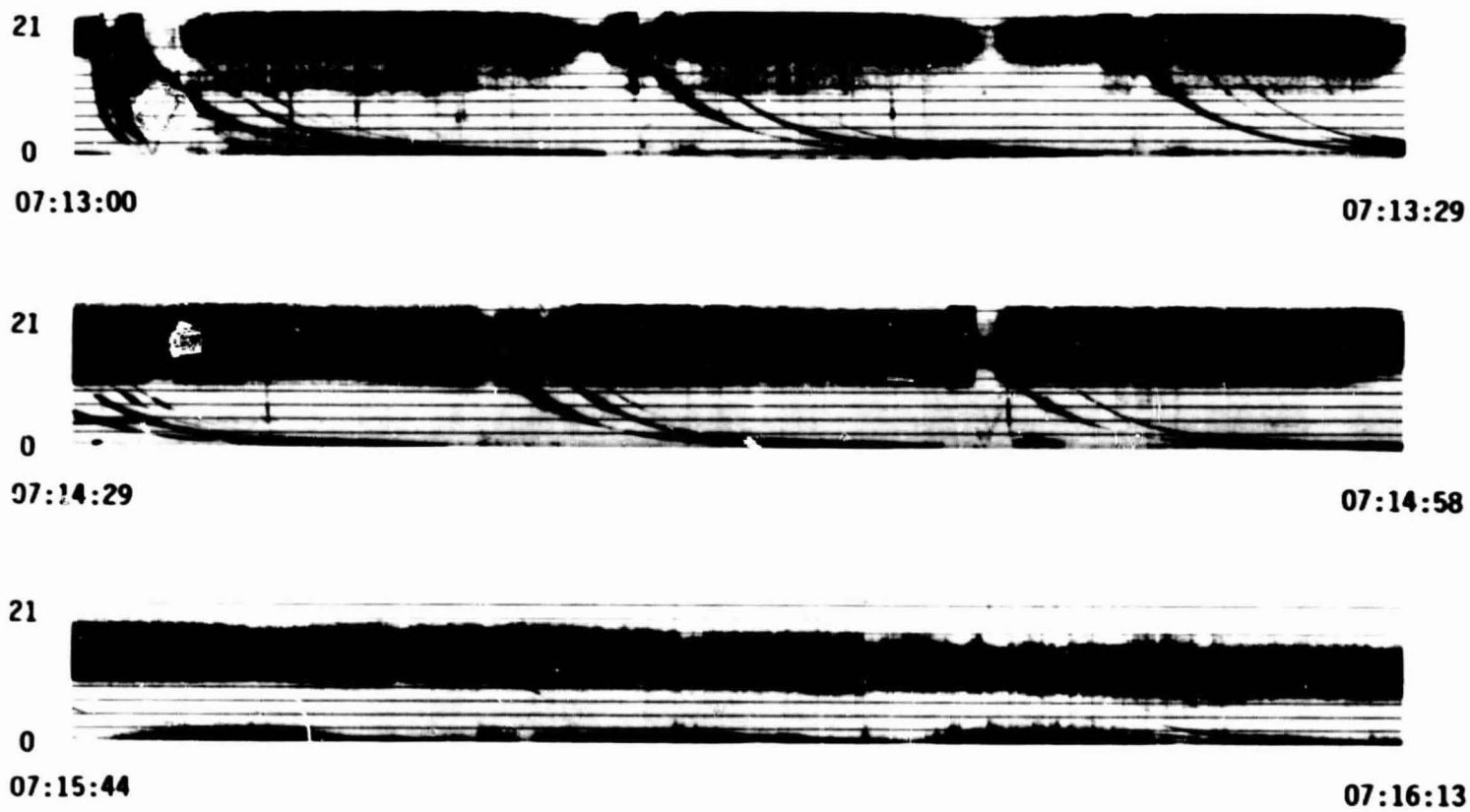

120

SET 15, FORMAT 11

72/164/0713

Excerpts of VLF Spectral film for the period 0713 - 0725

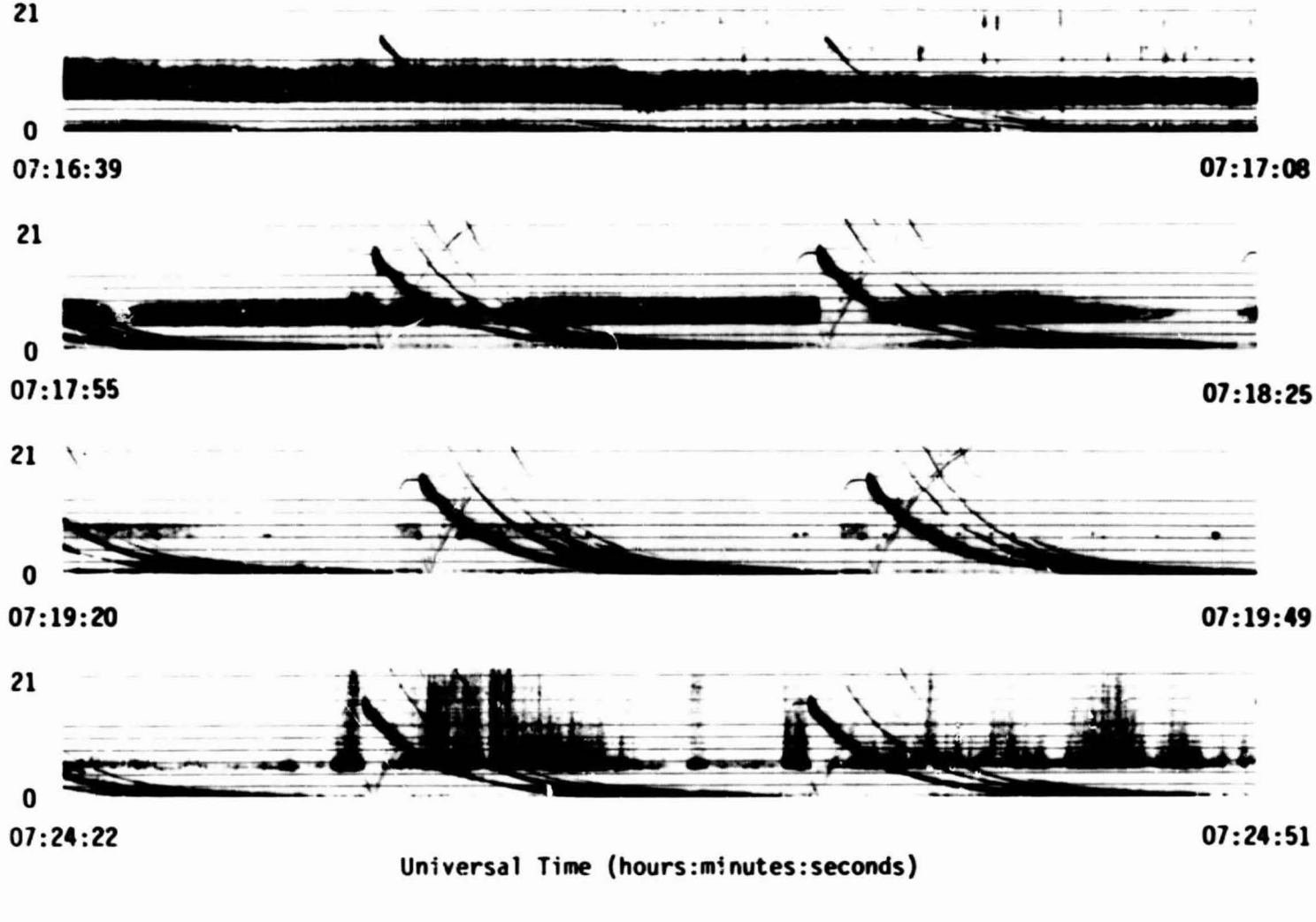

SET 15, FORMAT 11

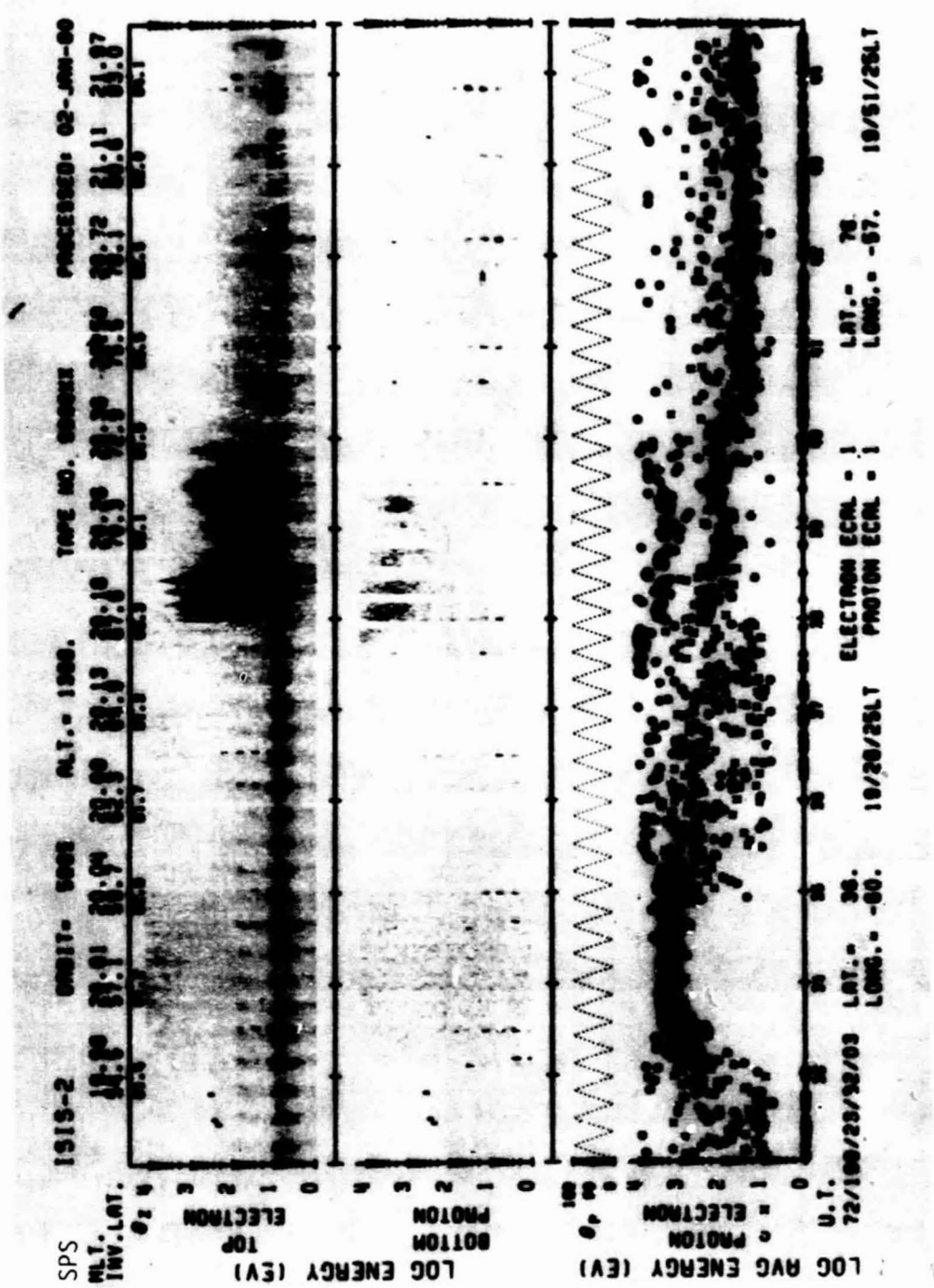

SET 16, FORMAT 6

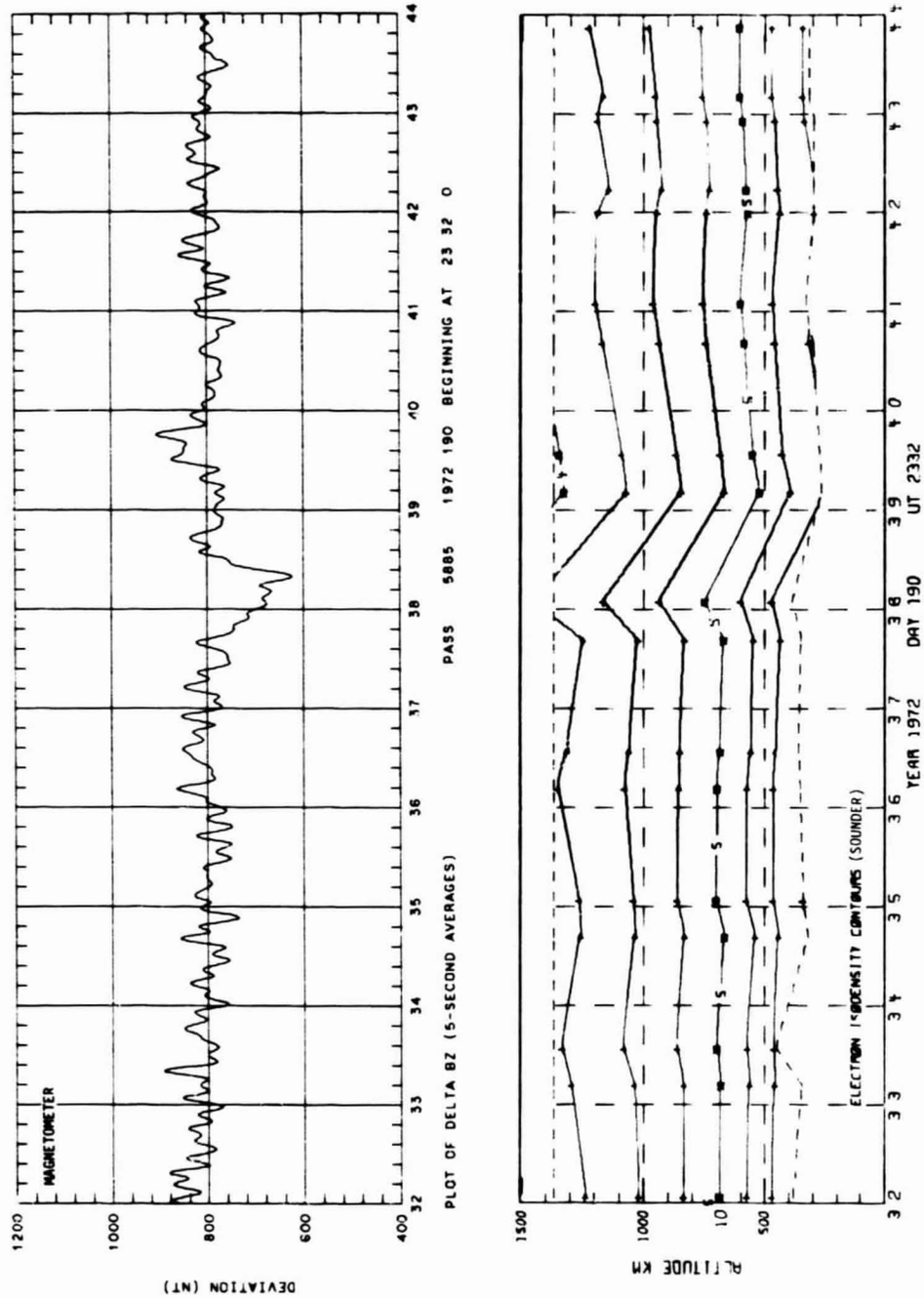

SET 16, FORMAT 2

SET 16, FORMAT 3

ORBIT 5885
DATE 720708
DAY 190

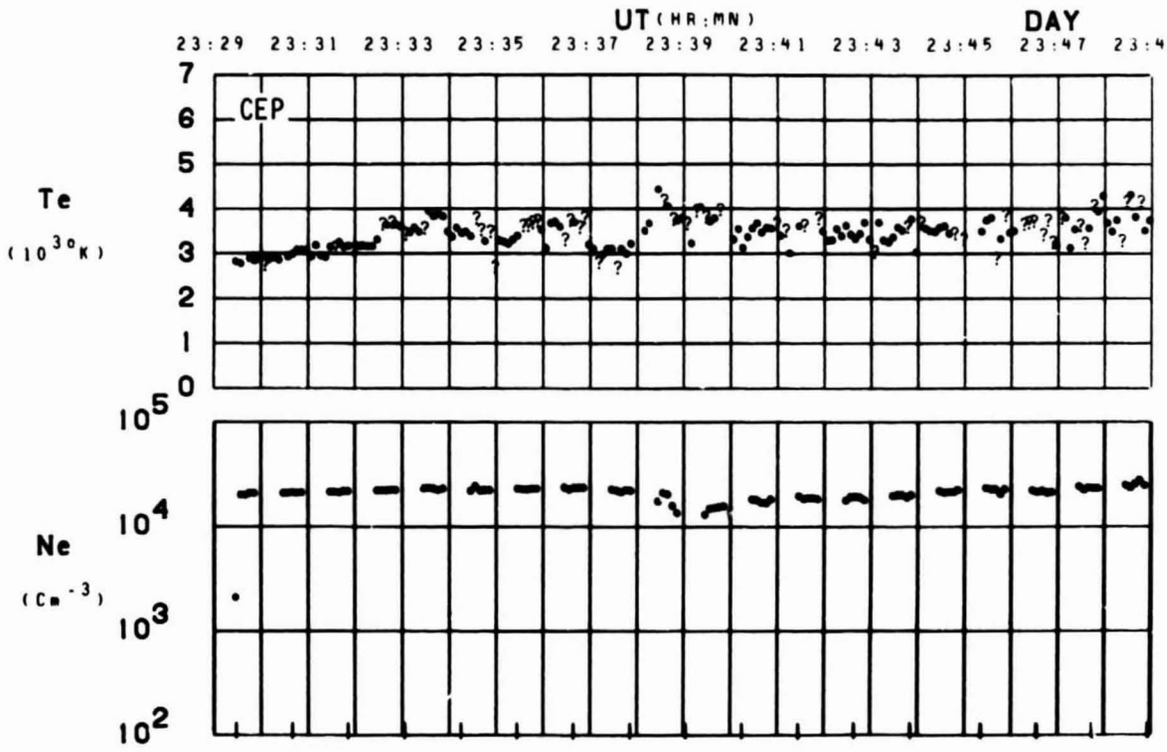

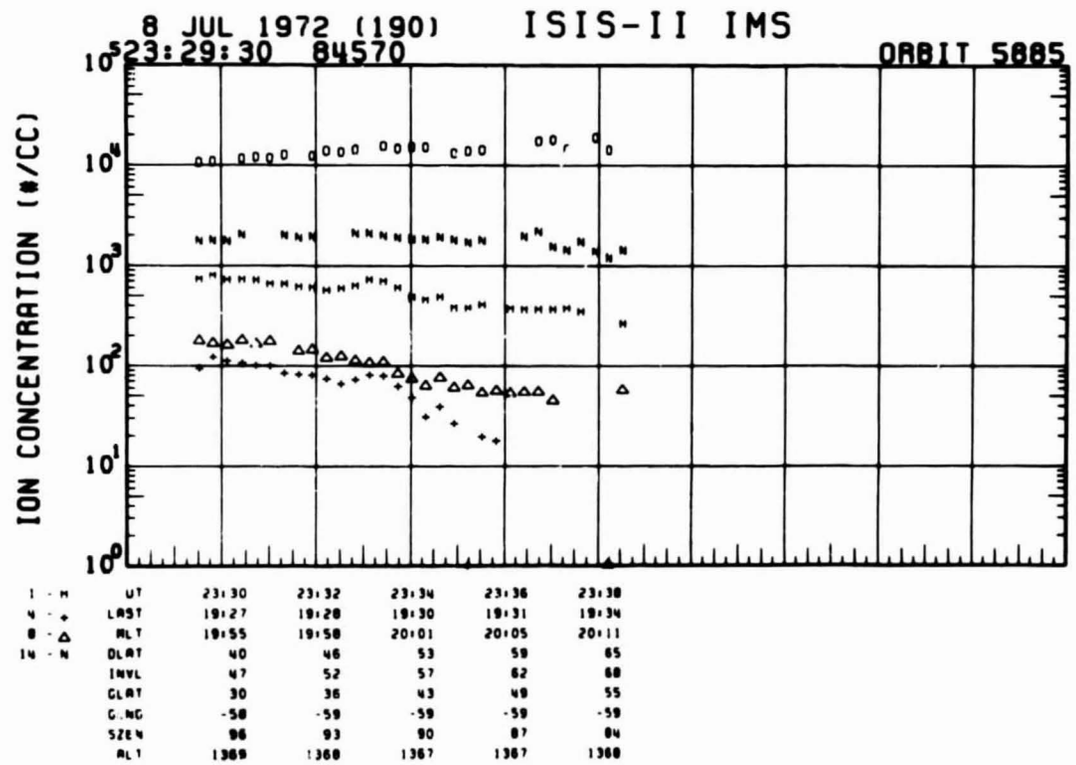

SET 16, FORMAT 4

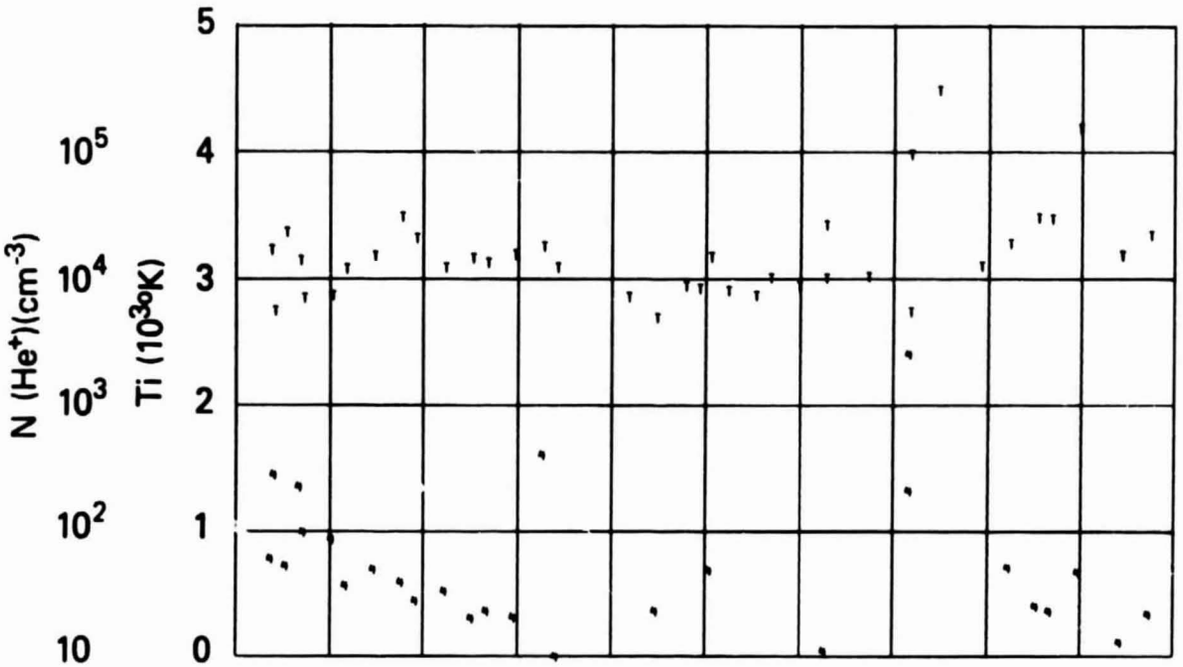

UT	23:30	23:32	23:34	23:36	23:38	23:40	23:42	23:44	23:46
LAST	19:27	19:28	19:30	19:31	19:34	19:37	19:41	19:49	20:08
MLT									
DLAT									
INVL	47	51	57	62	67	72	78	83	84
GLAT	30	36	43	49	55	62	68	74	81
GLNG	-59	-60	-60	-60	-60	-60	-59	-57	-53
SZEN	96	93	90	87	84	81	78	75	72
ALT	1369	1368	1367	1367	1367	1368	1369	1370	1371

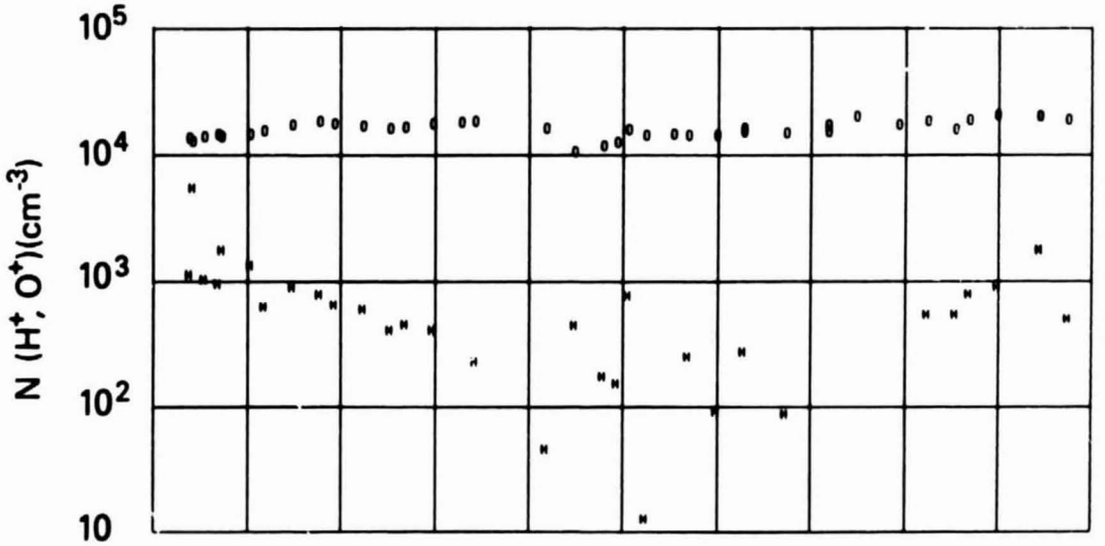

SET 16, FORMAT 5

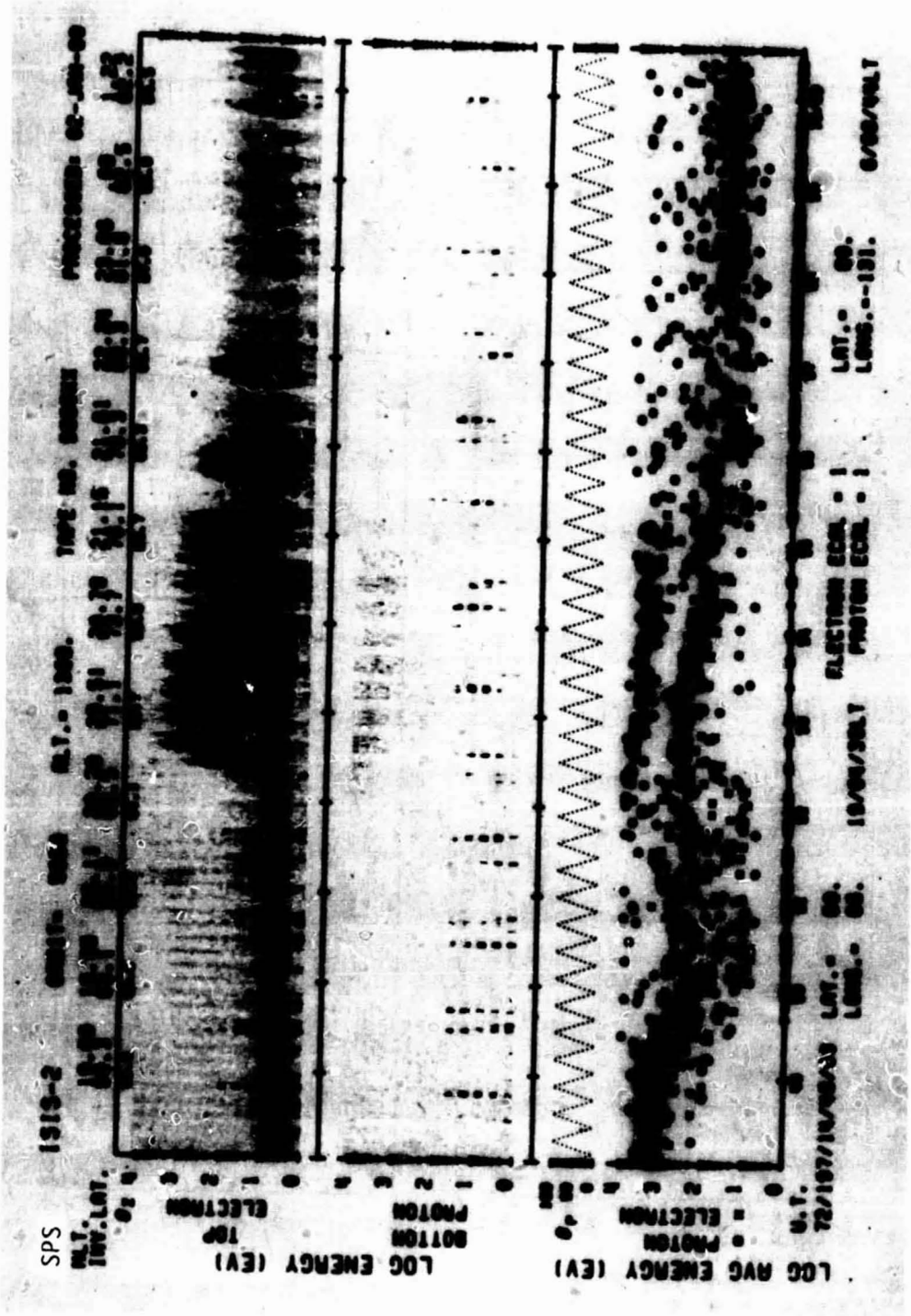

SET 17, FORMAT 6

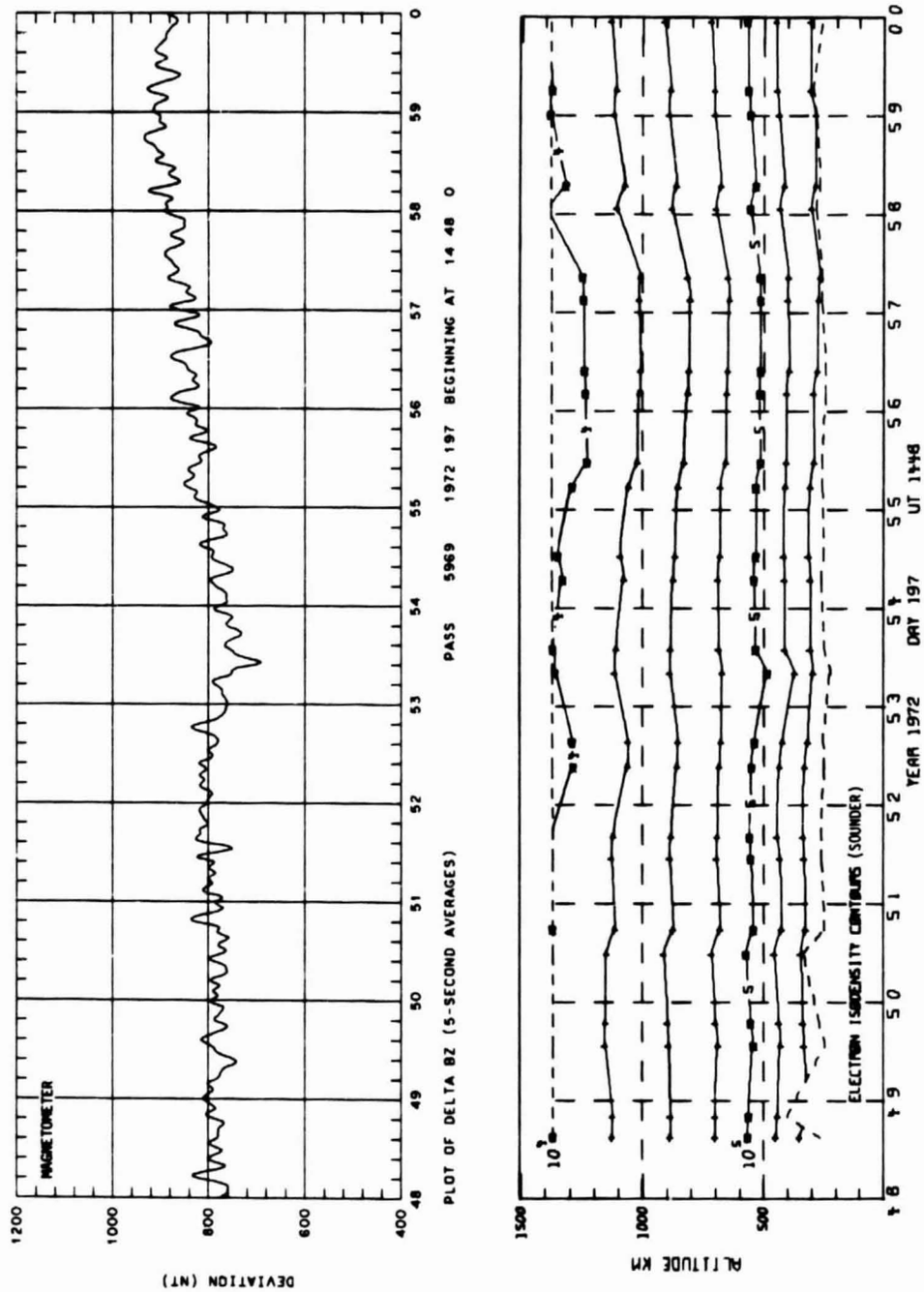

SET 17, FORMAT 2

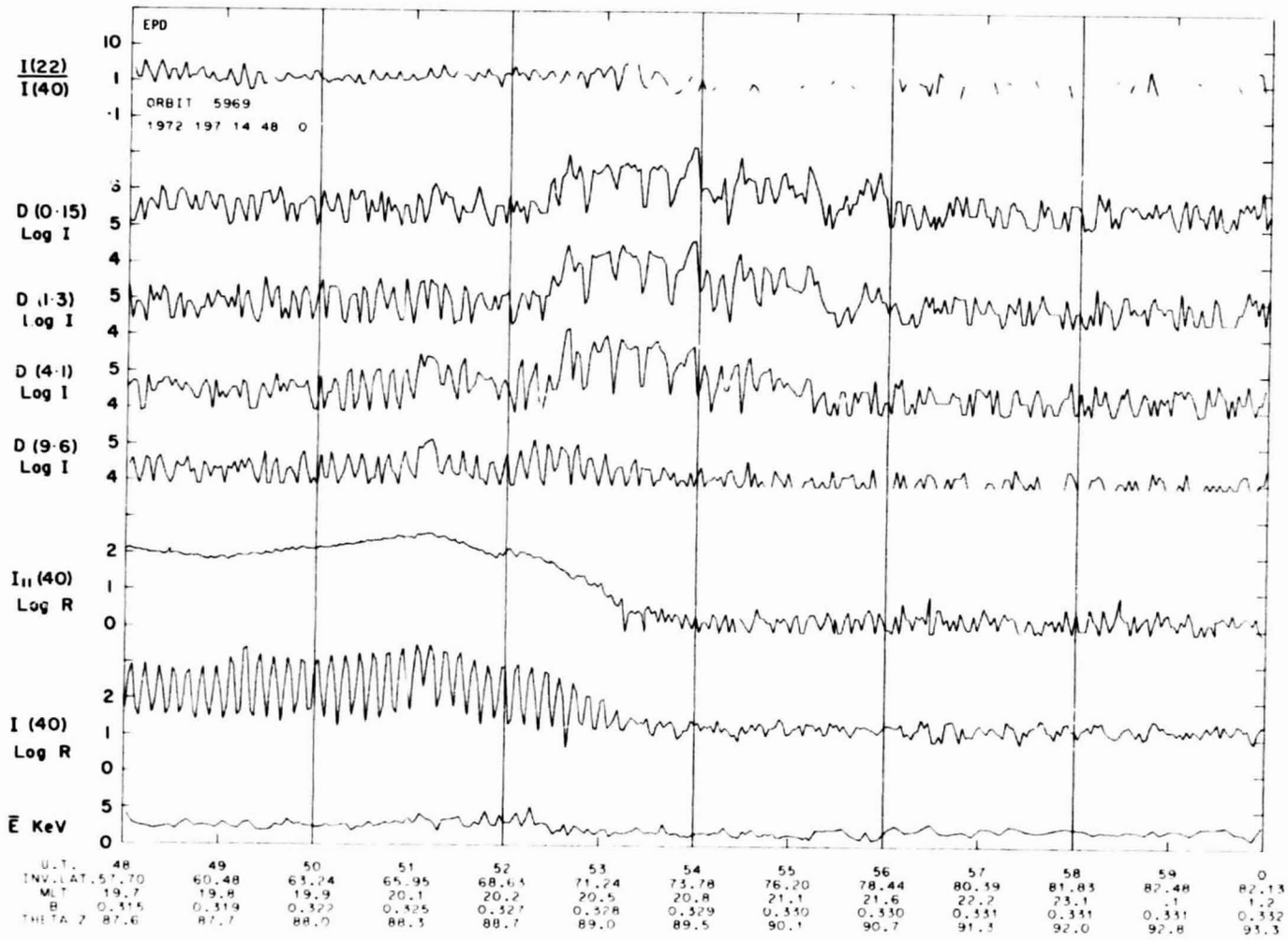

SET 17, FORMAT 3

ORBIT 5969
DATE 720715
DAY 197

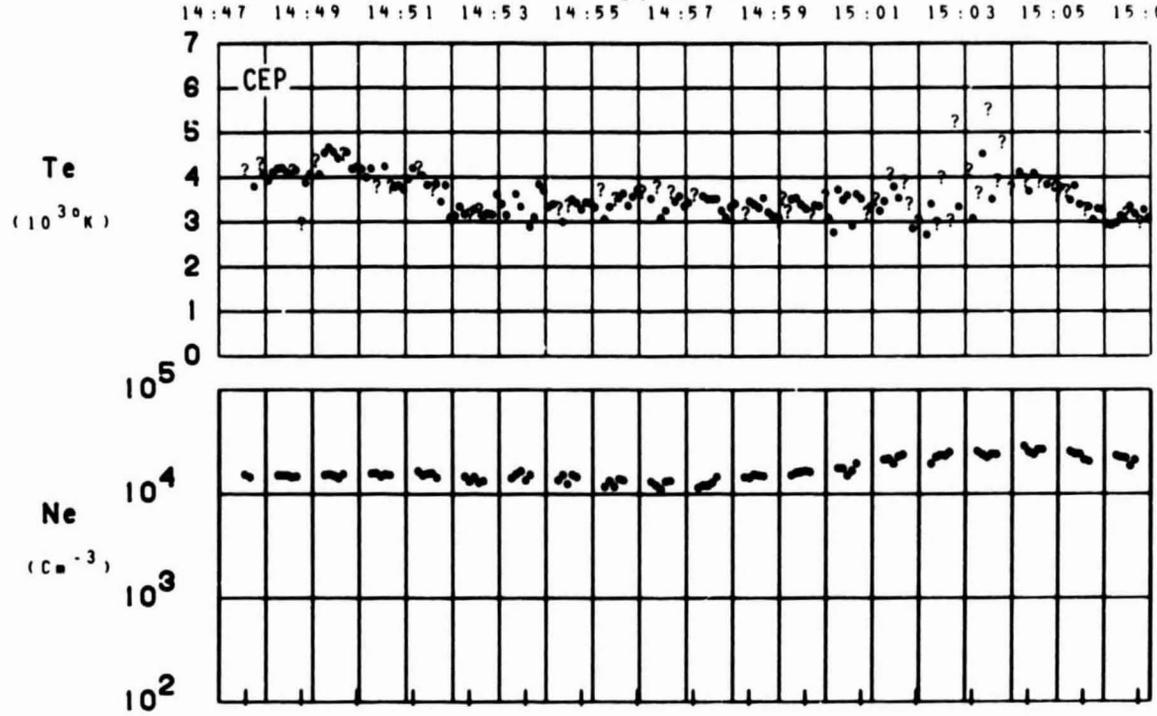

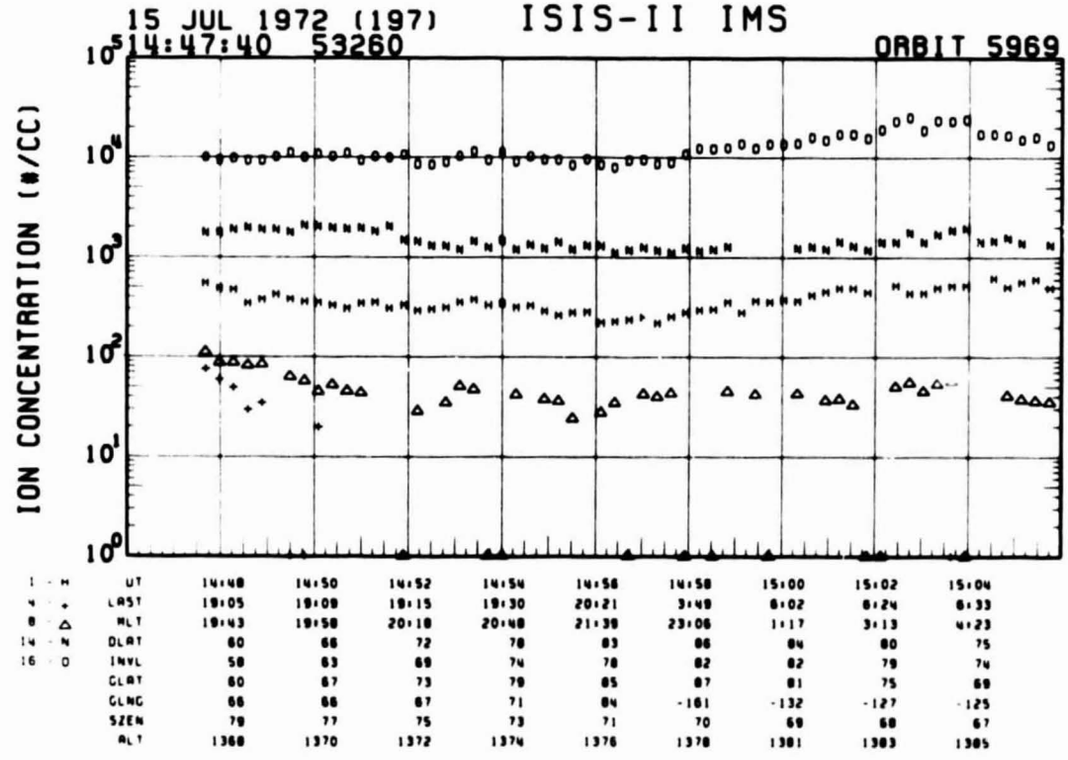

UT	14:48	14:50	14:52	14:54	14:56	14:58	15:00	15:02	15:04
LAST	19:05	19:09	19:15	19:30	20:21	3:49	6:02	6:24	6:33
MLT	19:43	19:58	20:18	20:48	21:39	23:06	1:17	3:13	4:23
DLAT	60	66	72	78	83	86	84	80	75
INVL	58	63	69	74	78	82	82	79	74
GLAT	60	67	73	79	85	87	81	75	69
GLNG	66	66	67	71	84	-161	-132	-127	-125
SZEN	79	77	75	73	71	70	69	68	67
ALT	1368	1370	1372	1374	1376	1378	1381	1383	1385

SET 17, FORMAT 4

RPA 720715

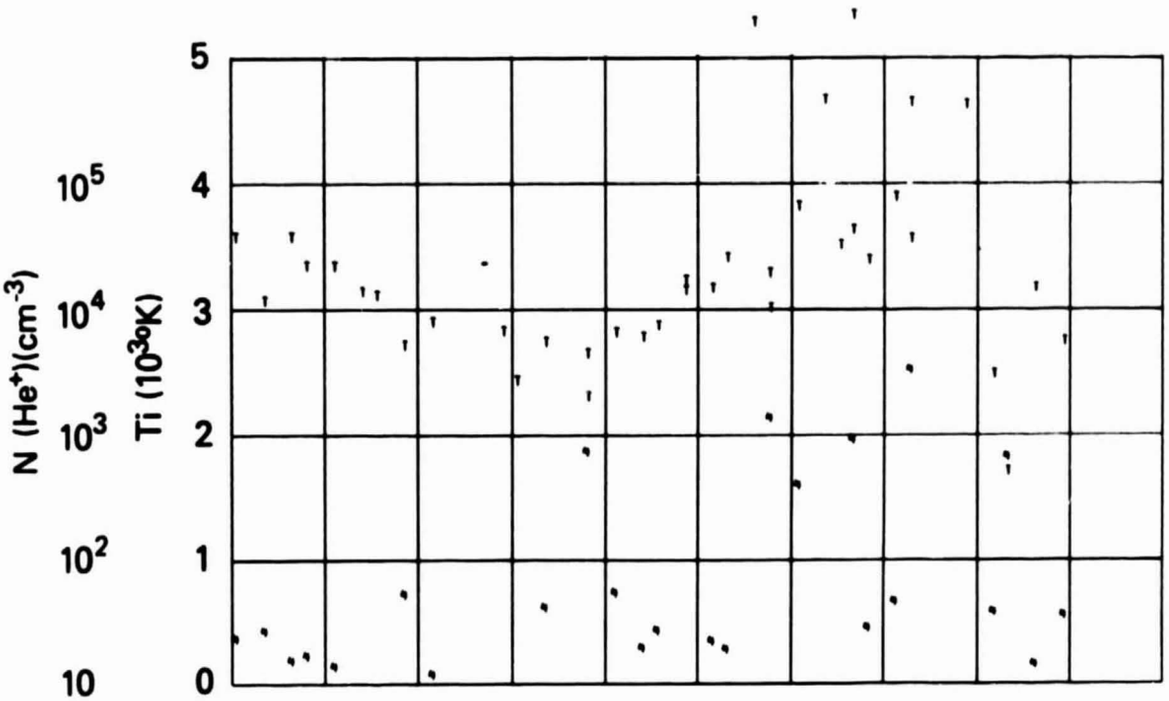

UT	14:48	14:50	14:52	14:54	14:56	14:58	15:00	15:02	15:04	15:06
LAST	19:05	19:09	19:15	19:30	20:21	3:49	8:02	8:24	8:33	8:38
MLT	19:43	19:58	20:18	20:48	21:39	23:06	1:17	3:13	4:23	5:03
DLAT	80	66	72	78	83	86	84	80	75	69
INVL	58	63	69	74	78	82	82	79	74	69
GLAT	80	67	73	79	85	87	81	75	69	62
GLNG	66	66	67	71	84	-161	-132	-127	-125	-125
SZEN	79	77	75	73	71	70	69	68	67	67
ALT	1368	1370	1372	1374	1376	1378	1381	1383	1385	1387

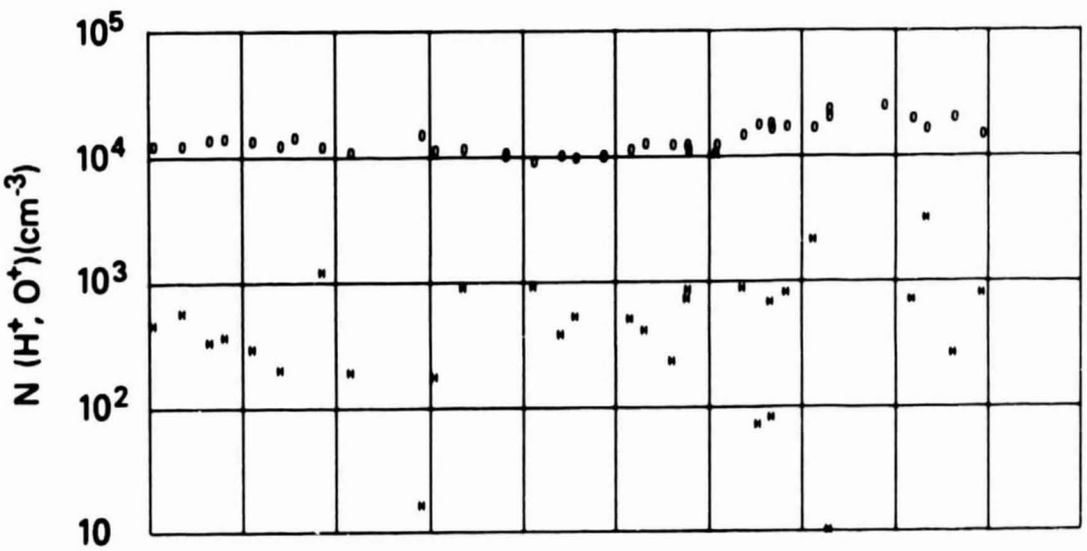

SET 17, FORMAT 5

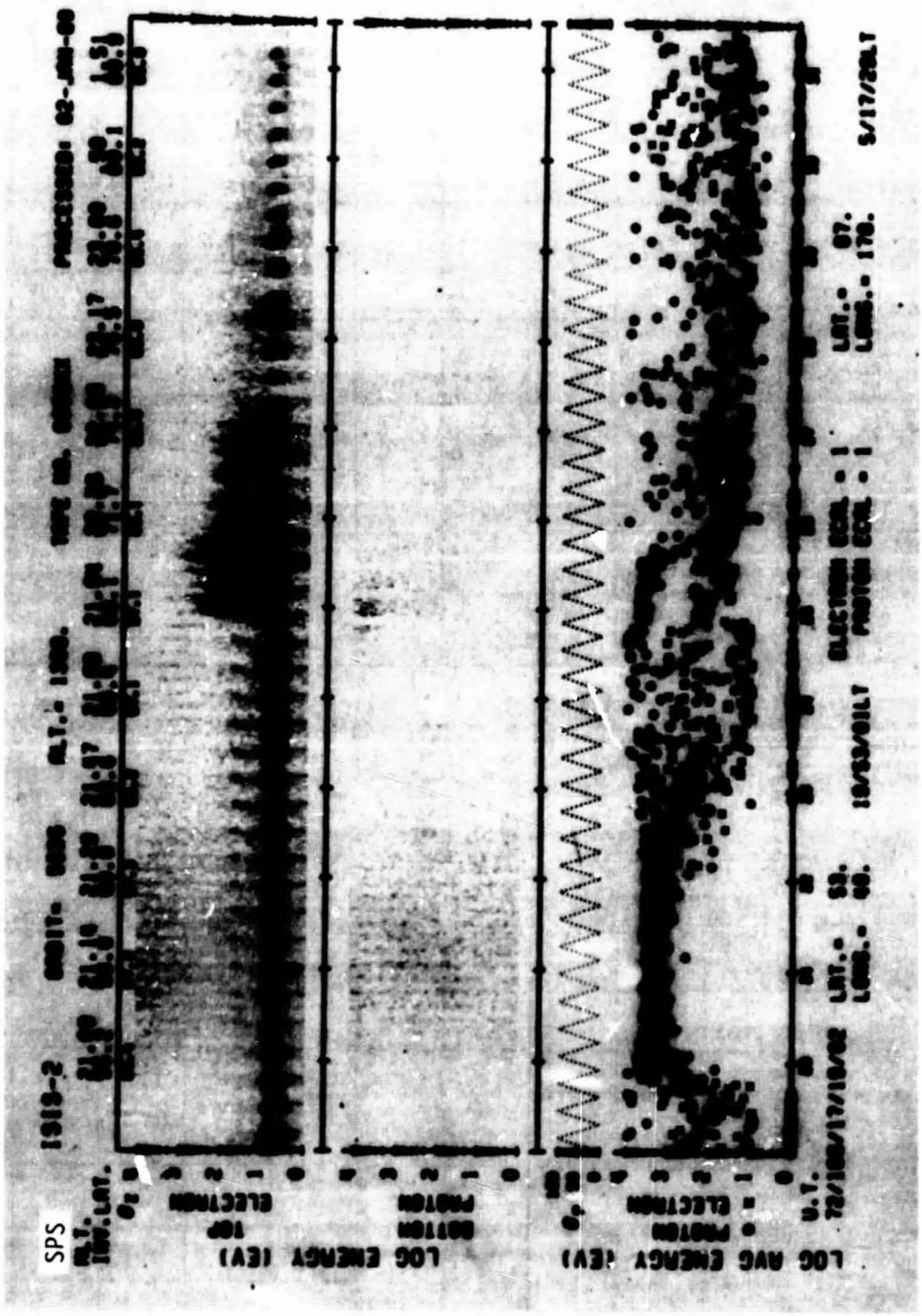

SET 18, FORMAT 6

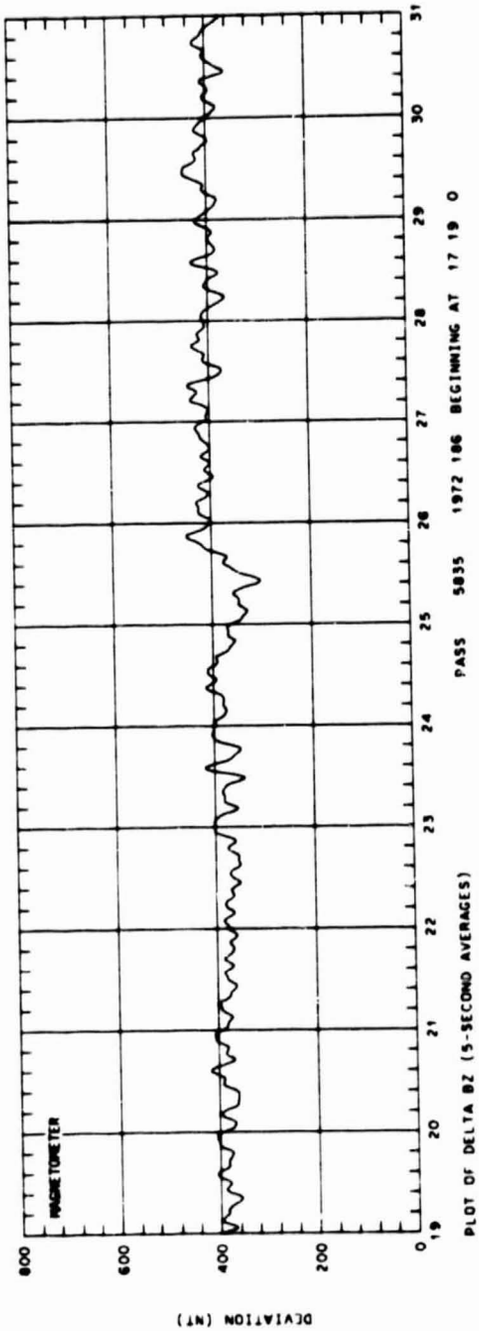

SET 18, FORMAT 2

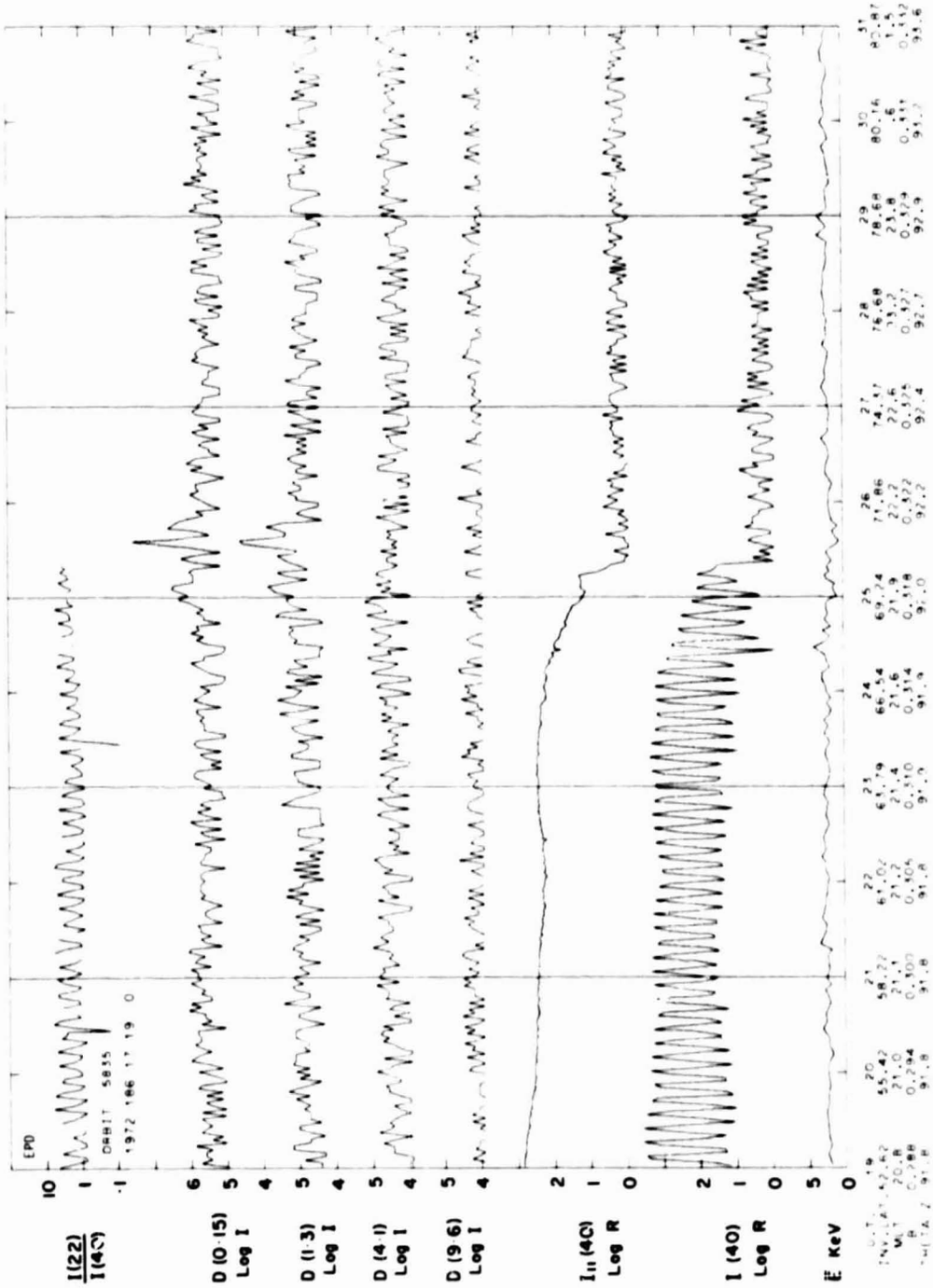

SET 18, FORMAT 3

ORBIT 5835
DATE 720704
DAY 186

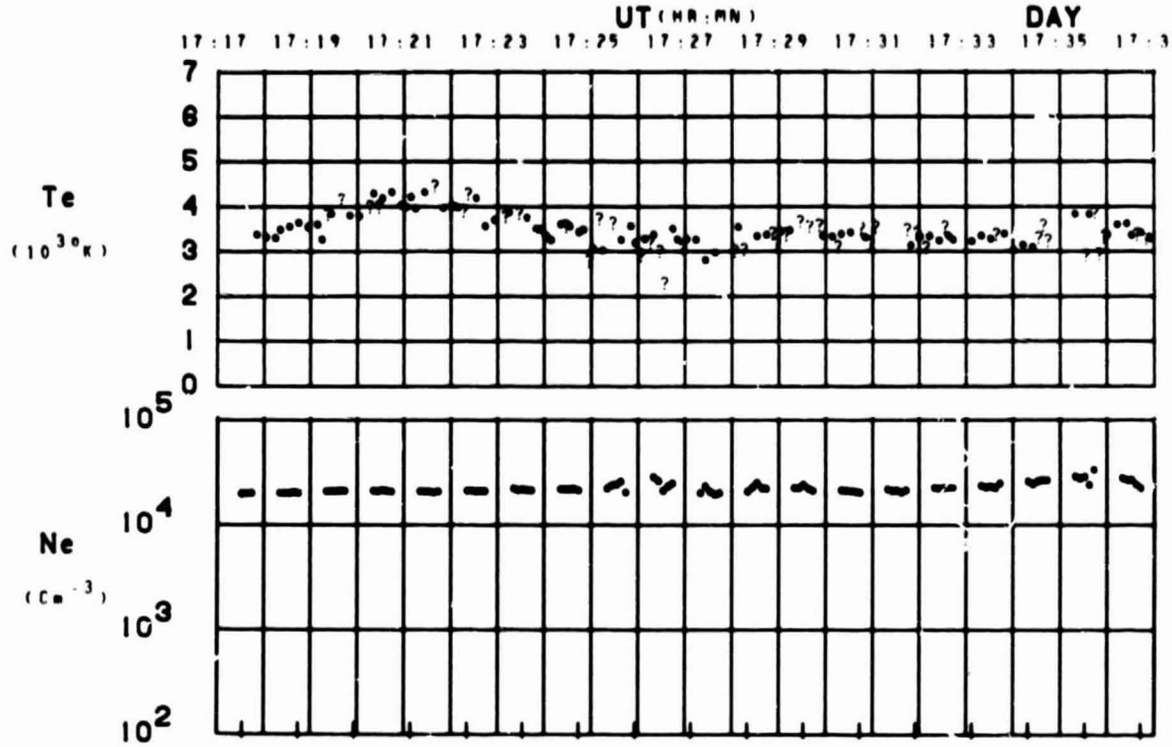

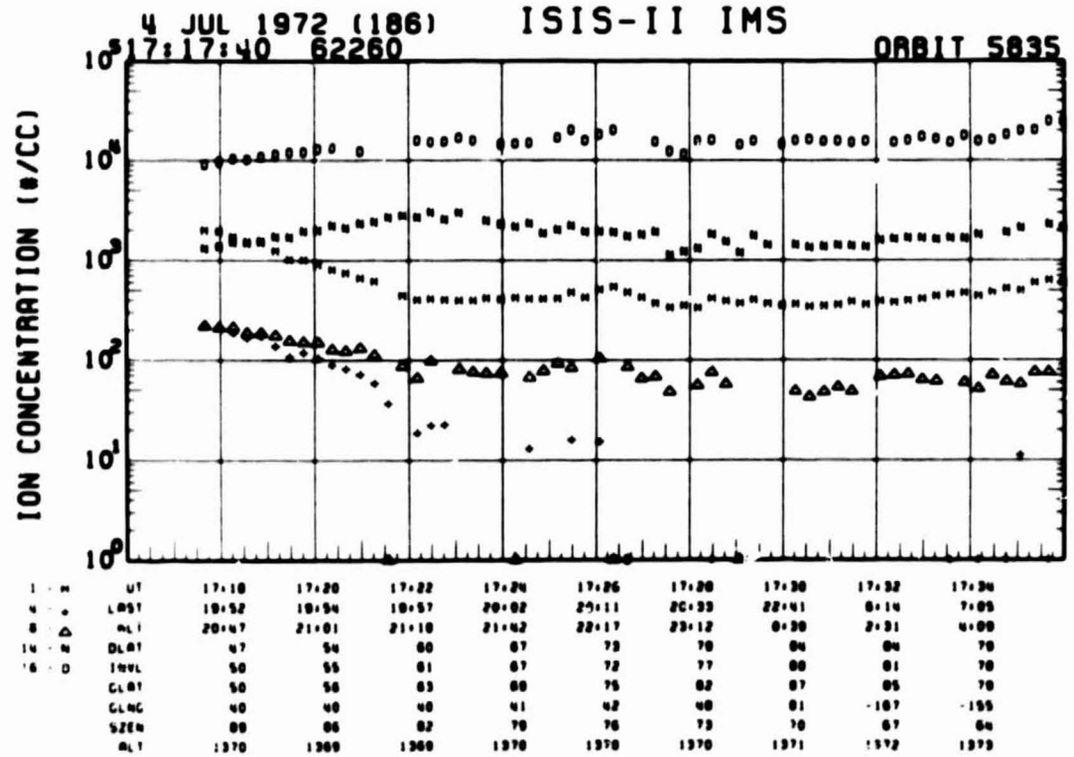

SET 18, FORMAT 4

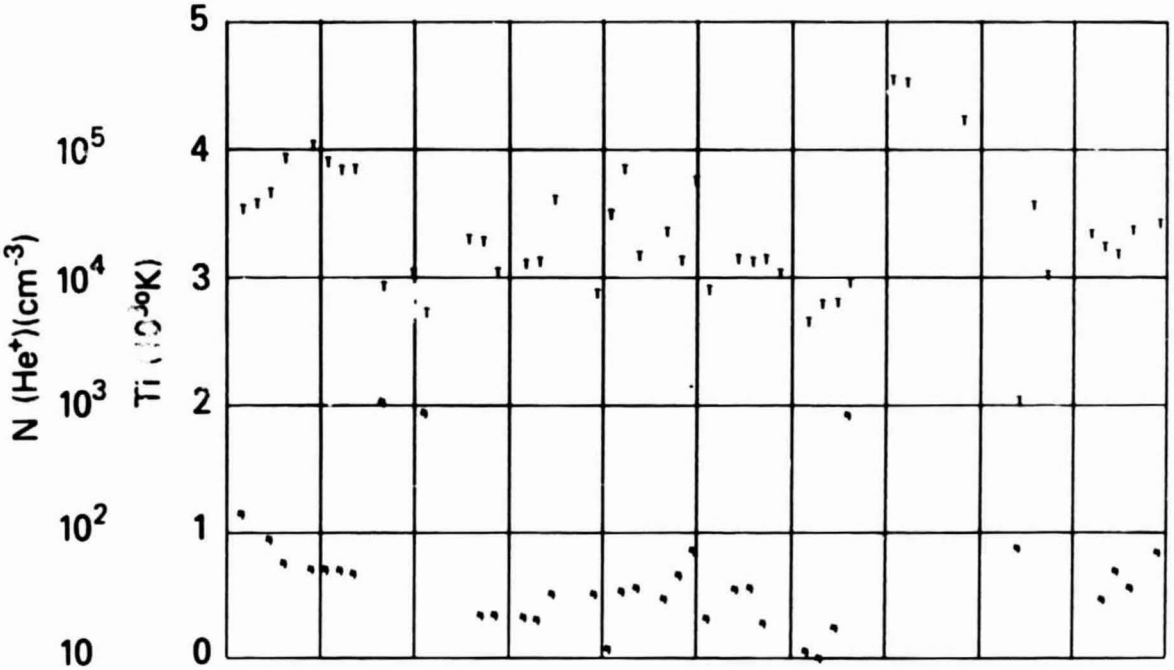

UT	17:18	17:20	17:22	17:24	17:26	17:28	17:30	17:32	17:34
LAST	19:52	19:54	19:57	20:02	20:11	20:33	22:41	6:14	7:05
MLT	20:47	21:01	21:18	21:42	22:17	23:12	0:39	2:31	4:09
DLAT	47	54	60	67	73	79	84	84	79
INVL	50	55	61	67	72	77	80	81	78
GLAT	50	56	63	69	75	82	87	85	79
GLNG	40	40	40	41	42	48	81	-167	-155
SZEN	89	86	82	79	76	73	70	67	64
ALT	1370	1369	1369	1370	1370	1370	1371	1372	1373

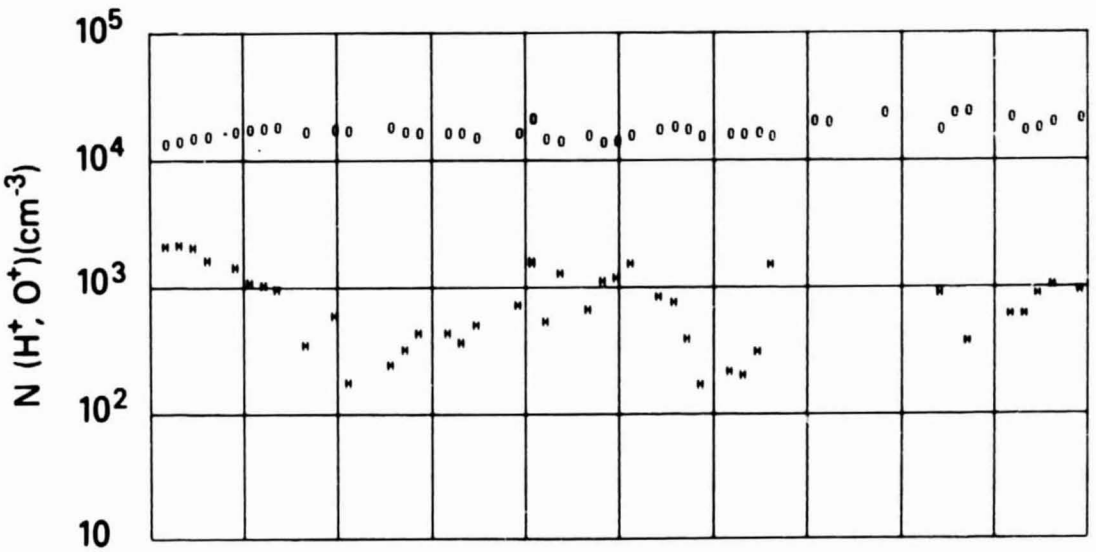

SET 18, FORMAT 5

72/186/1719

Excerpts of VLF Spectral film for the period 1719 - 1728

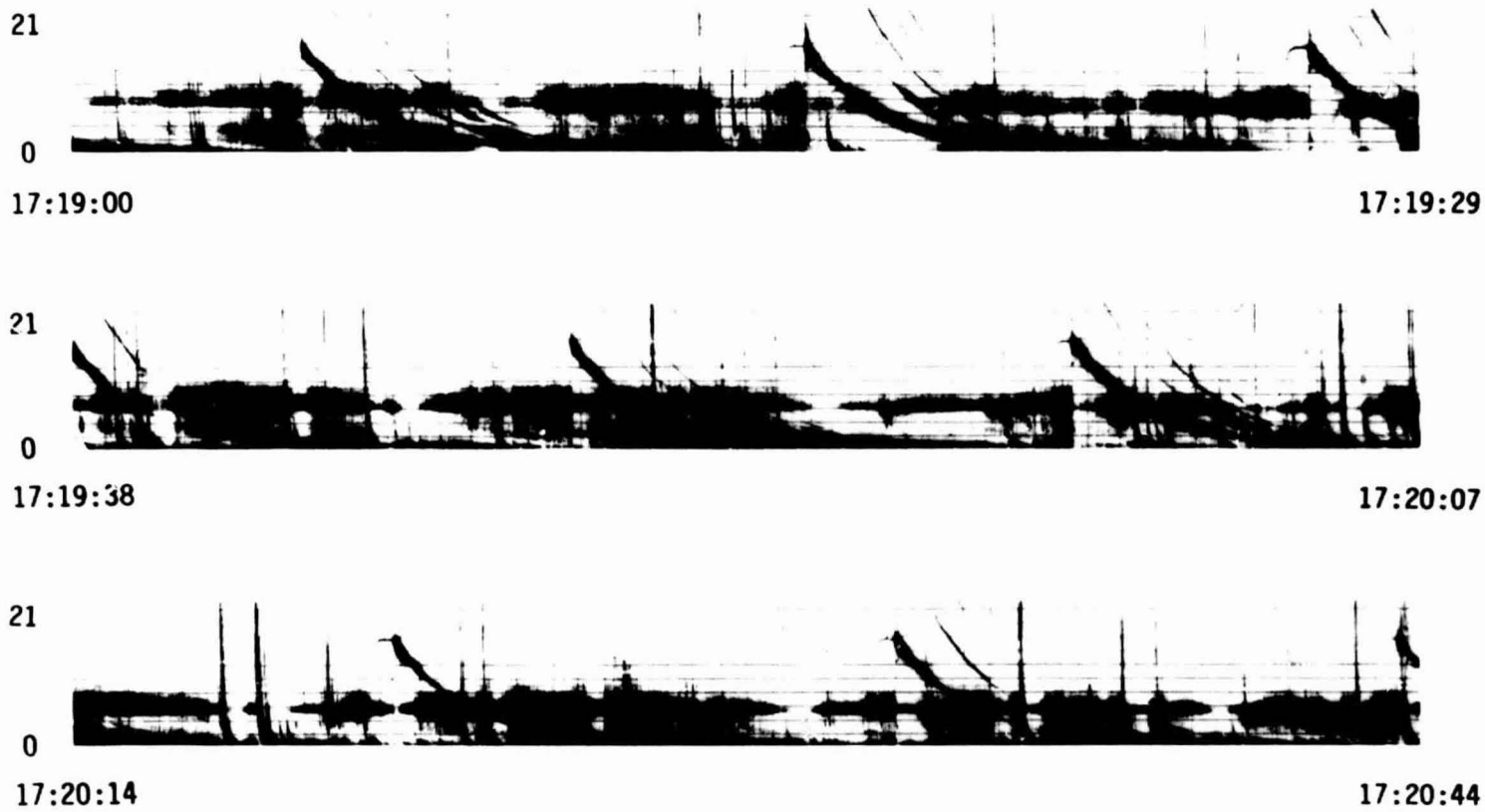

SET 18, FORMAT 11

72/186/1719

Excerpts of VLF Spectral film for the period 1719 - 1728

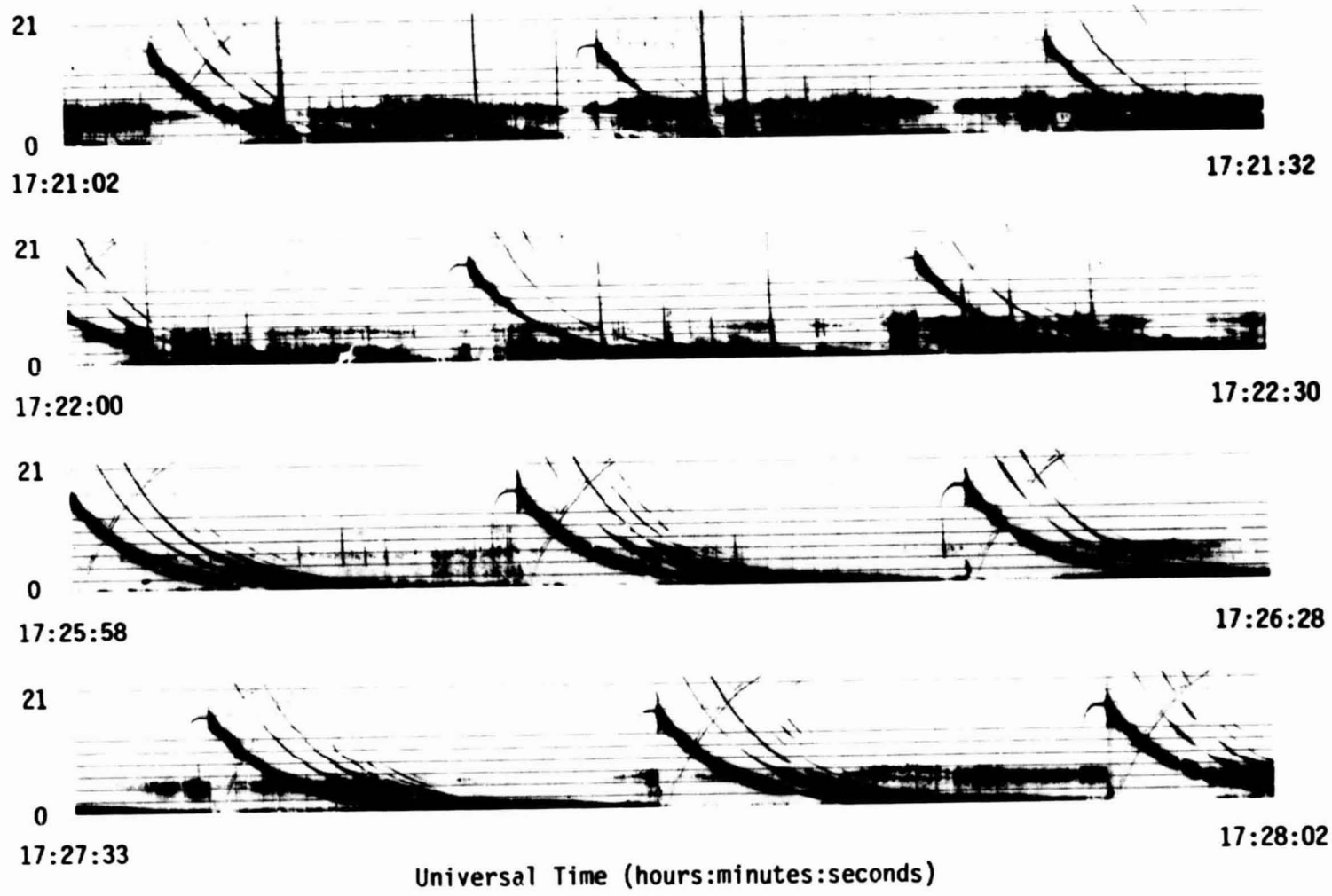

SET 18, FORMAT 11

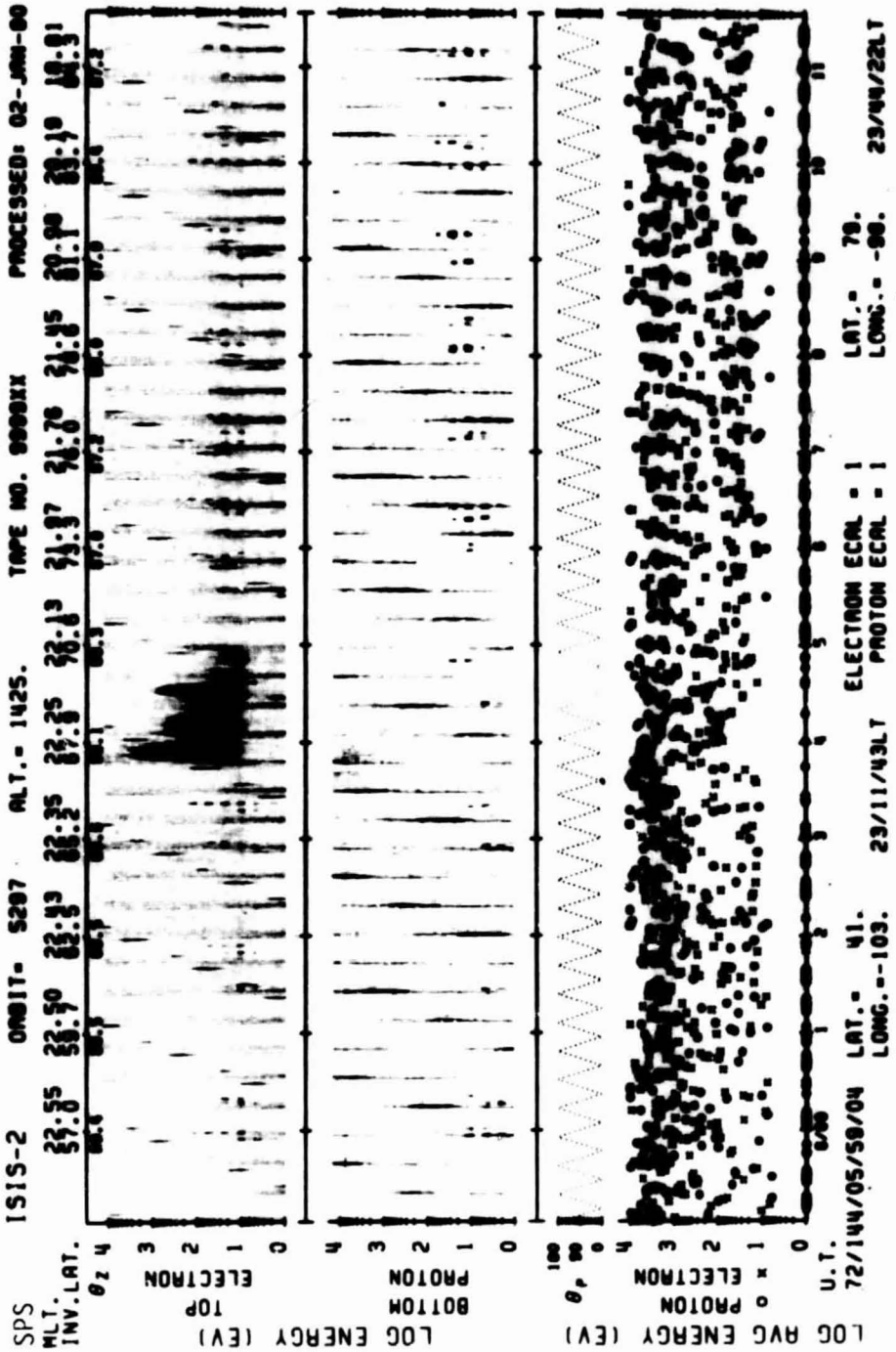

SET 19, FORMAT 6

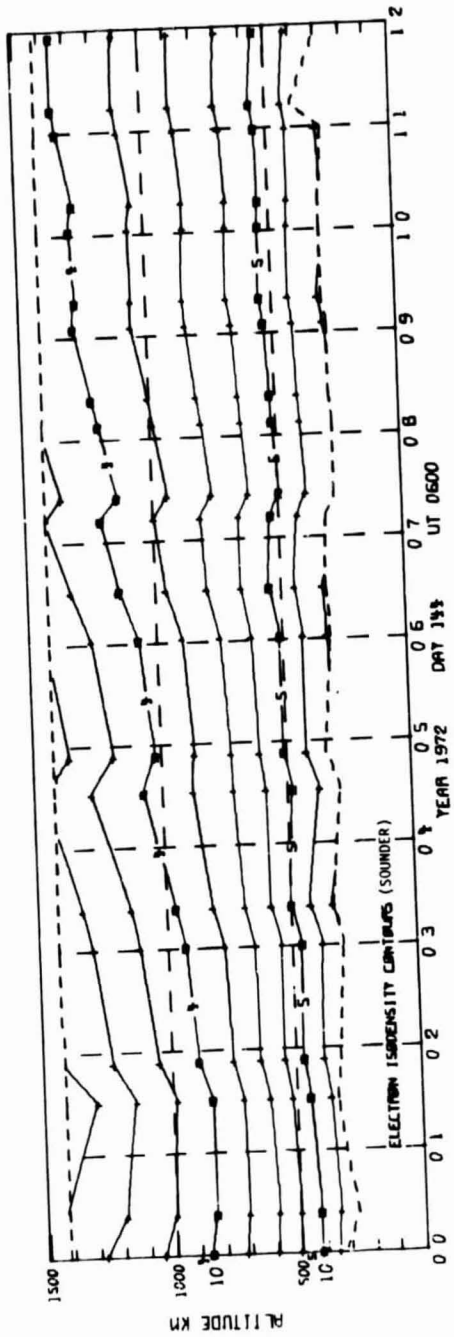

SET 19, FORMAT 2

SET 19, FORMAT 3

ORBIT 5297
DATE 720523
DAY 144

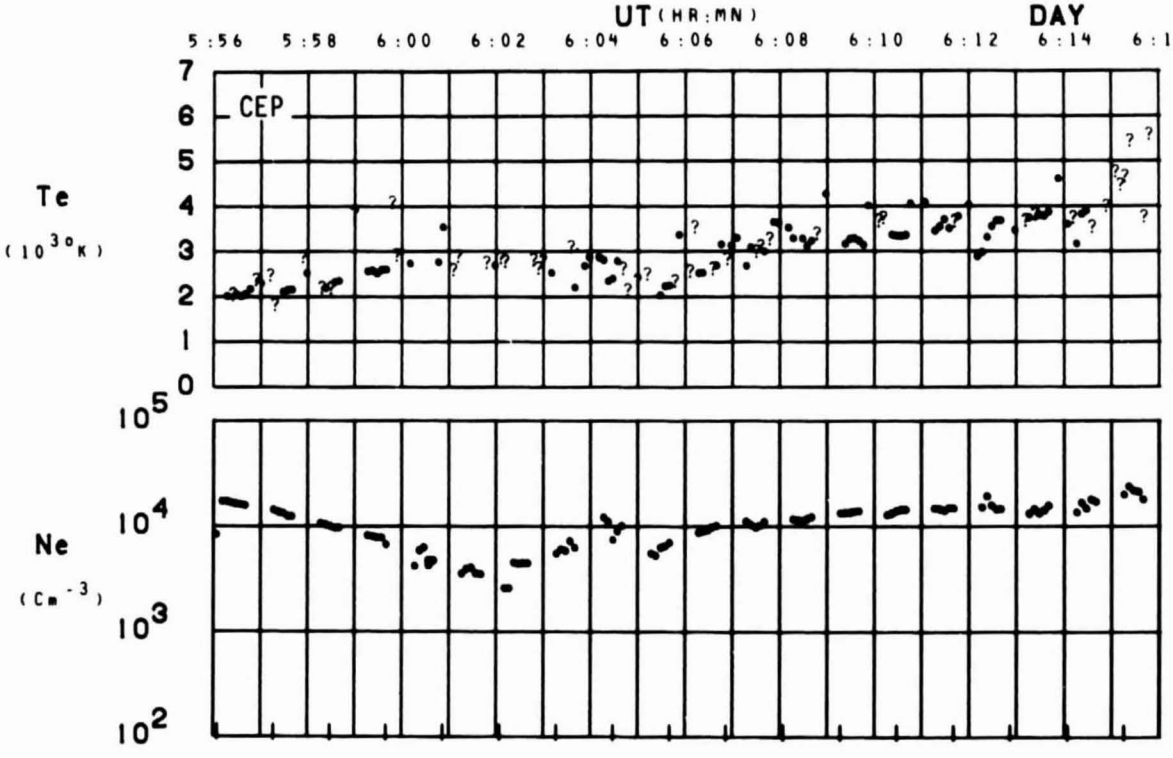

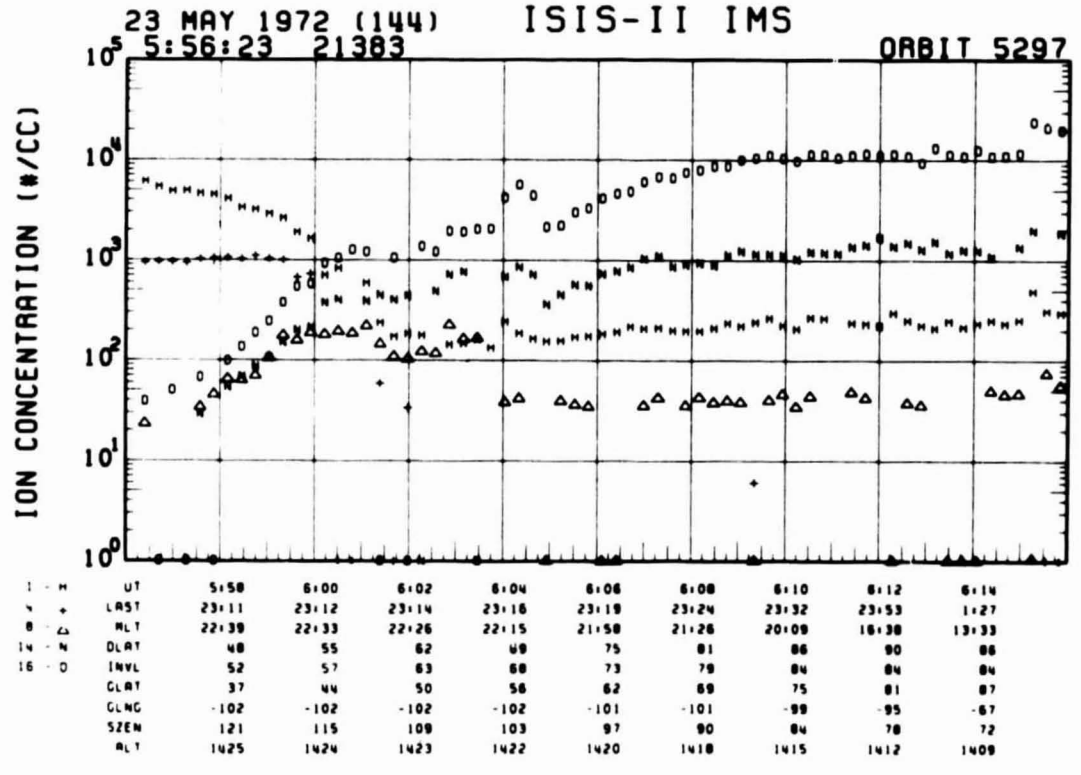

UT	5:58	6:00	6:02	6:04	6:06	6:08	6:10	6:12	6:14
LAST	23:11	23:12	23:14	23:16	23:19	23:24	23:32	23:53	1:27
MLT	22:39	22:33	22:26	22:15	21:58	21:26	20:09	16:38	13:33
DLAT	48	55	62	69	75	81	86	90	88
INVL	52	57	63	68	73	78	84	84	84
GLAT	37	44	50	56	62	69	75	81	87
GLNG	-102	-102	-102	-102	-101	-101	-99	-95	-67
SZEN	121	115	109	103	97	90	84	78	72
ALT	1425	1424	1423	1422	1420	1418	1415	1412	1409

I - H
+ - +
Δ - Δ
N - N
O - O

SET 19, FORMAT 4

RPA

720523

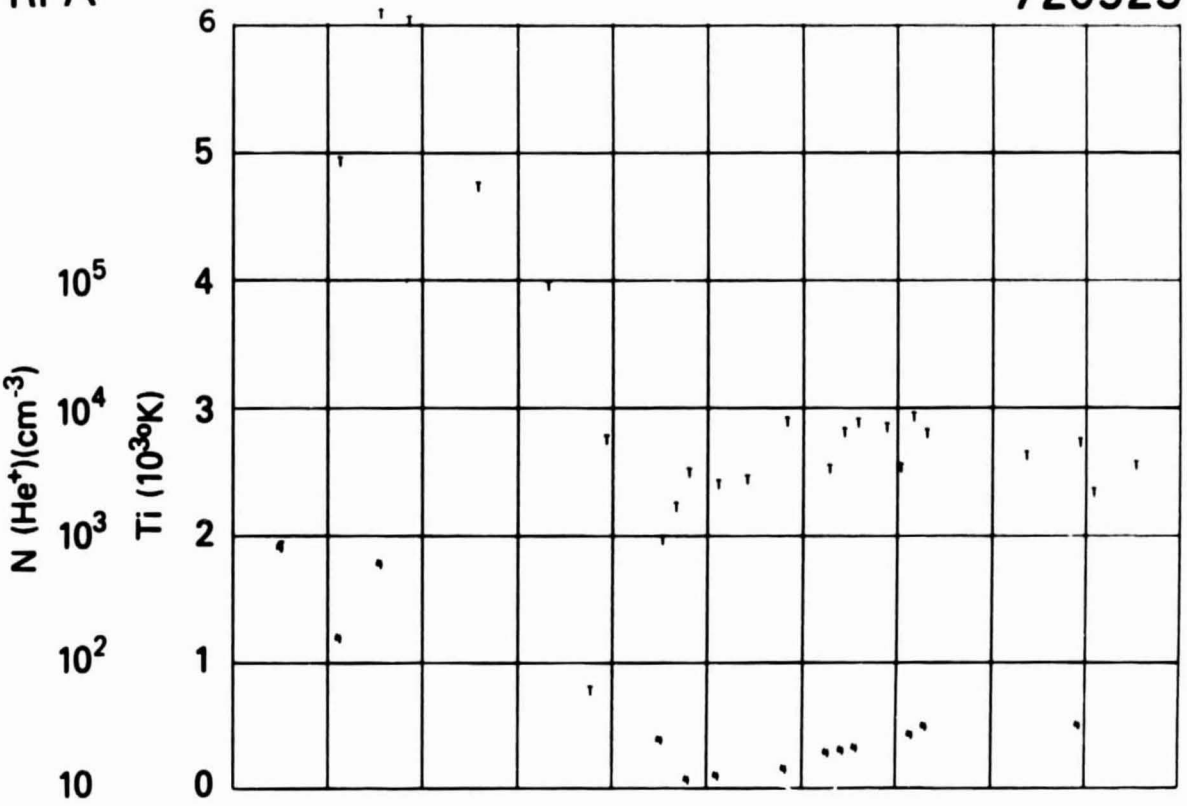

UT	5:58	6:00	6:02	6:04	6:06	6:08	6:10	6:12	6:14
LAST	23:11	23:12	23:14	23:16	23:19	23:24	23:32	23:53	1:27
MLT	22:39	22:33	22:26	22:15	21:58	21:26	20:09	16:38	13:33
DLAT	48	55	62	69	75	81	86	90	86
INVL	52	57	63	68	73	79	84	84	84
GLAT	37	44	50	56	62	69	75	81	87
GLNG	-102	-102	-102	-102	-101	-101	-99	-95	-67
SZEN	121	115	109	103	97	90	84	78	72
ALT	1425	1424	1423	1422	1420	1418	1415	1412	1409

SET 19, FORMAT 5

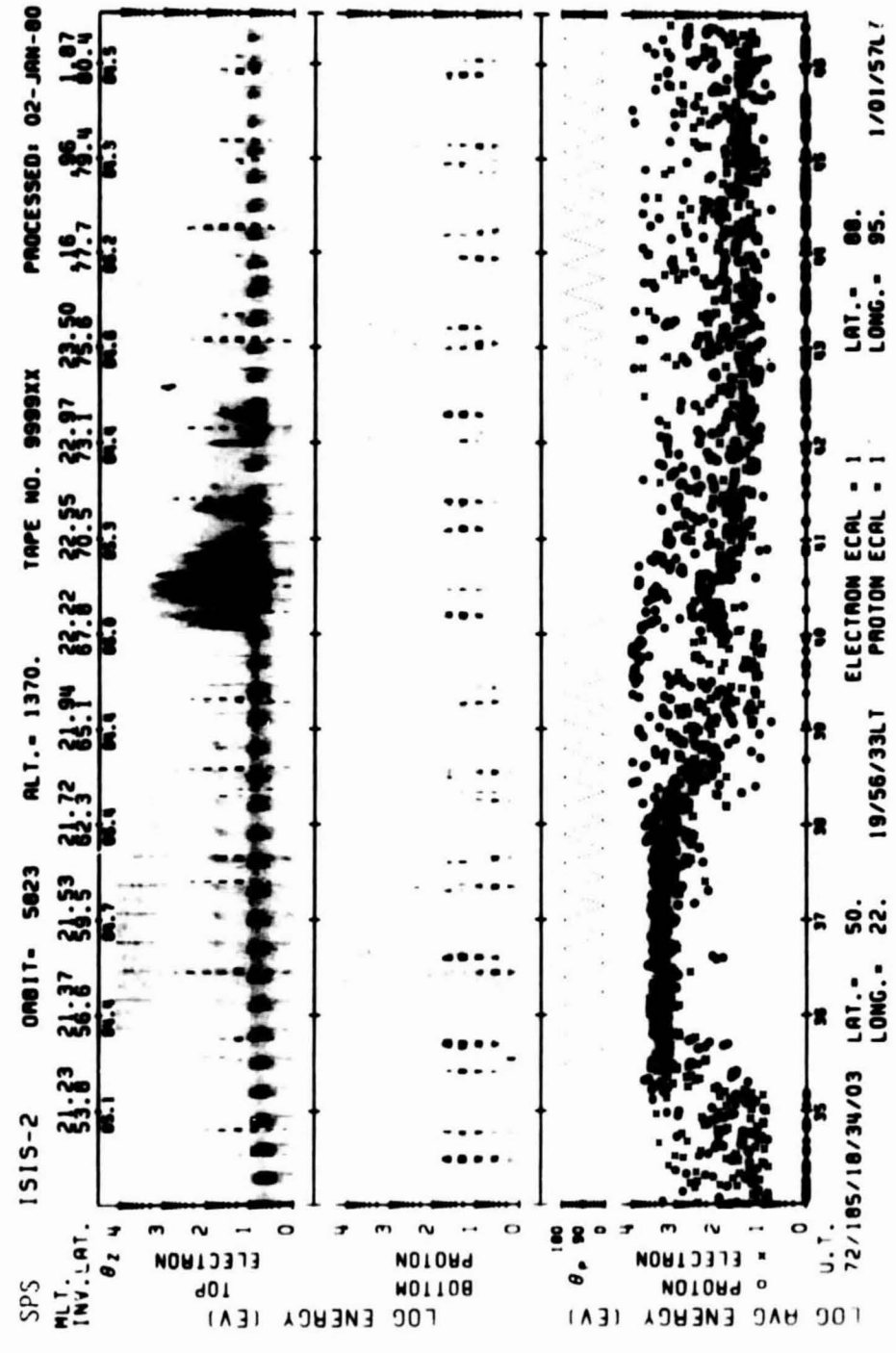

SET 20, FORMAT 6

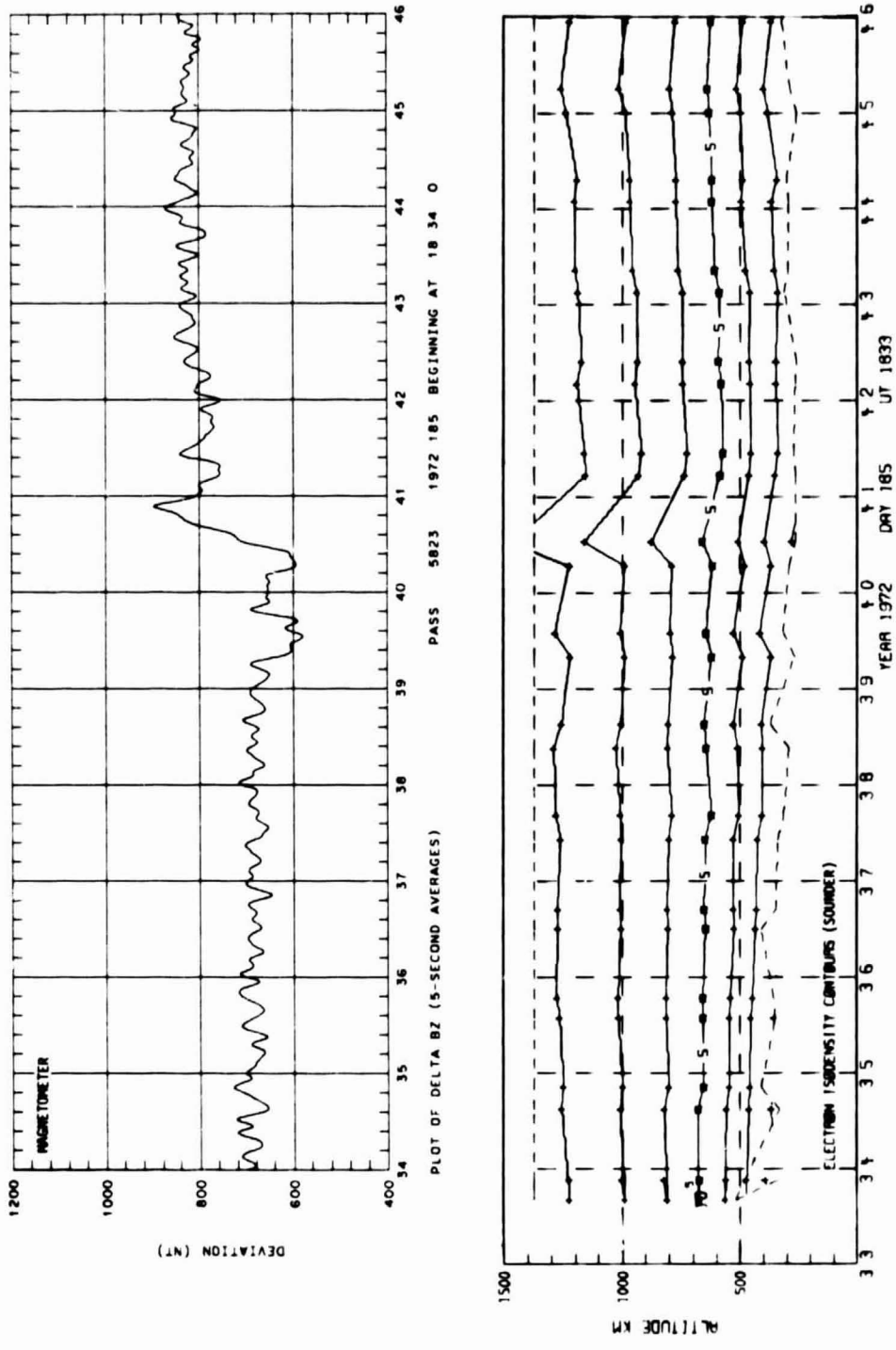

SET 20, FORMAT 2

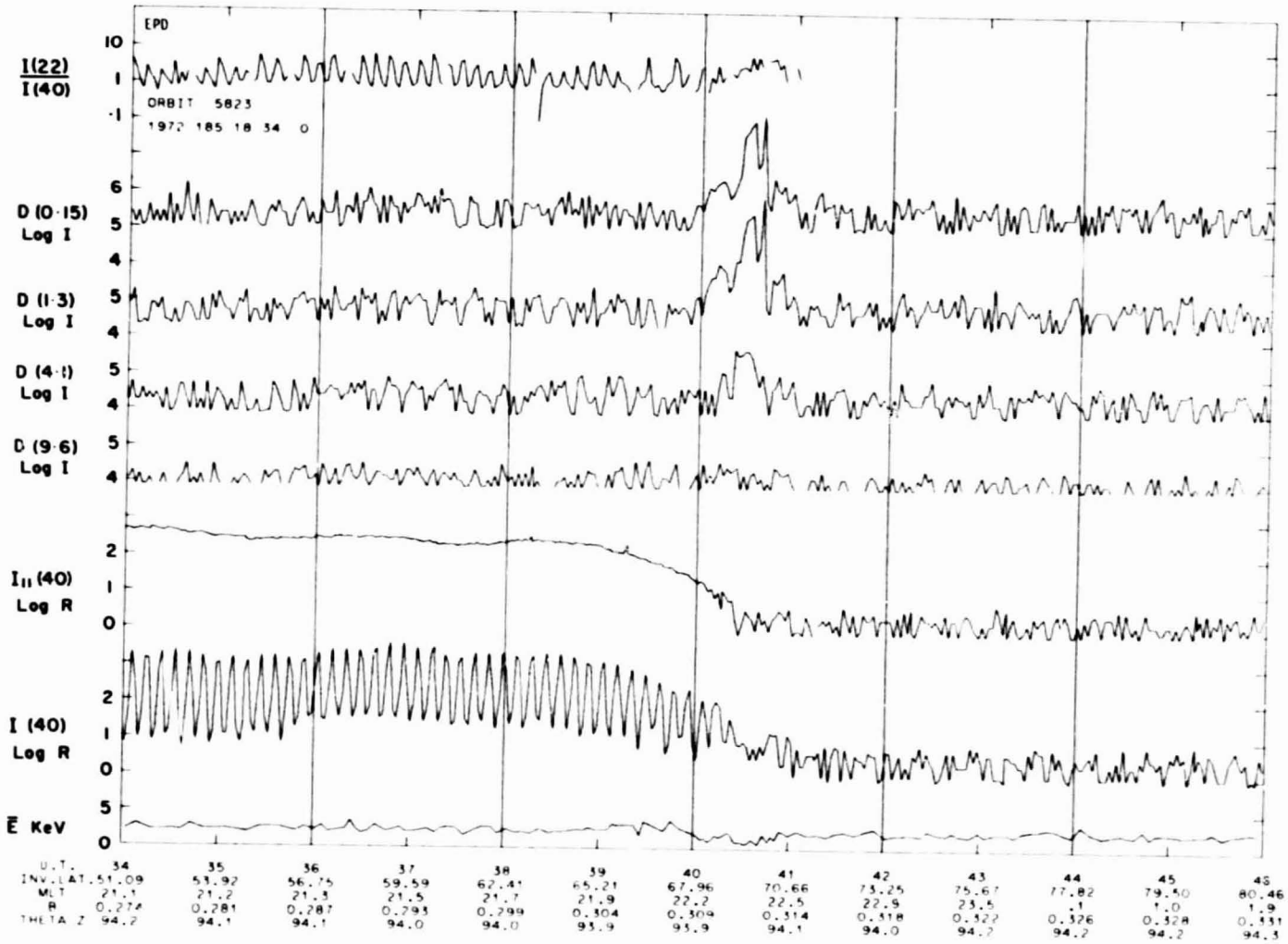

SET 20, FORMAT 3

ORBIT 5823
DATE 720703
DAY ;85

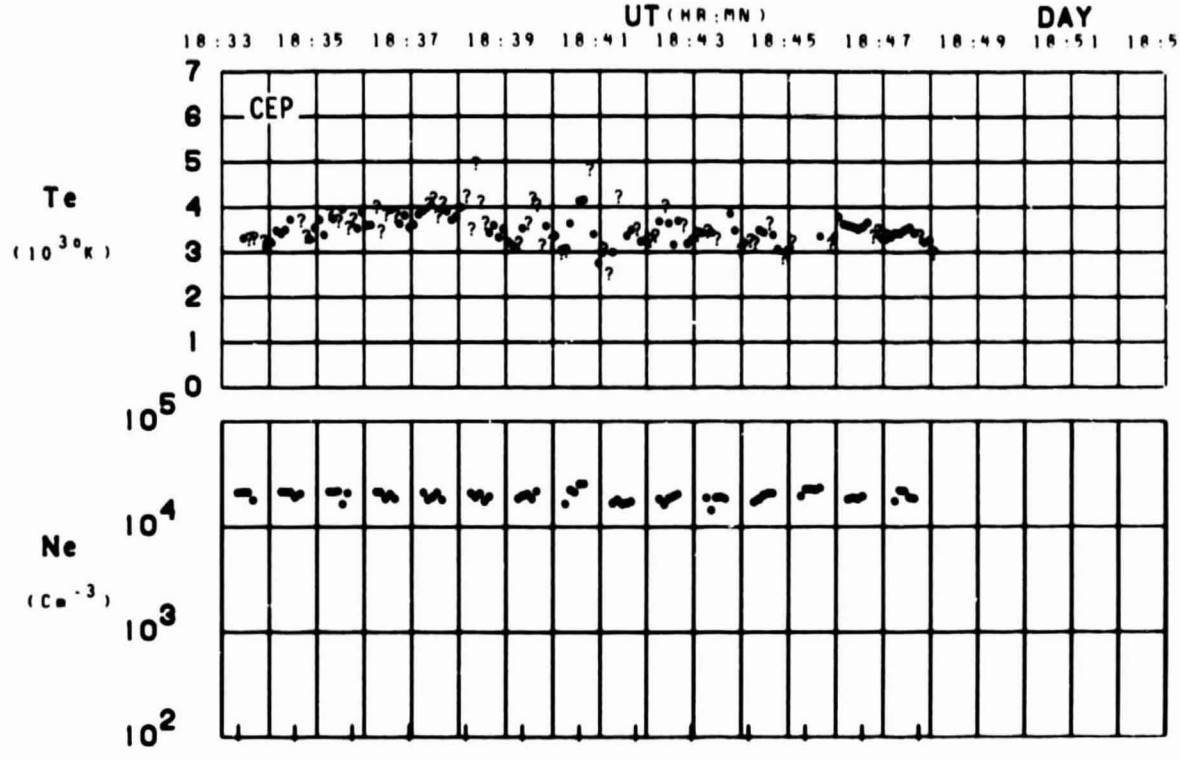

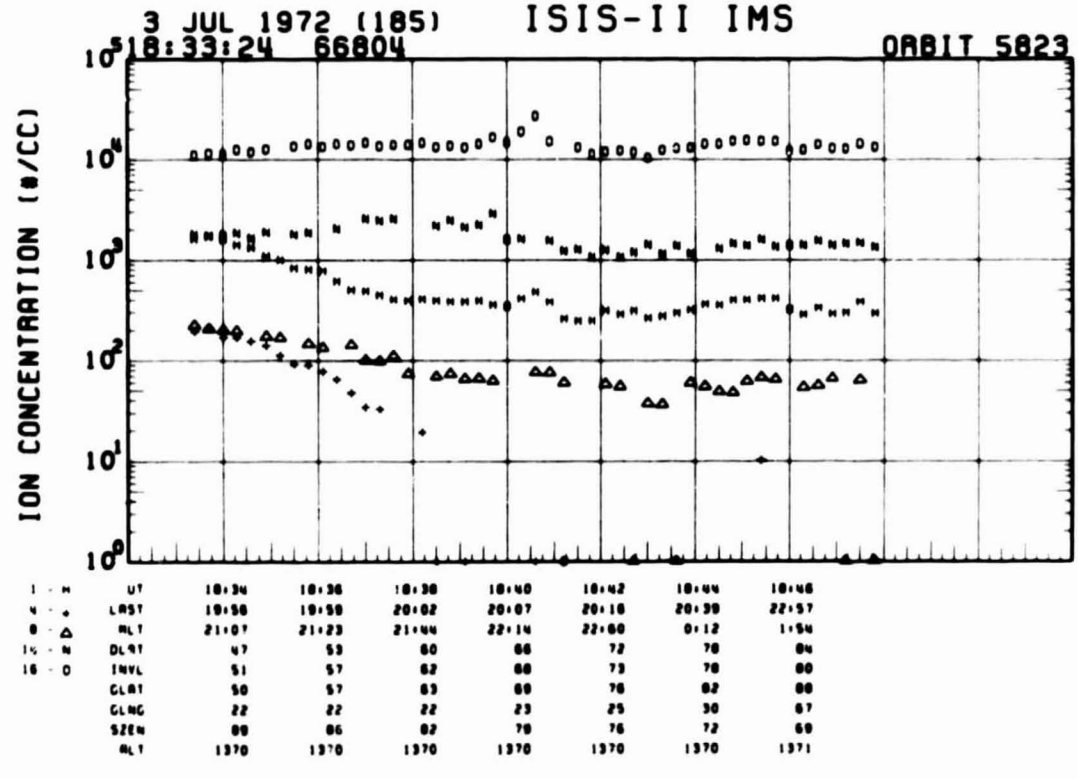

SET 20, FORMAT 4

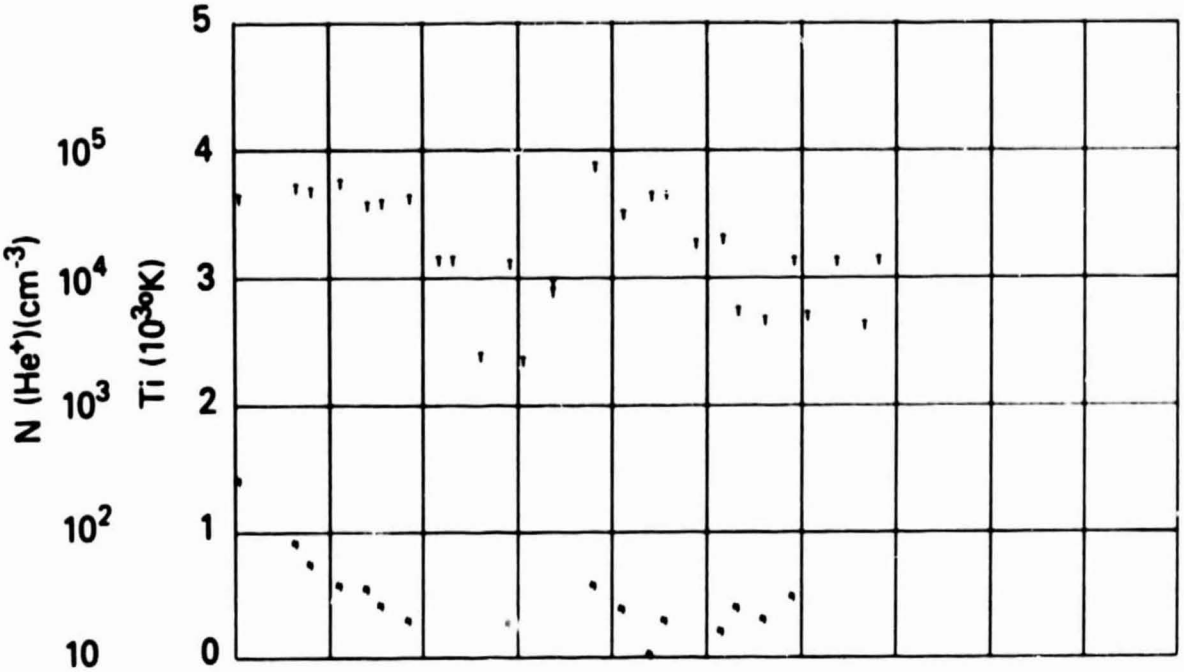

UT	18:34	18:36	18:38	18:40	18:42	18:44	18:46
LAST	19:58	19:59	20:02	20:07	20:16	20:39	22:57
MLT	21:07	21:23	21:46	22:14	22:60	0:12	1:54
DLAT	47	53	60	66	72	78	84
INVL	51	57	62	68	73	78	80
GLAT	50	57	63	59	76	82	88
GLNG	22	22	22	23	25	30	87
SZEN	89	86	82	78	76	72	69
ALT	1370	1370	1370	1370	1370	1370	1371

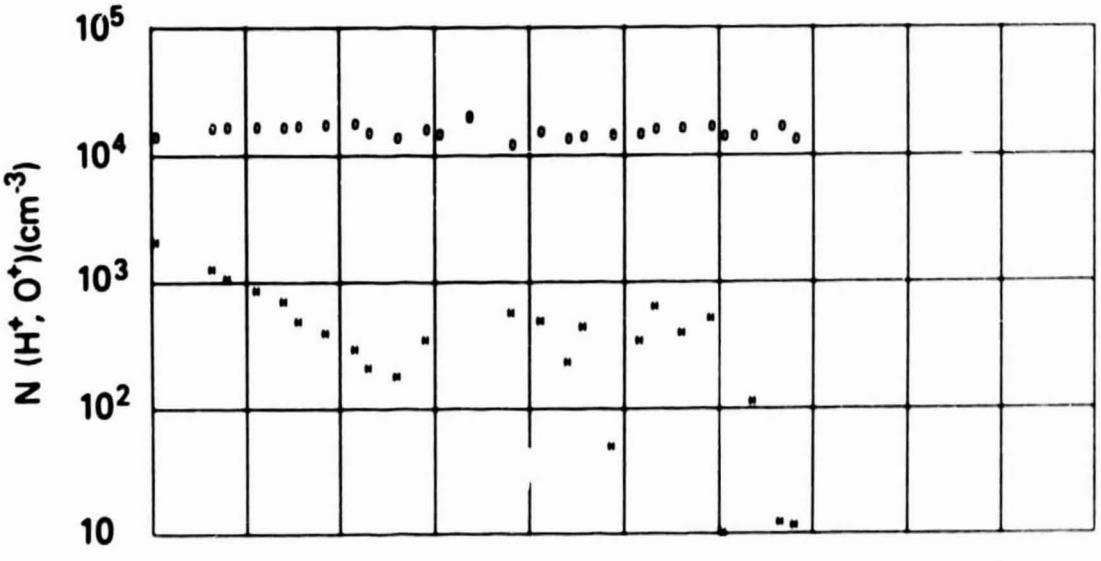

SET 20, FORMAT 5

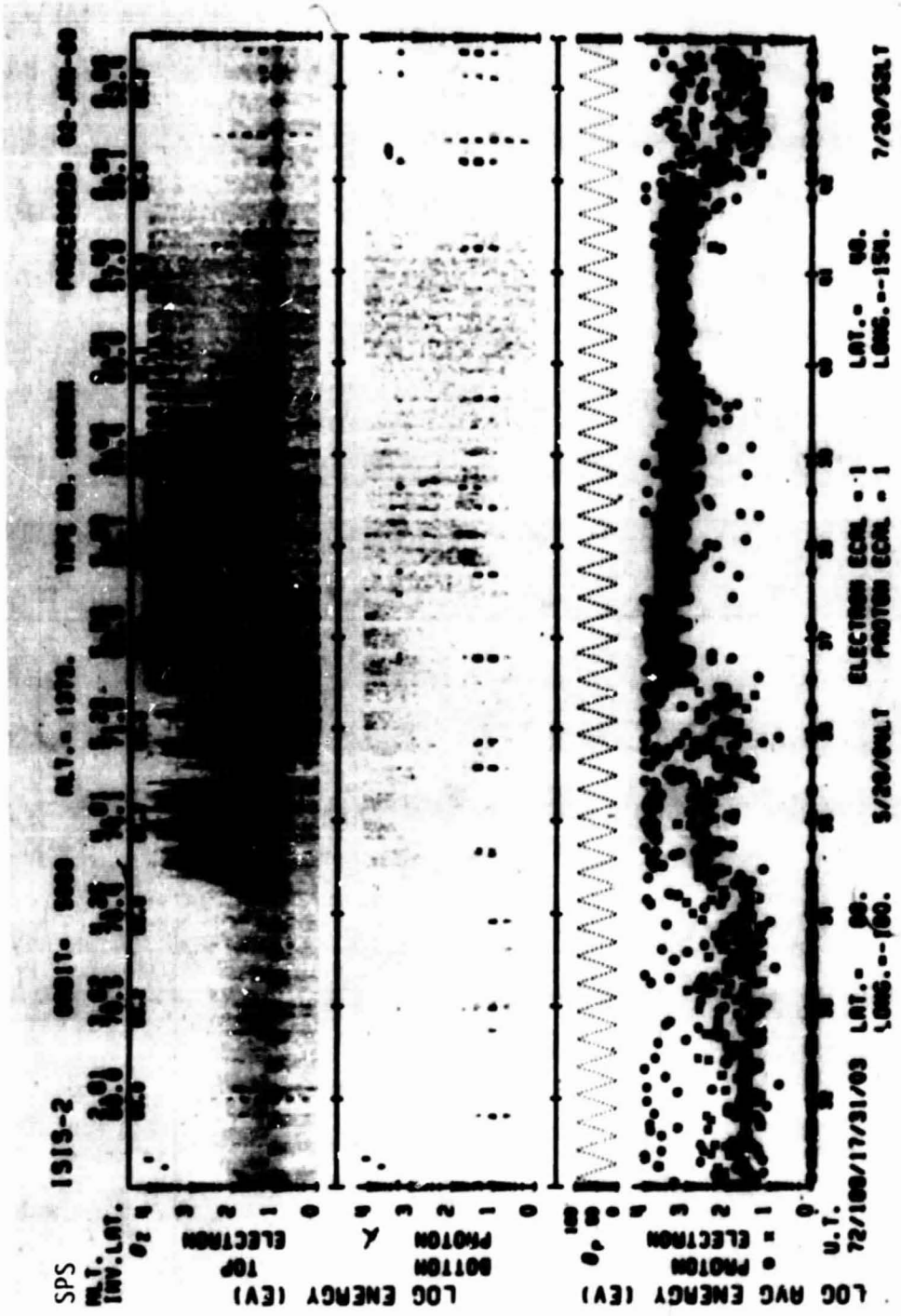

SET 21, FORMAT 6

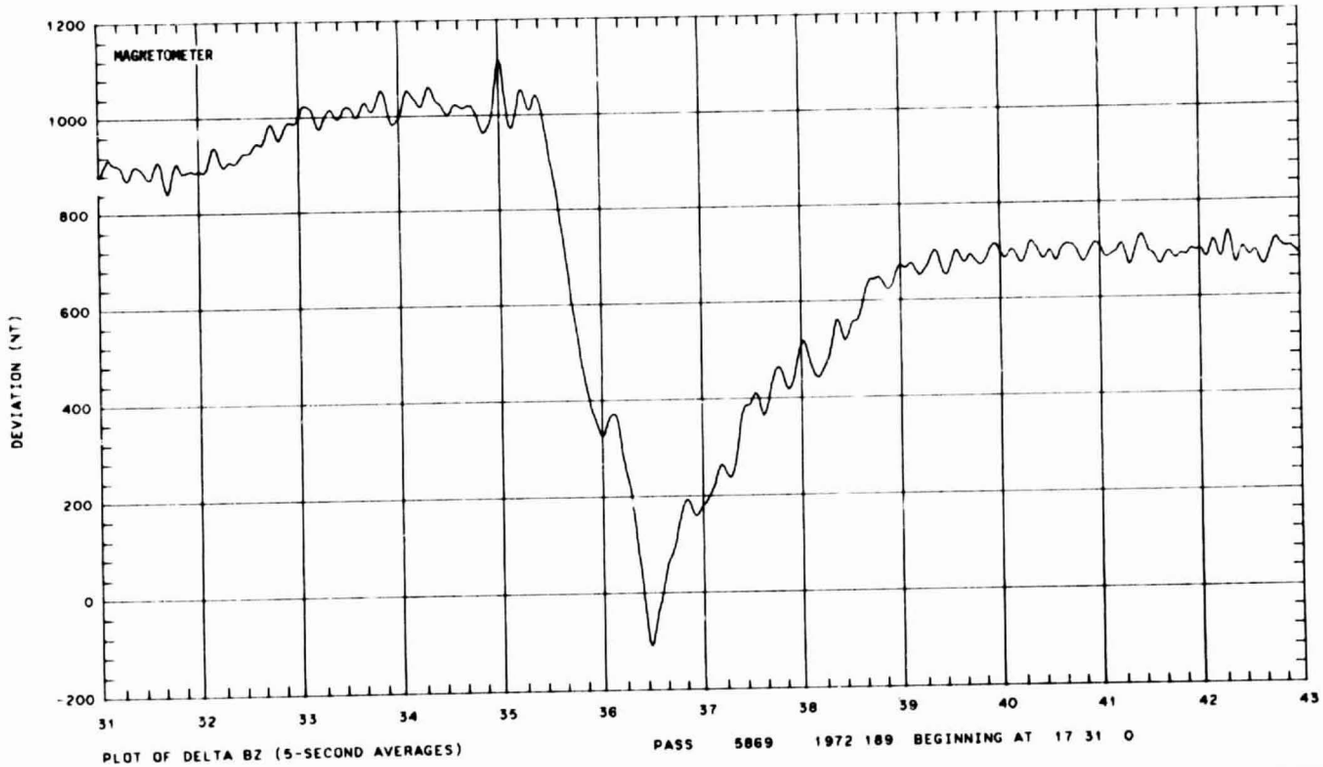

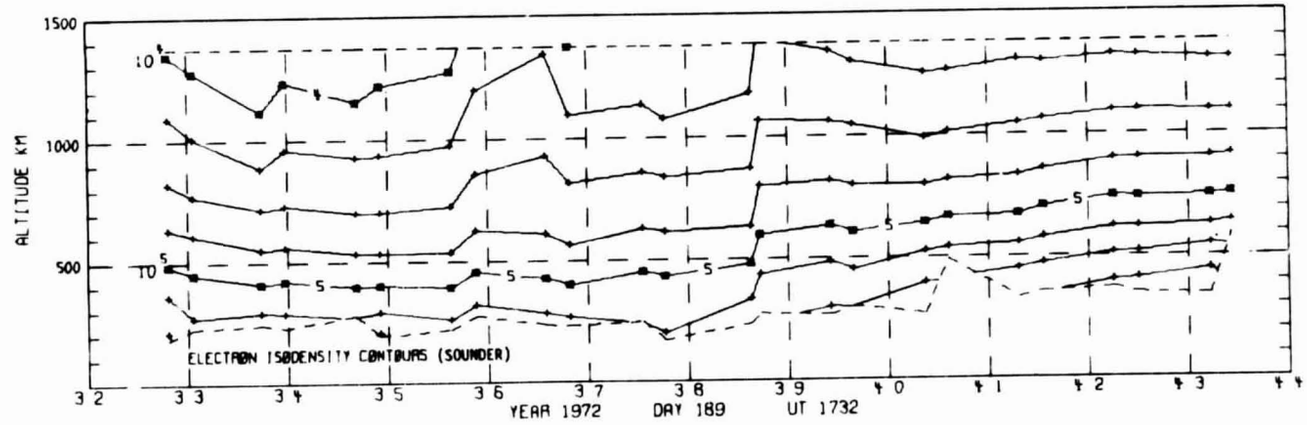

SET 21, FORMAT 2

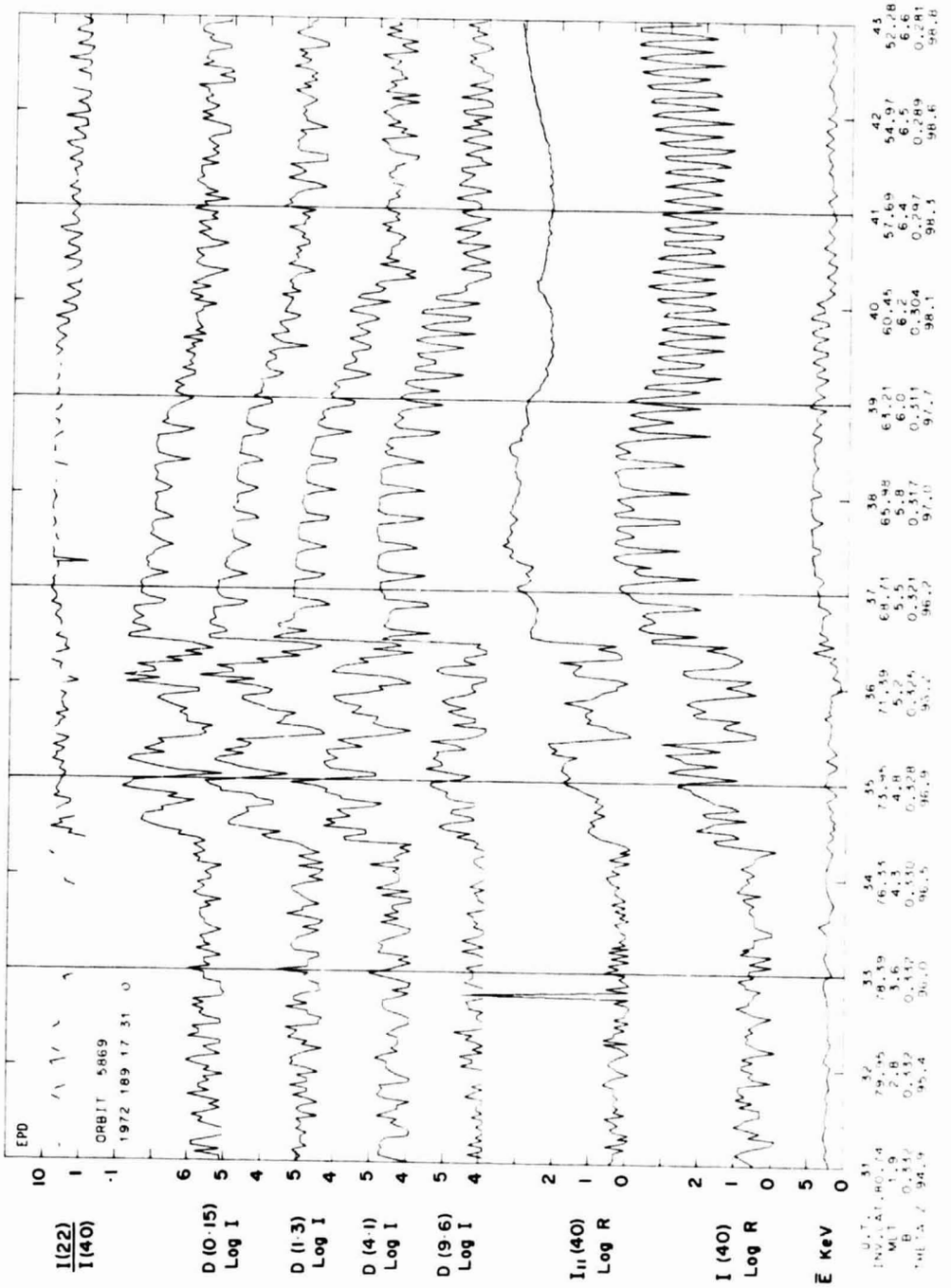

SET 21, FORMAT 3

ORBIT 5869
DATE 720707
DAY 189

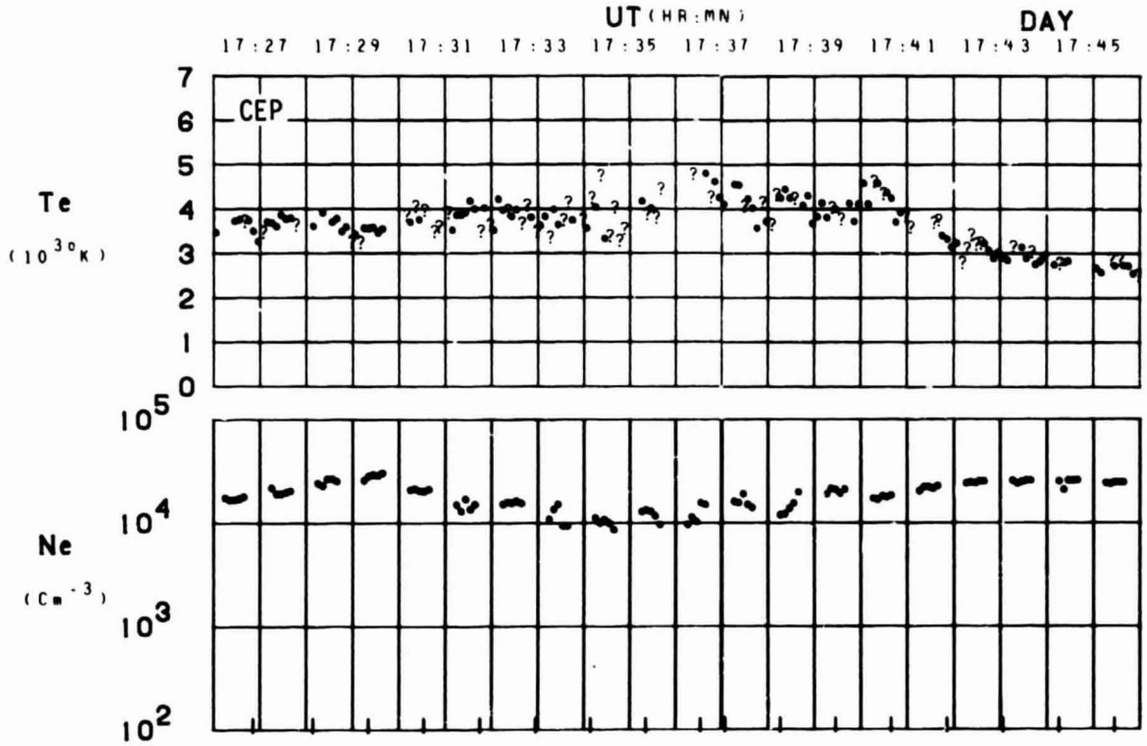

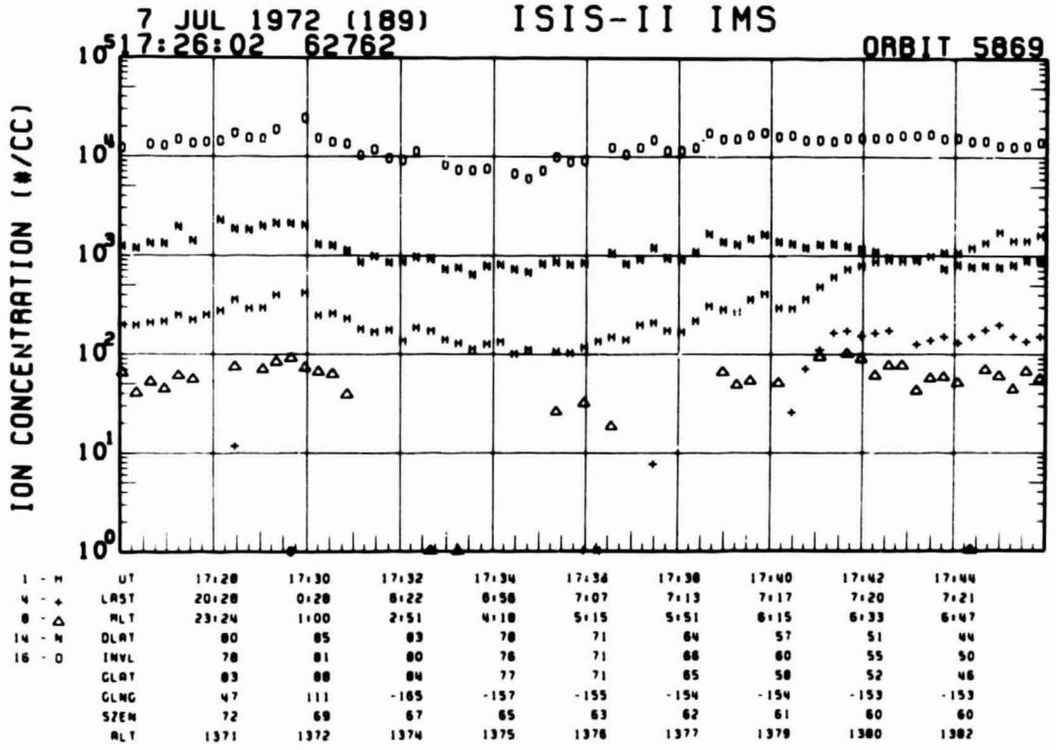

1 - H	UT	17:28	17:30	17:32	17:34	17:36	17:38	17:40	17:42	17:44
4 - +	LAST	20:28	0:28	8:22	8:58	7:07	7:13	7:17	7:20	7:21
8 - △	MLT	23:24	1:00	2:51	4:18	5:15	5:51	6:15	6:33	6:47
14 - N	DLAT	80	85	83	78	71	64	57	51	44
16 - O	INVL	78	81	80	76	71	66	60	55	50
	GLAT	83	88	84	77	71	65	58	52	46
	GLNG	47	111	-165	-157	-155	-154	-154	-153	-153
	SZEN	72	69	67	65	63	62	61	60	60
	ALT	1371	1372	1374	1375	1376	1377	1379	1380	1382

SET 21, FORMAT 4

RPA 720707

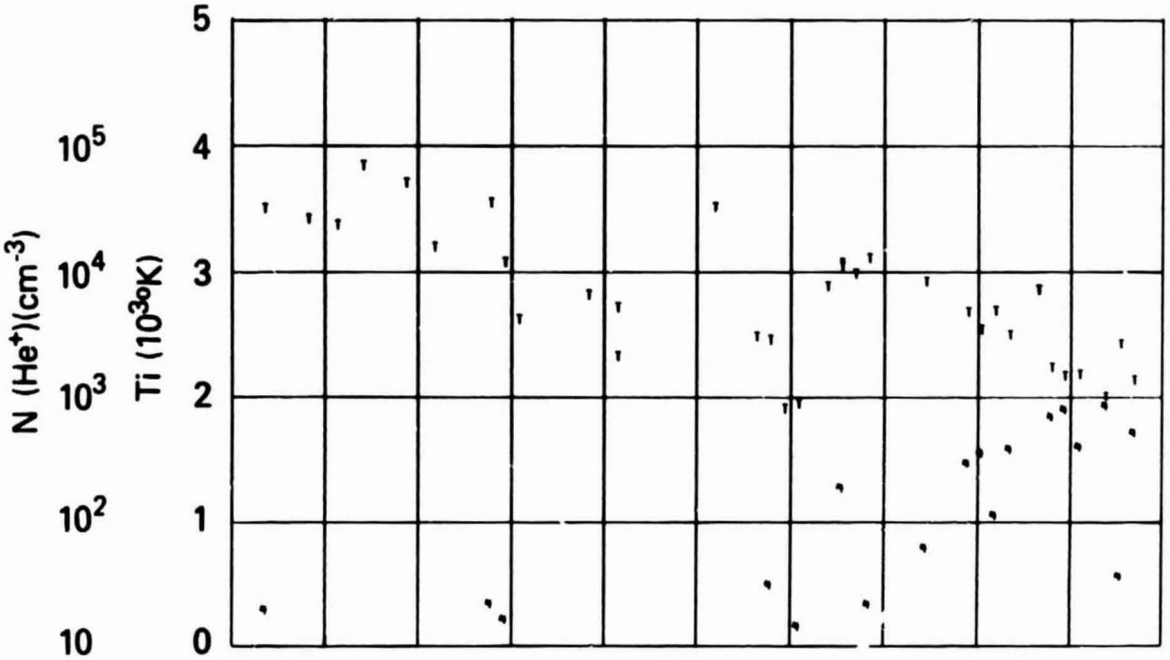

UT	17:28	17:30	17:32	17:34	17:36	17:38	17:40	17:42	17:44
LAST	20:28	0:28	6:22	8:58	7:07	7:13	7:17	7:20	7:21
MLT	23:24	1:00	2:51	4:18	5:15	5:51	6:15	6:33	6:47
DLAT	80	85	83	78	71	64	57	51	44
INVL	78	81	80	76	71	66	60	55	50
GLAT	83	88	84	77	71	65	58	52	46
GLNG	47	111	-165	-157	-155	-154	-154	-153	-153
SZEN	72	69	67	65	63	62	61	60	60
ALT	1371	1372	1374	1375	1376	1377	1379	1380	1382

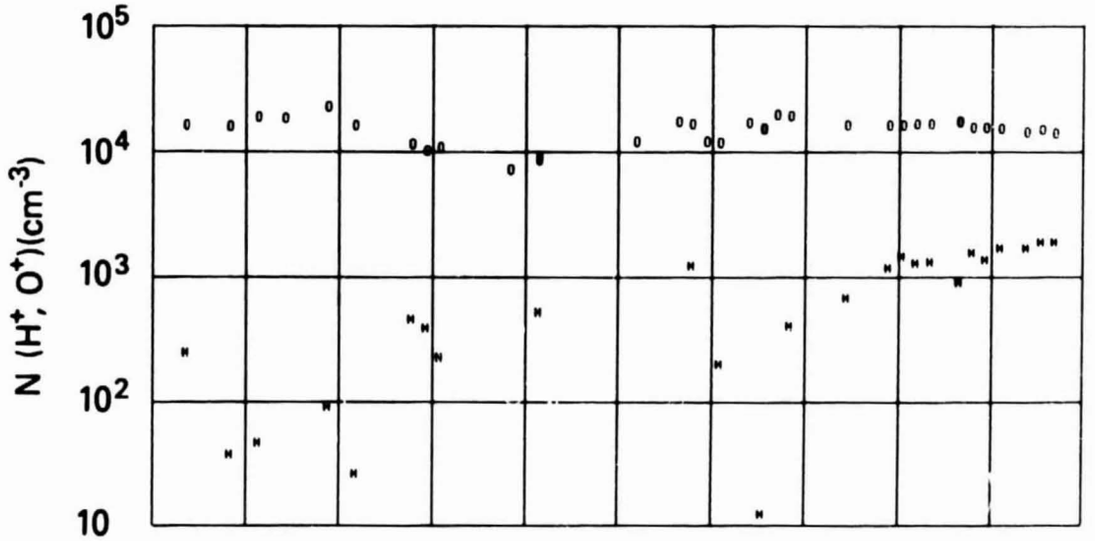

SET 21, FORMAT 5

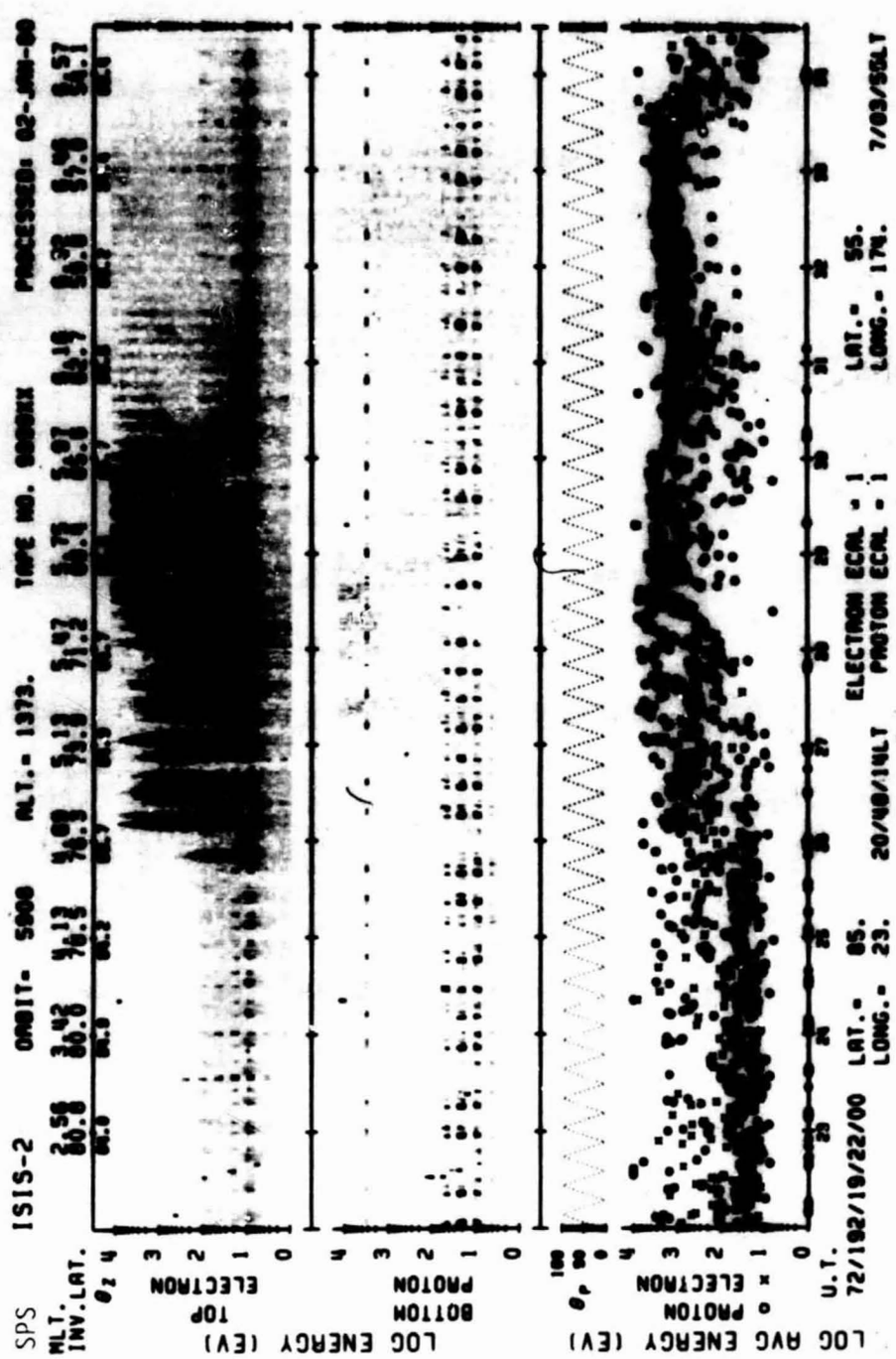

SET 22, FORMAT 6

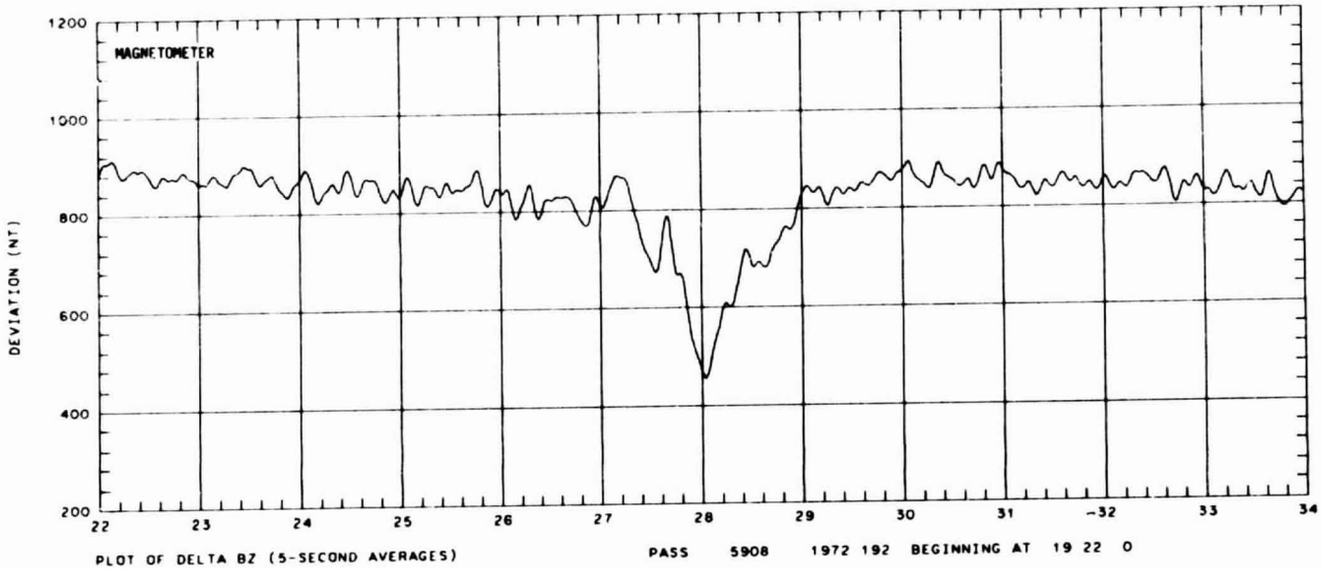

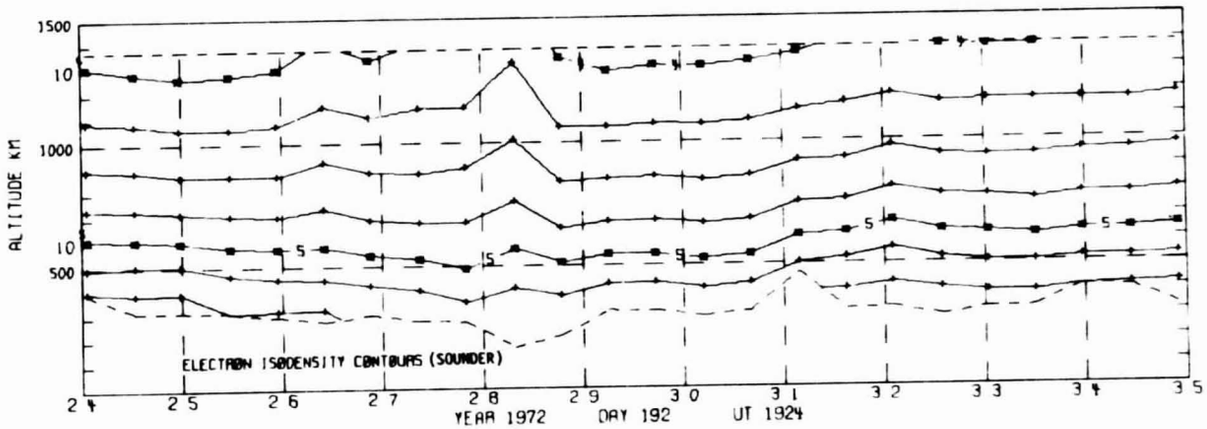

SET 22, FORMAT 2

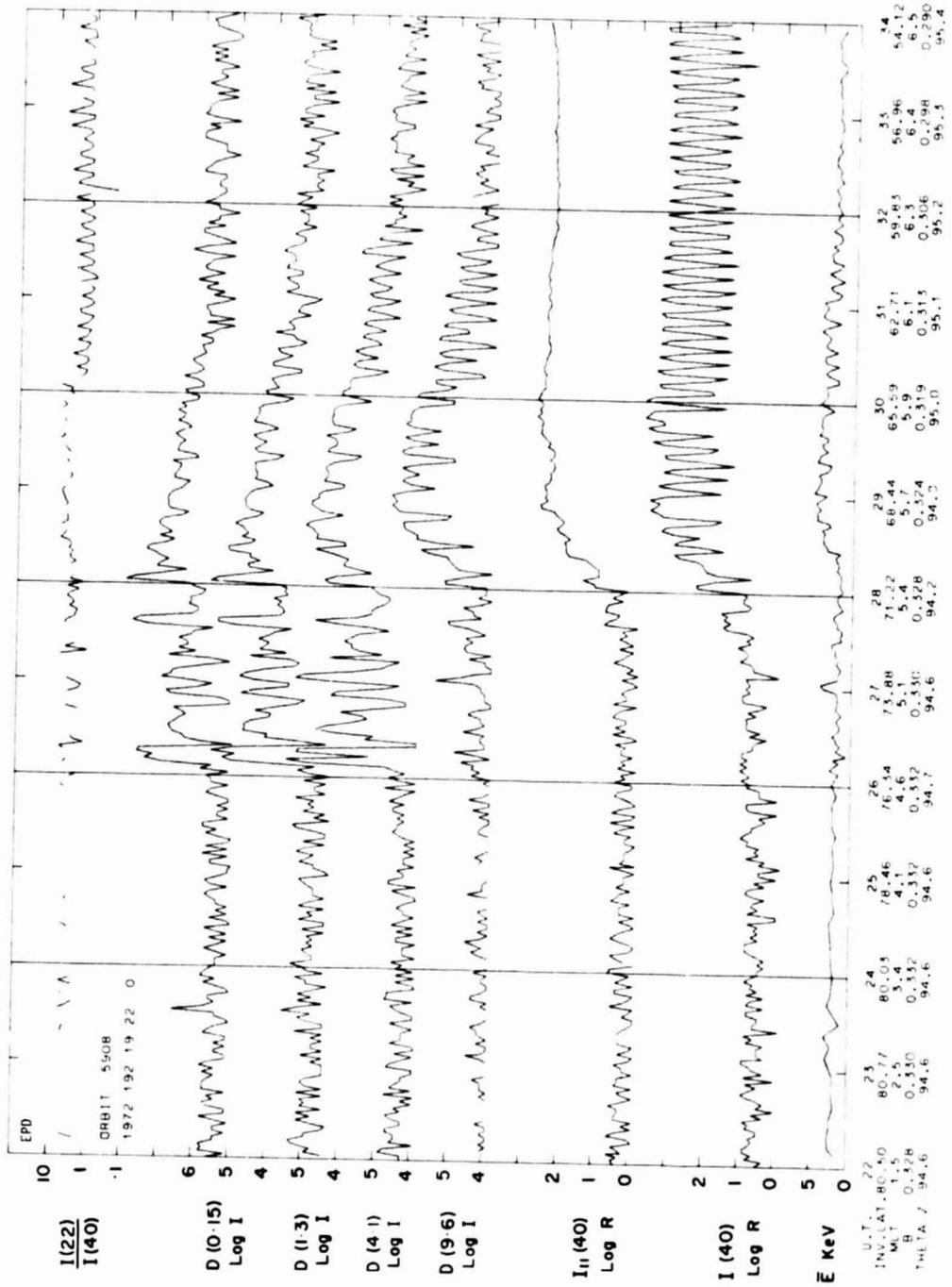

SET 22, FORMAT 3

ORBIT 5908
DATE 720710
DAY 192

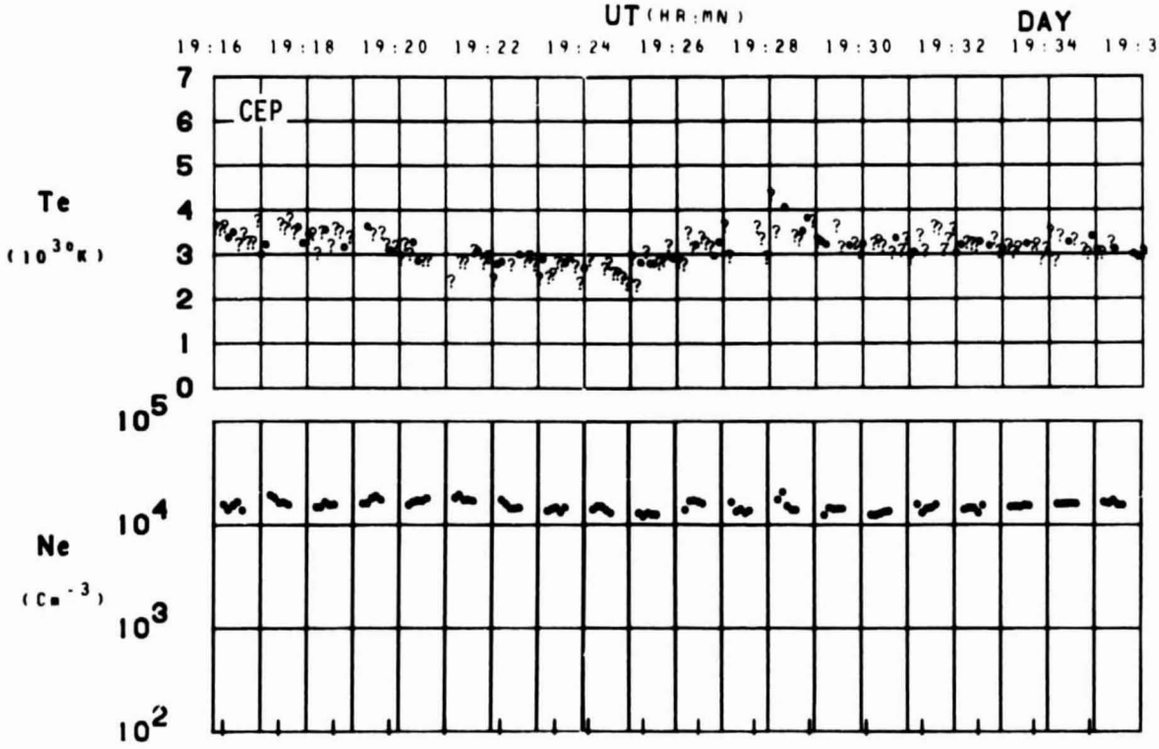

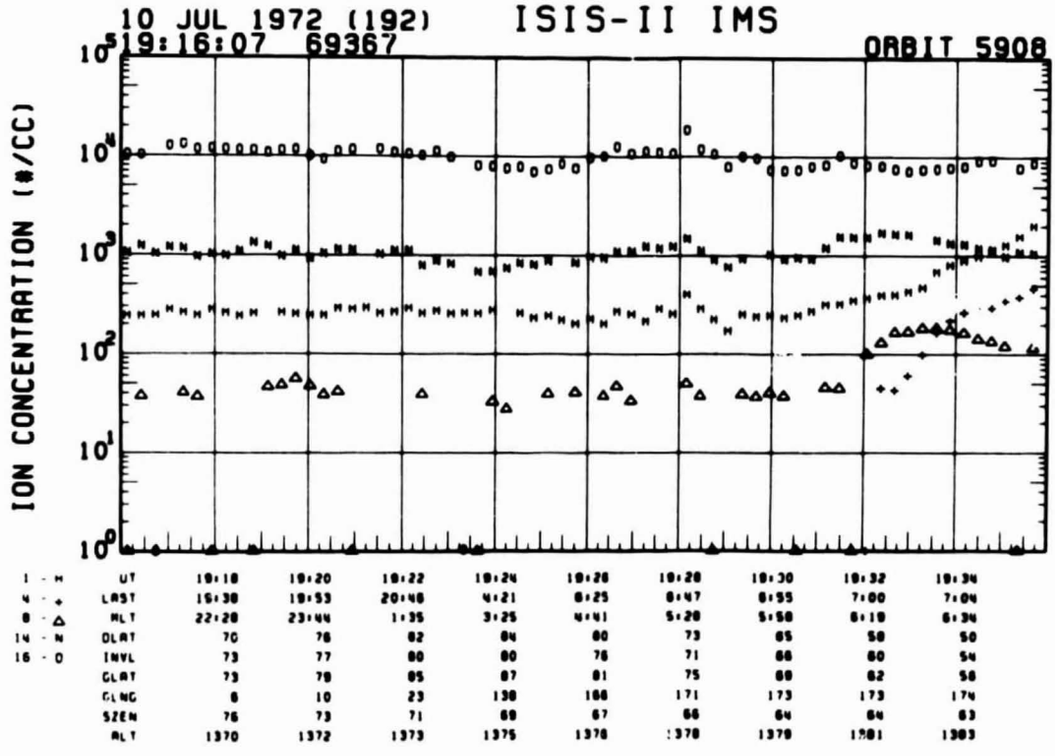

SET 22, FORMAT 4

RPA 720710

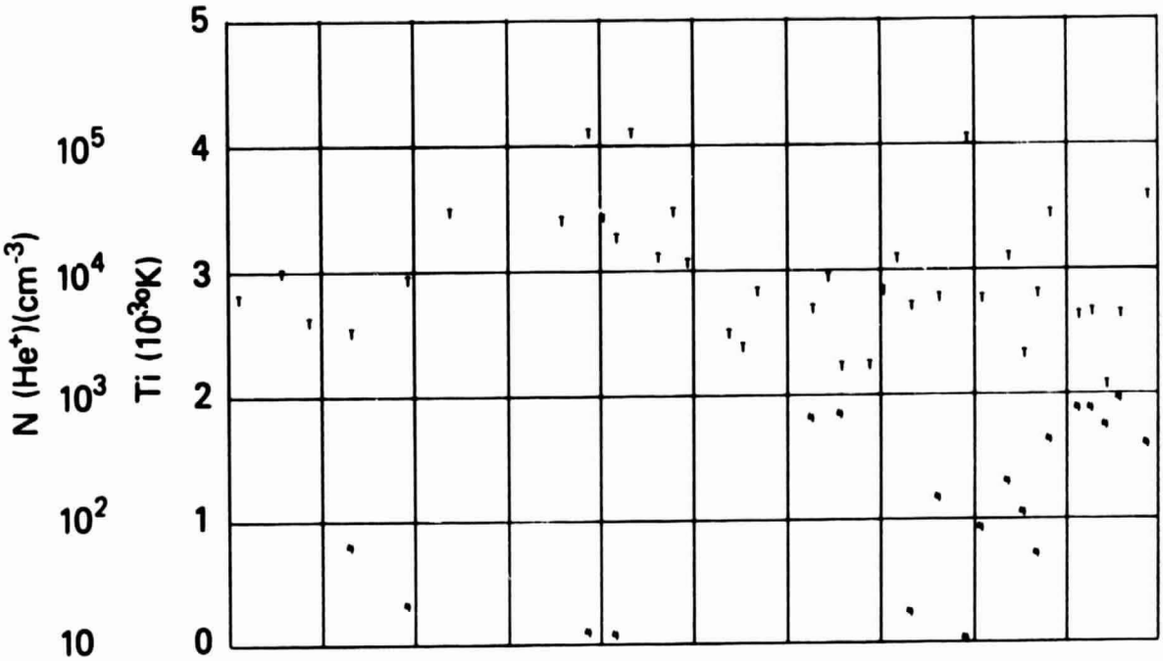

UT	19:18	19:20	19:22	19:24	19:26	19:28	19:30	19:32	19:34
LAST	19:38	19:53	20:46	4:21	6:25	6:47	6:55	7:00	7:04
MLT	22:28	23:44	1:35	3:25	4:41	5:28	5:58	6:19	6:34
DLAT	70	76	82	84	80	73	65	58	50
INVL	73	77	80	80	76	71	66	60	54
GLAT	73	79	85	87	81	75	69	62	56
GLNG	6	10	23	138	166	171	173	173	174
SZEN	76	73	71	69	67	66	64	64	63
ALT	1370	1372	1373	1375	1376	1378	1379	1381	1383

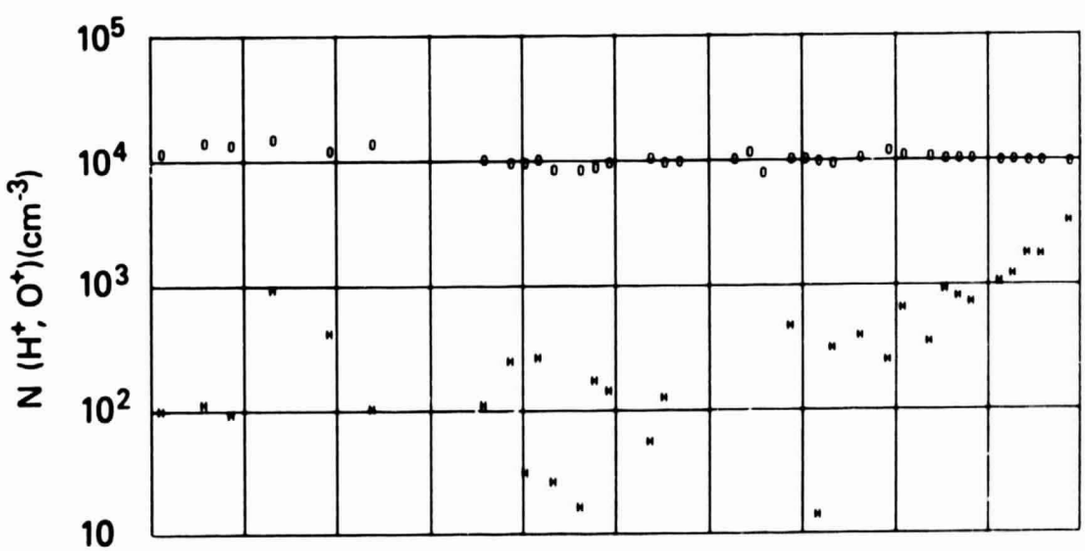

SET 22, FORMAT 5

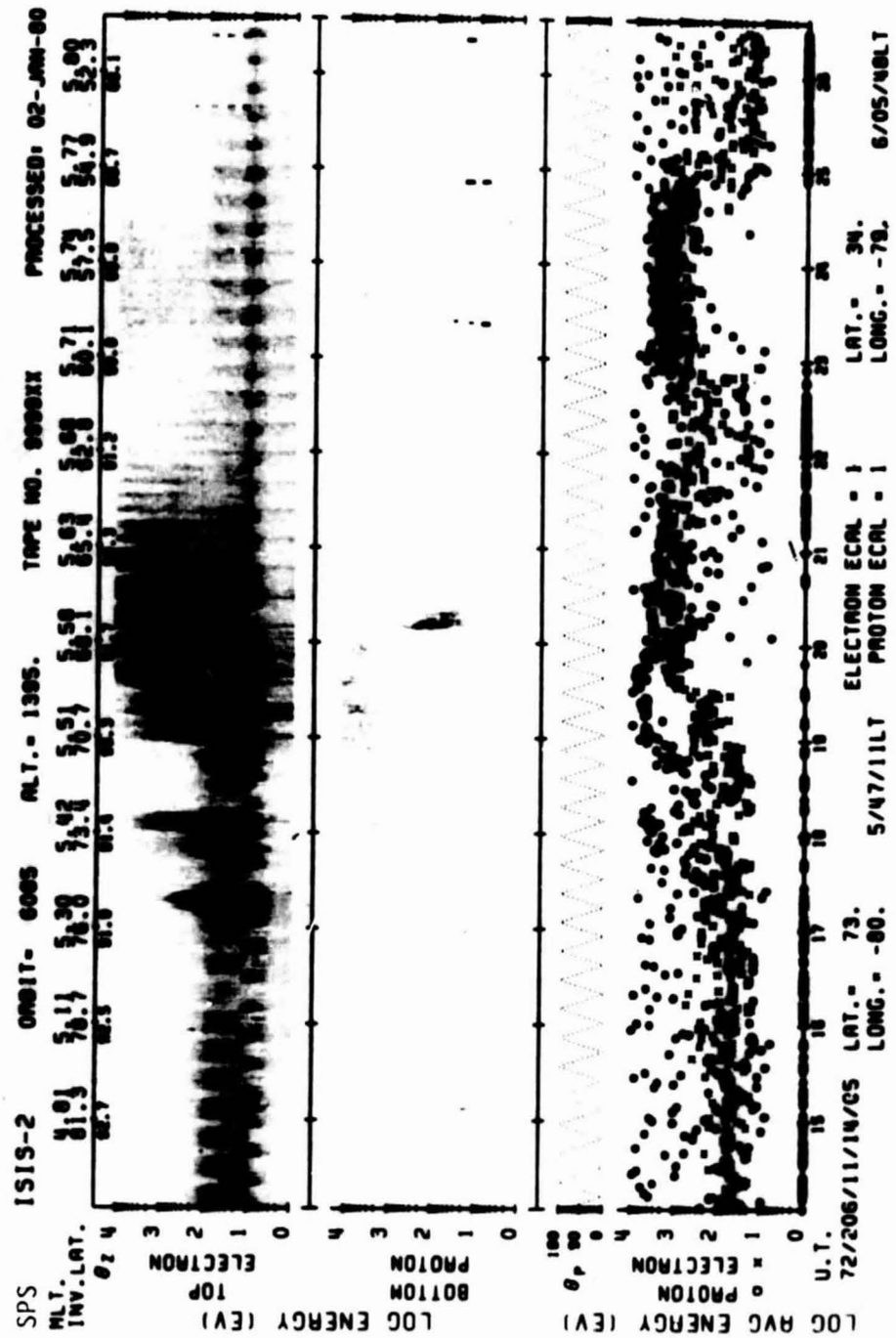

SET 23, FORMAT 6

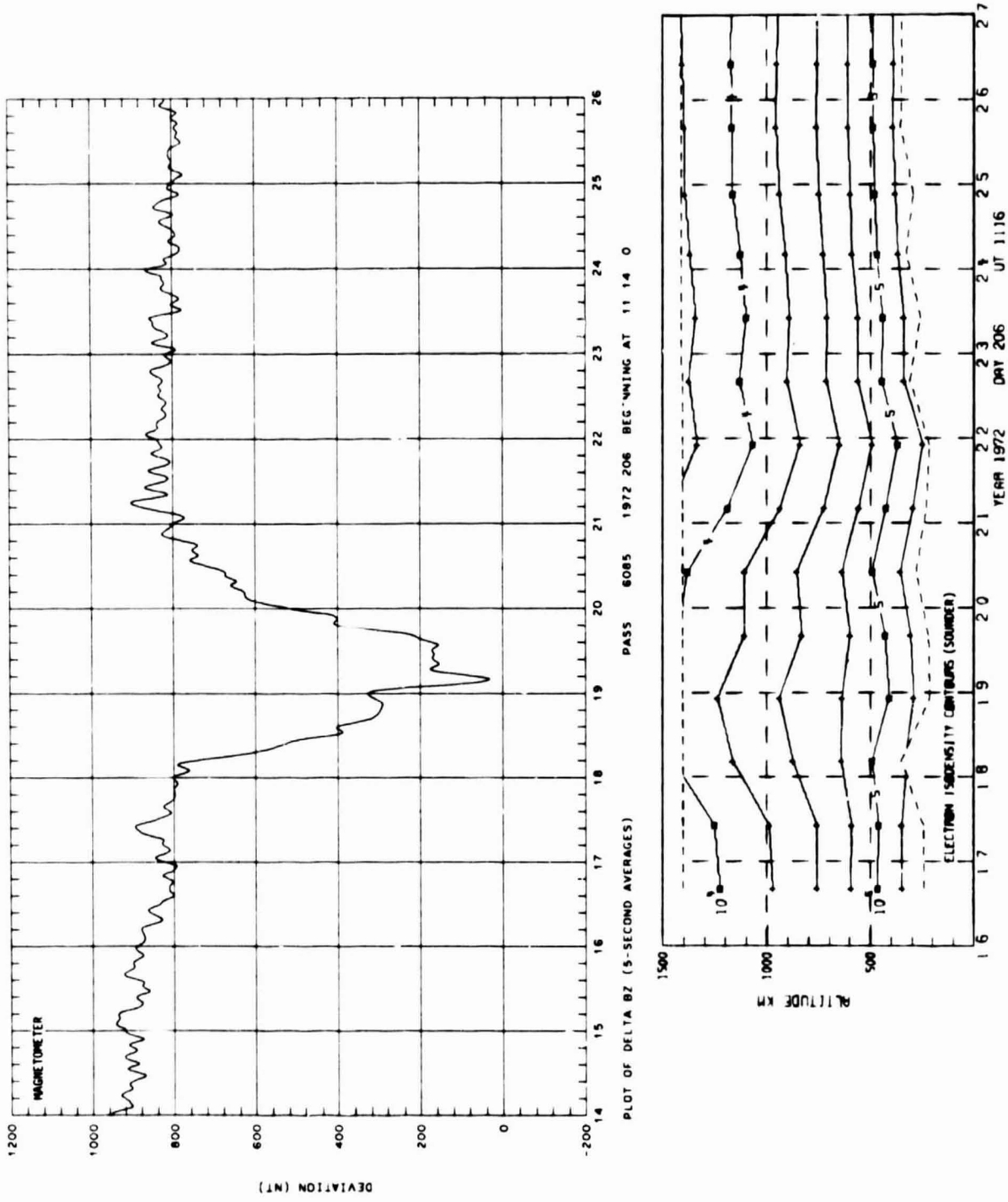

SET 13, FORMAT 2

SET 23, FORMAT 3

ORBIT 6085
DATE 720724
DAY 206

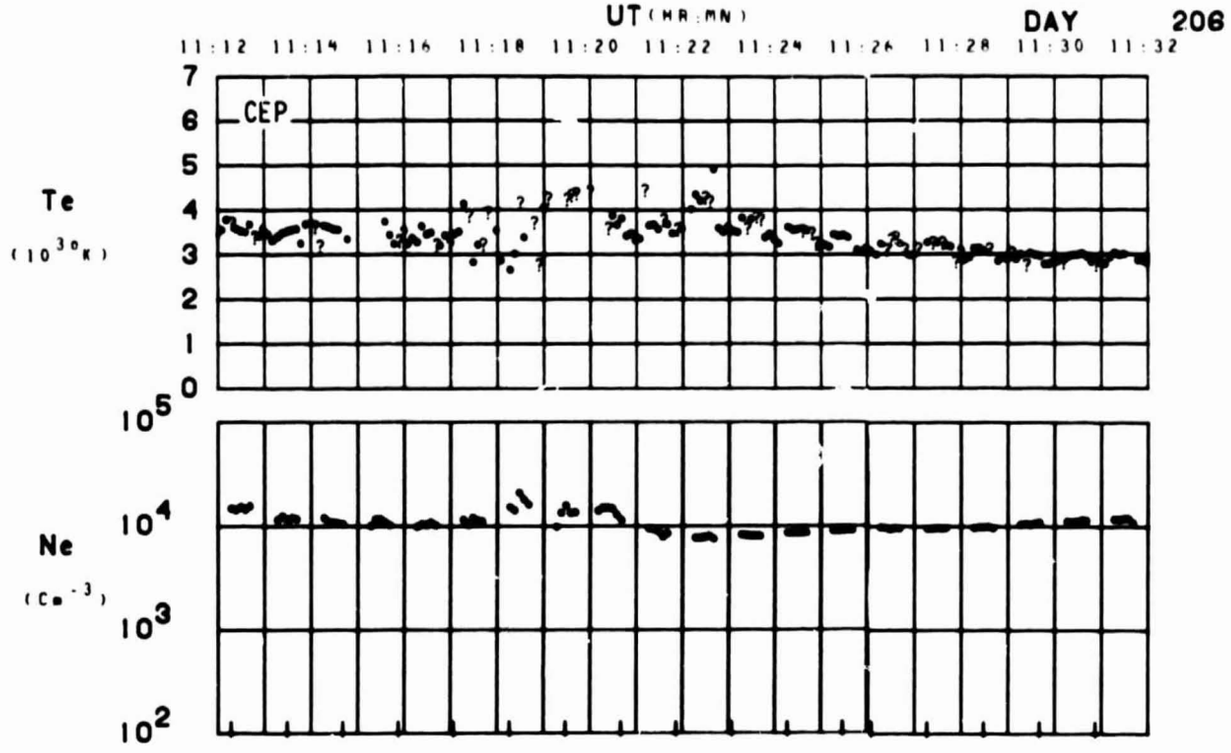

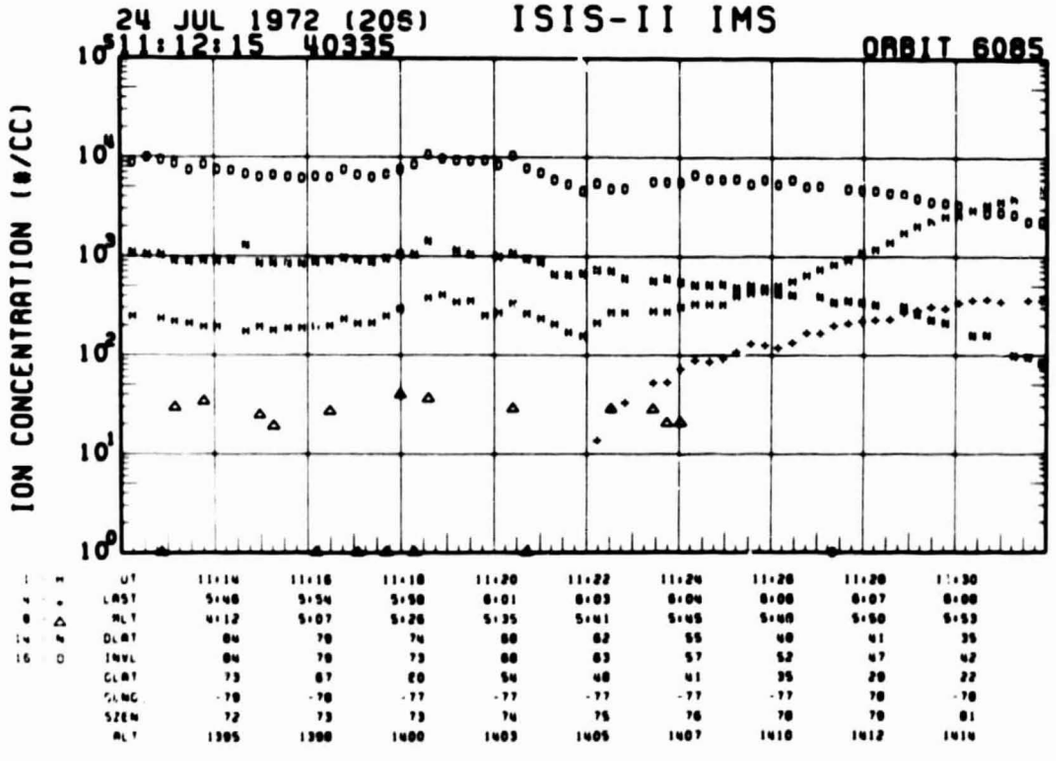

SET 23, FORMAT 4

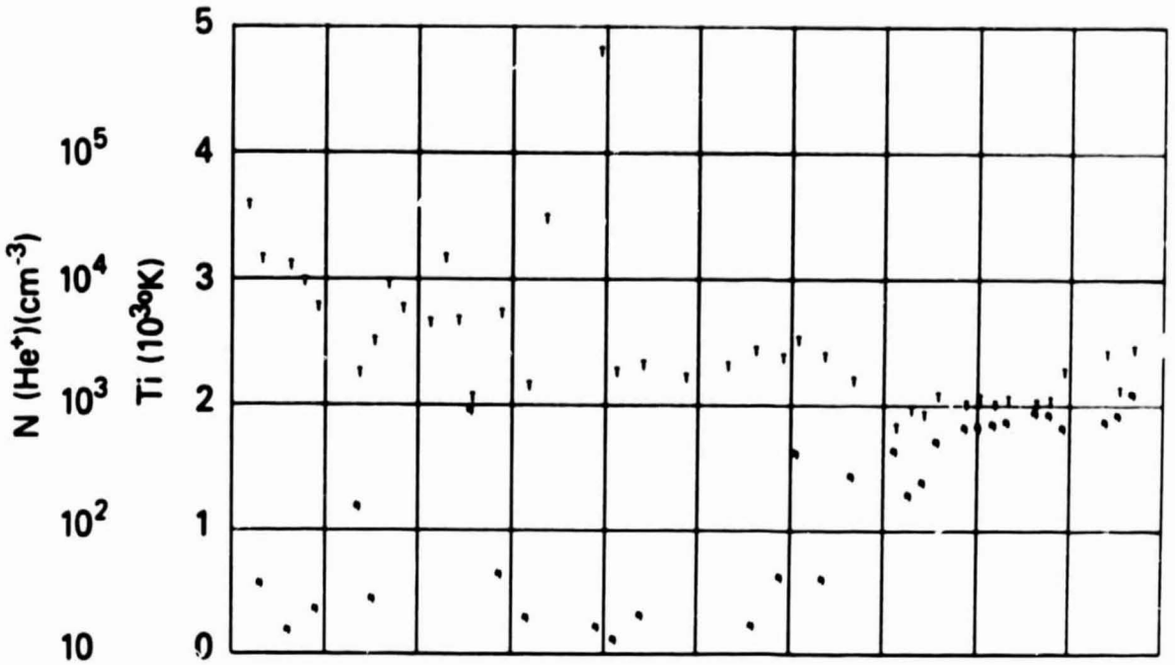

UT	11:14	11:16	11:18	11:20	11:22	11:24	11:26	11:28	11:30
LAST	5:46	5:54	5:58	6:01	6:03	6:04	6:06	6:07	6:08
MLT	4:12	5:07	5:26	5:35	5:41	5:45	5:48	5:50	5:53
DLAT	84	79	74	68	62	55	48	41	35
INVL	84	79	73	68	63	57	52	47	42
GLAT	73	67	60	54	48	41	35	29	22
GLNG	-78	-78	-77	-77	-77	-77	-77	-78	-78
SZEN	72	73	73	74	75	76	78	79	81
ALT	1395	1398	1400	1403	1405	1407	1410	1412	1414

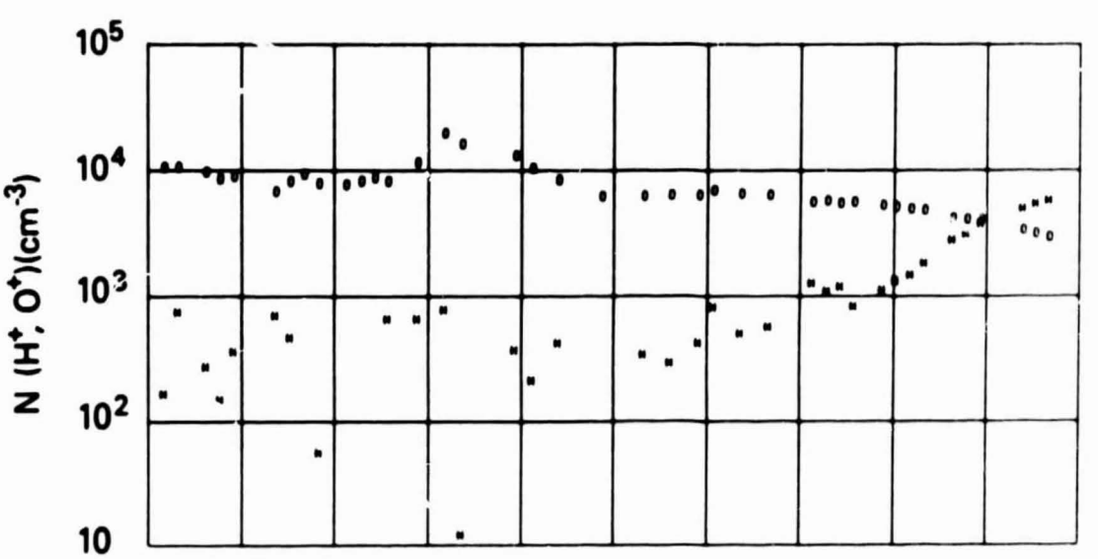

SET 23, FORMAT 5

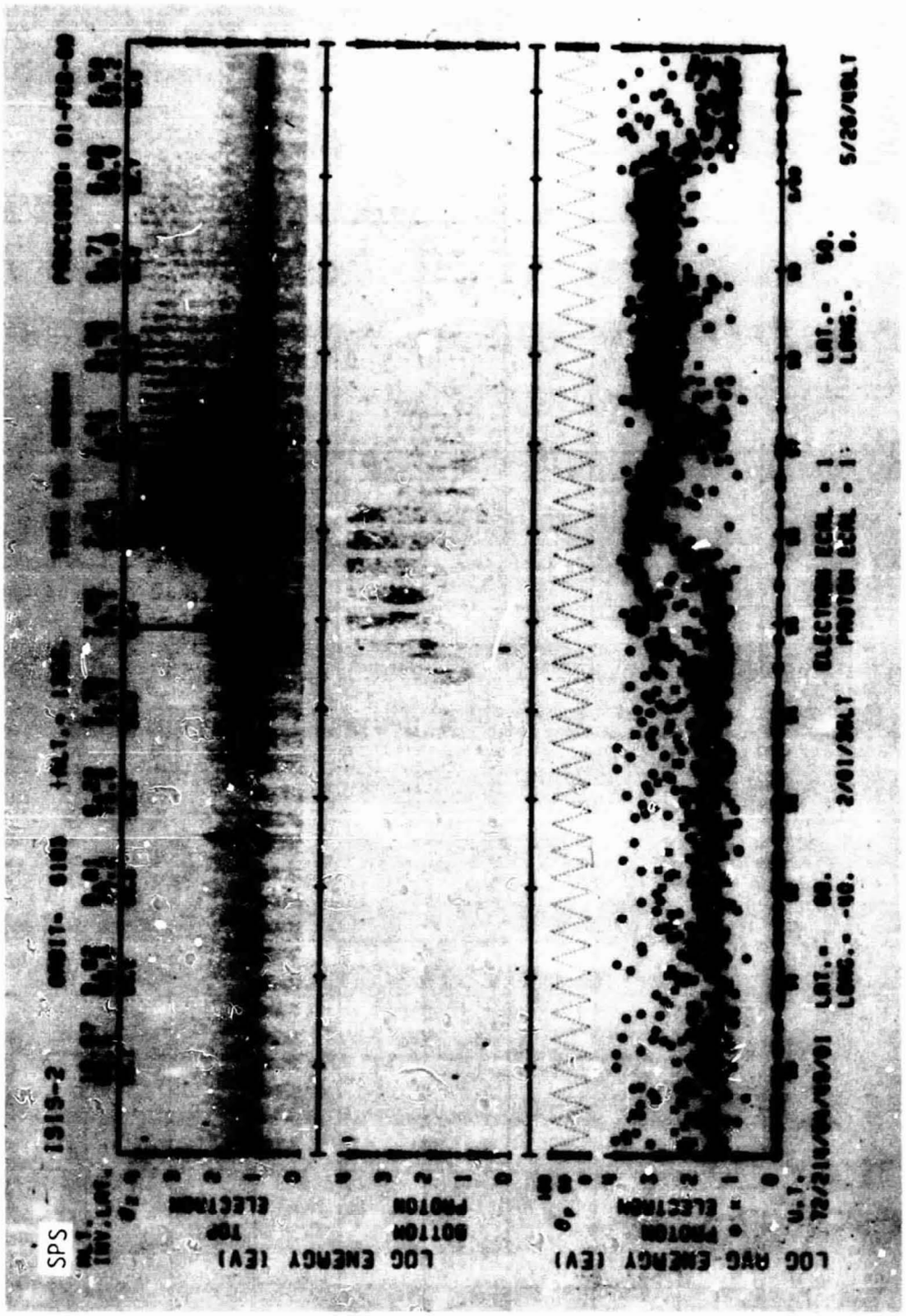

SET 24, FORMAT 6

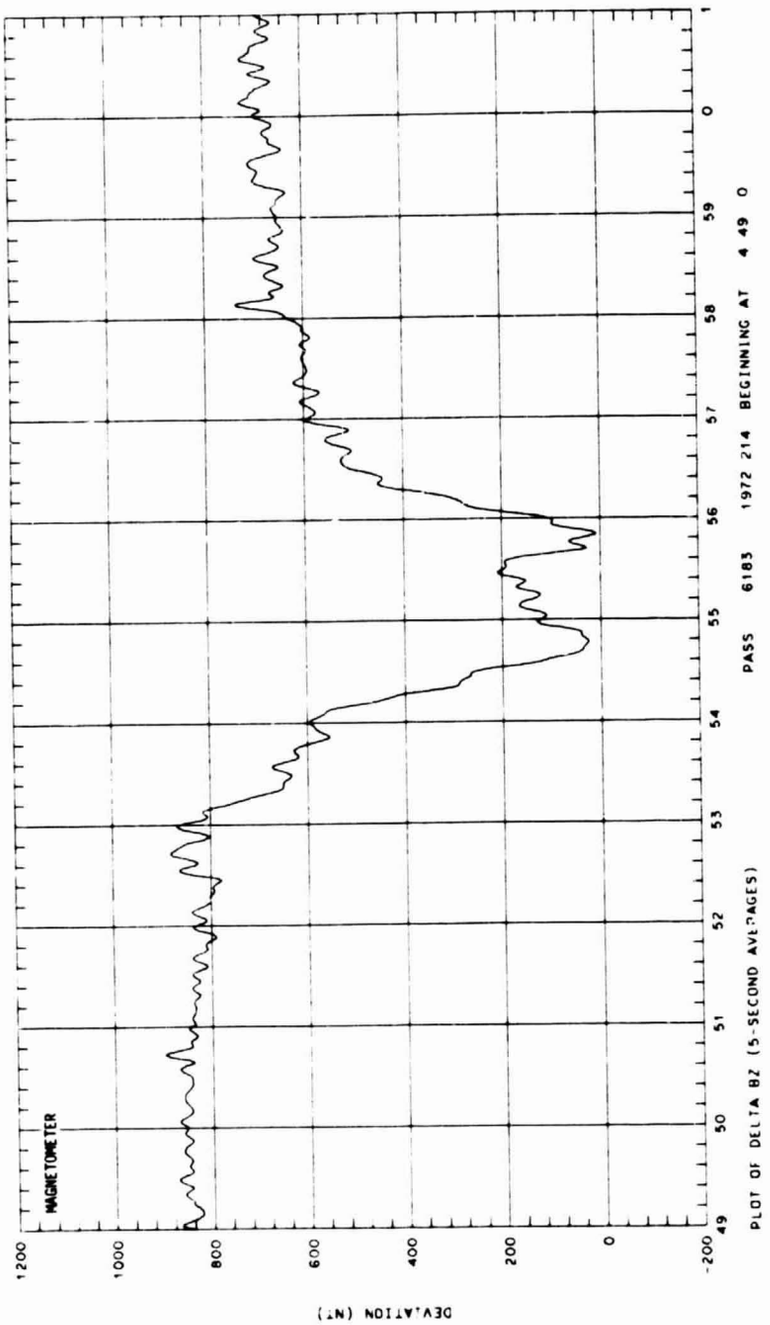

SET 24, FORMAT 2

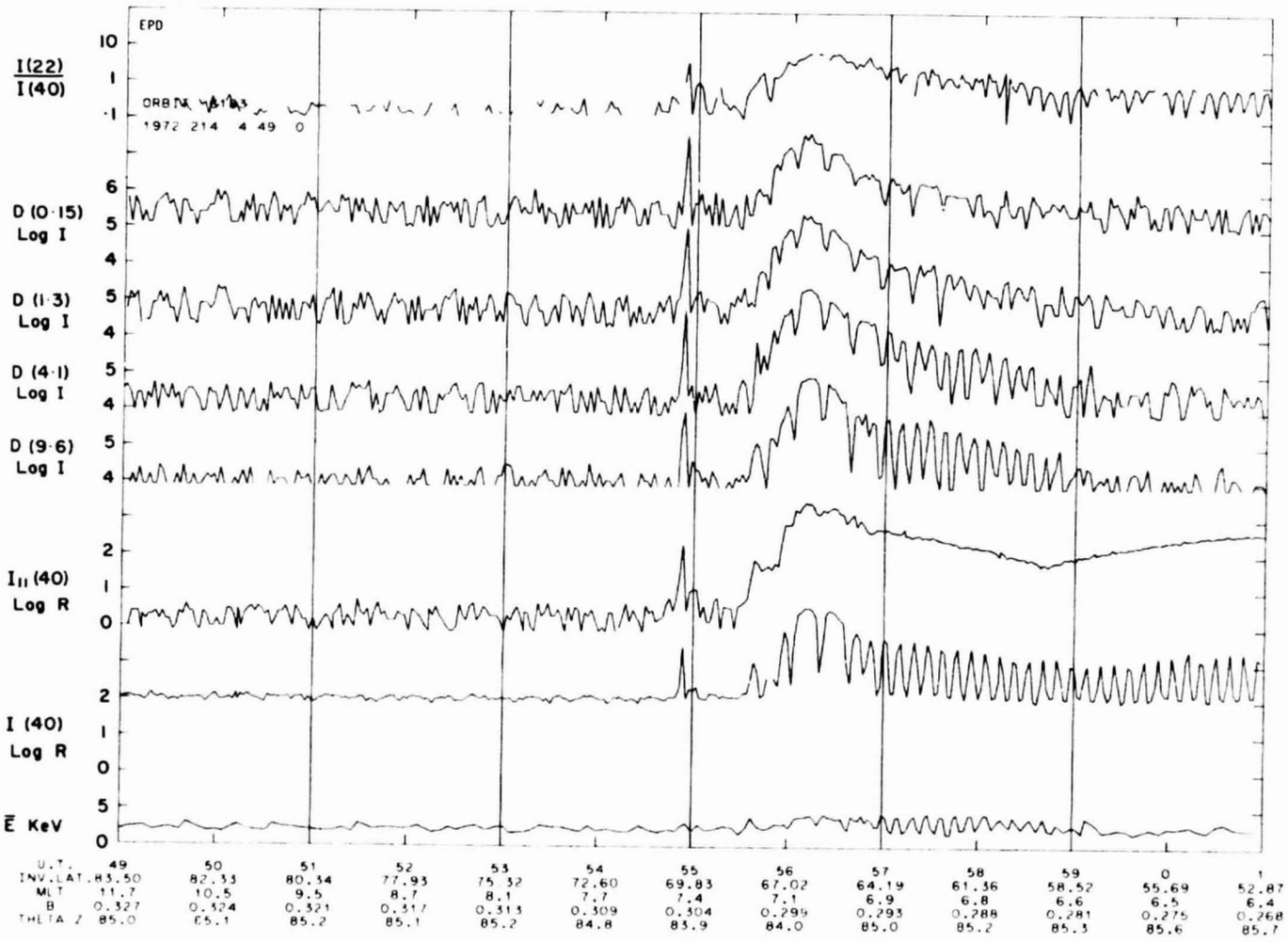

SET 24, FORMAT 3

ORBIT 6183
DATE 720801
DAY 214

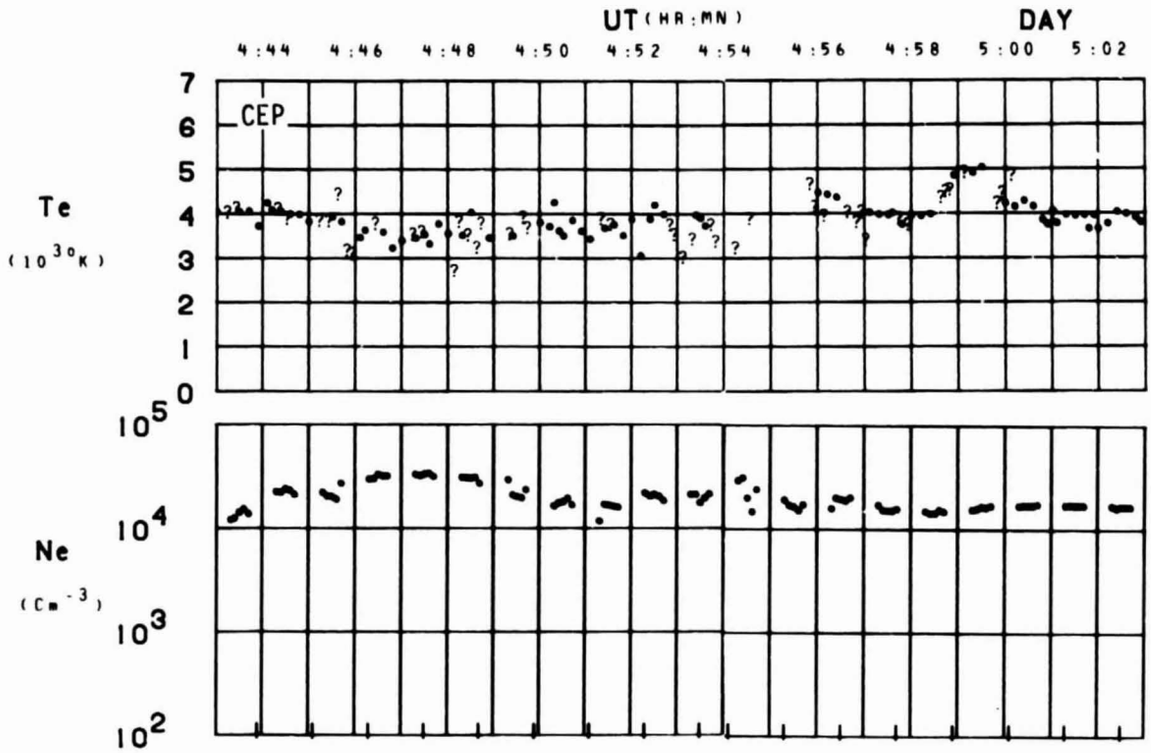

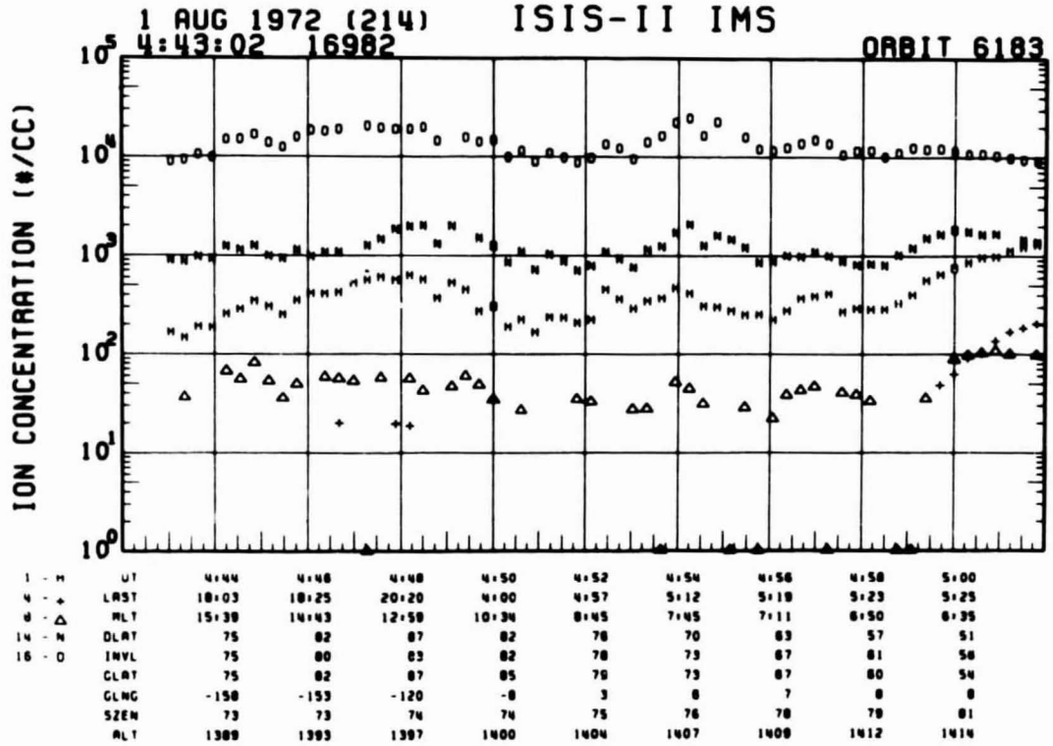

1 - H	UT	4:44	4:46	4:48	4:50	4:52	4:54	4:56	4:58	5:00
4 - +	LAST	18:03	18:25	20:20	4:00	4:57	5:12	5:19	5:23	5:25
8 - △	MLT	15:38	14:43	12:58	10:34	8:45	7:45	7:11	6:50	6:35
14 - N	DLAT	75	82	87	82	78	70	63	57	51
16 - O	INVL	75	80	83	82	78	73	67	61	56
	CLAT	75	82	87	85	79	73	67	60	54
	GLNG	-150	-153	-120	-8	3	8	7	8	8
	SZEN	73	73	74	74	75	76	78	79	81
	ALT	1389	1393	1397	1400	1404	1407	1409	1412	1414

SET 24, FORMAT 4

RPA

720801

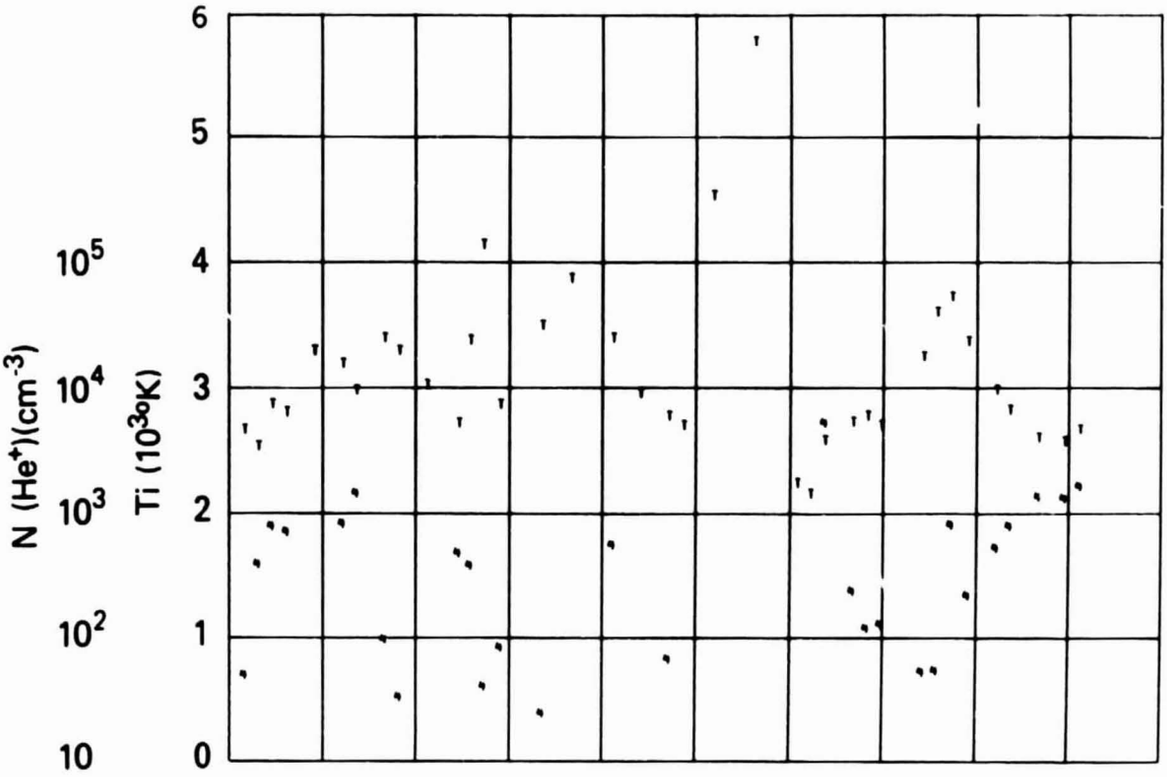

UT	4:44	4:46	4:48	4:50	4:52	4:54	4:56	4:58	5:00
LAST	18:03	18:25	20:20	4:00	4:57	5:12	5:19	5:23	5:25
MLT	15:39	14:43	12:59	10:34	8:45	7:45	7:11	6:50	6:35
DLAT	75	82	87	82	78	70	63	57	51
INVL	75	80	83	82	78	73	67	61	56
GLAT	75	82	87	85	79	73	67	60	54
GLNG	-158	-153	-120	-8	3	6	7	8	8
SZEN	73	73	74	74	75	76	78	79	81
ALT	1389	1393	1397	1400	1404	1407	1409	1412	1414

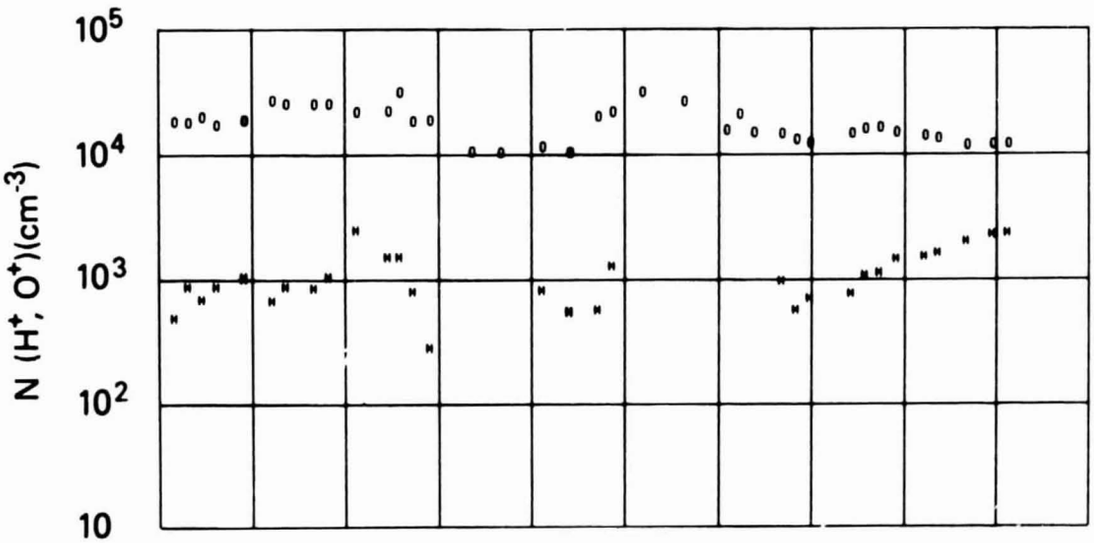

SET 24, FORMAT 5

72/214/0449

Excerpts of VLF Spectral film for the period 0452 - 0501

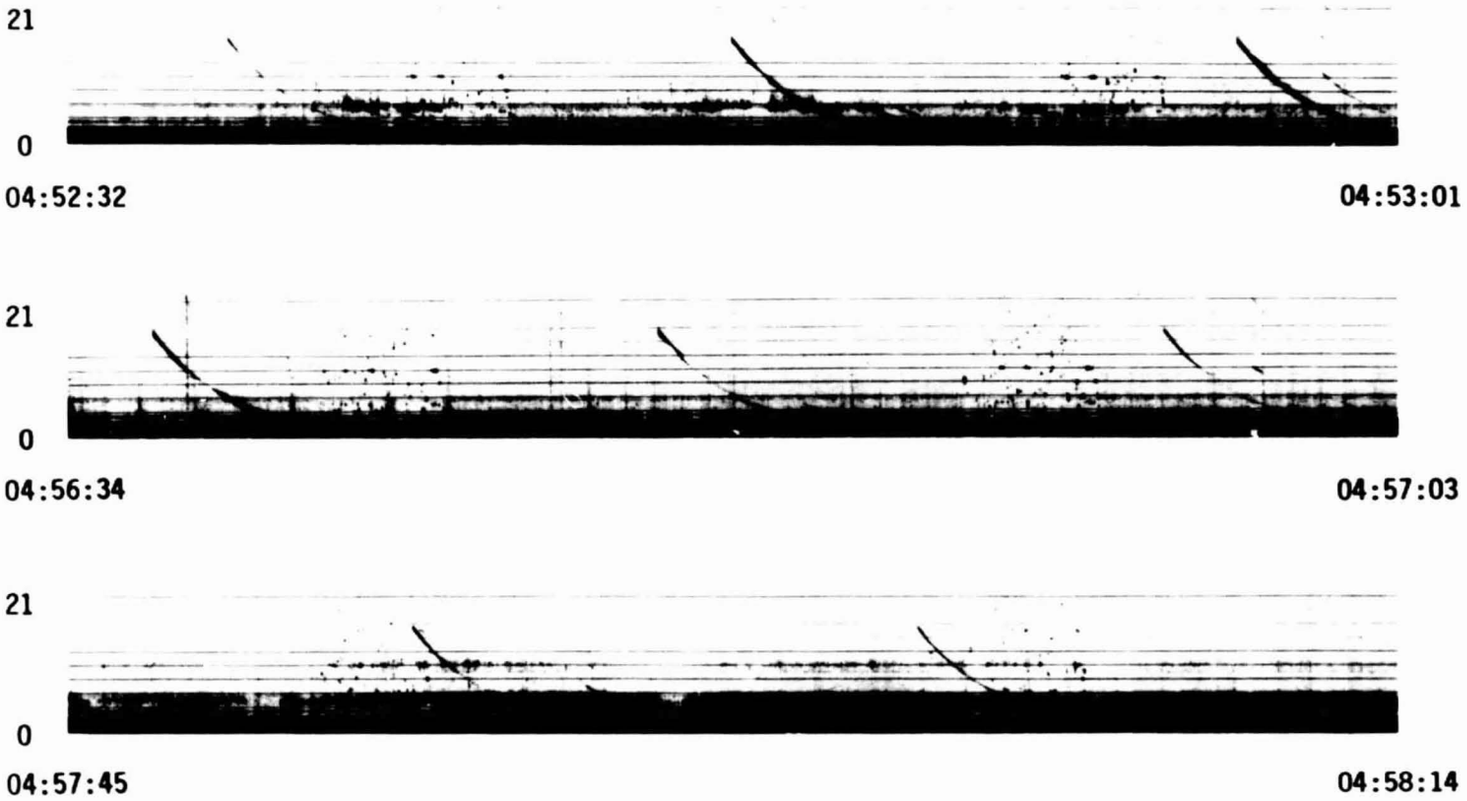

SET 24, FORMAT 11

72/214/0449

Excerpts of VLF Spectral film for the period 0452 - 0501

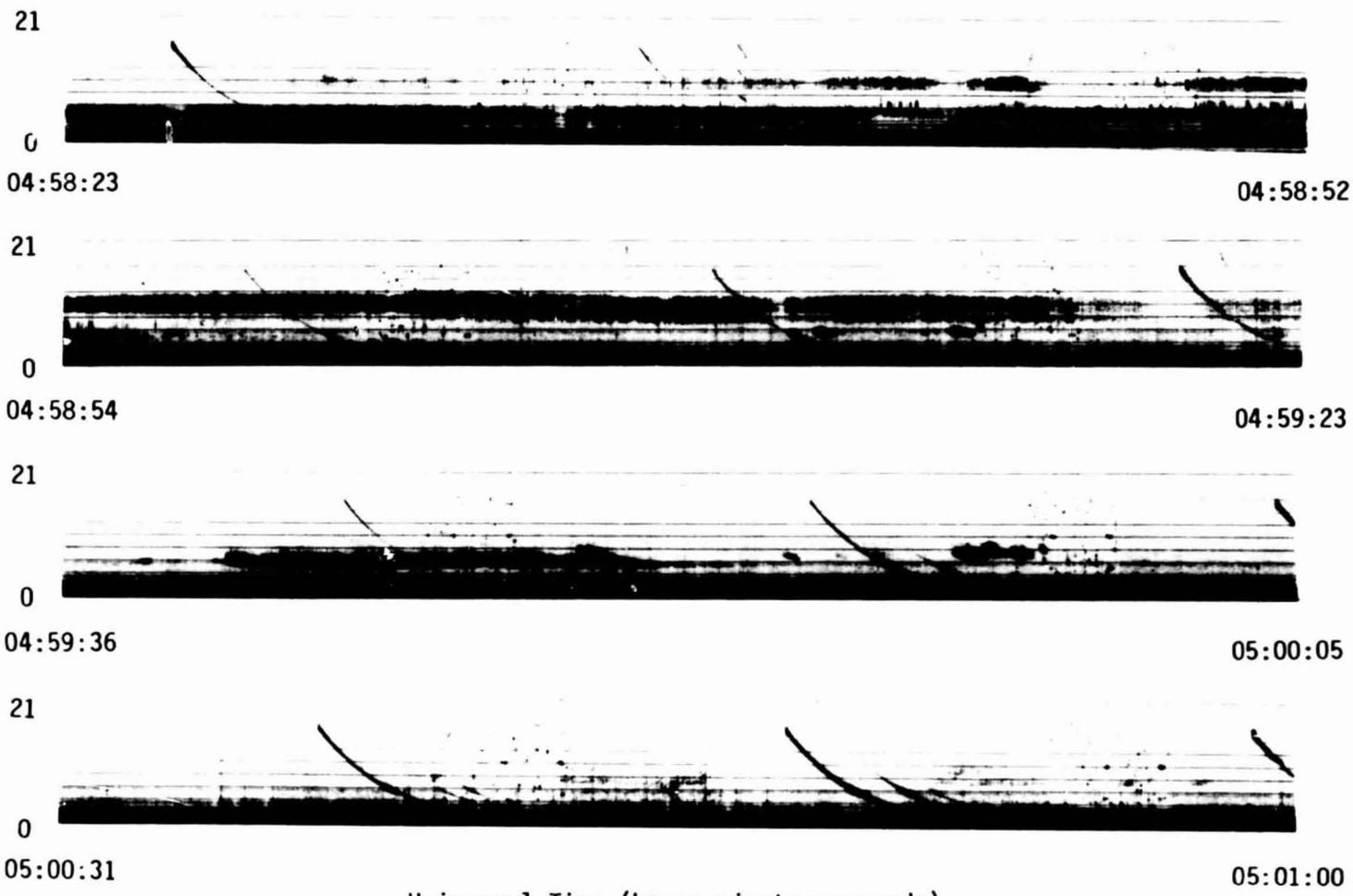

SET 24, FORMAT 11

SET 25, FORMAT 6

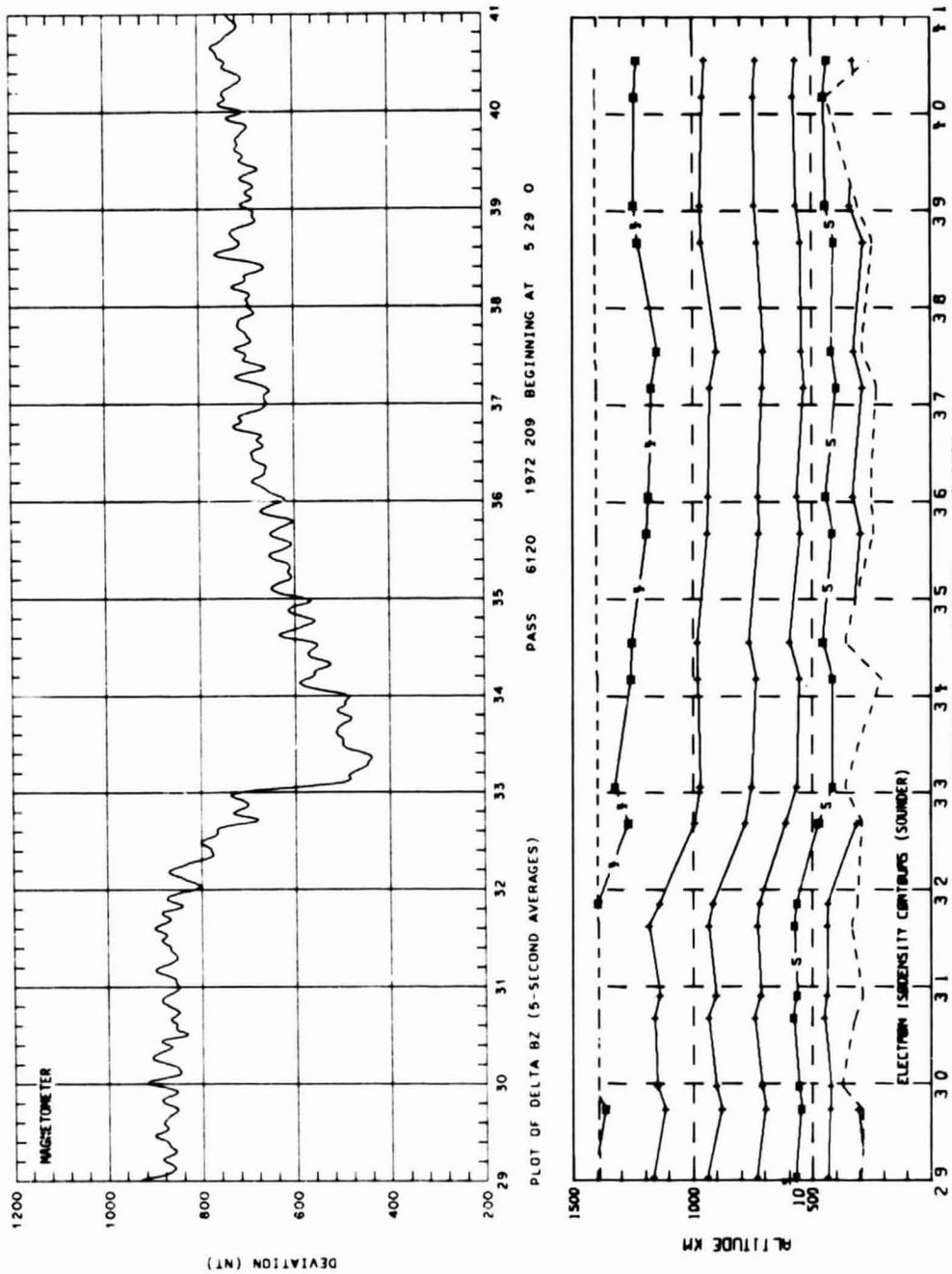

SET 25, FORMAT 2

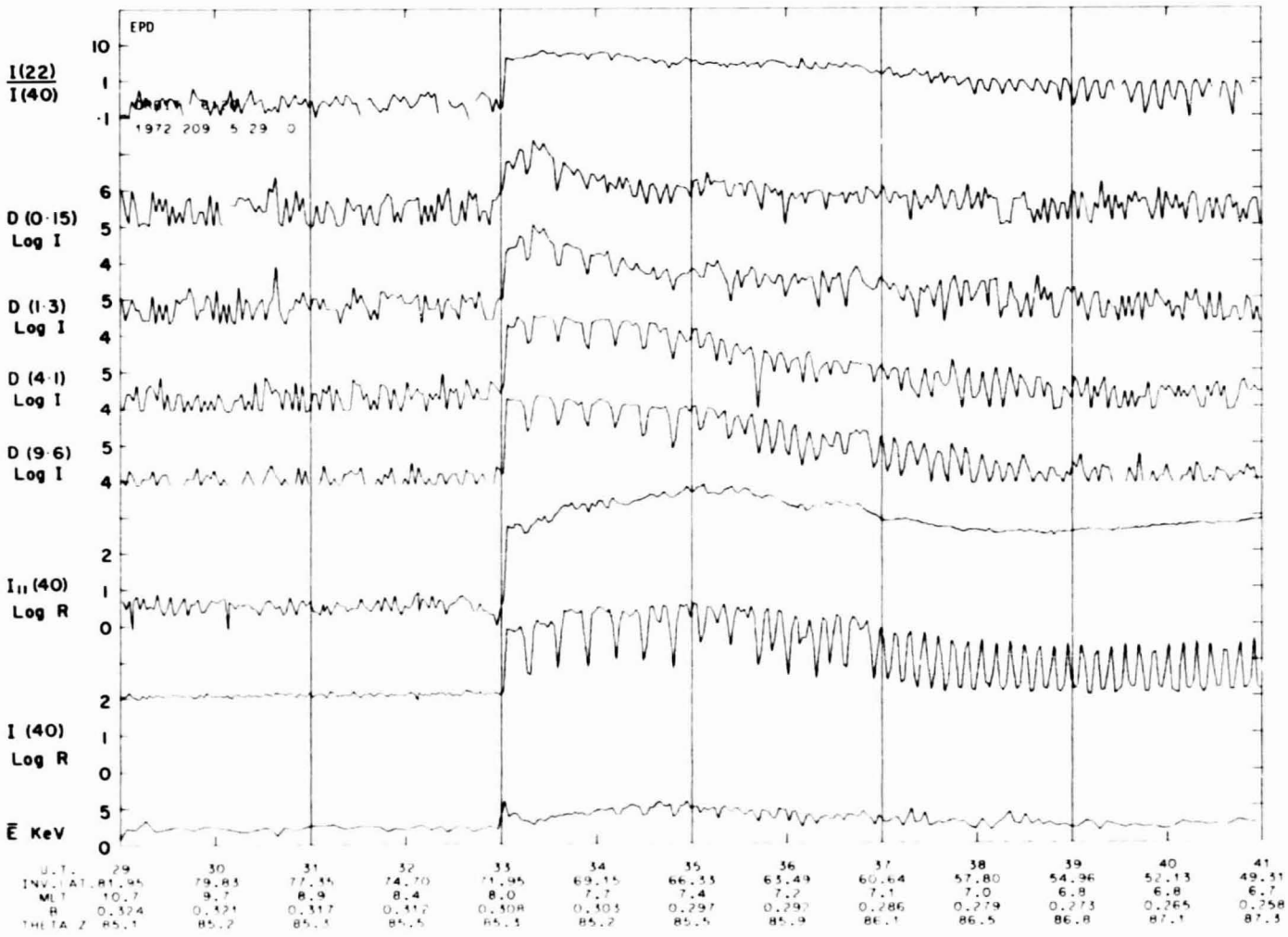

SET 25, FORMAT 3

ORBIT 6120
DATE 72072/
DAY 209

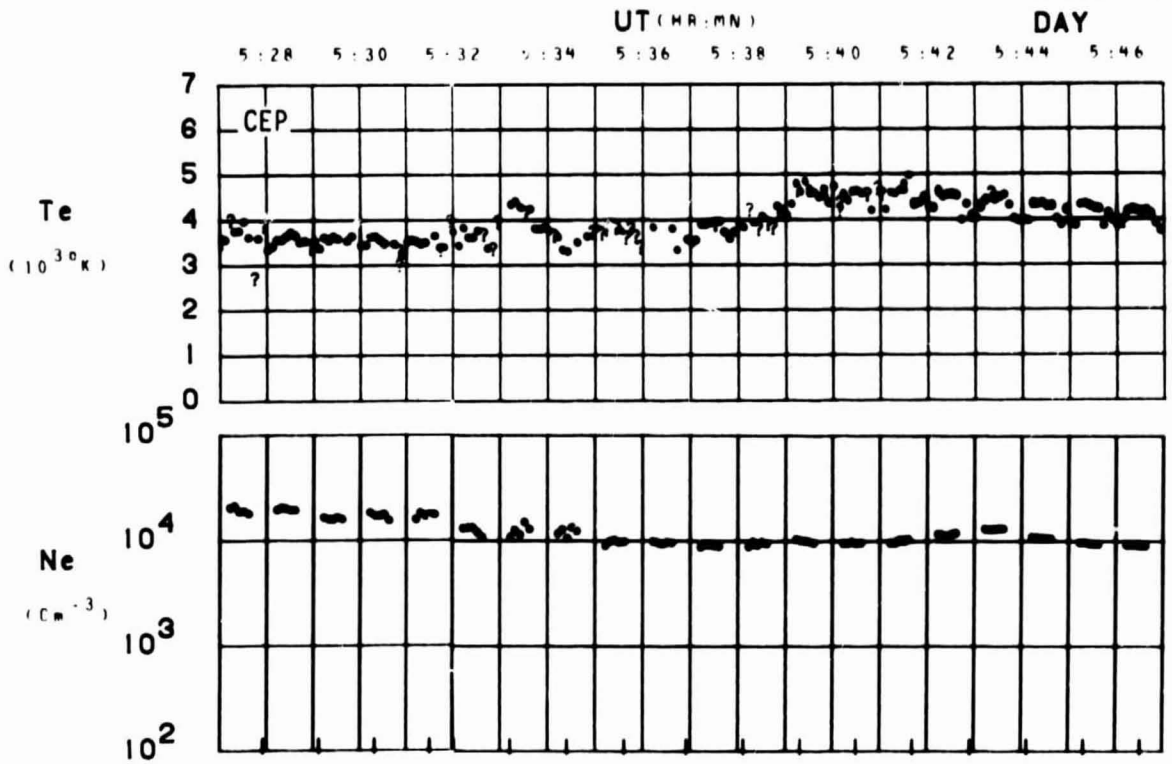

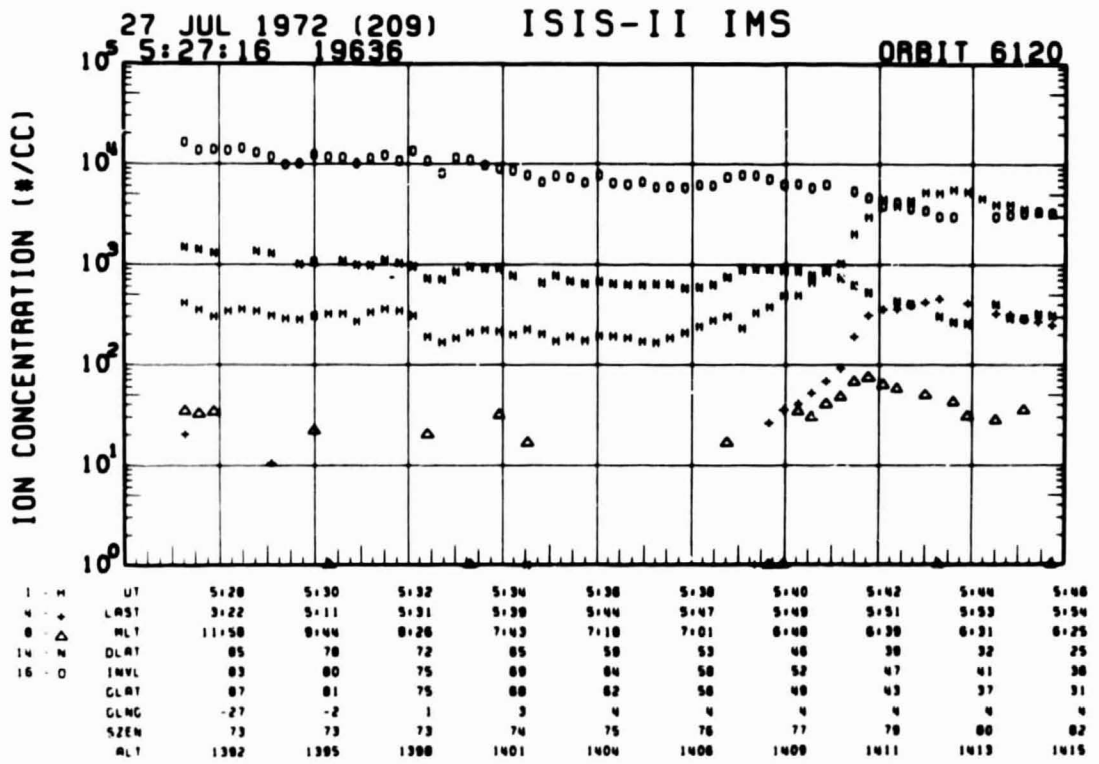

UT	5:28	5:30	5:32	5:34	5:36	5:38	5:40	5:42	5:44	5:46
LAST	3:22	5:11	5:31	5:38	5:44	5:47	5:48	5:51	5:53	5:54
MLT	11:58	9:44	8:26	7:43	7:18	7:01	6:48	6:39	6:31	6:25
DLAT	85	78	72	65	58	53	48	38	32	25
INVL	83	80	75	69	64	58	52	47	41	36
GLAT	87	81	75	68	62	56	49	43	37	31
GLNG	-27	-2	1	3	4	4	4	4	4	4
SZEN	73	73	73	74	75	76	77	78	80	82
ALT	1392	1395	1398	1401	1404	1406	1409	1411	1413	1415

1 - H
4 - +
8 - △
14 - N
16 - O

SET 25, FORMAT 4

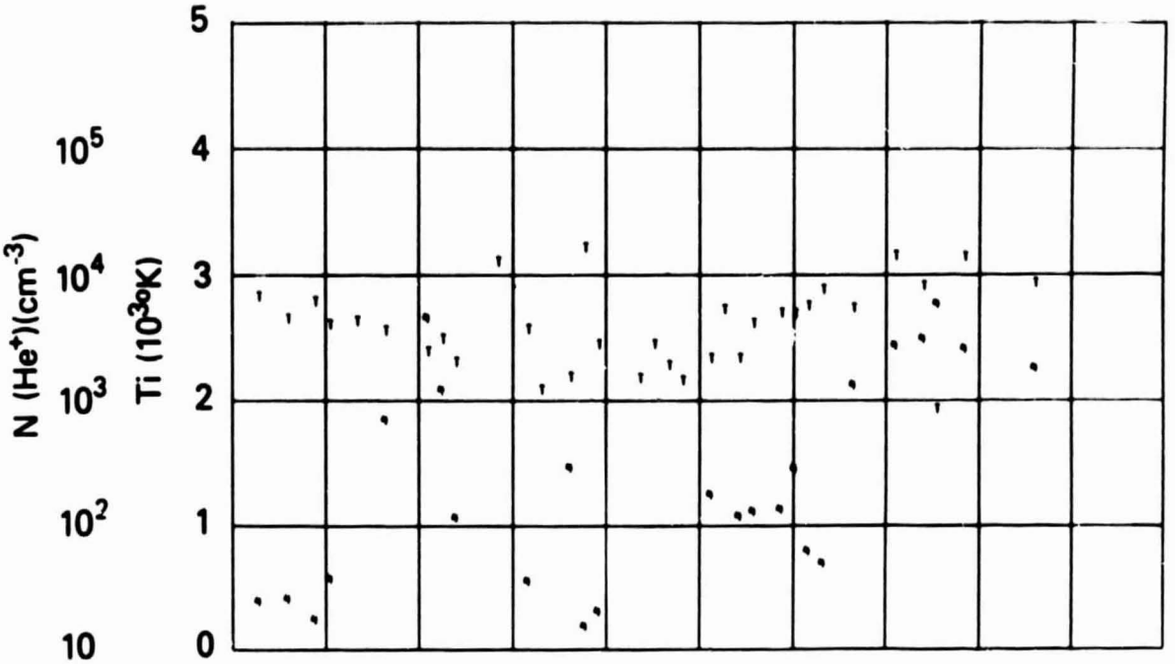

UT	5:28	5:30	5:32	5:34	5:36	5:38	5:40	5:42	5:44	5:46
LAST	3:22	5:11	5:31	5:39	5:44	5:47	5:49	5:51	5:53	5:54
MLT	11:58	9:44	8:26	7:43	7:18	7:01	6:48	6:39	6:31	6:25
DLAT	85	78	72	65	59	53	46	39	32	25
INVL	83	80	75	69	64	58	52	47	41	36
GLAT	87	81	75	68	62	56	49	43	37	31
GLNG	-27	-2	1	3	4	4	4	4	4	4
SZEN	73	73	73	74	75	76	77	78	80	82
ALT	1392	1395	1398	1401	1404	1406	1409	1411	1413	1415

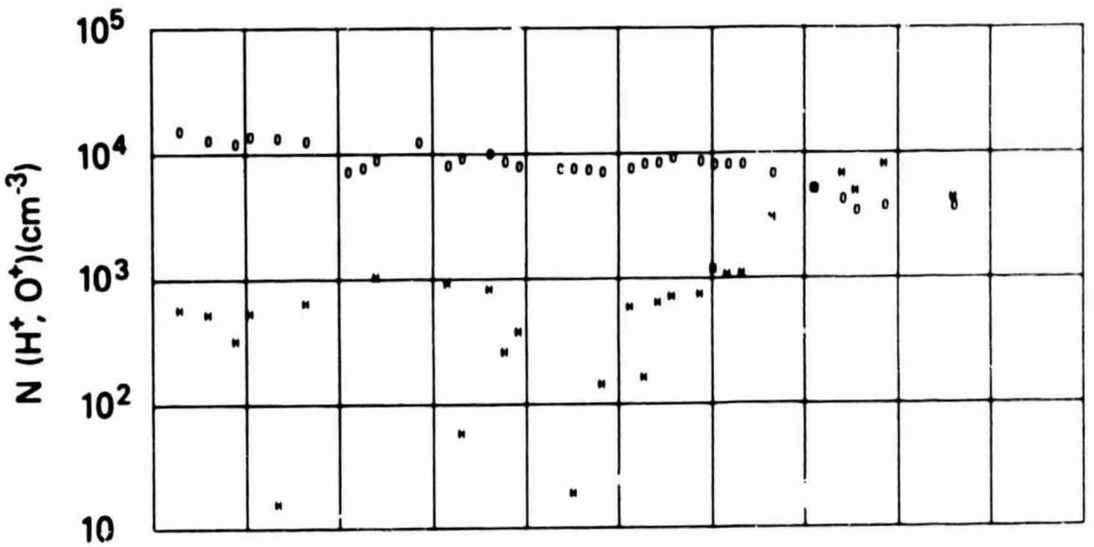

SET 25, FORMAT 5

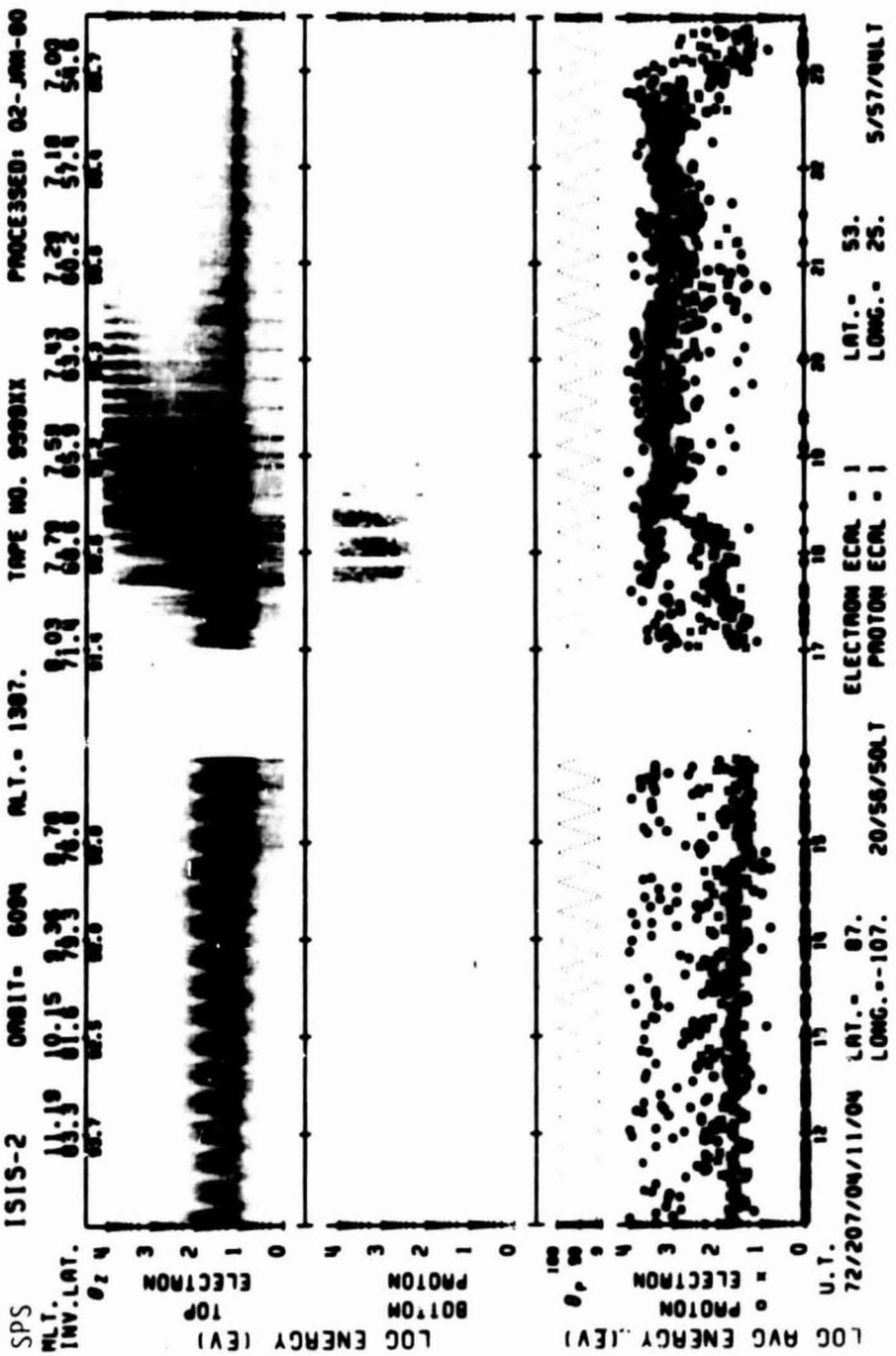

SET 26, FORMAT 6

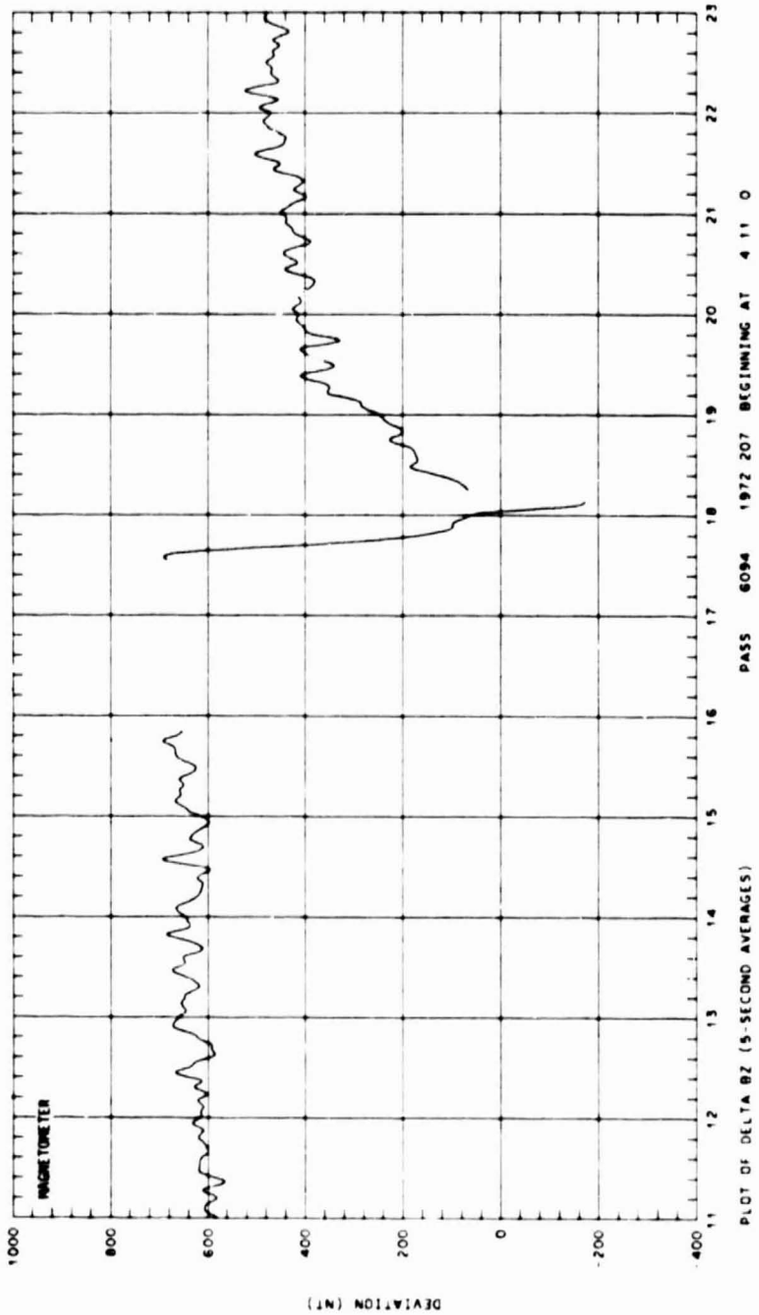

SET 26, FORMAT 2

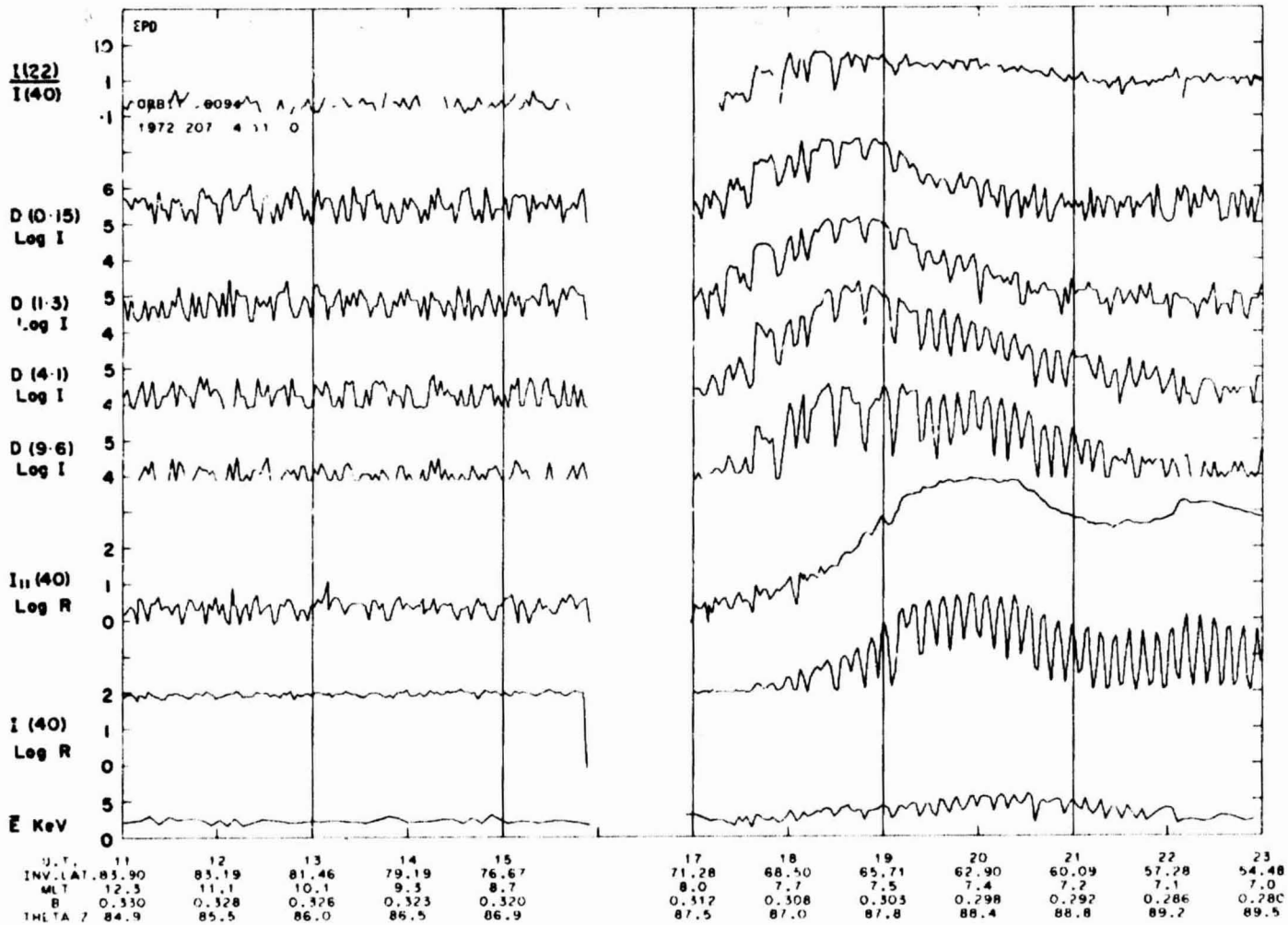

SET 26, FORMAT 3

ORBIT 6094
DATE 720725
DAY 207

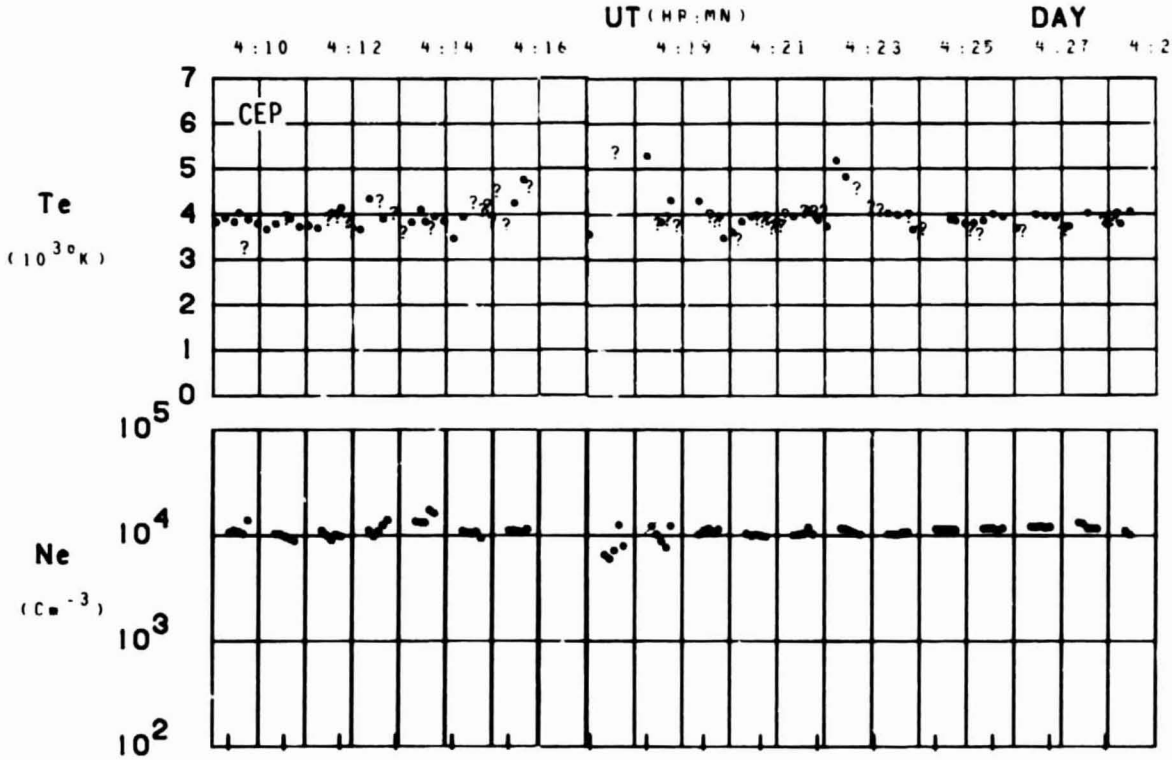

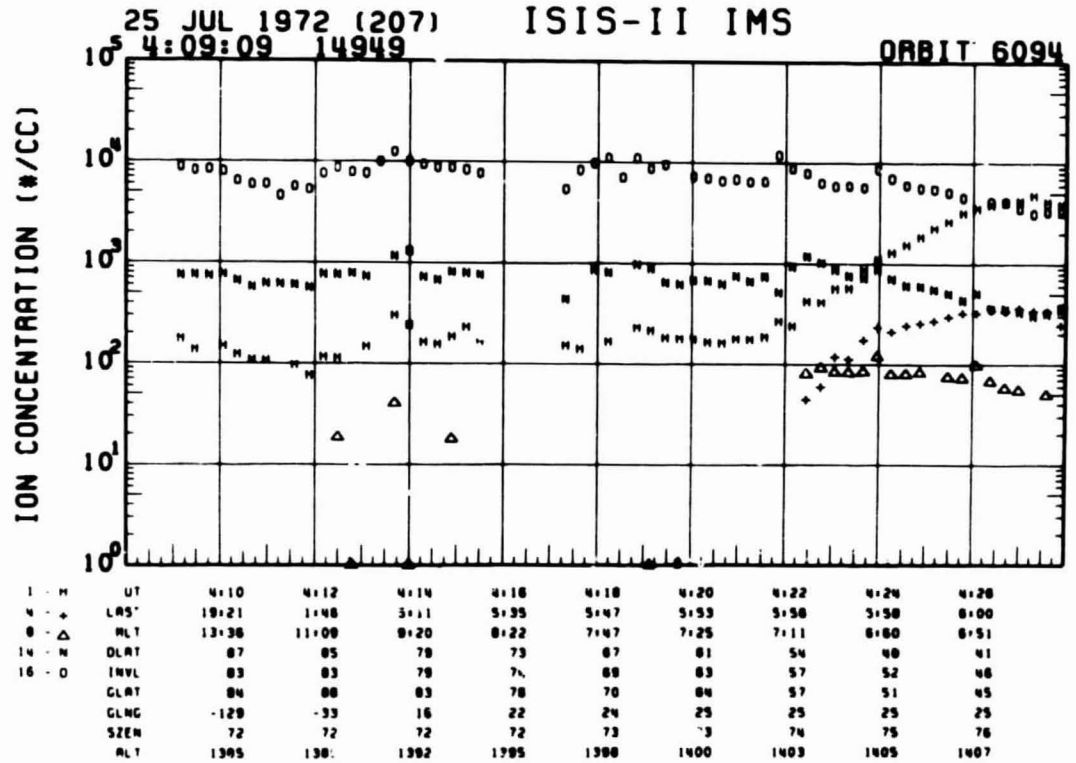

1 - H	UT	4:10	4:12	4:14	4:16	4:18	4:20	4:22	4:24	4:26
N - +	LAS*	19:21	1:48	3:11	5:35	5:47	5:53	5:58	5:58	6:00
O - △	MLT	13:36	11:09	9:20	8:22	7:47	7:25	7:11	6:60	6:51
14 - N	DLAT	87	85	78	73	67	61	54	48	41
16 - O	INVL	83	83	79	74	68	63	57	52	46
	GLAT	84	80	83	78	70	64	57	51	45
	GLNG	-129	-33	16	22	24	25	25	25	25
	SZEN	72	72	72	72	73	73	74	75	76
	ALT	1385	1381	1382	1385	1388	1400	1403	1405	1407

SET 26, FORMAT 4

72/207/0411

Excerpts of VLF Spectral film for the period 0416 - 0423

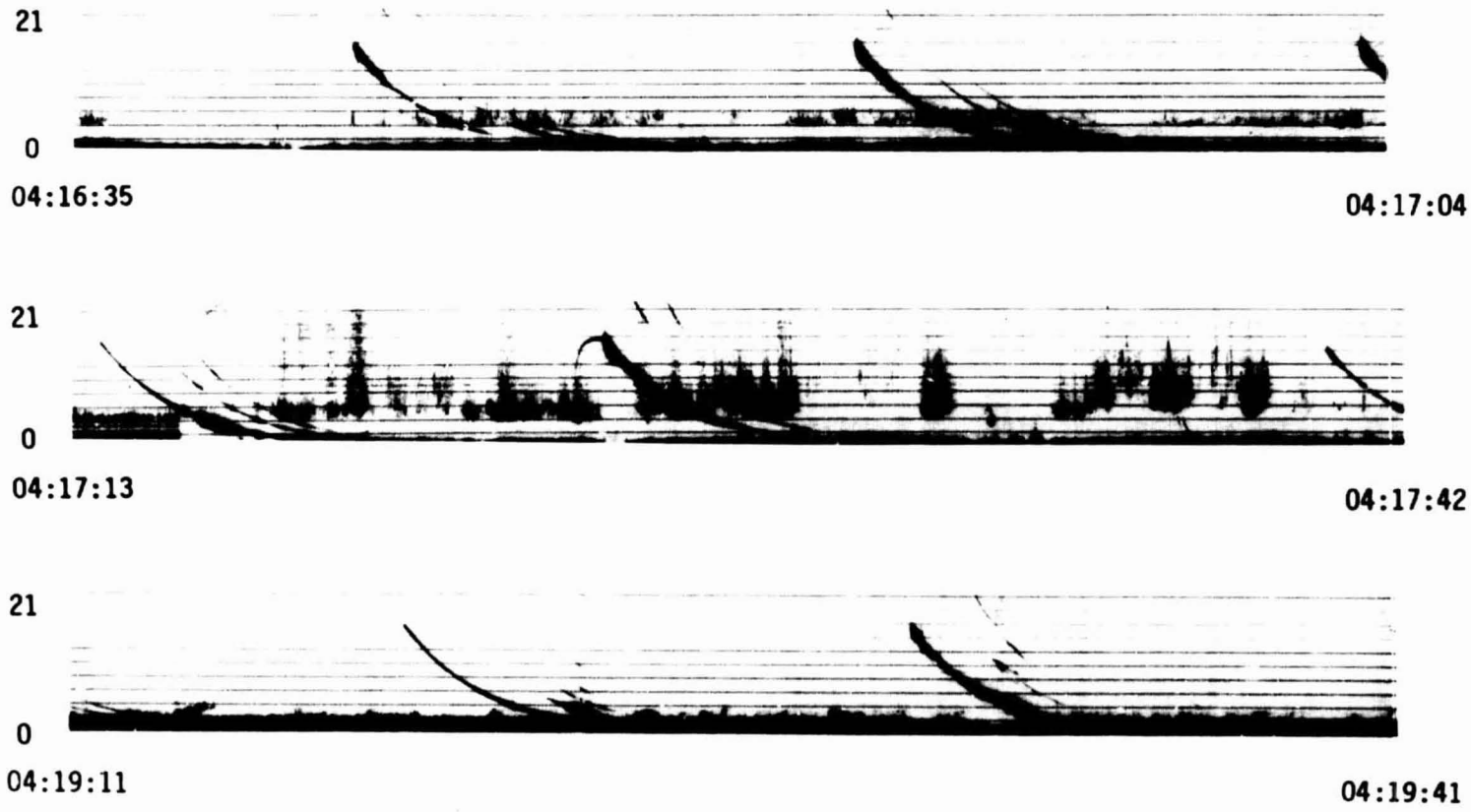

180

SET 26, FORMAT 11

72/207/0411

Excerpts of VLF Spectral film for the period 0416 - 0423

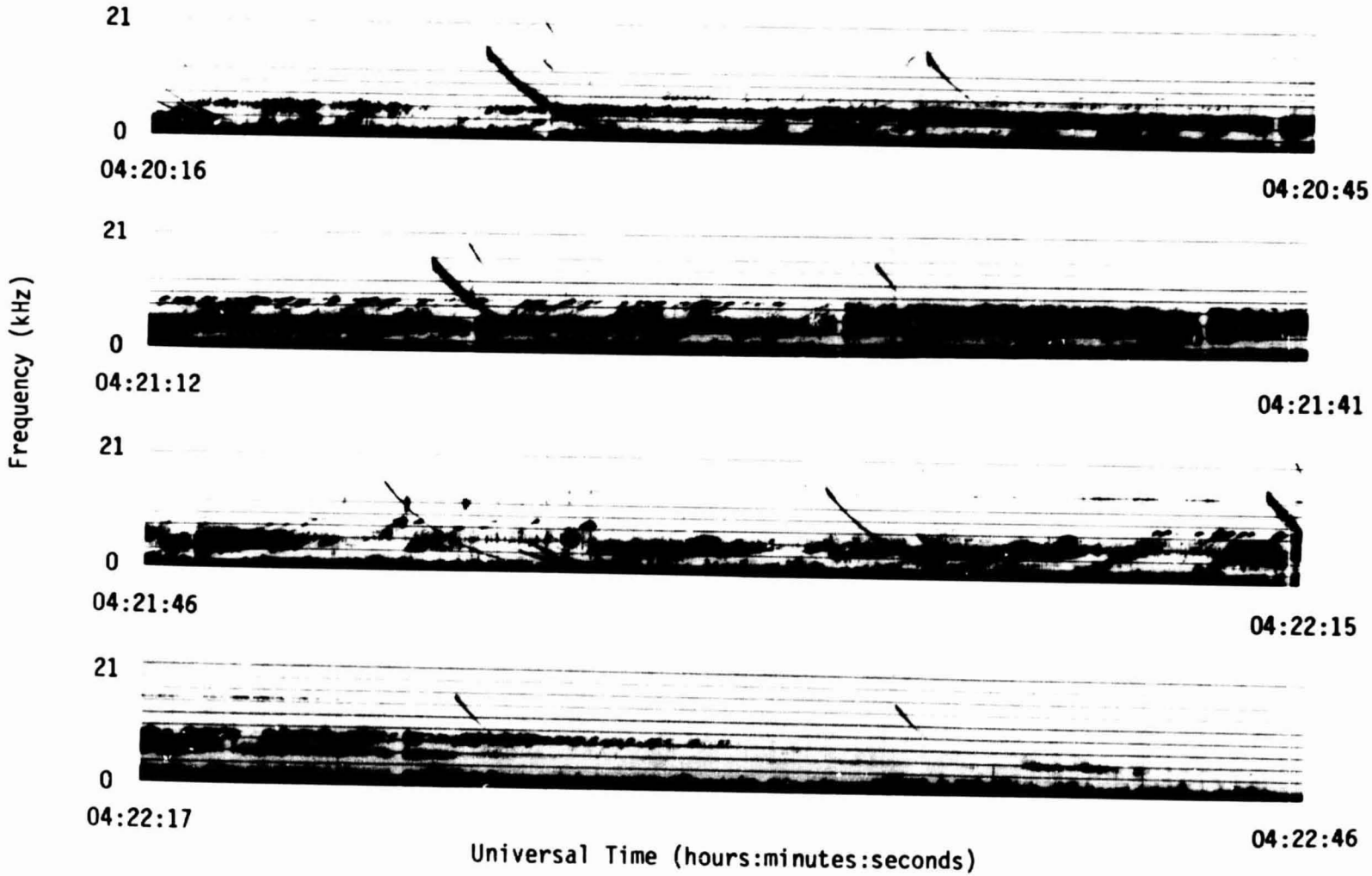

SET 26, FORMAT 11

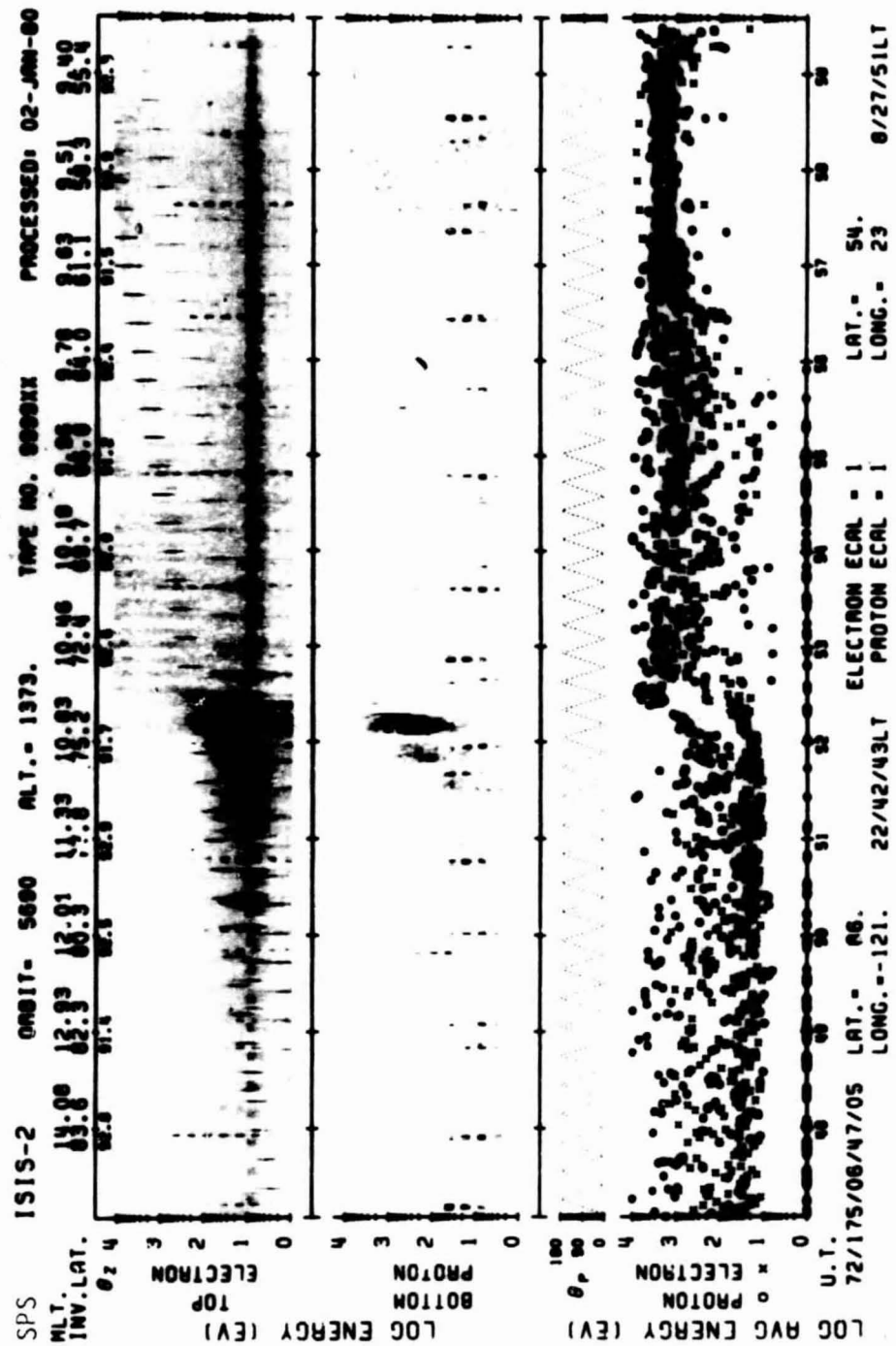

SET 27, FORMAT 6

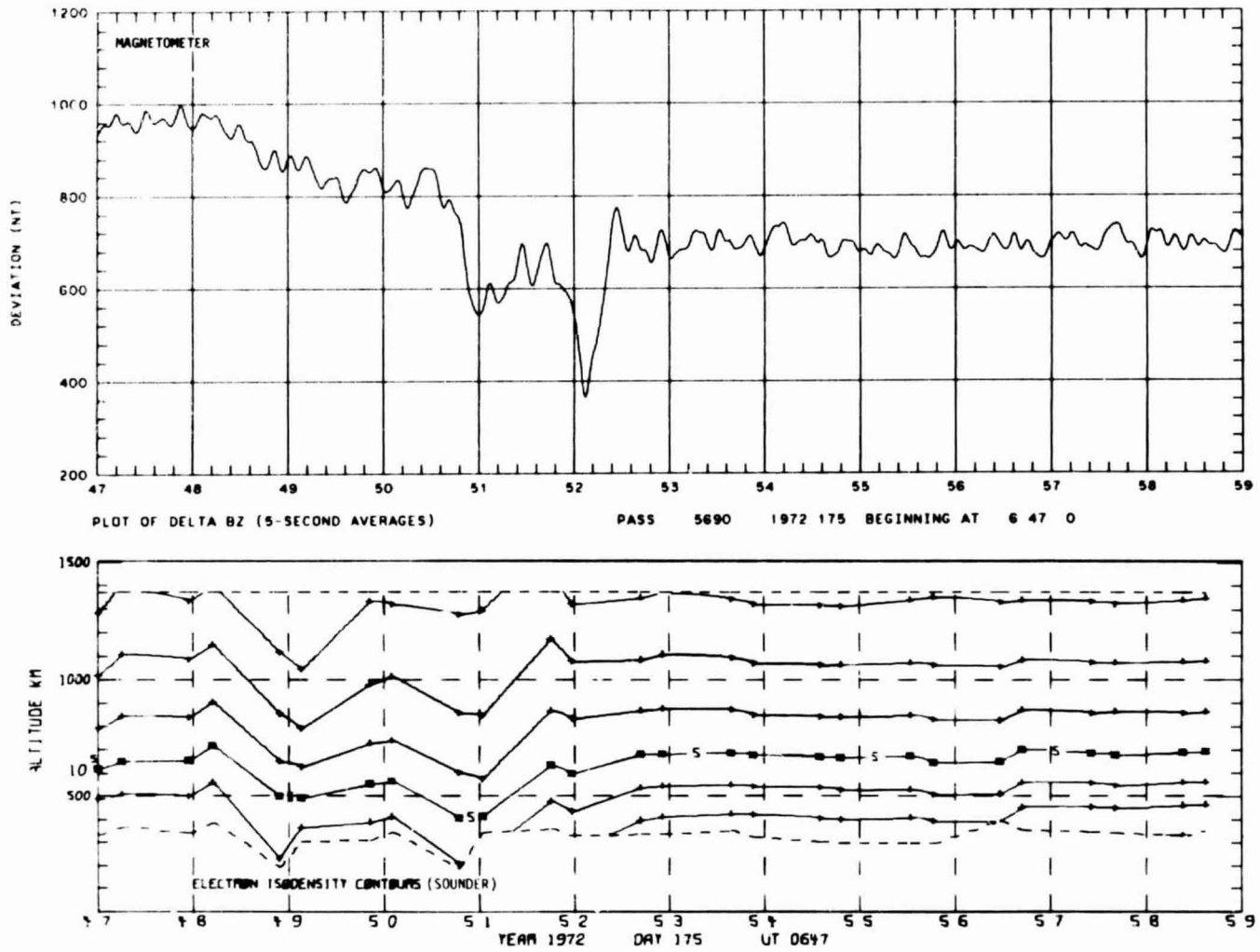

SET 27, FORMAT 2

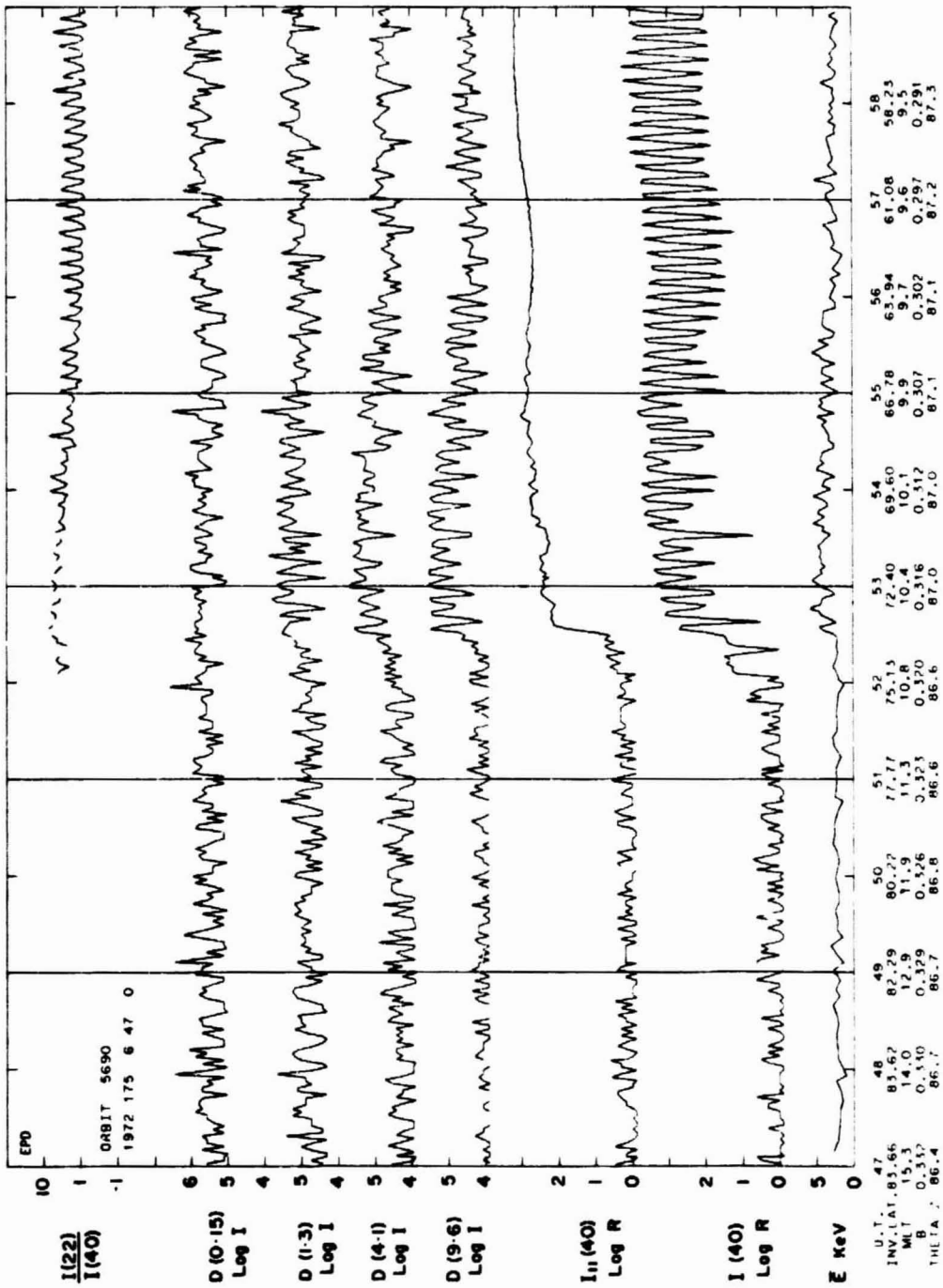

SET 27, FORMAT 3

ORBIT 5690
DATE 720623
DAY 175

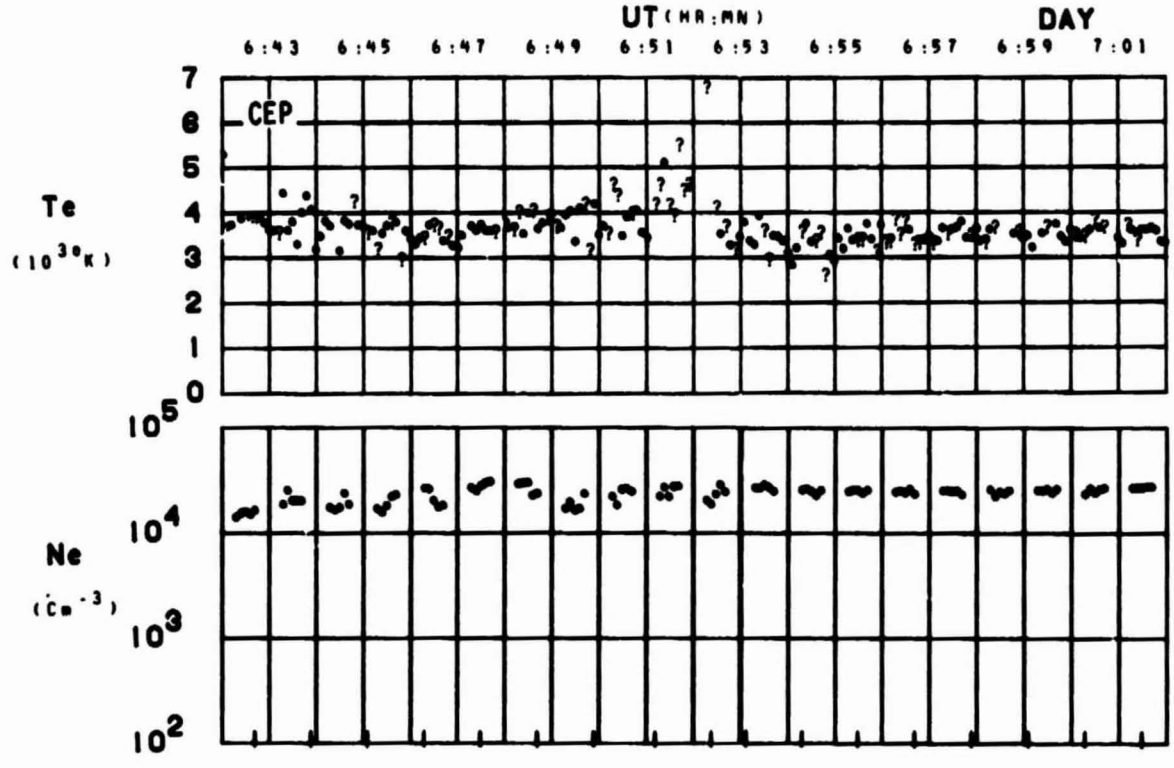

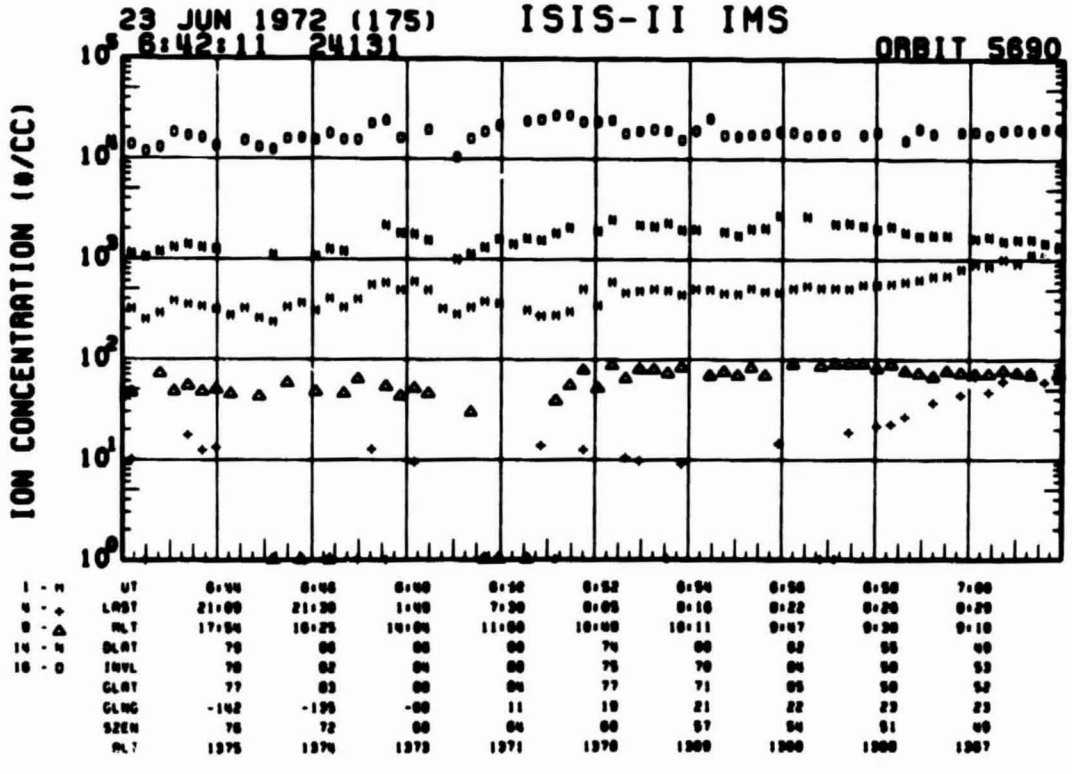

SET 27, FORMAT 4

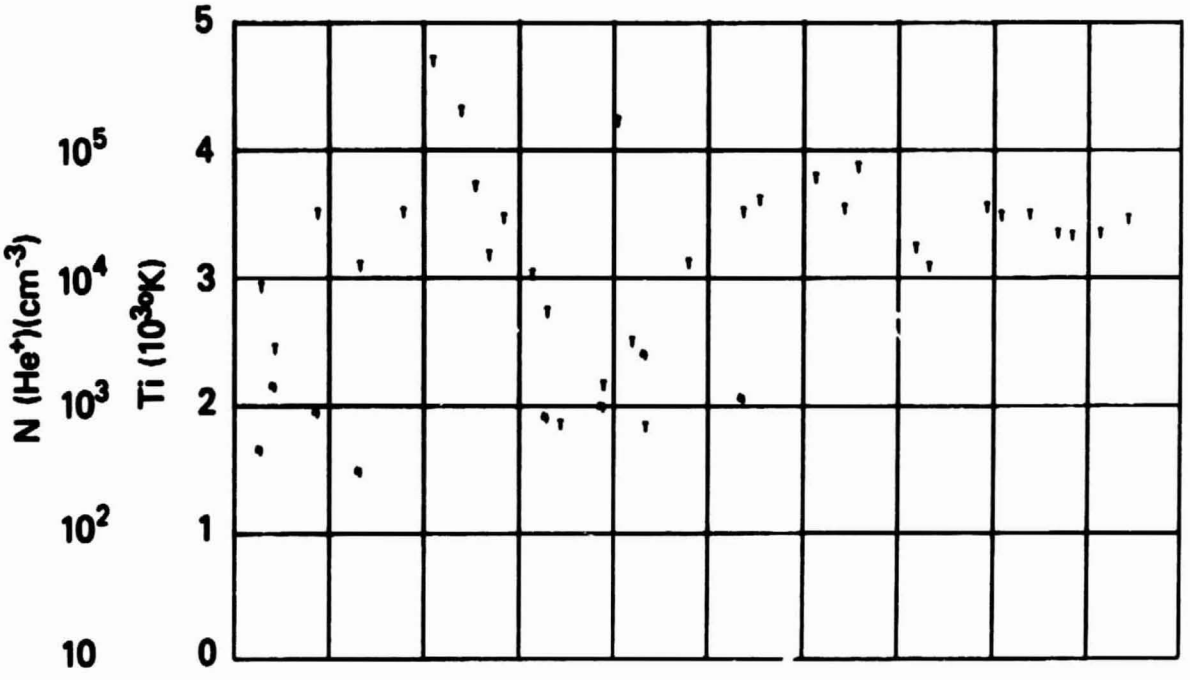

UT	6:44	6:46	6:48	6:50	6:52	6:54	6:56	6:58	7:00
LAST	21:09	21:30	1:49	7:30	8:05	8:16	8:22	8:28	8:29
MLT	17:54	18:25	18:04	11:00	10:49	10:11	9:47	9:30	9:10
DLAT	70	86	86	80	74	68	62	55	49
INVL	78	82	84	80	75	70	64	58	53
GLAT	77	83	88	84	77	71	65	59	52
GLNG	-142	-135	-88	11	19	21	22	23	23
SZEN	76	72	68	64	60	57	54	51	48
ALT	1375	1374	1373	1371	1370	1369	1368	1368	1367

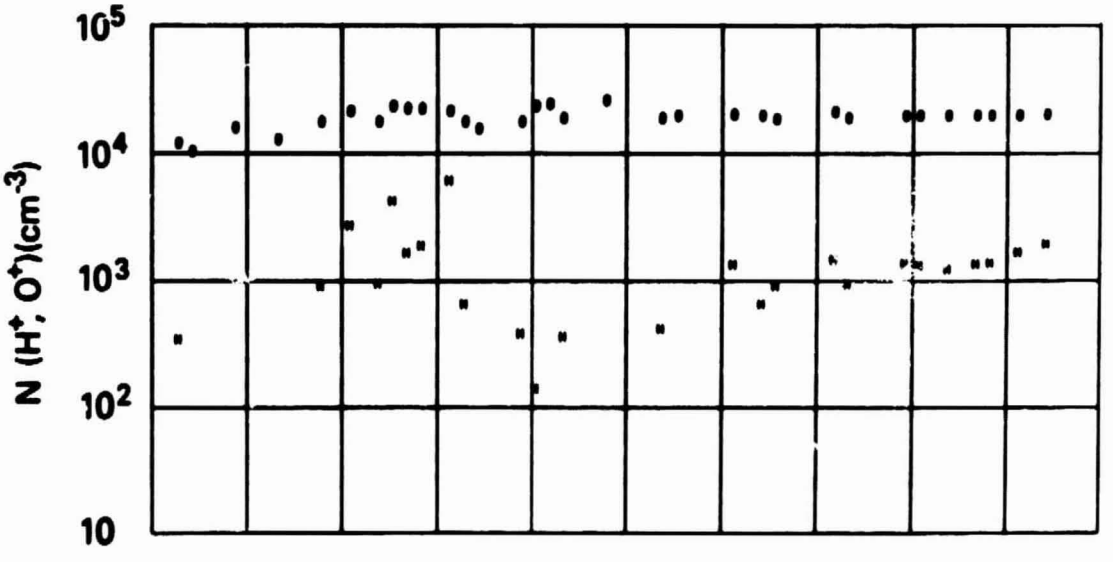

SET 27, FORMAT 5

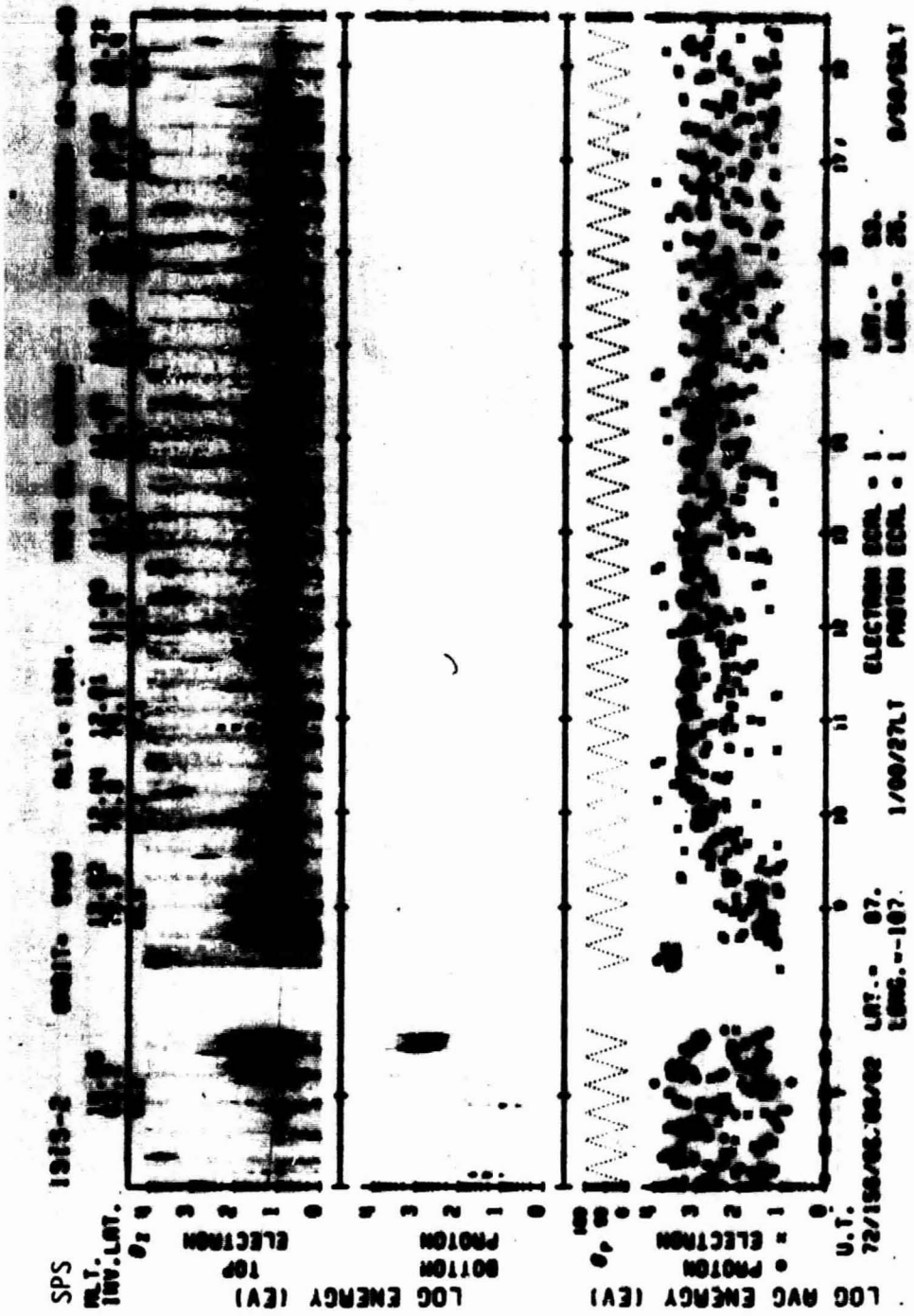

SET 28, FORMAT 6

SET 28, FORMAT 2

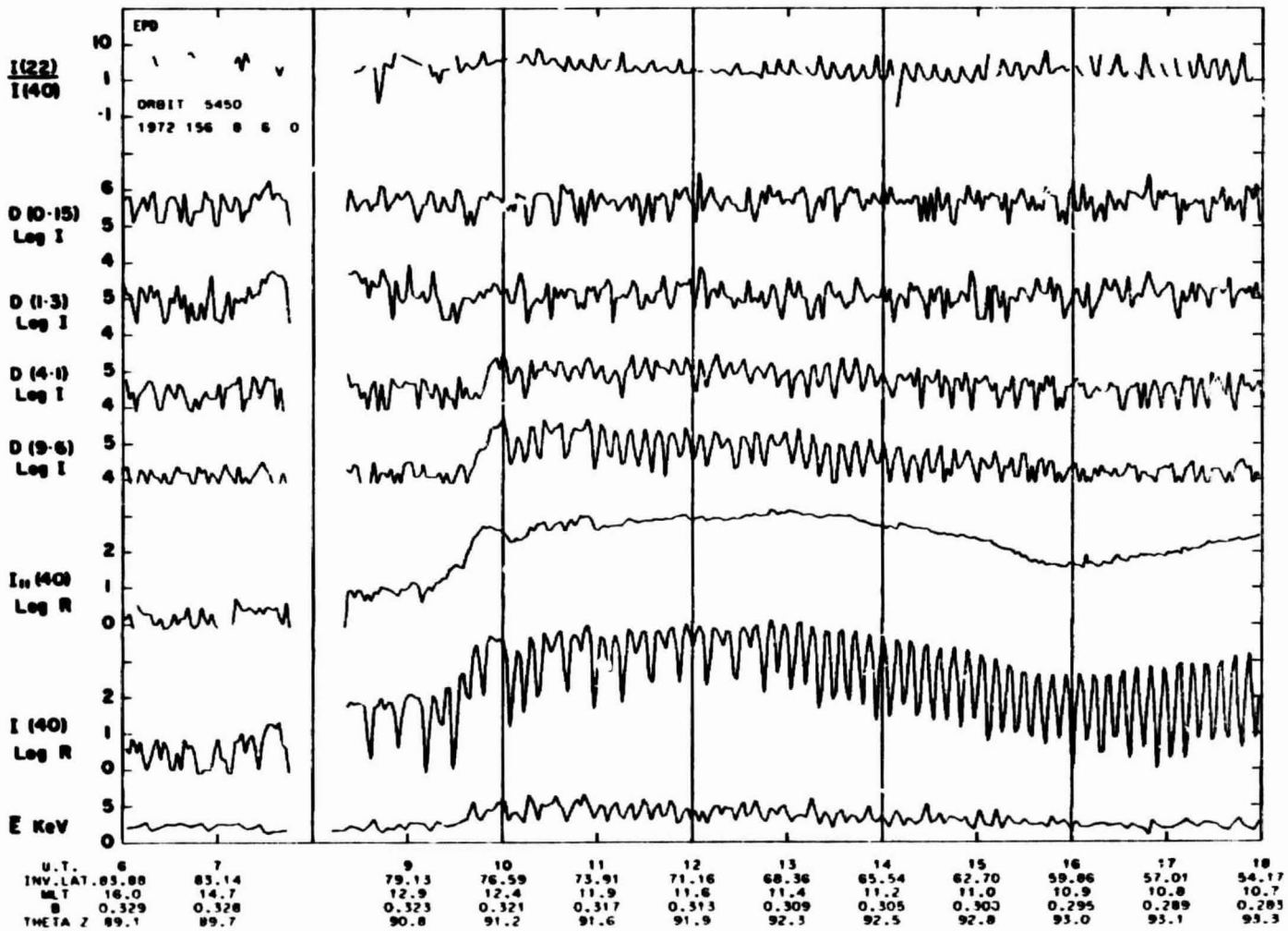

SET 28, FORMAT 3

ORBIT 5450
DATE 720604
DAY 156

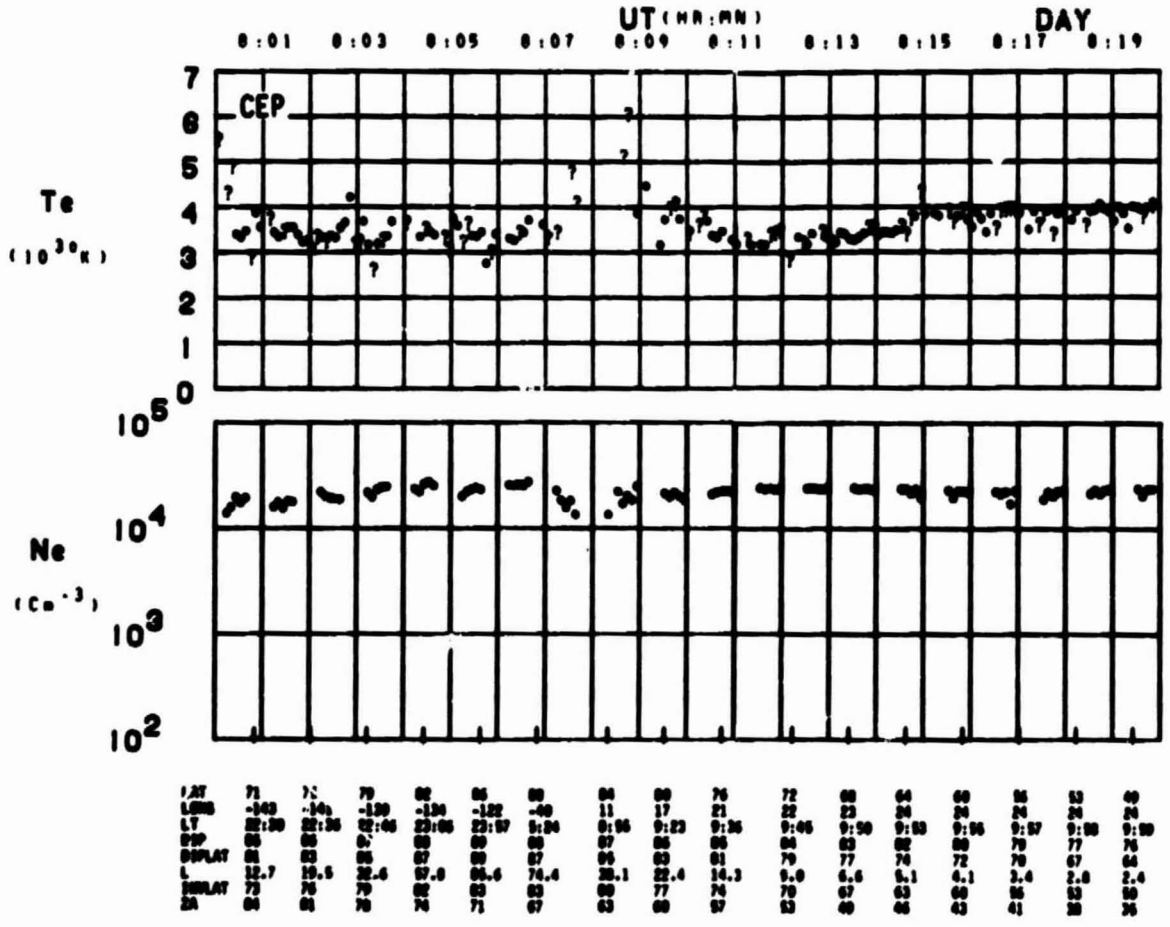

SET 28, FORMAT 4

RPA

720604

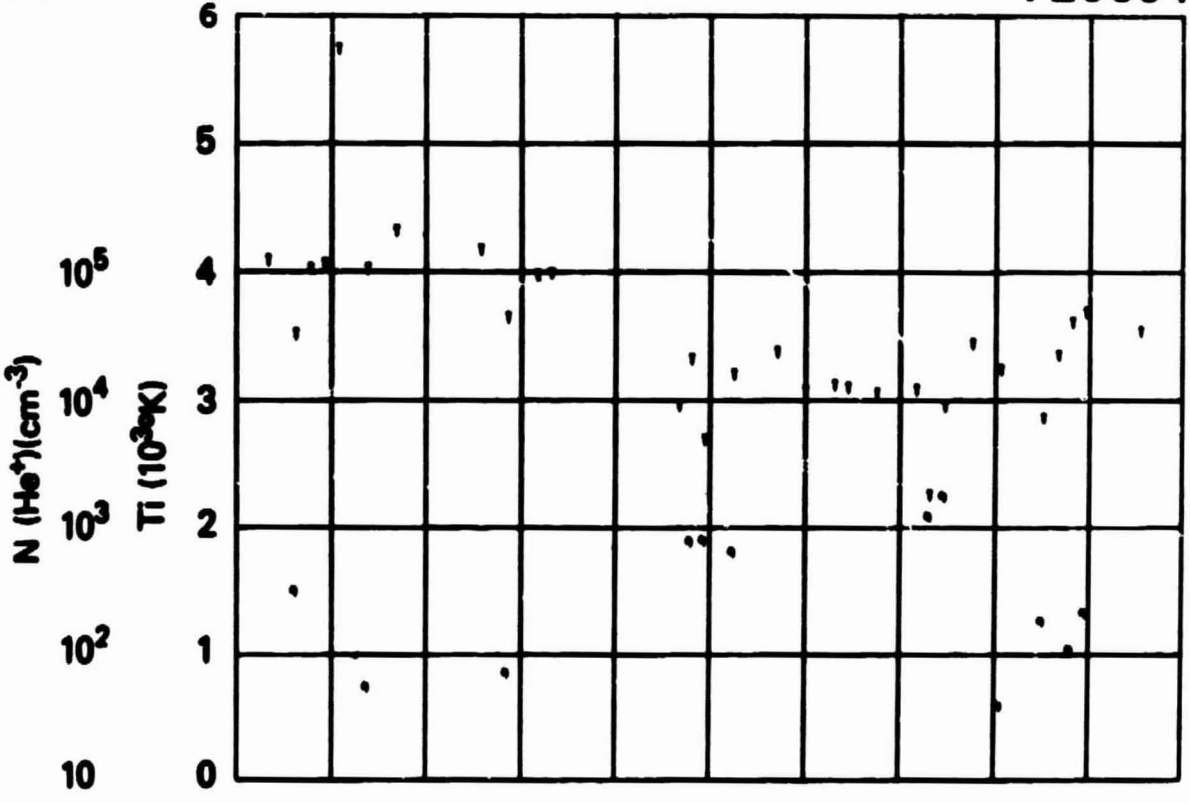

UT	00:02	00:05	00:08	00:08	00:10	00:12	00:14	00:16	00:18
LAST	22:36	22:57	00:17	00:36	00:20	00:44	00:52	00:56	00:58
MLT	19:57	18:39	15:20	13:00	11:46	11:12	10:53	10:40	10:31
GLAT									
GLON	77	81	84	81	77	73	68	69	64
GLAT	78	82	87	86	79	73	61	58	54
GLAS	-142	-137	-107	7	89	123	136	128	125
SZEN	81	75	70	64	59	53	48	43	38
ALT	1397	1394	1391	1388	1384	1380	1377	1373	1370

SET 28, FORMAT 5

SET 29, FORMAT 6

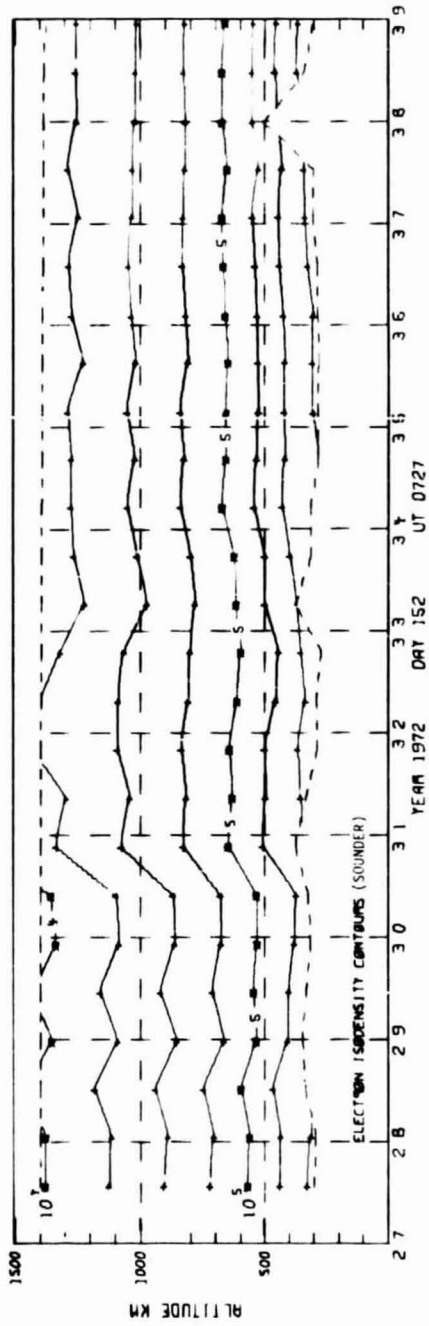

SET 29, FORMAT 2

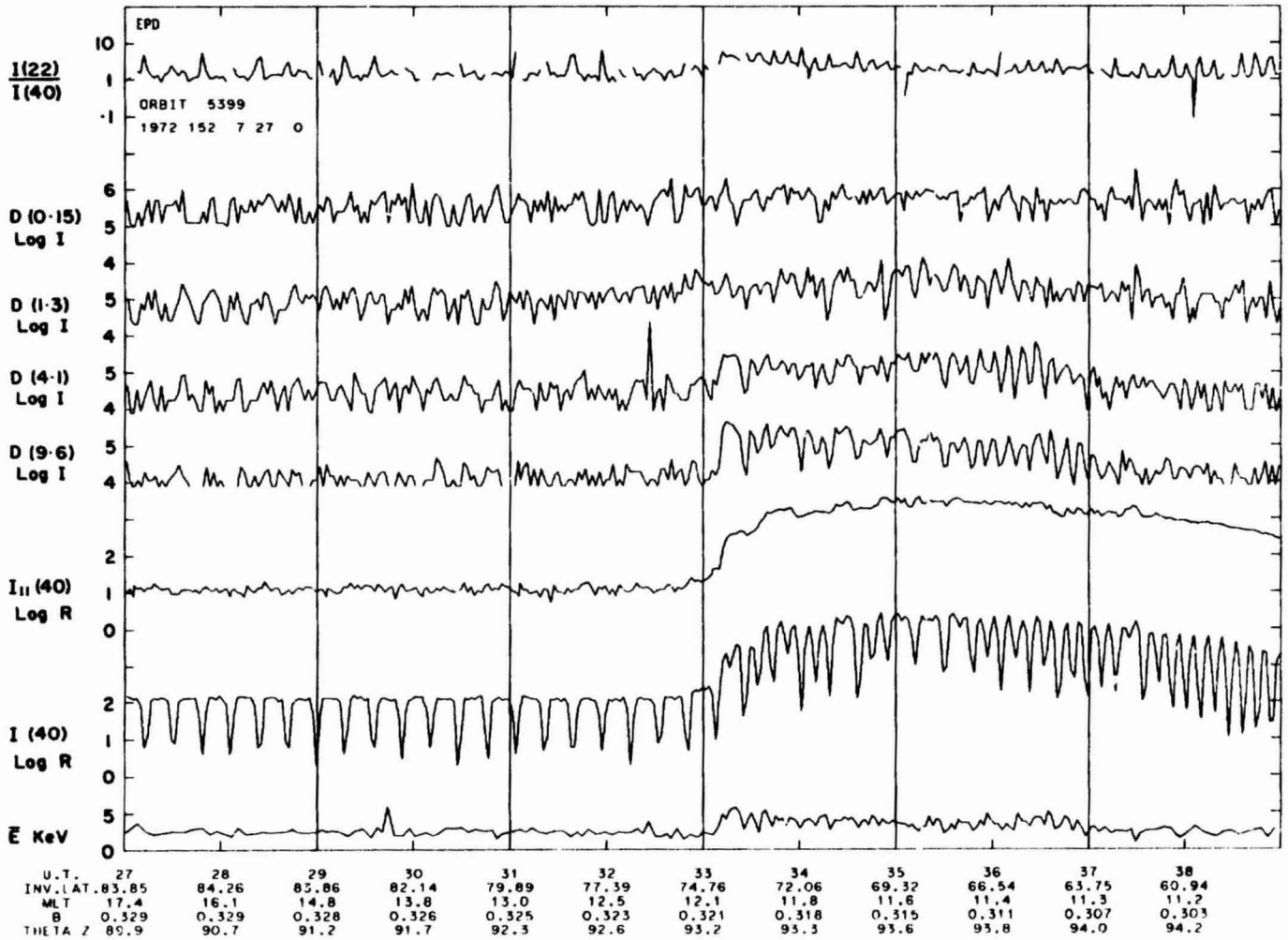

SET 29, FORMAT 3

ORBIT 5399
DATE 720531
DAY 152

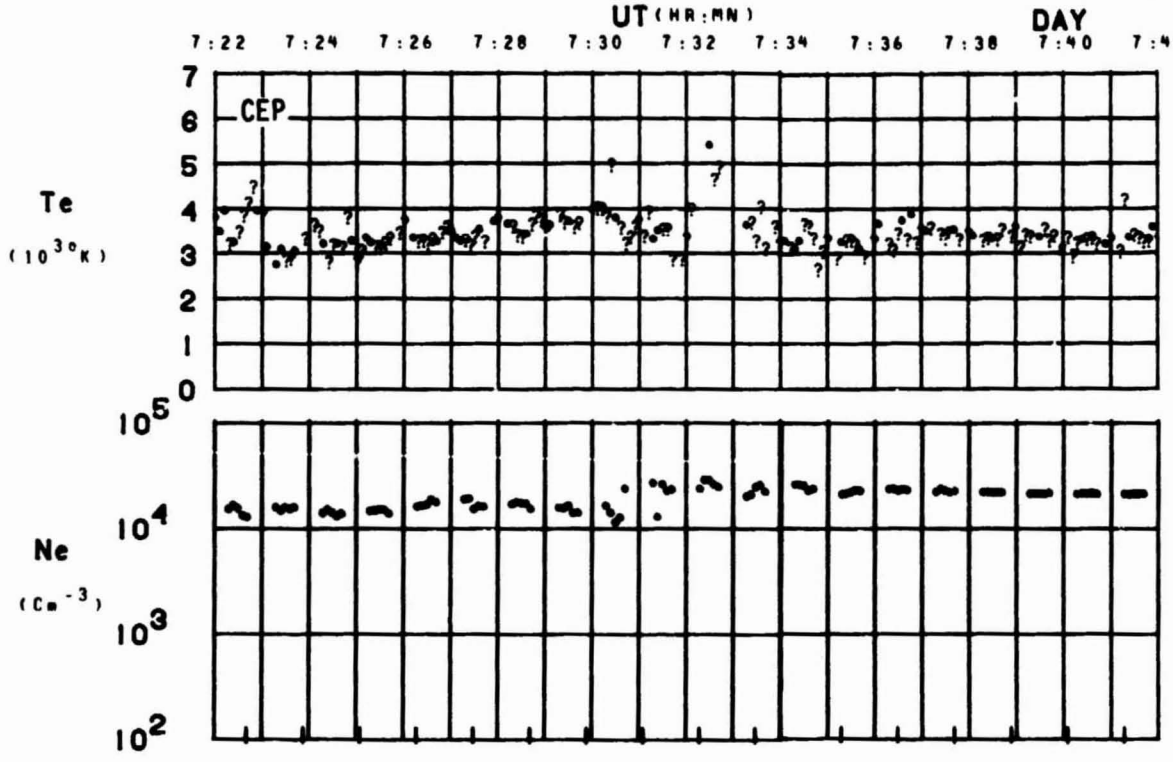

LAT	68	72	76	80	83	87	87	84	80	76	71	67	63	59	55	52
LONG	-129	-128	-127	-124	-119	-93	-4	25	32	35	37	37	38	38	38	38
LT	22:46	22:50	22:57	23:10	23:33	1:16	7:13	9:14	9:43	9:56	10:06	10:10	10:12	10:15	10:16	10:18
DIP	81	83	85	87	89	88	87	85	83	81	78	76	74	72	69	66
DIPLAT	74	77	81	84	88	87	84	80	77	73	68	64	61	57	53	49
L	13.0	20.0	33.6	62.8	96.7	94.5	57.2	31.2	18.8	12.4	7.5	5.7	4.5	3.7	3.1	2.6
INVLAT	73	77	80	82	84	84	82	79	76	73	68	65	61	58	55	51
ZA	88	84	81	77	74	70	67	63	60	56	51	48	45	41	38	35

SET 29, FORMAT 4

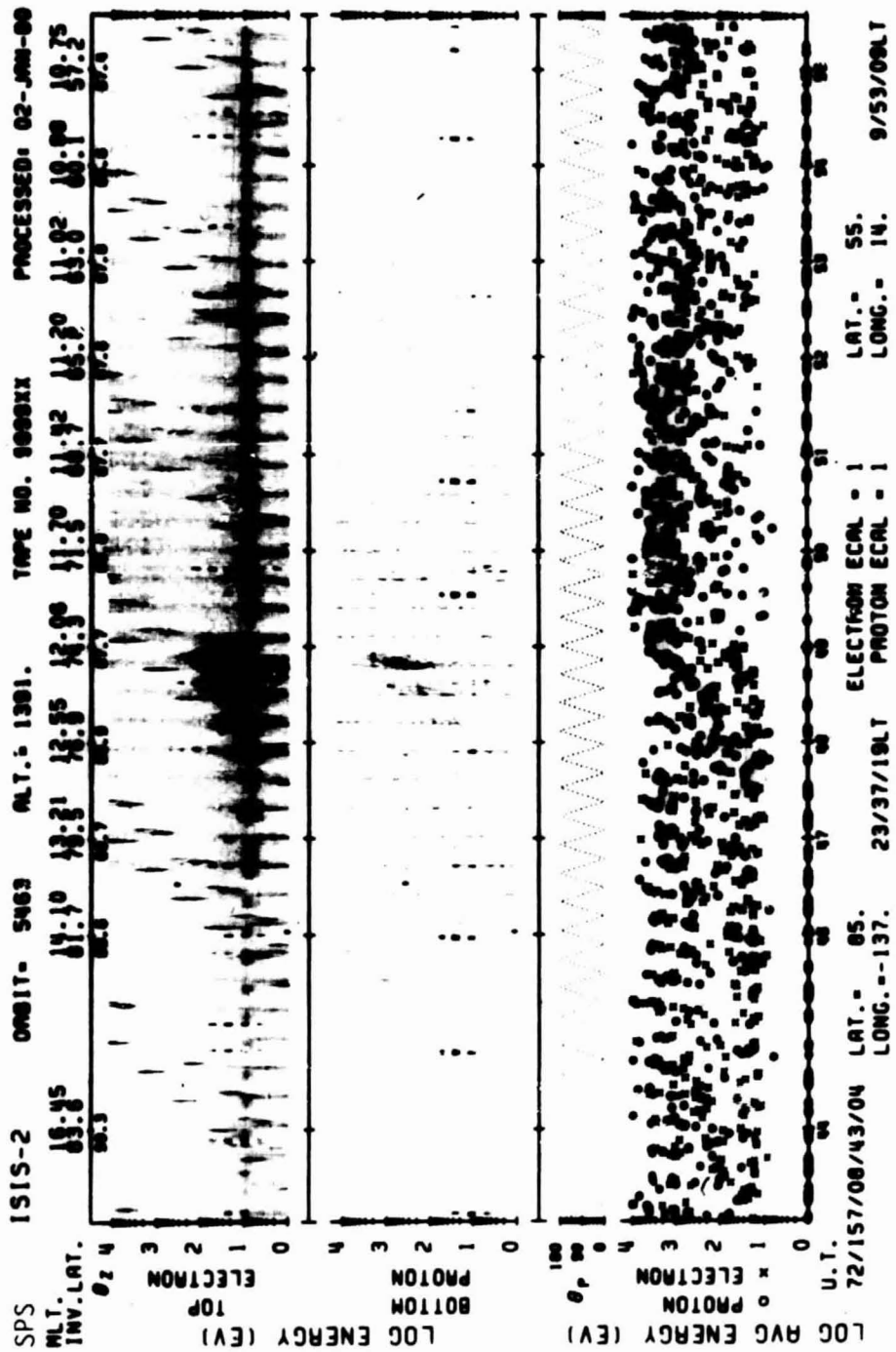

SET 30, FORMAT 6

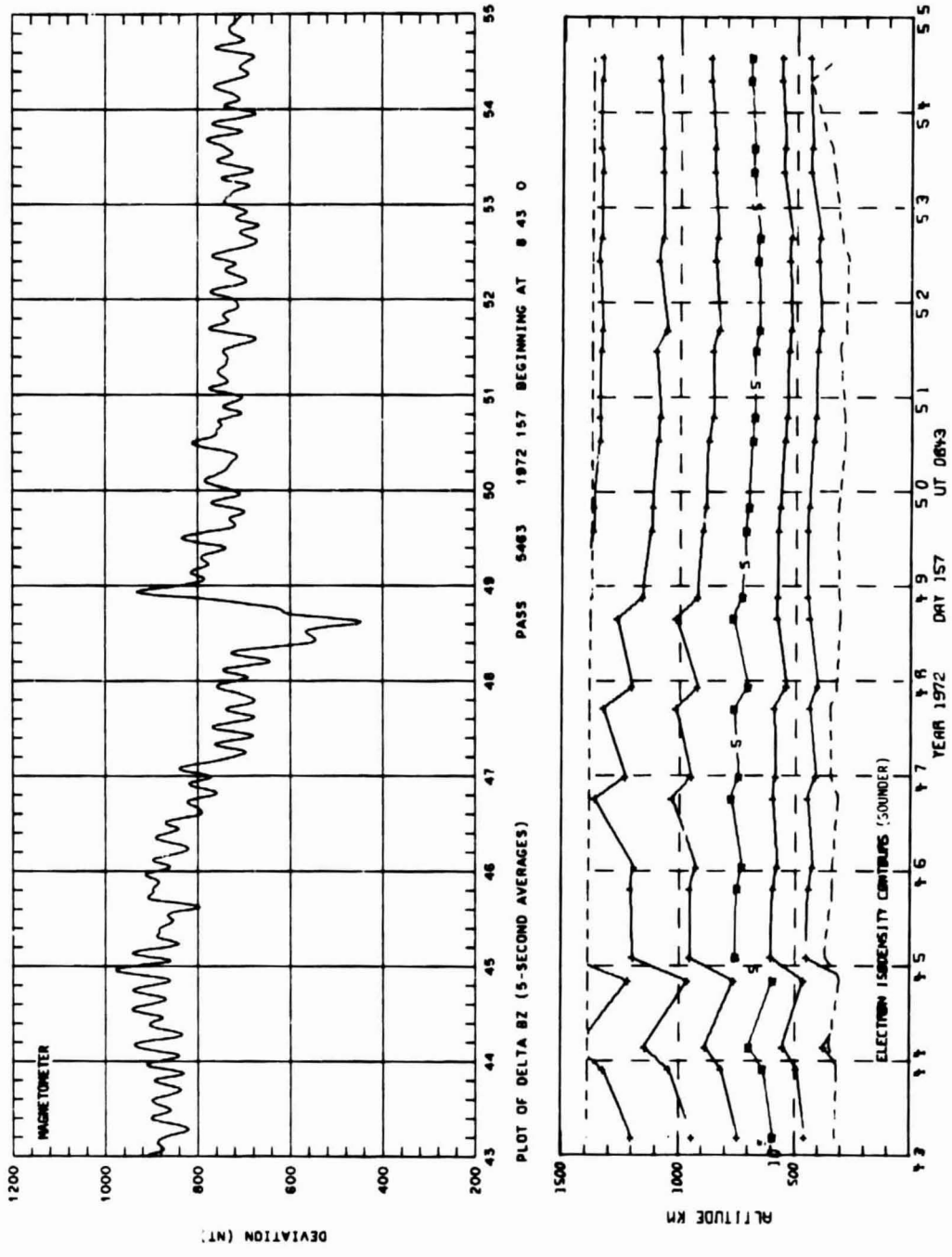

SET 30, FORMAT 2

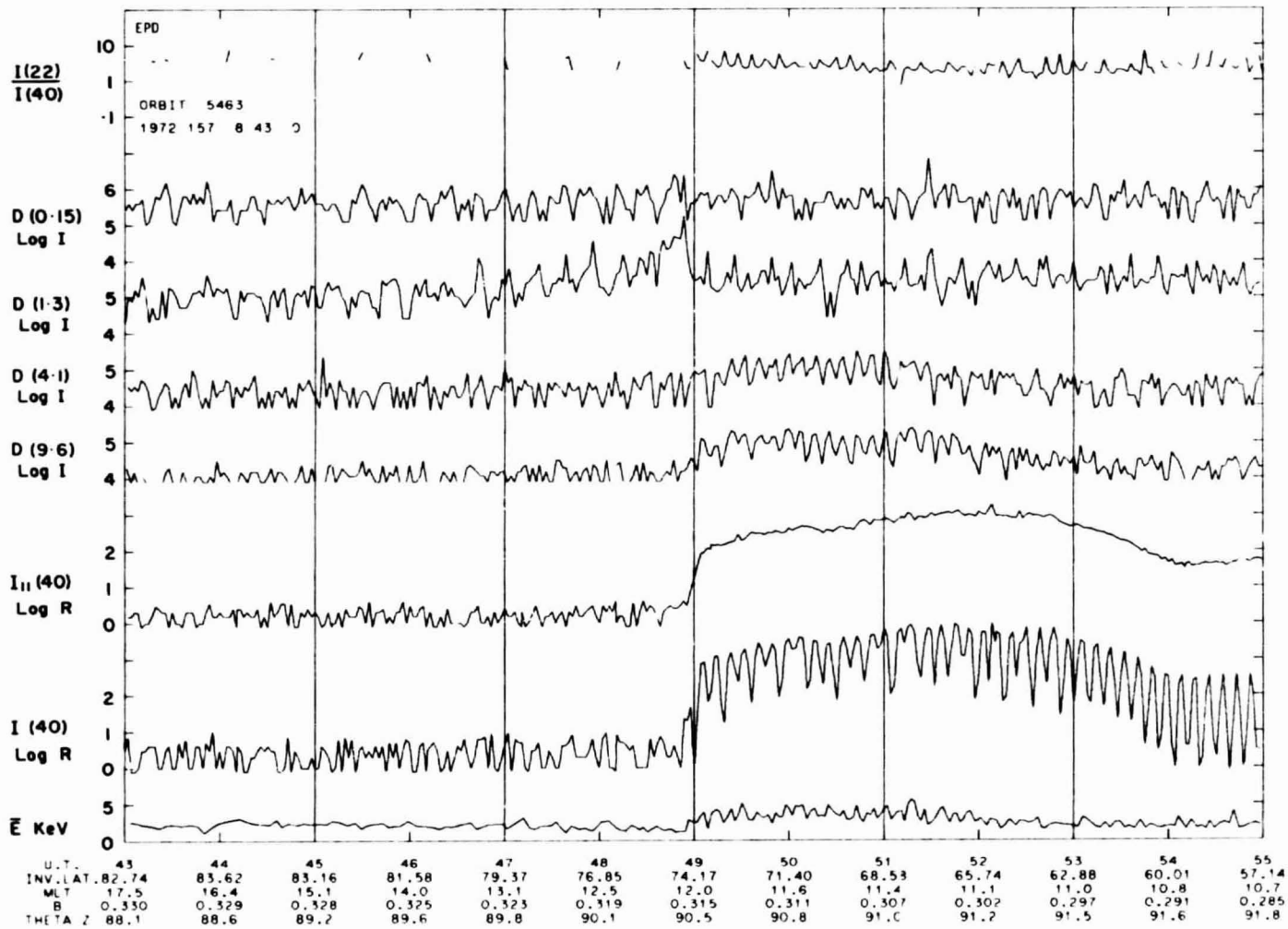

SET 30, FORMAT 3

ORBIT 5463
DATE 720605
DAY 157

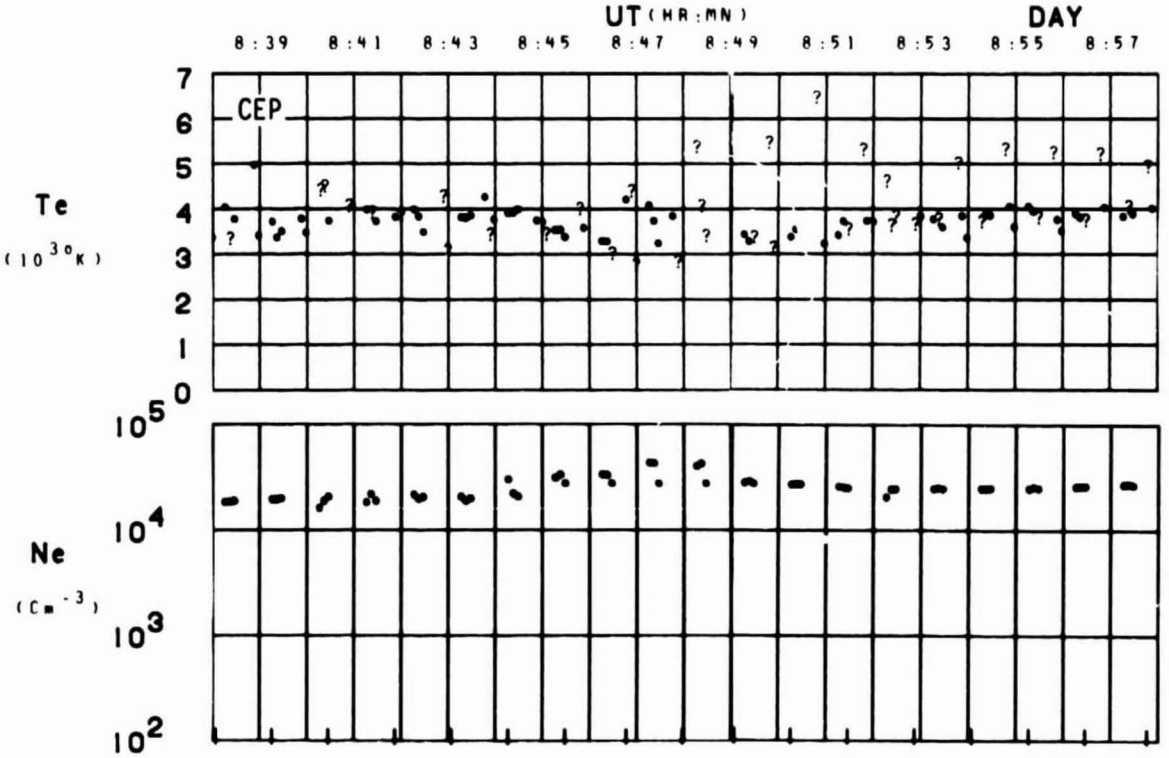

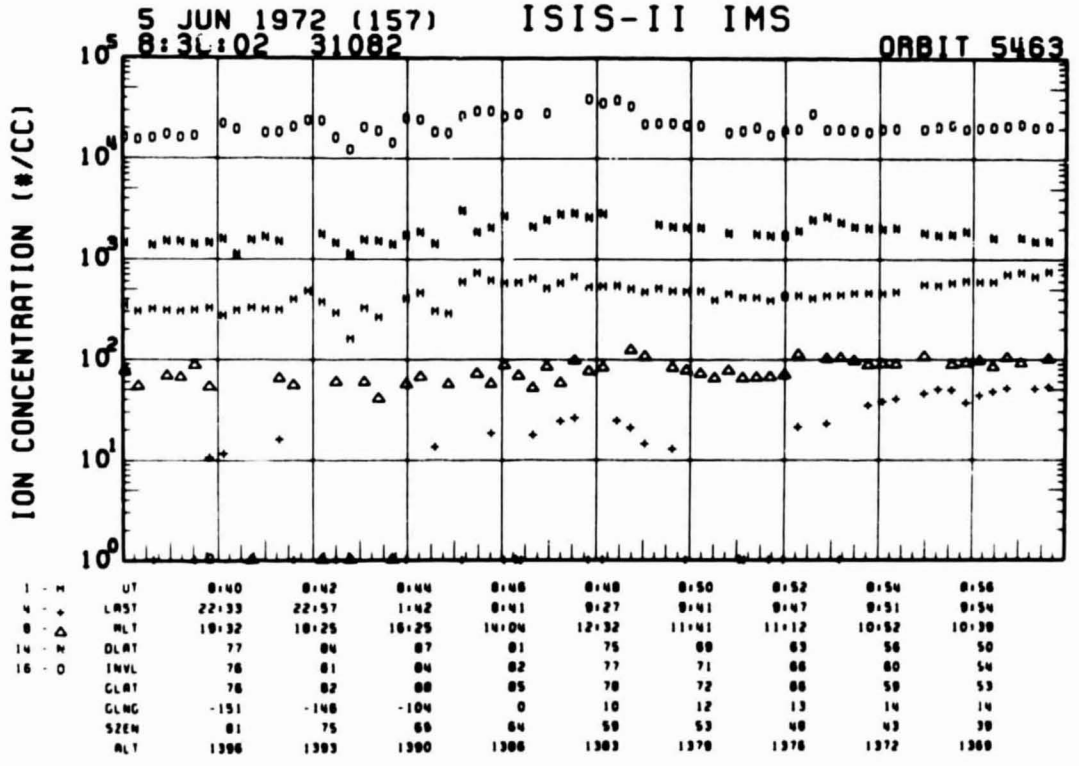

SET 30, FORMAT 4

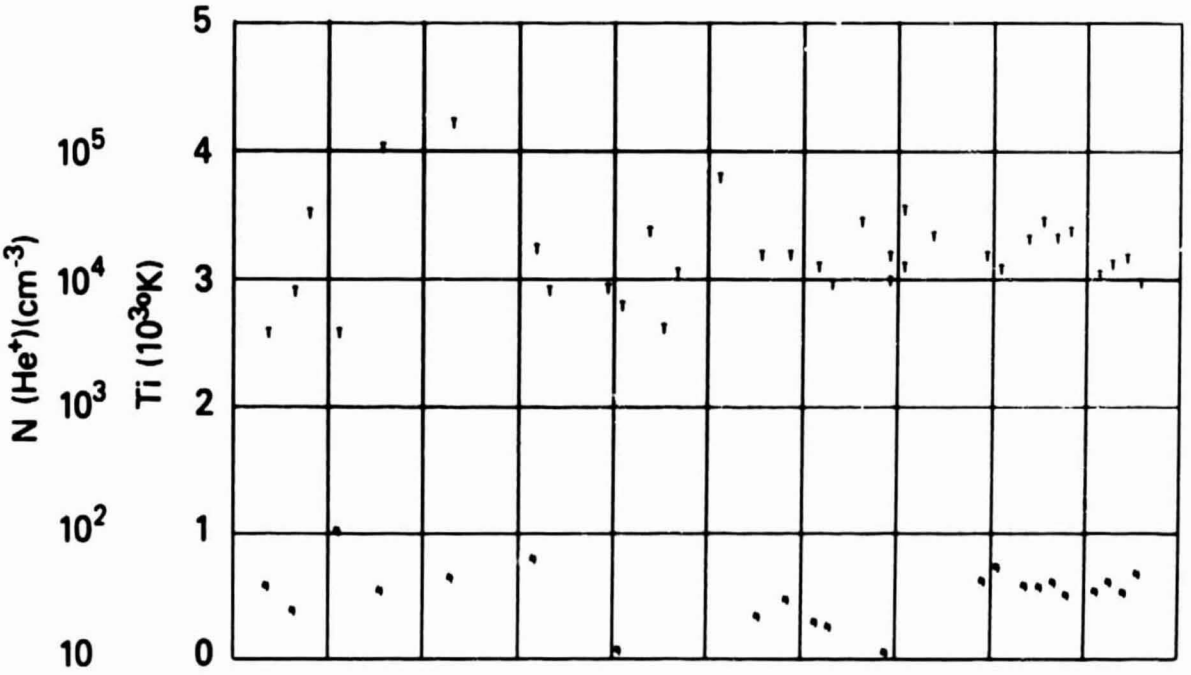

UT	8:40	8:42	8:44	8:46	8:48	8:50	8:52	8:54	8:56
LAST	22:33	22:57	1:42	8:41	9:27	9:41	9:47	9:51	9:54
ALT	19:32	18:25	16:25	14:04	12:32	11:41	11:12	10:52	10:38
DLAT	77	84	87	81	75	68	63	58	50
INVL	76	81	84	82	77	71	66	60	54
GLAT	76	82	88	85	78	72	66	59	53
GLNG	-151	-148	-104	0	10	12	13	14	14
SZEN	81	75	69	64	59	53	48	43	39
ALT	1396	1393	1390	1386	1383	1379	1376	1372	1369

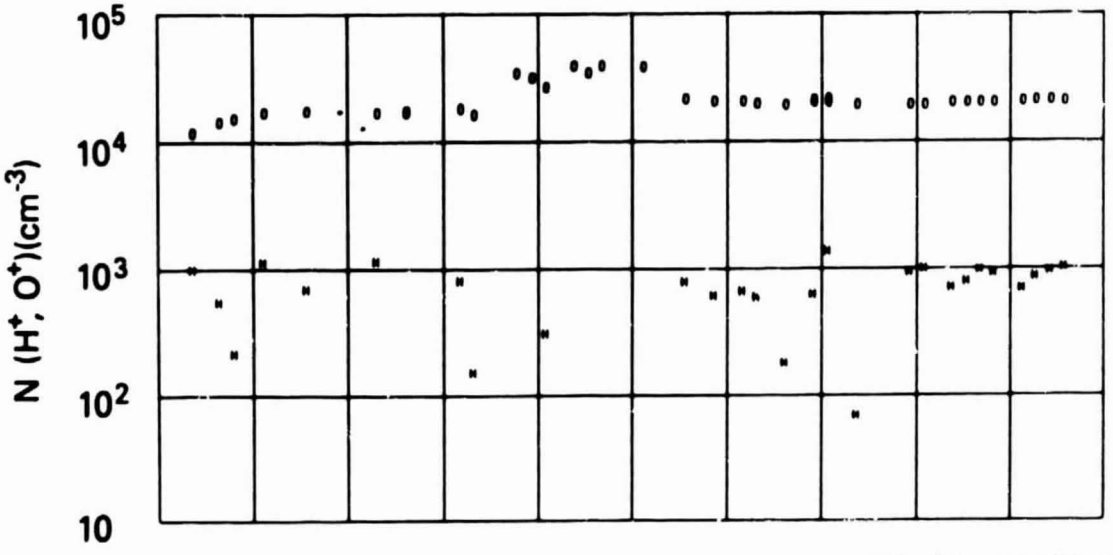

SET 30, FORMAT 5

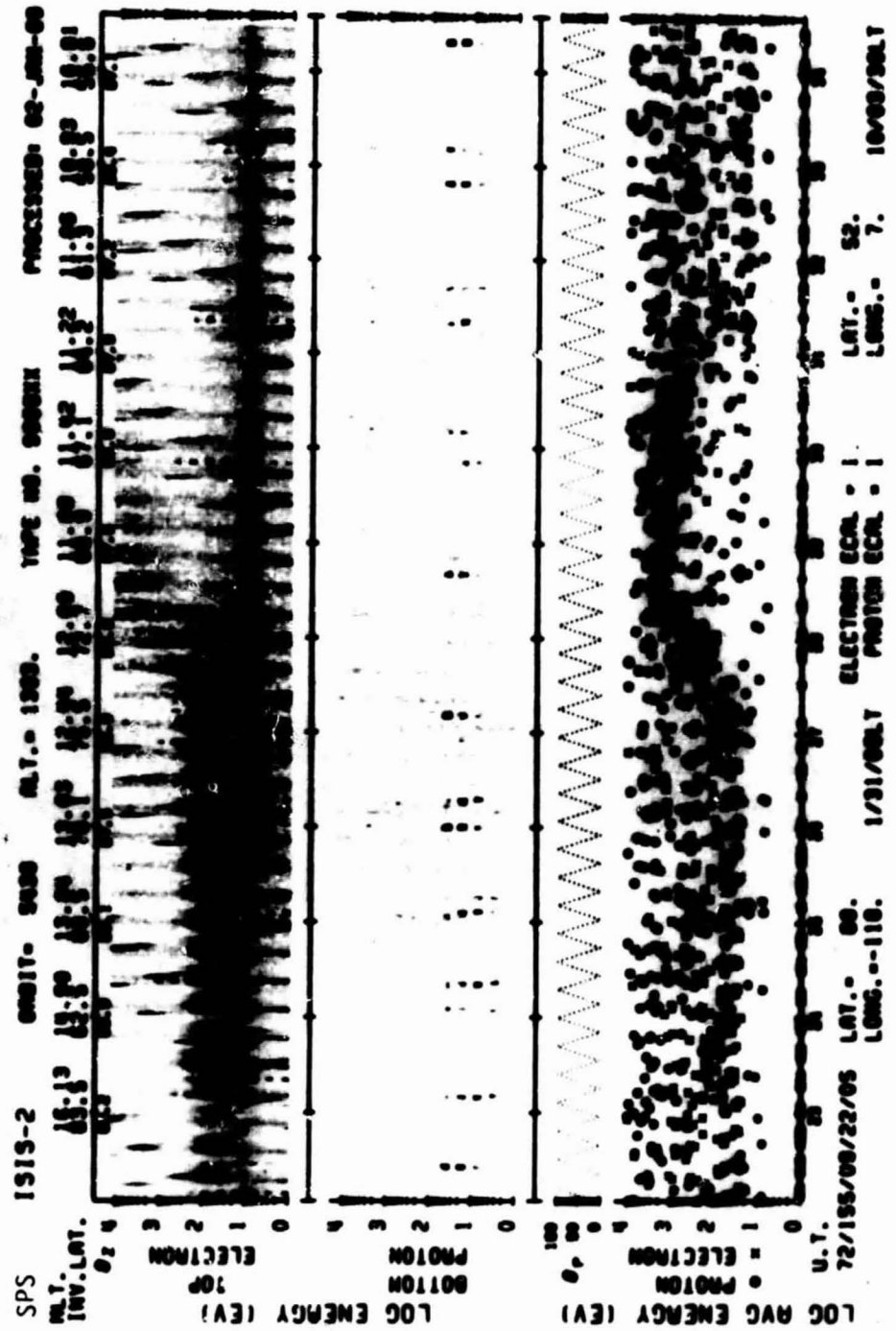

SET 31, FORMAT 6

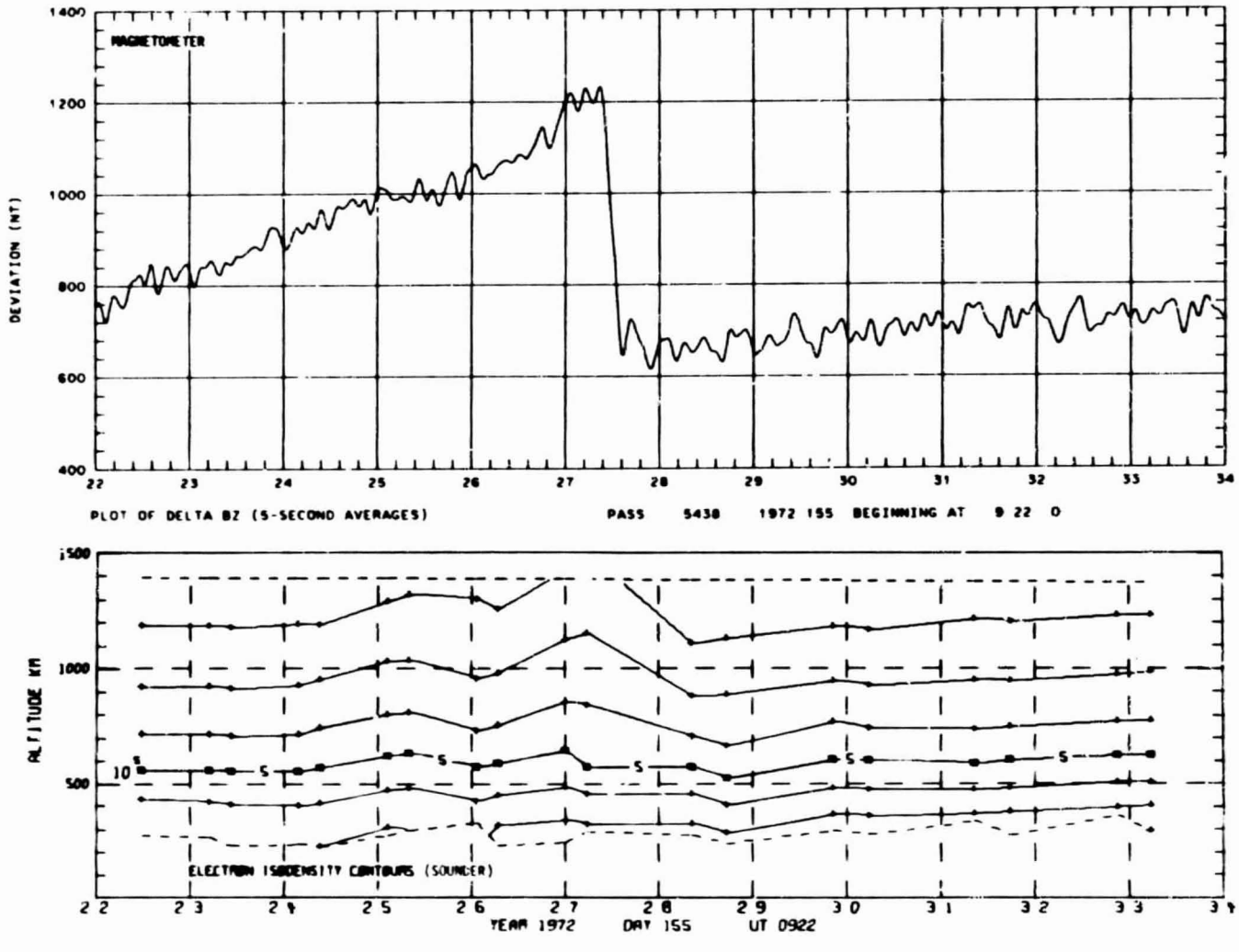

SET 31, FORMAT 2

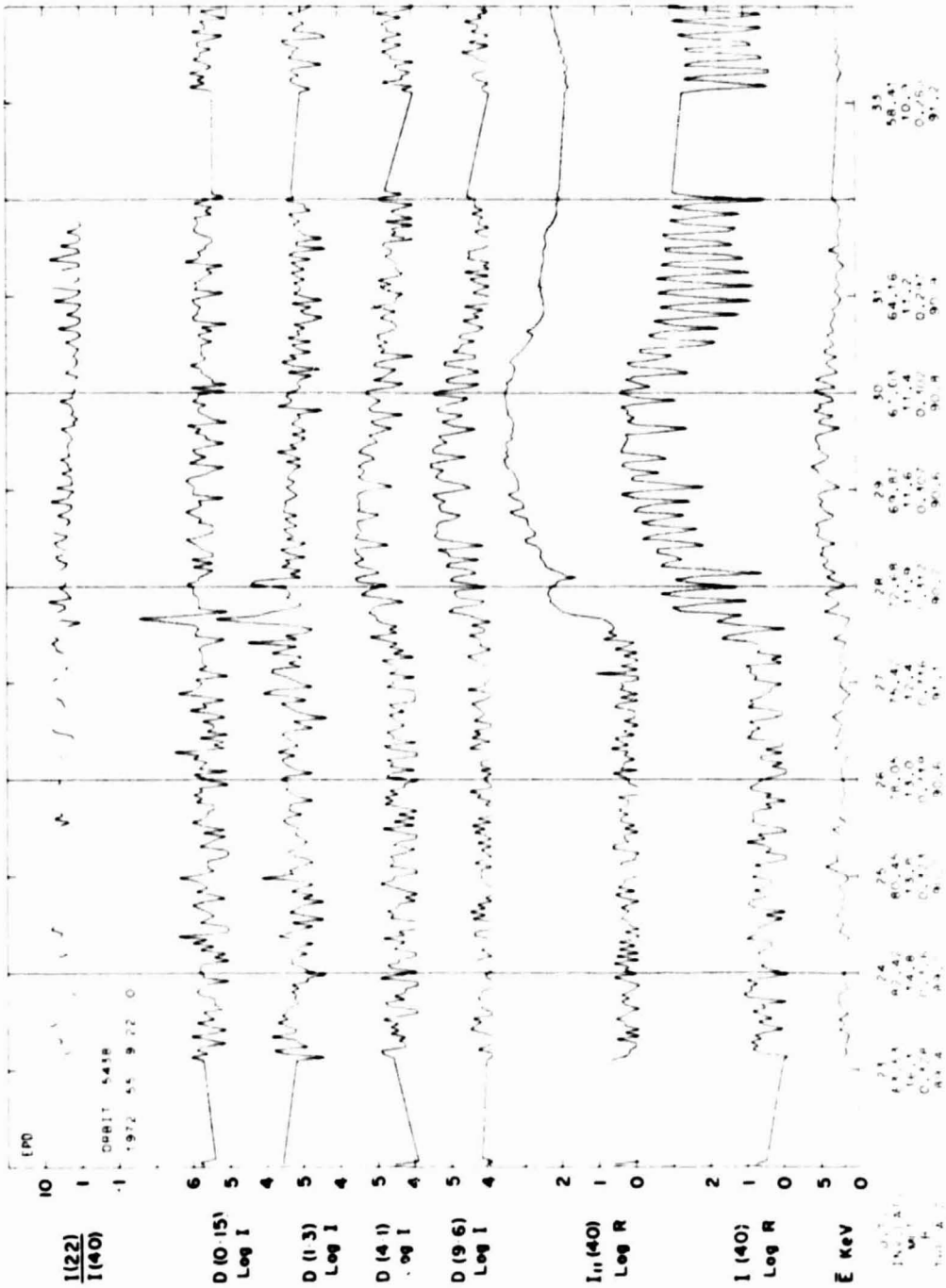

SET 31, FORMAT 3

ORBIT 5438
DATE 720603
DAY 155

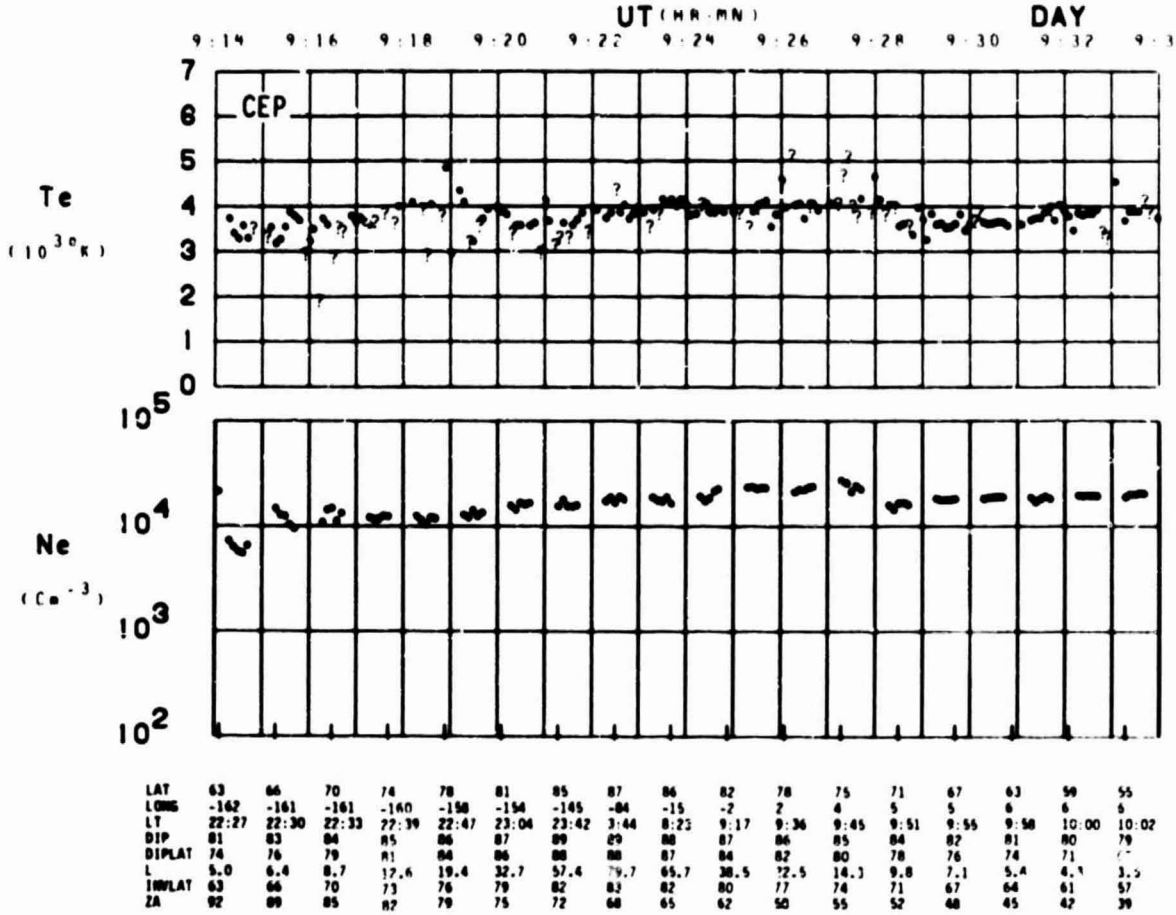

LAT	63	66	70	74	78	81	85	87	86	82	78	75	71	67	63	59	55
LONG	-162	-161	-161	-160	-158	-154	-145	-84	-15	-2	2	4	5	5	6	6	6
LT	22:27	22:30	22:33	22:39	22:47	23:04	23:42	3:44	8:23	9:17	9:36	9:45	9:51	9:55	9:58	10:00	10:02
DIP	81	83	84	85	86	87	89	89	88	87	86	85	84	82	81	80	79
DIPLAT	74	76	79	81	84	86	88	88	87	84	82	80	78	76	74	71	[illegible]
L	5.0	6.4	8.7	12.6	19.4	32.7	57.4	79.7	65.7	38.5	22.5	14.3	9.8	7.1	5.4	4.3	3.5
INVLAT	63	66	70	73	76	79	82	83	82	80	77	74	71	67	64	61	57
ZA	92	89	85	82	79	75	72	68	65	62	58	55	52	48	45	42	39

SET 31, FORMAT 4

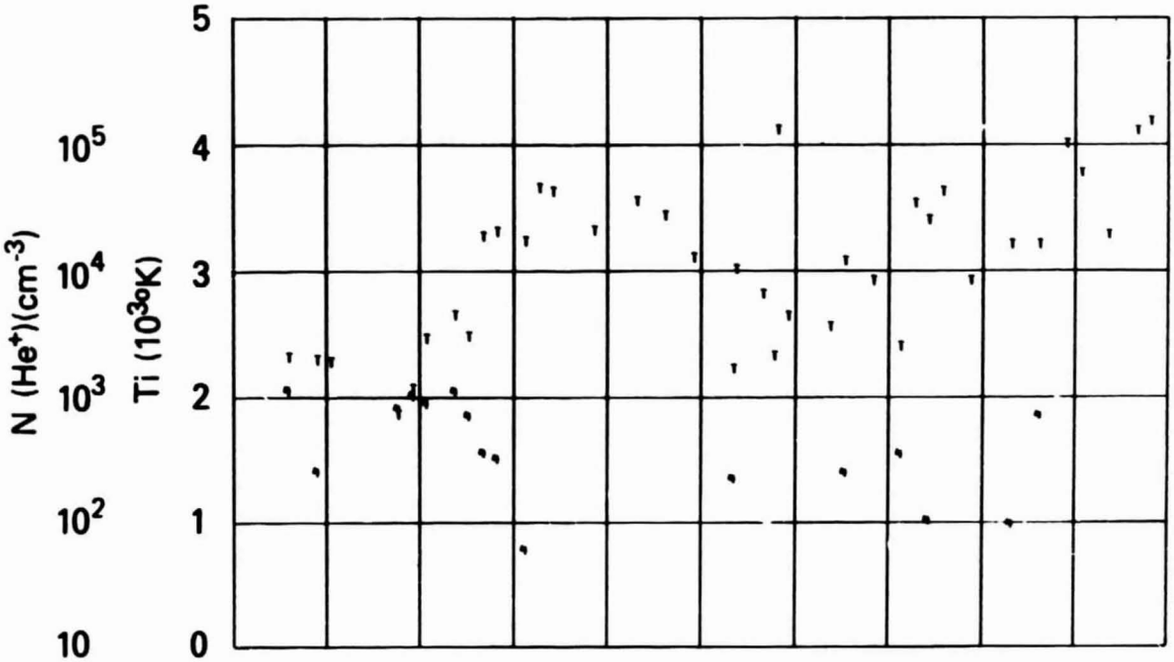

UT	09:16	09:18	09:20	09:22	09:24	09:26	09:28	09:30	09:32
LAST	22:32	22:41	23:03	01:17	08:45	09:35	09:50	09:56	10:00
MLT	21:32	21:06	19:03	16:47	13:57	12:18	11:31	11:05	10:48
DLAT									
INVL	69	74	79	83	82	78	72	67	61
GLAT	69	75	82	87	85	79	73	66	60
GLNG	-161	-160	-155	-124	-11	2	5	6	7
SZEN	87	-1	75	70	64	58	53	48	43
ALT	1402	1399	1396	1392	1389	1385	1381	1377	1374

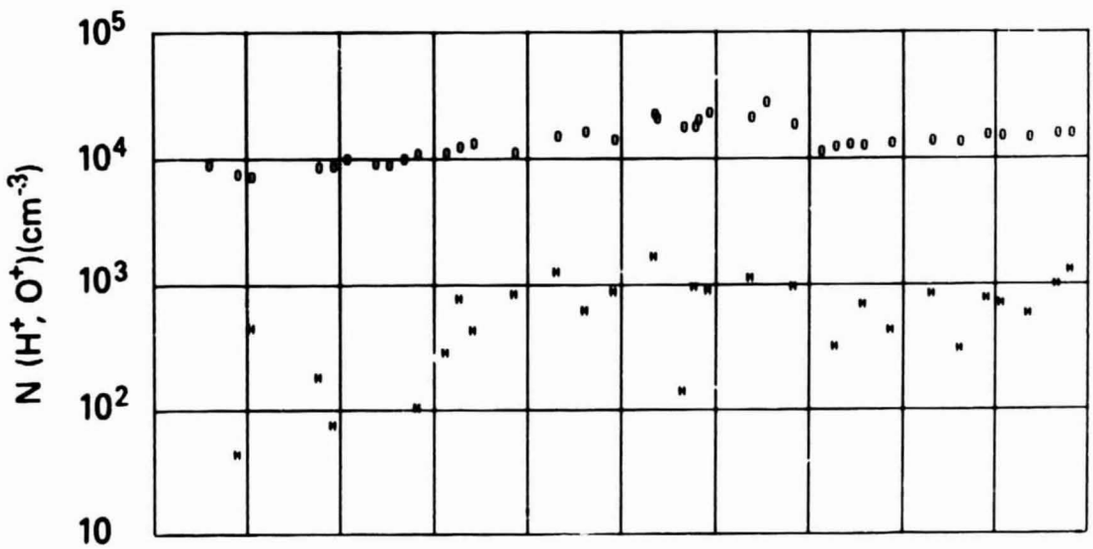

SET 31, FORMAT 5

SET 32, FORMAT 6

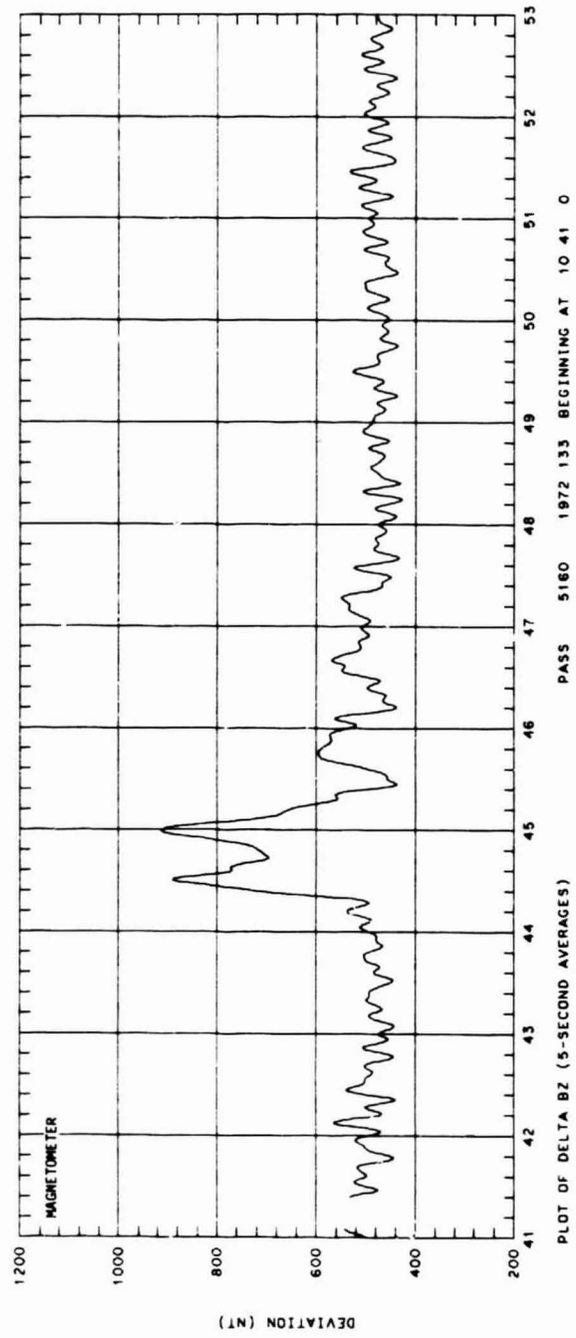

SET 32, FORMAT 2

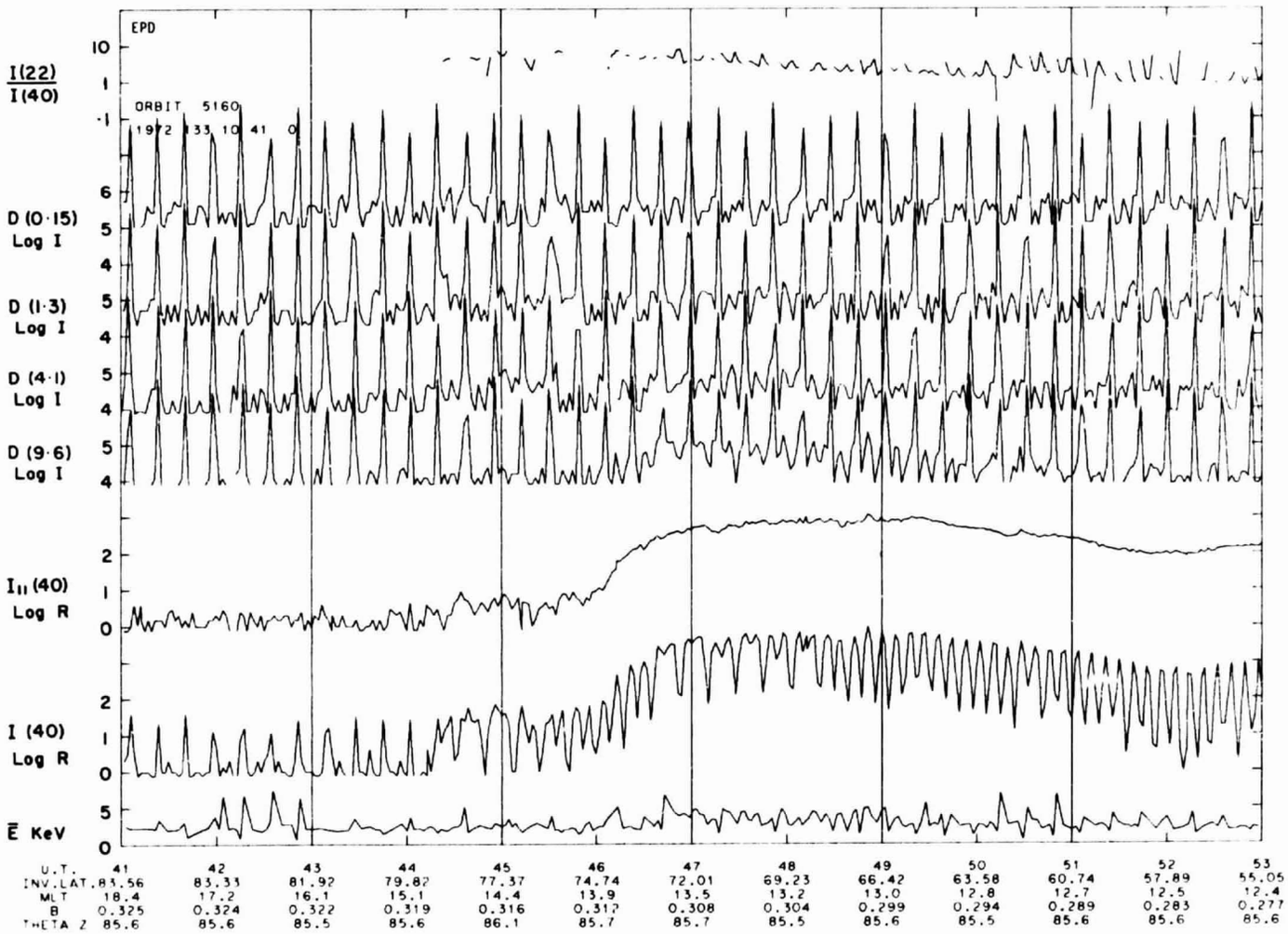

SET 32, FORMAT 3

ORBIT 5160
DATE 720512
DAY 133

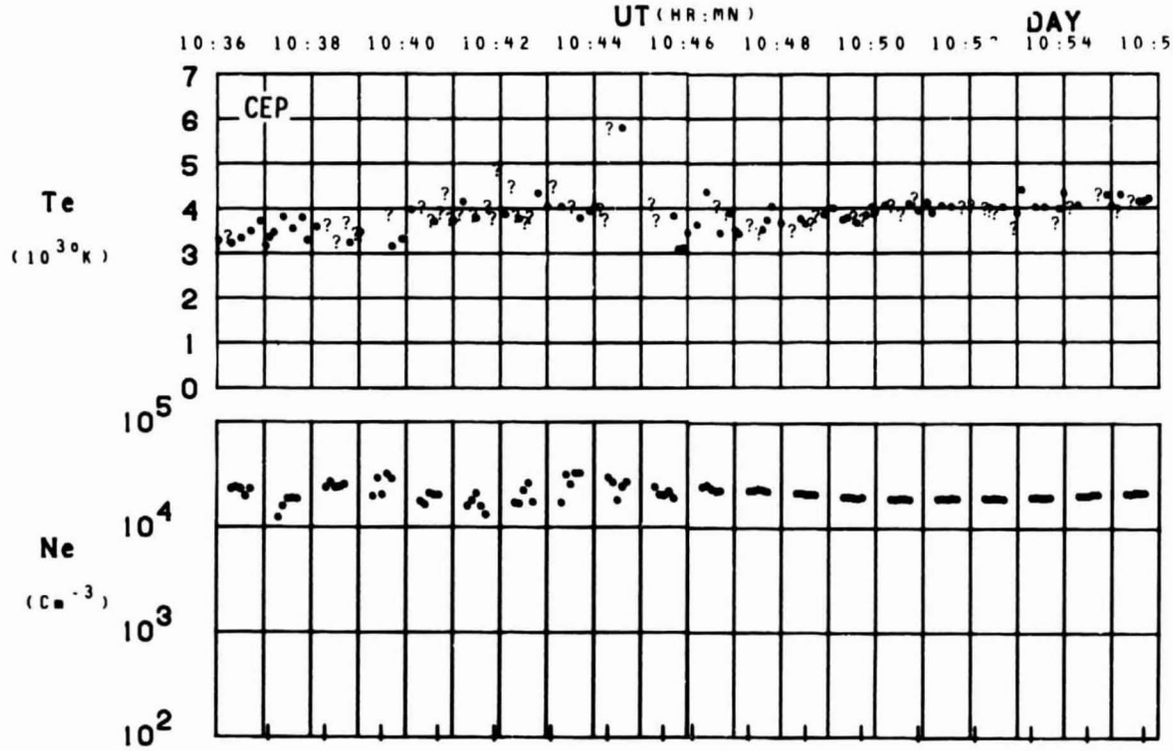

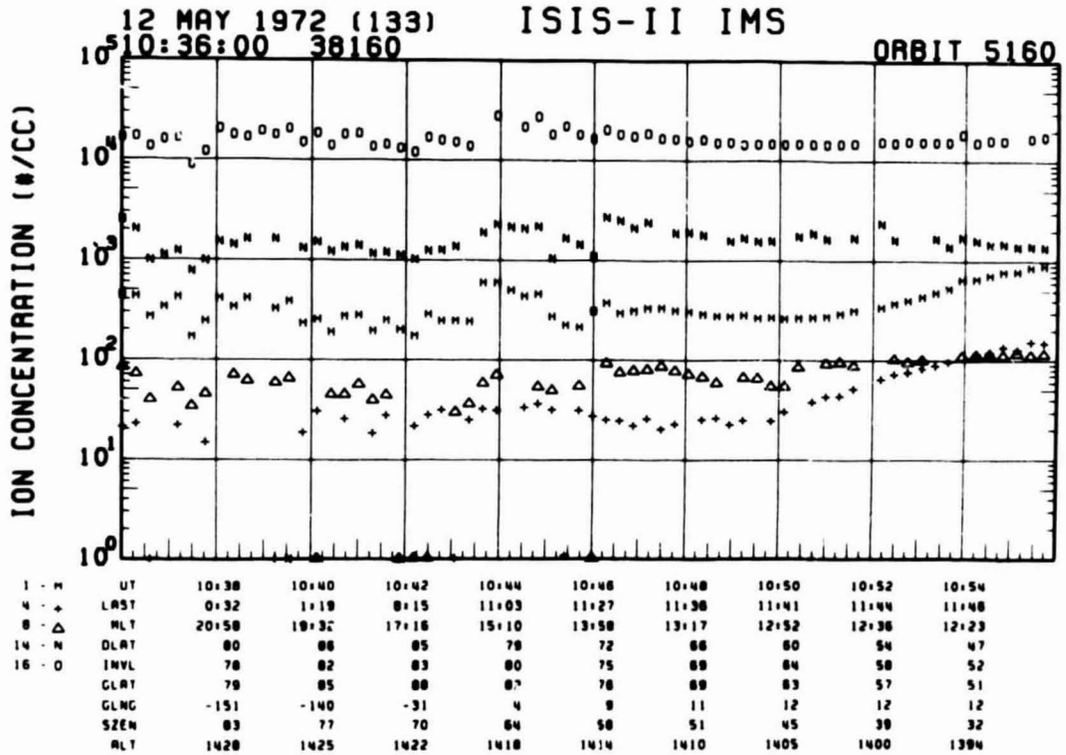

UT	10:38	10:40	10:42	10:44	10:46	10:48	10:50	10:52	10:54
LAST	0:32	1:19	0:15	11:03	11:27	11:38	11:41	11:44	11:48
MLT	20:58	19:32	17:16	15:10	13:58	13:17	12:52	12:36	12:23
DLAT	80	86	85	78	72	66	60	54	47
INVL	78	82	83	80	75	69	64	58	52
GLAT	79	85	88	87	78	69	63	57	51
GLNG	-151	-140	-31	4	9	11	12	12	12
SZEN	83	77	70	64	58	51	45	39	32
ALT	1428	1425	1422	1418	1414	1410	1405	1400	1394

SET 32, FORMAT 4

RPA

720512

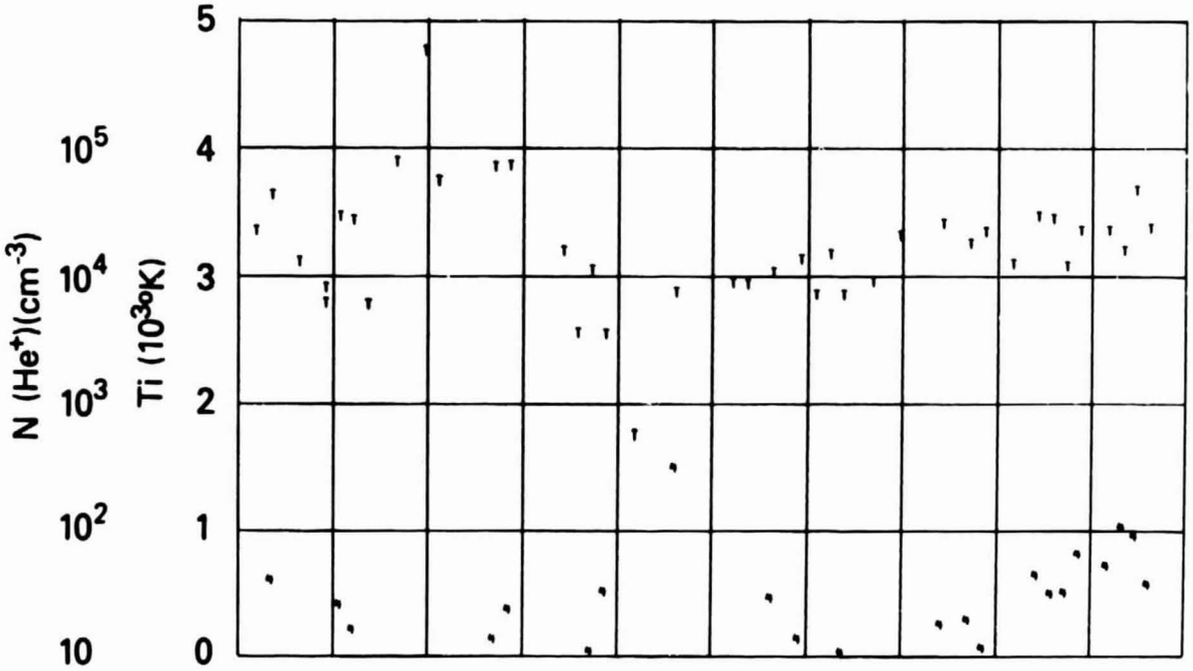

UT	10:38	10:40	10:42	10:44	10:46	10:48	10:50	10:52	10:54
LAST	0:32	1:19	8:15	11:03	11:27	11:36	11:41	11:44	11:46
MLT	20:58	19:32	17:16	15:10	13:58	13:17	12:52	12:36	12:23
QLAT	80	86	85	79	72	66	60	54	47
INVL	78	82	83	80	75	69	64	58	52
GLAT	79	85	88	82	76	69	63	57	51
GLNG	-151	-140	-31	4	9	11	12	12	12
SZEN	83	77	70	64	58	51	45	38	32
ALT	1428	1425	1422	1418	1414	1410	1405	1400	1394

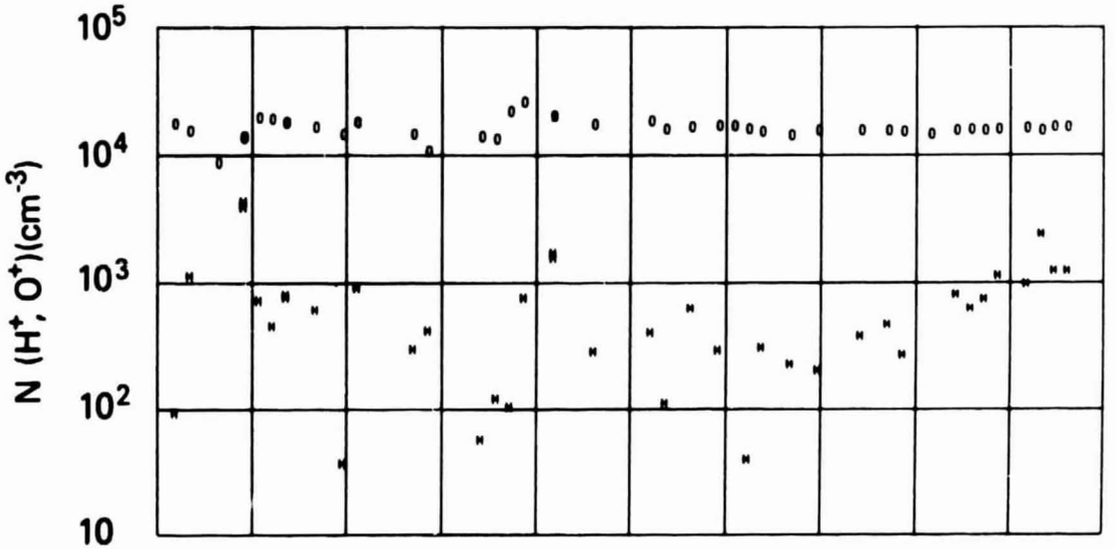

SET 32, FORMAT 5

72/133/1041

Excerpts of VLF Spectral film for the period 1043 - 1053

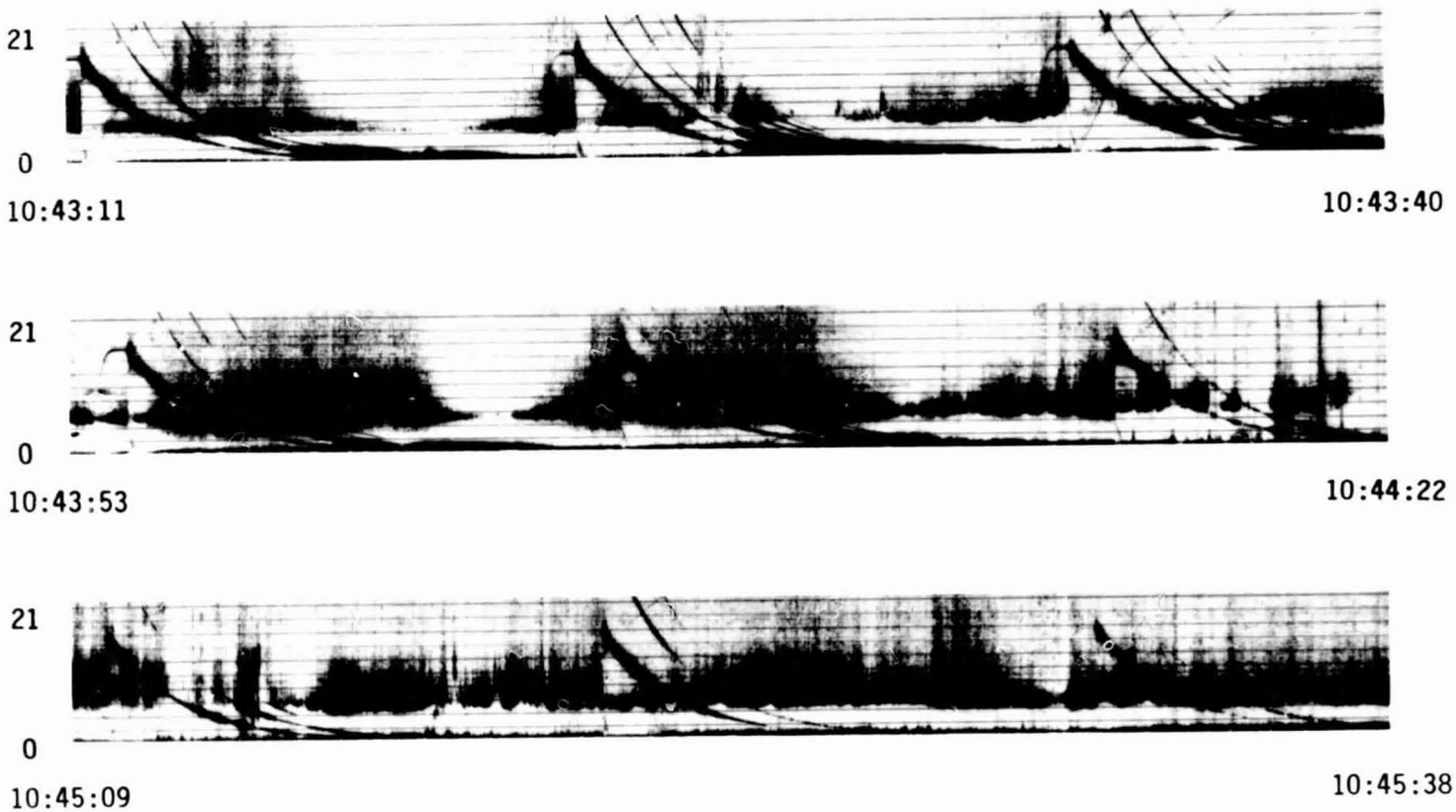

SET 32, FORMAT 11

72/133/1041

Excerpts of VLF Spectral film for the period 1043 - 1053

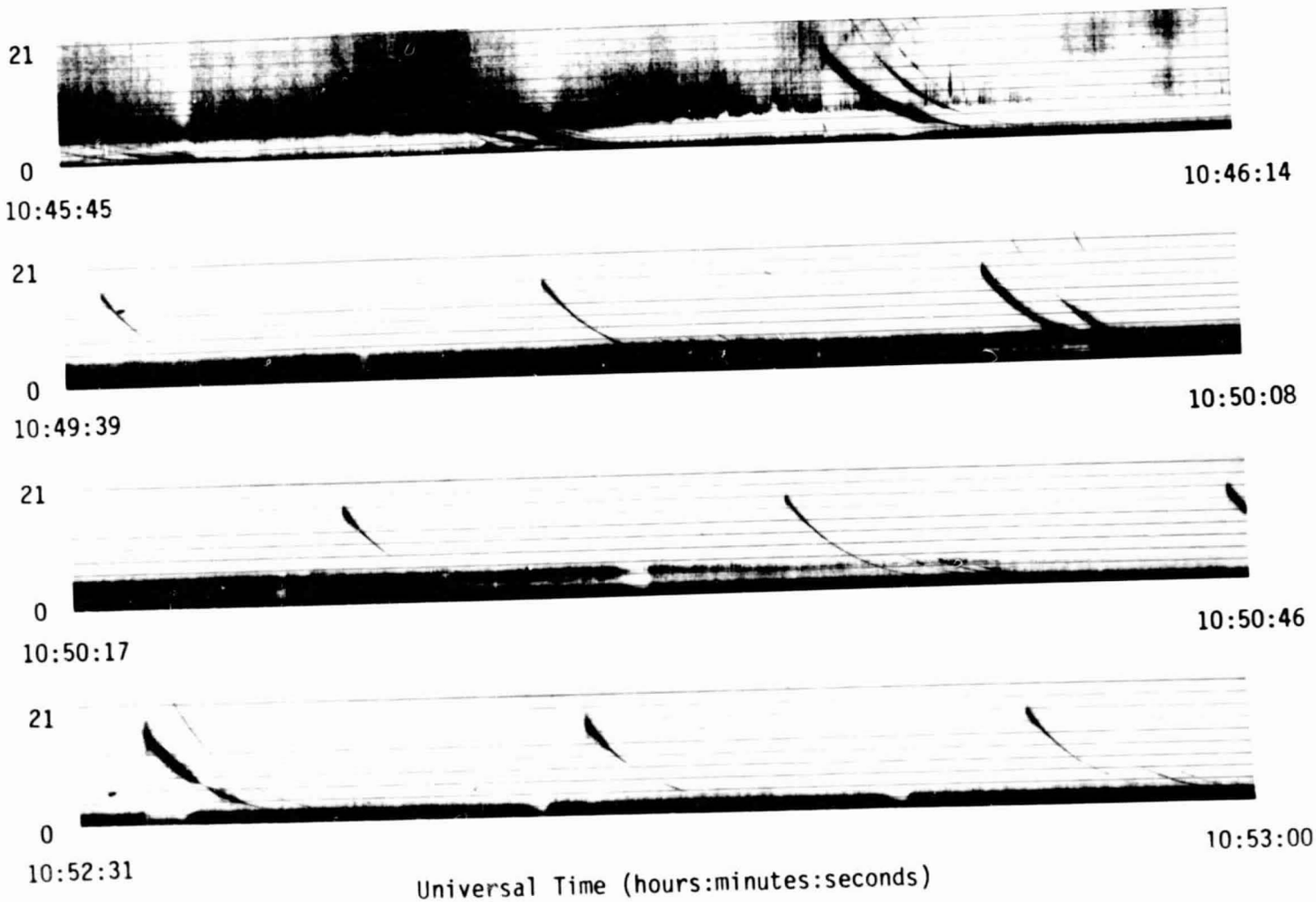

SET 32, FORMAT 11

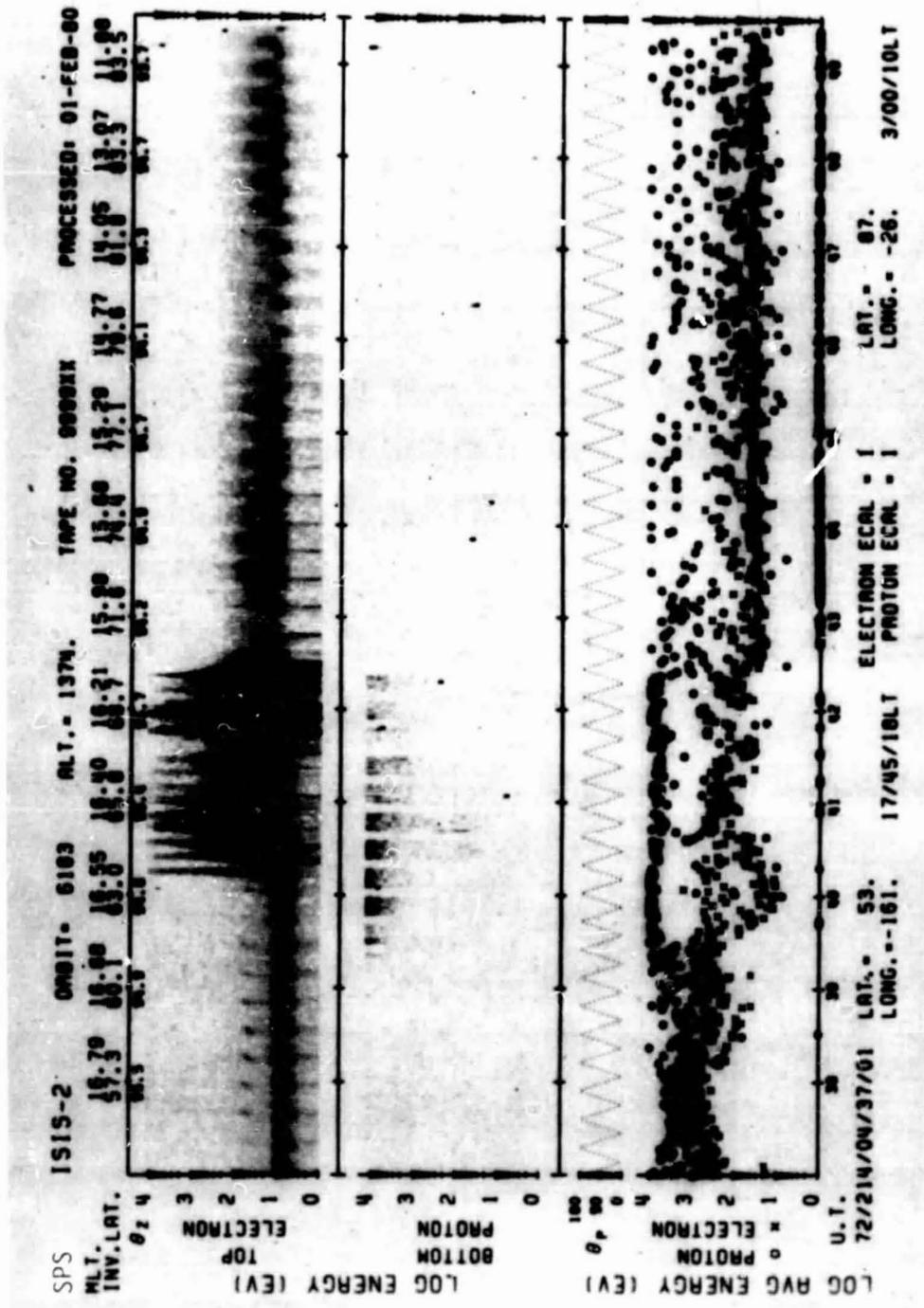

SET 33, FORMAT 6

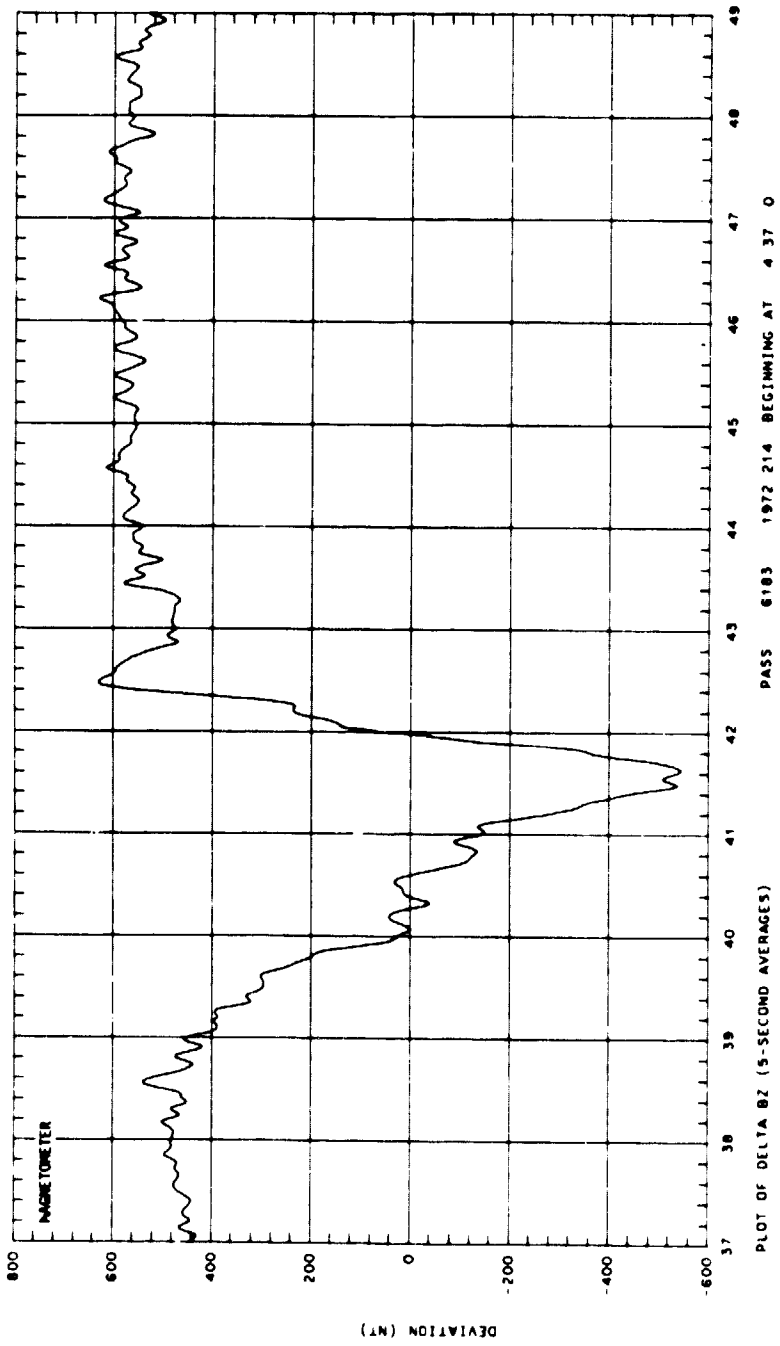

SET 33, FORMAT 2

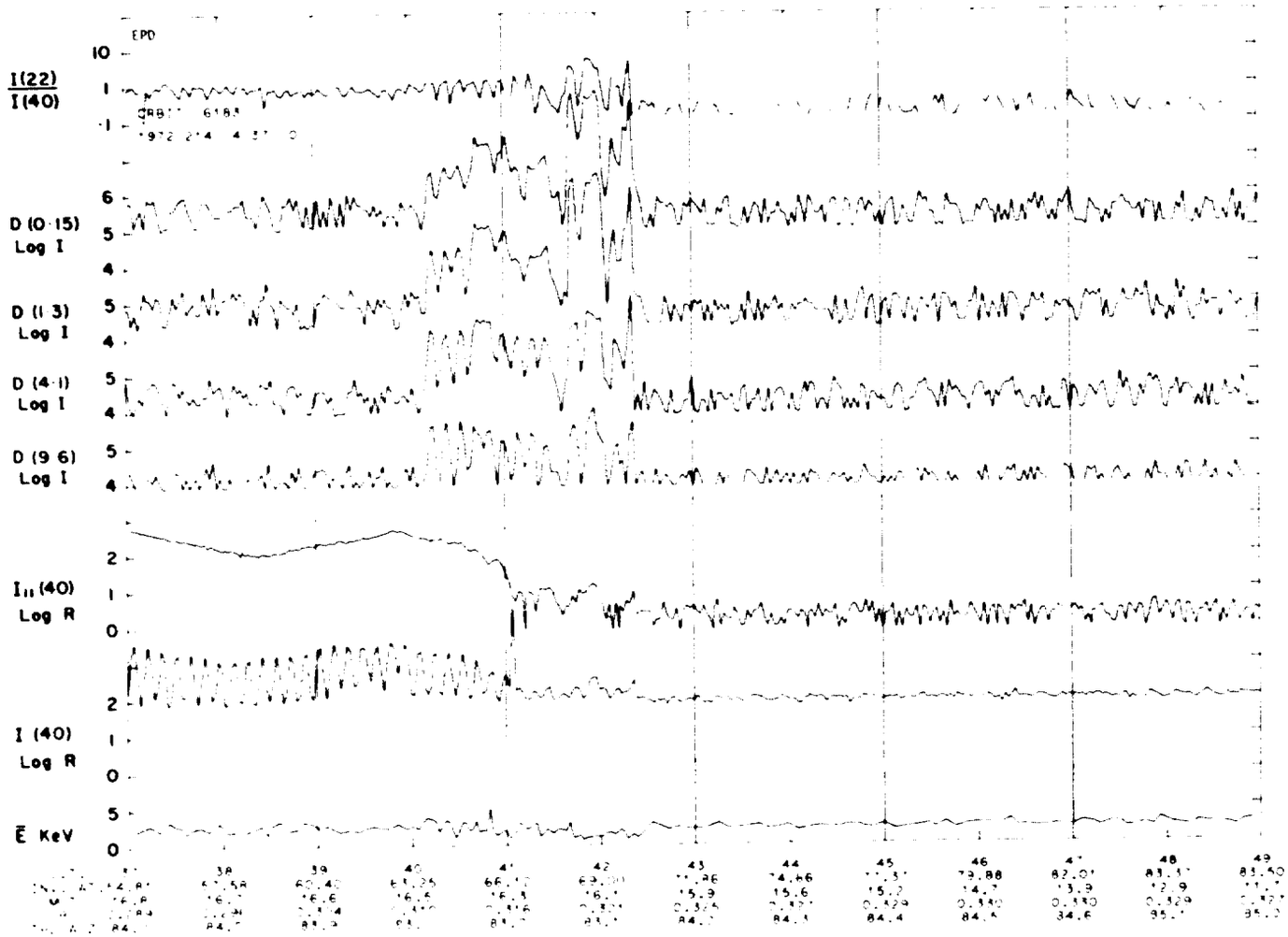

SET 33, FORMAT 3

ORBIT 6183
DATE 720801
DAY 214

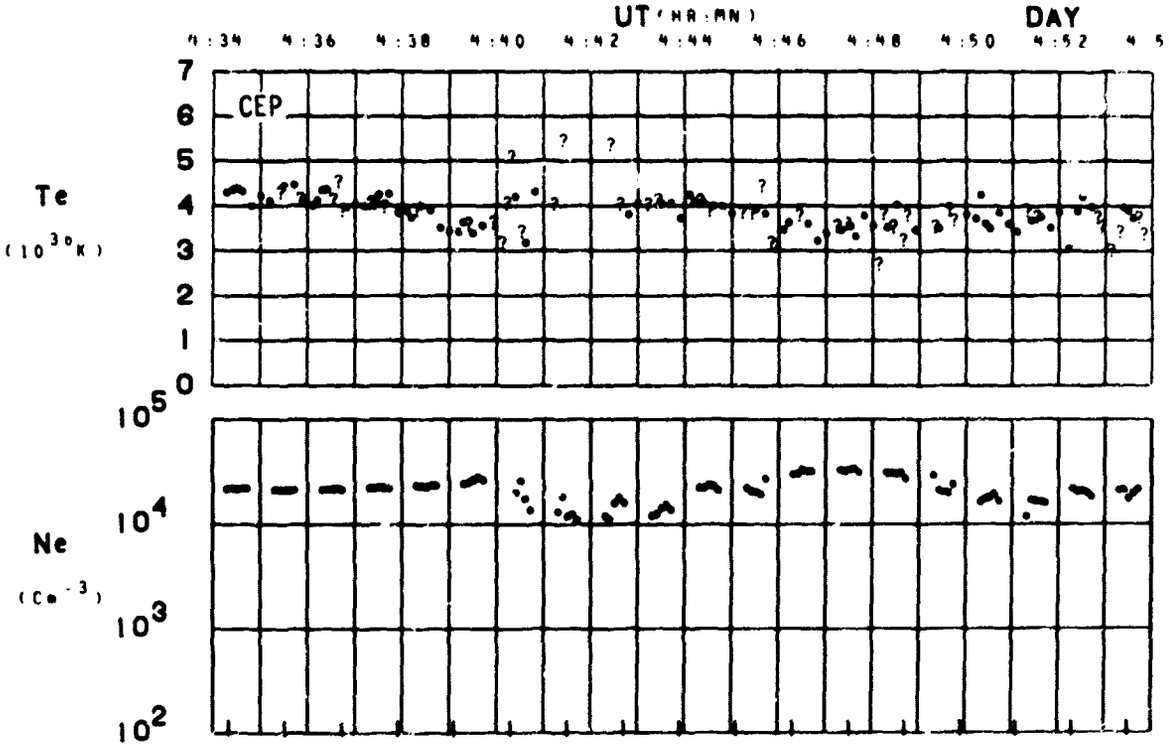

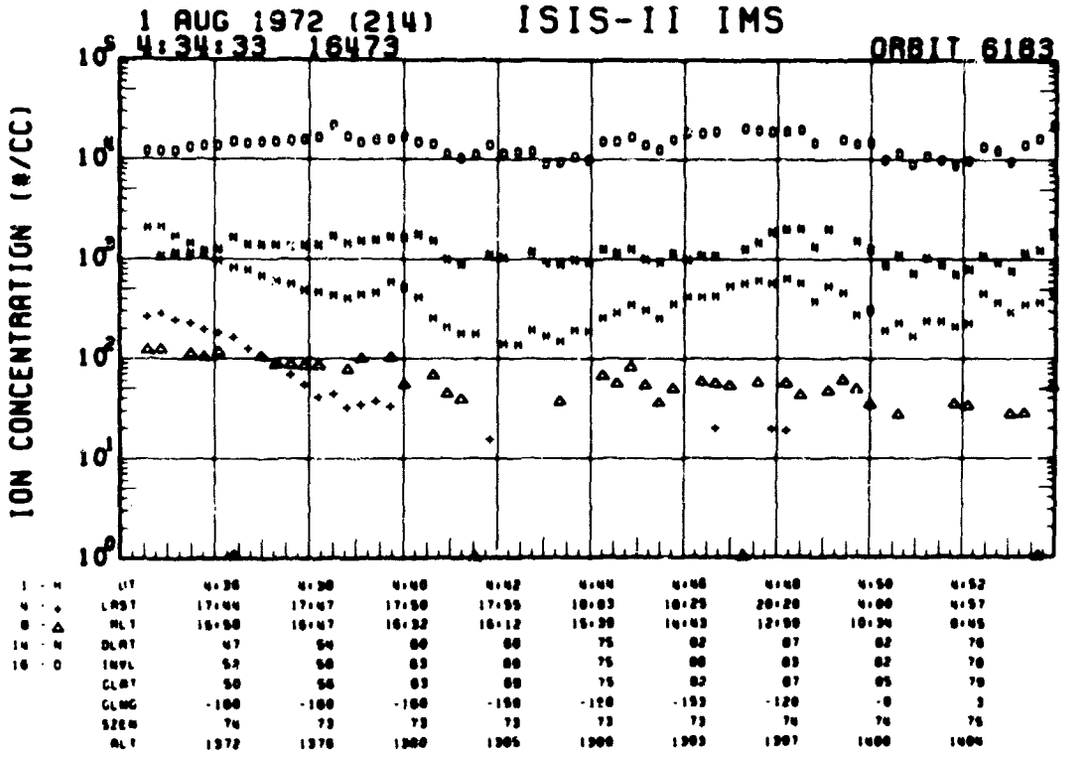

SET 33, FORMAT 4

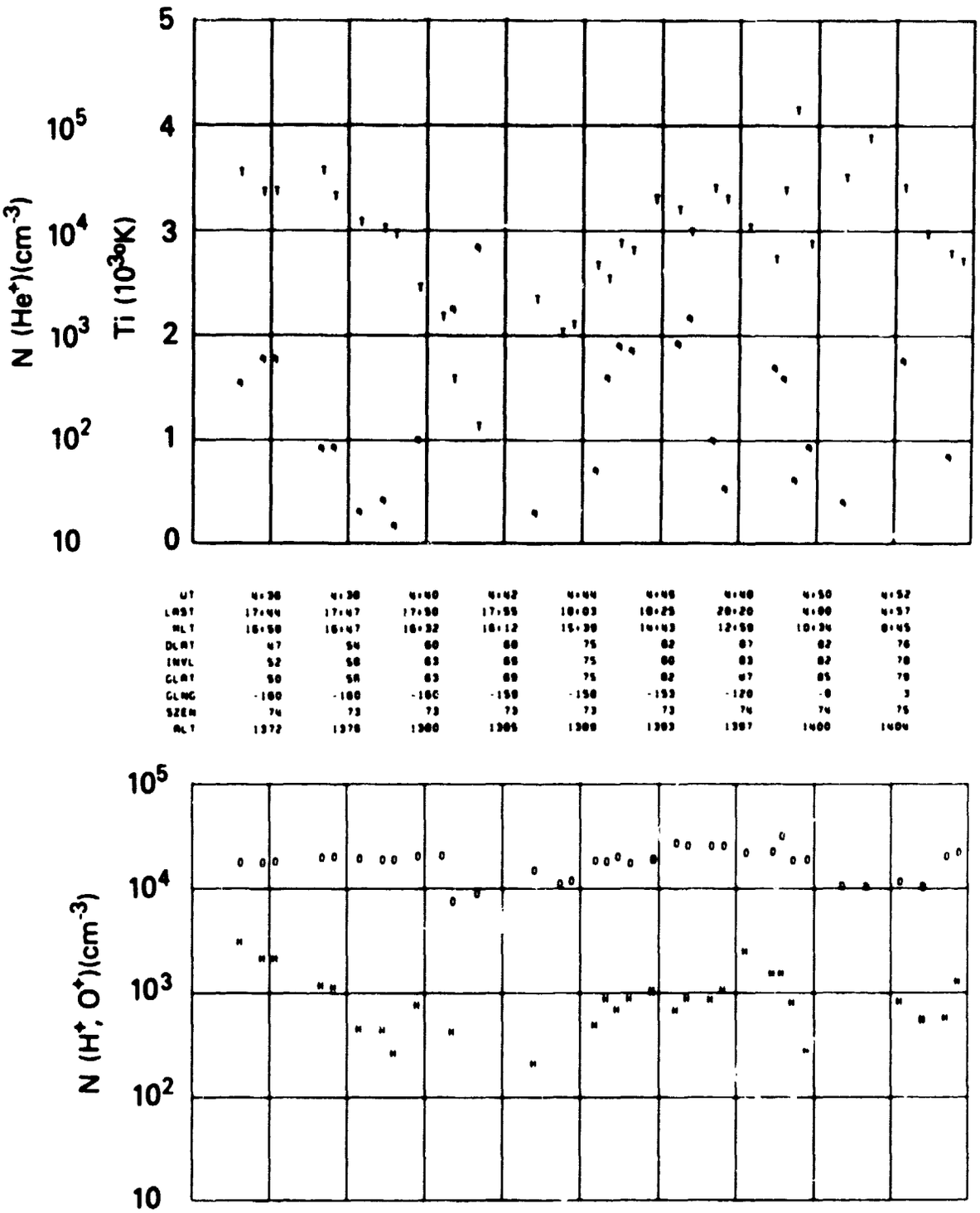

SET 33, FORMAT 5

72/214/0437

Excerpts of VLF Spectral film for the period 0437 - 0444

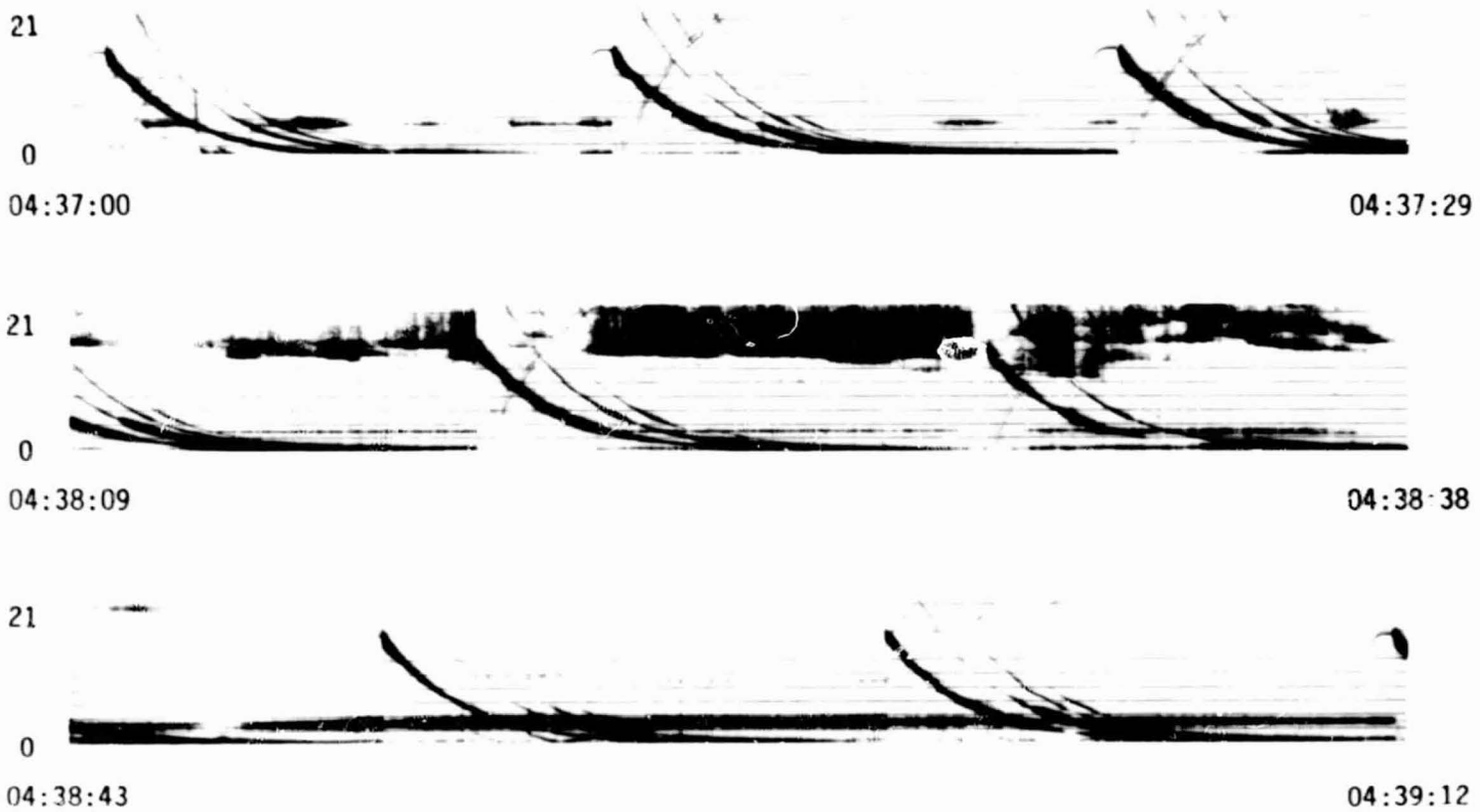

SET 33, FORMAT 11

72/214/0437

Excerpts of VLF Spectral film for the period 0437 - 0444

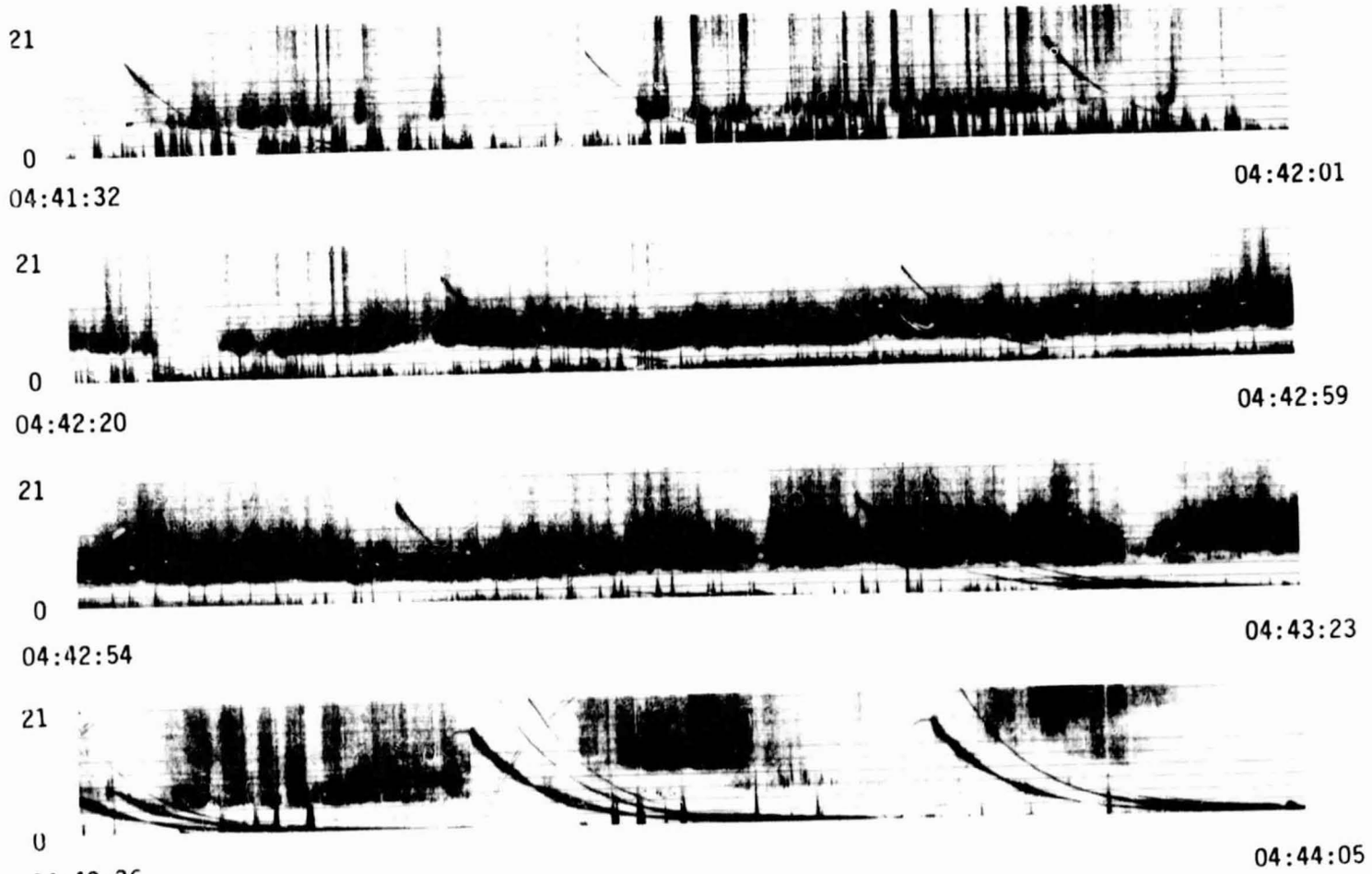

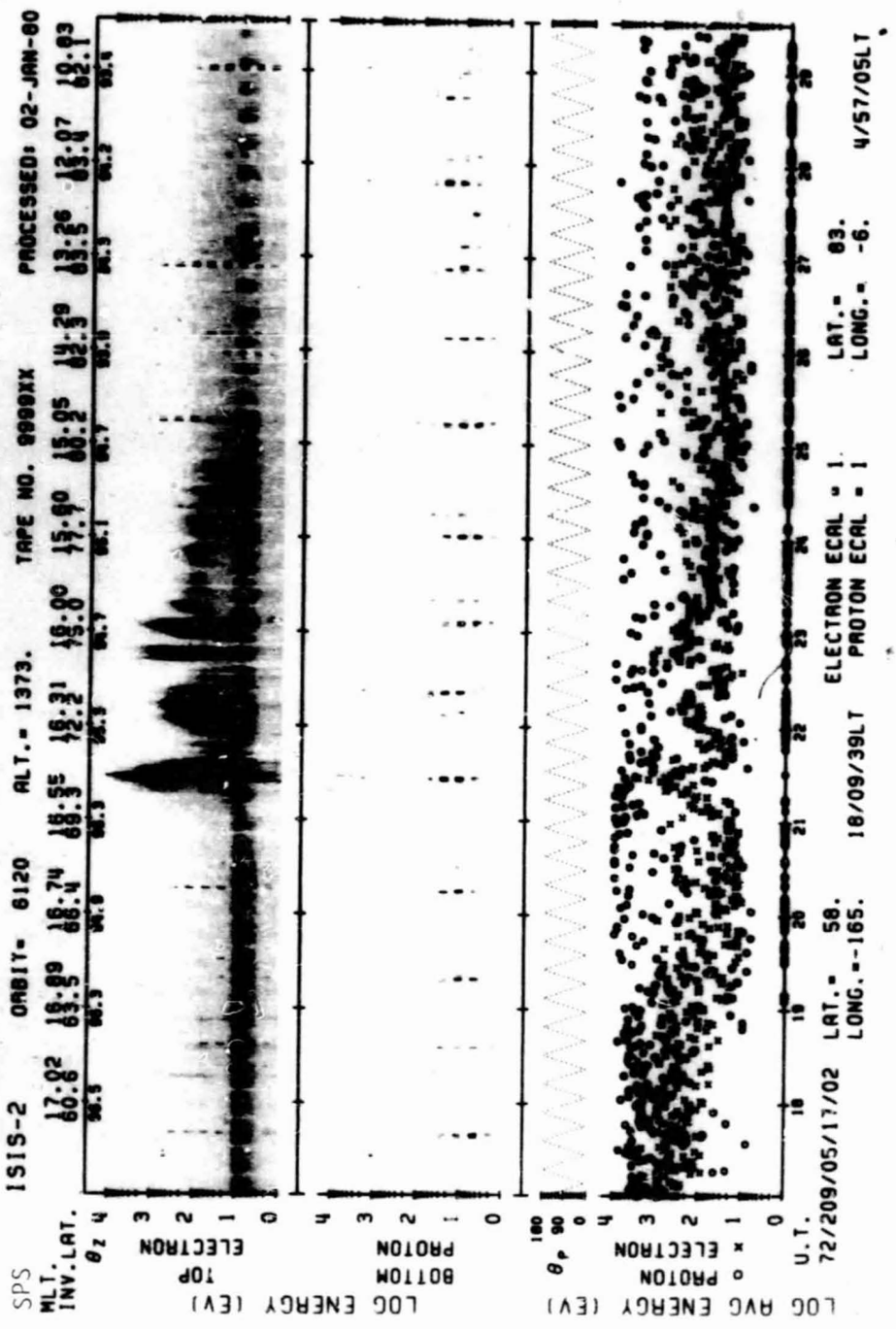

SET 34, FORMAT 6

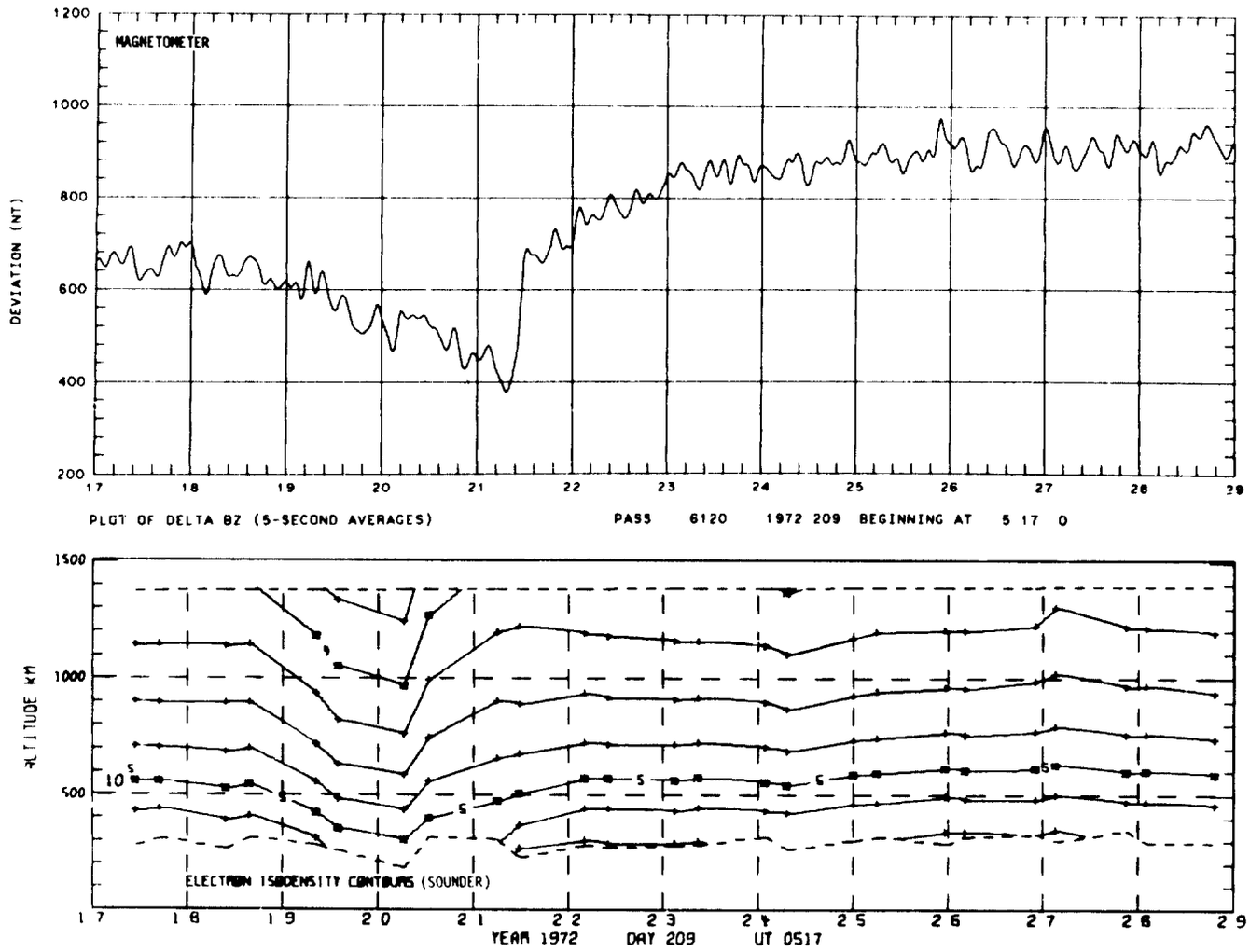

SET 34, FORMAT 2

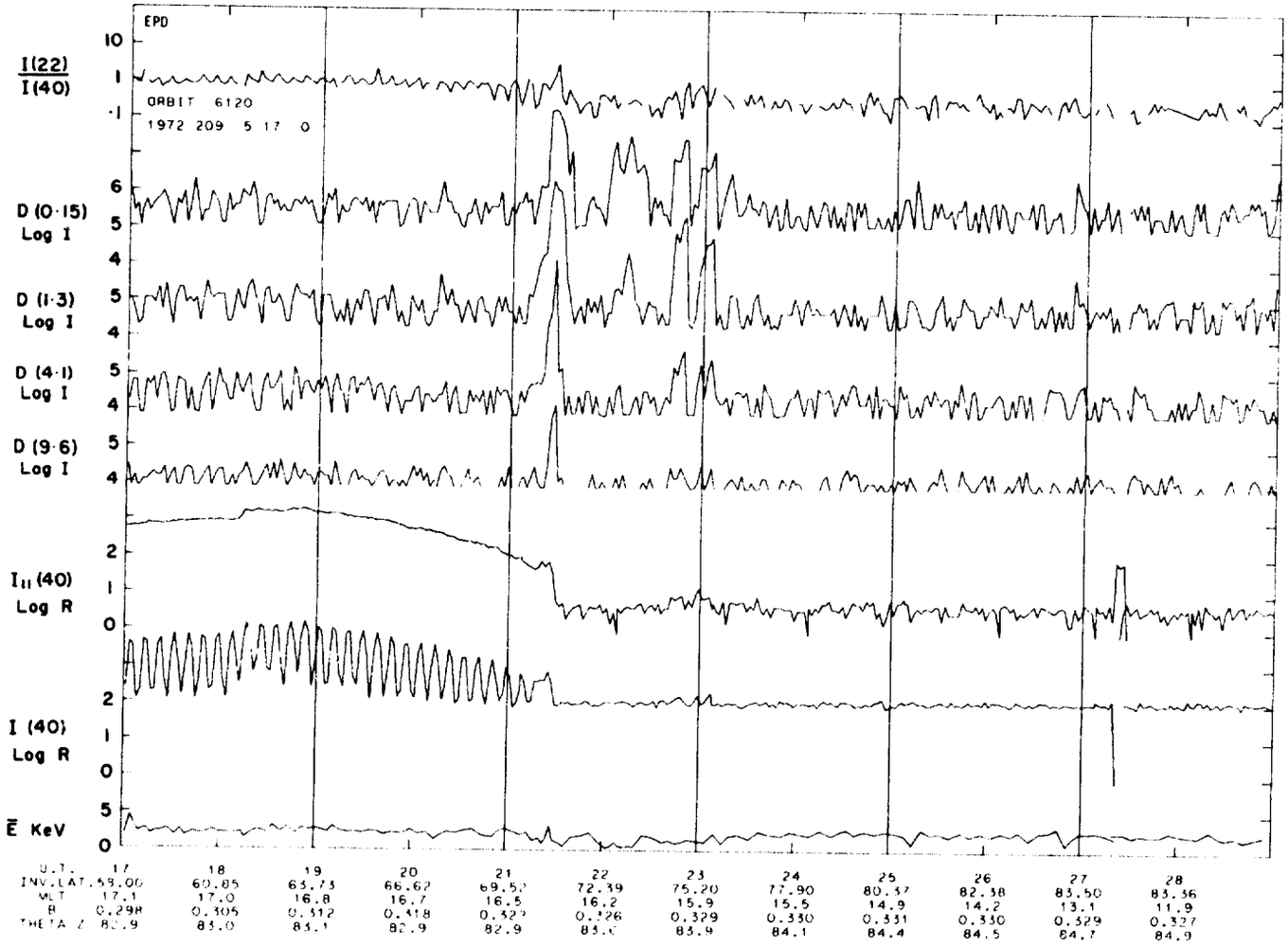

SET 34, FORMAT 3

ORBIT 6120
DATE 720727
DAY 209

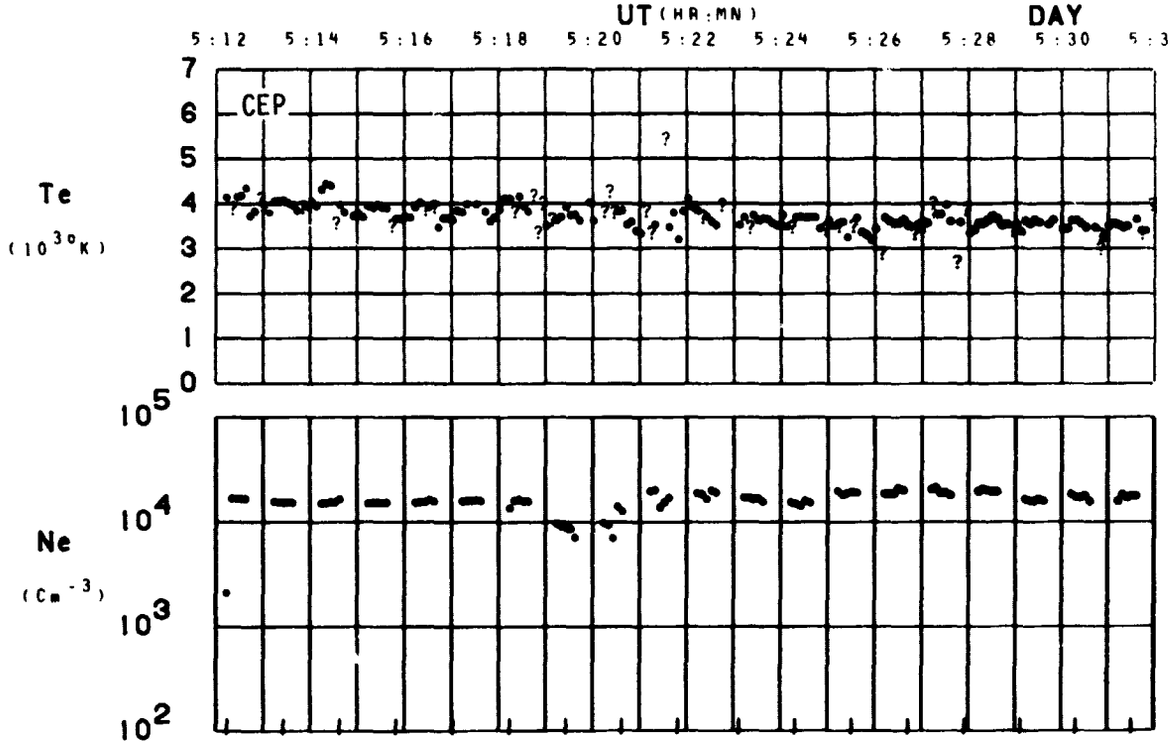

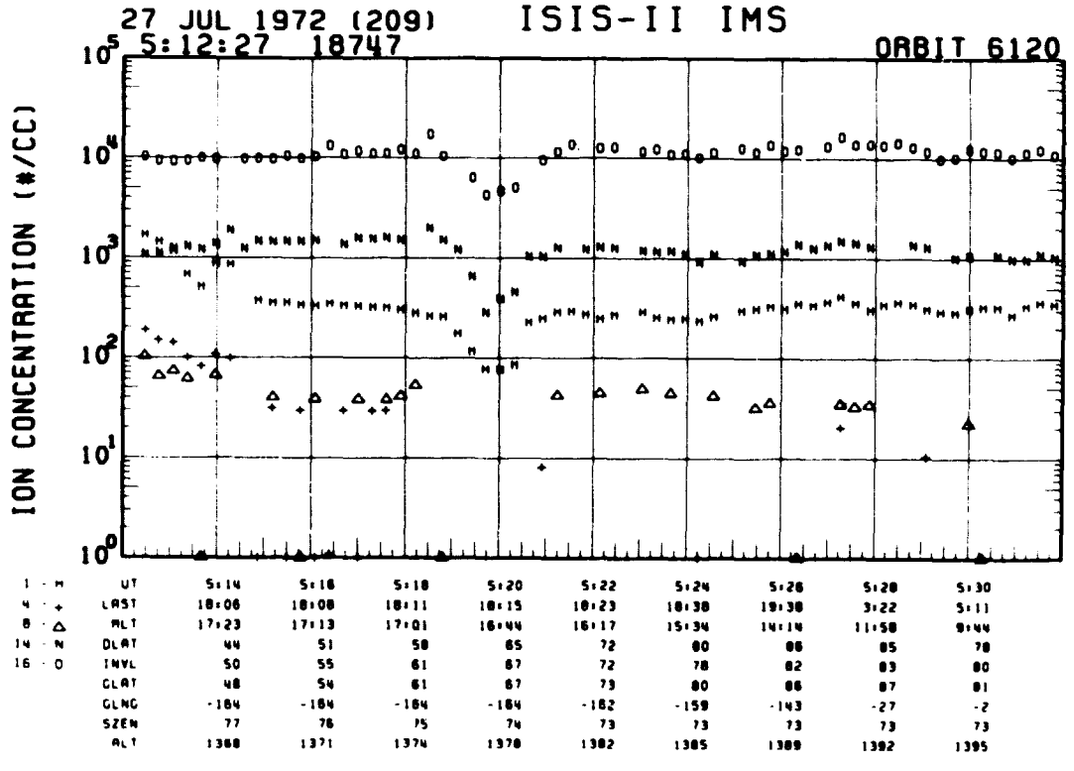

1 - H	UT	5:14	5:16	5:18	5:20	5:22	5:24	5:26	5:28	5:30
4 - +	LAST	18:06	18:08	18:11	18:15	18:23	18:38	19:38	3:22	5:11
8 - △	ALT	17:23	17:13	17:01	16:44	16:17	15:34	14:14	11:58	9:44
14 - N	DLAT	44	51	58	65	72	80	86	85	78
16 - O	INVL	50	55	61	67	72	78	82	83	80
	GLAT	48	54	61	67	73	80	86	87	81
	GLNG	-184	-184	-184	-184	-182	-159	-143	-27	-2
	SZEN	77	76	75	74	73	73	73	73	73
	ALT	1368	1371	1374	1378	1382	1385	1389	1392	1395

SET 34, FORMAT 4

RPA 720727

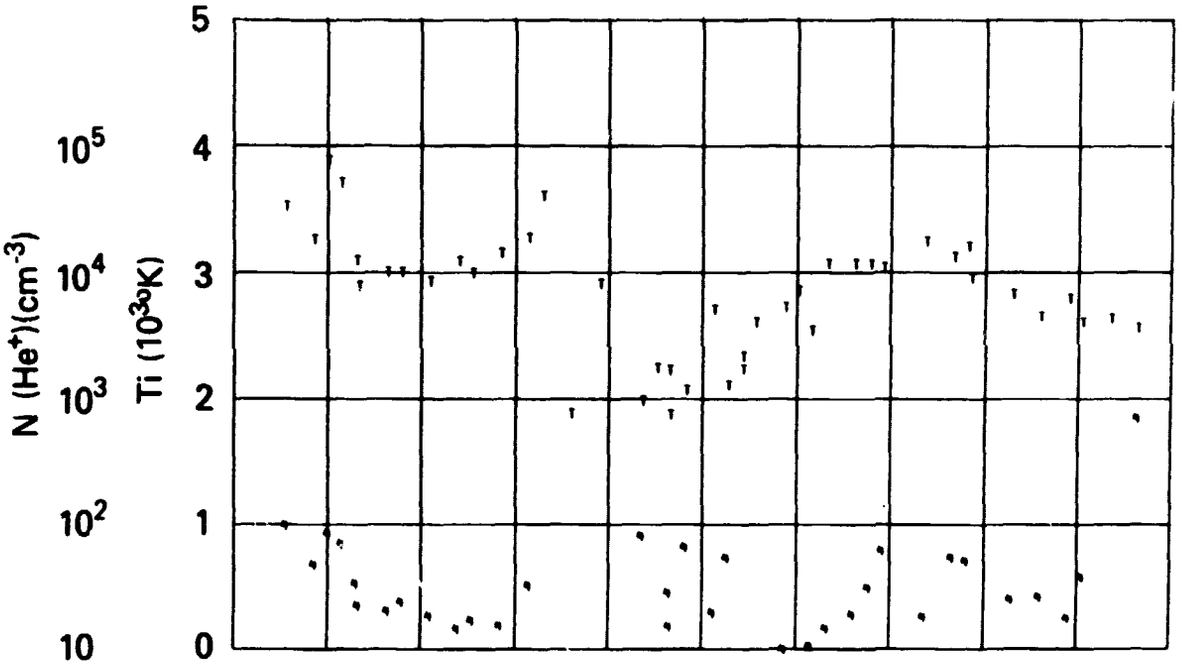

UT	5:14	5:16	5:18	5:20	5:22	5:24	5:26	5:28	5:30
LAST	18:06	18:08	18:11	18:15	18:23	18:38	19:30	3:22	5:11
ALT	17:23	17:13	17:01	16:44	16:17	15:34	14:14	11:58	9:44
DLAT	44	51	58	65	72	80	86	85	78
INVL	50	55	61	67	72	78	82	83	80
GLAT	48	54	61	67	73	80	86	87	81
GLNG	-164	-164	-164	-164	-162	-159	-143	-27	-2
SZEN	77	76	75	74	73	73	73	73	73
ALT	1368	1371	1374	1378	1382	1385	1389	1392	1395

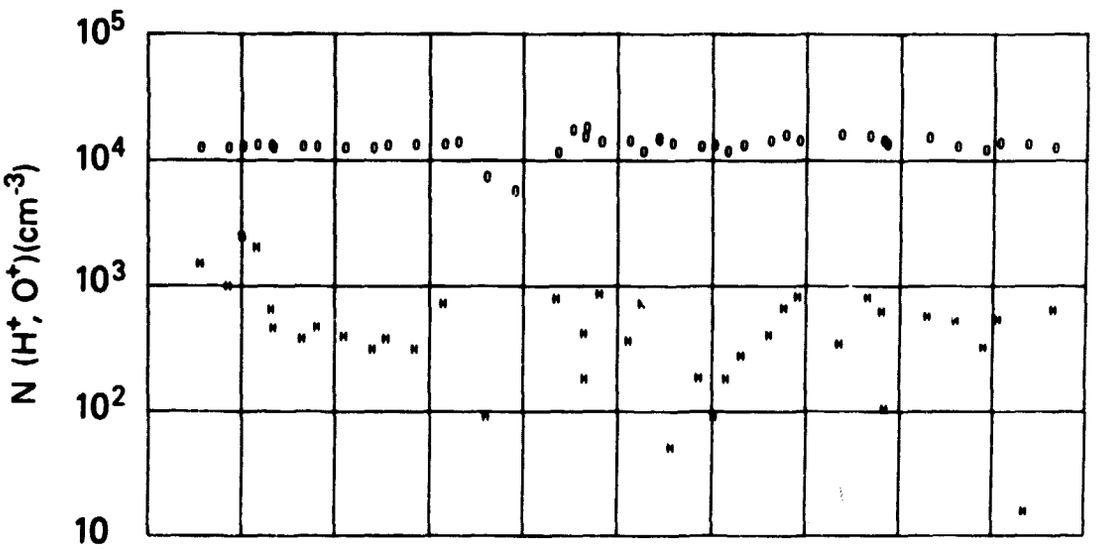

SET 34, FORMAT 5

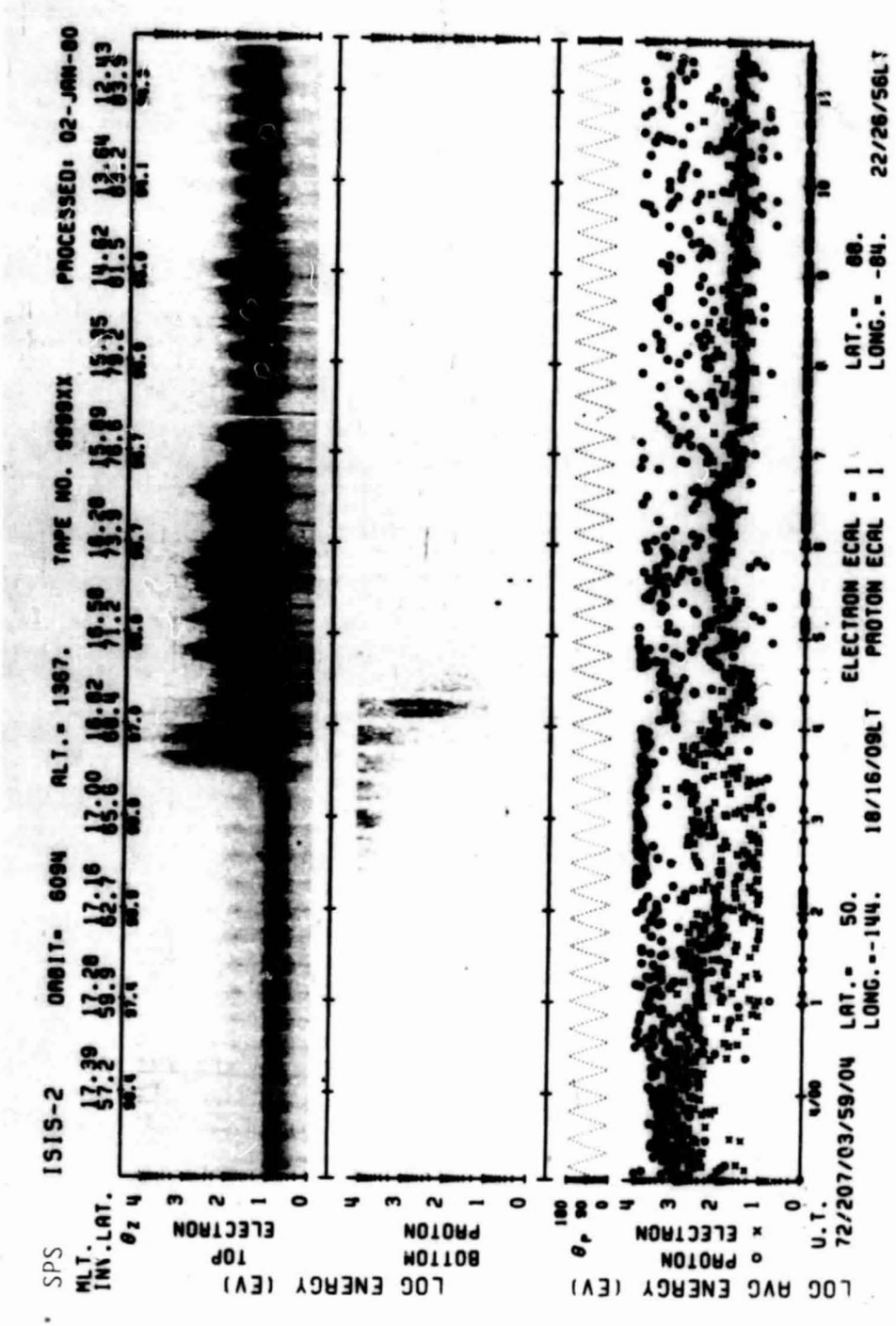

SET 35, FORMAT 6

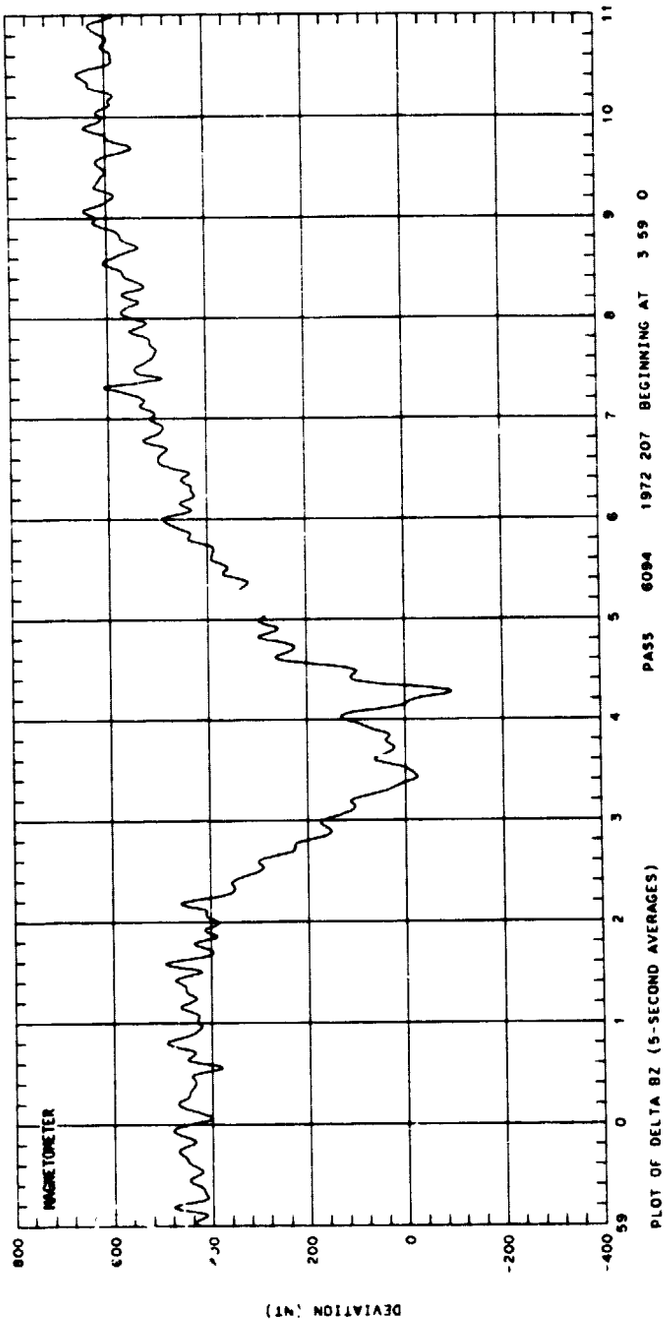

SET 35, FORMAT 2

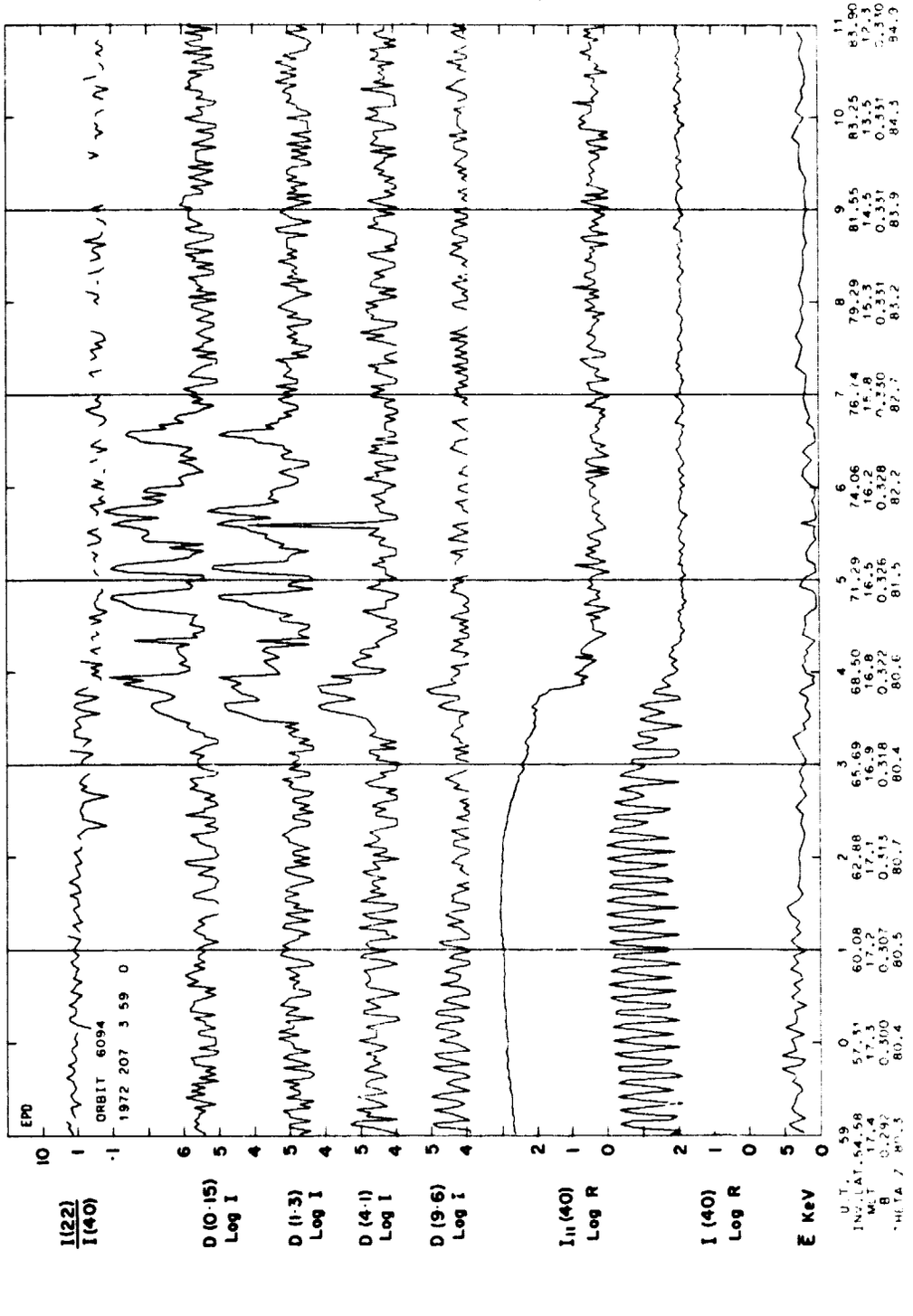

SET 35, FORMAT 3

ORBIT 6094
DATE 720725
DAY 207

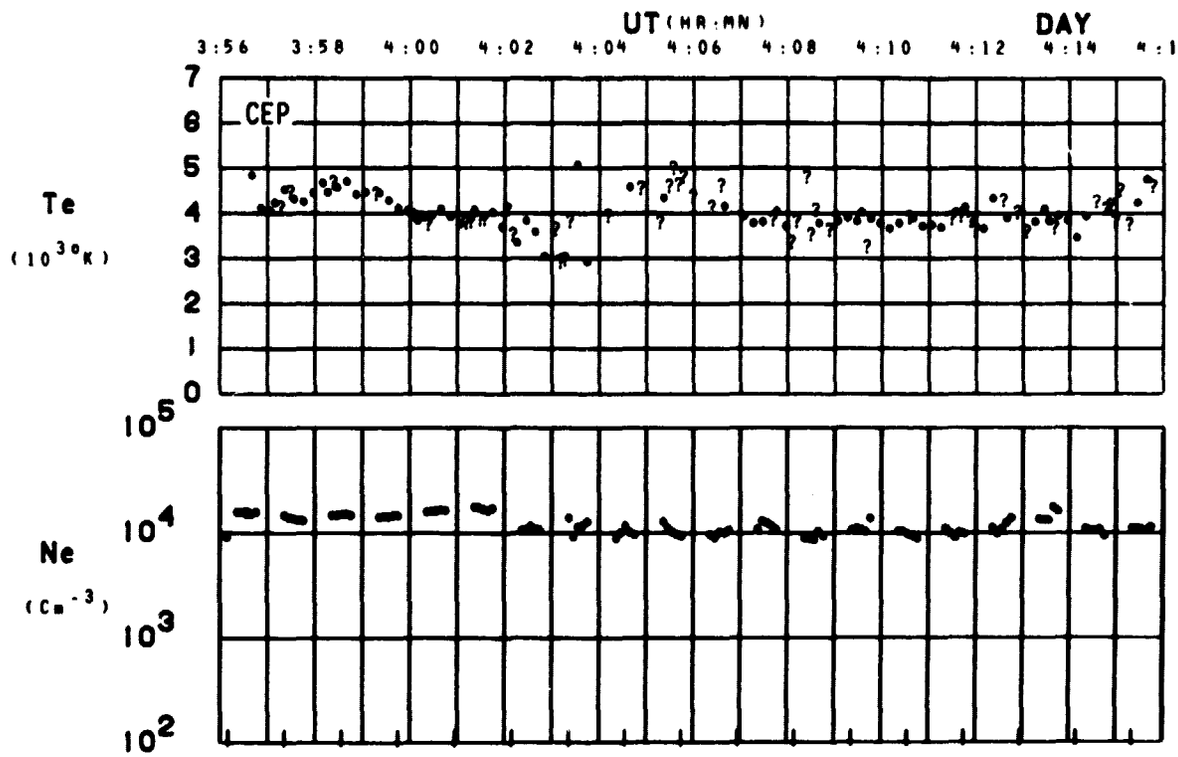

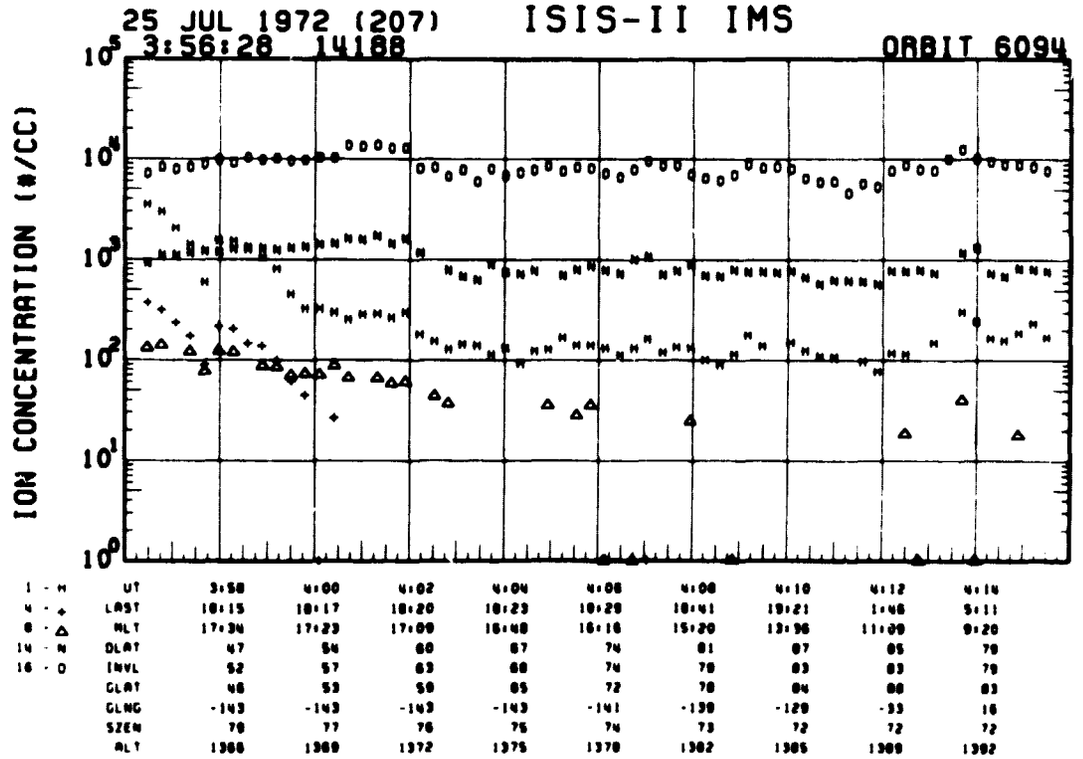

SET 35, FORMAT 4

72/207/0359

Excerpts of VLF Spectral film for the period 0359 - 0409

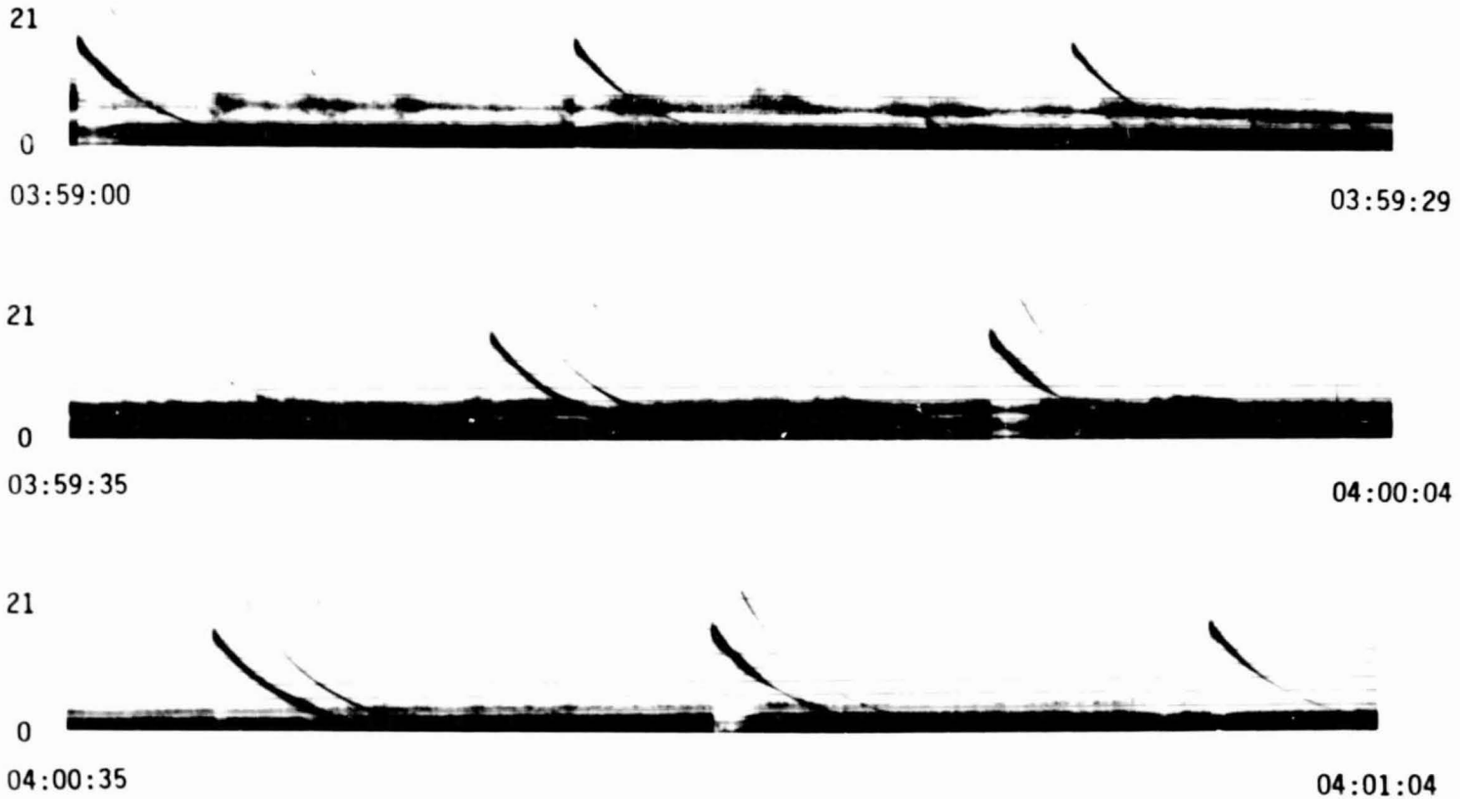

SET 35, FORMAT 11

72/207/0359

Excerpts of VLF Spectral film for the period 0359 - 0409

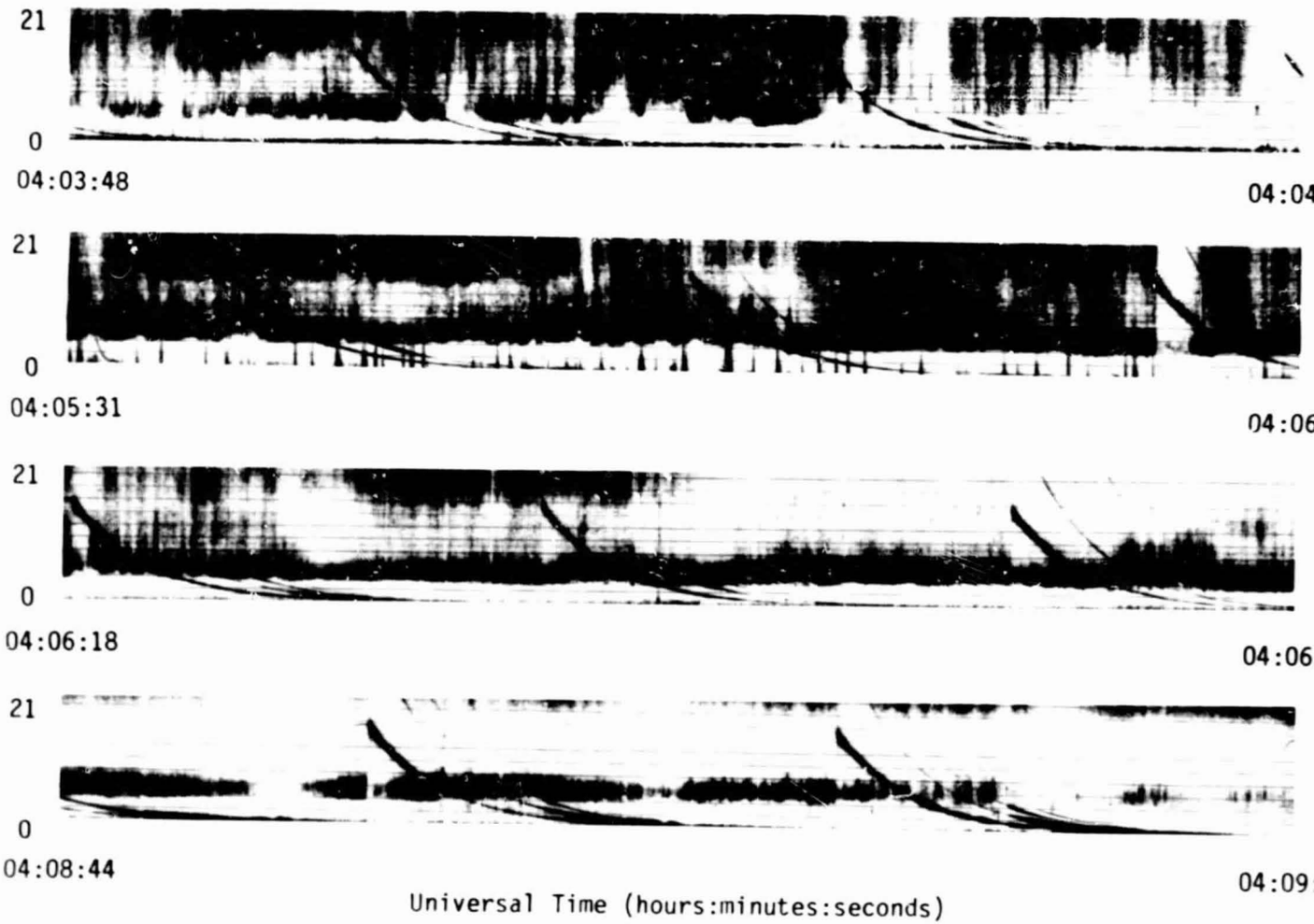

SET 36, FORMAT 6

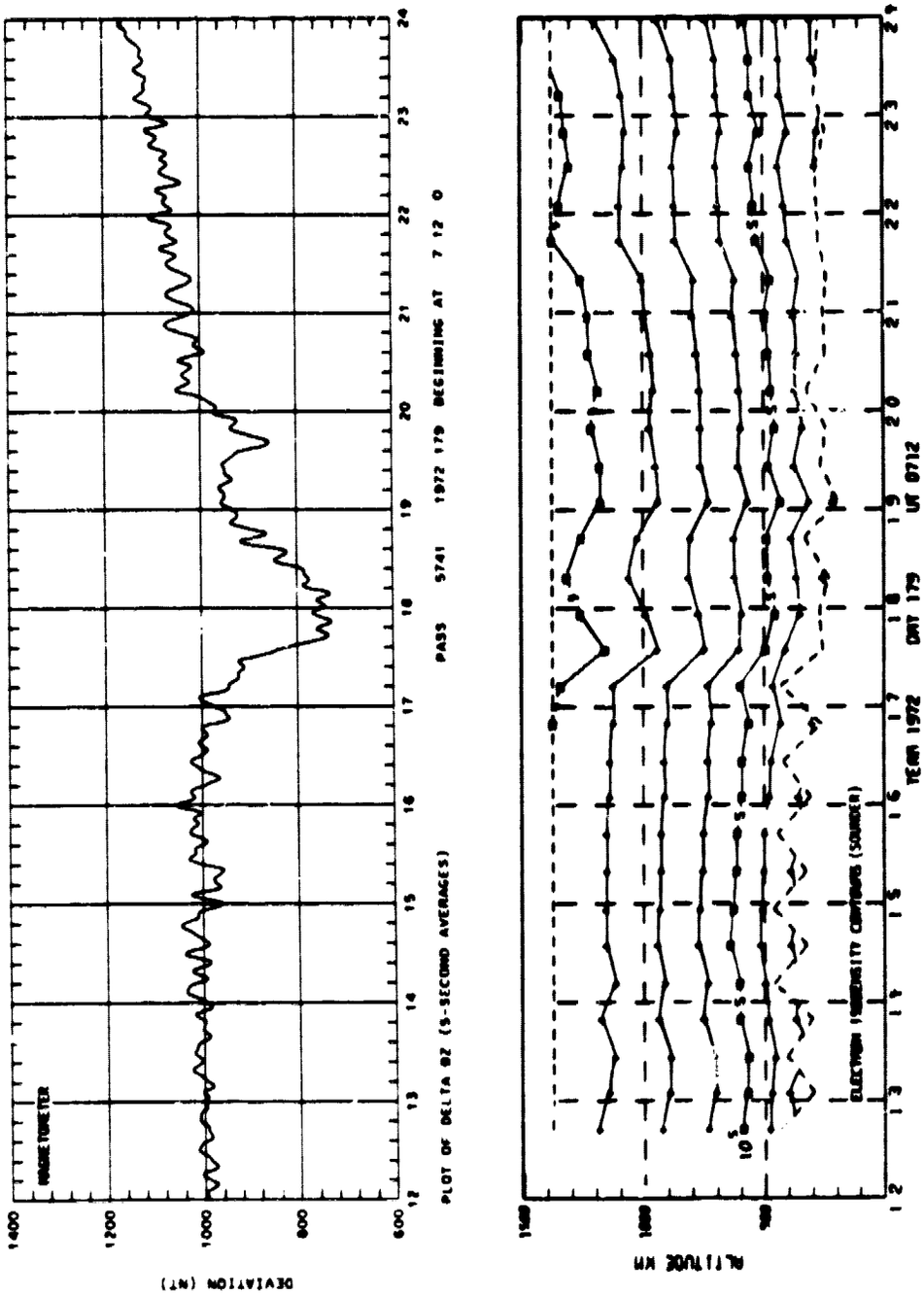

SET 36, FORMAT 2

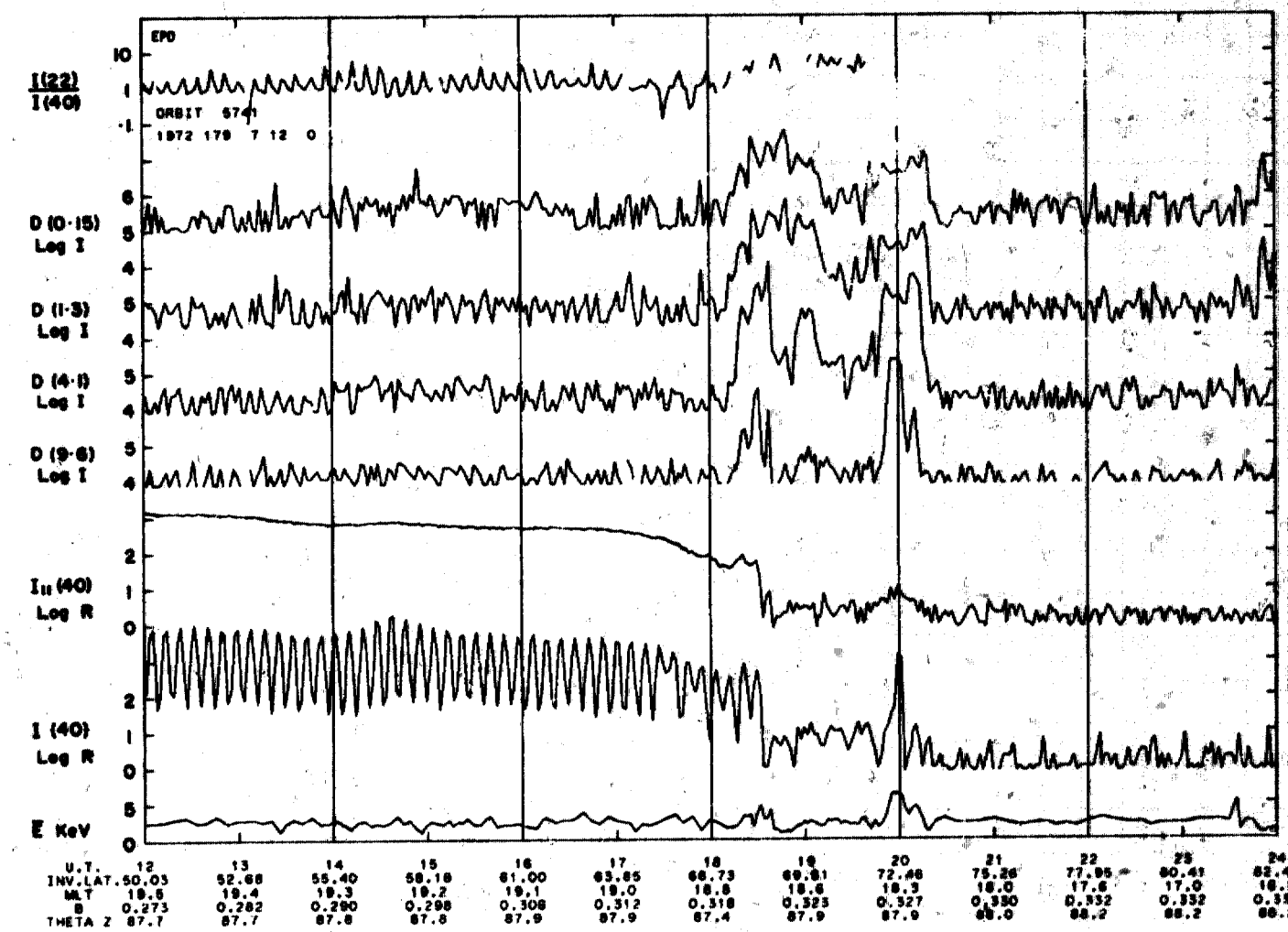

SET 36, FORMAT 3

ORBIT 5741
DATE 720627
DAY 179

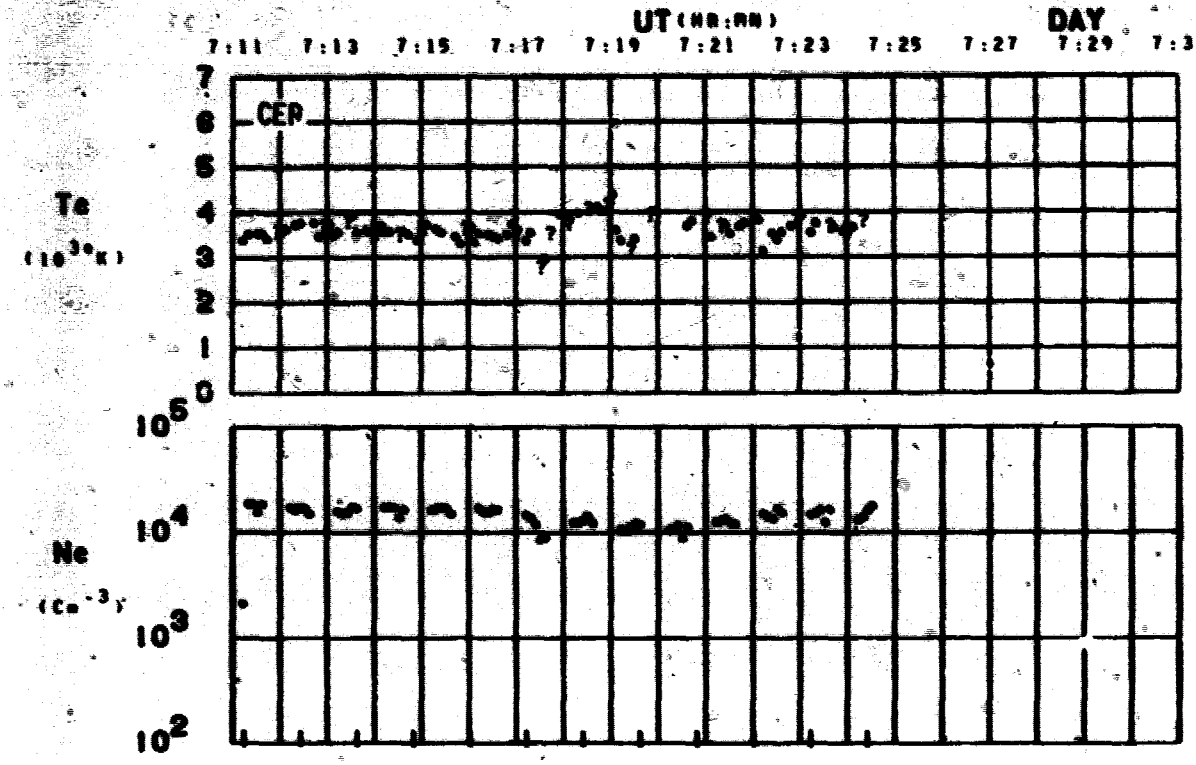

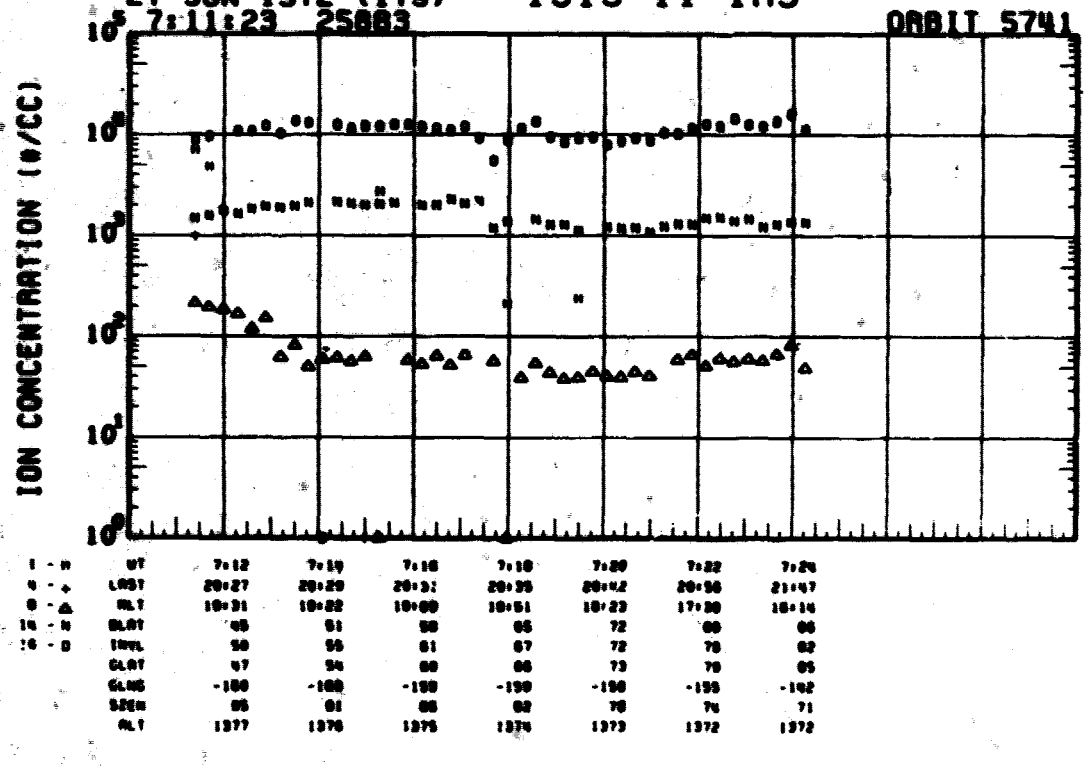

UT	7:12	7:14	7:16	7:18	7:20	7:22	7:24
LAST	20:27	20:29	20:31	20:35	20:42	20:50	21:47
MLT	10:31	10:32	10:00	10:51	10:23	17:30	18:14
GLAT	45	51	58	65	72	80	86
INVL	50	55	61	67	72	78	82
GLAT	47	54	60	66	73	79	85
GLNG	-150	-150	-150	-150	-150	-155	-102
SZEN	85	81	86	82	78	74	71
ALT	1377	1376	1375	1374	1373	1372	1372

SET 36, FORMAT 4

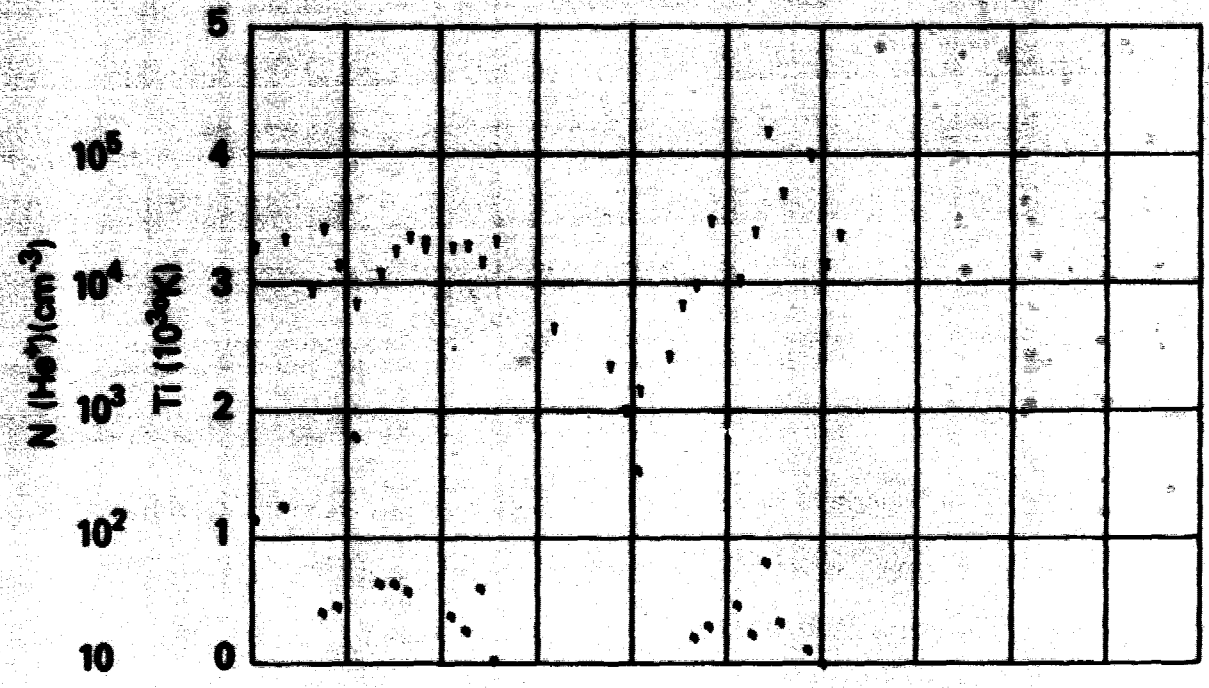

UT	7:12	7:18	7:18	7:18	7:20	7:22	7:26
LMST	20:27	20:29	20:31	20:35	20:42	20:58	21:07
MLT	19:31	19:32	19:00	19:01	19:22	17:30	19:16
GLAT	65	61	60	65	72	68	66
GLON	90	85	81	87	72	70	82
GLAT	67	64	60	66	73	70	65
GLAG	-100	-100	-100	-100	-100	-100	-102
SZEN	85	84	85	82	70	70	71
ALT	1377	1378	1375	1376	1373	1372	1372

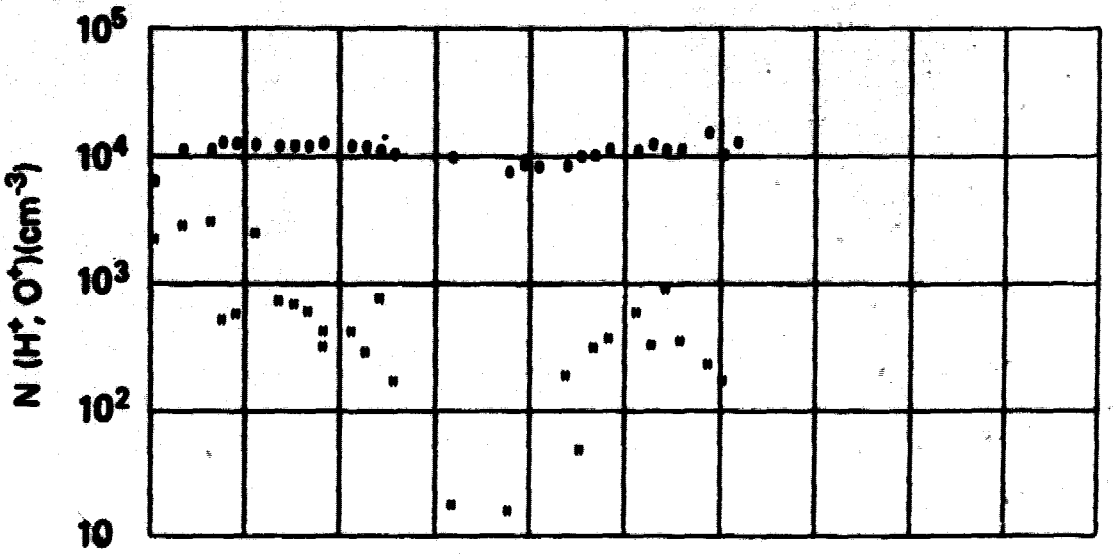

SET 36, FORMAT 5

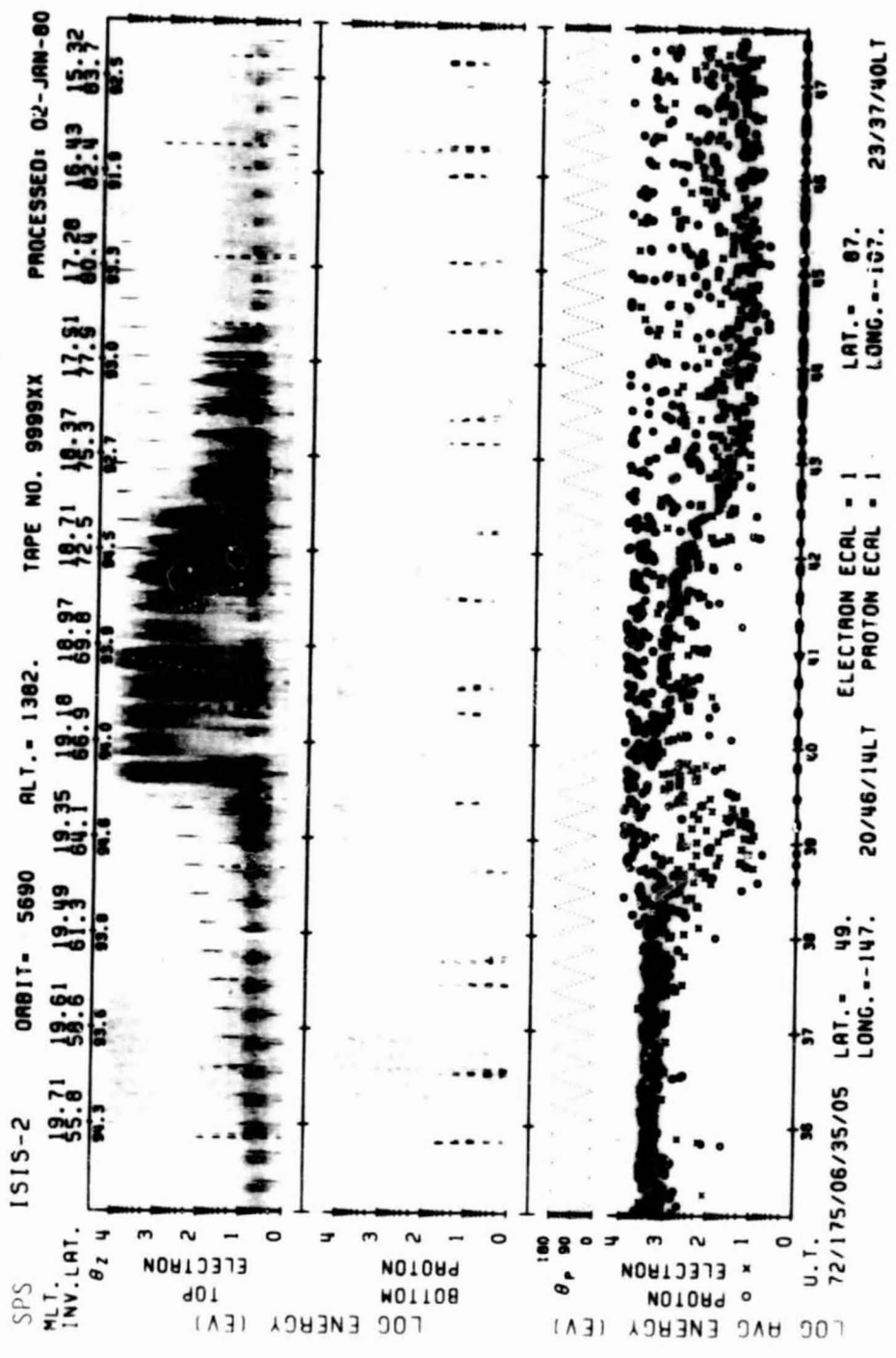

SET 37, FORMAT 6

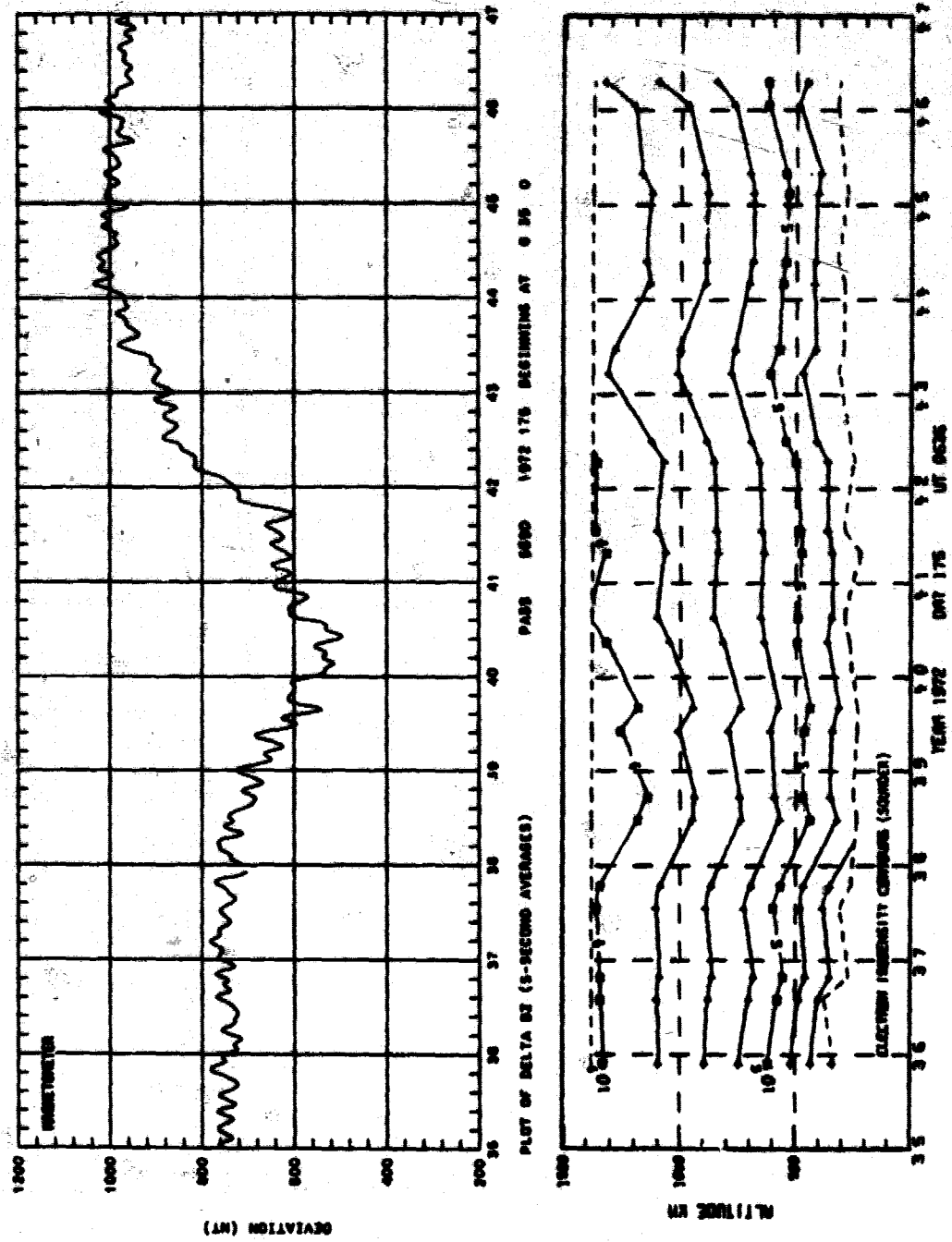

SET 37, FORMAT 2

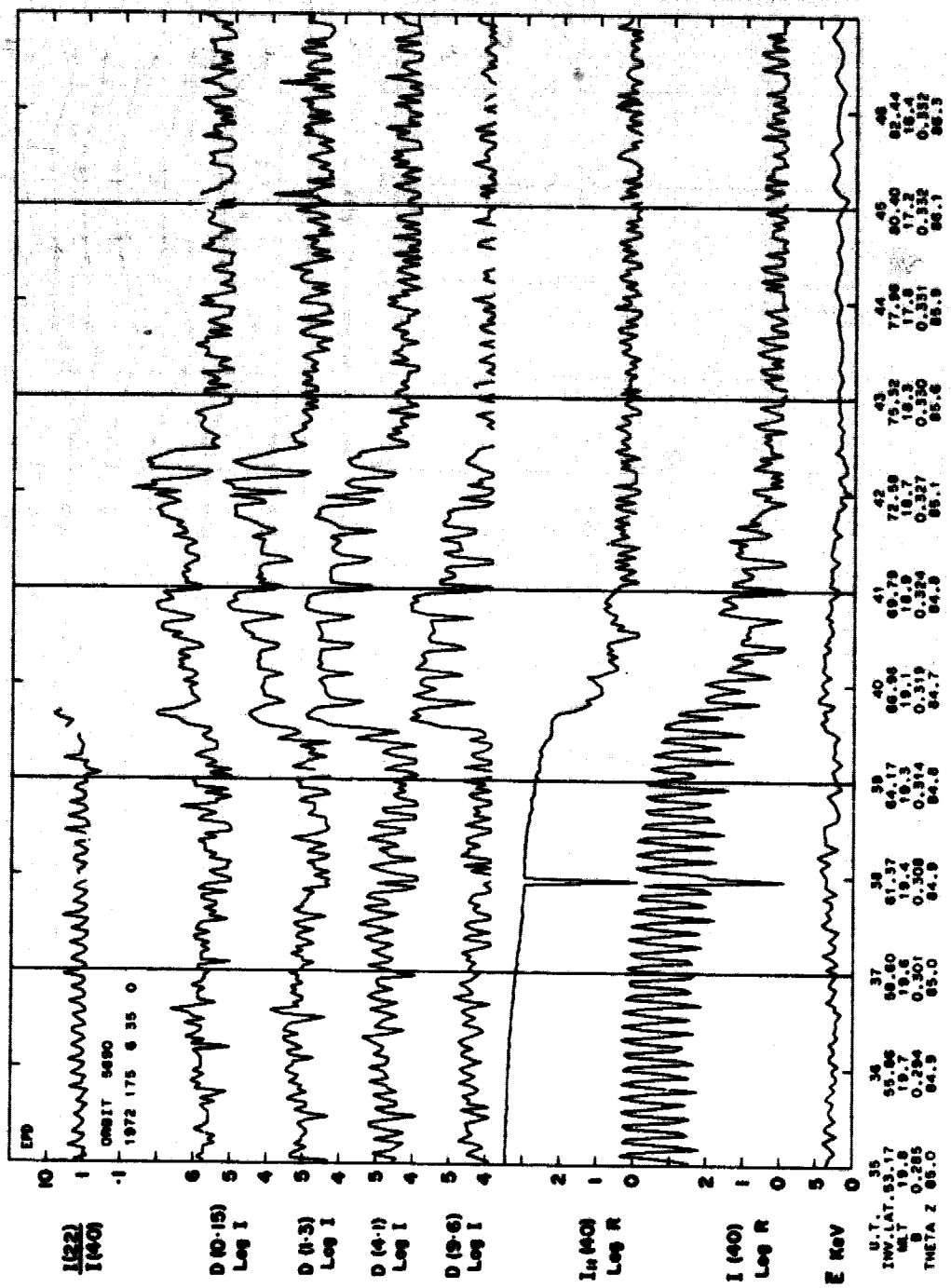

SET 37, FORMAT 3

ORBIT 5690
DATE 720623
DAY 175

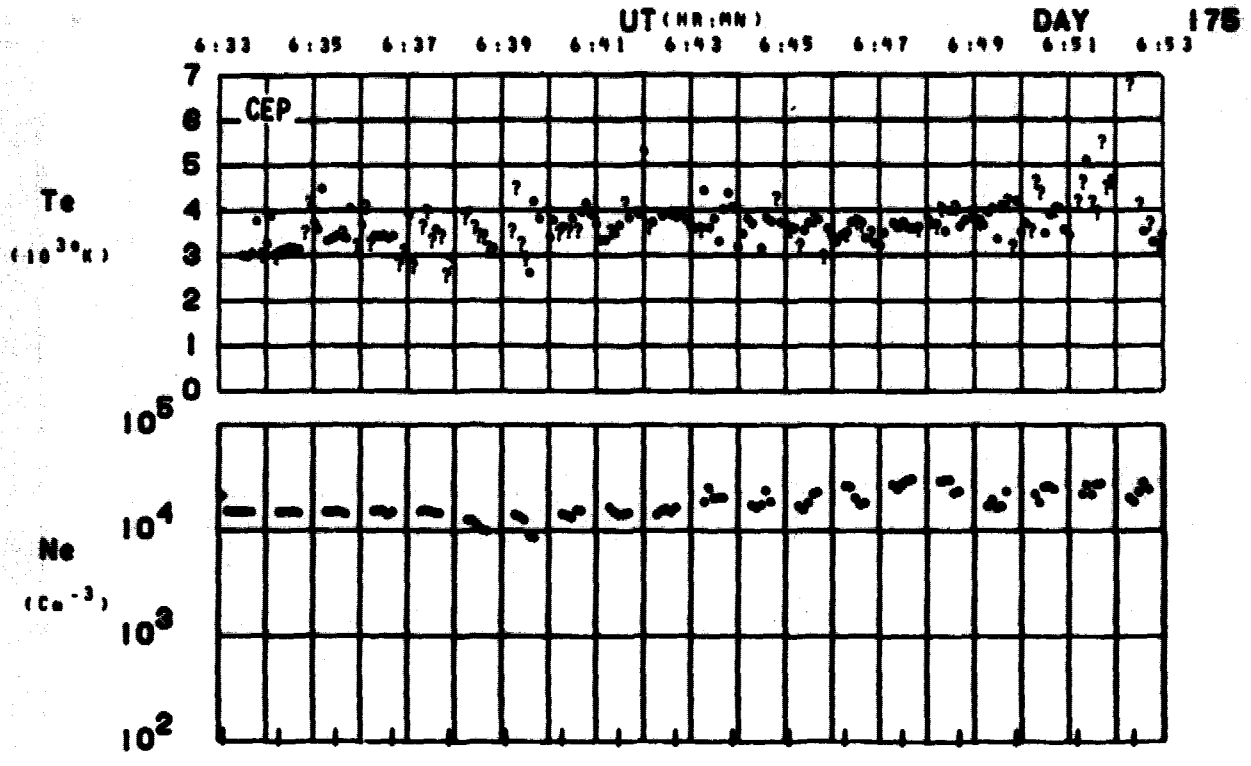

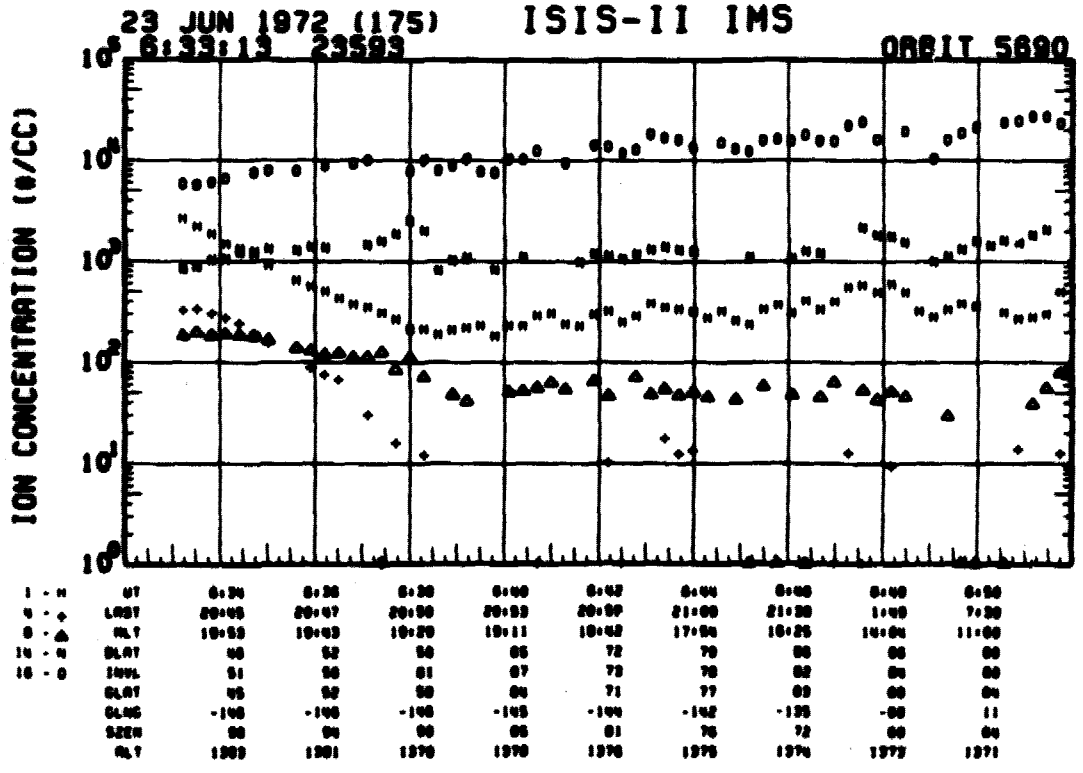

SET 37, FORMAT 4

UT	8:34	8:36	8:38	8:40	8:42	8:44	8:46	8:48	8:50
LOST	20:45	20:47	20:50	20:53	20:56	21:00	21:30	1:49	7:30
MLT	19:53	19:53	19:29	19:11	18:42	17:54	16:25	14:04	11:00
DLAT	46	52	58	65	72	79	86	86	86
INVL	51	58	61	67	73	78	82	84	86
GLAT	45	52	58	64	71	77	83	86	84
GLNG	-148	-148	-148	-145	-144	-142	-135	-86	11
SZEN	86	84	86	85	81	76	72	68	64
ALT	1383	1381	1379	1378	1376	1375	1374	1373	1371

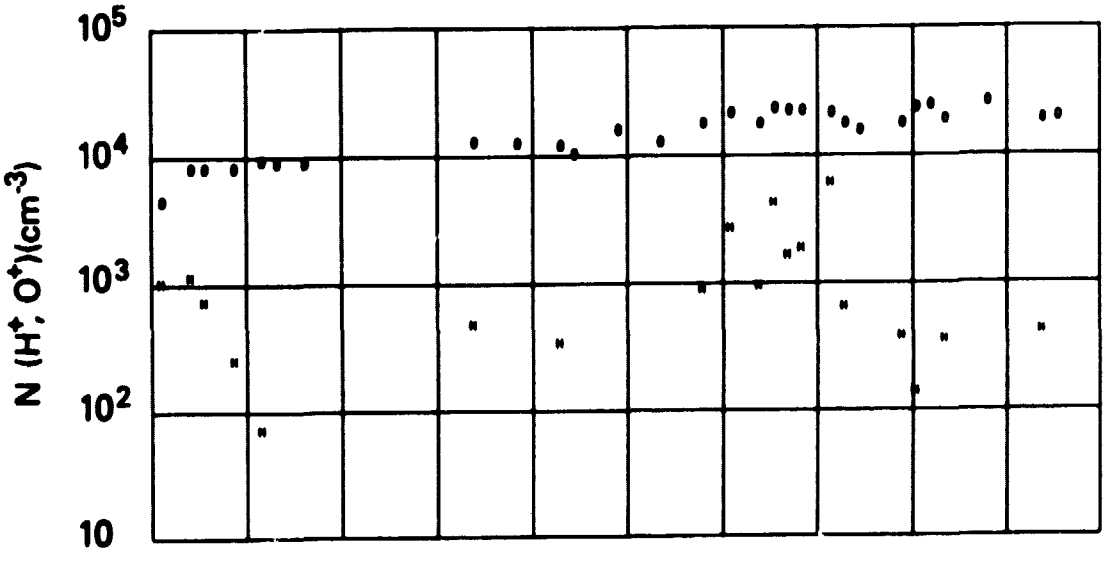

SET 37, FORMAT 5

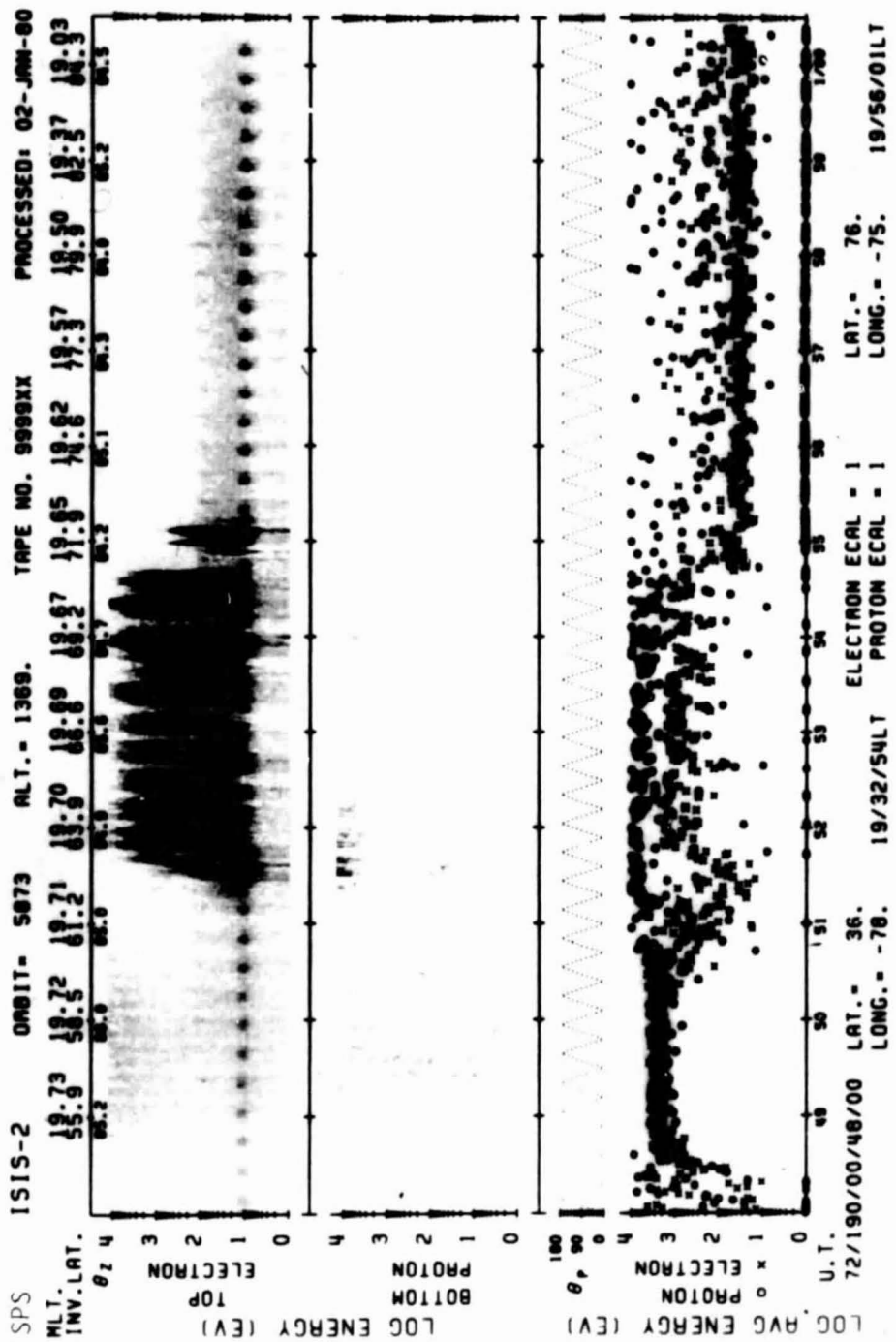

SET 38, FORMAT 6

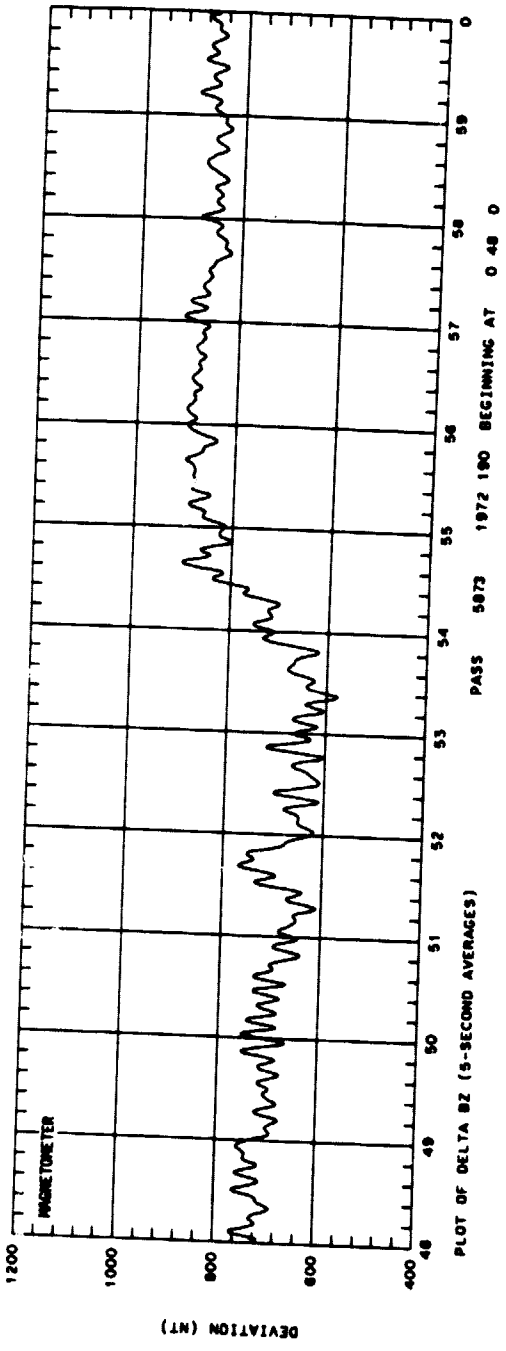

SET 38, FORMAT 2

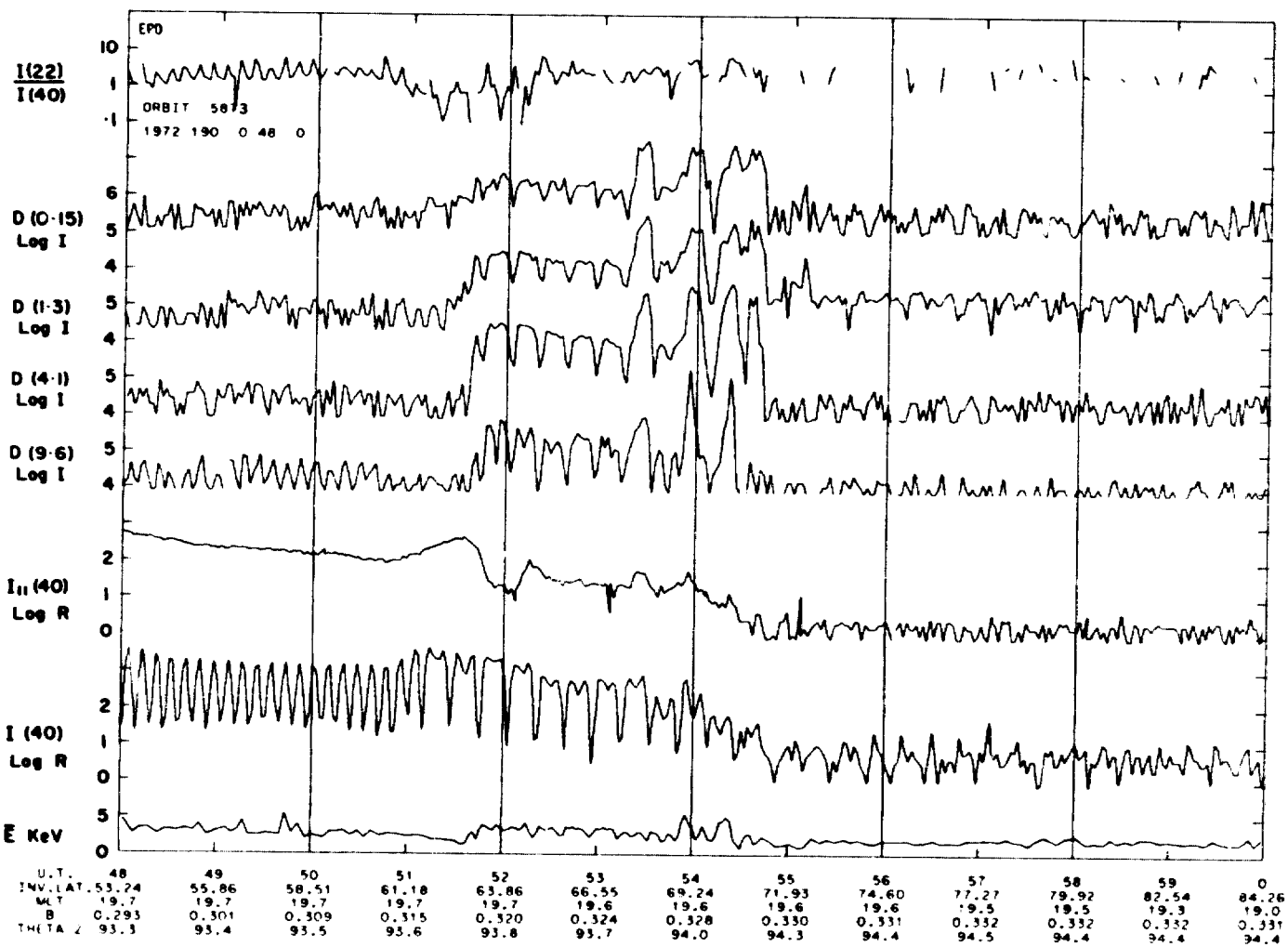

SET 38, FORMAT 3

ORBIT 5873
DATE 720708
DAY 190

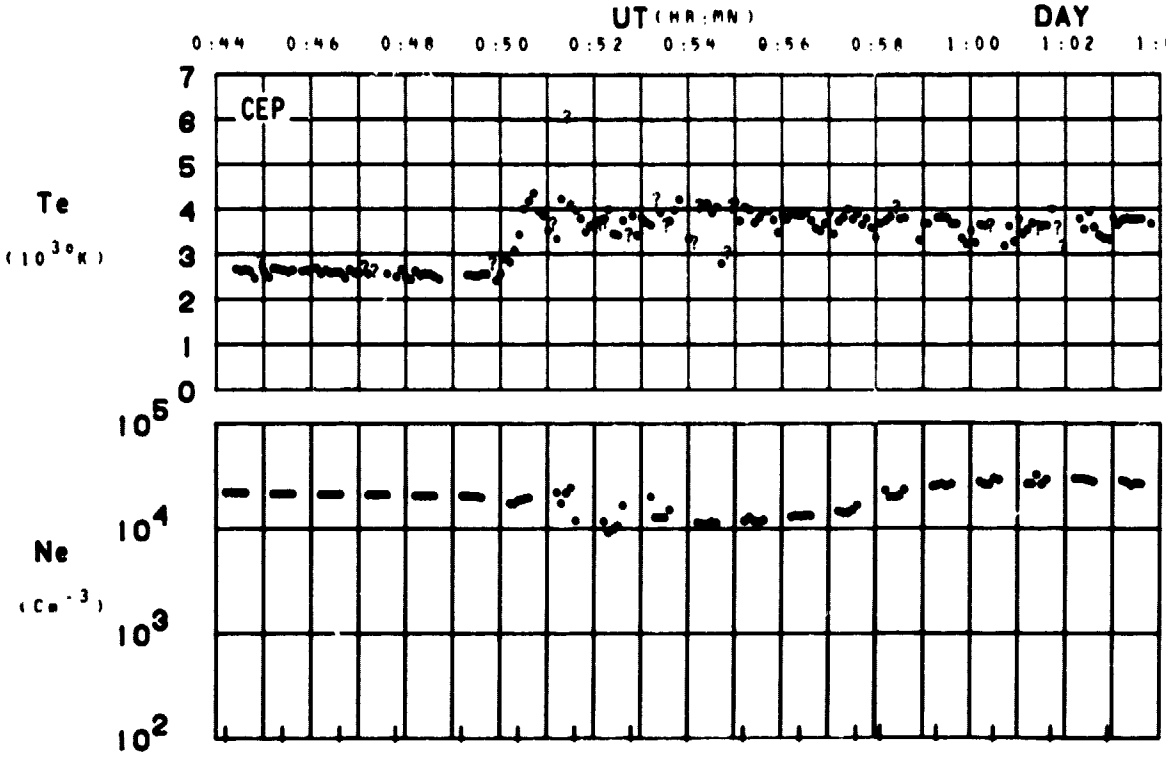

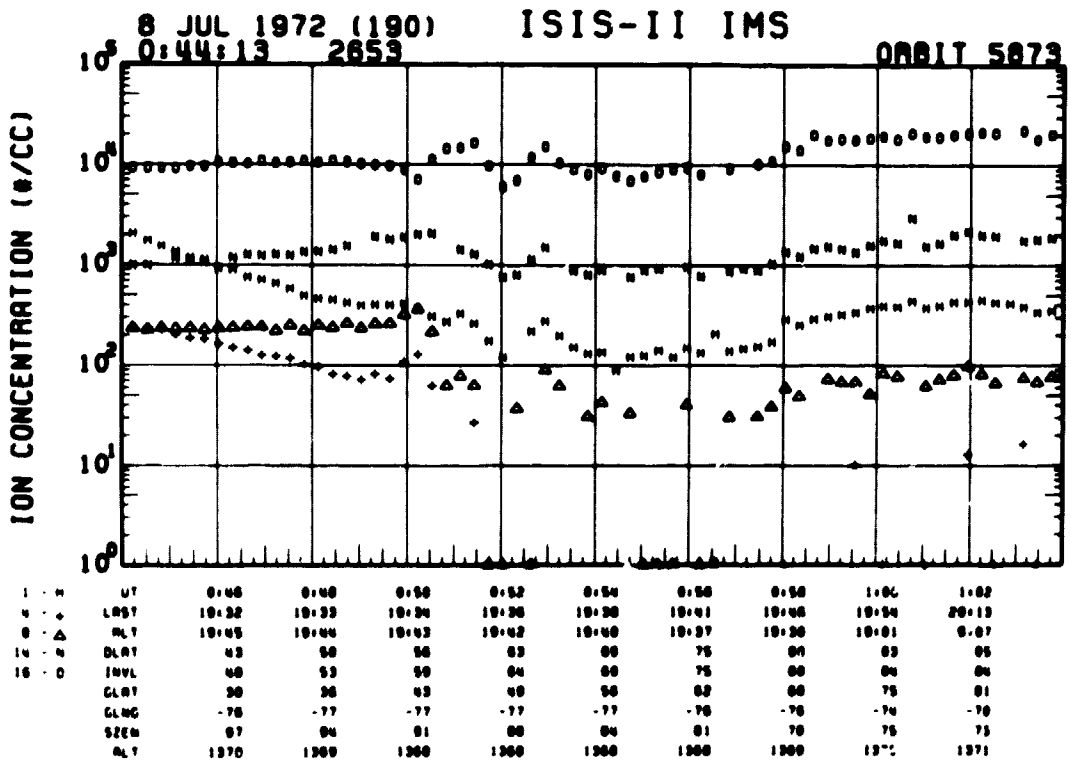

SET 38, FORMAT 4

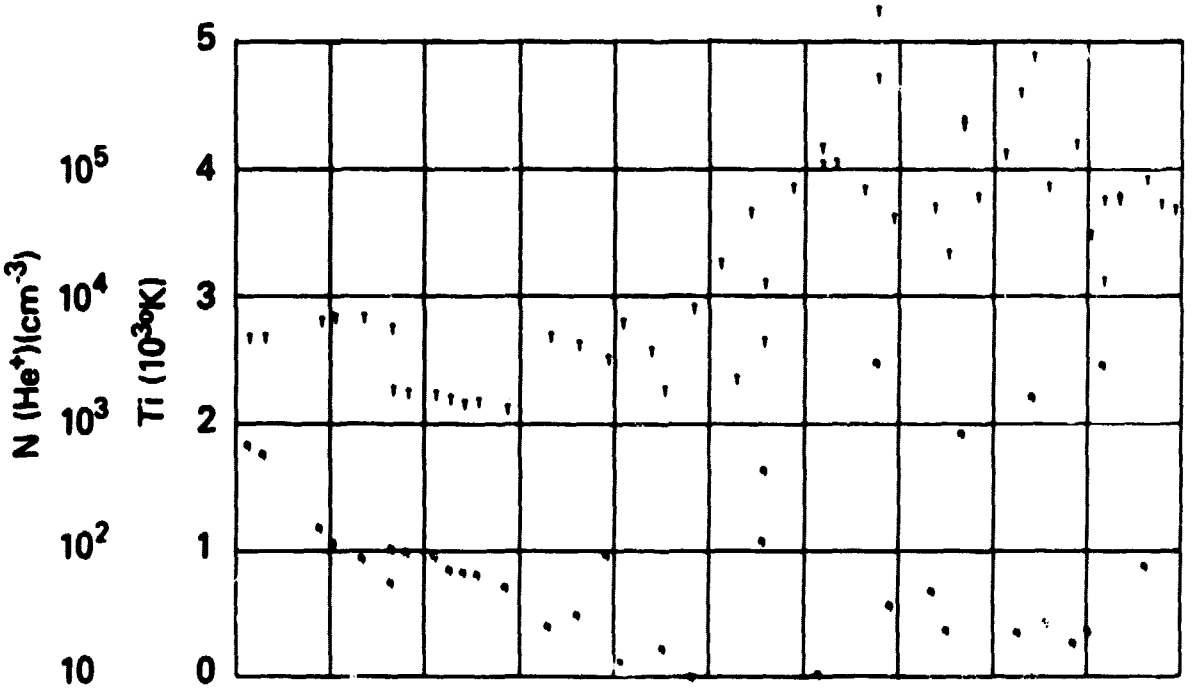

UT	0:46	0:48	0:50	0:52	0:54	0:56	0:58	1:00	1:02
LMST	19:32	19:33	19:34	19:36	19:38	19:41	19:46	19:54	20:13
MLT	19:45	19:46	19:43	19:42	19:40	19:37	19:30	19:01	0:07
DLAT	43	50	56	63	69	75	80	83	85
INVL	40	53	59	64	69	75	80	84	84
CLAT	36	36	43	49	56	62	68	75	81
GLNG	-78	-77	-77	-77	-77	-76	-76	-74	-78
SZEN	87	84	81	80	84	81	78	75	73
ALT	1370	1369	1369	1368	1368	1368	1369	1370	1371

SET 38, FORMAT 5

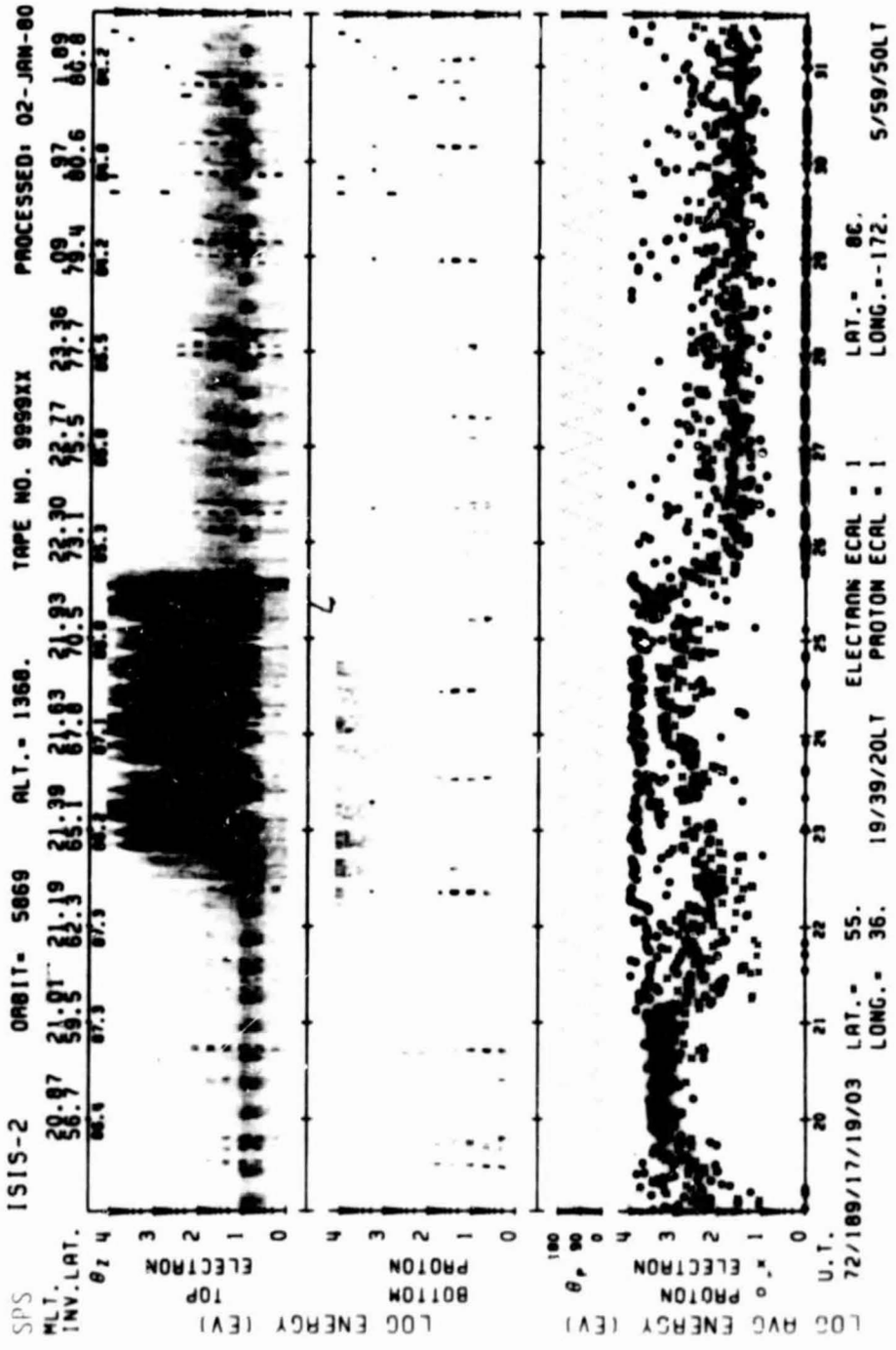

SET 39, FORMAT 6

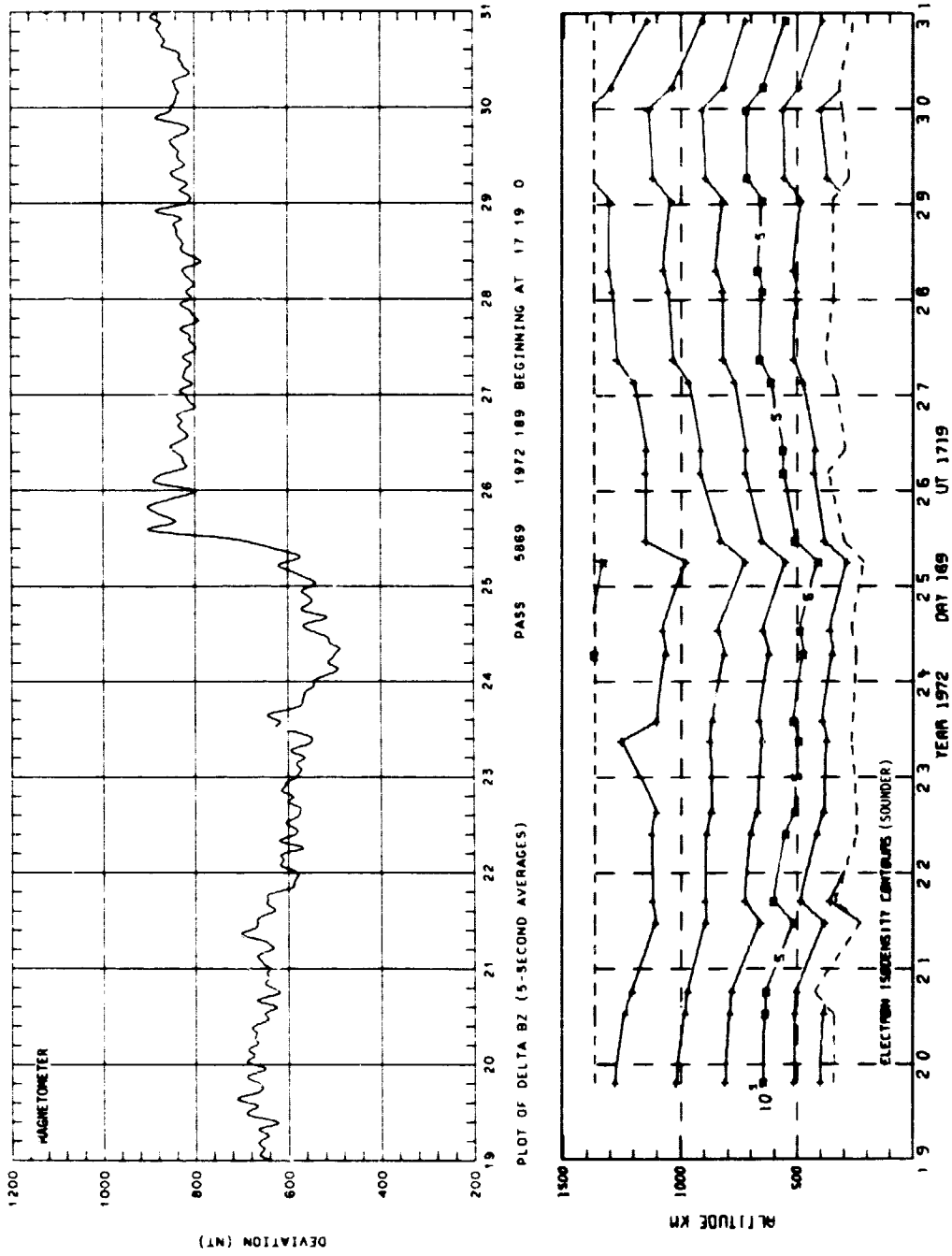

SET 39, FORMAT 2

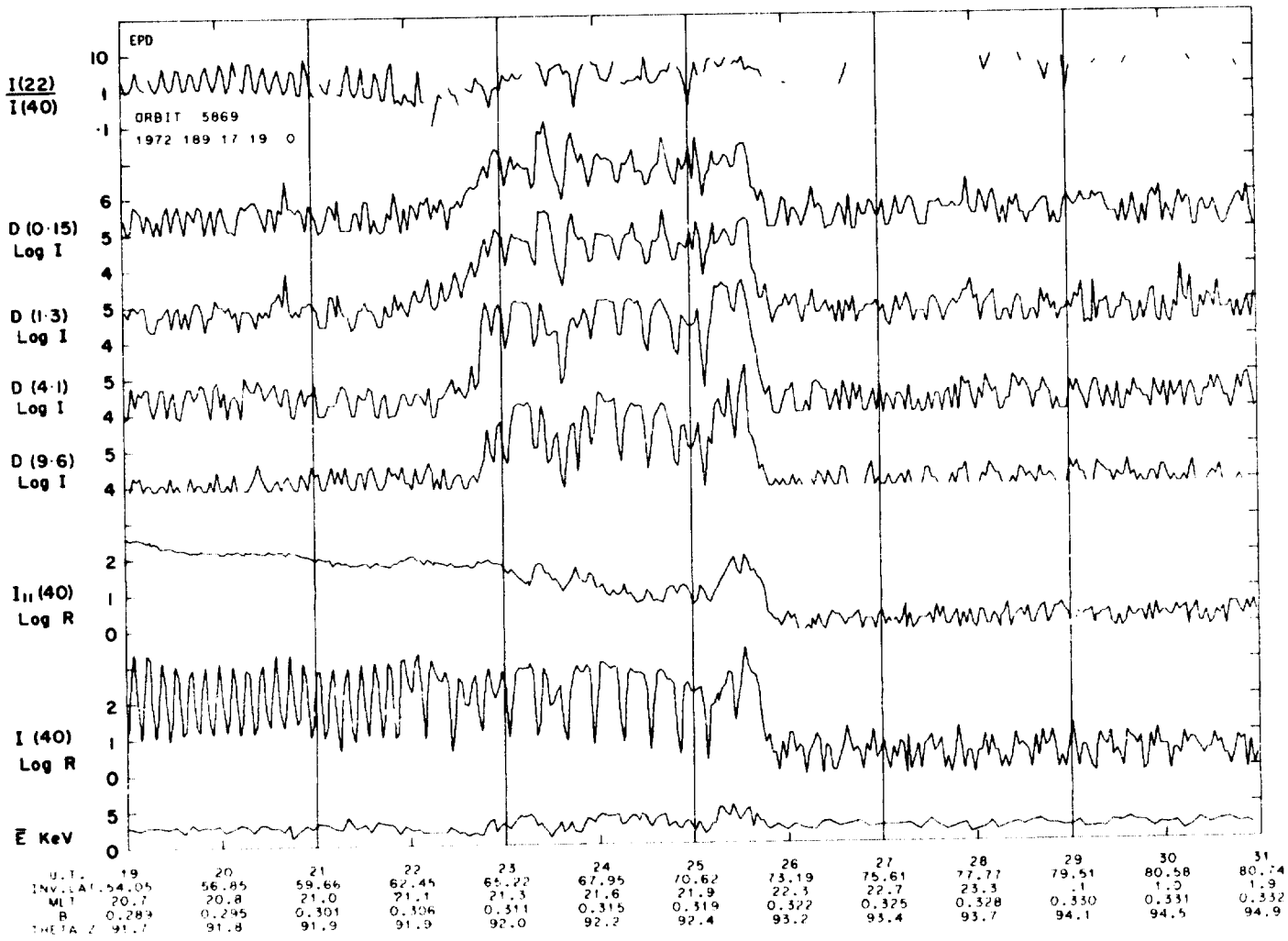

SET 39, FORMAT 3

ORBIT 5869
DATE 720707
DAY 189

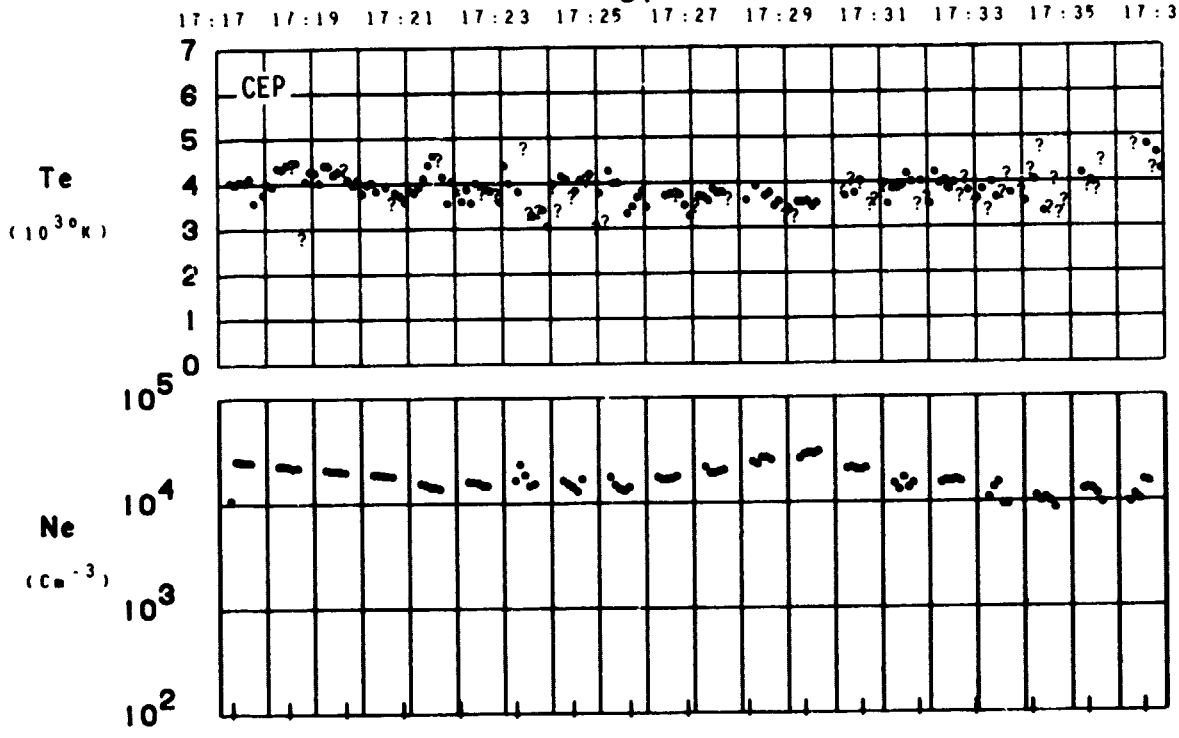

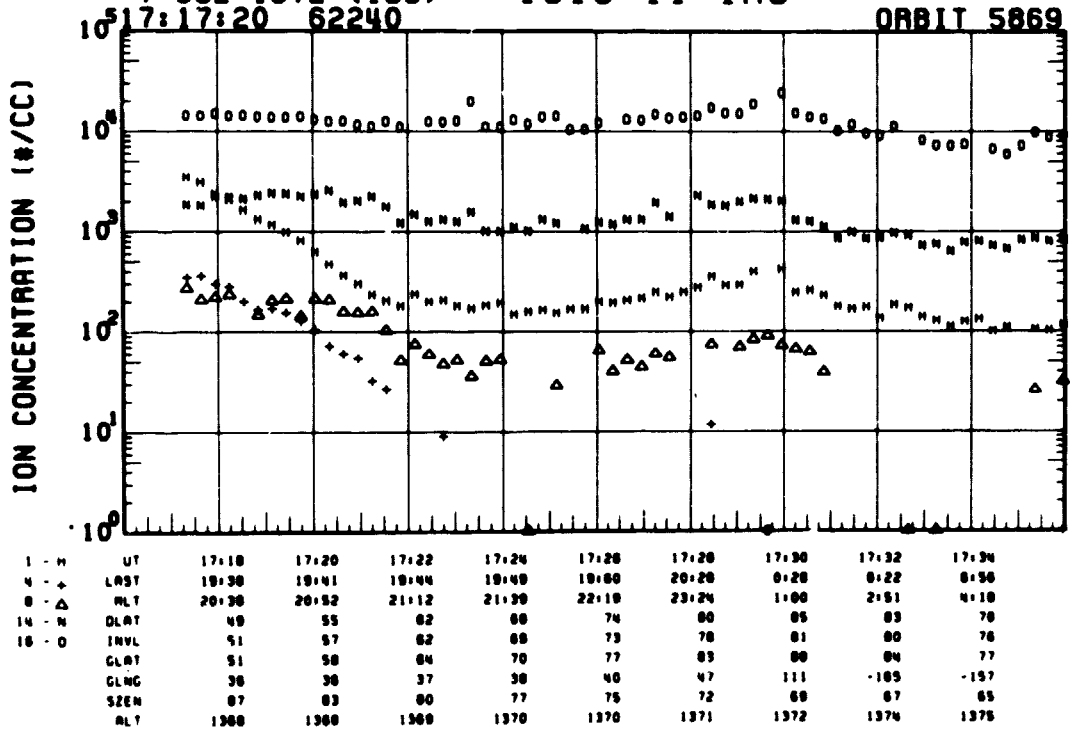

SET 39, FORMAT 4

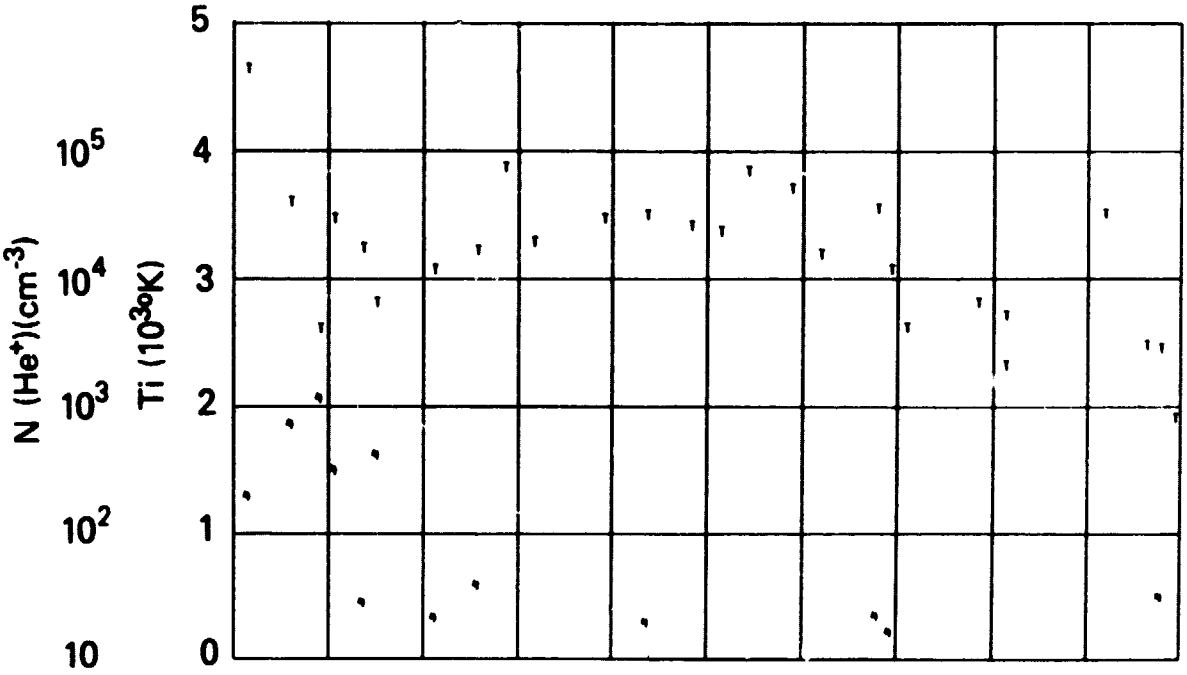

UT	17:18	17:20	17:22	17:24	17:26	17:28	17:30	17:32	17:34
LAST	19:38	19:41	19:44	19:49	19:60	20:28	0:28	6:22	6:56
ALT	20:38	20:52	21:12	21:39	22:19	23:24	1:00	2:51	4:18
DLAT	49	55	62	68	74	80	85	83	78
INVL	51	57	62	68	73	78	81	80	76
GLAT	51	58	64	70	77	83	88	84	77
GLNG	36	36	37	38	40	47	111	-165	-157
SZEN	87	83	80	77	75	72	69	67	65
ALT	1368	1368	1369	1370	1370	1371	1372	1374	1375

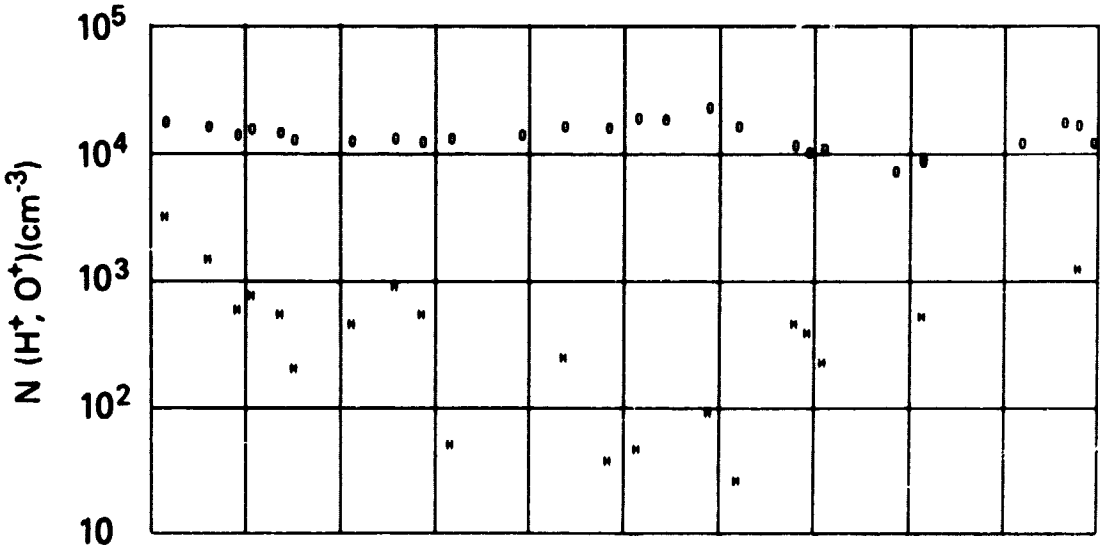

SET 39, FORMAT 5

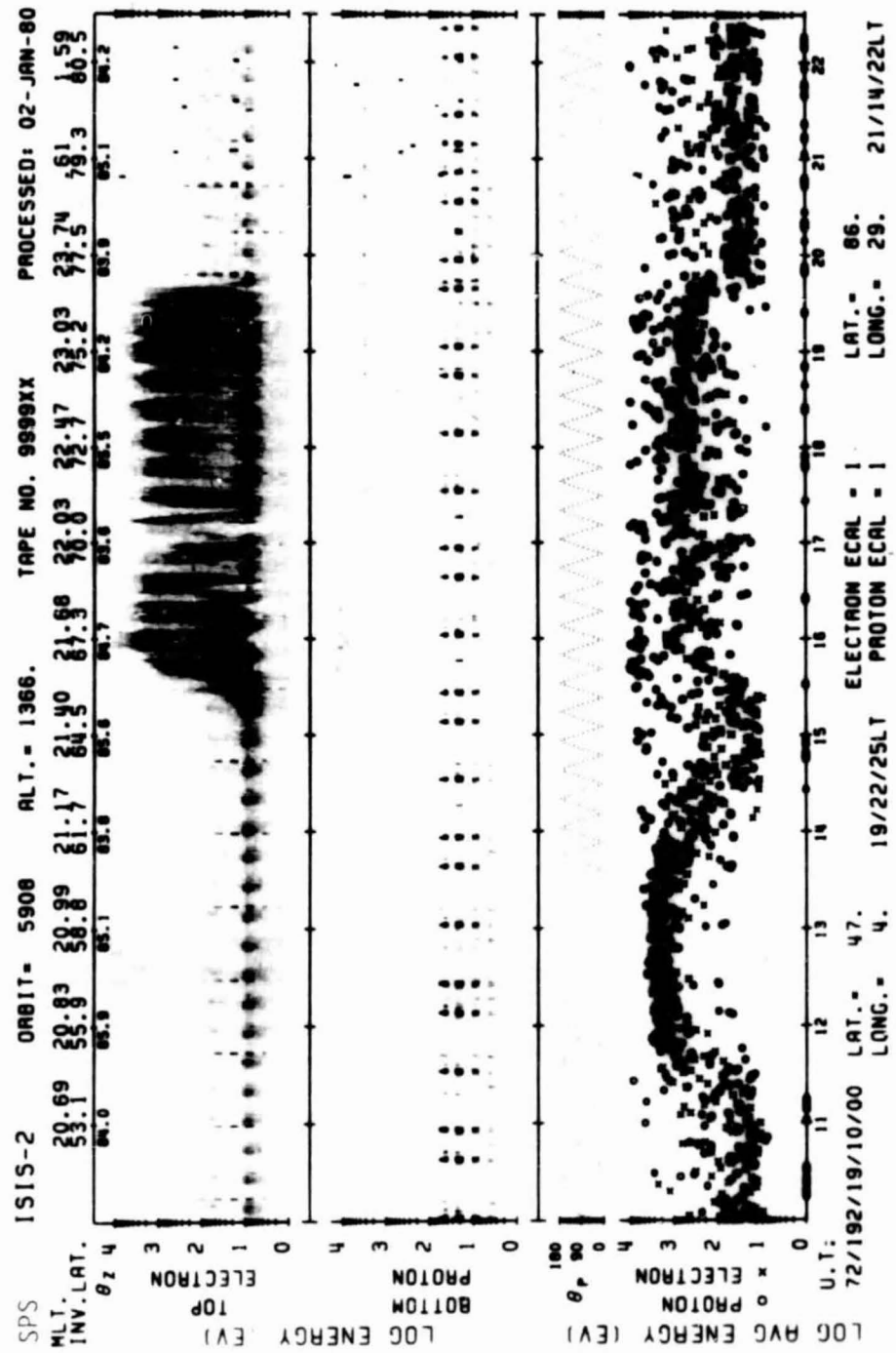

SET 40, FORMAT 6

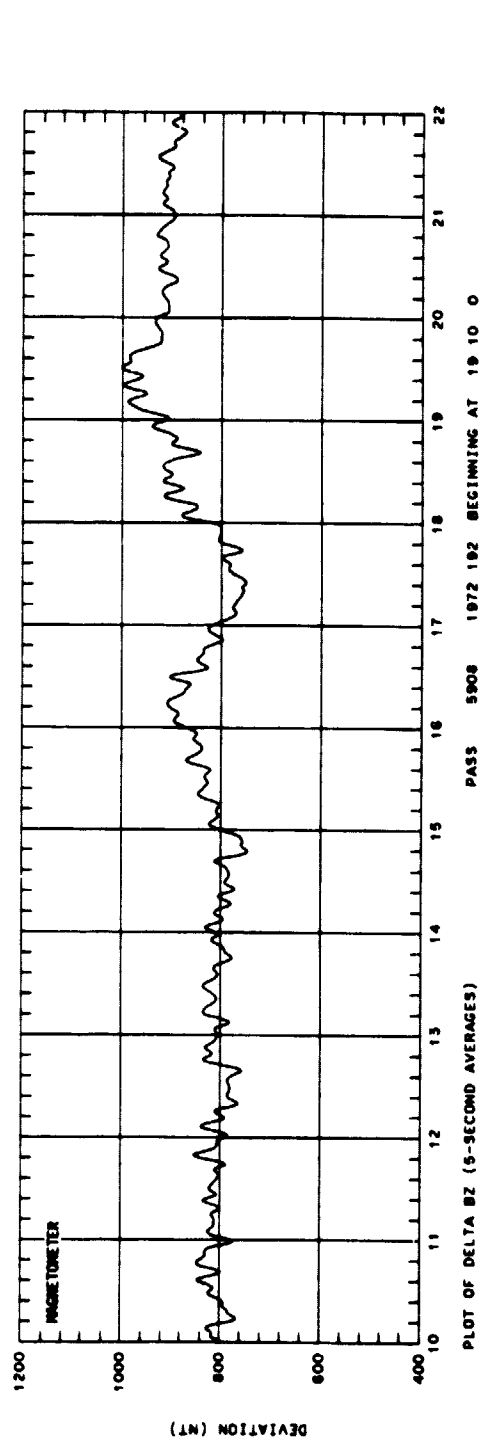

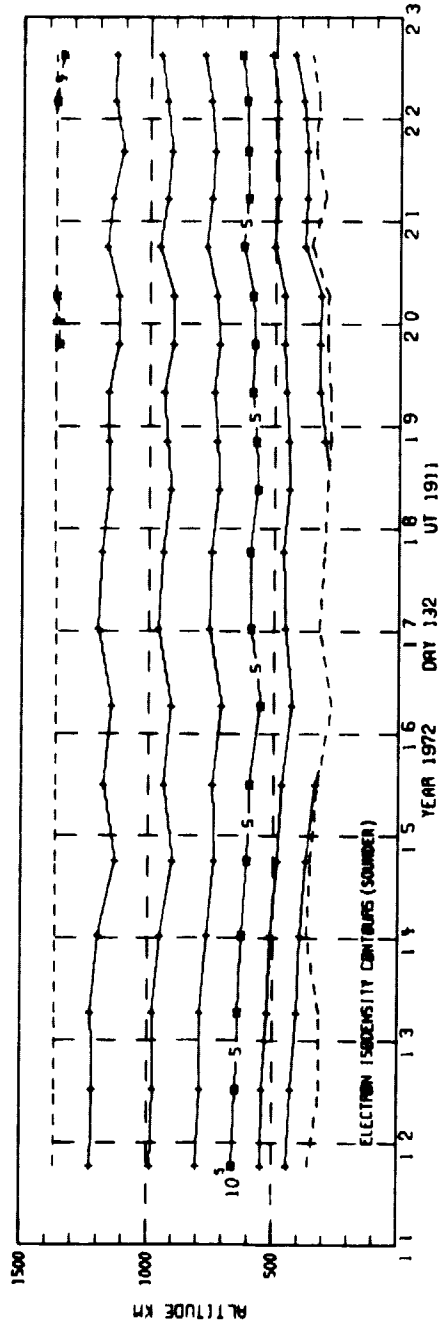

SET 40, FORMAT 2

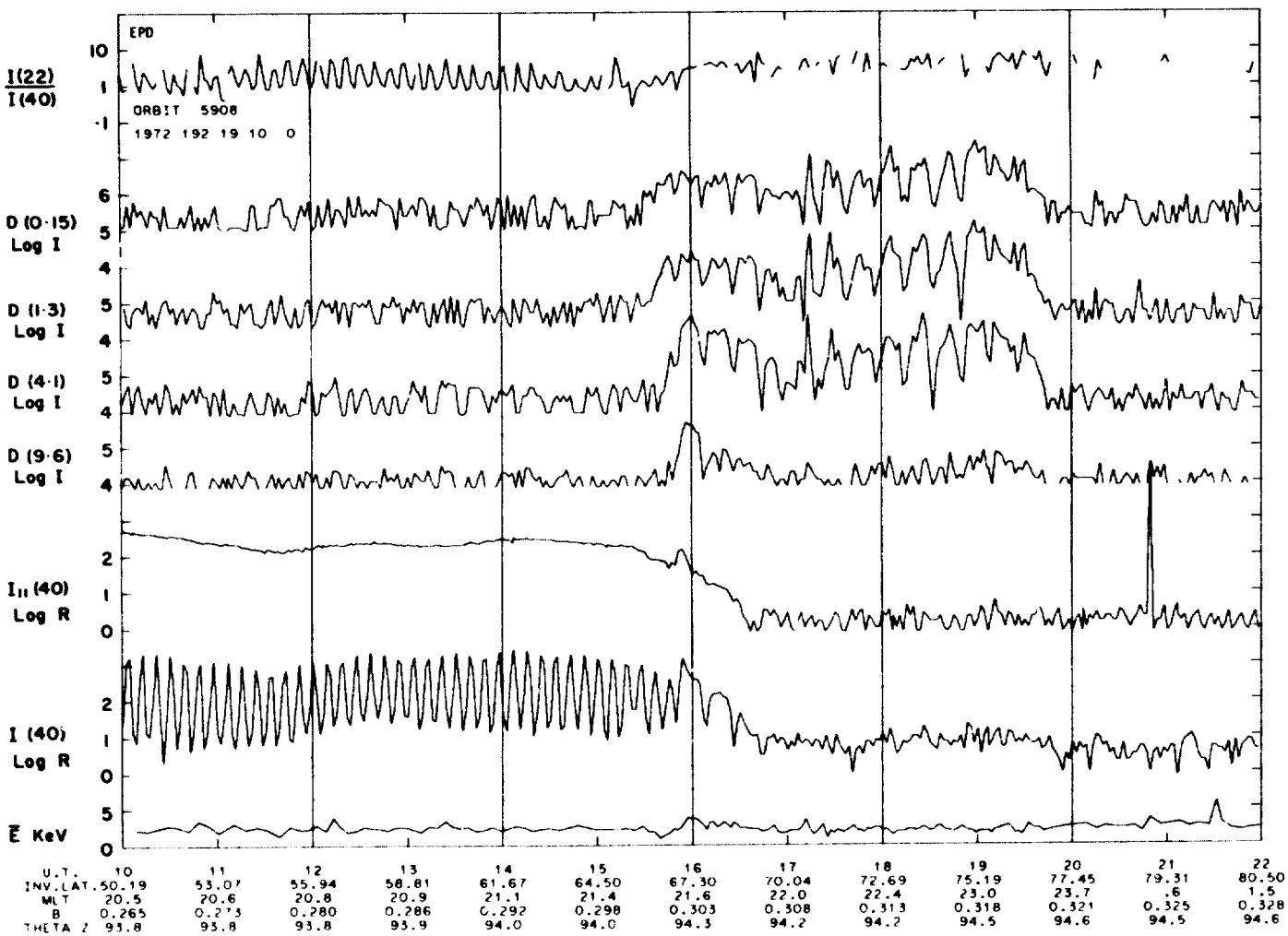

SET 40, FORMAT 3

ORBIT 5908
DATE 720710
DAY 192

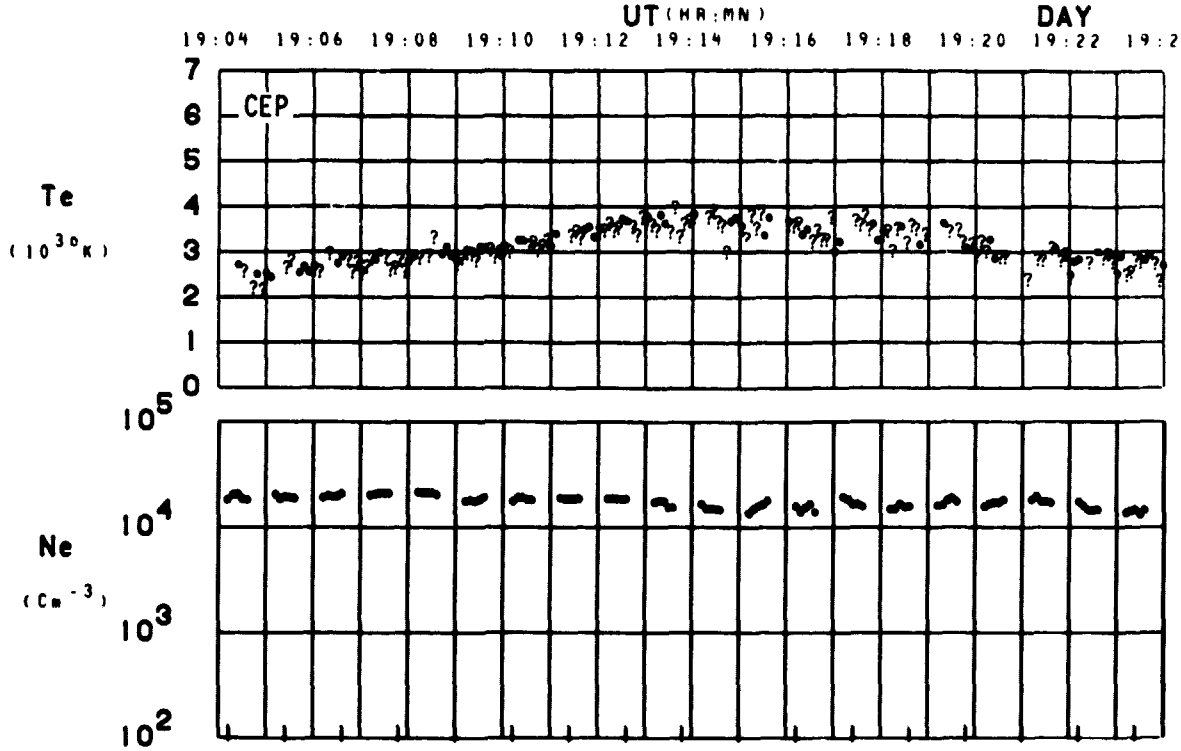

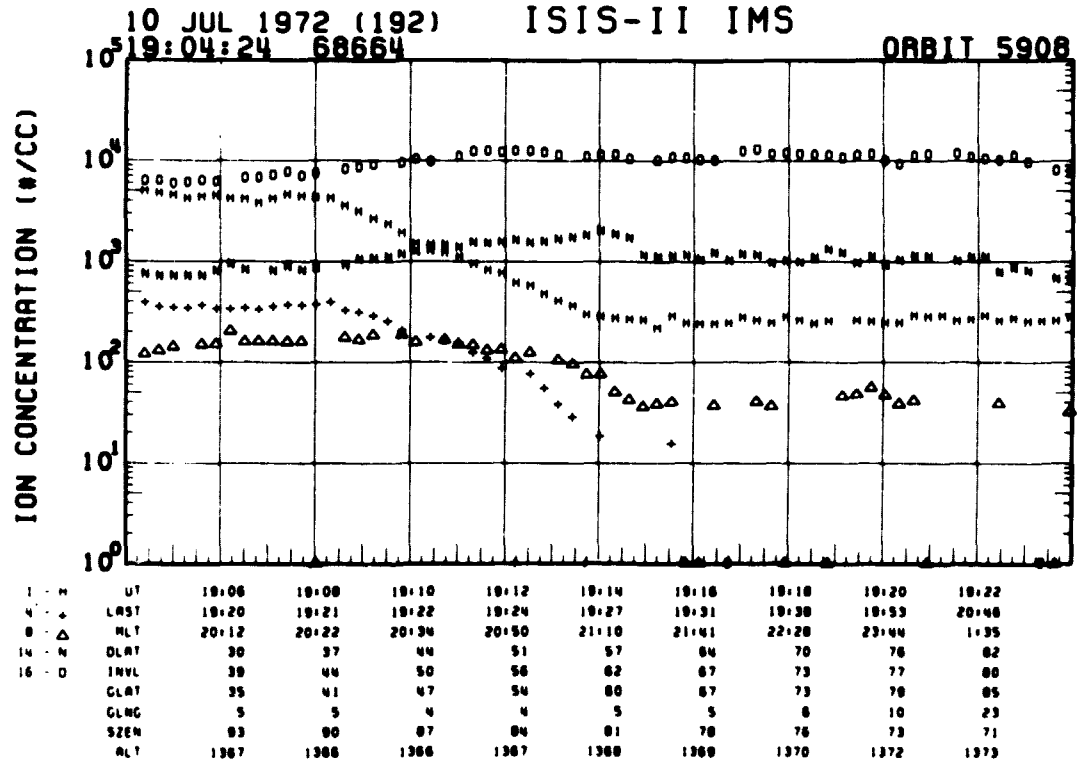

SET 40, FORMAT 4

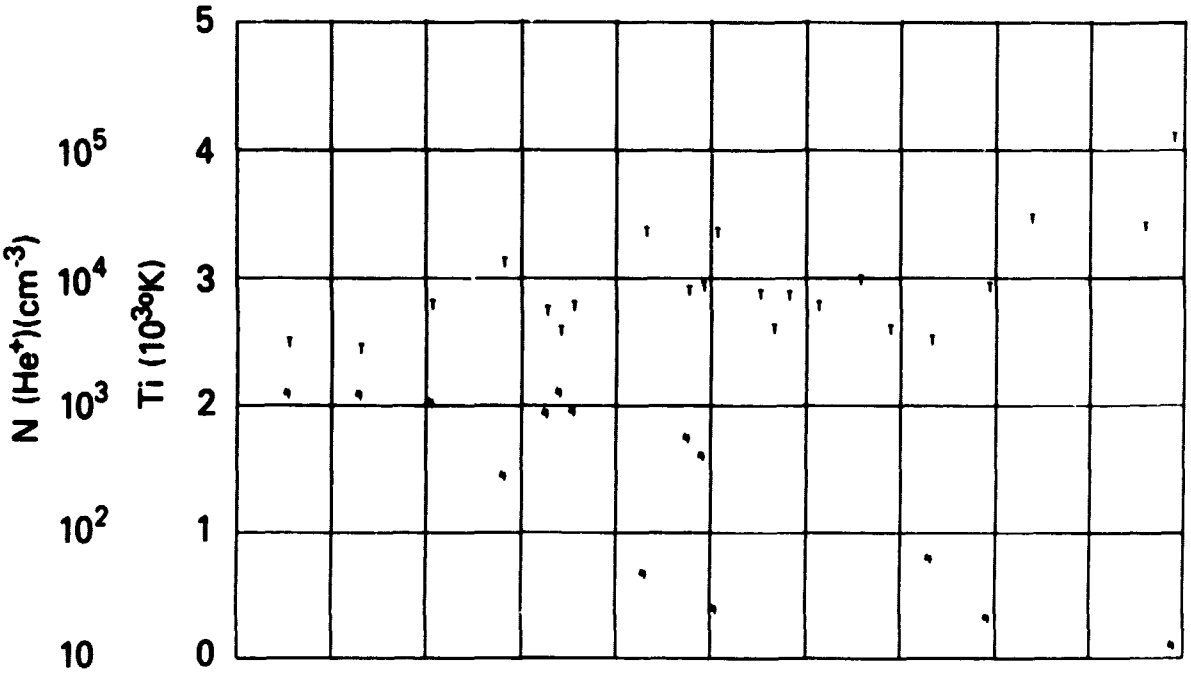

UT	19:06	19:08	19:10	19:12	19:14	19:16	19:18	19:20	19:22
LAST	19:20	19:21	19:22	19:24	19:27	19:31	19:38	19:53	20:48
MLT	20:12	20:22	20:34	20:50	21:10	21:41	22:28	23:44	1:35
DLAT	30	37	44	51	57	64	70	76	82
INVL	38	44	50	56	62	67	73	77	80
GLAT	35	41	[illegible]	54	60	67	73	79	85
GLNG	5	5	4	4	5	5	8	10	23
SZEN	83	80	87	84	81	78	76	73	71
ALT	1367	1366	1366	1367	1368	1369	1370	1372	1373

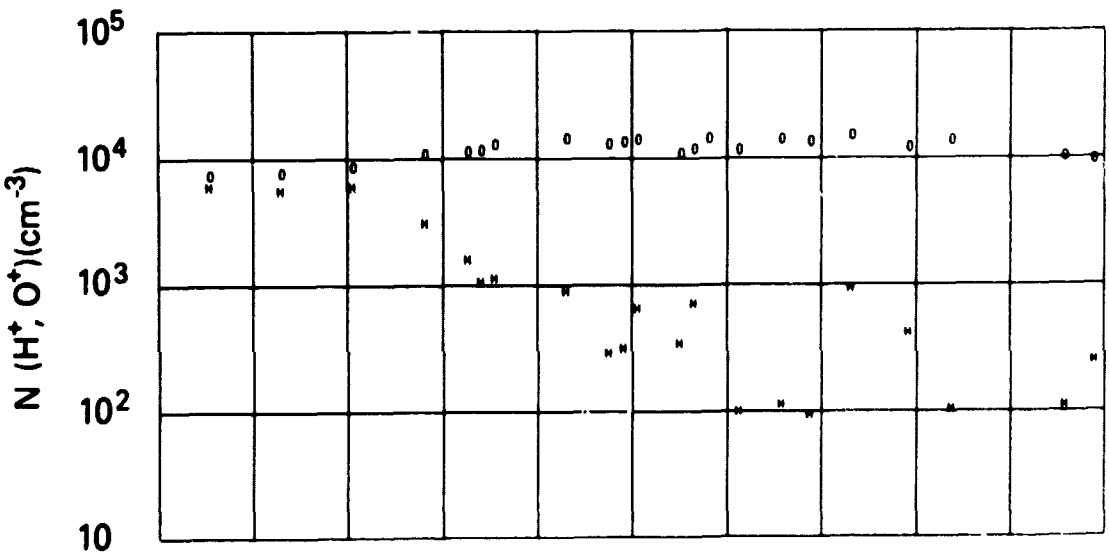

SET 40, FORMAT 5

National Aeronautics and
Space Administration

Goddard Space Flight Center
Greenbelt, Maryland 20771